DEPRESSURISATION OF A SUBCOOLED OR SATURATED LIQUID

by

PANAGIOTIS DELIGIANNIS

THESIS SUBMITTED IN ACCORDANCE WITH THE REQUIREMENTS

OF THE UNIVERSITY OF LIVERPOOL FOR

THE DEGREE OF DOCTOR OF PHILOSOPHY.

DEPARTMENT OF MECHANICAL ENGINEERING

LIVERPOOL UNIVERSITY

June 1990.

ABSTRACT

The present work is concerned with the theoretical and experimental modelling of the behaviour of the flow inside a storage tank during a hypothetical catastrophic structural failure of the vessel. This problem is very important in assessing the safety of storing and transporting high pressure liquified natural gases and refrigerants. During such pressure releases there is not enough time for phase transition phenomena to take place and consequently the liquid enters the metastable region where nucleation occurs to oppose a further pressure reduction and recover the pressure to a maximum.

A comprehensive review of the modelling of two phase flow with particular reference to the role of nucleation resulted in the one dimensional averaged governing equations for a two phase , bubbly, unsteady fluid flow with zero slip (between the phases) has been established.These are used in conjunction with appropriate expressions for the interfacial source terms i.e. interfacial mass and heat transfer, to predict the flow variation inside the vessel during a blowdown.

Based on the same equations and also on a pseudo-slip model for the free liquid-vapor interface , the case of a partially full vessel was also modelled.

To compliment the theoretical studies a series of experiments using freon 12 were performed as a part of a " Blowdown " simulation. Transient measurements of pressure, temperature and high speed photography were used to record the event.A small scale vessel was used so that non-equilibrium effects were emphasised.

Good agreement with the experiments was found provided non-equilibrium effects were included in the model together with an appropriate heterogeneous nucleation model.

The experiments in conjunction with theoretical modelling has allowed the heterogeneous factor ϕ to be determined.

An extension of classical nucleation theory has demonstrated the importance of interacting bubbles in the formulation of the rate of nucleation.

The effect of size, material and roughness of the interior of a vessel was evidenced from the experimental data to be important with respect to the two phase expansion in the vessel.

PREFACE

ACKNOWLEDGEMENT

I am indebted to Dr. J.C. Cleaver for his help, expertise and encouragement throughout the period of this study and the preparation of this thesis.

I gratefully acknowledge the help of Impact Research Group and in particular the patient help of Dr. B. Birch during the set up and performance of the experimental filming.

I also gratefully acknowledge the financial support for this study from the Greek Section of Scholarships and Research of " ALEXANDER S. ONASSIS " Public Benefit Foundation.

I thank Mr B. Baltzopoulos for his help about the computer analysis of the experimental results.

Many thanks to : Mr D. Smith, Mr D. Neary, Mr J. Hardcastle, Mr J. Haughie for their help.

TABLE OF CONTENTS

NOMENCLATURE

a_{gl}	relative acceleration
A	area
BCE	nucleation energy
C_o	flow distribution parameter
c	speed of sound
Cd	drag coefficient
C_d	discharge flow coefficient
f,f'	bubble distribution function, skin friction coefficient
$\vec{F}$	body forces,general force field
g,g_c	acceleration of gravity
g	specific free energy
G	free energy
$\dot{G}$	mass flow rate
H	total enthalpy,channel height
h	specific enthalpy, convection heat transfer coefficient
J	rate of nucleation per unit volume
K	Boltzmman constant
k	conductivity heat transfer coefficient
$\dot{m}$	mass transfer per unit volume
N,n	number of molecules,number of bubbles
Na	Avogadro number
p	pressure
$\vec{Q}$	heat transfer vector
$\dot{q}$	heat transfer per unit volume

r	bubble radius
S,s	entropy,specific entropy
$\tilde{T}$	stress tensor
u	phasial velocity
U',U	total internal energy
Uc	contact surface speed
$\vec{v}$	velocity vector
v	specific volume
V	velocity,volume
VE	slip ratio parameter

GREEK SYMBOLS

ρ	density
α	void fraction
σ	surface tension
μ	viscosity
$\tilde{\tau}$	shear stress tensor
θ	contact angle (nucleation)
ϕ	heterogeneous factor
λ	eigenvalues
χ	quality
ω	frequency

SUBSCRIPTS

k	phase k (=l or g)
b	bubble
i	interface
m	molecule

cr	critical
atm	atmospheric conditions
s	isentropic
w	wall
sat	saturation condition

CHAPTER 1

INTRODUCTION

1.1 DEFINITION OF THE PROBLEM

Over the last two or three decades many engineering problems have required a better understanding of the transient or steady state multiphase flows.In consequence a considerable body of experimental data now exists and many theoretical models developed. The main objectives have been associated with the safety of a plant and/or its economical operation.

Ishii (1975) summarised some of the major applications of two phase flow analysis which include, *1) power systems:* nuclear and conventional power plants,geothermal energy plants,liquid and solid propellant rockets. *2) heat transfer systems:* heat exchangers,evaporators,condensers,contact heat exchangers. *3) process systems:* extraction and distillation units,fluidised beds,chemical reactors. *4) transport systems:* pipeline transport of gas,oil mixtures,slurries,pulverised solid particles.

The theoretical base for calculating the flow field i.e. the velocity, pressure,temperature e.t.c. in all the above systems is the use of the three conservation equations,for mass,momentum and energy.

The rapid technological development,in these areas over the last two decades, requires a precise prediction of the above systems during both operation and potential hazardous

situation.The use of a well designed and instrumented experiment or a highly sophisticated mathematical model (depending on the applicability and availability of the above modelling to a given situation) is well documented in the literature.

Flows that can be encountered in the forementioned systems are generally: i)one component e.g.water-steam, ii)two components e.g. water-air, iii)three components e.g.water-air-particles.With respect to the phases involved: i)gas-solid, ii)gas-liquid, iii)liquid-solid.With respect to the phases interface, these flows can be on a i)developed flow regime and ii)transitional one.There are two distinguished developed flow regimes: i)dispersed and ii)separated flow. The dispersed flows can exist with either bubbly or droplet or particle dispersion. The separated flows can be either stratified or annular.The third category includes flows that pass from separated to dispersed regimes,especially during heat transfer processes,e.g.nuclear reactor core.

The present study is concerned only with a narrower range of the general multiphase and multicomponent problem, that is the two phase transient flows during fast pressure releases of storage tanks.During these releases the high enthalpy system feels the lower ambient pressure which results in a vigorous phase transition.Depending on the size of the rupture in the vessel, the system can be assumed to remain in equilibrium or not.For small holes in the structure of a pressure vessel,the mass flow rate is very small which gives a long time for the system to form vapor and so to remain in thermal equilibrium.On the other hand when the breakage is quite large the liquid enters the metastable region and nucleation will not take place until the liquid's superheat is sufficient. Theoretical models with or without provision for thermal disequilibrium are more or less successful depending on the type of opening.The thermal non-equilibrium aspect of fast pressure releases is the main subject of this study.

In the literature there are works performed to study both the two phase flow variation inside the pressure vessel and also the behaviour of the outflow from the break area.The better prediction of the dynamic behaviour of the mixture will result in a safer design of pressure release devices,and other components of neighbouring structures,which in turn will

minimise any potential risks.From figure 1,it is apparent that depending on the type of breakage,small hole or a catastrophic failure,and the part of the vessel where the breakage takes place,an outflow of either pure liquid or pure vapor or a two phase jet may occur.It is of great importance,for stored toxic,flammable e.t.c. substances,to be able to specify apriori the mass flow rate from the opening,the sizes of droplets in the two phase misty jet and the void fraction,so in conjunction with the local ambient velocity to predict the spread of the heavy gas to the surroundings.Even in the case where a special pool is used to concentrate any liquid outflow,during an accidental pressure release (see fig.1e),if the substance has a quite low saturation pressure for the ambient temperature,flash/evaporation may take place,which will lead to a vapor-air mixture which may disperse as a plume. Figure 1g illustrates the need for successfully designing the supports of the storage tank,to withstand the thrust produced by the momentum of the jet.Figure 1d depicts the general case of liquified gas jet escaping from the tank or attached pipework.

The main point here is that loads on structure will require knowledge of the transient momentum thrust from the break.The safety of the vessel will depend on how quickly a vessel can be vented to atmosphere.The extent of a plume of toxic or inflammable gas will depend on a knowledge of the transient mass flow rate from the rupture, also the structure of the two phase mixture.

1.2 LITERATURE REVIEW

The very important problem posed by the existence of the nuclear reactors energy plants was the main reason for the blossoming of transient two phase flow modelling over the last few decades.A sudden breakage in the cooling loop of the nuclear core of the LWR power generating systems would result in a vast pressure reduction of the water and vapor

production close to fuel rods.A "dry out" mode of heat transfer to the cooling system would then result in quite high temperature of the core and its melt.Therefore,careful predictions have to be made to provide certain information with respect to the mass flow rate of the water-steam mixture,the time interval available for any precautions to be taken (closing of certain valves or activating a secondary cooling system,e.t.c.). The expense involved in a full scale loss-of-coolant accident (LOCA) simulation has restricted the LOCA modelling to a theoretical consideration.Nevertheless there have been scale-down tests of the so called LOFT systems,reported by D.L. Reeder (1978) and M.I. Patton (1978).Less complex geometries,however, have been also experimentally modelled,in the form of pipe blowdown,where only the part of the loop,which includes the breakage is modelled,after it is isolated with a closed valve (closed end of the simulation pipe).

One way of checking the potential of the theoretical models was to run them for the initial conditions of the above both complex and less complex experiment. The base for all theoretical simulations was the solution of the conservation equations for mass,momentum and energy.Over the years different theoretical modes have been proposed,whose complexity depends on the assumption for either homogeneous,or thermal non-equilibrium or both thermal and mechanical non-equilibrium,or even different velocity,temperature and pressure for each of the phases,two phase flows.

Wolfert K.(1976) reported the two versions of DRUFFAN code,one with the homogeneous mixture assumption and the other with the thermal non-equilibrium one for dispersed flows.The last version incorporated an interfacial mass transfer model which included a slip between the phases.A simple model for calculating the bubble rising velocity was given as:

$$V_b = Kr_b \qquad (1.1)$$

where V_b is the bubble velocity,K a constant (sec -1) and r_b the bubbles radius. The above interfacial mass and heat transfer model had also one more free parameter (beside K) the number density of the bubbles.The code was checked against the experimental data reported by Edwards and O'Brien (1970).Most of the theoretical models reported over the years,often are run for the initial conditions of Edwards and O'Brien hot water,4.1 m long pipe blowdown experiments.The above theoretical model seemed to predict the metastable region quite accurately by carefully selecting the values for K = 1E2 sec-1 and N_b = 1E9 m-3.

W.H. Reed and W.L. Kirchner (1977),reported a 3-D UVUTEP computer code called TRAC.The slip model for this model was supplied by a drift-flux model.The advantage of the code was its ability to simulate two phase flows in detailed plant components such as,pipes,pumps,steam generators e.t.c.Like the other codes,of the new generation of two fluid flow assumption,appropriate models for the interfacial transfer terms were employed together with a detailed flow regime map which depending on the void fraction and the mass flow rate ,would activate a different model for the interfacial heat ,mass and momentum transfer terms.

FLASH-4 is another extensive LWR-LOCA simulation,which was built to complete the homogeneous model (RELAP4) reported by K.V. Moore and W.H. Retting (1973). The more sophisticated model,reported by R.W. Lyczkowski et.al. (1978),included slip between the phases.

S.Banerjee et.al. (1978) reported a simple homogeneous model called RODFLOW, which incorporated empirical expression for a superimposed slip and a steady state discharged model.They compared it with Edwards and O'Brien (1970) and other experimental data and they claimed a quite good agreement.The only deficiency was that the model could not predict the metastable depressurisation. This model was capable of simulating blowdown from heating pipes,by incorporating a 2-D thermal conduction equation for the heating tube.

Another major LWR code was reported by J.Loomis et.al. (1981).This is a 3-D UVUTEP model called THERMIT.Because of the complexity of the flow in the nuclear reactor,a flow regime map is also simulated to provide the appropriate relations for the interfacial transfer

terms.In 1982 J.E. Kelly and M.S.Kazimi reported a simplified flow regime map,which only depended on the pre- and post- dry out conditions and they claimed that the LWR practical operation conditions were fully covered.

Last is the LAURA reported computer code,by N.C. Markatos et.al.(1983). This is a 1-D UVUTEP model which incorporates a heat conduction equation for the fuel-rod temperature field calculation.

All the above computer codes are based on a very complicated mathematical modelling of the two phase flow.Considerable effort has been devoted to the development of the theory starting from the simple homogeneous model to the more complicated two fluid one.The first approach for mastering the formidable problem of the multiphase flow was to introduce the averaged process,which would result to more workable set of equations.Among others Ishii (1975) and D.A. Drew (1983) reported averaged conservation equations.Depending on the assumptions made,it is possible that the set of the governing equations is not of the hyperbolic type i.e. that the eigenvalues resulted from the forementioned set of equations are partially complex.This would result to uncontrolled growth of small perturbations,which is the result of important physical processes. Generally a homogeneous (EVETEP) and a thermal non-equilibrium (EVUTEP) model has real characteristics,where as a thermal and mechanical disequilibrium one does not.J.R. Travis et.al. (1976) built a multipurpose model for analysing LWR safety,dynamics of fluidised dust beds,raindrops or aerosol transport and other similar circumstances.His model was a drift-flux thermal equilibrium one and he claimed to have real characteristics.

Another drift-flux model was reported by R.W. Lyczkowski (1976) which made use of the two momentum equations (one for each of the phases) and he derived a slip equation for the flow field.Then by applying the necessary assumptions, he balanced the interfacial friction and gravity forces and with the use of an empirical steady state drift-flux expression he closed the set of the governing equations.

But in practical cases such as storage and transportation of liquified gases and during a LOCA,it was suggested by a great number of investigators,that both thermal and mechanical disequilibrium phenomena take place.However,these models have generally two complex roots resulting in an ill-posed problem. R.W. Lyczkowski et.al. (1977) suggested that a completely implicit centered difference numerical scheme can solve the ill-posed problem.The increased mesh spacing acts as a damping term for the growing instabilities and this is only possible in the finite deferences solution procedure.Where as for the method of the characteristics serious limitations exist that govern the dx/dt increment. That is why R.W. Lyczkowski removed the numerical instabilities by the addition of physically motivated differential terms.The $p\partial\alpha/\partial x$ term,omitted by many investigators,introduces a dynamic force acting on the interface and inclusion of which increases the region of real roots solution.This was also the main concept of W.T. Sha and S.L. Soo (1979),who discussed the $p\nabla\alpha$ term. Lyczkowski also suggested that the inclusion of transient flow forces enlarge even more the real characteristic region.These forces are related to fluctuations at the interface and they are called virtual mass or relative acceleration forces.

D.A.Drew and R.T. Lahey (1979) reported the objective form of the constitutive relations for the momentum equation and they included the general form of the virtual mass forces while D.A. Drew,L.Y. Cheng and R.T. Lahey (1979) underlined the importance of the virtual mass effects on the two phase flows.

A two phase two component incompressible flow was modelled by D. Gidaspow (1978).He also included the effect of the virtual mass forces.Since most of the former expressions of the relative acceleration are valid for dispersed flows ,Gidaspow suggested a two component incompressible flow one.His model was quite applicable to oil-water systems,slurry transport,geothermal energy generation ,e.t.c.

The inclusion of different pressures for each of the phases met also with success,with respect to the removal of the ill-posed problem.J.C. Rousseau and R.L. Ferch (1979) proposed an UVUTUP model for flat stratified flows.The phase interface pressure difference

was given with respect to the height occupied by each of the phases in a rectangular channel.They also claim to have managed to develop a set of equations with seven real roots.Like the former researchers S. Banerjee et.al. (1978) solved the general case of UVUTUP and reported real roots as well.Then assuming the cases of EVUTEP and EVETEP they compared their models with Edwards and O'Brien (1970) experimental data.

1-D UVUTUP models were developed for the case of separated and dispersed flows by W.T. Hancox et.al. (1978).A phase interface pressure difference expression was formulated,which depended on gravity for a stratified flow and on the drag force due to slip for a bubbly flow.In the case of a bubbly flow the virtual mass effects were included as suggested by Drew and Lahey (1979).

The rate of discharge of the water from a breakage in a nuclear reactor's loop is simulating by attaching a pipe,characterised by its L/D value to a quite large source vessel.The size of the vessel provides almost constant conditions at the upstream region of the pipe's inlet and a two phase flow expansion can be studied inside the pipe.

Edwards (1968) developed a model with zero slip based on a bubble growth theory being controlled by heat conduction from the surrounding superheated liquid.Empirical nucleation and delay time to nucleation expression also proposed,based on the degree of the liquid superheat and the surface tension.

The water metastability period also concerned D.L. Hunt (1970).He suggested that the delayed bubble growth governs the initial depressurisation region.He made use of an empirical power law expression depending on the liquid's superheat to estimate the number of bubbles nucleated at the vicinity of the pressure minimum. Experimental data were then used to determine the free parameters involved.A constant number density of bubbles will then grow to prevent any further depressurisation. The theory compared quite well with experimental data for the initial metastable region.

Later Edwards and Jones (1972) performed experimental work coupled with theoretical predictions for pipe discharge rates and its effect on the mixture level in the source pressure

vessel.The experimental measurements were compared with thermal equilibrium with and without slip critical discharge models.Their conclusion was that without restrictions of the flow downstream,the zero slip model was more accurate than the one with slip,but when a sharp-edge orifice was introduced at the exit the slip effect became important.

Pipe blowdown theoretical modelling,compared with available experiments was performed by Edwards and O'Brien (1970),W.T. Hancox et.al.(1978) and R.L. Ferch (1979).The common point in all the above works,was that the working fluid used to pressurise the vessel was water.Unlike W.S. Winters and H.Merte (1979),who used freon 12.A common assumption among the above theoretical models,except Hancox et.al.,was the thermal non-equilibrium behaviour of a bubbly mixture with no slip between the two phases.In all the above cases it was assumed that the heat was transfered from the liquid phase to the bubble which will be then used to evaporate liquid molecules from the interface.Where the other researchers made use of the two fluid conservation equations Winters and Merte conserved the energy through a bubble which was allowed to grow in a pressure changing environment,where any interfacial heat and mass transfer was affected by the detailed calculation of the liquid thermal boundary layer around it.Winters and Merte assumed a constant bubble number density of the order of 5-6E8 m-3 while Edwards and O'Brien used 2E11-2E14 m-3.Ferch preferred to introduce what he called a rate constant for the interfacial heat transfer process and by using Edwards and O'Brien experimental data he fitted his model to them using a constant of 2.5E-3 sec.Hancox et.al. used a homogeneous model to illustrate the method of characteristics technique and compared his theoretical results with Edwards and O'Brien water experimental ones.The theoretical long term depressurisation showed quite good agreement with the experiment but with the initial metastable region suppressed.

Ferch (1979) also performed a comparison of his model with another standard experimental test reported by Banerjee et.al.(1978).The difference from Edwards and O'Brien water experiments is that Banerjee's blowdown section of a vertical pipe is heated during the

event and also the water circulates in the test section (initial velocity not equal to zero) during the imaginary breakage. S.Banerjee and W.T. Hancox (1978) also reported a homogeneous model to quite well predict the long term of depressurisation of the above two standard problems.They also compared the more accurate and at the same time slower method of characteristics with faster numerical techniques.During LOCA cold water is injected on to the fuel rods.This event was found to be more precisely predicted with a thermal non-equilbrium model,by the above researchers for the Canadian nuclear reactor type.

Another reported research on the numerical method used to solve a homogeneous model set of hyperbolic equations,was performed by R.W. Lyczkowski et.al. (1978). They used an explicit finite difference form based on Lax's method.They reported quite accurate predictions for i) a shock wave ii) ideal gas discharge from a pipe and iii) water mixture discharge from a pipe (Edwards-O'Brien water experiments (1970)) problem.

An implicit finite difference scheme was reported by C.W. Solbrig et.al. (1978) to solve an 1-D UVUTEP LOCA simulation model.Theoretical-experimental comparison,with Edwards and O'Brien tests (1970),were also presented.

M.N Hutcherson et.al. (1983) formulated an experimental and theoretical modelling of a LOCA with a breakage in the inlet to the core loop.A complex internal geometry inside the pressure vessel was employed to simulate the core barrel of the nuclear reactor.Two load cells,pressure and temperature measurement systems instrumented the test section,with main aim to make measurements of the critical mass flow rate from the open end of a large diameter pipe attached to the main body.The main conclusion was that the transient flow rate from large diameter pipes is similar to steady state ones from smaller pipes.The initial wall surface nucleation made the presence of the internal configuration important.A theoretical quasi-steady single node model was also developed to simulate the above experiments.The novelty of this model was the breaking down of the blowdown event in three major regions:i) the subcooled liquid depressurisation,ii) the metastable nucleation and

bubble growth and iii) the homogeneous expansion of a droplet-vapor mixture.A Henry-Fauske critical mass flow rate model was assumed for the critical condition at the exit where for the subcritical flow a simpler model based on the pressure difference between the internal and ambient pressure was used.The comparison between theoretical and experimental results showed quite good agreement.The main conclusion to be drawn from this work,is that the available internal surface area to the volume ratio and the break area affect very much the degree of thermal disequilibrium of the system.

W.D. Ford et.al. (1971) conducted a different type of experiment,by studying the liquid freon 113 expulsion,during pressure releases.In his experiments a blockage of the channel was performed by a vapor slug produced due to liquid's superheat.A theoretical consideration of the problem was also performed by the numerical coupling of a form of the energy and momentum equations quite successfully.

B. Fletcher (1984) reported experimental results during pressure releases using freon 11.His aim was to find the factors that effect the mass flow rate from pipes and orifice,during discharge from storage tank below the liquid level. His conclusion was that the initial pressure and the length of the pipe are the only factors affecting the mass flow rate.Any nucleation process,depending on the initial condition could be delayed until outside the vessel (i.e. liquid jet at the exit) or started inside the vessel (i.e. two phase jet).

On the same type of experiments,with freon 12,H.E.A. van den Akker (1986) reported that instead of correlating the mass flow rate with the L/D quantity, as suggested by Fauske,the pipe length gives better results.He also defined a relaxation length,needed for the nucleation event to relief the liquid's superheat.For short pipes (not sufficient relaxation length) the flow alternates between a liquid superheat jet flow and a two phase one.Due to the liquid's superheat nucleation takes place resulting to a two phase flow and reduction of the mass flow rate,which in turn increases the mass hold up and the pressure. This in turn stops nucleation and results to a superheat liquid jet flow again. The long pipe discharges were observed to be more steady state and two phase at all times.

A.A. Kendoush (1989) reported experimental results with water depressurisation. Recognizing the importance of the initial metastable region,his aim was to determine the delay time in which the liquid is in a superheated state,before the nucleation process onsets.He made use of two different mechanism for depressurisation:i) sudden opening of a valve and ii) shower of cold water into the "hot" vapor region,which produced condensation.His conclusion was that the delay time decreases with the increase of the initial saturation pressure.He also developed a simple quasi-steady model,which takes into account the liquid's superheat and also utilises a steady state bubble rising velocity.The theoretical results seem quite close to the experimental ones.A constant bubble size had to be assumed apriori.

Much of the effort in modelling transient two phase flows,reviewed in this chapter has been directed towards the modelling and the more accurate representation of the interfacial transfer terms of mass momentum and energy.In the case where during the transient event the flow pattern of the flow changes,e.g.LOCA,a detailed flow map is needed to determine the right form of these terms.With respect to this,C.W. Solbrig et.al. (1978) and M. Ishii et.al.(1982) reported a complete flow map and also determine the form of the interfacial interaction terms as well as the form of the interfacial area concentration,very important for establishing the above expressions.It has to be said, at this point, that these terms have a steady state formulation i.e.they do not include any flow quantity gradients.However, S.Banerjee (1978), utilising the surface renewal concept, developed and proposed a form for the interfacial heat transfer, which includes the total pressure derivative.

1.3 PRESENT STUDY

The present investigations aim is to study the thermal non-equilibrium aspects of a pressure vessel blowdown,by means of both experimental and theoretical modelling.

The theoretical modelling includes, 1) a homogeneous model ,where the temperature and velocity is the same in both phases, 2) a thermal non-equilibrium model with and without the nucleation process included and 3) a thermal non-equilibrium model which incorporates a suitable scheme for the two phase mixture-vapor interface for the cases where the vessel is initially partially full with liquid.The theoretical modelling has been formulated from one dimensional volume averaged transient conservation of mass,momentum and energy equations. The set of equations has been solved by the method of characteristics.

Experimental modelling of the problem has been also performed using freon 12, and description and discussion of the experimental setup and results is also included.

A comparison between the theoretical and experimental results from the present work and other reported experiments is presented and possible explanations for any discrepancies between theory and experiment are also included.

Concluding statements are also presented with respect to the outcome from the present work.

CHAPTER 2

MULTIPHASE FLOW MODELLING-AVERAGING PROCESS

2.1 INTRODUCTION

From the engineering interest point of view both transient and steady state flows are of great importance for the every day application in power production plants such as nuclear, fossil fired, geothermal e.t.c., in chemical processes, transportation and storage of high pressure liquified gases. Furthermore assessment of accidents involved with the above installations ,require a better understanding of the physics if successful models are to be developed.Good modelling of these flows allows the design, the control and the safety of the overall system to be studied.

2.2 SINGLE PHASE FLOW

Many flows encountered in today's applications are multiphase and multicomponent.Multiphase flows consist of the same chemical species but different phases.For example,water and steam.Multicomponent means that the system consists of different chemical species which can occupy more than one phases.For example air with water and/or solid particles (rain).In many engineering applications it is only necessary to

assume single phase one component flows which simplifies all governing flow equations.The degree of accuracy of this assumption depends on the concentration of the less predominant chemical component or phase. Even for the most ideal conditions the flow equations can be very complicated, depending on whether the flow is assumed to be incompressible or not or laminar or turbulent.

For a compressible viscous turbulent flow,all flow quantities can be resolved into two constituent components,as it was suggested by Osborn Reynolds.The first component is the mean value of the flow quantity and the second is the superimposed fluctuations.Thus in some cases temporal and/or spatial averaging can be applied to filter out the turbulence quantities. Further simplification of the flow equations give rise to 2-D or even 1-D flow models. By means of a time or statistical averaging the high frequency quantities will cut off and the turbulent effect will be included in the mean flow equations in the form of the well known Reynolds stresses.During averaging information is lost so additional relationships must be specified for the "closure problem" to be removed. Any averaging with respect to the turbulent quantities must precede the space averaging,since turbulence is a 3-D phenomenon ,otherwise a serious error could be performed by excluding the turbulence effect,especially in cases where it is important.

2.3 MULTIPHASE FLOW

The main interest of this study lies in the physics and the handling of multiphase flow modelling. Whilst the governing equations for each phase are known ,the complex interactions between the phases render their solution impossible , except in the simplest of cases.Therefore to simplify the problem ,multiphase modelling relies on flow equations which describe how average quantities vary.Unfortunately the averaging process results in information being lost and this has to be established by suitable modelling.Averaged flow

equations, reported in the literature ,have been obtained by averaging the local and instantaneous conservation equations with respect to space time over an ensemble or in some combination of these (Ishii (1975),Vernier & Delhaye (1974),Drew (1983)).

The mathematical model consists of the averaged conservation equations,the state relation for each of the phases,the auxiliary and secondary jump conditions,the constitutive relations for the pressure and the stresses,energy and mass transfers and the boundary conditions.A multiphase model is far more complicated than a single one,since now all flow quantities have been doubled or tripled depending on the number of phases involved and also extra information is needed for the interfacial transfer terms.

This type of multiphase modelling,the so called "multifluid model" has been used as a benchmark against experimental data,with considerable amount of success.The averaged flow quantities,described by the flow equations,are especially favourable for comparing with experimental measurements.The physical size of the sensor used for example ,pressure or temperature measurements and their response time usually involve some kind of spatial and time averaging.

2.4 EXPERIMENTAL AVERAGE PROCEDURE

The most commonly used experimental averaging procedures are:1) volume or area averaging,2) time averaging with no averaging in space,3) ensemble averaging with no averaging in space,4) time or ensemble and space averaging.

The main averaging rule is that the averaging procedure should lead to continuous flow quantities with continuous first derivatives.This rule is violated during the area average,each time the interface becomes tangent to the cross sectional plane.For the time point averaging, however, the time derivative of the void fraction becomes discontinuous.Therefore double

averaging e.g. time/space, are usually used.Experimental averaging reported by Banerjee et.al. (1979) suggests that the volume/ensemble averaging is more accurate and straight forward,but for large experiments the ensemble averaging can only be obtained at prohibitive expense.For example a void fraction averaging can be performed by trapping flow between two quick closing valves and measuring the proportion of each phase.The ensemble procedure involves repetition of the same experiment by starting from the same initial condition and by closing the valves after the same elapsed time.

2.5 MATHEMATICAL AVERAGING

2.5.1 THE AVERAGED CONSERVATION EQUATIONS

In this section the averaged flow equations will be derived,resulting in a multifluid model.

The conservation equations applied to each of the phases of a multiphase flow can be averaged with respect to turbulence.For the same purpose as the single phase flow the randomness of the fluctuating part of a flow quantity has to be excluded from the conservation equation without excluding,however, its effect on the mean flow.

If $<>$ denotes an averaging process and $f(\vec{x},t)$ is a flow quantity,then $<f(\vec{x},t)>$ corresponds to the mean value of $f(\vec{x},t)$.To filter out the microscopic field the following processes can be used:

1) time averaging

$$<f(\vec{x},t)>_1 = \frac{1}{T}\int_{t-T}^{t} f(\vec{x},t)\ dt \qquad (2.1)$$

where T is suitable time interval.

2) space averaging

$$<f(\vec{x},t)>_2 = \frac{1}{V(\vec{x},t)} \int_{V(\vec{x},t)} f(\vec{x},t)\ dV \qquad (2.2)$$

where $V(\vec{x},t)$ is the average control volume

3) ensemble averaging

$$<f(\vec{x},t)>_3 = \frac{1}{n} \sum_{1}^{n} f(\vec{x},t) \qquad (2.3)$$

where n is the number of repetitions.

A number of rules are also used during averaging.If f and g are two different flow quantities:

1) $<f+g> = <f> + <g>$ (2.4a)

2) $<<f>g> = <f>\ <g>$ (2.4b)

3) $<\frac{\partial f}{\partial t}> = \frac{\partial <f>}{\partial t}$ (2.4c)

4) $<\frac{\partial f}{\partial x_i}> = \frac{\partial <f>}{\partial x_i}$ (2.4d)

The equations of motion applying to each of the phases are (White 1974)

1. conservation of mass

$$\frac{\partial \rho}{\partial t} + \nabla . \rho \vec{v} = 0 \qquad (2.5)$$

2.conservation of linear momentum

$$\frac{\partial \rho \vec{v}}{\partial t} + \nabla . \rho \vec{v}.\vec{v} = \nabla . \tilde{T} + \rho \vec{F} \qquad (2.6)$$

3.conservation of energy

$$\frac{\partial \rho U'}{\partial t} + \nabla . \rho \vec{v} U' = \nabla . \vec{v}.\tilde{T} + \rho \vec{v}.\vec{F} - \nabla . \vec{Q} \qquad (2.7)$$

In these equations ρ is the density, $\vec{v}$ is the field velocity,$\tilde{T}$ the stress tensor,$\vec{F}$ the body force density,U' the total internal energy or $U' = U + \vec{v}^2/2 - g.\vec{x}$,$\vec{Q}$ the field heat transfer,which could be described by Fourier's law.

In the case of a multiphase flow some difficulty may arise by the fact that averaging has to be limited by the interface and the physical limits as well (e.g.vessel or pipe wall) plus the fact that some provision has to be made concerning the required information caused by the interfacial link with the other phases.It is therefore necessary to introduce a new quantity $X_k(\vec{x},t)$, called the phase function which has the following properties,

$$X_k(\vec{x},t) = \begin{bmatrix} 1 \text{ if } \vec{x} \text{ is in the phase k} \\ 0 \quad \text{otherwise} \end{bmatrix} \qquad (2.8)$$

Since X_k is constant in the interior of phase k,the conservation of the X_k quantity gives rise to:

$$\frac{\partial X_k}{\partial t} + \text{Div}\, X_k \vec{v}_i = 0 \qquad (2.9)$$

or

$$\frac{\partial X_k}{\partial t} + \vec{v}_i \,.\, \nabla X_k = 0$$

Since X_k Div $\vec{v}_i = 0$ (in the interior of phase k,Div $\vec{v}_i = 0$). The concept of the phase function is very useful since X_k picks out the individual phases and ∇X_k the boundaries i.e. the interfacial or physical ones.∇X_k has the direction of the normal to the interface pointing inwards to the phase k i.e.

$$\nabla X_k = -\vec{n}_k \frac{\partial X_k}{\partial n_i} \qquad (2.10)$$

where $\vec{n}_k$ is the unit vector normal to the interface pointing outwards from phase k.In the above expression $\vec{v}_i$ is the field velocity of the boundaries.Drew (1983) also defined the void fraction α as

$$\alpha = \langle X_k \rangle = \frac{1}{t}\int_{t-T}^{t} X_k \, dt \qquad (2.11)$$

using a time averaging process.

By multiplying equations (2.5) to (2.7) with X_k and averaging with respect to time yields:

1.conservation of mass

$$\frac{\partial <X_k \rho>}{\partial t} + \nabla . <X_k \rho \vec{v}> = <[\rho \nabla X_k . (\vec{v} - \vec{v}_i)]> \qquad (2.12a)$$

2.conservation of momentum

$$\frac{\partial <X_k \rho \vec{v}>}{\partial t} + \nabla . <X_k \rho \vec{v}.\vec{v}> - \nabla . <X_k \tilde{T}> +$$

$$<X_k \rho \vec{F}> = <[\nabla X_k . \{\rho \vec{v} . (\vec{v} - \vec{v}_i) - \tilde{T}\}]> \qquad (2.12b)$$

3.conservation of energy

$$\frac{\partial <X_k \rho U'>}{\partial t} + \nabla . <X_k \rho \vec{v} U'> - \nabla . <X_k \tilde{T} . \vec{v}> +$$

$$\nabla . <X_k \vec{Q}> - <X_k \rho \vec{v} . \vec{F}> = <[\nabla X_k . \{\rho U' (\vec{v} - \vec{v}_i) - \vec{v} . \tilde{T} + \vec{Q}\}]> \qquad (2.12c)$$

Making use of equation (2.9) the first term of equation (2.5) is

$$X_k \frac{\partial \rho}{\partial t} = \frac{\partial \rho X_k}{\partial t} - \rho \frac{\partial X_k}{\partial t} = \frac{\partial \rho X_k}{\partial t} + \rho \vec{v}_i . \nabla X_k$$

In the same manner the rest of the equations can be written in the above form (2.12).All the interfacial and wall transfer terms for mass,momentum and energy are on the right-hand side of the equations.

Equations (2.12) apply to the whole flow domain for all k phases involved.In the above equations $<X_k A>$ denotes a X_k-weighted average of the flow quantity A.This means that "A" quantity has a mean value over the k phase which depends on space and time.Taking into account (2.11) this gives,

$$<A> = \frac{<X_k A>}{\alpha} \qquad (2.13)$$

Terms in the conservation equations of the type $,<X_k\ B\ \rho>$,are the mass-weighted averages,where B is a flow quantity.Using (2.13),

$$<B> = \frac{<X_k B \rho>}{<\rho>\ \alpha} \tag{2.14}$$

In the general form $<\tilde{T}>$ can be written as

$$<\tilde{T}> = <-p>\ \tilde{I} + <\tilde{\tau}> \ , \tag{2.15}$$

where $\tilde{I}$ is the unit tensor.It has been a custom to replace the instantaneous interfacial pressure,$p_{i,k}$ at the k phase side of the interface with an average part and a fluctuation one,so

$$p_{i,k} = <p>_{i,k} + p'_{i,k} \tag{2.16}$$

It is also customary to define $p'_{i,k}$ as

$$p'_{i,k} = p_{i,k} - <p>_{i,k} \ , \tag{2.17}$$

It is convenient to define the following quantities,

$$\dot{m}_{i,k} = <[\rho \nabla X_k.(\vec{v} - \vec{v}_i)]>_{i,k} \tag{2.18a}$$

$$\dot{m}_{i,k}\vec{v}_{i,k} = <[\nabla X_k \rho \vec{v}.(\vec{v} - \vec{v}_i)]>_{i,k} \tag{2.18b}$$

$$\dot{m}_{i,k}U'_{i,k} = <[\nabla X_k.\rho U'\ (\vec{v} - \vec{v}_i)]>_{i,k} \tag{2.18c}$$

$$U' = H - \frac{p}{\rho} \ . \tag{2.18d}$$

For the case when the wall friction and heat transfer is negligible and if there is no mass transfer at the wall, (2.13) to (2.17) allow equations (2.12) to be written as,

1. k phase conservation of mass

$$\frac{\partial \alpha_k <\rho>_k}{\partial t} + \nabla . \alpha_k <\rho>_k <\vec{v}>_k = \dot{m}_{i,k} \qquad (2.19a)$$

2. k phase conservation of momentum

$$\frac{\partial \alpha_k <\rho>_k <\vec{v}>_k}{\partial t} + \nabla . \alpha_k <\rho>_k <\vec{v}>_k . <\vec{v}>_k - \alpha_k \nabla <p>_k$$

$$= \nabla . \alpha_k (<\tilde{\tau}>_k + \tilde{\tau}'_k) - \alpha_k <\rho>_k <\vec{F}>_k + (<p>_{i,k} - <p>_k) \nabla \alpha_k$$

$$+ \dot{m}_{i,k} <\vec{v}>_{i,k} + <(p_{i,k} - <p>_{i,k}) \nabla X_k - \tilde{\tau} . \nabla X_k>_{i,k} \qquad (2.19b)$$

3. k phase conservation of energy

$$\frac{\partial \alpha_k <\rho>_k <H>_k}{\partial t} + \nabla . \alpha_k <\rho>_k <\vec{v}>_k <H>_k - \alpha_k \frac{\partial <p>_k}{\partial t}$$

$$= \nabla . \alpha_k (<\tilde{\tau}>_k + \tilde{\tau}'_k) <\vec{v}>_k - \nabla . \alpha_k <\vec{Q}>_k + \alpha_k <\rho>_k <\vec{v}>_k . <\vec{F}>_k -$$

$$(<p>_{i,k} - <p>_k) \frac{\partial \alpha_k}{\partial t} + \dot{m}_{i,k} <H>_k -$$

$$<(p_{i,k} - <p>_{i,k}) \frac{\partial X_k}{\partial t} + \vec{v} . \tilde{\tau} . \nabla X_k - \vec{Q} . \nabla X_k>_{i,k} \qquad (2.19c)$$

In the above equations the subscript k denotes a flow quantity in the bulk of phase k and i,k denotes a flow quantity at the k side of the interface. $\tilde{\tau}$ is the viscous stresses and $\tilde{\tau}'$ the Reynolds ones.

In the same manner the conservation of mass,momentum and energy on the interface requires that:

$$\sum_{1}^{k}\dot{m}_{i,k} = 0 \tag{2.20a}$$

$$\sum_{1}^{k}\dot{m}_{i,k}<\vec{v}>_{i,k} + <p>_{i,k}\nabla\alpha_k + <(p_{i,k} - <p>_{i,k})\nabla X_k$$

$$- \tilde{\tau}.\nabla X_k>_{i,k} = \sigma R'\nabla\alpha_k \tag{2.20b}$$

$$\sum_{1}^{k}\dot{m}_{i,k}<H>_{i,k} - <p>_{i,k}\frac{\partial\alpha_k}{\partial t} - <(p_{i,k} - <p>_{i,k})\frac{\partial X_k}{\partial t}$$

$$+ \vec{v}.\tilde{\tau}.\nabla X_k - \vec{Q}.\nabla X_k> = \begin{bmatrix}\text{interfacial energy}\\ \\ \text{source term}\end{bmatrix} \tag{2.20c}$$

where R′ is the average interfacial curvature.Equations (2.20) are the so called jump conditions.A. Biesheuvel and L.van Wisngaarden (1984) suggested that the surface tension forces can have the form of, $\sigma\vec{n}_l.\nabla\vec{n}_g$,where σ is the coefficient of the surface tension.According to Ishii (1975) the surface tension consists of a mean part and a fluctuating one,due to the relative motion between the phases.Assuming zero fluctuating part the simplest form of interfacial power consumption can be given as:

$$\begin{bmatrix}\text{interfacial energy}\\ \\ \text{source term}\end{bmatrix} = \sigma R'\frac{\partial\alpha_k}{\partial t} \tag{2.21}$$

Furthermore Benson (1966),suggests that any surface change requires an energy and mass absorption by the interface.This would result in an extra source term for the energy jump condition.In the present study it is assumed any energy source term involved with the interfacial build up is negligible.

In the case of a bubbly mixture, $R' = 2/r_b$,where r_b is the bubble radius. With zero motion both momentum and energy jump conditions give

$$<p>_{i,g} - <p>_{i,l} = 2\frac{\sigma}{r_b} \tag{2.22}$$

which is the mechanical equilibrium equation for the bubble. The interfacial source terms on the right-hand side of equations (2.19) may be physically interpreted as follows:

1) $\dot{m}_{i,k}$: This is the mass transfer term through the interface,due to nucleation ,evaporation and diffusion.

2) $\dot{m}_{i,k}<\vec{v}>_{i,k}$ (or $\dot{m}_{i,k}<H>_{i,k}$): this term represents the interfacial momentum (or energy) transfer term,due to the phase change process across the boundary.

3) $(<p>_{i,k} - <p>_k)\nabla\alpha_k$ (or $(<p>_{i,k} - <p>_k \partial\alpha_k/\partial t)$): This is the averaged pressure difference between the bulk of the phase and the k side of the interface.It is an important term whenever the spatial (or time) derivatives of the void fraction are important or whenever the averaged pressure difference is important.For example,in dispersed flows this term is negligible for the dispersed phase,since the pressure gradients developed in the small bubble or droplet voids are very small.For the continuous phase, however, this is not true and the Rayleigh equation can be used to link the two averaged pressures.

4) $<(p_{i,k} - <p>_{i,k})\nabla X_k>_{i,k}$ (or $<(p_{i,k} - <p>_{i,k})\partial X_k/\partial t>_{i,k}$).This term is the fluctuating part of the interfacial pressure.Slip between the phases is the reason,which results in the appearance of this term.The relative motion is the source of interfacial forces such as:1) aerodynamic force,which can be split into the drag (viscous effect) and the form drag force (pressure variation on the dispersed phase interface),2) virtual mass force (due to relative acceleration of the phases) and other less important forces such as the lift force,which is due to changes of the flow field perpendicular to the relative motion direction. The lift force is not important in fast inviscid flows.The Basset force,which carries the effect of the flow field evolution in the momentum equation is not generally considered to be important.

5) $<\tilde{\tau}.\nabla X_k>_{i,k}$ (or $<\vec{v}.\tilde{\tau}.\nabla X_k>_{i,k}$): This term involves viscous and turbulent stresses at the k side of the interface.

6) $<\vec{Q}.\nabla X_k>_{i,k}$.This is the heat transfer term from the interface into the k phase.

Equations (2.20) represent the interfacial conservation of mass,momentum and energy.The interface has often been treated as a discontinuity where the local and instantaneous flow equations hold for each of its sides.In analogy with the single phase shock wave,the quantity conserved over the interface,remains unchanged on both sides of the interface unless,an appropriate interfacial source term is present.It can be noticed that each of the terms of the interfacial jump condition is the same as in the main flow equation,representing the reaction of the interface.

An interesting term in both energy and momentum jump condition, is $<p>_{i,k}\partial\alpha_k/\partial t$ (or $\nabla\alpha_k$) which is called the buoyant force (Drew (1983)).The reason for this is because it depends on the pressure distribution around the interface and also on the time/space local phase distribution.

For a two phase flow,equations (2.20) become:

$$\dot{m}_{i,g} = -\dot{m}_{i,l} \tag{2.23a}$$

$$\dot{m}_{i,g}(<\vec{v}>_{i,g} - <\vec{v}>_{i,l}) + (<p>_{i,g} - <p>_{i,l})\nabla\alpha_g$$

$$+ <\{(p'_{i,g} - p'_{i,l}) - (\tilde{\tau}_g - \tilde{\tau}_l)\}\nabla X_g>_i = \sigma R'\nabla\alpha_g \tag{2.23b}$$

$$\dot{m}_{i,g}(<H>_{i,g} - <H>_{i,l}) + (<p>_{i,g} - <p>_{i,l})\frac{\partial\alpha_g}{\partial t} -$$

$$<(p'_{i,g} - p'_{i,l})\frac{\partial X_g}{\partial t} + (\tilde{\tau}_g.\vec{v}_g - \tilde{\tau}_l.\vec{v}_l).\nabla X_g$$

$$-(\vec{Q}_g - \vec{Q}_l).\nabla X_g>_i = \sigma R'\frac{\partial\alpha_g}{\partial t} \tag{2.23c}$$

Forces due to the interfacial pressure difference are important when the surface tension (for dispersed flow) or/and the interfacial mass transfer or/and the spatial and/or temporal derivatives of the void fraction are important.

2.5.2 CONSTITUTIVE RELATIONSHIPS

In fluid mechanics the primary concern is with the fluid velocity field. First the most convenient origin must be chosen which allows the flow field ($\vec{v}(\vec{x},t)$) to be modelled and second the solution i.e the knowledge of $\vec{v}$ with respect the space and the time.To do so Newton's second law can be employed,

$$\vec{F} = m\vec{a} \tag{2.24}$$

For the Eulerian approach the acceleration $\vec{a}$,describes the so called "total" or "material" change of the velocity field,where on the left-hand side $\vec{F}$ stands for all the forces acting on the field.From equation (2.24),

$$\vec{a} = \frac{d\vec{v}}{dt} = \frac{\partial\vec{v}}{\partial t} + \vec{v}.\nabla.\vec{v} \tag{2.25}$$

$\vec{v}.\nabla.\vec{v}$,includes the effect of the non-linear ($\vec{v}.\vec{v}/2$) and ($\nabla \times \vec{v}$) terms and it is equal to all forces acting on the system.These forces can be separated into two categories,the body forces and the surface ones.The first ones are due to any external field i.e.gravity,magnetic,

electromagnetic,e.t.c.,where the second ones are due to internal interactions of the fluid with itself.The major difficulty with all flows,single or multiphase,is to find the appropriate relationship to describe the link of these interactions with the change of the velocity field i.e. $\partial u_i/\partial x_i$.This relationship is the well known constitutive relationship.

For a multiphase flow,the problem of finding constitutive equations,is more difficult,since there is fluid interaction in all phases in addition each of the sides of the interface have to be related to the velocity field.For the momentum equation to be solved (together with the energy and mass equations) certain terms have to be transformed into their velocity functions.These terms are:

$$(<\tilde{\tau}>_k + \tilde{\tau}'_k)\ ,\ (<p>_{i,k} - <p>_k)\ ,\ p'_{i,k}\ ,\ <\tilde{\tau}>_{i,k}$$

Sometimes it is not worth referring to the viscous stresses of the mean flow ,in comparison with the stresses resulting from the highly energetic Kolmogorov eddies,which transfer the momentum by collisions in greater quantities.

In the case of a bubbly flow,when the size of the bubbles is quite small the bubbles follow the flow pattern sufficiently closely that no slip between the phases can be noticed and no additional forces from the interface result i.e. $p'_{i,k} = 0$ and $<p>_{i,k} - <p>_k = 0$. As soon as there is some slip at the interface,then each and everyone of the bubbles act as an obstacle for the continuous phase,which adds to the flow a distinct turbulence frequency and so the coexistence of the two (or more) phases is a turbulence source.In 1845 Stoke made three postulations,concerning the setting of the relations between stress and strain.One of these,refers to the objectivity of these relations.According to the objectivity postulate,the fluid is isotropic i.e. its properties are independent of direction and therefore the deformation law is independent of the axis direction on which it is expressed.It is obvious that the same postulate holds in the case of a multiphase flow for both the phase and interface relations.These relationships include the void fraction and its temporal/space derivatives,the velocity field and its derivatives,the geometry of the interface (e.g.the bubble's size) and

physical properties such as density,viscosity e.t.c.Drew (1979) reported all the flow quantities that can be used in the constitutive equations,by proving their objectivity.These quantities are,the material derivatives of the scalar flow quantities e.g.$d\alpha/dt$,the slip velocity,between the phases,the relative acceleration i.e.

$$\vec{a}_{gl} = \frac{\partial(\vec{v}_l - \vec{v}_g)}{\partial t} + \vec{v}_g.\nabla\vec{v}_l - \vec{v}_l.\nabla\vec{v}_g$$

and finally the strain tensor,

$$D_{k,b} = \frac{1}{2}(\nabla\vec{v}_k - \nabla^t\vec{v}_k) \ .$$

The turbulence stress tensor ($\tilde{\tau}'_k$) consists of

$$\tilde{\tau}'_k = \text{Reynolds stresses} + \text{multiphase effect stresses} \qquad (2.26)$$

In well mixed multiphase flows the turbulence stresses are due to slip but in separated flows can be caused also by the interface wavy instability (Kelvin-Helmholtz).By analogy with the viscous stresses,the eddy viscosity stress can be model as $2\mu'_k D_{k,b}$,where μ'_k is the so called eddy viscosity which can be calculated using Prandl's mixing length model.The second part of equation (2.26) is a function of $(\vec{v}_l - \vec{v}_g)$.For bubbly mixtures,Drew and Lahey (1979) separated the induced eddy pressure due to $|(\vec{v}_l - \vec{v}_g)^2|$ from the two phase effect stress due to $(\vec{v}_l - \vec{v}_g).(\vec{v}_l - \vec{v}_g)$ and they presented the following model,

$$\tilde{\tau}'_k = 2\mu'_k D_{k,b} + c_1\tilde{I} + c_2(\vec{v}_l - \vec{v}_g).(\vec{v}_l - \vec{v}_g) \qquad (2.27)$$

where μ'_k, c_1, c_2 depend on the void fraction,the bubble size and the relative velocity field.$\tilde{\tau}_k$,is the viscous stress term.For newtonian flows is given as

$$\tilde{\tau}_k = 2\mu_k D_{k,b}$$

where μ_k is the viscosity (physical property) of the fluid.Ishii (1975) argued that this term is not enough to describe the viscous stresses in a multiphase flow and he suggested that

$$\tilde{\tau}_k = 2\mu_k D_{k,b} + \mu_k \frac{b_k (1-\alpha_k)}{1-\alpha_k} [\nabla\alpha_k(\vec{v}_l - \vec{v}_g) + (\vec{v}_l - \vec{v}_g)\nabla\alpha_k] \quad (2.28)$$

where b_k is called the mobility of phase k.

Both $\tilde{\tau}_k$ and $\tilde{\tau}'_k$ models are usually applied to the continuous phases where in the dispersed one (e.g.bubbles),it is assumed that the turbulence stress is zero and that the viscous stress,sometimes is zero too.In the case where the above assumption is not true,analogous models can be used for the other phase.All above models are functions of $D_{k,b}$, $(\vec{v}_l - \vec{v}_g)$, α_k , $\nabla\alpha_k$,which are all objective quantities.

Next the pressure constitutive relations will be discussed.In the general case of a two phase flow model,with different phase and interfacial pressures, different phase velocities and different phase temperatures,the three equations of mass,momentum and energy are sufficient to provide a solution for the two velocity fields,providing a constitutive relation is known for the pressure field.The simplest and more often encountered assumption is that all pressures are equal i.e. $p_l = p_{i,l} = p_{i,g} = p_g$. There are cases when the above assumption is almost true,when it can be assumed that the phase speed of sound is so much greater than the flow velocity,that any flow change information travels very fast in all directions,resulting in a pressure equalisation.For example,in bubbly mixtures with small slip,no surface tension and small dr_b/dt (speed of contraction/ expansion),the above assumption is sufficient.When the slip between the bubbles and the liquid increases,the liquid pressure adjacent to the

interface is much greater than the bulk liquid pressure.For dispersed flows the term ($<p>_{i,k} - <p>_k$) (for the continuous phase k), can be modelled using Rayleigh's equation. Stuhmiller (1977) suggested that the above pressure difference can be calculated as a function of ($|\vec{v}_l - \vec{v}_g|^2$) (form drag force).

Nigmatulin (1979) and L. van Wijngaarden (1984) studied the effects of the liquid on the bubble interface,when terms like,dr_b/dt and ($\vec{v}_l - \vec{v}_g$) and also the crowded effect,due to the presence of other bubbles,is not negligible. By assuming a potential flow,surrounding a bubble they tried to theoretically evaluate the pressure difference between the liquid interface and the bulk. Nigmatulin made use of his cell theory and he managed to adjust Rayleigh's equation to accommodate the effect due to the increased bubble population. Nigmatulin takes into account also the slip and he proposes the following expression for the liquid pressure difference,

$$<p>_{i,l} - <p>_l = (1 - 1.1\alpha^{1/3})\rho_l r_b \frac{d^2 r_b}{dt^2} + (1 - 1.47\alpha^{1/3} + 1.33\alpha)\frac{3}{2}\left(\frac{dr_b}{dt}\right)^2 \rho_l$$

$$- (1 + 0.67\alpha)(\vec{v}_l - \vec{v}_g).(\vec{v}_l - \vec{v}_g)\frac{1}{4} \qquad (2.29)$$

In the case of separated flows,the interfacial pressure fluctuation term is due to the wavy behaviour of the interface (Kelvin-Helmholtz),which for high inertia flows can cause plug or slug flow.The interfacial momentum exchange,due to these irregularities is far more complicated and it involves forces like the virtual mass,which can be important even for an assumed inviscid flow.The gravitational force (body force) is very important in this case,since it opposes any interfacial instability.On the other hand,the gravitational force creates another pressure difference,often presented as

$$<p>_{i,k} - <p>_k = \frac{g\alpha H\rho_k}{2} \qquad (2.30)$$

where H is the vertical size of the pipe.

The pressure difference between each of the side of the interface is due to the surface tension effects and the interfacial mass transfer,in case of a vigorous phase change.For bubbly flows in which surface tension is important, the pressure difference is often given as

$$<p>_{i,g} - <p>_{i,l} = \frac{2\sigma}{r_b} \tag{2.31}$$

For the interfacial pressure fluctuations and the stresses, analogous constitutive relations have to be found.Ishii(1975) and Drew (1983), concentrated all the above terms to what they called interfacial force density term.Drew (1979) postulated a form for the sought relationship containing only objective functions of the velocity field.If M is the interfacial force density ,

$$M = \Lambda_1(\vec{v}_l - \vec{v}_g) + \Lambda_2\vec{a}_{gl} + \Lambda_3(\vec{v}_l - \vec{v}_g).D_{l,g} + \Lambda_4(\vec{v}_l - \vec{v}_g).\nabla(\vec{v}_l - \vec{v}_g) \tag{2.32}$$

where Λ_1 to Λ_4 are scalars function of the velocity field and the fluid properties. The first term is the drag force and

$$A_1 = \frac{3}{8}\alpha\rho_l\frac{Cd}{r_b}|\vec{v}_g - \vec{v}_l|$$

where Cd is the drag coefficient.The combination of the second and fourth term is the virtual mass force.

$$A_2 = \alpha\rho_l Cvm$$

$$\Lambda_4 = \Lambda_2(1 - L)$$

where Cvm is the virtual mass coefficient and L is a void fraction function. Theoretical or empirical correlations for Cvm have been derived by Zuber(1964), Nigmatulin (1979),Wijngaarden(1976),Mokeyev(1977).All the above investigators concluded that,

$$Cvm \rightarrow \frac{1}{2} \text{ as } \alpha \rightarrow 0$$

The third term is due to the lift force effect.A3 is a function of the local void fraction.There are very little experimental data to suggest that this force exists in the usual multiphase flows.

2.5.3 AVERAGED TWO PHASE EQUATIONS FOR ONE DIMENSIONAL FLOW

Equations (19) and (20) are the 3-D form of multiphase flow equations, where all flow quantities are free of their high frequency part.If,now,all averaged signs (< >) are dropped and equating k with either g (vapor phase) or l (liquid phase),these equations can be reaveraged over the cross section area or a thin flow slice of volume V(x,t).Taking the dot product with the unit x direction vector $\vec{n}_x$,of the momentum equation, the 1-D form of the two phase flow equations with all flow quantities varying with x and t can be established. Engaging the averaging rules (2.4) and also defining the new averaging quantities as

$$< \alpha_k A_k >_x = \frac{1}{V} \int_{V(x,t)} \alpha_k A_k \, dV \qquad (2.33)$$

where A denotes a flow quantity.The flow equations can be rewritten as,

1.k phase conservation of mass

$$\frac{\partial V<\alpha\rho>_k}{\partial t}+\frac{\partial V<\alpha\rho u>_k}{\partial x} = V<\dot{m}_{i,k}>_x \qquad (2.34a)$$

2.k phase conservation of momentum

$$\frac{\partial V<\alpha\rho u>_k}{\partial t}+\frac{\partial V<\alpha\rho uu>_k}{\partial x}+\frac{\partial V<\alpha p>_k}{\partial x}=\frac{\partial V<\alpha(\tilde{\tau}+\tilde{\tau}')>_{k,x}}{\partial x}-V<\alpha\rho\vec{\Gamma}>_{k,x}$$

$$+V<\dot{m}_{i,k}\vec{v}_{i,k}>_x+V(<<p\nabla X_k-\tilde{\tau}.\nabla X_k>_{i,k}>_x) \qquad (2.34b)$$

3.k phase conservation of energy

$$\frac{\partial V<\alpha\rho H>_k}{\partial t}+\frac{\partial V<\alpha\rho uH>_k}{\partial x}-\frac{\partial V<\alpha p>_k}{\partial x}=$$

$$\frac{\partial V<\alpha\vec{v}.(\tilde{\tau}+\tilde{\tau}')>_{k,x}}{\partial x}-\frac{\partial V<\alpha\vec{Q}>_{k,x}}{\partial x}+V<\alpha\rho\vec{v}.\vec{F}>_{k,x}+V<\dot{m}_{i,k}H_{i,k}>_x$$

$$+V<<p\frac{\partial X_k}{\partial t}-\vec{v}.\tilde{\tau}.\nabla X_k+\vec{Q}.\nabla X_k>_{i,k}>_x \qquad (2.34c)$$

Making use of the definition for ∇X_k,

$$\nabla X_k = -\vec{n}_k\frac{\partial X_k}{\partial n_i} \qquad (2.35)$$

and for 1-D case

$$\nabla X_k = -\vec{n}_k \qquad (2.36)$$

and together with the interfacial source term definitions and assuming that the average process control volume does not vary with x and t,equations (2.34) yield,

1.k phase conservation of mass

$$\frac{\partial <\alpha\rho>_k}{\partial t} + \frac{\partial <\alpha\rho u>_k}{\partial x} = \dot{m}_{i,k} \tag{2.37a}$$

2.k phase conservation of momentum

$$\frac{\partial <\alpha\rho u>_k}{\partial t} + \frac{\partial <\alpha\rho uu>_k}{\partial x} + \frac{\partial <\alpha p>_k}{\partial x} = \frac{\partial <\alpha(\tilde{\tau} + \tilde{\tau}')>_{k,x}}{\partial x}$$

$$- <\alpha\rho\vec{F}>_{k,x} + \dot{m}_{i,k}u_{i,k} + << (p\tilde{I} - \tilde{\tau}).\nabla X_k >_{i,k} >_x \tag{2.37b}$$

3.k phase conservation of energy

$$\frac{\partial <\alpha\rho II>_k}{\partial t} + \frac{\partial <\alpha\rho uII>_k}{\partial x} - \frac{\partial <\alpha p>_k}{\partial t} = \frac{\partial <\alpha\vec{v}.(\tilde{\tau} + \tilde{\tau}')>_{k,x}}{\partial x}$$

$$- \frac{\partial <\alpha\vec{Q}>_{k,x}}{\partial x} + <\alpha\rho\vec{v}.\vec{F}>_k + \dot{m}_{i,k}H_{i,k} + << p\frac{\partial X_k}{\partial t} - \vec{v}.\tilde{\tau}.\nabla X_k >_{i,k} >_x \tag{2.37c}$$

and the interfacial jump conditions are:

$$\sum_1^k \dot{m}_{i,k} = 0 \tag{2.38a}$$

$$\sum_1^k \dot{m}_{i,k}u_{i,k} + << (p\tilde{I} - \tilde{\tau}).\nabla X_k >_{i,k} >_x = \sigma R' \frac{\partial \alpha_k}{\partial x} \tag{2.38b}$$

$$\sum_{1}^{k}\dot{m}_{1,k}II_{i,k}+<<p\frac{\partial X_k}{\partial t}+\vec{v}.\tilde{\tau}.\nabla X_k-\vec{Q}.\nabla X_k>_{i,k}>_x=\sigma R'\frac{\partial \alpha_k}{\partial t} \qquad (2.38c)$$

2.5.4 DISTRIBUTION PARAMETERS

Studying equations (2.37) one may notice that they cannot be solved in their present form.The average of the products has to be replaced by the product of the averages.The concept of the distribution parameter aims to overcome this problem.There are two such parameters involved with the time/space derivatives of the flow quantities and one involved with the interfacial source term. Flow quantities such as $<\alpha\rho u>_k$ or $<\alpha\rho II>_k$ e.t.c. have to be separated,first with respect to the void fraction and then to one another i.e.

$$<\alpha\rho uII>_k=C_o^{\alpha}<\alpha>_k C_o^{f}<\rho>_k<u>_k<II>_k$$

where C_o^{α} is the void fraction distribution parameter and C_o^{f} is the flow field one, which for the given example takes into account the ρ,u and II distribution on the cross section area.

The interfacial exchange quantities e.g. the interfacial heat transfer,are usually modelled,using empirical coefficients and steady state relationships i.e.

$$<<\vec{Q}.\nabla X_k>_{i,k}>_x=<\dot{q}>_{i,k}=<\Lambda_i h_i\Delta T>_i$$

where A_i is the interfacial area concentration,h_i the heat transfer coefficient and ΔT the phasial temperature difference.Furthermore

$$<A_i h_i\Delta T>_i=C_o^{I}<A_i>_i<h_i>_i<\Delta T>_i$$

where C_o^{I} is the distribution parameter for the interfacial terms.The interfacial friction,the virtual mass force e.t.c. can be treated in the same manner. Strictly speaking, all coefficients

used to model the interfacial terms,vary with the flow regime and the flow changes,but often it has been assumed that,

$$C_o^I = 1$$

It is customary to assume a power law distribution on a cross section area (or in a thin slice),in the case where C_o^s , C_o^f , C_o^I are to be calculated.Their calculation however must depend on the flow regime,especially for C_o^s and C_o^I which are directly dependent on the geometry of the interface.The geometry of the physical limits of the flow also affect the forementioned calculation of the parameters.Experimental information on the void fraction and the flow variables distribution is vital for the C_o modelling and calculation. Unfortunately,there is very little work performed in this area and all data involve steady state measurements.It has to be said,here,that any profile measurements in a non-fully developed flow regime can result to erroneous conclusions.A great deal of analytical modelling has been performed by S.G. Bankoff(1960) and later on improved by N. Zuber and S.A. Findlay(1965) and N. Zuber and F.W. Staub and G.Bijwaard(1966).In the last paper they suggest that if the flow-regime was ignored,C_o could be assumed constant. They actually proved their suggestion by comparing theoretical results with water experimental data, obtained from water flow in circular ducts.

By analogy with a single phase flow,where it is proved that there is similarity between the temperature and the velocity profiles,in multiphase flows it can be assumed that the void fraction is similar to the flow variable profile.The latest assumption simplifies the C_o modelling very much.

An entirely different approach to the distribution parameter concept has been suggested by researchers on the field,reviewed by S.Banerjee and A.M.C. Chan (1984).In cases of very different velocities or temperatures, in one of the phases,instead of determining a C_o for the distribution across the cross section area,the phase can be assumed split up in two components with $C_o = 1$.The latest suggestion avoids the evaluation of the distribution

parameter,but complicates the two phase modelling,because ,now,more transfer terms for the "new" phases are required to be modelled.

2.5.5 SIMPLIFIED 1-D TWO PHASE BUBBLY FLOW EQUATIONS

For a well mixed bubbly flow regime,it can be assumed that:

1) $C_o^a = C_o^f = C_o^I = 1$

2) the effect of the spatial heat transfer derivative can be assumed negligible compared to the flow changes,

3) in the case of small bubbles $<u>_l = <u>_g = <u>$ (no slip) which implies that any interfacial pressure fluctuations are zero as well,

4) for bubble sizes greater than the critical,the effect of the surface tension is negligible and assuming that,

$$\frac{dr_b}{dt} = 0 \text{ and } \frac{d^2r_b}{dt^2} = 0 \text{ (no contraction/expansion)} ,$$

$$<p>_l = <p>_{i,l} = <p>_{i,g} = <p>_g$$

5) any viscous,turbulent and body forces effects are negligible.

The simplified form of the flow equations is (dropping the, < > , avcraging signs)

1.k phase conservation of mass

$$\frac{\partial \alpha_k \rho_k}{\partial t} + \frac{\partial \alpha_k \rho_k u}{\partial x} = \dot{m}_{i,k} \qquad (3.39a)$$

2.k phase conservation of momentum

$$\frac{\partial \alpha_k \rho_k u}{\partial t} + \frac{\partial \alpha_k \rho_k u^2}{\partial x} + \alpha_k \frac{\partial p}{\partial x} = \dot{m}_{i,k} u \tag{2.39b}$$

3.k phase conservation of energy

$$\frac{\partial \alpha_k \rho_k I I_k}{\partial t} + \frac{\partial \alpha_k \rho_k u I I_k}{\partial x} - \alpha_k \frac{\partial p}{\partial t} = \dot{m}_{i,k} I I_{i,k} + \dot{q}_{i,k} \tag{2.39c}$$

and the simplified form of the interfacial jump condition is:

$$\sum_1^2 \dot{m}_{i,k} = 0 \tag{2.40a}$$

$$\sum_1^2 \dot{m}_{i,k}\, u = 0 \tag{2.40b}$$

$$\sum_1^2 \dot{m}_{i,k} I I_{i,k} + \dot{q}_{i,k} = 0 \tag{2.40c}$$

CHAPTER 3

NUCLEATION KINETICS

3.1 INTRODUCTION

Vapor production can occur a) during a temperature increase (with constant pressure) or b) during rapid pressure releases (with constant temperature). In this chapter the second case will be discussed.A blowdown accident which may occur in different industrial processes can trigger an irreversible phase transition in the bulk of the liquid system.In such processes the pressure falls so rapidly to almost atmospheric levels,that the liquid does not have the time to follow an equilibrium path,which leaves the fluid in a superheat state.Its temperature is much higher than the saturation one,depending on the local pressure,and its thermodynamic state is called a "metastable state".

Depending on the stability of the environment the residence time of the system in this state may vary.Nucleation is the phenomenon observed when the liquid (in its metastable condition) produces an irreversible phase transition,which helps the liquid's superheat relief.There are two modes of nucleation related to the degree of superheat of the system in this condition. A) The homogeneous nucleation,where "flashing" of the liquid takes place in the bulk and B) the heterogeneous nucleation,where any nucleation activities are helped by the presence of foreign articles e.g. the wall cavities,dissolved inert gases,dispersed particles e.t.c.As will be shown later homogeneous nucleation requires high degrees of superheat and

long residence times for the nucleus to be created whereas heterogeneous nucleation does not.As reported by Skripov (1974),the residence time of the system in the unstable condition,depends on the rate of nucleation,which in turn depends on how rich the system is in molecules,the size of the system and the size of the nucleus. Nucleation is a random event,which can be described by a Poisson distribution of the maximum work required for nucleation. Any nucleation promotion is a result of pressure and temperature fluctuations ,which provide enough energy for "liquid" molecules to become "vapor" ones.The size of the nucleus is related to the liquid's superheat.Less superheat,means bigger sizes,i.e. more molecules to fill up the bubble void.It also means fewer fluctuations.All these result in longer residence times for homogeneous nucleation, whereas for heterogeneous nucleation, the bubble voids are much smaller resulting in fewer required molecules and of course less residence time.

3.2 THEORY OF STABILITY

It was shown by Benson (1966) that for an isolated system (plus its surroundings) to be in a stable equilibrium,any possible variation of its state would produce a negative change in entropy,which is against the second law of thermodynamics.On the other hand a spontaneous change of a system would produce an entropy increase.Equilibrium is only reached when the entropy is maximum.For the equilibrium state,the system balances any tendencies for a change.Bearing the above stability rules in mind,it will be shown,that spontaneous change occurs when a liquid is in the metastable region.

For a system at a given pressure and temperature but with its volume allowed to change,the first law of thermodynamics states that,

$$dh = \delta q - \delta w , \qquad (3.1)$$

where h is the specific enthalpy,q the heat transfer to the system and w the work performed by the system.For an irreversible process:

$$dh < T\,ds - \delta w \ , \tag{3.2}$$

where T is the temperature of the system,p the pressure and s the specific entropy. It is well known,however,that dh = du + pdv + vdp,where u is the specific internal energy so that,

$$\delta w < T\,ds - du - pdv - vdp \ . \tag{3.3}$$

Making use of the specific free energy function,g = u + pv-T s,

$$dg = du + pdv + vdp - T\,ds - s\,dT \tag{3.4}$$

From (3.3) and (3.4)

$$\delta w < -dg - s\,dT \tag{3.5}$$

For a constant temperature process,

$$\delta w < -dg \tag{3.6}$$

In conjunction with the stability criteria,any spontaneous change (e.g flashing) produces an increase in entropy,a decrease in the free energy function and results in the system returning to an equilibrium state.

There are three types of equilibrium state,namely,the stable,the metastable and the unstable.Any remarks with respect to the strength of the stability for each of the above states will be drawn in conjunction with the nucleation process of a liquid system.In this respect the stability of each of the above equilibrium states depends on the size of the temperature and pressure perturbations, needed to move the system from this state.The size of these perturbations will determine the size of the critical nucleus.The well known definition for the critical nucleus is:*"the size of the nucleated molecular cluster that can survive and spontaneously grow afterwards"*.For the stable state the critical size tends to infinity which means that equation (3.6) becomes $dg=0$ or the free energy function has its minimum value.For the metastable case,the critical size depends on the degree of penetration into the metastble region of the liquid.The smaller the critical size the less the system can hold on to its state.Figure 89 illustrates a p-v diagram making use of the important van der Waal's equation of state for an ideal substance.Assuming that a liquid initially in the "A" state undergoes a constant temperature process it follows the path "A-B",which crosses the equilibrium (binodal) line and its limit is the spinodal line.The limit for any nucleation phenomenon is the spinodal line.Following the above stability discussion,the closer it comes to the spinodal line the greater its superheat and the smaller the critical size. So nucleation is unavoidable.It was proved by Zel'dovich and Todes (1940) that in the metastable region the specific heat Cp is negative and the $(\partial p/\partial v)_T < 0$ .At the spinodal line Cp remains negative and $(\partial p/\partial v)_T = 0$. The spinodal line belongs to the unstable region.Because of the negative Cp, from the heat conduction equation, the temperature differences grow exponentially , resulting in the liquid's decomposition, without nucleation.That is why the spinodal line is referred as the theoretical nucleation limit.

3.3 NUCLEATION ENERGY BARRIER

The weak stability of the metastable state of the superheat liquid is due to the fact that the chemical potential of the liquid phase is greater than the corresponding vapor's one,for the local conditions.For a given pressure and temperature the chemical potential is equal to the free energy function and denotes the ability of the molecules to produce work.Recalling equation (3.4) together with the first law of thermodynamics for an isothermal process

$$dg = v\,dp\,. \tag{3.7}$$

or

$$v = \left[\frac{dg}{dp}\right]_T \tag{3.8}$$

From figure 89 it is apparent that g is equal to the area under van der Waal's isothermal path.Figure 90 is an illustration of this area integration.Branch "A-E" corresponds to the subcooled liquid state (fig 89),"E-B" corresponds to the metastable region and branch "E-D" corresponds to the stable vapor region. From figure 90,it can be noticed that for a given pressure the chemical potential of the liquid is greater than the corresponding vapor one for a stable state. It is also obvious that the lower the pressure the greater the potential difference between the "E-B" and "E-D" branches.

The definition of nucleation with respect to the molecular action is as follows. For simplicity "liquid" molecules are the molecules in the liquid phase,where their thermal motion is restricted by the liquid molecular bonds.When locally there is an accumulation of energy due to thermal and pressure fluctuations the molecular potential can reach the limit to break these liquid bonds and replace them with the less restricting vapor ones.This phenomenon is called nucleation.The protection of the new phase is managed by the formation of the

liquid-vapor interface.The forementioned free energy difference will be directed towards the work needed for the interface build up and the filling up of the void with "vapor" molecules.The surface tension is a very important thermodynamic parameter during flashing since the vapor cavity is quite small (of the order of a few microns).As mentioned by Skripov (1974) for very low nucleation pressures the critical bubble is totally empty and energy transfer as work is directed towards the build up of the interface. At the point of the bubble's formation a random predomination of the molecular evaporation process over the condensation process will result in its growth,and the opposite procedure will result to its collapse, since the reduction of the critical size even by one molecule will increase the surface tension effect which will then collapse the vapor cavity.The critical cluster is thus in mechanical and chemical equilibrium and hence,

$$p_g - p_l = \frac{2\sigma}{r_{cr}} \quad , \tag{3.9}$$

$$g_g(p_g, T) = g_l(p_l, T) \quad , \tag{3.10}$$

where r_{cr} is the critical radius and σ the surface tension.p_l is the pressure of the liquid outside the bubble and p_s is the saturation pressure for the given temperature.

If within the metastable liquid phase (mother phase) ,a new phase (vapor phase) is created in the form of a small nucleous , then from the stability criterion characterised by equation (3.6) , irreversible energy transfer as work is produced and the chemical potential reduced.In the general case when a V volume of superheat liquid (with free enthalpy equal to $G_{initial}$) , is transformed to a V volume of vapor (with free enthalpy equal to G_{final}) ,the size of the bubble produced r_b , will generally be different from the critical bubble of radius r_{cr} ,i.e.

$$r_b \neq r_{cr} \tag{3.11}$$

In consequence equation 3.6 gives rise to

$$0 \geq 4\pi r_b^2\sigma - \frac{4}{3}\pi r_b^3 (p'_g - p_l) - N(g_l(p_l, T) - g_g(p'_g, T)) \qquad (3.12)$$

where p'_g is the pressure inside the bubble ,with a size different from the critical one and N the number of molecules in the bubble.The righthand side of equation (3.12) is the work needed for the creation of this bubble and is given as

$$W = G_{final} - G_{initial} \quad . \qquad (3.13)$$

In the special case of a critical cluster ,$\Delta g = 0$ in equation (3.12).

From equation (3.7) ,

$$N\Delta g = N(g_l(p_l, T) - g_g(p'_g, T)) = \frac{4}{3}\pi r_b^3(p_g - p'_g) \qquad (3.14)$$

From equations (3.12) ,(3.13) and (3.14) ,it can be shown that ,

$$W = 4\pi r_b^2\sigma - \frac{4}{3}\pi r_b^3 dp_{sat} \qquad (3.15)$$

where dp_{sat} indicates the degree of superheat.From the above equation and for a given superheat the free energy change is a function of the molecular cluster. Figure 91 illustrates this function and it is apparent that there is a certain r_b for which the nucleation work becomes a maximum.This is the size of the critical cluster.In theory any bubbles with smaller sizes will collapse and with bigger ones will carry on growing spontaneously.The whole

nucleation process can be illustrated as the equilibrium state of a sphere on a convex surface (fig.91).Nature always follows the quickest way to the stable state.From the stability criterion (3.6),all the bubbles , with sizes less than the critical, will reduce their free energy by simply reducing their size and eventually collapsing and the opposite happens with the bigger ones. The sphere on the convex surface example is a quite good one,since it can explain why not all of the critical bubbles can survive,as it was quoted by Skripov (1974).The summit of the convex surface is not a stable position for the sphere, and the same is valid for the critical cluster.Any random domination of the condensation process resulting in the bubble's collapsing.From equation (3.9),it can be seen that the critical size degreases as dp_{sat} increases.

3.3.1 HOMOGENEOUS MODE OF NUCLEATION

From equation (3.13) any temperature and/or pressure fluctuations due to rapid pressure reduction processes and/or turbulent flows can result in an increase in dG. There is,however,one value of dG that will trigger the nucleation phenomenon and this is the maximum for the given thermodynamic conditions. If equation (3.15) is differentiated with respect to r_b, after the dp_{sat} is replaced by equation (3.9),and equating the resulting expression to zero,it can be shown that,

$$\text{for } r_b = r_{cr} \quad dG_{max} = W_{cr} = \frac{4}{3}\pi r_{cr}^{\,2}\sigma \ , \tag{3.16}$$

or in terms of the liquid superheat

$$W_{cr} = \frac{16\,\pi\sigma^3}{3\,dp_{sat}^{\,2}} \ , \tag{3.17}$$

where W_{cr} is the maximum work required for nucleation.

3.3.2 HETEROGENEOUS MODE OF NUCLEATION

I.WALL EFFECT

In everyday applications the effect of the container or the pipe wall is present.Small irregularities or cavities on the surface help the nucleated bubbles,by allowing only a small spherical segment to grow on the wall.But from equations (3.16) and (3.17) it can be seen that this reduces the required work for nucleation making it easier for the superheat liquid to nucleate.

If σ_{lg}, σ_{ls} and σ_{gs} are the surface tensions of the interfaces between the liquid and the vapor,the liquid and the solid,and the vapor and the solid, and θ is the contact angle between the bubble interface and the wall,

$$\cos\theta = \frac{(\sigma_{gs} - \sigma_{ls})}{\sigma_{gl}} \quad , \tag{3.18}$$

and the volume of the sphere's segment can be shown (Skripov (1974),Blander and Katz (1975)),to be

$$V' = \frac{1}{3}\pi r_b^{\,3}(1+\cos\theta)^2(2-\cos\theta) \quad , \tag{3.19}$$

or

$$V' = V\phi \quad , \tag{3.20}$$

where ϕ is the so called heterogeneous factor given as

$$\phi = \frac{1}{4}(1+\cos\theta)^2(2-\cos\theta) \quad . \tag{3.21}$$

From equation (3.16) the critical nucleation work for the equivalent bubble with volume equal to V′ is given as,

$$W'_{cr} = V'\frac{\sigma}{r_{cr}} \tag{3.22}$$

where V′ is the volume of the segment of the critical cluster and V its total volume.From equations (3.22),(3.20) and (3.16)

$$W'_{cr} = W_{cr}\phi \tag{3.23}$$

From equation (3.20) it is readily shown that ϕ is the ratio of the volume of the segment of the bubble to the total one,so the value of ϕ is less than unity. This shows how much less nucleation work is needed. From equation (3.22) it can be seen that W_{cr} is directly proportional to the bubbles volume.For example if the segment's volume is half of the total,only half of the work is needed.

II. THE EFFECT OF DISSOLVED INERT GASES

In the case of dissolved gases ,the partial pressure of the gas helps in reducing the nucleation energy barrier which makes it easier for the system to nucleate.Assuming there exists a vicinity where there are N "liquid" molecules and N_{gas} gas molecules with a partial pressure of p_{gas}.Then after nucleation, N_{gas} molecules are mixed up with the vapor ones. So the free energy change can be given as

$$G_{final} - G_{initial} = -(dg\,N + dg_{gas}N_{gas}) + 4\pi r_b^2\sigma - \frac{4}{3}\pi r_b^3(p'_g + p_{gas} - p_l) \quad . \tag{3.24}$$

As it has been said before,dg for the liquid-vapor system is negative,since the chemical potential of the liquid is greater than the vapor's and dg_{gas} is also negative,for the same reason.

The mechanical equilibrium for the critical cluster,now,becomes

$$dp = p_g + p_{gas} - p_l = dp_{sat} + p_{gas} \quad , \tag{3.25}$$

so the critical work is,

$$W_{cr} = \frac{16}{3}\pi\frac{\sigma^3}{(dp_{sat} + p_{gas})^2} \quad . \tag{3.26}$$

From the above equation,the critical work decreases,as the pressure difference between the liquid's one and the one inside the bubble increases. For the purpose of modelling it may be assumed that the gas behaves as ideal and

$$p_{gas} = (\rho RT)_{gas} \quad , \tag{3.27}$$

where ρ,is the density,R its gas constant and T the temperature of the system during the isothermal nucleation process.

3.4 THE RATE OF NUCLEATION

Based on the Gibbs concept,the critical work for the cluster formation shows how stable the metastable liquid is.If the work,that is required is enormous then the system can remain to that state for ever.Volmer and Weber (1926) and Frenkel (1955),made use of this concept for the formulation of the rate of nucleation of a metastable liquid.Keeping in mind that the nucleation mechanics relies on the favourable local increase of the energy by fluctuations,the main feature of their formula for the rate of nucleation was the randomness,described by an exponentiation term.Assuming a steady state process i.e. J = const.,where J is the so called rate of nucleation or the flux of nuclei,their expression can be given as,

$$J = R_{cr} f_{cr} \ , \tag{3.28}$$

where R_{cr} is the rate of transition of the critical bubbles to the next size and f_{cr} is the number of critical nuclei per unit volume.For the development of the classic nucleation theory there are two bubble distribution functions assumed. f denotes the first and it represents the number of bubbles of a given size r_b. The other is f' and called pseudoequilibrium distribution function.This means that,if a stable state liquid condition is assumed i.e. a balance between the number of bubbles transmitting from neighbouring sizes then J = 0.f' denotes the distribution function for this condition.A link is also assumed to exist between f and f' and is of the form,

$$f = z_1 f' \quad , \tag{3.29}$$

where z_1 is the nonequilibrium factor and its value is less than or equal to 1, depending on the bubble size.For $r_b << r_{cr}$, where J can be assumed zero, $z_1 = 1$. These sizes of bubbles are created and then collapse.For $r_b >> r_{cr}$ no bubbles exist.This is because even if large r_b means very much less surface tension work,the work associated with pumping in of molecules is enormous for such voids. So since $f' \to 0$, $z_1 = f/f' \to 0$,and so z_1 is assumed to be zero.Skripov (1974) suggests that since the nucleation work increases so sharply at $r_b = r_{cr}$,it can be assumed that $z_1 = 1/2$. Including in the J formulation the "Poisson" character of the process,

$$f' = N \exp(\frac{-W(r_b)}{KT}) \quad , \tag{3.30}$$

where K is the Boltzmman constant,T the system's temperature and N the number of molecules per unit volume.This allows equation (3.28) to be written as,

$$J = N R_{cr} z_1 \exp(\frac{-W_{cr}}{KT}) \quad . \tag{3.31}$$

Often B denotes the product of R_{cr} times z_1 and it is called preexponential factor,so

$$J = N B \exp(\frac{-W_{cr}}{KT}) \tag{3.31a}$$

Later other investigators developed the quantity B by involving a detailed evaporation/condensation molecular process into it,but the exponentiation factor form was retained.Part of the effect of the degree of penetration of the liquid into the metastable region,on the J,is included in this term.

Doring (1937) and Volmer (1939),first introduced the evaporation/condensation concept,at the bubbles interface.The molecular cluster is first created because of the thermodynamic state of the liquid,described by the f and then it grows depending on the number of molecules that join/leave its interface. Their main equation was given as,

$$J = [A f q_{n_b}] - [A f a_{n_b+1}] \tag{3.32}$$

where A is the bubble's surface,q is the mean rate of vaporisation and a the mean rate of condensation and n_b is the number of molecules in the cluster.Next they assumed that the driving force for both vaporisation and condensation is the chemical potential difference of the vapor between any cluster size and the critical.This brings in the effect of diffusion of bubbles with $r_b < r_{cr}$ to $r_b > r_{cr}$.Of course for smaller or bigger bubbles than the critical the mechanical and chemical equilibrium rules (3.9,3.10),are not valid and the nucleation work is given by,(Skripov (1974),Blander and Katz (1975),Kagan (1960)), as

$$W = W_{cr} - 4\pi\sigma(r_b - r_{cr})^2 b \ , \tag{3.33}$$

where $b = 1 - 1/3(1 - p_l/p_g)$. This b factor takes into account the mechanical and chemical disequilibrium effects,i.e.when there is a rapid evaporation of molecules,the chemical equilibrium is reached so $p_g = p_l$ and b= 1.On the other hand if the bubble's size adjustment is quite fast,$p_g >> p_l$ and b can be assumed equal to 2/3. In reality the typical equilibrium

state of the bubble is somewhere in between. Both Doring (1937) and Volmer (1939),ended up with an expression for the nucleation flux like equation (3.31a).Their B was given as

$$B = \left(\frac{2\sigma}{\pi mb}\right)^{1/2} \exp\left(\frac{-l}{KT}\right) , \tag{3.34}$$

where m is the mass of a molecule and l is the molecular latent heat.

Zel'dovich (1942) formulated the most general diffusion equation to describe the nucleation mechanics. f' bubbles will nucleate for each of the sizes depending on the chemical potential difference between the vapor and the liquid phase (see equation3.24). However it may be noted that the real f distribution is different to f',because of thermal fluctuations at a molecular level. So any random loss or gain of molecules results in a diffusion of bubbles with size r_b (and n_b number of molecules) to either side i.e. $(n_b + 1)$ or $(n_b - 1)$. The diffusion equation,therefore,can be given as,

$$\frac{\partial f}{\partial t} = \frac{\partial}{\partial r_b}\left[D\frac{\partial f}{\partial r_b} - Df\frac{\partial Lnf}{\partial r_b} \right] . \tag{3.35}$$

In the above equation the term in the brackets is the rate of nucleation.Assuming the transport theorem to valid in this situation, the total f does not change and hence,

$$\frac{\partial f}{\partial t} + \frac{\partial fR}{\partial r_b} = 0 , \tag{3.36}$$

where R is the rate of transmission from one bubble size to the neighbouring. For the application of the transport theorem R is the "velocity" with which f flows into the viewing window.From (3.28) J = f R.So,

$$\frac{\partial f}{\partial t} + \frac{\partial J}{\partial r_b} = 0 \quad , \tag{3.37}$$

Kagan (1960) assumed that f does not change with time.This last assumption is not unrealistic.Skripov (1974) suggests that the time interval during which the nucleation process is unsteady is of the order of 1E-9 seconds. Experiments from the present work and also the work of other researchers showed a time for the first surviving bubble to appear to be of the order of a few hundreds of microseconds.So equation (3.37) gives,

$$J = \text{constant} \quad . \tag{3.38}$$

This is an assumption considered also by Skripov(1974),Doring (1937), Volmer (1939),Frenkel (1955),Blander and Katz (1975),J. Fisher (1948). Using equations (3.36),(3.37) and (3.38), Kagan (1960) managed to formulate the rate of nucleation. He allowed for the bubble's size to be affected by viscous and inertial forces and he also took into account the thermal boundary layer developed around each of the clusters.Assuming a chemical equilibrium the general form of his B was given by Skripov (1974) as

$$B = \frac{1}{4\pi}\left[\frac{KT}{\sigma}\right]^{1/2}\left[\frac{d\dot{n}}{dr_b}\right]_{cr} \tag{3.39}$$

Omitting any inertial,viscous and thermal boundary layer effects,Skripov (1974) showed that B can be given as

$$B = a\left[\frac{2\sigma}{m\pi}\right]^{1/2}\exp\left[\frac{-1}{KT}\right] \tag{3.40}$$

where a is the rate of condensation from the bubble's interface.This quantity is assumed to be equal to 1 in Doring's expression for J.Depending on whether viscous effects or inertial or thermal boundary layer ones are important (3,40) may take a more complicated form (see Skripov (1974)).

A simpler method to calculate B and through equation (3.31) the nucleation rate, is suggested by Skripov (1974).By assuming that z_1 is equal to unit,B = R_{cr} and

$$R_{cr} = \Lambda_{cr} q \quad . \tag{3.41}$$

From (3.41),the rate of transmission of the clusters in the neighbouring size,is equal to the vaporisation rate times the critical interfacial area.Vaporisation is due to the molecular collisions with the interface.Hence for an ideal gas molecules,

$$q = \frac{p_g}{(2\pi mKT)^{1/2}} \quad . \tag{3.42}$$

He also suggested that a constant value for B can be assumed to be approximately equal to 1E12 sec-1.

In the present study the nucleation model used is given by equation (3.31a) with B given from equation (3.39).For the ideal gas the number of molecules in the bubble is,

$$n = \frac{p_g}{KT} V_b \quad , \tag{3.43}$$

where V_b is the volume of the bubble.So,

$$n = \frac{4\pi p_g r_b^{\,3}}{3KT} \quad . \tag{3.44}$$

Differentiating (3.43) first with time and then with r_b,it can be shown (Skripov (1974) or Kagan (1960)),that

$$\left[\frac{d\dot{n}}{dr_b} \right]_{cr} = 2\pi a \left[\frac{8KT}{\pi m} \right]^{1/2} \frac{\sigma}{KT} \quad , \tag{3.45}$$

giving,

$$B = \left[\frac{6\sigma}{3\pi m} \right]^{1/2} \quad . \tag{3.46}$$

This form of B was also reported by Blander and Katz (1975). The above expression for B was rederived using equation (3.39) and the effect of mechanical or chemical equilibrium was included.It was assumed that there is a mechanical equilibrium, so b=2/3.In any case the difference in values between unity and 2/3 is negligible for the calculation of J.

3.5 THE LIMIT OF SUPERHEAT

As mentioned earlier the theoretical maximum superheat is close to the spinodal line.Practically the liquid system is liable to nucleate any where along its isothermic path.A way to locate the theoretical maximum superheat and with it the spinodal limit is to use the rate of nucleation expression (30a). From this expression r_{cr} can be given as

$$r_{cr} = \left[\frac{3KT}{4\pi\sigma} \mathrm{Ln}\left[\frac{N B}{J} \right] \right]^{1/2} , \qquad (3.47)$$

and from equation (3.9),dp_{sat} can be given as

$$dp_{sat} = \left[\frac{16\pi\sigma^3}{3KTLn(B\ N/J)} \right]^{1/2} . \qquad (3.48)$$

From the Clausious-Clapeyon equation together with the assumption that $\rho_l >> \rho_g$

$$dp_{sat} = \frac{dT_{sat}\, h_{gl}\, \rho_g}{T} , \qquad (3.49)$$

Where h_{lg} is the latent heat for vaporisation. From equations (3.48) and (3.49),

$$dT_{sat} = \frac{T}{\rho_g h_{lg}} \frac{16\pi\sigma^3}{3KT\ Ln(B\ N/J)} , \qquad (3.50)$$

a steady state nucleation process can be assumed to start when the first surviving critical cluster appears.For J = 1 and an initial liquid temperature the required superheat for homogeneous nucleation can be calculated.Calculated values from the above equation are of the order of 100 degrees,which agree quite well with experimental measurements (see e.g. Skripov (1974)).This means that for homogeneous nucleation the liquid has to penetrate quite deeply into the metastable region.This is unliky to happen in the everyday applications

where the degree of penetration is very much less.This implies that heterogeneous nucleation is present.

The dependence of the nucleation process on the wall roughness and the effect of its characteristics on the reproducibility of the activation of the nucleation sites,was studied by D.B.R Kenning and K. Thirunavukkarasu (1970). They reported that for metal surfaces the nucleation phenomenon was highly non-reproducible,where after a special treatment of the surface stable nucleation sites could be observed.They suggested that by cleaning the surface thoroughly the degree of wetting the surface cavities had increased and that was the reason for a more stable nucleation process.Also by using a PTFE-coated surfaces they proved that the different surface characteristics affect the nucleation process as well.They also suggested that there is a great number of sites that rely on being activated by neighbouring existing activated sites.

From the above it is obvious that, the heterogeneous factor is rather difficult to determin without the knowledge of the surface characteristics extracted in the form of experimental data for a given set up.

Y. Lee and W.Q. Shen (1987) reported their experimental results for the effect of the surface roughness on the rewetting process.Once a bubble has been nucleated,grown and left the nucleation site,fresh liquid refills the cavity,and so another bubble will be evaporated.Of course, the rate of rewetting of the nucleation spots,determines the whole nucleation process on the wall. The above researchers concluded that the roughness of the surface plays an unimportant role for the rewetting process.

3.6 THE CROWDED EFFECTS ON NUCLEATION

The nucleation process as a mean of relieving the liquid's superheat , has been discussed in the previous sections and this discussion was based on the molecular free energy (chemical potentials) change or in other words the nucleation energy barrier.The classical nucleation theory was studied by many researchers,aiming to improve the prediction of the nucleation rate by taking into account the thermal boundary layer around the single critical cluster and also the viscous and inertial effects (see Kagan 1960).None of these researchers,however,took into account the effect of the presence of other bubbles,in the two phase mixture,on the rate of nucleation.

For simplicity the complex motion of a bubbly flow will be broken down to three simpler motions:i) the mean motion,which is characterised by the physical size of the flow e.g. the diameter of the pipe,ii) the macromotion,which is characterised by the size of the growing bubbles in the mixture and iii) the micromotion,which is characterised by the size of the critical bubbles.In the present study,in the critical bubbles category are included both the surviving and the collapsing critical bubbles and their number density is given by equations (3.29) and (3.30).

The crowded effects can be divided into two categories:i) macromotion and ii) micromotion crowded effects.

3.6.1 MACROMOTION CROWDED EFFECTS

In the case of a bubbly flow modelling where the nucleation process is included,the liquid energy equation takes into account the effect of the growing bubbles on the temperature in the bulk of the liquid phase ,since each bubble acts as a heat sink during its growing period.The mechanical equilibrium for the critical bubble is given as,

$$p_{sat}(T_l) - \langle p \rangle_l = \frac{2\sigma}{r_b} \qquad (3.51)$$

where $<p>_l$ is the averaged liquid pressure.Biesheuvel and van Wijngaarden (1984) ,however,proposed an expression to link the averaged liquid pressure with the averaged mixture one.Models with the assumption of a constant phasial/intefacial pressure are not so accurate with respect to equation (3.51).

Biesheuvel and Wijngaarden expression can be written as:

$$<p>_l = <p> - \alpha\rho_l\{\frac{3}{2}\left[\frac{dr_b}{dt}\right]^2 + r_b\frac{d^2r_b}{dt^2} - \frac{1}{4}(|u_g - u_l|)^2\}\ , \tag{3.52}$$

where r_b is the bubbles radius and u_g,u_l the vapor and and liquid velocities respectively.With the assumption that the second derivative is negligible and with,

$$r_b = \left[\frac{3\alpha}{4\pi N_b}\right]^{1/3}\ , \tag{3.53}$$

and also assuming that the vapor/liquid slip is due to the vapor drift,i.e.

$$u_g - u_l = 1.41\frac{\left[\frac{(\rho_l - \rho_g)g_c\sigma}{\rho_l^2}\right]^{1/4}}{(1-\alpha)} \tag{3.54}$$

(see Lyczkowski (1976)),equation (3.52) can be written as,

$$dp_{sat} = p_g - <p> + \alpha\rho_l\left[\frac{0.064}{N_b^{2/3}\alpha^{4/3}}\left[\frac{d\alpha}{dt} - \frac{\alpha}{N_b}\frac{dN_b}{dt}\right]^2\right]$$

$$-\left[\frac{0.5\,\alpha\,\rho_l}{(1-\alpha)^2}\left[\frac{(\rho_l - \rho_g)g_c\sigma}{\rho_l^2}\right]^{1/2}\right] \tag{3.55}$$

A more complicated model for the slip velocity can be used with equation (3.52) taking into account any interfacial momentum transfer terms (e.g.virtual force). When the void fraction

is large both $d\alpha/dt$ and dN_b/dt are quite small,so the velocity slip term becomes greater and so the dp_{sat} becomes smaller ,predicting a larger critical bubble size and therefore an increased nucleation barrier and smaller nucleation rate.

3.6.2 MICROMOTION CROWDED EFFECTS

From the nucleation theory section discussion it is apparent that f_{cr} number of critical bubbles are nucleated per unit volume of the liquid,but only $f_{cr}R_{cr}$ critical bubbles per unit volume and time,manage to survive.In this section the interest is concentrated on all f_{cr} critical bubbles,since their nucleation requires energy consumption,extracted from the liquid phase.Assuming that all these critical clusters are heat sinks with respect to the liquid's superheat and a steady state heat transfer process,compared to the fast nucleation one, the total heat transfer to f_{cr} number of critical bubbles per unit volume can be given as,

$$\dot{q} = a_i h_i (T_l - T_{li}) \ , \tag{3.56}$$

where a_i is the interfacial area per unit volume,which is given as

$$a_i = f_{cr} 4\pi r_{cr}^2 \ . \tag{3.57}$$

h_i is the heat transfer coefficient,T_l the temperature in the bulk of the liquid and T_{li} the temperature of the liquid adjacent to the critical bubble's interface. From (3.56) T_{li} can be given as

$$T_{li} = T_l - \frac{\dot{q}}{4\pi r_{cr} f_{cr} h_i r_{cr}} \ . \tag{3.58}$$

T_{li} is the temperature the critical cluster feels and affects its collapse or survive.Kagan (1960) had included the heat transfer effect in the nucleation rate by making use of the Fourier's conduction heat transfer equation given as ,

$$k_l\left[\frac{\partial T_l}{\partial R}\right]_{R=r_b} = \frac{\dot{n}\,l}{A} = \frac{\dot{q}}{A} \quad , \tag{3.59}$$

where A is the bubble interfacial area,k_l is the heat conductivity coefficient for the liquid,l the molecular laten heat and $\dot{n}$ the rate of vaporisation of the molecules which is given as (Skripov (1974)),

$$\dot{n} = \frac{\pi a\left[\frac{8\,K\,T_l}{\pi\,m}\right]^{1/2} r_b^{\,2}}{K\,T_l}\left[p_g(T_{li}) - p_g(T_l)\right] \quad . \tag{3.60}$$

He also assumed that there is a coefficient d, which determines the temperature dependence of the saturated vapor pressure in a small region of states and hence,

$$p_g(T_{li}) - p_g(T_l) = d\,(T_{li} - T_l) \quad . \tag{3.61}$$

Hence by substituting the temperature difference in (3.61) from (3.59) and in turn the pressure difference in (3.60) from (3.61), the new form of $\dot{n}$ can be substituted in equations (3.45) and (3.39).As shown by Kagan (1960) the nucleation rate is given by

$$J' = \frac{J}{(1+Z)} \quad , \tag{3.62}$$

where Z is given as

$$Z = \frac{adl\left[\frac{8\,K\,T_l}{\pi m}\right]^{1/2} r_{cr}}{4\,k_l\,K\,T_l} \quad . \tag{3.63}$$

Following his method a new Z has been derived which includes the crowded effects as well,and is given as:

$$Z' = \text{adl}\frac{\left[\frac{8\,K\,T_l}{\pi m}\right]^{1/2}}{4K\,T_l f_{cr} h_i} \quad . \tag{3.64}$$

for heat transfer to a spherical object in a flow, with no slip, the Nusselt number is given by

$$Nu = \frac{h_i 2r_{cr}}{k_l} = 2 \quad . \tag{3.65}$$

From (3.63),(3.64) and (3.65)

$$Z' = Z(f_{cr})^{-1} \tag{3.66}$$

and

$$J' = \frac{J}{(1+Z')} \quad . \tag{3.67}$$

According to Skripov (1974) f_{cr} is given as

$$f_{cr} = \frac{1}{2} N \exp\left[\frac{-16\pi\sigma^3}{3\,K\,T_l\,dp_{sat}{}^2}\right] \quad . \tag{3.68}$$

When the superheat is not sufficient for nucleation $f_{cr} = 0$ and from (3.67) $J' = 0$.

In the case of heterogeneous nucleation ϕ can be included in the same way as discussed earlier in the chapter.

CHAPTER 4

THEORETICAL BLOWDOWN MODELLING

4.1 PHASE EQUILIBRIUM MODELLING

4.1.1 PROBLEM DESCRIPTION

The first approach for modelling a sudden depressurisation process from a vessel with a constant cross section area,is to consider the two phase fluid to be in thermal and mechanical equilibrium.The model is able to simulate the blowdown of a liquid system,initially at rest,and in either a saturation or subcooled condition.At zero time one of the two closed ends of the pipe opens permitting the liquid to feel the lower atmospheric pressure.The result of this,is an instantaneous superheat of the liquid and an expanding two phase mixture.The present model treats the two phase mixture as a homogeneous one,i.e.no slip and no temperature difference between the phases.Because of the very short times involved in this kind of transient release the effect of the heat transfer from the pipe wall and the body forces are neglected.Furthermore it is assumed that the effect of any skin friction forces are small compared to the rapid changes effects.The pressure in both phases is assumed to be the same.Both liquid and vapor are in a saturation state corresponding to the mixtures pressure.

As one of the pipes end is instantaneously removed a simple one dimensional and ideal rarefraction wave family propagates down the pipe lowering the system's pressure.The speed

of sound used by the present model is the isentropic frozen one (the appropriate expression will be derived later on).

4.1.2 TWO PHASE EQUILIBRIUM MODEL FORMULATION

For homogeneous flow the three one dimensional averaged conservation equations, described in chapter 2, reduce to the following.

i) mass conservation equation for the mixture

$$\frac{\partial \rho}{\partial t} + \frac{\partial (\rho u)}{\partial x} = 0, \tag{4.1}$$

ii) momentum conservation equation for the mixture:

$$\frac{\partial (\rho u)}{\partial t} + \frac{\partial (\rho u^2)}{\partial x} + \frac{\partial p}{\partial x} = 0, \tag{4.2}$$

iii) energy equation for the mixture:

$$\frac{\partial (\rho H)}{\partial t} + \frac{\partial (\rho u H)}{\partial x} - \frac{\partial p}{\partial t} = 0, \tag{4.3}$$

where $H = h + u^2/2$ and ρ and u the mixture density and velocity respectively. It is more convenient to rearrange the above equations algebraically to get

$$\tilde{A}_2 \frac{\partial \vec{U}}{\partial t} + \tilde{A}_1 \frac{\partial \vec{U}}{\partial x} = 0 \qquad (4.4)$$

Making use of the state equation

$$\rho = \rho(p,h) \quad . \qquad (4.5)$$

where $\vec{U}$ is a vector and $\tilde{A}_1$ and $\tilde{A}_2$ are matrices corresponding to the dependent variables,

$$\vec{U} = \begin{bmatrix} u \\ h \\ p \end{bmatrix} , \quad \tilde{A}_1 = \begin{bmatrix} u & 0 & 1/\rho \\ c^2 & u & 0 \\ \rho c^2 & 0 & u \end{bmatrix} , \quad \tilde{A}_2 = \tilde{I} \quad .$$

The above conservation equations together with the equation of state for the system complete the set of equations required to formulate the homogeneous model.

The assumptions used for the present modelling are,

(1) A pure substance is assumed,i.e. no foreign gases and particles present.

(2) On a given cross section all flow quantities i.e. u,p,ρ e.t.c. have the same value for both phases and equal to their averaged one.

(3) Body forces are assumed to be negligible.

(4) No wall heat transfer and friction effects.

(5) The liquid phase is assumed incompressible ($\rho_l = \text{const}$ and $c_l = \text{const.}$)

(6) A perfect fracture of the membrane,which separates initially the liquid in the vessel from the atmosphere,is also assumed.

4.1.3 METHOD OF SOLUTION

If all eigenvalues of the above set of equations are real, then the above equations are classified as hyperbolic.For the homogeneous model case the above equations are indeed hyperbolic in nature.In order for the eigenvalues to be determined

$$\det\ [\tilde{A}_2\lambda - \tilde{A}_1] = 0\ . \tag{4.6}$$

where λ is the eigenvalue. For the present case,there are three eigenvalues

$$\lambda = u,\ u + c,\ u - c \tag{4.7a}$$

where c is the local speed of sound for the mixture.On a x,t plane λ can be written as

$$\lambda = \frac{dx}{dt} \tag{4.7b}$$

A well known numerical technique used for the solution of the hyperbolic partial differential equations is the so called 'method of characteristics'. During transient phenomena the flow information travels by means of high amplitude disturbances with the speed of sound through the given medium.This is utilised by the method of characteristics to solve the three conservation equations along the information travel paths.Along these 'characteristic' paths the above set of equations reduce to an ordinary differential set of equations,which are called compatibility equations and can be written as follows

$$\text{along}\ \ \frac{dx}{dt} = u + c \quad \frac{dp}{dt} + \rho c \frac{du}{dt} = 0\ , \tag{4.8a}$$

along $\frac{dx}{dt} = u - c \quad \frac{dp}{dt} - \rho c \frac{du}{dt} = 0$, (4.8b)

and along $\frac{dx}{dt} = u \quad \frac{dh}{dt} - \frac{1}{\rho}\frac{dp}{dt} = 0$. (4.8c)

The local speed of sound for the homogeneous case is the so called 'isontropic frozen' speed of sound.By definition

$$c^2 = \left[\frac{\partial p}{\partial \rho} \right]_s , \tag{4.9}$$

and by making use of the caloric state equation

$$\rho = \rho(p, \chi) \ , \tag{4.10}$$

where χ is the flow quality,c can be written as

$$\frac{1}{\rho^2 c^2} = \frac{\chi}{\rho_g{}^2 c_g{}^2} + \frac{(1-\chi)}{\rho_l{}^2 c_l{}^2} - \left[\frac{1}{\rho_g} - \frac{1}{\rho_l} \right] \frac{\partial \chi}{\partial p} \tag{4.11}$$

and since it is assumed a frozen sound speed $\partial\chi/\partial p = 0$.The meaning of the 'frozen' concept is that the 'sound' disturbances travel so fast,that the system does not have the time to change the quality at a given point during the time a sound wave passes by. So the speed of sound expression becomes:

$$c = \left[\frac{1}{\rho^2 \left[\frac{\chi}{\rho_g{}^2 c_g{}^2} + \frac{1-\chi}{\rho_l{}^2 c_l{}^2} \right]} \right]^{1/2}, \tag{4.12}$$

where ρ_k and c_k (k = g,l) are the density and speed of sound for phase k respectively.

4.1.4 SOLUTION TECHNIQUE

The three compatibility equations (4.8) hold along the right and left propagated waves and along the material path,respectively.In theory the three characteristic curves are not straight lines ,on the (x,t) plane,but for quite small time and space advances the wave propagation is locally deemed as a straight line.A general solution algorithm is shown in figure 83.The propagated procedure with time and space is used for all dependent variables to be evaluated at point "3".By knowing the values of all flow properties at points "1","4" and "2",equations (4.8) can be written in finite difference form as follows,

along (R) right propagated waves

$$\frac{x_3 - x_1}{t_3 - t_1} = u_1 - c_1 \,, \quad \frac{p_3 - p_1}{t_3 - t_1} - \rho_1 c_1 \frac{u_3 - u_1}{t_3 - t_1} = 0 \tag{4.13}$$

along (L) left propagated waves

$$\frac{x_3 - x_2}{t_3 - t_2} = u_2 + c_2 \,, \quad \frac{p_3 - p_2}{t_3 - t_2} + \rho_2 c_2 \frac{u_3 - u_2}{t_3 - t_2} = 0 \tag{4.14}$$

along (M) the material path

$$\frac{x_3 - x_4}{t_3 - t_4} = u_3 \,,\, \rho \frac{h_3 - h_4}{t_3 - t_4} - \frac{p_3 - p_4}{t_3 - t_4} = 0 \qquad (4.15)$$

Theoretically the characteristic paths depend on all known points "1","4" and "2" and the unknown one "3",thus equations (4.8) are implicit in nature.However, it was noticed, during the trial "runs" of the model, that by keeping the time advance small, the above equations can be assumed explicit, performing quite accurately.Making use of equations (4.13),(4.14) and (4.15) the values of x,t,u,p,h,which correspond to the point "3" can be readily evaluated.The rest of the flow properties i.e. χ,ρ,c,T (mixture's temperature) are calculated by making use of the state equation.R.W.Haywood(1969) proposed a series of expressions,which he called "characteristic functions" of the state.So a way to determine the saturation properties for a given saturated state, is to either make use of Haywood's expressions or to perform an interpolation between the tabulated saturation values by G.F.C. Rogers and Y.R. Mayhew (1980).

4.1.5 TYPE OF SOLUTION

The hyperbolic equations allow for a propagation solution to be performed when suitable boundary conditions are applied to the system.By adopting this propagated procedure there are two ways of making use of the method of characteristics.First,is the type of solution used by W.T.Hancox et.al.(1978) when they tried to simulate a water blowdown

phenomenon.With this technique, the three characteristic curves i.e.dx/dt=u,u+c and u-c,are traced on the (x,t) plane starting from a series of simple rarefraction waves produced at the open end of the pipe at the zero time when the membrane was suddenly removed (see fig. 84).According to the above "tracing down" method the left and right propagation waves meet at an unknown and random point of plane (x,t).This last feature of the method introduces a difficulty in case one prefers to calculate the evolution of a given flow property e.g.pressure at a given point.For example,one of the purposes of the present model is to compare the theoretical pressure history with the experimental one at given locations along the pipe's axis.With the first method,this requires an interpolation procedure to be employed which is time consuming and tedious.

The second type of solution,which was used in the present work,relies on the construction of a constant space and time interval mesh (see fig.85). From the next time interval and from each of the mesh points the characteristic paths are extrapolated back to the previous time interval where all flow quantities are known.The calculating procedure is well illustrated in figure 86. In order for the interception points "1","4" and "2" to be determined the values of all flow quantities are linearly extrapolated between the known ones at the mesh points.Unfortunately there isn't any theoretical criterion to suggest what the space and time intervals have to be for more accurate presentation of the model.So one has to rely on trial runs to determine the most efficient and accurate selection of the mesh size.There is however,a stability criterion which can be given as:

$$(c+|u|)\frac{dt}{dx}\leq 1 \qquad (4.16)$$

The main difference with the first procedure is that the space and time locations for the phenomenon evolution are known and they can be initially specified so the purposes of this theoretical work are served.

4.1.6 INITIAL AND BOUNDARY CONDITIONS

The values of all flow quantities of the system at zero time,namely,the enthalpy,h,the pressure,p,the quality,x,the velocity,u,must to be specified a priori for each of the mesh points,except the two boundaries. i) The closed end: At the closed end of the vessel,figure 87 the velocity is zero and hence the particle path is traced by a line perpendicular to the x-axis and hence:

$$x_3 = x_4 = x(\text{bottom}) \tag{4.17}$$

The left propagated wave intercepts the wall and it is coupled with a simplified version of the right propagating wave equation :

$$u_3 = 0 \tag{4.18}$$

ii) The opened end: At the opened end the missing left propagated wave equation (see fig.87) is replaced by the condition:

$$p_3 = p(\text{atm}) \tag{4.19}$$

when the local mixture speed of sound is greater or equal to the local mixture velocity or

$$u_3 = c_3 \tag{4.20}$$

when the flow is sonic.

For the last boundary condition,when the flow is sonic the pressure at the exit plane cannot be evaluated explicitly,so an iteration subroutine is activated with aim of determining the choking flow pressure.

4.1.7 CALCULATION OF THE SATURATION PROPERTIES

As it has been pointed out in section 4,an interpolating subroutine has been written to provide the main computer code with all the saturation information required,given only the value of the pressure.The 'saturation' subroutine utilises a simple linear interpolation model,which is used to extract data from the tabulated saturation states by G.F.C. Rogers and Y.R. Mayhew (1980).

4.1.8 SIMPLE CENTRAL WAVE SYSTEM -EXPANSION FAN

For a vessel suddenly opened into a low pressure reservoir,in the present case the atmosphere,an expansion fan calculation has been used.This is similar to the case of the well known shock tube problem (M.J.ZUCROW,J.D.HOFFMAN (1976)).At zero time ,when the membrane is removed a family of central left propagating waves is originated at the open end.An expansion fan computer program has been written to simulate and calculate the values of all flow quantities affected by the expansion as a result of the $dx/dt = u-c$ characteristics travel down the vessel.It is assumed by the code that the sudden release to the atmospheric pressure,p_{at},is done by small pressure drops as follows,

$$\Delta p = \frac{p_{in} - p_{at}}{N} \tag{4.21}$$

where N is the number of pressure drops, at the zero time.The above code makes use only of the left (L) and material (M) paths equations (4.14) and (4.15) respectively.The leading wave propagates with a speed of sound equal to 500m/sec for the freon 12 substance and 1200m/sec for the water.The speed of sound of the following disturbances is calculated by the isentropic frozen relationship. The code runs until either the pressure at the exit reaches the atmospheric one or the flow becomes choked,which ever comes first.At the end of this run all expanded properties of the flow at the exit are known and are utilised by the main code to trigger the blowdown simulation.At any mesh point,except the exit plane,the values of the flow properties are equal to the saturation or subcooled state of the liquid at rest.This expansion fan program,assumes that the shock wave,produced at the other side of the removed membrane,has quickly left the exit plane,so it does not affect the transient flow inside the vessel.However, in the case of a blowdown from a vessel with extension pipework which is studied later on, and also the simulation of the explosion of glass spheres,full with freon 113,the present code takes into account the effect of the shock wave,which imposes a pressure behind it greater than the atmospheric.

4.1.9 COMPUTER PROGRAM

A computer program has been written in "FORTRAN 77" for the digital computer, making use of the step type tracing solution.By altering the saturation subroutine and the initial conditions,it is possible for the code to simulate one dimensional 'Blowdowns" of any

pure substance from a pipe of arbitrary dimensions.A complete listing of the computer code including all the appropriate subroutines can be found in appendix A.All computations ,for the present work,were performed on the VAX digital computer at the University of Liverpool.

4.2. THERMAL NON-EQUILIBRIUM MODELLING

4.2.1 INTRODUCTION TO THE PROBLEM

The modelling of a seemingly explosive depressurisation of a system (saturated or subcooled liquid or liquid and vapor in equilibrium),which allows for the temperature to be different in the two phase will be presented next.During fast pressure releases e.g total failure of a storage vessel containing high enthalpy system,the time allowed for the system to follow an equilibrium phase transition process e.g. evaporation from the free interface,is so much restricted ,that the liquid crosses the binodal line and it enters the metastable region as the pressure reduces without any thermal relief of the liquid.

The minimum requirement from the modelling point of view,is for a temperature difference to be allowed between the phases,if one requires a satisfactory simulation of the initial depressurisation.The effect of the different velocities between the phases is not included in the present model.The no-slip assumption is believed to be quite accurate in the cases of small vessels and also in cases of slower expansions of the system.

The present thermal non-equilibrium model assumes that a bubbly mixture with uniformly dispersed bubbles of the same size occupies any cross section plane of the vessel,which is assumed to be of constant cross section area.On a given plane both vapor and liquid flow quantity values correspond to an averaged value,over each of the two phases separately. For bubble sizes which can be assumed big i.e.greater than the critical diameter the surface tension effect can be assumed negligible and so the pressure on each of the interface sides is the same,as given by the following relation:

$$\Delta p = 2\frac{\sigma}{r} \tag{4.22}$$

Furthermore since the vapor phase is restricted by spherical voids of quite small radius,it can be assumed,that any pressure changes are transmitted so fast in the vapor medium,that the pressure difference between the vapor side of the interface and the bulk of the bubble is zero.The same assumption holds for the liquid side of the interface as well,since any pressure difference produced by the form drag force is zero,since a no-slip assumption has been previously made and also any pressure disturbances travel quite fast with the liquid speed of sound,compared to the local material velocities. Hence the pressure constitutive relation simplifies to:

$$p_l = p_{il} = p_{ig} = p_g \tag{4.23}$$

The general description of the model is: a multifluid flow simulation, where conservation of mass ,momentum and energy equations are solved for each of the phases separately.The only link between the two phases is the interfacial heat and mass transfer.The void fraction change relies on the phase change process and the pressure change,formulated as a mechanical equilibrium relation,which allows for no bubble growth oscillations.

In the sections that follow,a complete formulation will be presented for i) a constant bubble size model ii) a nucleation model and iii) a thermal non-equilibrium blowdown simulation from a partially full vessel with or without vent pipework attached to its exit.

4.2.2 FORMULATION OF THE THERMAL NON-EQUILIBRIUM MODEL

According to the assumptions reported in the previous section the averaged equations governing the motion of a one dimensional two phase flow described in chapter 2 can be modified to give:

$$\frac{\partial \alpha_k \rho_k}{\partial t} + \frac{\partial \alpha_k \rho_k u}{\partial x} = \dot{m}_{ik} \tag{4.24}$$

$$\frac{\partial \alpha_k \rho_k u}{\partial t} + \frac{\partial \alpha_k \rho_k u^2}{\partial x} + \alpha_k \frac{\partial p}{\partial x} = \dot{m}_{ik} u - \tau_{wk} \tag{4.25}$$

$$\frac{\partial \alpha_k \rho_k (h_k + \frac{u^2}{2})}{\partial t} + \frac{\partial \alpha_k \rho_k u (h_k + \frac{u^2}{2})}{\partial x} - \alpha_k \frac{\partial p}{\partial t} = \dot{q}_{ik} + \tau_{wk} u + \dot{m}_{ik} (h_k + \frac{u^2}{2})_i \tag{4.26}$$

The subscript k (=l or g) denotes the phase (liquid or vapor). $\dot{m}$ and $\dot{q}$ are the rates of mass and heat transfer per unit volume and τ is the shear force per unit volume.The subscripts w and i denote transfer from the wall and the interface respectively.In the formulation of the above equations,it is also assumed that any effect of the wall heat transfer and body forces are very small during fast transient phenomena.

The equations that link the conservation equations across the interface are:

$$\dot{m}_{ig} + \dot{m}_{il} = 0 \quad , \tag{4.27}$$

$$\dot{m}_{ig}u + \dot{m}_{il}u = 0 \quad , \tag{4.28}$$

and

$$\dot{q}_{ig} + \dot{m}_{ig}(h_g + \frac{u^2}{2})_i + \dot{q}_{il} + \dot{m}_{il}(h_l + \frac{u^2}{2})_i = 0 \quad . \tag{4.29}$$

By making use of the state equation

$$\rho_k = \rho_k(p,h_k) \tag{4.29a}$$

equations (4.24) to (4.26) can be rearranged to a matrix form like equation (4.4). $\vec{U}$,$\tilde{A}_1$,$\tilde{A}_2$ and the non-zero right hand side $\tilde{A}_3$ are:

$$\vec{U} = \begin{bmatrix} u \\ p \\ \alpha \\ h_g \\ h_l \end{bmatrix}, \tilde{A}_1 = \begin{bmatrix} u & 1/\rho & 0 & 0 & 0 \\ \alpha\rho_g & \alpha u/c_g^{\,2} & \rho_g u & 0 & 0 \\ (1-\alpha)\rho_l & (1-\alpha)u/c_l^{\,2} & -\rho_l u & 0 & 0 \\ 0 & -\alpha u & 0 & \alpha\rho_g u & 0 \\ 0 & -(1-\alpha)u & 0 & 0 & (1-\alpha)\rho_l u \end{bmatrix},$$

$$\tilde{\Lambda}_2=\begin{bmatrix} 1 & 0 & 0 & 0 & 0 \\ 0 & \alpha/c_g^{\,2} & \rho_g & 0 & 0 \\ 0 & (1-\alpha)/c_l^{\,2} & -\rho_l & 0 & 0 \\ 0 & -\alpha & 0 & \alpha\rho_g & 0 \\ 0 & -(1-\alpha) & 0 & 0 & (1-\alpha)\rho_l \end{bmatrix}, \tilde{\Lambda}_3=\begin{bmatrix} C_1 \\ C_2 \\ C_3 \\ C_4 \\ C_5 \end{bmatrix}$$

where

$$C_1 = \frac{-\tau_w}{\rho}$$

$$C_2 = \dot{m}_{ig} - \frac{1}{\rho_g}\left[\frac{\partial \rho_g}{\partial h_g}\right]_p C_4$$

$$C_3 = -\dot{m}_{ig}$$

$$C_4 = \Gamma_{eg} - (H_g - u^2)\dot{m}_{ig} - u\Gamma_{fg}$$

$$C_5 = \Gamma_{el} + (H_l - u^2)\dot{m}_{ig} - u\Gamma_{fl}$$

where $\Gamma_{ek} = \dot{q}_{ik} + \dot{m}_{ik}(h_k + \frac{u^2}{2})_i$, $\Gamma_{fk} = (-\tau_{wk} + \dot{m}_{ik}u)$, $H_k = h_k + \frac{u^2}{2}$

Like the homogeneous model the eigenvalues of the matrix are

$$\frac{dx}{dt} = u, u, u, u + c, u - c \qquad (4.30)$$

and the compatibility equations which apply along these characteristics are:

$$\text{along } \frac{dx}{dt} = u + c \quad dp + \rho c du = (C_2 + \rho c C_1)dt \tag{4.31a}$$

$$\text{along } \frac{dx}{dt} = u - c \quad dp - \rho c du = (C_2 - \rho c C_1)dt \tag{4.31b}$$

$$\text{along } \frac{dx}{dt} = u \qquad d\alpha - B dp = (C_3 - BC_2)dt \tag{4.31c}$$

$$\alpha \rho_g dh_g - \alpha\, dp = (\rho_g C_4 - C_2)dt$$

$$(1 - \alpha)\rho_l dh_l - (1 - \alpha)\, dp = (\rho_l C_5 - C_2)dt$$

where c is the isentropic frozen speed of sound in the mixture and is given as:

$$c = \frac{1}{\left[\rho\left[\frac{\alpha}{\rho_g c_g^{\,2}} + \frac{(1-\alpha)}{\rho_l c_l^{\,2}}\right]\right]^{1/2}} \tag{4.32}$$

and B is given as:

$$B = \frac{\alpha(1-\alpha)(\rho_g c_g^{\,2} - \rho_l c_l^{\,2})}{(\rho_g c_g^{\,2} \rho_l c_l^{\,2})}$$

For the construction of the thermal non-equilibrium model it was assumed that the liquid density and speed of sound are constant throughout the event and that the specific heat for both the vapor and the liquid phase are also constant.

The method of solution,the solution technique and the type of solution are exactly the same as in the phase equilibrium case. Furthermore the boundary conditions used for the homogeneous model can be applied to the non-equilibrium one as well.

4.2.3 INTERFACIAL HEAT TRANSFER MODEL

The missing information associated with the averaging process of the flow conservation equations is related to interfacial quantities and in general with mass,momentum and energy transfer terms from the boundaries i.e. interface and wall.Vital information for the model is the interfacial heat transfer and this is addressed in this section.

Banerjee (1978) was one of the first investigators to propose a heat transfer model which would include both algebraic and derivative terms.The main concept behind his model was the surface renewal theory.This theory considers that turbulent eddies in the continuous phase,renew the material close to the interface by bringing fresh fluid at averaged intervals t (sec).So by solving the heat conduction equation for the thermal boundary layer of the dispersed phase,he managed to formulate the interfacial heat interaction involving total derivatives.Boure' (1975) had summarised the progress towards interfacial constitutive relations and he had shown that the above relations must include derivative terms as well as algebraic ones. As is well known derivatives on the right hand side of the conservation equations will result in different eigenvalues, which may render the equations non-hyperboilic. Furthermore the proposed model by Banerjee includes a turbulent quantity,the renewal time, which is quite difficult to be established.He proposes also that the heat transfer from the vapor phase to the interface is negligible since experiments with steam-water,showed a less than 5% vapor heat transfer,of the liquid one. The later assumption will be one of the main assumptions of the present interfacial heat transfer model.

Other quasi steady heat transfer models have been proposed by a number of investigators.Ishii (1982) reported a general form of the steady state model given as

$$\dot{q}_i = a_i F_d \tag{4.33}$$

where a_i is the interfacial area concentration and F_d the driving force.

C.W. Solbrig et.al. (1978) summarised the models for i) interfacial phenomena i.e. heat,mass and momentum transfer,ii) wall face interactions and iii) interfacial area concentration.All the above models were given with different formulation for different flow regimes.

The base,for most investigators,for calculating F_d is given as,

$$F_d = h(T_k - T_i) \tag{4.34}$$

where h is the heat transfer coefficient and T_k and T_i the temperature of the k phase and the interface respectively.The value of h,can be found in the literature to be given as constant or to vary,depending on the flow regime, the thermodynamic properties of the phase,the Reynolds number,e.t.c (J.E. Kelly and M.S. Kazimi (1982)).Wolfert (1976) proposed a heat transfer model which was a sum of a zero slip part and a non-zero slip one.He assumed the bubble velocity to be the product of its size times a constant (1/sec).A quite different approach to the problem was suggested by both M.N. Hutcherson et.al.(1983) and Winters (1978).They included the energy equation and the interfacial heat and mass transfer in a bubble growth model. Their main assumption was that the inertia dominated growth period takes place in the first few microseconds and so its effect is negligible.The interfacial heat transfer,however,is the most important mechanism of the bubble growth and that was the one they modelled as a heat conduction phenomenon from the liquid to the vapor phase.

The main aim of the present model is to reflect quite realistically the interfacial interactions without losing its simplicity.Hence the main assumption is that the heat transfer from the vapor phase to the interface is zero (which is backed up by Banerjee (1978)).Since the vapor thermal diffusivity is far greater than the liquid one any temperature changes will quickly balanced out inside the bubble, to give

$$T_g = T_i \ . \tag{4.35}$$

Therefore the form of the heat transfer model is given as:

$$\dot{q}_i = a_i \, h \, (T_i - T_g) \ , \tag{4.36}$$

For a mixture consisting of spherical bubbles,

$$a_i = N_b 4\pi r_b^{\,2} \ , \tag{4.37}$$

where N_b is the number density of the bubbles.By definition the void fraction is given as:

$$\alpha = N_b \frac{4}{3} \pi r_b^{\,3} \ , \tag{4.38}$$

and hence

$$\dot{q}_i = 3 \frac{\alpha}{r_b} h(T_l - T_g) \ . \tag{4.39}$$

The heat transfer coefficient is a function of the Nusselt number Nu,the thermal conductivity k,and the bubble radius r_b ,hence

$$h = Nu \frac{k}{2r_b} \quad (4.40)$$

The Nusselt number is usually obtained through experimental correlations.For the present study the following value is used (Bird (1960)):

$$Nu = 2 + 0.6 \frac{2r_b U_s \rho_l}{\mu_l} \frac{C_p \mu_l}{k_l} \quad , \quad (4.41)$$

where μ_l, k_l, C_p, U_s are the dynamic viscosity,the conductivity coefficient,the specific heat (constant pressure) of the liquid phase and the slip ratio respectively.For zero slip

$$\dot{q}_i = \frac{1.5}{r_b^2} \alpha \, Nu \, k \, (T_l - T_g) \quad . \quad (4.42)$$

The present model does not provide an equation for the bubble size change and the assumption is that r_b is constant and the number density of the bubbles changes through the void fraction equation.The latest assumption is equivalent to the one made by Edwards and O'Brien (1970) when they assumed that N_b was constant.Similar forms of the above equation can be found in the published work of other investigators,for example Ferch (1979) made use of a constant with the dimension of time.He considered this parameter to be the constant rate of the interfacial heat transfer.In the following sections,when comparison between

theory and experiments has been performed the value of r_b has been adjusted to fit the experimental data with quite realistic values for the bubble size. Any void fraction change,from the beginning of the event, is because of the growth of the already existing and uniformly dispersed bubbles.As it was reported by Ferch (1979) a deficiency of the averaged process of the flow field equations requires that the void fraction has to be different than zero at the beginning of the event.So the value of 1E-6 has been assumed,which is close to zero.It can be thought effectively as proportional to the number of existing nucleation sites.

4.2.4 WALL FRICTION MODEL

This section is concerned with the modelling of the missing information associated with the wall friction stresses.As in the previous section the model which will be used is of a quasi steady nature.The general form of the skin friction model is given in the literature as:

$$\tau_{wk} = \alpha \rho_k F \quad , \tag{4.44}$$

where F is given as:

$$F = \frac{4f}{2D} u|u| \quad . \tag{4.45}$$

D is the pipe diameter,u,the material velocity,and f a friction factor. For the single phase flow f is given as:

$$f = 0.46Re^{-0.2} \quad , \tag{4.46}$$

for turbulent flow and as

$$f = \frac{64}{Re} \quad , \tag{4.47}$$

for the laminar flow.In the present model a two phase multiplier will be used, developed by Hancox and Nicoll (1972) and published by Hancox et.al. (1978).The concept associated with a two phase multiplier is to relate the effect of the single phase flow with a two phase one.This multiplier is given as:

$$\tau^* = 1 + \chi(b-1)[1 + 3.57\exp(-0.00884g)][1 - \exp(-4.96(1-\chi))] \tag{4.48}$$

where

$$b = \frac{\rho_l}{\rho_g}\left[\frac{\mu_g}{\mu_l}\right]^{0.2} \tag{4.49a}$$

$$g = \frac{\dot{G}}{(g_c\rho_l(\rho_l - \rho_g)\mu_l)^{1/3}} \tag{4.49b}$$

where $\dot{G}$ is the mass flow rate per unit area and g_c the acceleration of gravity. If the total skin friction for the mixture is given as,

$$\tau_w = \rho F \tau^* \tag{4.50}$$

the individual friction parts for each of the two phases is weighted with the help of the void fraction as,

$$\tau_w = (\rho_g \alpha + \rho_l (1 - \alpha)) F \tau^* = \tau_{wg} + \tau_{wl} \tag{4.51}$$

4.2.5 THE CHOKED FLOW PLANE MODELLING

The actual flow near the exit is not one dimensional, slip and friction between the phases occur and in addition the effect of less than 100% opening produced by the membrane's rupture, discussed in the experimental chapter, requires careful modelling of this boundary condition.

The difficulty lies in relating the theoretical boundary condition to the actual exit flow condition.This is achieved by assuming that a steady flow exists between the theoretical and actual flow planes at the exit region.To account for the effects of slip, friction and three dimensionality of the flow a pseudo discharge coefficient is defined. For steady flow R.P.Benedict (1974) suggested a generalised discharge coefficient,assuming a single phase flow.His expression is adopted in the present study assuming a homogeneous flow with no slip.His C_d depends on the Reynolds number and it can be calculated to be around 0.55 for 10% blockage.This value agrees with the values reported by Fletcher (1984) and H.E.A. van den Akker (1986) who suggested that for high Reynolds numbers C_d can be smaller.

A form of the mass flow rate equation proposed by F.J.Moody (1964)can be given as

$$\dot{G} = |2g_c \frac{dh}{v^2}|^{1/2} \tag{4.52}$$

From the first law of thermodynamics it follows that,

$$Tds = dh - vdp \tag{4.53}$$

where s is the specific entropy and T the temperature of the system.For an isentropic process

$$ds = 0 \text{ and } dh = vdp \tag{4.54}$$

and hence

$$\dot{G}_{is} = (2g_c \rho dp)^{1/2} \tag{4.55}$$

which is a well known form used by H.E.A. van den Akker(1986),Fletcher(1984) and others.For a nonisentropic process,however $\dot{G}$ may be given as follows

$$\dot{G}_{nis} = \{2g_c \rho[dh - T\ ds\ rho]\}^{1/2} \tag{4.56}$$

A reason for an increase in the system's entropy is the slip between the phases. A form of the drag force per unit area of the interface,as the slip's result, for a two phase flow is given by Drew (1983) as

$$F_{drag} = \frac{3}{8}\alpha\frac{Cd}{r_b}\rho_l u_l^2(k-1)^2 \qquad (4.57)$$

where Cd is the drag coefficient and k the slip ratio and hence,

$$T\,ds\,\rho = F_{drag} \qquad (4.58)$$

For bubbly flows he suggests that Cd is equal to 1 and for bubbles of 1mm in diameter and void fraction of 0.3 the constant part of the above expression is 225 and for the case of freon 12 where ρ_l is about 1300 Kg/m^3 the interfacial stress is 73 bar (in pressure units) for a liquid velocity of 5 m/sec and a slip ratio of 2.

According to B.T.Arnberg et.al.(1974) the actual mass flow rate during a nonisentropic process is defined as

$$\dot{G}_{act} = C_{d_{nis}}\dot{G}_{th} \qquad (4.59)$$

from equations (4.52),(4.56) and (4.59)

$$C_{d_{nis}} = \left[\frac{dh\,\rho}{dh\,\rho - F_{drag}1E-5}\right]^{-1/2} \qquad (4.60)$$

where $C_{d_{nis}}$ is the nonisentropic discharge coefficient.From the above simple numerical example it was shown how much the slip can affect the mass flow rate and in turn the discharge coefficient. If one assumes,however an isentropic slip model for the mass flow rate with incompressible liquid phase and a constant slip ratio for high quality ,it can be shown

using the R.E. Henry model (1968) that the slip affects C_d very little, because of the mechanical disequilibrium ($C_d = 0.93$ for quality equal to 0.9 where $C_d = 0.53$ for quality of 0.3 and for the both cases $k = 3$). In the case of choked flow,

$$\dot{G}_{th} = \rho c_{th} \tag{4.61}$$

and

$$\dot{G}_{act} = \rho c_{act}$$

where c_{th} and c_{act} is the theoretical and experimental mixture speed of sound and assuming that both the actual and theoretical densities are equal.If now it is assumed that there is a total C_d that includes the mechanical and thermal disequilibrium effects,then this can be given as,

$$C_d = \frac{c_{act}}{c_{th}} \tag{4.62}$$

The latest equation was reported also by Winters (1978),claiming that his C_d covers any nonisentropic effects and also two dimensional effects at the exit. With respect to equation (4.62) the exit boundary condition when the flow is choked can be written as

$$u_{exit} = C_d\, c_{th} \tag{4.63}$$

The effect of the equal theoretical-experimental density values assumption, is thought to be included in the value of the C_d. A value of a multiphase flow discharge coefficient, C_d, is

difficult to be evaluated, but as was shown from the numerical example based on equation (4.60), the interfacial drag force can be very important resulting in values as low as 0.1.

4.2.6 NUCLEATION MODE OF PHASE TRANSITION MODELLING

With respect to the present thermal non-equilibriun model,it is obvious that no provision has been made for the formation of the critical bubbles in the onset of the event.In the literature it is normally assumed that a given constant number of bubbles exists from the beginning of the phenomenon and that they grow through heat transfer interfacial interactions (e.g.see the work published by Winters (1978) and Edwards and O'Brien (1970)).In the present model a first approach to solve this problem was performed,by introducing a non-constant population of constant size bubbles,where their number density changes through the void fraction equation.As will be seen from the theoretical comparisons with experimental data,this is not enough.The pressure minimum is very much underpredicted and so is the rate of the pressure recovery. From the above,it is apparent for the need of a nucleation model to predict the initial phase transition during the fast pressure undershoot into the metastable region.

In the published work by A.R.Edwards (1968) an empirical exponentiation law formulation was assumed to predict the number of bubbles per unit mass of the fluid nucleated at the inlet to the pipe,depending on the local conditions. The delay time to the onset of nucleation was also used in the model. This was based on the theory suggested by Kantrowitz (1951).He argued that in very rapid expansions the energy barrier is not the key element for nucleation but the time it takes for the first molecules to diffuse into the critical nuclei.The delay time proposed by Kantrowitz is of the order of 100 microseconds while Hodgson (1984) suggested several microseconds or less.D.L. Hunt (1970),also used a power law equation for the number density and then used a bubble growth theory to predict the vapor phase change of the predicted critical bubble population depending on the liquid's

superheat.Malnes (1975) followed a different approach.He assumed that the chief role in depressurisation events is played by the dissolved gases initially in the system.He did not use a classical nucleation model, but he assumed a constant number of foreign gas bubbles.The quantity of gas,assumed to be dissolved initially in the liquid,had to be quite large,in order for the experimental data to be favourably compared with the theory.In none of the above cases is the number density of the bubbles conserved.The initial calculated bubble population number is just used for further vapor production,through interfacial heat and mass transfer.Only recently J.R.Rizinic and M. Ishii (1989) made use of the bubble number density conservation equation reported by G.Kocamustafaogullari and M.Ishii (1983).Their main aim was to predict the axial change of the void fraction for a steady state flow.The bubble number density conservation equation was used together with an empirical active wall nucleation site relation.

As evidenced from the literature no nucleation model has been used before in two fluid models to account for the sudden flashing of the superheat liquid during transient pressure releases of high enthalpy liquids from pressurised vessels and pipes.

The remaining part of this section is devoted to the development of the nucleation model which supports the EVUT5 computer program.Comparison with experimental data and discussion are included in a later section.

Starting with the postulate of Ishii et.al. (1982) and employing the transport theorem it follows that,

$$\frac{dn_b}{dt} = \int_v \frac{\partial N_b}{\partial t} dV + \int_s N_b \vec{u} ds \ , \qquad (4.64)$$

where V is the control volume,n_b is the total number of bubbles,N_b is the number density and $\vec{u}$ the flow field velocity.It is therefore follows that for an infinitesimal control volume,

$$\frac{\partial N_b}{\partial t} + \text{div} N_b \vec{u} = \text{Total change of } n_b \tag{4.65}$$

The change in N_b arises from homogeneous nucleation in the bulk of the liquid (N_{hom}),heterogeneous nucleation on the foreign surfaces (N_{het}) and the rate at which bubbles coalesce (N_{coal}).In the general conservation equation of the bubble population another term also enters the relation,associated with the disintegration of the larger bubbles.For the purpose of the present study,it is thought that this term is negligible for the sizes likely to be encountered in the initial phase of an expansion.The number density for one dimensional flow is given by

$$\frac{\partial N_b}{\partial t} + u\frac{\partial N_b}{\partial x} + N_b\frac{\partial u}{\partial x} = N_{hom} + N_{het} + N_{coal} \tag{4.66}$$

The next step is for equation (4.66) to be transformed in a form compatible with the rest of the characteristic equations (4.30).

Utilising equation (4.24) for the vapor phase results in,

$$\alpha\frac{d\rho_g}{dt} + \rho_g\frac{d\alpha}{dt} + \rho_g\alpha\frac{\partial u}{\partial x} = \dot{m}_{ik} \tag{4.67}$$

The vapor state equation in differential form is given as,

$$\frac{d\rho_g}{dt} = \left[\frac{\partial \rho_g}{\partial p}\right]_{h_g} \frac{dp}{dt} + \left[\frac{\partial \rho_g}{\partial h_g}\right]_p \frac{dh_g}{dt} \tag{4.68}$$

Equations (4.66),(4.67),(4.68) and the vapor energy equation (4.30) result in the following form of the bubble number density conservation equation:

$$\frac{dN_b}{dt} - \frac{N_b}{\rho_g c_g^{\,2}} \frac{dp}{dt} - \frac{N_b}{\alpha} \frac{d\alpha}{dt} = N_{hom} + N_{het} - N_{coal} - \frac{N_b}{\alpha \rho_g} \dot{m}_{lg}$$

$$+ \frac{N_b}{\alpha \rho_g^{\,2}} BCE \left[\frac{\partial \rho_g}{\partial h_g}\right]_p \tag{4.69}$$

where BCE is the energy transferred to the vapor during flashing.The above equation requires that the nucleation rate be given. Making use of the homogeneous rate of nucleation equation,the force balance equation on the interface of the critical cluster and the Clausius-Clapeyron equation,it can be shown (H.E.A. van den Akker (1986)),that the degree of superheat,for one critical cluster to nucleate homogeneously is 100 K. Such a value is in good agreement with experimental data (see Skripov (1975)). In most experimental studies of rapid depressurisations the temperature difference is less than the homogeneous limit.This indicates that bubble generation does not occur in the bulk of the liquid but mainly on the wall of the container or impurities in the liquid.Therefore N_{hom} can be considered zero.At the beginning of the depressurisation N_{coal} might also be considered small. The rate of nucleation is evaluated from the expression suggested by Blander and Katz (1975) and referred in the nucleation chapter earlier on. The present model assumes that all bubbles nucleate on the wall but averaged over the bulk of the liquid.No drift model is used to account for the relative motion of the bubble from the wall to the bulk. From the void fraction point of

view,given the N_b ,the averaged size of the bubble is calculated,for the given cross section. Blander's expression involves a quantity called the heterogeneous factor.This is defined as the percentage of the bubble segment,which is being nucleated on the wall, compared to the total size.In the present model the value of "ϕ" is an averaged one,corresponding to the whole event.The present model can be used,to determine the value of "ϕ" for a given experiment.By matching the pressure minimum the optimum value of "ϕ" can be also found.Alamgir et. al.(1980) made use of the rate of depressurisation to calculate a value of "ϕ",by integrating the nucleation rate equation for the time duration of the given depressurisation.The present model is thought to be a more accurate way for the above integration since all flow quantities are allowed to change.The superheat of the liquid is calculated by subtracting from the liquid temperature the saturation temperature for the given pressure.It is also assumed that the vapor in the critical cluster is in saturation condition,which is not far from the reality.

For the nucleation model the interfacial heat transfer is given as,

$$\dot{q}_i = 3.9 N_b^{2/3} \alpha^{1/3} Nu\, k\, (T_l - T_g) \tag{4.70}$$

where the usual assumptions for constant bubble size or number density have been removed.The interfacial mass transfer term encountered in the flow equations, now includes the nucleation transfer term which is given as,

$$\dot{m}_{nu} = N_{het} \frac{4\pi}{3} r_{cr}^{\ 3} \rho_{g_{sat}} \phi \tag{4.71}$$

and BCE is given as,

$$BCE = N_{het} \frac{4\pi}{3} r_{cr}^{2} \sigma\phi \qquad (4.72)$$

The only free parameter linked to the present nucleation model is "ϕ".This model can be used in two ways.First,to predict the "ϕ" during the first explosive nucleation near the minimum pressure,by adjusting "ϕ" to match the minimum pressure to fit the experiments and second to predict an averaged "ϕ" for the total pressure history.In reality,however "ϕ" is not the only parameter that affects heterogeneous nucleation.Kenning et.al (1970) showed that the phenomenon of nucleation is not necessarily reproduced when tests with the same surface and initial conditions are carried out.It has been suggested that the rewetting rate of a surface affects the number of available nucleation sites (Y.Lee,W.Q.Shen (1987)).

4.2.7 PARTIAL FULL VESSEL WITH EXTENSION PIPEWORK MODEL

In this section a transient two phase blowdown from a partially full vessel with liquid,model will be presented.The additional effect, of a vent pipe of the same cross section area as the vessel, has been also included in the model.

Most of the theoretical and experimental work concerning the transient pressure releases from pipes or vessels,has been performed assuming that the liquid,initially in equilibrium,occupies 100% of the storage space.There is, however work performed in the Health & Safety Executive (personal communication) where a partial full case was assumed.A further analysis on their result will be presented later on.In reality storage tanks with e.g.LNG,LPG,refrigerants e.t.c. are almost always partially full.This makes the 100% fullness assumption of the models somewhat inaccurate, since the effect of the interface and the vapor layer initially in the vessel is not included in the transient behaviour of the flow quantities.

The vapor layer in equilibrium (initially) with the liquid smooths down the rapid pressure changes the system is subjected to.So the pressure changes are milder even at the neighbourhood of the interface,which separates the liquid from the vapor,where the reflection of the pressure waves on it,makes the pressure effect more severe.

The most important part of the present model is the modelling of the interface. As noted from the filming of the blowdown,during the present experimental work (see experimental chapter),bubbles were produced on the wall of the vessel and then as they move towards the free interface,they slip through it.At the same time,the vapor generation in the bulk of the liquid pushes the interface outwards.The flow on the other side of the interface is a vapor-droplet mixture flow.There is a point when the void fraction is quite large and the interface disappears and the flow pattern on both sides of the interface looks the same.

The present model incorporates a subroutine,which simulates the escape of the vapor from the interface (see fig.23).It does not distinguish between the evaporation escaping mode and bubble slip.The interface acts effectively as a porous piston pushing its way out of the "cylinder" i.e. pipe.The front of the piston produces a source term which is the escaping vapor and its velocity is simplified to the following form:

$$u_{vapor} = \frac{u_{interface}}{VE} \qquad (4.73)$$

where VE is a slip ratio parameter,which is assumed to be constant throughout the event.Different forms of bubble slip model have been tried e.g.the sum of the interfacial velocity plus a constant escaping velocity or a constant escape vapor velocity,which resulted to a break down of the program. However,the very simple assumption presented by equation (4.73),proved to work quite well.

In the most generalised case,the model can predict a blowdown from a partially full vessel with a vent pipe attached to it.In this case it is assumed that there are two separate interfaces.One between the liquid or the two phase mixture and the vapor and the

second,between the vapor and the air.For the models simplification,it is assumed that the vapor and the air are in a quite pure gaseous state i.e. no droplets are assumed to co-flow in either gases.It is also assumed that no vapor diffuses through the vapor-air interface.An inclusion of a typical diffusion equation would not allow for the method of characteristics to be used,since a higher order differential terms had to be included.

The EVUT6 computer code supported by the mixture-vapor interfacial model and also including the nucleation model as well,can simulate any partially full blowdowns.This problem is similar to a shock tube problem,when a vent pipe is also included.Inside the vessel there are two wave action domains,namely the two phase and the vapor one (see fig. 23).The complexity of the model lies on the "porous" interface.The basic concept is the same as described in sections 4 and 5.The interface is the material path where waves from both domains partially reflect and transmit through it.An added boundary condition is given by equation (4.73).A complex interpolation subroutine is employed to calculate the flow quantities when on either one or both sides of the interface the waves intercept the line (on (x,t) plane) that links the "next" with the "previous" position of the interface i.e. the material path.Outside the vessel i.e. on the other side of the membrane,the air is accelerated,the pressure increases and a mild shock wave is formed. Both gases are assumed perfect.A special subroutine is employed when the interface approaches the exit.At that point the right extrapolated wave,to the previous time step (see fig.86) is extended beyond the exit. The above subroutine iterates between the "known" and "unknown" flow quantities ,in order to calculate the wave action,until the "known" solution converges.

4.2.8 THREE PHASE MODELLING OF A TWO PHASE FLOW

A first approach to model the interface between the liquid and the vapor, has been attempted with little success.The EVUT3 computer program was written,assuming the bubble interface to be the third phase.All three equations of motion,namely mass momentum

and energy conservation,were employed to calculate the flow quantities of the interface. No runs of this model are included in the present work.The conservation equations look the same as the ones for the vapor phase,but instead of the void fraction,α,$\alpha'$is used.For this model it follows that,

$$1 = \alpha + \alpha' + (1 - \alpha - \alpha') \tag{4.74}$$

where α, α' and $(1-\alpha-\alpha')$ is the vapor,the interface and the liquid void fraction,respectively.Also α' can be given as

$$\alpha' = 3\alpha \frac{\delta}{r_b} \tag{4.75}$$

where δ is the thickness of the interface.

Experiments,however,with pure liquids in equilibrium with their own vapor have shown that some of the interfacial heat transfer goes towards the build up of the interface and any interfacial area change is accompanied by a heat absorption. It is thought that the surface tension term in both the energy and momentum equations is important and therefore exclusion of it produces inaccurate results.

4.2.9 MAIN GENERAL ASSUMPTIONS OF THE MODELS

The main assumptions used to formulate the above models are:

1) A pure substance is assumed i.e. no foreign gases and particles present.

2) Slip between the phases is assumed zero.

3) Surface tension is neglected.

4) Body forces are neglected.

5) Constant liquid properties (ρ_l,c_l,k_l).

6) Constant specific heat (constant pressure) for both phases.

7) Bubbly mixture,formed of uniformly dispersed,non-interactive,spherical bubbles

8) The temperature of the interface is equal to the vapor one.

4.3 SHOCK TUBE THEORETICAL CONSIDERATION

In section 4.1 a simple central wave action model was used to calculate the pressure reduction at the exit.This section is devoted to the theoretical evaluation of the expansion velocity and pressure at the exit and the effect of the produced shock wave on them.Also a comparison of the theoretical expansion velocities to the experimental ones will be performed.

Theoretically it is assumed that at time equal to zero the diaphragm at the exit is removed and this action produces a series of waves,which have the same origin.The waves that travel in the pressurised region are rarefraction waves while those traveling to other side of the membrane are compression waves (see fig.23).The last ones,increase the pressure and the temperature of the medium as they travel through,resulting in an increase of the speed of sound. This increase results,in turn, in the formation of the shock wave.Depending on the pressure difference between high and low pressure regimes,the strength and the speed of the shock wave changes.In the present section the material velocity at the exit of the high pressure section is of interest,dictated by either the strength of the shock wave,or ,when this is very weak,by the choked flow at the exit point.

Making use of the momentum and mass conservation equations across the shock wave,the material velocity behind the shock wave can be given as,

$$Uc = c_{air}(CPR - 1)\left[\frac{2}{3.36CPR + 0.56}\right]^{1/2} \tag{4.76}$$

where Uc is the material velocity at the end of the expansion,the so called contact surface velocity,c_{air} is the speed of sound in the air,CPR is the ratio of the pressure at the exit to the atmospheric pressure.For the above expression it is assumed that the specific heats ratio is 1.4.

With the assumption of a homogeneous flow,in the driving section first,and second, with a thermal non-equilibrium one,the simple wave action program was run for freon 12 and for a range of pressures from 2 bar to 10 bar,assuming an initial saturation liquid.This program is capable of calculating the flow quantities at the exit plane,where the expansion takes place,and also detect whether the flow is restricted by the shock wave or a critical flow and determine the velocity and pressure at the exit.

Figure 87 illustrates the effect of the initial pressure ,on the pressure ratio between the expansion pressure and the atmospheric one.In the case of the phase thermal non-equilibrium model,it is apparent that the system always expands to atmosphere.In comparison with the homogeneous one, which always has a pressure at the exit higher than the atmospheric one.The explanation for this is that the vapor production is much higher in the homogeneous case,since it is forced by the pressure change. Since the vapor's inertia is greater than the liquid's one,this accelerates the system faster and results in higher velocities and stronger shock waves or critical flows.It is interesting to notice in the above figure that for the homogeneous model there are two regions.In the first the pressure ratio increases slower than the second one.The first corresponds to the shock wave effect while the second one to the choked flow.Up to about 7 bar,the expansion velocity is insufficient to produce a choked flow before the compression waves have the time to build up the effective shock wave.Beyond the 7 bar,the material velocity is getting so much excessive that the choked flow occurs first allowing the effect of the shock wave not to passe down the critical flow plane.

Another interesting comparison is the initial pressure versus the (2+logUc) for both models (see fig.88).The profile of the curves looks the same but the values of the velocity are quite different as mentioned before.On the same plot the experimental velocity measurements,performed in the present work and presented in the experimental chapter,are also included.As one can see from this figure,the measured velocities lay between the two predictions and closer to the homogeneous one.For the phase thermal non-equilibrium model it is assumed that any phase transition mechanism is not possible for the so short time it is involved for the removal of the membrane.On the other hand evaporation is inevitable for the homogeneous model.Based on the experimental results,it is thought that the membrane's blow off is quite slow,compared to the time intervals required for any kind of phase transition i.e.nucleation and evaporation.So the vapor produced during the opening of the exit plane was enough to bust the material front to velocities quite higher than the predicted ones,using a phase thermal non-equilibrium model.

A series of experiments,have been performed in the establishments of the Health & Safety Executive,using twenty litter glass sphere.Their main aim was to model the end part of a bullet-shape storage tank blowdown during a total structural failure.The glass spheres were initially full or partially full with liquid freon 11 and they were hit at the base with a special spring mechanism,in order to explode.Measurements of the pressure, temperature and velocity of the fragments were performed.These experiments were performed to assess the energy carried by the fragments and the shock wave. Analysis of their experimental results,showed no shock wave present.

Typical material velocities at the time of blowing off,for a full sphere is 15m/sec (for $p_{in}=4$ bar).The above thermal non-equilibrium model was run for freon 11 and the experimental conditions.It was possible to predict the central wave action produced from the explosion,since at time equals to zero the 1/r terms in the spherical coordinated flow equations are zero. The model predicted 1) the nonexistence of a shock wave and 2) an initial material velocity of 0.415m/sec. It is believed that for the same reason as before,there is an

increased phase transition,during the creation of the central waves.Since,in this case,the exposed area to the ambient condition is much greater than during a vessel blowdown,the vaporisation phenomenon is even greater.The computation was repeated assuming spheres full of vapor in the experimental conditions for the partially full spheres.For an initial pressure of 5.2 bar,the experimental typical velocity was 144m/sec and the strength of the shock wave 1.8.The theoretical predictions are exactly the same.This means that 1) the fragments had the velocity of the material path,since there were only small light glass pieces and 2) a partially full vessel produces worse results during blowdown, from the inertia point of view.

CHAPTER 5

FREON-12 BLOWDOWN EXPERIMENTS

5.1 INTRODUCTION

The experimental data produced from a series of tests in the present work will be now presented and discussed.The main feature of these tests is the use of a refrigerant,namely freon 12 (dichlorodifluoromethane).The present tests are similar to those performed by Winters (1978) for freon 12 and Edwards and O'Brien (1970) for water.The main differences lies in the size of the vessel used and the differing orientations of the vessel.This provides a contrast to the longer vessels used by Winters. From the scaling point of view it adds to the current literature experimental information with respect to quite short vessel blowdowns,where thermal-nonequilibrium effects are more severe in comparison to the slip effects between the phases.

In addition to pressure and temperature time histories two further observations have been made.

1) Two different types of high speed camera have been used. The first was used to provide information about the type of flow encountered in these tests and the line averaged void fraction history.The second was used to provide information about nucleation on the thermocouple hot junction.

2) A low power laser set up has been also used to provide some information on the rising velocity of the bubble front.

Freon 12 was used as the working fluid,because: 1) The thermodynamic properties of the saturated state of R 12 are well-known e.g. G.F.C Rogers and Y.R Mayhew (1980). 2) The vapor pressure of R 12 is quite low,which allowed the use of thin melinex film,to be used as a diaphragm.

Another advantage of the low working pressure was the simplicity of the experimental set up,since the working temperature was almost equal to the ambient.A simple heating tape was used to increase the temperature up to 36°C. Also problems associated with high pressures e.g. safety,leakages e.t.c. were minimised.Since the working temperature were so similar to the atmospheric one the use of a thermal insulation was not necessary and the initial temperature of the liquid in the vessel was quite uniform (within 0.8°C for the vertical orientation and 0.2°C for the horizontal one).

5.2 DESCRIPTION OF THE EXPERIMENTAL SET UP

Figure 2 illustrates the experimental set up. The experimental system consisted of a 0.2m long vessel with a 0.034m diameter.At the open end of the vessel a melinex membrane was fitted.Prior to each test the vessel was pressurised with R 12 liquid,and allowed to reach a uniform temperature before rupturing the diaphragm.The diaphragm removal was achieved by melting off the melinex film.

Any pressure,temperature and laser outputs were amplified and displayed on a four channel transient recorder with a built in printer,which could provide a hard copy of the display.

The individual parts of the experimental apparatus are described in more detail in the following sections.

5.2.1 PRESSURE VESSEL

Two different vessels were built,one made of perspex and the other of mild steel.There were three experimental sessions performed with the mild steel vessel.In each of them a different roughness of the internal surface of the vessel,was used,to assess the effect of roughness on nucleation and vapor production and in turn on the initial and long term depressurisation. The three different roughness were:1) 3.2, 2) 0.8 and finally 3) 0.2 μm RMS.The above selection of the wall roughness was made on the basis that Winters reported that his blowdown experiments were independent of surface roughness when the RMS roughness height was greater than 4 μm.

The effect of different materials could be assessed from the information provided by both the perspex and the steel tests.

There were three pressure stations along the vessel axis for measuring the transient pressure history and in particular one of them was located at the base (closed end) where the effect of the rarefaction wave reflection could be recorded.

Three temperature stations were used to measure the initial temperature of the system before the initiation of the test.Two extra ports on the vessel's wall were used for the transient temperature measurements, one located close to the bottom pressure transducer and the other opposite to the middle one (see fig.2).

The good "finish" of the perspex vessel made it transparent and hence it was possible for a movie film to be produced for individual experiments.

At the open end a teflon flange was used to keep the diaphragm in position. Four clamps secured the pressurised vessel at the top.

The R 12 supply and exhaust valve were located at the top of the vessel together with a pressure gauge for measuring the initial pressure. The top flange was fitted with a heater-wire for the purpose of rupturing the diaphragm by melting and provision was made to fit varying lengths of extension pipe.

The vessel was screwed on a steel machined plate which could be clamped securerly on vertical or horizontal surfaces depending on the orientation selection.

5.2.2 DIAPHRAGM BURSTING MECHANISM

Based on the plastic nature of the diaphragm a melting mechanism was developed to provide the triggering of the phenomenon device.This way of rupturing the membrane was selected because of simplicity of use. It proved to be quite reliable, inexpensive,safe with little interfere with the flow .This device consisted of a so called "resistance" wire,made of a nickel , coupled to a 30 volt power supply unit and an electric switch. A fine groove was machined on the inner surface of the teflon ,around the vent,where the wire was seated.Because of the burned remnants of the membrane on the wire,after each test, the wire had to be changed regularly.

5.2.3 MEASUREMENT OF THE SYSTEM PRESSURE PRIOR THE BLOWDOWN

The initial static pressure of the liquid or liquid-vapor (in equilibrium) system was measured with a commercial freon 12-22 pressure gage,designed and calibrated to provide a ± 0.14 bar accuracy.Since it was made only for freon measurements,it was not possible to be dead weight tested.However,it was tested during the trial test runs,when the vessel was charged with vapor freon 12, against the calibrated pressure transducers. Both pressure gage and transducers showed a quite good agreement to a 0.2 bar accuracy.

5.2.4 TRANSIENT RECORDER

Transient voltage signals were first amplified and then directed and displayed on a 1604 Gould digital storage oscilloscope.The present transient recorder was preferred because it could provide a powerful combination of signal capture,coupled with extensive data analysis capability.Its main facilities utilised in the present work are: 1) the internal autocalibration of the device,which could be forced prior to any tests, 2) four channel data acquisition simultaneously, 3) 10 K word memories on every channel,which made possible to any of the traces to be stored and compared with others, 4) 20 MHz Bandwidth real time operation,5) horizontal trace expansion up to 200 times, 6) ability to capture events from 50 ns to 2,000 sec, 7) ability to store pre-trigger information,8) cursor facilities provide automatic measurements of the captured trace and finally 9) a built in colour plotter for permanent records.

5.2.5 HIGH SPEED CAMERA SYSTEM

Two different high speed cameras have been used to perform two different purposes.First the flow pattern characteristics during the event was filmed and interesting information about the initiation of nucleation was provided.Second, information was gathered about the nucleation from a single site (thermocouple hot junction), the bubble growth on the site, departure diameter and rising velocity.

For the first purpose a Hadland HYSPEED cine camera was used.The speed limit of this camera is 10,000 frames per second,where for the present experiments the speed of 7,000 frames per second was used.A timer unit, built in the University of Liverpool,controlled the triggering of the vessel and the start of the camera by closing the circuit of the heater-wire.The precision of the timer unit was 5 ms.For the selected speed the wind up time

to the nominal speed for the camera was 0.8 sec,which was the delay between triggering the camera and the initiation of the phenomenon.Two constant light sources of 1 KW were switched on just prior to start of the experiment.

The second was an Hadland Imagon 700 ultra high speed photography with a limit of 1E6 frames per second.The present speed used was 2.5E4 frames per second. This camera system also incorporated of a Hadland 3 channel delay generator triggering device.This instrument was designed to allow precision sequencing of events from 70 ns to 20 sec in 10.ns steps.The triggering signal for the above unit came from a secondary electric circuit.The main component of this circuit was a fine coated copper wire,stretched over the diaphragm.The bursting of the membrane broke the wire,changing the voltage at its ends from 0 V to 12 V.A pair of Hadland flashs were also used. This unit consisted of a CU-1 flash control and two FH-1 flash heads. The duration time for the flashes is 2 ms and the stored energy 60J per head. The rise time for the flashes was 50 microseconds,hence the flashes had to start before the camera.The television principal was adopted by the camera and so a sequence of frames appeared on a t.v. screen,which could be photographed using a conventional polaroid camera.

5.2.6 FREON 12 SUPPLY

Freon liquid and vapor,in equilibrium was stored in a commercial 60 Kg cylindrical tank.The tank was fitted with two valves,one for liquid and the other for vapor supply (for the pressure instrumentation calibration).A supply line connected the reservoir with the pressure vessel.A 2 W heating tape was placed at the outside of the reservoir,for the purpose of increasing the pressure just beyond the initial pressure in the vessel.This small pressure increase was enough to drive the liquid in the vessel.So no refrigerant pumps were needed.Furthermore a special filter was inserted into the feed line,to hold any foreign particles and any dissolved moisture.

5.2.7. TRANSIENT PRESSURE MEASUREMENTS

Kistler 7031 quartz crystal pressure transducers were employed for the transient pressure measurements.This was a logical selection since the times involved in the present work were of the order of 100 ms for the long term depressurisation and a few hundreds of microseconds for the metastable region. The quoted natural frequency by the manufacturer is 80 KHz,which makes it appropriate for coping with both the early nucleation region and the long term one.

The only disadvantage of these measurements was the effect of the transient temperature changes on the pressure.For constant temperature measurements the manufacturer quotes a temperature coefficient,in case the field temperature is different than the calibration one.However in the case of transient temperature changes the thermal contraction of the crystal housing can produce erroneous pressure readings.In a personal communication with the manufacturer,they proposed a thin coat of silicone rubber solution to protect the head from any temperature effects.A thickness of less than two millimetres produced a significant improvement of the pressure trace.While the early stages of the depressurisation where very well measured,the long term pressure measurements where very much overpredicted.A comparison of the initial depressurisation ,with and without the silicone layer,showed no effect on the response and the actual measurement,produced by the silicone rubber.

The pressure transducer output was then amplified by a 5007 Kistler charge amplifier.Based on the transducer operating principal the circuit has to have an insulation resistance of 1E13 ohms.Hence all the connections had to be cleaned regularly with pure alcohol.The pressure transducer itself was baked on a regular bases,for several hours at a temperature of 100°C,so that any moisture would evaporate.

All three pressure transducers were dead weight calibrated and their linearity was checked for the whole working pressure range.Furthermore a series of vapor tests were run and comparison between the initial pressure shown on the static pressure gage and the final atmospheric one,indicated a quite good measurement ability of the present pressure measurement system.

5.2.8 TRANSIENT TEMPERATURE MEASUREMENTS

The static temperature measurement was performed with three copper-constantan home-made thermocouples of 0.1 mm in diameter.The hot junction was achieved by twisting first the two wires together and then melting them using an oxegen- acetylene flame.The outputs where recorded by a Comark 1625 electronic thermometer with an accuracy of 0.05°C between -200°C and 400°C and a 0.1°C resolution.

The transient measurements were performed using a copper-constantan home-made thermocouple of 25 μm in diameter.A robust hot junction could be easily produced by simply tight both ends to form a knot.In this fashion the two wires were in contact with each other.These thermocouples proved to have quite fast response times. The reason is that the temperature measurement did not rely on the hot junction blob of sometimes three times the diameter of the wire, produced during soldering or melting the two wires together,but on a very narrow contact surface.The output was directed to a CEC 1-165 DC amplifier and then to the transient recorder.

All thermocouples were calibrated on the ice melting point and the water boiling one with the help of a glass mercury thermometer.

5.2.9 LASER MEASUREMENTS

A low power laser tube,of 5 mW used in conjunction with a photomultiplier and an isotope developments E.H.T unit type 532/D,to provide the laser measurements. No calibration of the unit was needed,since only the time delay for the blockage of the laser beam by the bubble swarm,was measured.The voltage output was displayed on the transient oscilloscope.

5.3 EXPERIMENTAL PROCEDURE

Prior to any test initiation a new membrane was replaced and the heater-wire was checked.The top flange was then securerly closed and the vessel was pressurised up to 2 bar with vapor R 12 and the vessel was checked for any leakages using a butane flame.The exhaust and the feeding valves were then opened,allowing liquid to charge the vessel and at the same time vaporise vigorously so that any air in the vessel was mixed with the vapor R 12 and expelled from the vessel.When the vessel was full of liquid the exhaust valve was closed.After the pressure had reached the appropriate level the feeding valve was closed too.The system was then left to settle to a uniform temperature.The transient recorder was then internally calibrated,the charge amplifiers and the laser system were switched to operate and the blowdown was then initiated.

5.4 PRESENTATION AND DISCUSSION OF EXPERIMENTAL RESULTS

The bulk of the experimental work,performed in the present project,can be divided into five stages with respect to the material the vessel was made of and the roughness of its wall.328

tests were completed.From these 255 were performed with the "perspex" vessel and the rest with the "mild steel" one.For the first 70 of the "perspex" tests the internal wall of the vessel was very smooth but for the rest the internal surface had become scratched.Three different roughness have been tested with the "mild steel" vessel,with RMS roughness of 3.2, 0.8 and 0.2 μm.The aim of the present experimental work is to assess the effect of the 1)different wall material,2)different wall roughness, 3)different liquid level initially in the vessel,4)different length of extension pipework,5)different orientation and 6)different ambient conditions.

In all the above tests the liquid initially in the vessel is saturated with temperature in the range 15-36°C.

5.4.1 GENERAL DESCRIPTION OF THE BLOWDOWN PHENOMENON

Figures 5,6 and 7 show "typical" transient decompression traces at three axial locations during blowdown test No.123.Much of the thermal non-equilibrium behaviour of the system,is encountered in all the blowdown tests. This nonequilibrium behaviour is similar to that noted by Edwards,O'Brien (1970),and Winters(1978) in their blowdown experiments.The main features of the above pressure traces in all the pressure stations are,the sharp decrease of pressure to a minimum far below the saturation pressure,the seemmingly explosive pressure recover to a maximum lower than the initial pressure,followed by a much slower pressure reduction to atmospheric pressure.In figure 5 the initial short term depressurisation history is illustrated.As the membrane at the exit is blown off the material accelerates outwards producing a rarefaction wave family which propagates rapidly down the vessel reducing this way the local pressure.The bottom pressure station always records a pressure minimum much lower than the atmospheric.From figure 8 it can be seen that in the area close to bottom there is a complex wave interaction between the waves propagating from the exit and the ones reflected on the bottom. This causes the much lower pressures near the bottom.The effect of the reflected rarefraction waves is also recorded by the middle

pressure station. Because the speed of sound in the liquid is quite high (compared to gases) the wave family occupies a narrow band (see fig.8),resulting in a constant pressure area between the down and up propagating waves.From figure 5, the characteristic double minimum caused by the forementioned double wave action can be seen. However,the theoretical constant pressure part is not pictured in the middle pressure trace and this is because nucleation starts somewhere before the minimum which manages to increase the pressure until the reflected waves arrive and reduce it again to the second minimum.The nucleation phenomenon effect can be seen by comparing the pressure minimum between the middle and top pressure stations.From figure 5,it can be seen that the middle pressure is not expanded to the minimum pressure recorded by the top pressure transducer.Since the top pressure station is close to the exit it is thought that it records the pressure at the exit quite accurately.Almost always its minimum pressure is greater than the atmospheric which means that the flow at the exit is probably choked from the beginning.This was also noted by Winters in his filming tests of the exit.The effect of the reflected rarefraction waves cannot be seen in the top pressure trace.The two phase mixture produced by the nucleation and evaporation phase transition increases the compressibility of the medium which in turn tends to damp out the reflected waves.Because the vessel is quite short (.2m) the rate of depressurisation in all three pressure stations is similar. Temperature measurements showed that the liquid retains its initial temperature during the initial rapid depressurisation where the pressure approaches the atmospheric one.This means that the liquid is metastable and somewhere in the vicinity of the pressure minimum starts nucleating.The nucleation is of the heterogeneous type and this because the liquid superheat is much less (approx.25°C) than the required one for homogeneous nucleation.

Figures 6 and 7 show the rapid increase of the pressure to a maximum due to nucleation and thereafter the continuing phase transition which slows down the pressure reduction to its final value.Since the flow is believed to be choked at the exit,caused by the quite low speed of sound of the two phase mixture,the mass hold up in the vessel helps further to slow down

the depressurisation.An effect which may increase the mass hold up is also the slip between the two phases and their complex interactions.

An interesting phenomenon was observed in some of the blowdown tests.As it is illustrated in figure 8,in some of the tests the depressurisation slope was not smooth and the double pressure minimum in the middle pressure trace was missing.The latest characteristic was caused by the poor diaphragm opening. Instead of melting instantly sometimes it was torn off depending on the contact of the melting wire with the membrane. A slow opening of the exit resulted in a broadening of the wave family.So a complex wave interaction area takes the place of the constant pressure one recorded by the middle pressure station (see fig.8).

5.4.2 REPRODUCIBILITY

The reproducibility of the R-12 experiments performed in the present study is demonstrated in figures 9 and 10.Multiplots have been produced by superimposing the pressure history trace of two different tests.The tests ,in question, have been performed with almost identical initial conditions of pressure and temperature.Furthermore these tests have been performed by using the same vessel (made of either perspex or mild steel).Three pairs of experiments have been used to show the degree of reproducibility.In figure 10 three different plots one for each of the pressure stations in the vessel show a quite good reproduction of the long term pressure histories.As can be seen from the plots,the maximum pressure recovery is well duplicated in all three stations and in both materials.In figure 9 the short term pressure histories of the same experiments have been plotted to illustrate the reproducibility of the initial depressurisation region.The result is a very poor reproduction of the pressure history and the further from the bottom,the poorer it becomes.The level of the pressure undershoot,the steepness of the depressurisation,the explosive character of the pressure recovery and the pressure maximum tended to vary from test to test.The reason is the non-reproduced bursting of the membrane.The melting mechanism for rupturing the

diaphragm produces unpredictable openings. When the heat of the melting wire is not uniform or when there is a bad contact between the wire and the membrane,the membrane tears instead of blowing off instantly,with result the rarefraction wave family to be widely spread and so the steepness of the decompression to be smoothed down.Depending on the opening time the reproducibility was sometimes a lot worse than the one observed in figure 9.One thing is,however,evidenced from both figures,the low degree of reproduction of the initial metastable region does not affect the long term pressure history.However,the pressure trace recorded near the vessel exit is always affected by the poor opening of the diaphragm and this is because of the remainders of the diaphragm which affect the mass flow rate from the exit and hence the recorded pressure.

5.4.3 ROUGHNESS-MATERIAL EFFECT

During fast pressure releases the key feature is the flashing of the liquid system after the pressure minimum has been reached.For heterogeneous nucleation the surface is the most important factor because all the existing cavities and irregularities on the surface increase nucleation by decreasing the required critical work for nucleation.

In the present section the role of different materials and roughness of the surface is investigated.The role of the heterogeneous nucleation has long been recognised e.g. Winters and Merte (1978) conducted experiments with two different roughness (4 and 12 E-6 m) and they reported no effect on the pressure traces.Their explanation was that there was already enough nucleation on the wall,so an increase of the surface roughness would not make any difference.In the present work mild steel vessels with roughnesses of 3.2,0.8 and 0.2 μm were used. Figure 11 shows different tests with almost the same initial conditions,to indicate how the change in roughness affects the long term pressure trace.In the top plot,it is well demonstrated that a reduction in roughness from 3.2 to 0.8E-6 m (test No 199 and 215) increased the pressure plateau,which most probably is a result of an increase of the

nucleation process.The middle plot shows the effect of the roughness reduction from 0.8 to 0.2E-6 m (test No 215 and 221 respectively).The fact is that no great difference can be observed and the slight discrepancy can be easily attributed to reproducibility.The bottom plot,however, illustrates a quite different pressure history, when roughness decreases from 3.2 to 0.2 μm (test No 199 and 221 respectively).A conclusion from the above results, is that quite rough surfaces result in large cavities and generally speaking,irregularities.But the bigger the cavity,the harder is for a bubble to nucleate in it.This is because,the critical work required for nucleation is proportional to the volume of the bubble.The geometrical factor attached to the heterogeneous mode of nucleation is ϕ,which is a function of the contact angle between the wall and the bubble surface.ϕ,however,increases as the contact angle decreases,increasing the required critical work.For critical clusters trying to nucleate in large pits the contact angle gets quite large and that is why nucleation may decrease with the increase of roughness beyond an upper limit.

Furthermore the material of the wall affects the nucleation because some materials provide more irregular surfaces than other.In the present study a profilometry of the inner surface of the vessel wall has been carried out (figure 12),for both materials (perspex and mild steel) and for the different roughness as well.In the above figure the difference in material is very well illustrated,where one can notice the smooth profile of the perspex ,free of any irregularities,where the mild steel one is more like a "zic-zac" type of profile.As roughness decreases it should result in higher probability for nucleation.Figure 13 enhances the conclusion drawn from the profilometry,that the two materials provide different number of nucleation sites and hence different degree of nucleation.Superimposing test No 8(perspex) and 216(mild steel),with almost identical initial conditions,it can be seen that in the mild steel case,the nucleation is more vigorous,than for the perspex which rise to a greater maximum pressure and longer plateau.Since the vapor production is so much greater it is to be expected that the event time for the mild steel tests to be much shorter (see figure 13).

Finally,the experimental work performed with the perspex vessel can be divided into two groups,performed in two different time periods.It is a well known fact that the perspex is one of the easiest materials to loose its smooth profile of its surface with the time.As it was proved by the statistical analysis and figure 14,the added scratches on the inner wall have affected nucleation.In the above figure the slight increase of the pressure plateau and the much shorter event time of the experiment,show an increased nucleation for the test with the less smooth vessel wall (test No 129),than the one with perfectly smooth surface (test No 8).

Concluding,the present experimental work showed that the different material of the vessel affects heterogeneous nucleation,by changing the wall surface features and furthermore roughness also affects nucleation by altering the sizes and the number of pits on the surface in question.However,according also to Winters and Merte (1978) findings,there must be an upper roughness limit beyond which nucleation is not affected.From the present study,also,it is evidenced that there is a lower limit as well.Hence as the roughness tends to reach the limits of a smooth surface the number of the nucleation sites is reduced which decreases the vapor production.The main effect of the roughness is longer pressure plateaus and shorter event times.

5.4.4 THE EFFECT OF ORIENTATION

Figures 15 and 16 demonstrate the effect of varying the orientations of the vessel with respect to the axis of the vessel.In the present study the bulk of the experimental data have been obtained with the vessel positioned vertically,with the open end facing upwards.However,a number of tests have been preformed with the vessel horizontal,so the change of the orientation effect to be assessed.

In theory,in the case of vertical orientation gravity opposes the pressure difference,between the pressure in the vessel and the atmospheric one,which pumps material out of the vessel.In the case of horizontal orientation,however, gravity i) tends to separate liquid from vapor and

ii) helps the material to freely flow out of the vessel.Winters and Merte (1979) reported that they observed bubbly flow during their experiments.The latest comment is typical of an agitated flow due to vast vapor production on the wall.Probably the size of their vessel was not long enough for a stratified flow to be established.

Figure 15 and 16 illustrate the comparison between "vertical" and "horizontal" tests,for the initial and long term decompression. In these plots the pressure traces recorded by the middle pressure station (test No 228 "vertical" and 233 "horizontal") and the bottom one (test No.51 "vertical" and 14 "horizontal") show a slighter faster expansion of the mixture in the "horizontal" test than in the "vertical" one.This can be attributed to the positive contribution of gravity.From the bottom pressure trace for the "horizontal" test,a much flatter pressure plateau that ends on a hump is recorded,which results to a longer total time.An explanation for this can be found in the figure 15 (top plot) which illustrates the short term depressurisation corresponding to the same experiments.While the top plot (fig. 16) shows a quite good similarity of the pressure traces,the one of figure 15 shows a great difference. This is attributed to the poor opening of the diaphragm.Figures 17 and 18 show a typical pressure history during blowdown from a horizontal vessel,at both pressure stations (close end and middle),for a group of tests with a bad opening. From the rapid depressurisation plots a two step depressurisation resulted from the tearing of the diaphragm instead of blowing off.The typical long term pressure history always has a flatter pressure plateau which ends on to a hump.It is believed that remaindering parts of the membrane produce a mass hold up,which in turn affects the flow and the pressure.These latest features do not accompany tests with fairly good opening.

In all vertical experiments there was almost always a vapor pocket adjacent to the membrane.It is believed that the higher vapor inertia resulted in faster openings,unlike the horizontal set up,where liquid was attached to the exit.

Concluding,the opening of the exit of the horizontal set up,is not as good as the vertical one,and this produces additional features to the pressure history. Depending on the degree

of the success of the bursting of the diaphragm,the above features are more or less intense and the pressure history closer or much different from the tests performed with a vertical vessel and identical initial conditions.

5.4.5 LIQUID FREON 12 SPEED OF SOUND MEASUREMENTS

The speed of sound in the liquid freon 12 is a property not well documented in the open literature.For an isentropic process it is given as:

$$c_l = \left[\frac{\partial p}{\partial \rho} \right]_s^{1/2}$$

For the use of the above expression,thermodynamic data in the compressed liquid region are needed.Unfortunately there is not such data,but R.W. Haywood (1969) reported a form of the equation of state which can be used to provide an expression for any thermodynamic property.

Winters(1978) reported a number of researchers who tried to measure the liquid R-12 speed of sound for a quite large range of temperatures (117-279°K). In the present study,measurements of the speed of sound were performed by measuring the time it takes the rarefraction wave to travel between two pressure stations.A special cursor facility,available on the 1604 Gould transient recorder,has been utilised for the accurate measurement of the time interval involved.However,this type of measurement carries many uncertainties,because of the physical size of the pressure transducer and the difficulty to recognise when the first rarefraction wave passes by.

The above measurements showed that the averaged speed of sound in the temperature range 17 to 36°C,was 493.24 m/sec,for a sample of 71 experimental measurements,with standard deviation of 38 m/sec.The speed of sound was also measured by Winters (1978) and

it was found to be 502 m/sec at 26°C.He also made use of the following expression based on the law of corresponding states,

$$c_l = \left[\frac{f\rho}{MW} \right]^3$$

where ρ is the density,MW is the molecular weight and f is a coefficient which depends on the liquid's molecular structure.From the above expression and for the R-12 he calculated a value of 491 m/sec for the sound speed,which is quite close to the value measured in the present experimental work.

5.4.6 THE EFFECT OF VARYING THE INITIAL TEMPERATURE

The effect of varying the initial temperature of the liquid R-12 system is demonstrated in figure 19.Test No 19 and 58 have the same initial pressure but initial temperature 17.75 and 19.9°C respectively.It is apparent from their pressure history comparison,in both pressure stations (bottom and middle),that even a small temperature increase affects the pressure maximum,the pressure plateau and the total event time.Given the same wall characteristics, nucleation increases with an increase of the temperature,since the molecular kinetic energy increases as well.The bubble growth is also affected by the liquid temperature and there is a tendency for the system to approach the saturation pressure,corresponding to the initial temperature after the pressure minimum.This never happens since the liquid gets colder as the phase change proceeds.From the above it is apparent that the temperature affects the vapor production,which in turn sustains the pressure in the vessel and affects the value of the pressure recovery and the phenomenon duration.

Since the bulk of the experiments had an initial saturation condition ,the comparison between test 19 and 58 is a typical of only the few of the tests with subcooled initial

conditions, illustrating the effect of the temperature variation.Similar temperature effects were also observed by Winters (1978).

5.4.7 LASER MEASUREMENTS FOR BUBBLE RISING VELOCITY CALCULATION

The laser measurements have been performed to provide additional information about,i) the type of nucleation (homogeneous or heterogeneous),ii) the type of the nucleation sites (on the wall or on the impurities in the bulk of the liquid) and iii) the rising velocity of the bubble swarm front.Using the perspex vessel,a thin low power laser beam was shot through the centre of the vessel.The beam was then received and amplified from the other side of the vessel by a photomultiplier and the output was then displayed on the transient recorder. A typical output was a steep change of the light intensity,due to the bubbly two phase obstruction, to almost no received light from the photomultiplier.

Figure 20 shows the pressure vessel,with the first set of plugs 15mm from the close end and the second ones 74 mm.It also shows the locations where the laser beam was directed to the vessel wall during both "double" and "single" laser tests.

All laser experiments are grouped into i) bottom and ii) middle laser tests. Bottom laser tests are the ones performed with the laser beam passing below the second set of plugs.For these tests a delay time was measured between the arrival of the first rarefraction wave at the bottom and the sharp change of the laser output.Middle laser tests are the ones performed with the laser beam over the second set of plugs.For these tests a delay time was measured with respect to the first rarefraction wave arrival at the middle pressure station.

A typical laser output is shown in figure 21.For the single laser beam tests a lot of effort was directed for almost the same initial conditions to be achieved.Since the R-12 reproducibility has been shown to be quite good, it was assumed that an averaged velocity

can be calculated,based on the delay time and the distance of the beam laser from two different experiments.All the experimental data are tabulated in tables 1 and 2.

Depending on the same conditions and the laser beam set up the bottom laser tests are divided into 3 groups.It is apparent from the tabulated results in table 1,that the delay time for all the tests is quite large compared to the pressure history at the bottom.Figure 22 illustrates a typical initial depressurisation history with the delay time for each of the tests of group 3 marked on it.It is obvious that first nucleation occurs at the bottom and the bubble swarm produced propagates upwards and blocks of the laser light at each of the different laser stations.From the above it is clear that there is no nucleation happening in the bulk of the liquid or on the perspex wall.The tests of group 2 have been performed by shooting the laser beam over the first set of plugs.The delay times measured for these tests are much shorter than the ones mentioned before.This can only be explained if nucleation takes place on the first set of plugs.

From table 1 and group 3,it can be seen that the velocity of the bubble swarm increases with the distance from the bottom,starting from zero right at the vessel's base.From table 1 it is also well illustrated that their velocity decreases as they approach the first set of plugs.An explanation for this is the bubble collision that takes place at this vicinity between the up rising bubble population from the base and the one nucleated on the plugs.

Based on the above conclusion the middle single laser tests give an indication of the bubble population front velocity,which comes from the second set of plugs,since the laser beam passes over these plugs.

Making use of the equation for bubble rising velocity in a constant pressure field,proposed by Collier (1972),

$$U_r = 1.18\left[\frac{\sigma g_c(\rho_l - \rho_g)}{\rho_l^2}\right]^{1/4}$$

for the given conditions,U_r should be equal to 0.15 m/sec,which in comparison with the values in table 1,is very small.The great difference between the velocity evaluated from the experiments and the one calculated by the above expression is due to the fact that the flow inside the vessel is a transient one with variable pressure field and also the crowded effect associated with the interaction of bubbles.

Table 2 includes two set of tests,one for the bottom laser tests and one for the middle ones, performed by using a laser splitter.Hence by measuring the time it takes for both of the laser beams to get blocked of and also by knowing the distance between the two laser beams the bubble front rising velocity can be calculated for each test.This way the assumption for reproduced tests with the same initial conditions,can be checked as well as the accuracy calculating an average velocity with the above method. For test No 168,its space range overlaps with 4-10 mm (from bottom,group 3) and the calculated velocities are almost the same.Tests 169 and 170 demonstrate the reproducibility of the calculated rising velocity.From almost the same conditions it can be seen,from table 2,that the rising velocity is almost the same with only 8% difference. The space range of tests 169,170 overlaps with the upper limit of the space range of tests 116,117 and the calculated velocity agreement is quite good.

From the middle laser tests (table2),one can observe an increase of the rising velocity until 129 mm from the base.Then the velocity decreases. This could be due to i) the choked flow conditions at the exit,which increase the mass hold up by decreasing the velocity or ii) a massive bubble production right ahead of this point in the mild steel part of the vessel located at the top of the perspex.

Concluding,the laser measurements provide information of the bubble production mechanism in the vessel.Since the vessel was made of perspex,no serious nucleation could be held on the wall.Hence,the only nucleation sites where the bottom the first and second set of plugs ant the top mild steel part. Bubbles nucleate on these sites and then they detach to form a rising front, which accelerates upwards until it arrives at the next nucleation site.Then

a complex bubble interaction takes place,which results in a deceleration. Finally from figure 22 it can be noticed,that as the bubbles get away from the bottom plug,the pressure recorded by the bottom pressure transducer,indicates a pressure reduction.

5.4.8 PRESSURE MEASUREMENTS IN THE EXTENSION PIPE

An extra pressure transducer had been fixed in the extension pipework with its measuring surface flush with the internal wall.These pressure measurements were performed to provide more information about the two phase flow behaviour in the extension pipe.In figure 24 a typical pressure history is shown,while in figure 23 the wave action inside the vessel and the extension pipe is demonstrated.A sudden pressure increase can be noticed,following the diaphragm bursting (figure 24),which is caused by the shock wave passing by (fig 23) produced by the acceleration of the material out of the vessel.Since,there was almost always a vapor pocket attached to the membrane,as it is illustrated in figure 23 the rarefraction waves propagate first in the vapor phase and then they partially reflect and transmit through the interface.The reflected waves will then reduce the pressure in the extension pipe below the atmospheric (fig. 24).It is believed that the product of the complicated wave interaction with the vapor-liquid interface and the accelerating contact surface,is a set of compression waves,which will then increase the pressure in the pipe to atmospheric level.The pressure will retain a plateau until the two phase flow arrives,to increase the pressure further.Depending on how close to the exit the liquid-vapor interface is,the pressure plateau can be shorter or longer.

The two phase mixture consists of vapor as the continuous phase and droplets as the dispersed phase,as it is evidenced from the filming of the event. Figure 25 shows the two pressure histories recorded by the pressure transducer 20 mm from the exit,in the vessel and 60 mm from the exit in the extension pipe. In figure 25,it is well illustrated that the two

traces look alike,after the pressure maximum,which suggests that the flow condition in the vessel and in the vent pipe are linked together.

Figure 26 shows the effect of changing the length of the extension pipe, on the pressure 60 mm from the exit.For almost identical initial conditions and lengths of the extension pipe 0.2 and 1 m,the explosive character of the pressure increase due to the nucleation in the vessel,is recorded by the extension pipe pressure transducer and it is identical for both tests.The long depressurisation,however is affected by the different mass hold up due to the increased length of the pipe.The length of the pipe is important from the i) interfacial mass and heat transfer ii) slip between the phases and iii) skin friction on the wall,point of view.The above factors will affect the pressure in the vent pipe in the long run.

A further use of these pressure measurements is the approximate calculation of the material velocity in the extension pipe.The shock wave recorded in the vent pipe is a weak one and its velocity can be given as:

$$c_s = (\gamma R T)^{1/2}$$

assuming an isentropic process with $\gamma = 1.4$ and the gas constant for air is 287 j/kg °K.Knowing the ambient temperature the compression wave speed of sound is readily evaluated.This together with the distance of the pressure transducer from the exit,determines the time of opening.Next the time the material arrives at the pressure station has to be defined.Figures 27 show comparisons between tests with the same initial conditions,the same length of the extension pipe,but different percentage of liquid initially in the vessel. After the initial pressure oscillations due to the wave action,the different level of liquid initially in the vessel affects the time the pressure increases to its maximum value.An explanation for this is that the two phase mixture has to travel different distances,depending on the position of the liquid-vapor interface initially in the vessel.

Figures 27 also illustrates how the pressure maximum and the total area under the pressure trace,recorded in the vent pipe,reduce as the percentage of liquid initially in the vessel reduces.

Tests with the same initial conditions and length of the pipework,but with the pressure transducer moved close to the exit of the vent,proved further that the pressure increase in the pipework is due to the arrival of the two phase mixture.Figure 28 show comparisons of two pressure traces, one close to the diaphragm (test No 188) and the other close to the exit (test No 189),for the initial and the long term depressurisation respectively. The above experiments (188 and 189) have been performed with extension pipe length equal to 0.2 m and in these figures the delay time it takes the two phase front to travel from one pressure station to the other is well illustrated. The same can be seen in figures 29 and 30 with extension pipe lengths equal to 0.5 and 1.0 m.

Furthermore figures 28,29 and 30 show how much the pressure history changes along the pipe for 0.2,0.5 and 1.0 m lengths.As the pressure station moves outwards the increased length of the pipework,make the pressure losses even larger,because of the skin friction and also the deceleration of the fast moving droplets (with respect to the vapor motion) due to gravity. The size of the droplets also gets smaller due to the evaporation and small droplet mixture has small slip between the phases,a fact which decreases the static pressure of the flow as well.

Figure 31 illustrates the effect of different roughness of the vessel's wall,on the flow in the vent pipe.The pressure traces are quite similar and small discrepancies can attributed to the effect of the reproducibility.

Table 3 shows the velocity,with which the material front escapes from the vessel once the membrane has been removed.From the above table one may notice that the initial condition (for the given range of the temperature and pressure) does not affect the value of this velocity.In theory this velocity depends on the initial pressure in the vessel.For the tests 193 and 222,the calculated velocity is 36.7 and 20.73 m/sec respectively.Since the initial

conditions are the same,the great difference in the velocity,can only be explained by the different pressures the system might expand to.In figure 32 the initial depressurisation history,recorded by the top pressure transducer in the vessel ,is compared for both tests (193 and 222).It is apparent from the above figure that the pressure in the test No 193,decreases more rapidly to a lower pressure than the test No 222.Also the size of the vapor pocket initially in the vessel and the type of bursting (instantaneous or slow) are other factors that could affect the material front velocity.

Finally figure 32 illustrates the different minimum pressure the system in the vessel expands to,to account for the velocity discrepancy between test No 209 and 219.An averaged value for the material front velocity deduced from the data of table 3 is 25.67 m/sec with a standard deviation of 5.16 m/sec .

5.4.9 VESSEL EXPANSION EXPERIMENTS TO VACUUM EXTERNAL CONDITIONS

A number of fast pressure release experiments have been performed by making use of a vacuum tank.A special bent pipe had been constructed to fit on top of the pressure vessel,while the other end is firmly connected on to the vacuum tank.Special care had been taken for the two joints,of the connecting pipe to be well sealed with special vacuum flanges.The pressure inside the vacuum tank could go down to about 120 mm Hg,by using a vacuum pump and the tank's seals could hold this pressure for approximately 20 minutes.The experimental procedure was the same as the rest of the vertical tests. First a new membrane is replaced and then the top flange ,which accommodated the bursting mechanism ,is clamped on to the bent pipe. The vessel is then filled up with freon 12 and the liquid is left ,for approximately 30',to reach a more or less uniform temperature.Afterwards the vacuum pump is started and as soon as the vacuum pressure in the tank is just below the

operating one (around 150 mmIIg),the pump is then stopped.The rest of the procedure is identical to the vertical test one and it has been mentioned before.

Figures 33 and 34 illustrate the long term and the initial depressurisation history respectively.Figure 33 shows a comparison of two typical pressure traces with and without the use of the vacuum tank.Pipe blowdowns to atmosphere, and almost the same initial conditions as the ones performed with external vacuum conditions,have been performed in order for the effect of the connecting pipe and the lower external pressure,at the exit, to be assessed.The two tests are coploted on figure 33.Both pressure stations in the vessel,seem similar as far as the pressure profile is concerned.However,the level of the pressure plateau is higher in the "no vacuum" test than in the "vacuum" one and this is probably attributed to the much different external pressures.The effect of the bent pipework is pictured on the very much similar pressure profile,which is common to all tests.Of course the final pressure the system expands to and the total event times are different because of the different conditions at the exit.Figure 35 shows a comparison of the long term expansion trace,recorded at the middle pressure station, between tests with same initial conditions and with or without the bent pipe. The effect is dramatic.The bent extension pipe has an internal diameter of 25.4 mm,where the vessel's exit diameter is 34mm.The combined effect of the exit area restriction and the bent pipe,increases the mass hold up in the vessel and results to greater and flatter pressure plateaus and longer event times.It is a well known fact,even in the single phase case,that any flow restrictions propagate compression waves up stream and increase this way the pressure and decrease the flow velocity.

The most interesting find from the present tests,is pictured in figure 34. In both tests it can be seen that the "no vacuum" test,experiences a less steep depressurisation,but with deeper pressure minimums than the "vacuum" one,in both pressure stations.Furthermore,for the "vacuum"test at the middle pressure station,once the pressure reaches its first minimum,it retains the same pressure until the reflected rarefraction waves propagate back from the bottom to reduce it further.In the case of the"no vacuum"test,after the pressure reaches its

first minimum,it begins to increase again until the reflected rarefraction waves reduce it to a second minimum.It is thought that,this pressure increase is caused by local nucleation which began somewhere in the vicinity of the first minimum.This phenomenon has not been observed in the case of the "vacuum" test.A probable explanation is that,as the membrane bursts, the vacuum tank sucks the material from the vessel so fast,resulting in a choked condition at the exit.The choked pressure the system expands to,is the first pressure minimum recorded by the middle pressure station.For the given initial temperature and nucleation sites on the vessel wall,nucleation process is not possible to begin at this pressure so in fact there is nothing to affect the pressure at this time and this is why the pressure retains a small plateau.Also the steeper depressurisation,in the case of the "vacuum" tests,can be explained in terms of the better opening,since with a very low pressure,applying at the outside of the membrane the bursting was faster and clearer.

5.4.10 THE EFFECT OF PARTIALLY FULL VESSEL

The effect of reducing the mass of the liquid initially in the vessel , on the pressure history trace in the vessel,has been studied.A series of experiments with 75%,50% and 25% of liquid in the vessel have been performed. The use of the perspex vessel made possible the measurement of the liquid level in the vessel prior to each blowdown.

Figures (36),(37),(38) and (39)demonstrate the effect of different levels of liquid and show comparisons between tests with almost the same conditions and 100% and 50% of filling and 75% and 25% of filling respectively.The above pressure traces are typical of all partially full pressure releases. For the tests chosen to demonstrate this effect,(tests No 143 (75% full) and 137 (50% full)),the bottom and the middle pressure stations are covered with liquid while the top one is not and for test No 145 (25% full) only the bottom pressure station is in the liquid phase.In figures 37 and 39 the long term pressure histories are plotted.A general observation from the above plots is that the event times involved,are very much

reduced.From figure 37,which demonstrates the two extreme situations (75% and 25% full),one can observe lower pressure maximums ,less flat and much shorter plateaus.Less liquid in the vessel means less nucleation,as it is clearly stated by Skripov (1974).Furthermore less nucleation means less phase transition phenomena.Since the top pressure station is always in the vapor phase,the pressure maximum is more or less the same but with a delay time introduced in the case of 25% full experiment.This is because the two phase mixture (vapor-droplets),takes longer time to reach the top.By making use of this information and also knowing the distance between the liquid levels in the 75% and 25% full cases (100 mm),an averaged velocity of the two phase front can be estimated to be 16.67 m/sec.

In figures 36 and 38 the wave action and the effect of the liquid-vapor interface movement can be observed.The general observations are: 1) the delay time for depressurisation to begin at all pressure stations, except the top one,increases as the level of the liquid decreases.This is because the liquid is substituted with vapor,which has a much lower speed sound. 2) For the same reason as before,the slope of depressurisation is less steeper as the liquid level decreases. 3) For the top pressure trace,there is a pressure drop followed by a constant pressure part followed by another pressure drop.This is caused by the expansion wave fan,which reduces the pressure to a minimum and then as it partially reflects on the liquid-vapor interface,it reduces the pressure further.This is a quite usual phenomenon encountered in all gas expansion processes.This is not observed in the 75% full case (fig.36),because the expansion fan is spread so much in the vapor phase,that before the whole expansion is completed the first reflected rarefraction waves come back for a further reduction of the pressure. 4) For the pressure station initially in the vapor phase the pressure minimum the system expands to,is much lower than the one observed when the liquid phase covers the pressure transducer.The cause of this phenomenon is the presence of the liquid-vapor interface,which partially reflects back the rarefraction waves ,which result to lower minimums.In figures 36 and 38,for the top pressure trace,the minimum recorded,for test No 142 (full) and the minimum before the constant pressure parts for tests No 137 and

145 (50% and 25% full respectively) ,is not equal to the atmospheric pressure,fact that suggests,that the flow at the exit is choked.It is well known, that $du = dp/(c_g \rho_g)$,where u is the material velocity,p the pressure,c_g and ρ_g the vapor speed of sound and density respectively.For constant dp drop from the initial pressure to the atmospheric one,the vapor temperature decreases and so do the vapor speed of sound and the density.Hence du increases.For the given test the initial temperature is 290.5° K,the speed of sound is 167 m/sec and the density 11 kg/m³. Even with the assumption of constant temperature,during the expansion,u can be calculated to be equal to 233.5 (for dp=4.29 bar) at the end of the expansion fan.This value is far greater than the speed of sound in the vapor,so the flow gets choked somewhere in the middle of the expansion.When the top pressure station is in the vapor phase the choked pressure is approximately 2 bars,while when it is in the liquid one,the choked pressure is almost 1 bar (fig38 top pressure trace),since for the liquid is more difficult to get accelerated to choked conditions. 5) The double pressure minimum that characterises the middle pressure trace, during the full vessel blowdowns,is not present in these tests.Even in the tests where the pressure station is in the liquid phase,the transmitted rarefraction waves,through the liquid-vapor interface,is so much spread,so there is not a clear distinction between the waves transmitted from the interface and the ones reflected from the base of the vessel. 6) For the bottom pressure station, it is evidenced that the pressure minimum increases as the liquid level decreases.The reason for this is,again,the quite low speed of sound in the vapor phase,which slows down the depressurisation and provides longer time intervals for nucleation to become important.The lower pressure maximums observed in figures 36 and 38, for the bottom pressure station,must be the result of the quite high minimum pressure,which in turn result to lower nucleation rates and so the balance of the vapor extraction from the vessel with the vapor production is not enough to produce higher pressure maximums. 7) For the bottom station,the liquid-vapor interface interaction with the rarefraction waves,is more apparent in the 25% full case.This is because,when there is a

lot of liquid in the vessel the fast travelling waves do not allow for any interfacial effect to show.

In figure 38 (bottom) for the 25% full case,it is illustrated the way the rarefraction waves interact with the interface,as the pressure drops ,slightly increases and then drops again,as the waves come back after a partial reflection on the interface.After the pressure minimum the oscillating character of the trace reflects the movement of the interface. Gradually,however,all this wave action gets damped down by nucleation and the more complex interactions with the bubble's interface. 8) In figure 37 test No 145 (bottom) and 143 (middle) and also figure 39 test No 137 (middle),low frequency oscillations can be observed after the pressure has recovered to its maximum.In figures 36 test No 145 (top) and 143 (top) and also in figure 38 test No 137 (top),however,high frequency oscillations are recorded after the pressure minimum.It is not a coincidence that all low frequency oscillations are recorded by pressure stations in the liquid phase,where the higher ones are recorded by vapor stations in the vapor phase.It is believed that the low frequency oscillations are produced by the interfacial movement (oscillation frequency of a few milliseconds),where the higher ones are produced by the wave action and they are quite common in gas expansions.Their frequency is given (Ardron and Duffey (1978)) as:

$$\omega = \frac{c}{4L}$$

where L is the distance the waves travel with speed of sound equal to c.

5.4.11 THE EFFECT OF THE EXTENSION PIPEWORK

The effect of the pipework on the source term i.e. the vessel which experiences the blowdown,is studied in this section.A series of experiments have been performed making use

of both the perspex and mild steel vessels and also using three different lengths of pipe i.e. 0.2,0.5 and 1.0 m. The extension pipe was of the same diameter as the vessel and it was made of perspex as well.A combination of different liquid levels initially in the vessel,with different extension pipe lengths,tests have been performed to study both effects as well.

A considerable amount of work has been performed by H.E.A. van den Akker (1986) at a Shell laboratory in Amsterdam,on the discharge of saturated liquid R-12 from a pressure vessel through short and long pipes.He stated that the mass hold up in the vessel,due to the pipe located at the exit,was due to 1) the vena contracta phenomenon,happening at the inlet to the pipe, 2)nucleation of the superheated liquid,which starts at the vena contracta, where the pressure is low and the turbulent pressure and temperature fluctuations are favourable and 3) friction along the pipe's wall.As it was evidenced from his experiment the mass hold up increases rapidly as the pipe length increases to a certain value (for the given conditions and fluid) and then there are only small changes as the pipe length increases further.He called this length, the relaxation length and he defined it,as the required pipe length for the superheated liquid to return to equilibrium.After this, friction is the only affecting factor.

In the present experimental work,a cine camera film showed that the flow in the inlet to the vent pipe is a vapor-droplet mixture.As it was evidenced from the film the liquid interface breaks and great agitation produces lumps of liquid to be carried away by the vapor phase.

To show the effect of the extension pipe on the vessel pressure history,a comparison between tests of the same initial condition and different pipe length have been performed.A preliminary comparison showed that the pressure traces are affected in the same way and the same degree in each of the pressure stations,for all the tests and so it was chosen the middle pressure transducer trace to show the effect of the extension pipework.

Figure 41 shows the initial and long term depressurisation histories.From the initial expansion comparisons,it can be seen that the pressure traces are unaffected by the use of different lengths of pipe.This was thought to be due to the fact that the wave action and nucleation,responsible for the look of the initial depressurisation region,are so fast that the

information of the extension pipe presence comes later.As it was evidenced from the pressure data analysis,from the pressure station in the vent pipe,the flow is initially choked,so again any information travelling upstream of the pipe cannot get through the choked plane .The similarity of the metastable region (fig. 41) proves the above remark.

Figures 40 and 41 illustrate very well the effect of the extension pipe on the long term pressure history.It is quite obvious the effect of the vent pipe on the level and duration of the pressure plateau.The changes in the pressure histories start straight after the pressure maximum,caused by the growing bubbles.In both figures the tests with the extension pipe on,form a quite separate region away from the "no pipe" test.In particular,the difference in pressure plateau between the test with 0.0 and 0.2 m pipework is quite distinguished.A further increase of the length of the vent,however,to 0.5 m or even to 1.0 m,produces very little change.

The cine film of the extension pipe flow,revealed that from the beginning until the end of the event,the whole pipe cross section area,was occupied by a very dense mixture of vapor and droplets.Furthermore,no vena contracta region was observed,which can be explained by the fact,that the pipe had the same diameter as the vessel.From the above,it can be safely deduced that the vena contracta is not one of the reasons for a mass hold up increase,in the present work.

Careful study of all pressure minimums, recorded by the top, pressure station, revealed that the choked pressure, at the exit, is not affected by the presence of the pipework.If this was the case the choked flow conditions would give another reason for changing the mass hold up.Hence the only factor remaining to affect the flow behaviour in the vessel is the friction and the phase transition phenomena due to nucleation and evaporation. It was shown by van den Akker (1986),that the effect of the friction is rather linear.From figure 40,it is obvious that a pipe length increase from 0.0 to 0.2 m produces far greater changes than the increase from 0.2 to 0.5m or 0.5 to 1.0 m.Hence the reason must be the liquid,in the form of droplets, which did not have the time to relieve its superheat in the vessel,and since the

two phase jet is now enveloped by the pipe the effect of any action (nucleation/evaporation) towards thermal equilibrium between liquid and vapor, is directly linked to the flow behaviour in the vessel.

As the length of the pipe increases the residence time for the droplets in the pipe increases and more of the liquid phase gets back to saturation state. As the relaxation length for thermal equilibrium is approached,the effect of the phase transition phenomena becomes weaker and then friction remains the dominating factor.

Furthermore,in figures 42 and 43,the effect of both different liquid levels and different lengths of the vent pipe is demonstrated.It can be seen that the added pipe effect becomes less and less severe as the liquid quantity initial in the vessel reduces.For example in figure 43,in the case of 25% full vessel,the 0.2 m pipe produces almost no change on the pressure trace recorded by the middle pressure station.This can be explained,since less liquid produces less vapor i.e fewer bubbles which are the driving force for the liquid to escape from the liquid interface in the form of droplets. So fewer droplets travelling longer distances (lower liquid level in the vessel),return to equilibrium easier.Hence this proves further that the phase transition phenomena affect mainly the mass hold up,which in turn affects the pressure maximum and the pressure plateau.

Figure 44 illustrates the extension pipe effect in the case of the mild steel vessel.Closer study of the above figure shows that for all three pipe lengths the pressure plateau is the same.In conjunction with figure 40,there is a distinguished difference between the level of pressure plateau for 0.2 and 0.5 m pipe lengths.This last difference between "perspex" and "mild steel" vessel test,can be attributed to the increased nucleation process in the case of the mild steel due to the increase of the number of the nucleation sites.So liquid loses much easier its superheat and the 0.2m length suffices for the return of the liquid drops to equilibrium.

For both vessel tests,from the long term expansion,it may be observed that after the pressure plateau the "0.5 m" pressure trace holds up a bit longer than the "0.2 m" one and

also by the end of the event the "1.0 m" test holds up a bit longer than the "0.5 m" one.This is explained with respect to the void fraction increase (beyond approximately 0.7),when a vapor-droplet mixture is established in the vessel as well and so any phase transition (in the vent pipe) effect becomes unimportant and hence friction (which increases with the pipes length) takes over.Since the orientation of the the vessel was vertical gravity becomes important as well.

Further experimental data,with different vent pipe materials are needed,to further prove the importance of the phase transition,on the mass hold up and the flow behaviour in the vessel.

5.4.12 TEMPERATURE MEASUREMENTS

Transient temperature measurements have been also performed making use of a T type thermocouple (copper-constantan), made of 25 μm, in diameter ,wires.Temperature measurements were performed in both perspex and mild steel vessel experiments.In the case of the perspex tests,transient temperature histories have been recorded both in the middle height of the vessel (opposite the middle pressure station) and near the bottom of the vessel (14 mm from the bottom pressure station).For the bottom temperature measurements, the hot junction of the thermocouple was very close to the vessel wall (2 mm from the plug) and for the middle ones two different lengths of thermocouple were used: 1) 16 mm and 2) 2 mm from the wall.

Figure 45 illustrates typical pressure and temperature transient traces at the same height in the vessel (74 mm from the base) and demonstrates that the temperature history follows quite closely the pressure one.Since it is well known that the pressure transducer response time is quite good,this implies that the response time of the thermocouple is similar.

Figure 46 illustrates two temperature histories from two different tests with almost the same initial conditions.The length of the thermocouple was 2 mm, i.e.the hot junction was

located 2mm from the wall. From the above figure it can be seen that both traces are very smooth but the one corresponding to the bottom pressure station, is shifted to lower temperatures.Since both tests were performed with the perspex vessel, the only nucleation sites were located on the plugs and at the base of the vessel,since this was the most difficult part for the tool to reach,during the vessel construction.Hence more nucleation produces greater relief to the superheat liquid,resulting in lower temperatures.Another reason is that the bottom is the most remote part of the vessel,with respect to the exit,where all transient changes are slower and therefore longer time intervals are available for the metastability of the liquid to be shorted out.This can be shown better by comparing the temperature output with the calculated saturation temperature ,corresponding to the local pressure output.Figures 50 and 51 show comparisons of the above type for the bottom and middle pressure stations respectively (perspex).It is obvious from the above figures that the temperature measurements are closer to the saturation ones for the bottom case than the middle one.These experiments have been performed with the 2 mm thermocouple. The rest of the figures 47 (perspex), 48 (steel), 49 (steel) and 52 (perspex) are comparisons of the same type as above.The thermocouple used for the last experiments was the 16 mm one at the middle temperature station.

The effect of the two different materials is next assessed.Figures 48 and 49 show two "mild steel" tests,where 47 and 52 show two perspex ones. Closer observation of the four set of traces (by measuring the vertical shift of the two traces in the same plot) shows a slight decrease of the difference between the saturation temperature and the measured one,in the case of the mild steel.Also the temperatures measured at the end of the blowdown are lower in the mild steel case than the perspex case.The effect of different material does not seem to have a very severe impact on the temperature measurements near the centre line,which could well mean that the added nucleation action on the wall,affects very little the liquid's superheat in the bulk.On the other hand,however,figures 50 and 51 show very low measured temperatures (short thermocouple) near the wall for both bottom and middle temperature

stations.The same can be noticed in figure 53,where two tests,one with the short and the other with the longer thermocouple,at the middle station are compared.The initial temperatures of the system are slightly different but this does not seem to affect the overall history.At each instant the temperature measured,closer to the wall is lower than the one measured near the centre line and by the completion of the phenomenon the bulk temperature stops at 1.96°C,where the one near the wall goes down to negative values (-14.85°C). An explanation for this observation can be the vast nucleation on the plug,which affects the local temperature more than the passing of bubbles by the hot junction.From figure 53 also,it can be seen that the temperature trace closer to the wall is much smoother than the one in the bulk and also it does not pick up the phase alternation around the hot junction.By the middle of the blowdown,the longer thermocouple records temperature oscillations (fig.53),which must be due to the arrival of the bubble front from the bottom and this is the only point the two temperature traces (with 16 and 2 mm thermocouple) are approaching each other.

In the present experiments,the temperature measurements show higher values than the saturation ones at all instants,even when the vapor was the continuous phase.The higher temperature by the end of the test could be explained with respect to the air entrainment into the vessel.During the bubbly mixture flow, higher temperatures can be expected,since the thermocouple always measures the continuous phase temperature (because of its physical size).No explanation can be offered,however,for the period when vapor is the continuous phase other than the fact that the vapor is superheated as well (if the heat transfer process is faster than the mass transfer one).

Figure 54 illustrates the difference in the flow pattern extracted from the comparison of the temperature measurements in both mild steel and perspex cases.The mild steel temperature trace looks smoother,without picking up the up rising bubble front from lower nucleation sites,unlike the perspex one.This is probably because more uniform nucleation on the wall of the vessel offers a more uniform bubbly mixture in the bulk,so any phase alternation is

not so distinguished.Other than this,the temperature is a bit higher,in the mild steel test than the perspex one,until the middle of the event,when the continues phase is the vapor and so the temperature suddenly drops to lower values compared to the perspex test measurement.Figure 53 in conjunction with figure 54 show a temperature difference between the bulk and the wall and between perspex and mild steel tests,close to the end of the phenomenon when vapor is the continues phase.Also from the films it was obvious that a vapor-droplet mixture was occupying the bulk while liquid was dripping down on the vessel wall.So this could mean that even when vapor occupies the bulk, phase transition phenomenon,takes place on the wall,resulting in lower temperatures.In the case of the mild steel,the phase transition phenomenon is even more vigorous so it results in cooling down the core further.

Finally,figure 55 illustrates a long term temperature history (short thermocouple) at the bottom,prolonged long after the pressure had reached atmospheric value.This last plot shows that the temperature reaches its minimum value (-15.34°C) at atmospheric conditions and then retains a constant value until all the liquid is evaporated.Then the warmer air entrainment increases the temperature again.

Temperature measurements were also performed by Winters (1978).His experimental apparatus involved a bigger vessel.He claimed,that soon after the initial decompression period,the temperature recorded by the thermocouple follows quite closely the saturation one,corresponding to the local pressure. An explanation could be that the size effect on the thermal non equilibrium phenomenon is quite important.

5.4.13 HIGH SPEED CAMERA (IMACON) MEASUREMENTS

A series of tests have been performed making use of a very fast camera (2.5E6 frames/sec). The initial temperature trace behaviour was able to be clarified as well as providing

information about the bubble size,averaged bubble rising velocity and generally more information about the nucleation and growth of a bubble.

Figure 56 includes three sequences of different tests with almost the same initial conditions.A special triggering device allowed a different delay time for the camera to operate so starting from the top photograph, one can see the bubble growing on the thermocouple,reaching the departure diameter and then detaching from the hot junction and flow away.The sequence of frames is alternately up and down,starting from the left bottom corner.

Photograph from test No 5PH,which is not presented here,includes the period of no nucleation on the hot junction and the period when a bubble starts to appear.The bubble is very small and the whole image is very dim for successful reproduction of the photograph.The sequence of frames from test No 5PH together with the temperature trace leave no doubt,as to what causes the initial temperature decrease.It is obvious from the present tests that as soon as a bubble nucleates on the thermocouple,the temperature starts reducing.The temperature continues to decrease as the bubble grows bigger. When the bubble reaches the departure diameter dictated by the local conditions, it starts detaching and moving away,the temperature starts increasing again.A very good example to show the above procedure is test No 14PH.It so happened,for this test,that the camera operation time included the temperature minimum (see fig 57).The arrows on the short time plot indicate the camera time range and together with the photograph,one can see that up to frame 5 the temperature reduces. In this frame,however,a tail (observed in all detached bubbles see photograph 17) starts forming.From the temperature trace,one can see that after 160 microseconds from the camera's triggering,the temperature starts increasing again,which coincides with the bubble departure (frame 5).If for some reason no nucleation occurs in the vicinity,the temperature of the hot junction will not change until the bubble front rising from the bottom,reaches the temperature station (see fig.58).

Furthermore one could show that any temperature changes are not caused by the liquid expansion,but only by the phase transition.The energy equation for the liquid phase,when the void fraction is zero reads:

$$\frac{1}{\rho_l}\frac{dp}{dt} = \frac{dh_l}{dt}$$

For the test 14PH initial conditions dp/dt = 8.33E8 N/m2 sec,which results to $dh_l/dt = 638.8$ kj/sec kg and so $dT_l = 0.34°C$,which is very small compared to the temperature decrease recorded during test 14PH.

Assuming that the pressure recorded by the pressure transducer is also the vapor pressure inside the bubble,then the temperature measured at the time of nucleation and bubble growth is higher than the saturation one,corresponding to the local pressure (see fig.59).In fact the thermocouple measures the temperature of the liquid adjacent to the bubble,since its physical size does not allow it to penetrate the bubble.

As it was evidenced from all the present tests,a typical detached bubble (see photograph test 17PH-fig 56) has almost always a vapor tail,which partially shades the light under the bubble.It is thought that this tail consists of small bubbles nucleated in the wake of the bigger bubble.Calculation of the Reynolds number,for the conditions of the test and the averaged calculated rising velocity,of the bubble,showed a turbulent flow around it (Re = 23000).It is well known that the critical work for nucleation,is equal to the free energy change,which in turn depends on temperature and pressure fluctuations.Hence a turbulent flow favours such fluctuations and so the nucleation under the bubble.

In table 4,the delay time between the points when pressure and temperature start decreasing,is displayed together with the corresponding test number.Even though the initial conditions for all the tests are not much different,one can notice a randomness with respect to these delay times.It has been stated by Skripov (1974) that nucleation is a random event

depending locally on the flow fluctuations.In the present experiment,since the nucleation sites are so much fewer (only on the thermocouple),this randomness shows more.

An early nucleation means that the bubble grows and detaches quicker so the temperature reaches again a high level,before other local phase transition (e.g. on the plugs e.t.c.) cools down the system.From figure 60 and 61, it can be seen the difference in the temperature maximum (after the first minimum) for tests 6PH (delay time 200 microseconds) and 17PH (delay time 600 microseconds) respectively.

From table 4 and 5,it can be seen,that for tests with an early nucleation (test 1PH and 16PH),the detached bubble size is bigger than in tests with almost the same conditions and greater delay times for nucleation (e.g.test 17PH).During an early nucleation the bubble growth is favoured by the rarefraction wave action,which reduces the external pressure,so the bubble can grow bigger.This is opposite to the later nucleation,during which the pressure increases and restricts the bubble growth.Bigger bubbles also mean higher relief of the superheat of the liquid i.e.lower minimum temperatures (see fig.61).

Another measurement involved with the present experiments was the bubble size determination.Making use of the polaroid photographs and a traveling microscope with a grid,it was possible for the bubble size to be measured with some accuracy.Also the bubble displacement from the "hot junction" was measured in the same way as the bubble size.Data from both measurements can be found in tables 5 and 6.By knowing the speed of the camera and making use of the data of table 6,an averaged bubble rising velocity could be calculated.The velocity calculations are tabulated in table 7.The time range also included in the above table,is the time with respect to the point in time the first rarefraction wave arrives at the middle pressure station.The velocities calculated for all the present tests look very much the same.Except test 1PH,in the rest of the tests the detached bubble does not rise freely in the bulk of the liquid and it looks as if its upwards movement is restricted by the transient flow .For the series of tests 15-18PH,the initial conditions were very much the same and the bubble appearance quite delayed,in comparison with test 1PH (see table 4).It is

believed that local nucleation and bubble growth on the plugs,propagates waves into the liquid,affecting its pressure and velocity and this wave action affects the up rising movement of the bubble coming from the hot junction.So there are two reasons why the bubble of test 1PH does not show any deceleration:1) it is too large to follow any local flow fluctuations and 2) the initial wave rarefraction action favours its upwards movement.From table 5,one can see that for tests 15-18PH,the bubble growth event has been captured by the camera in its early time and so bubble oscillation with respect to its size are apparent,unlike test 1PH.

In table 8 a comparison of the bubble rising velocity with the theoretical averaged mixture velocity prediction (making use of the thermal nonequilibrium model with nucleation) is shown.The experimental calculated velocity of table 8 is the averaged value over the time range in table 7.From table 8 it can be seen that i) both theoretical and experimental velocities are of the same order and ii) for the early time (test 15PH) the agreement is closer.As the time progresses and wave action due to phase transition is added to the system the velocity differences increase to 38% (test 16PH).The bubble size also affects the formentioned velocity difference.Comparing tests 16 and 17PH ,test 17PH has smaller bubble size and therefore the experimental velocity agrees more to the zero slip assumption than test 16PH,with larger bubble size.

Since test 14PH includes the bubble departure event,making use of a theoretical model for the bubble growth,in a constant pressure field,the contact angle between the solid surface and the bubble interface can be evaluated.In literature there are two kinds of growth domination, i) the inertia one and ii) the surface tension one.In the case of the surface tension growth domination the bubble keeps a spherical shape,due to surface tension forces.Since in the present experiments the bubbles look very much spherical,the formula for the departure diameter estimation reads:

$$d_D = 0.0208\,\theta\left[\frac{\sigma}{g_c(\rho_l - \rho_g)}\right]^{1/2}$$

From test 14PH it is believed that $d_D = 1.75$ mm,so from the above equation $0 = 94.746°$.Since the 0 for the departure diameter is 95°,0 for the critical size must have been even bigger.

Making use of the rising bubble velocity,in a constant pressure field,formula stated by Tong (1965),

$$U_b = 1.18\left[\frac{\sigma\, g_c(\rho_l - \rho_g)}{\rho_l^2}\right]^{1/4}$$

so $U_b = 0.11$ m/sec,which changes very little, with ρ_g changing between 0.2 and 12 kg/m3.Comparison of this velocity with the experimental one, shows more than ten times underprediction caused by the transient pressure field.

Making use of the bubble growth formula,reported by Winters (1978),for a constant pressure field,yields

$$d(t) = 4\,\frac{k_s}{\sqrt{3}}\,a_l^{1/2}\,Ja\,t^{1/2}$$

where k_s is a geometrical factor and is equal to $\sqrt{3}$,a_l is the thertmal diffusivity and Ja is the Jakob number. Assuming the initial condition of test 14PH,the measured bubble size after 1.12 msec of the depressurisation begining,is 1.5 mm,where the calculated one is 1.22 mm.After 1.28 msec the measured one is 1.75 mm and the calculated one is 1.3 mm and after 1.4 msec the experimental one is 2 mm and the theoretical 1.37 mm.

It is apparent from the above that the bubble growth,in a constant pressure field calculation,is much slower than the one provided by the experimental data.Making use of the same formula and allowing for the vapor quantities to change,with respect to pressure,the bubble growth history has been calculated for the conditions of test 14PH and it is shown in figure 62.From the last plot,it can be seen that the measured bubble sizes (test 14PH) are underestimated up to 10 times.

5.4.14 HIGH SPEED CAMERA RESULTS

A high speed camera has been used to film the whole Blowdown event from a "perspex vessel".The fact that the perspex is transparent allowed a very good monitoring of the phenomenon for quite an extended viewing area.The camera was placed at the side perpendicular to the centre line of the vessel,so the viewing area was covering the whole cross section area.Since the height of the vessel portion that could be filmed was about 3cm,four separate filming have been performed recording the Blodown event at different parts of the vessel.

FILM I.

The filming area of the first film covered 31mm in height close to the bottom of the vessel.The aim of this film was to monitor the type of phase transition i.e.nucleation and bubble growth,the nucleation sites,the flow patterns encountered during the blowdown from a small vertical vessel and the behaviour of the two phase flow close to the base.The viewing window included the bottom pressure station plug and the bottom side ones.For the present film the average speed of the camera was 438E-6 sec/frame.

The general observations from the film are: 1)Frame 1,which corresponds to t=.44E-3sec. coincides with the vicinity of the pressure minimum recorded by the bottom pressure station.From frame 1 nucleation starts on the plugs where the rest of the vessel wall and the bulk of the liquid are totally free of any nucleation event. 2)The bubbles that grow on the plugs expand into the liquid.The bubbly flow coming from the side plugs follows a spherical expansion,so its velocity is not exactly vertical but it has a radial component too. 3)At the point where the bottom rising bubble front meets the lower part of the side one ,its velocity reduces. 4)The bubbles behinds the rising front seems to coalesce and produce strips of

vapor so it looks as if the dark background (bubbly mixture) cracks up. 5)By the time t=51.7E-3sec.,frame 118 the whole viewing portion of the vessel is occupied by a bubbly mixture. 6)From the few first frames the bottom pressure transducer looks to be covered by a vapor layer.

With respect to the pressure trace recorded by the bottom pressure station (fig.63) at time t=.44E-3sec,frame 1,the bottom starts nucleating and the pressure is at the vicinity of the pressure minimum.From that moment and up until t=5.25E-3sec.,frame 12,the bubbles expand freely into the metastable liquid and they move away from the plug.In the meanwhile nucleation on the plug carries on.At frame 12,the two expanding bubble populations,from both the side and the bottom plugs meet.The rest of the frames show a high void fraction mixture close to bottom where anywhere is a bubbly mixture with vapor cracks in between.At time t=61.3E-3sec.,frame 140,bubbles coalesce to produce vapor as the continues phase and this starts from the bottom and slowly propagates upwards. Frame 213,t=93.3E-3sec.,the whole viewing vessel portion is dominated by vapor with fine droplets.Frame 223,t=97.7E-3sec.,close to bottom the droplets becoming denser.From this frame some droplets coalesce to produce bigger ones and some others they just vanishe from frame to frame because of the phase transition.At this region,where the pressure is almost atmospheric,the droplets drop into the vessel.A general observation is that no intermediate phase transition e.g.annulus or slug flow occurred.

Making use of a film analyser the bubble front which rose from the bottom plug was tracked up to the point where the side one got in the way(t=17.2E-3sec). Figure 64 shows a time profile of the propagation of the bubble front.To clarify more the way the bubble front moves outwards,e.g.accelerates or slows down e.t.c. a simple backwards step method has been used to evaluate the rising velocity of the bubble front at each data point.The results of this evaluation are presented in figure 65.In this figure it can be seen the oscillating character of the transient rising velocity affected by the wave action and the local phase transition. Initially the bubble front seems to accelerate (during the first frame) which is the

result of the explosive nucleation on the plug.There is a slow down period in which the bubbly layer grow close to the pressure transducer.At this time the velocity reduces and the pressure reaches its maximum,at t= 2E-3sec. after the blowdown initiation.From figure 65 it is apparent that in the time period between 2 and 3E-3sec. there is an acceleration of the front which partially causes the pressure reduction after the pressure maximum (fig.63). Then as the side bubble populations grow and expand into the liquid they push out compression waves resulting to a further slow down of the bubble front which comes from the bottom.The complex interaction between the growing bubbles is pictured on the velocity history plot (fig 65) after the first 5.25E-3sec. At this time bubbles from the base and the side meet.

A preliminary void fraction measurement was made possible by making use of the film analyser.By knowing the total length of the vessel diameter ,at each frame the dark portion of it was measured and then divided by the total diameter.So a line averaged void fraction of the mixture could be calculated at 2cm from bottom. It is well known that a void fraction measurement is one of the most difficult ones.All known up to date methods have some short of inaccuracy.The method proposed in the present experimental analysis is applicable to cases where a transparent vessel material is used. Since the present experimental results will be compared with theoretical ones later on and since the conservation equations are averaged with respect to volume,for the above comparison to have a meaning, the line averaged measurements have to be translated to a volume averaged ones. It was evidenced from the present film that the vapor portion was growing as two half spheres from the pressure plugs on the wall. Hence the control volume for the volume averaged void fraction was chosen to be equal to $\pi D^3/4$ where D is the vessel's i.d., which results in the following expression between the volume and line averaged void fractions,

$$\alpha_v = \frac{2}{3}\alpha_l^3.$$

A void fraction history plot can be seen in figure 66,where one can see a slow increase of the void fraction initially (6E-3sec),followed by a greater increase ,when the bubble front arrives at the given point.The reason for the quite sharp void fraction increase up to 15E-3sec,which is then followed by a slower one,is because,initially the side spherical bubble fronts expand too fast into the liquid and then they reach a point when the radial propagation slows down and the vertical one becomes the dominant motion.

The inaccuracy involved with this method when dark portion of the cross section area is measured by "the eye" is that small liquid gaps between the bubble cannot be seen and so the above measurements slightly overpredict the real values. Nevertheless,it gives a very good indication on how the void fraction changes. The void fraction history profile from the present experiments agrees quite well with the one measured by A.R.Edwards and T.P.O'Brien (1970), in "water" experiments making use of the "X" ray method.

FILM II

The viewing window for this film includes the middle pressure station plugs. For the present test the liquid interface initially in the vessel is at 10cm from the bottom.The liquid interface is also included in the filmed portion of the vessel.The aim here is to monitor the movement of the interface and how the bubbles escape from it.

The main observation was that the liquid is literally at rest and the bubbles slip through the interface.Since the liquid hardly moves the flow pattern beyond the interface is a vapor-droplets mixture.As the phase transition proceeds the clear liquid phase is followed by a bubbly and then by a droplet mixture.No slug or annulus flow pattern could be seen during the whole depressurisation event.

In more detailed the main observations are: 1) At time t= 1.13E-3 sec.,frame 7,nucleation begins on the pressure transducer. From this point in time a bubbly layer grows on the plug forming a spherical front which expands into the bulk of the liquid.The pressure recovers to its maximum value while this bubbly layer is only a few millimetres thick (approx. 3mm).

At time t= 1.431E-6 sec.,frame 9 the pressure maximum has been reached and this coincides with the fact that the bubble front is removed from the plug leaving a vapor layer attached to it.This affects the pressure by decreasing to a lower value where it retains a pressure plateau,caused by the phase transition phenomenon. 2) At time t= 1.91E-3 sec.,frame 12,evaporation starts from the liquid interface. One can see bubbles nucleating adjacent to the liquid interface.The events of nucleation in the bulk of the liquid take place in a narrow zone 5mm attached to the liquid interface. The only explanation for this bulk nucleation,is that there might be suspended particles in the liquid (e.g.dust) and because of the turbulent character of the agitated interface and the quite low local pressure,caused by the reflection of the rarefraction waves on the interface,the local conditions favoured nucleation.From frame to frame this bubbles grow bigger and at the same time flow towards the interface and they just slip through it.The size of those bubbles is about 1mm and by tracking down individuals the growth velocity was measured to be about 1m/sec.Their traveling velocity was noticed to increase with the time e.g. for frames 13,14 the velocity was about 4m/sec and for frames 21,22 it went up to about 8m/sec. 3) At time t= 12.88E-3 sec.,frame 81,the bubble front from the base plugs arrives at the middle ones.This is the point where,with respect to the pressure trace,fig 67, the pressure oscillations are dumped out and a short pressure plateau can be observed. It is believed that these pressure oscillations are caused by the liquid interfacial movement and any wave action produced by this movement is absorbed by the bubbly mixture.

All the frame numbers mentioned above in conjunction with distinguished events are pictured in figure 67.

FILM III

During this filming the vessel was full of liquid freon 12 and a fifty centimetres long extension pipe was placed at the exit of the vessel.The viewing window for this film includes

the exit of the vessel and a few centimetres from the lower part of the extension pipe.As it was evidenced from the last film the liquid interface hardly moves,so this affected the flow pattern in the extension pipe. In general lines right from the beginning vapor-droplet mixture occupied the whole cross section area of the extension pipework.

In more detail,from frame 1 vapor flows up the pipe and droplets seemed to become denser and expand from the wall to the centre of the pipe.The drops are not uniformly dispersed initially and they occupy the one side of the pipe.This is believed to be caused by the non-uniform bursting of the membrane.From frame 10 ,t= 1.53E-3sec.,the drops are densely and uniformly dispersed in the pipe.By the frame 850,t= 130E-3sec,the droplet mixture gets less dense and by the frame 976, t= 146E-3sec,which is the end of the phenomenon,the droplets are fewer restricted to the wall where the vapor phase seems to occupy the centre of the pipe.

FILM IV

This experiment has been performed with the vessel initially full with liquid freon 12. The viewing window for this film is the middle part of the vessel (middle plugs). For this test a thermocouple is accommodated in the middle plug opposite the pressure transducer.The "hot junction" of the thermocouple is close to the centre line of the vessel (1.6cm from the wall).The aim of this filming is to determine as accurate as possible what temperature exactly the thermocouple measures,the liquid or vapor one. It was suggested by Winters that his temperature measurements were mostly affected by the vapor. It is believed that in the present experiments the thermocouple measures the temperature of the continues phase.

In more detail the observations made from this film are: 1) Nucleation starts on both plugs the same time,which is approximately .45E-3sec, frame 3.This means that the metastable conditions produced by the depressurisation are the same for the given cross section area and so plugs of the same material and which have been machined in the same way provide similar

nucleation sites and so they have to nucleate at the same time. At this time no phase transition action can be seen on the "hot junction".Like in the previous films a spherical bubble expansion can be seen coming from the plugs. At about t=2.85E-3sec.,frame 19,a growing bubble can be seen leaving the temperature sensor.At about t=4E-3sec.,frame 27,there is a lot of local nucleation going on which causes a lower temperature environment and also a string of bubbles can be seen to leave the "hot junction".There size is about 1.5mm.The latest phase transition event can be seen to affect the temperature measured by the thermocouple ,see fig.68.At time t=8.85E-3sec.,frame 59,the sensor is enveloped by small bubbles, but still liquid is the continues phase.At time t=10E-3sec.,frame 66,a two phase mixture arrives at the sensor.From figure 68 it is apparent that at that moment the temperature drops very fast.At frame 72 ,which is at the middle of the temperature drop the vapor phase looks very dense around the sensor.At this point it has to be said that the two phase bubbly mixture mentioned before is not the one from the bottom plugs, but the one expanded from the lower part of the middle plugs.At t=15.3E-3sec,from the beginning of the event,frame 102,liquid again covers the sensor and its temperature increases,tending to reach its initial value.A string of bubbles can be seen rising from the "hot junction" (frame 154) which decreases its temperature slowly (fig.68). At time t=38.4E-3sec,frame 256,the bottom bubble front arrives at the middle position. At this point no great temperature change can be noticed, and this is because this bubbly mixture is the one coming from the side bottom plugs and occupy mostly the wall area.A few milliseconds later the second bubble population (bottom plug) arrives at the middle of the vessel and the effect on the temperature is apparent.From figure (68) it can be seen that at this time the middle pressure transducer experiences a pressure increase (pressure hump). Behind the two phase front which advances outwards,bubbles coalesce and so there is a gradual transition from a bubbly flow to a droplet one.This is more apparent at frame 413(t=61.95E-3sec.) where from figure 68 ,it can be seen that the temperature drops dramatically. From this point any temperature increase

is caused by a dense droplet patch passing by the sensor(e.g.frames 465,615 and 733).No evidence of a annulus or slug flow were given by this film.

5.5 STATISTICAL ANALYSIS OF EXPERIMENTAL DATA I

Making use of the initial phase of the metastable region pressure history a statistical analysis has been carried out in order for the experimental parameters affecting the liquid superheat to be established.Namely the initial metastable region can be described by two quantities:1) the pressure vicinity where nucleation is most likely to set off and 2) the pressure maximum to which pressure recovers.

In the present analysis the "SPSSX" statistical computer package was used to carry out a multiple regression analysis and provide the correlation coefficient "r",which shows how well the experimental data are described by a linear relationship.A probability level is also provided ,which shows the degree of significance of the independent variables contribution and the goodness of fit of the data around the regression line.The constant and the slopes with respect to each of the independent variable for the given regression line are also provided.

In the present analysis the effect of the different material,namely "steel" and "perspex" and different roughness will be assessed.As it has been mentioned in previous chapter,in the case of "perspex" there is the "perspex old" (smooth internal surface) and the "perspex new" (scratched internal surface).In the case of "steel",there is the "ms1" (roughness=3.2 μm rms),the "ms2" (roughness =0.8 μm rms) and the "ms3" (roughness=0.2 μm rms).

The present statistical analysis,like any analysis of this type,is subjected to errors due to: 1) experimental data extraction from the experimental traces, 2) the restricted number of data and 3)the theoretical modelling used by "SPSSX".

5.5.1 THE EFFECT OF NUCLEATION ON THE PRESSURE MINIMUM

It is evidenced from the experimental data that the pressure minimum at the middle pressure station was almost always higher than the exit one (recorded by the top pressure station).So it was thought that somewhere in the vicinity of the first pressure minimum nucleation starts.The production of the vapor at this point it is thought to produce the opposite effect of the depressurisation. Prior to nucleation the wave action in a suddenly depressurised vessel is sufficiently fast for any spatial changes to be small.In addition during this period, little liquid will be expelled and thus any changes in volume of vapor arising from nucleation can be translated into pressure changes given by the liquid compressibility equation:

$$dp = -\left[\frac{E}{V}\right]dV \tag{5.1}$$

where E is the liquid compressibility coefficient and V the volume of the liquid. In terms of pressure and volume changes rate the above equation reads,

$$\frac{dp}{dt} = -\left[\frac{E}{V}\right]\frac{dV}{dt} \tag{5.2}$$

The rate of liquid volume decrease per unit volume can be given as:

$$\frac{1}{V}\frac{dV}{dt} = J\,V_b\,\phi \tag{5.3}$$

where J is the rate of nucleation V_b is the volume of one bubble and ϕ is the heterogeneous factor. J can be given by the following equation:

$$J = \frac{\rho_l\,Na}{MW}\,B\exp\left[\frac{-W_{cr}\,\phi}{T_{in}\,K}\right] \tag{5.4}$$

where ρ_l is the liquid density,Na the Avogadro number,MW the molecular weight, W_{cr} the minimum work required for nucleation ,K the Boltzmann constant and B is the molecular interactions per second which Skripov (1974) suggests can be assumed constant and equal to 1E12 sec-1. Making use of equations (5.2) and (5.3) and also of the measured depressurisation rates from the present tests,"ϕ",can be calculated. If nucleation is assumed to start in the region where dp/dt = 0,the rate of depressurisation just prior to nucleation can be approximated by dp_{sat}/dt , where $dt = t(p_{min})-t(p_s(T_{in}))$. For the present case of freon 12 it is assumed that the liquid density,compressibility coefficient and surface tension are constant in the given temperature range. "ϕ" has been statistically correlated with 1)the liquid superheat dp_{sat}, 2)T_{in} and 3)the depressurisation rate.For the present experimental work "ϕ" showed a very strong dependance on dp_{sat} (see fig.69) and a less strong dependence on T_{in}/T_{cr} (see fig.70). This is not unexpected,because

$$dp_{sat} = \frac{2\sigma}{r_{cr}} \qquad (5.5)$$

where the above equation means that as dp_{sat} changes r_{cr} changes too.For the same nucleation sites ,however,since "ϕ" is a function of the contact angle between the bubble and the wall,any change in the value of r_{cr} means a change of the value of the contact angle and hence a change of the "ϕ".The rest of the experimental parameters were found to have no effect on "ϕ".

The strength of nucleation,in the present study,is called the pressure difference between the pressure minimum and the pressure the system would have expanded to if nucleation had not occurred.This theoretical pressure is assumed to be the pressure minimum recorded at the exit of the vessel.A statistical analysis of the strength of nucleation with respect to the material and the roughness of the vessel wall showed no correlation at all. Since the initial nucleation is not affected by the different material and roughness ,it is believed that the initial metastable behaviour of the liquid recorded by the pressure transducer probably is only affected by the pressure transducer presence.

A similar work has been performed by Alamgir et.al.(1980). Making use of "water" test results,he tried to evaluate a value of "ϕ".Unlike the present study,Alamgir assumed that nucleation starts as soon as the system crosses the binondal line. He reported that in his work "ϕ" was found to be correlated with the initial temperature "T_{in}" and the rate of depressurisation. The rate of depressurisation strongly depends on the opening characteristics which in turn reflect their effect on the value of "p_{min}".Figure 76a illustrates the temperature dependence of "p_{min}" for both water and R 12 experiments.For Alamgir water tests (1980) the dependence is quite strong since the bias of the opening characteristics was not present , since the opening mechanism provided almost the same opening time.For the R 12 tests three different set of experiments are illustrated in the above figure, Winters (1978),Friedel (1986) and the ones from the present work.The depressurisation slopes involved with Winters tests are of the order of 3-10 E4 bars/sec , for the present tests 0.1-2 E4 bars/sec and for the (Friedel (1986)) tests 5-11.5 bars/sec.In the above figure the three different R 12 regions can be seen clearly.But even for the same set of experiments , in the case of Winters and the present work tests, there is a lot of scatter.It is believed that this is caused by inconsistent opening characteristics produced by the diaphragm bursting method (a ball valve was used for the Friedel (1986) tests). "dp_{sat}" is plotted against (Δt_{min}) in figure 76b.From the above two figures it is apparent that the quite strong correlation of "ϕ" with "dp_{sat}" , is because "dp_{sat}" includes both the temperature and the opening characteristics effects.

A multiple regression analysis revealed that for the present freon 12 tests, "ϕ" can be given as follows (with regression coefficient equal to 0.999),

$$\phi = -3.9E-4 + 5.22E-5\,[dp_{sat}]^{2.3} + 9.63E-4\left[\frac{T_{in}}{T_{cr}}\right]^{2}$$

The above relationship is valid for freon 12 and for T_{in} in the range 15.8-36.8°C and dp_{sat} in the range 2.6-5 bar.

5.5.2 THE EVALUATION OF THE HETEROGENEOUS FACTOR FOR THE WATER TESTS

Making use of the water experiments reported by Alamgir et al. (1980) and applying the above method a value of "ϕ" has been determined for each of the test initial conditions.For the "water" test temperature range it is assumed that a linear relationship exists with respect to the temperature for the liquid density and compressibility coefficient.For the surface tension a temperature relation has been employed , proposed by Alamgir and Lienhard (1981). The correlation between "ϕ" and "dp_{sat}" is given in figure 72. Using Alamgir's equation,for the same initial conditions, his "ϕ" can be calculated and compared with the one from the present study (fig.74).From the above figure one can see that the calculated "ϕ" is quite similar.This similarity strengthens the concept of the calculated "ϕ" with the above two different methods,both having as base the nucleation theory.Furthermore the quite good "dp_{sat}" and "T_{in}/T_{cr}" correlation with "ϕ" for both methods (fig.72 and 73),means that the system internal energy and the degree of its superheat are the main parameters affecting the nucleation and "ϕ".

Unlike the freon12 tests,the water tests show a very good agreement between "ϕ" and the initial temperature.The reason must be the quite constant opening characteristics of the exit which leaves "ϕ" to depend only on the temperature. Both temperature and superheat dependence on "ϕ" were expected since both affect the size of the critical bubbles and so the size of the contact angle and in turn the value of "ϕ".

For the water tests, a multiple regression analysis showed that "ϕ" can be calculated by the following expression (with a regression coefficient equal to 0.998),

$$\phi = 0.15\left[\frac{T_{in}}{T_{cr}}\right]^{24} + 2.14E-8\,[dp_{sat}]^{4}$$

for a temperature range 117-260°C and a dp_{sat} range 0-16 bar.

A comparison of the calculated value of "ϕ",between freon 12 and water tests, for the same "dp_{sat}" and "T_{in}/T_{cr}" (see fig.69,70,72 and 73) can show larger values of "ϕ" for the same degree of superheat and initial temperature, for the freon 12 case.This means that the probability for a critical bubble , with bigger size,to survive,is higher for the freon 12 case than it is for the water one.As it is well discussed in Skripov's textbook (1974), nucleation is more probable in liquids richer in molecules e.g.freon 12,since the molecular collisions responsible for the nucleation,now are more numerous.

5.5.3 THE EFFECT OF THE LIQUID SUPERHEAT ON THE MAXIMUM PRESSURE

In the present study "p_{max}". is the maximum pressure regained in the vessel after nucleation starts and it must depend on the number of nuclei and how fast these grow to relieve the liquid's superheat.Quantities extracted from the experimental data,such as T_{in} (initial temperature) ,p_{min1} (first pressure minimum the local pressure expands to), t_{min1} ,e.t.c. and also combination of them have been checked to see whether they affect the p_{max}.

A qualitative statistical analysis has also been carried out with respect to "material" and "roughness". Taking care of the initial condition bias instead of the "p_{max}" the quantity "$(p_{sat}-p_{max})/p_{sat}$" was used as the dependent variable ,where "p_{sat}" is the saturation pressure with respect to "T_{in}".The result of the analysis showed that the "material" affects "p_{max}"(probability level> .9999). As for the "roughness" it was found to be also significant only in the case of the "steel" experiments (probability level >0.9999).The case of the "perspex new" had to be rejected because of its very narrow temperature range.

A multiple regression analysis has been carried out for each of the materials and roughness categories which showed that the only independent variable affecting "p_{max}" is "T_{in}".This was in fact suggested also by Alamgir et al.(1980) and Brown (1959) as a result of their "water" tests.The only difference is that Alamgir temperature relation is not linear where the one

observed from the present experimental work (temperature rang:15.8-35.8°C) is linear.In figure 77 the experimental relationship "p_{max}" vs "T_{in}" is illustrated.

The results of the statistical analysis can be found in table 9.From the above table it can be seen that,for the "steel" tests, roughness decreases the effect of "T_{in}" on "p_{max}",by simply decreasing the slope of the regression line.This could be resulted in the decrease of the wall area as roughness decreases. This implies that less nucleation sites are available and so smaller number of growing bubbles sustain the "p_{max}" pressure.

The same analysis was applied to Winters (1978) results from his experiments. The roughness of his vessel wall is 4 μm rms. The results from the above analysis are also tabulated in table 9.Even if the number of his data was not enough,one can see that the slope of regression line is quite similar to the ones correspond to the present "steel" tests.The quite low correlation coefficient is because most of his experiments reported had the same initial temperature (27°C).

5.6 STATISTICAL ANALYSIS OF EXPERIMENTAL DATA II

5.6.1 FACTORS AFFECTING THE AVERAGE PRESSURE IN THE VESSEL

The pressure history during blowdown is useful,because together with other information (e.g. temperature measurements e.t.c.) it gives a detailed view of the process during pressure releases,i.e. the metastable region,the nucleation region,the bubble growth region and finally the approach to equilibrium region. However in practise,an averaged value of the pressure inside the vessel during the phenomenon would be more appropriate.Assuming that there is a uniform constant pressure throughout the process,this pressure must be an average value of the instant pressure with respect to time.Applying the Bernoulli equation at the exit of the vessel yields:

$$\dot{G}_{av} = C_d\sqrt{2\,\rho_{av}\,(p_{av} - p_{at})}$$

where $\dot{G}_{av}$ is the averaged value of the mass flow rate per unit area,ρ_{av} is the averaged mixture density,p_{at} is the atmospheric pressure and C_d is the discharge coefficient.The thrust also on to the vessel can be given as,

$$F = \dot{m}\,u = A_{exit}\,\frac{\dot{G}_{av}^{\,2}}{\rho_{av}}$$

It is apparent from the above an averaged value for the density could give a rough idea of what the flow rate from the vessel and the thrust are.For example in a complex nuclear reactor cooling system in case of an accident (breaking of an inlet or outlet from the core pipe) the knowledge of the mass flow rate is a vital information,because then the time before the core "burns out" can be calculated.

Using the experimental data from the present study as well as Winters experiments, a correlation has been sought using statistical means between, the averaged pressure in the vessel and the initial conditions as well as geometrical factors of the vessel.The averaged pressure is defined as the ratio of the area under the pressure history trace divided by the total time of the experiment.The independent variables are,$p_{sat}(T_{in})$,material,roughness ,size,filling,length of the extension pipe.In the present study,a series of experiments have been used, namely a) three different lengths of extension pipe (.2,.5,1 m) with the same internal diameter as the vessel,and b) four different levels of liquid (full , 75% , 50% and 25%full) initially in the vessel.The size parameter is provided by Winters experiments.All correlations were quantitative ones except the material and the roughness for the perspex case.The evaluation of the area under the pressure history trace has been performed by the use of a "Graf Bar " mark I sonic digitiser which was used to read and store more than 500 points extracted from each experimental print out.A "cubic Splines" interpolation routine was used

,then,to define the curve passing from these points and a "Simpson's rule" routine was used to evaluate the integral.

Making use of the "SPSSX" statistical computer program a linear regression analysis has been performed for each of the categories involved in the tests. It was found that $p_{sat}(T_{in})$ is very well correlated with "p_{av}",i.e the initial temperature of the system is quite an important factor.A further analysis of 95 experimental data showed a quite good correlation between the standardised value of "p_{av}" and the material the vessel was made of.Since,the initial temperature dependance on "p_{av}" was found to exist the temperature bias was excluded from the correlation between "p_{av}" and "material" by using instead of "p_{av}","$(p_{sat} - p_{av})/p_{sat}$".It is this last quantity that is defined as standardised "p_{av}".This qualitative relationship turned out to be important with probability level greater than 0.9999.Furthermore a roughness correlation has been performed for each of the material categories (perspex and steel).It was found that for the "perspex" case the added scratches on the vessel wall do affect the dependent variable.Unlike,in the "steel" case where the change in the wall roughness did not show to have an important effect on the average pressure. Even if the probability level,for the "roughness" correlation in the "perspex" case,is greater than 0.9999,it is believed that this correlation was strengthened by the fact that there were only two different roughness categories and also because the roughness change was very large,since the first part of the perspex tests was performed with a very smooth wall,with literally no nucleation sites at all. For the "steel" tests,three different vessel sizes were involved in the analysis.It is well known that:

$$\dot{G} = \frac{1}{A_{exit}} \frac{dm}{dt}$$

where m is the mass of the liquid in the vessel.Since all test were performed by using the same working liquid freon 12 (same density),the change of the liquid's volume will be proportional to the instant mass outflow.So the volume of the vessel was selected to represent the "size" variable in the "standardised p_{av}"- "size" correlation.The three different volumes involved in

the analysis are: 0.2E-3 , 1.4E-3 , 2.8E-3 m^3.The above correlation resulted in a correlation coefficient equal to 0.939 with probability level greater than 0.9999,which means that there is a quite good relationship.This relationship is not linear for the present experimental data and it can be given as follows,

$$SURFsts = -2.07\,(size)^3 + 0.742$$

where SURFsts is the "standardised p_{av}" for short. According to the above classification for the "material","roughness" and "size",a "$p_{av} = f(p_s)$" relationship is sought for each of the roughness categories for the perspex tests and each of the size categories for the steel tests.All the results from the present analysis are tabulated in table 10.

Figure 78 shows the "$(p_{sat} - p_{av})/p_{sat}$" dependence on the "size" (for "material="steel").In figure 79 the three different regions of the "size" parameter are illustrated,on the p_{av} (SURFt) versus p_{sat} plot,for all the experiments.

The $p_{av} = f(p_{sat})$ relationship for the perspex and steel (size=0.2E-3) cases is not linear.The general form of the equation is:

$$p_{av} = B_1\, p_{sat}^{\,5} + B_o$$

where B_1 is the slope of the linearized form of the above equation and B_0 the interception on the "p_{av}" axis. For the Winters experiments,however,the relationship is linear.Figure 80 shows the $p_{av} = f(p_{sat})$ relations for the three important categories of table 10.

From table 10 it can be seen the low correlation coefficient for the "new perspex"(scratched surface) tests,which resulted to a non important correlation.The possible reason for this is the very narrow rang of "p_{sat}"(5.2-5.5 bar).

Next,the rest of the geometrical parameters will be correlated with the "standardised p_{av}".Making use of the experiments performed in the present study,the effect of the "filling" (level of liquid initially in the vessel) and the "extnpipe" (the length of the extension pipe attached to the vessel at the exit) will be sought for each of the two materials,since it was

proved from the preliminary statistical analysis that the "material" factor affects "$(p_{sat} - p_{av})/p_{sat}$".

For the case of perspex a multiple regression analysis showed that the "filling" parameter is more influential,with a regression coefficient equal to 0.85,than the "extnpipe" one (regression coefficient equal to 0.125). For the present analysis no roughness distinction is need since all test data have been provided using the "new perspex" vessel.

A bivariate regression analysis was then employed to each of the "extnpipe" value (1 , 0.5 , 0.2 , 0.0 m) seeking a SURFsts= f(filling) and the same analysis was repeated for each of the "filling" values (full=1 , 75 % full=0.75 , 50 % full=0.5 , 25 % full=0.25), seeking a SURFsts=f(extnpipe). The results are tabulated in tables 11 and 12.

For the steel experiments the analysis was much simpler since no "filling" data could be established for the steel vessel.A bivariate regression analysis showed that the "standardised p_{av}" in the steel vessel during blowdown is not affected by the different lengths of the extension pipework.

From table 12,one can see that for the cases of 25% and 50% full vessel there is not any relationship between the averaged pressure and the length of the extension pipe.This means that all experimental data are too much scattered around a constant value of the dependent variable.In the case of the 75 % and 100 % full vessel , however , there is a quite good fit of all experimental data around 0.546 for "full" and 0.616 for "75 % full" since the slope of the relationship is almost zero and the probability for the slope to be zero is almost 1 (>0.9999).

From table 10,11 and 12 the relationships between "p_{av}" and a) "p_{sat}",b) "size", c) "material",d) "filling" and e) "extnpipe" show a high probability level which can only mean that for all important relations there is a quite good fit of the experimental data.Since the experimental points involved in the above analysis compose a sample and samples sometimes behave in a slightly different manner from the whole population,the above analysis could not

be a universal one until more data are entered the analysis.The qualitative concept of the analysis,however,is very much universal.

5.6.2 DISCUSSION

In the previous section a statistical analysis has been carried out,using information extracted from a series of experiments performed in the present study and also a number of experiments performed by Winters.The common point between these experiments is the working liquid used,which was freon 12.

In the present work a very important chapter of the "safety" of storage and transportation of high pressure liquified gases industry has been researched,by looking into the relations between an averaged pressure in the vessel during rapid pressure releases and i) the initial conditions,ii) the material of the vessel,iii) the size of the vessel,iv)the roughness of the wall, v)the % of filling and vi) the length of the extension pipework attached to the exit of the vessel in question.

As it was mentioned before by using the steady state mechanical energy equation (Bernoulli),one can see that the averaged mass outflow depends on Δp where Δp is the pressure difference between the averaged pressure in the vessel and the atmospheric one.The $\dot{G}_{av}$ is important from i) the spread of the material in the surrounding area point of view ,ii)the waste of the material prediction point of view and iii) the prediction of the thrust applying to the adjacent structures.

The above analysis showed high dependence of "p_{av}" on p_{sat}, so this means that the storage and transportation are safer as long as the temperature of the system is kept down,e.g. vessel storaging LNG next to heat sources could result to hazardous situations.

In the case of the material dependence, it was suggested from the present statistical analysis that "SURFsts"decreases as the "material" changes from perspex to steel and as "SURFsts" decreases "p_{av}" increases.This means that for the "steel" vessel,which is richer in nucleation sites,the vast phase transition phenomena tend to increase "p_{av}" in the vessel.But for more

accurate assessment of the "material" dependence on "p_{av}", more experiments are needed involving more materials.

The roughness showed to have no effect on p_{av} in the case of "steel".It was only when a change from a very smooth wall (perspex old) to a less smooth one (perspex new) that the roughness affected in some way the p_{av}.

From figure 78,one can see the nonlinear dependence of the "size" on "p_{av}". Smaller sizes mean smaller "p_{av}".This could mean that smaller containers are safer from an accident point of view because they would result to a less hazardous situation.

From figure 81 and 82 it is evidenced that the % of liquid initially in the vessel affects very much the averaged pressure.If a vent pipe is attached to a safety valve on top of a storage tank and in case of emergency the valve blows off,the present analysis showed that there is an optimum vent pipe length that smooths down the effect of the "filling" on "p_{av}".In the present case it was found that for 1m extension pipe the relationship

$$\left[\frac{P_{sat} - P_{av}}{P_{sat}} \right] = f(\text{filling})$$

is linear,unlike for the 0.0,0.2,0.5 m long ones where the same relation is cubic. But in any case of extension length,the more liquid is stored in the vessel the higher the resulted "p_{av}" during an accident is.This suggests that is much safer to use partially full storage tanks than 100% full ones.

Finally from table 12 it is apparent that for a given % of liquid initially in the vessel any changes on the extension pipe length produced no changes on the "p_{av}",in the present tests.

Concluding,

1) The averaged pressure over the whole depressurisation phenomenon in the event of an accident of a pressurised vessel,is a significant quantity which affects both the mass outflow from the vessel and the thrust on the surrounding structures.

2) The averaged pressure is mostly affected by:

i) the initial temperature of the system

ii) the material the vessel is made of

iii) the size of the vessel

iv) the % of liquid initially in the vessel

3) For a universal quantitative relationship between "p_{av}" and the forementioned independent variables to be determined,if one exists,more experiments are needed with vessel sizes and material similar to the ones used in practice and also liquids in conditions,they are normally stored.

4) The present statistical work is ment to give a robust proof that there is a relationship which links the above variables,observed from the experiments.

CHAPTER 6

COMPARISON OF TWO PHASE FLOW MODELS WITH EXPERIMENTAL DATA

In this chapter the interest is concentrated on the comparison of i) the phase equilibrium model ii) the phase thermal non-equilibrium model with constant radius,iii) the phase thermal non-equilibrium model with nucleation and iv) the phase thermal non-equilibrium model with nucleation and initially partially full vessel with R12 and water experiments.

The empirical parameters attached to each of the model formulation are discussed and the degree of their influence on the two phase blowdown predictions will be shown.Any deviations from the experimental data observed will be also discussed.

For the present comparisons, the blowdown of an initially saturated liquid pressurised to the pressure of approximately 5.3 bars (T= 17.54°C) was used as a reference.The ability of the model to predict different initial conditions was tested by comparing the theoretical results with data from 8.51 bars blowdown of saturated liquid (T= 35.1°C).The experimental data was provided from the test print-outs by selecting distinguished points from the flow quantities histories plots,at the points of any slope changes.Both experimental and theoretical data points were presented by using the "GINO" computer package.

6.1 COMPARISON OF THE PHASE EQUILIBRIUM MODEL

Figures 92 and 93 illustrate the theoretical-experimental comparison,of the phase equilibrium model.As can be noted from the above plots the prediction of the system's expansion is very poor and unrealistic.The same was reported also by Winters (1978),but in his case the comparison was somewhat better than the one in the present work.This is believed to be due to the fact that his pressure vessel was far bigger than the one in these tests,which resulted in a less profound disequilibrium phenomena between the phases.The degree of disequilibrium is closely related in the time available to the system for phase transition, which in turn will result in the liquid's relief of its superheat.Any phase change is initially due to happen by nucleation and as it can be shown, (Skripov (1974)) the volume of the liquid plays a very important role.The same was reported by Winters and Merte (1978),only they related any disequilibrium effects to the volume to exit area ratio.The greater the exit area the shorter the time allowed for any disequilibrium balances.On the other hand the smaller the volume,the fewer bubbles that nucleate with less evaporation,which gives the same result as before.Comparison between Winters volume to exit area ratio and the one from the present work,showed a ratio over three times smaller in these tests than in Winters ones,which means far greater thermal non-equilibrium effects.The phase equilibrium model assumes that the two phase mixture is in equilibrium,to do so an enormous amount of phase transition has to take place,responding to any pressure reductions.This is the reason why this model predicts far to short expansion times (for both the bottom and the middle pressure stations, fig. 92 and 93 respectively), a non-existing i) pressure recovery from the liquid's metastable pressure minimum and ii) pressure plateau.

From the above it is obvious for the need to use a model which will take into account the thermal disequilibrium effects between the two phases. A C_d (exit loss coefficient) equal to unity was used with the above model,since the effect of any smaller values and the

improvement of the prediction was small ,covered by the unrealistic effect of the phase equilibrium assumption.

6.2 COMPARISON OF THE THERMAL NONEQUILIBRIUM MODEL (CONST. BUBBLE SIZE)

For this model the use of two empirical constants was needed.These two constants are: i) the size of the bubble in terms of the radius, ii) the C_d exit loss coefficient.The influence of the bubble size,on the system expansion ,is illustrated on figure 94.As it can be noted by increasing the size of bubble the pressure recovery is slower,the maximum pressure is lower and the pressure plateau longer.Even if a bigger bubble size means a greater heat and mass transfer,which in turn means generally higher pressures and rates of pressure recovery,it also means that for a given void fraction there are fewer bubbles.The number density of the bubbles,N_b,is also proportional to the heat transfer and it so happens that N_b decreases faster than the increase of the interfacial area,which results in less interfacial transfer phenomena,so important during fast releases.Furthermore lower pressures in the vessel result in lower mass flow rates at the exit and that is how the prolonged pressure plateau is explained.

Figure 95 illustrates the effect of the different exit loss coefficients with values less than unity.Strictly speaking,C_d,in this model, does not have the meaning of a classic fluid mechanics coefficient.As it was discussed in chapter 4 this coefficient covers for the less than 100% opening of the diaphragm and the mechanical and thermal effects of this on the flow of the mixture. A decrease of C_d produces a flatter pressure plateaus and therefore increases the long time pressure history.This is because it restricts the outflow,increasing the mass hold up and eventually the pressure.From figure 95,it is apparent that its effect starts at a certain time,no matter what the value of C_d is.This is because C_d becomes effective only when the

flow is choked,as it was discussed in the theoretical development of the C_d coefficient in previous chapter.

A trial and error process was used for establishing the optimum values of the two constants to fit the experimental data as closely as possible.This process resulted in :$C_d = 0.4$ and $r_b = 1.5E\text{-}4$ m.For the initial conditions,mentioned before, the theoretical model provided the data illustrated in figures 96 to 103.In figures 96 to 98,the three pressure histories are plotted.The main characteristic of these predictions is the slow recovery of the pressure from the pressure minimum.This can be attributed to the fact that the initial mode of phase transition,i.e. nucleation,in the present model is omitted.For the bottom and middle way pressure traces (fig.96 and 97 respectively) once the pressure reaches the pressure maximum the overall pressure prediction is quite satisfactory, with respect to the pressure plateau and the total time the event lasts.Again at the end of the phenomenon,when the void fraction is large,the main assumption of the model,i.e.bubbly flow,fails to cope with the probable droplet-vapor mixture flow,resulting in a theoretical completion of the phenomenon faster than the experimental one.Close to the exit,the pressure prediction is not as good as for the rest of the pressure stations.It is believed that all discrepancies except the slow pressure recovery rate,which was discussed previously,are due to the fact the flow at the exit is very much multidimensional and the averaged value for the flow quantities,assumption no longer valid.Plus the fact that the non-ideal break of the diaphragm increases these discrepancies.Furthermore it was evidenced from the experimental filming that there is a non-zero slip between the phases at the exit.The overprediction of the pressure plateau at the exit can be attributed to the two dimensional velocity distribution at the exit plane and the developed flow patterns other than bubbly,e.g. annular.

In figure 99,the experimentally measured temperature is compared with both the theoretical liquid and vapor ones.Since initially the sensor is in the liquid phase,the temperature it measures is that of the liquid and from the above figure one can see that initially the experimental temperature is quite close to the theoretical liquid's.As the

expansion of the two phase mixture progresses i)the liquid cools down and ii) the void fraction increases, resulting in the vapor being the continuous phase.So the measured temperature approaches the theoretical vapor trace.A general observation from fig.99 is that the vapor temperature is underpredicted.This could be the result of the constant specific heat assumption,since Cp theoretically depends on the temperature and the pressure of the system.

It is thought that for a more realistic prediction of a blowdown from the perspex vessel,which provides considerably fewer nucleation sites located only on the measurement stations,is to increase the bubble size.As it was mentioned before this will result in a decrease of the number density of the bubble population.Since the main aim of this work is not to perfect the flow predictions by adjusting the free constants,but to underline their effect and their physical significance,a random increase of the bubble size to 2E-4 m,has been chosen.Figures 100 and 101,illustrate the pressure histories at the bottom and 7.4 cm from the bottom respectively.The result is a decrease in the heat and mass transfer,which produces a quite good agreement for both stations. A slight overprediction of the pressure plateau at the bottom pressure trace is observed and it may require a further decrease of the interfacial exchanges,by increasing the bubble size.This latest conclusion is based on the same reason that makes a thermal non-equilibrium model important,the lack of sufficient vaporisation which results in a pressure maximum far lower than the saturation pressure with respect to the initial temperature for both the theory and the experiment ,which is an indication of the degree of the thermal nonequilibrium phenomenon. It is an interesting fact that the C_d kept its previous value ,which it is something one should expect,since the diaphragm bursting mechanism was the same.

The effect of different initial temperatures of the liquid on the model predictions will be next examined.To do so, extreme experimental initial conditions have been chosen.The liquid is saturated and pressurised to 8.5 bars. Again for these runs the empirical parameters retain their previous values i.e. $C_d = 0.4$ and $r_b = 1.5E\text{-}4$ m.The characteristics of this comparison

are the same (see fig.102 to 104), slow pressure recovery from the metastable region, quite good agreement on the pressure plateau and this time even more accurate prediction of the total time of event completion.The exit pressure trace is again overpredicted especially by the end of the phenomenon where the flow pattern must be other than bubbly and the two dimensional effects are even more important.

A general conclusion from the above predictions is that,a simple constant bubble size heat transfer model can predict most of the long term depressurisation quite well.Of course r_b is not the exact bubble size but more like an averaged value which takes into account the constant values of the Nusselt number and the conductivity coefficient involved in the heat transfer expression.

Water experimental data reported by Edwards and O'Brien (1970),will be next simulated.Figure 105 and 106 illustrate the pressure history at two different locations along the pipe axis (10 and 150 cm from the closed end respectively). The values of C_d and r_b,found to provide quite good agreement with the test,are: $C_d = 0.5$ and $r_b = 4.5E\text{-}4$ m.The value of C_d is believed to be realistic since,thick glass diaphragms were used and are known to provide less than 100% breaking area.Furthermore the surface tension for the water conditions is greater than R12 so this means less surviving bubbles.Similar to the R12 pressure predictions,the rate of the pressure recovery is slow,because the nucleation phenomenon is omitted.Once the pressure reaches its maximum value the depressurisation history looks reasonably close to the experimental one.Just before the 350th msec the void fraction becomes unity (see fig.107) and the pressure rapidly reduces to the atmospheric.This is the region where the bubbly flow assumption collapses, resulting in somewhat shorter total event times.Figure 107,shows the void fraction history.It is apparent from the above figure that the phase transition is overpredicted.The theoretical void fraction prediction performed by Edwards and O'Brien (1970) looks very similar to the one predicted in the present work.Both theoretical curves,however,bear a quite good resemblance to the general profile of the

experimental trace.Both lack the initial rapid increase of the void fraction,as a result of the nucleation process.

Figure 108 illustrates the temperature history at the same position as the void fraction one.The theoretical temperature prediction for both the liquid and the vapor phase are also coplotted.From the above figure one can notice that the experimental temperature is always between the two theoretical ones.In the beginning the temperature measured by the thermocouple is close to the liquid's.As the void fraction increases,the phase transition cools down the liquid and so the recorded temperature starts getting away from the liquid's and approaching the vapor's trace.But when the theoretical void fraction becomes unity the single phase vapor expansion produces a very fast pressure and temperature reduction.In reality the void fraction does not reach unity for approximately the next 100 msec and this allows the temperature to follow a milder reduction.

Runs of all the above models with and without consideration to the wall friction term showed small effect on the flow prediction and only for quite large void factions.So any discrepancies mentioned before,it is unlikely to be due to the wall friction model.

6.3 COMPARISON OF THE PHASE NON-EQUILIBRIUM MODEL (NUCLEATION PROCESS)

From the previous section it is apparent that the nucleation process needs to be included in the two phase modelling if the initial metastable region is to be predicted accurately.The experimental parameters used in conjunction with this model are the C_d and the ϕ i.e. the heterogeneous factor.C_d retains its previous value (0.4).Figure 109 and 110 (the initial and long term depressurisation respectively) illustrate the effect of the different ϕ on the pressure prediction. A large value of ϕ means a large nucleation work term and therefore a small number of nucleated critical bubbles,while small ϕ has the opposite effect. The direct result

of small ϕ is the quite large minimum and maximum pressure (see figure 109).From figure 110,the larger the pressure maximum,the steeper the overall depressurisation and the shorter the total event times.This is the result of the massive bubble production.Following the same trial and error process as before,the value of ϕ was able to be established,in order to provide a quite close fit to the experimental data.The value of ϕ selected for the present experimental conditions is 1.3E-3.Figures 111 to 116 illustrate the pressure history prediction at three locations along the vessel's axis.For the pressure measurements at the bottom and the middle of the vessel (fig.111 to 114) the rate of depressurisation , the minimum, the pressure recovery and the pressure maximum are predicted quite well.The theoretical pressure follows the experimental one quite well,especially the bottom trace,up to the point where the void fraction is quite large and the nucleation process is negligible. From figures 97,98,112 and 114 one can notice that a combination of the two models can provide very good results.Physically this means that bubbles nucleate initially and then they grow to provide the flat part of the pressure plateau. The exit pressure prediction is met with somewhat less degree of success.Generally the same characteristics,mentioned for the other two pressure histories, valid for this one as well,but the effect of the exit flow conditions i.e. probably different flow pattern than the one assumed,two dimensional effects e.t.c could be responsible for any further discrepancies.

From the point of view of the reference to the perspex run with the previous model,a "partial" nucleation version of the present model was developed.This model provides the facility for the nucleation region along the vessel's axis to be specified.Assuming that nucleation takes place only on the measurement stations, the results are illustrated in figures 117 to 120.Generally the rate of depressurisation,the minimum pressure,the rate of pressure recovery and the maximum pressure are predicted quite satisfactorily.The accuracy of the prediction is not as good as for the previous test,which means that a simple assumption for one dimensional distribution of the nucleation sites is not enough.The value of ϕ chosen for this run was the same as before (1.3E-3).

The blowdown of saturated liquid R12 pressurised to 8.5 bars was also simulated. As it was discussed before, ϕ depends on the initial temperature of the liquid.ϕ increases with temperature,so the value of ϕ for this run was chosen to be equal to 3.7E-3.Figures 121 to 126 illustrate the pressure history in the vessel.A comparison with figures 102 and 103,show an improvement of the pressure recovery,observed experimentally,and also for the initial depressurisation history (see fig. 121 and 123) the pressure slope is predicted quite well.By comparing the prediction of the minimum pressure in both 5.3 an 8.5 bars, it can be noticed, that for the 8.5 bars case,theory underpredicts it. In an attempt to predict as closely as possible the total pressure history, the averaged value of ϕ,happened to be larger than the one needed during the initiation of the nucleation.Skripov (1974), suggested that after the first nucleated bubbles have appeared, the temperature of the liquid and generally its superheat decreases, and so all thermodynamic properties change including the surface tension.But greater surface tension (for smaller temperature) means higher nucleation barrier and therefore fewer nucleated critical bubbles.It may be noticed that for both the high and low enthalpy liquid,initially in the vessel,the degree of superheat,represented by the dp_{sat} is almost the same and equal to approximately 4 bars,but the molecular energy,mainly responsible for the nucleation process,is much less for the saturation liquid pressurised to 5.3 bars than it is for the other case. So nucleation is more vigorous for the high enthalpy liquid,resulting to a fast cool down of the superheat liquid and an increase of the surface tension.

The nucleation computer program can be used for the evaluation of this initial ϕ quantity,which results in a much higher minimum pressures.By fitting the minimum pressure,the optimum value of ϕ can be determined,for the local conditions (this is similar to a work performed by Alamgir).

Generally the pressure prediction looks quite well up to the point where nucleation process becomes negligible.

Figures 125 and 126,present the initial and total pressure history comparisons for the exit pressure station.Like the previous comparisons the complex flow situations at the exit,affect the theoretical prediction of the pressure.

It has to be said,at this point,that the value of ϕ,used in conjunction with the nucleation program,is an averaged value depending on the average contact angle between the nucleated critical bubble and the surface of the wall. Making use of the empirical expression for ϕ,developed in a previous chapter, the degree of the crowded effect can be shown to vary with the initial temperature. For the case of the blowdown of R12 initially pressurised to 5.3 bars (T=290.7°K),the calculated ϕ from the above expression, which is based only on the pressure minimum, is 1.5E-3, which is quite similar to the value used during the nucleation model run (1.3E-3).However, for an increase of the initial temperature (T_{in}=308.25°K), the ϕ expression provides the value of 1.98E-3 which is far smaller than the one used in the present model (3.7E-3).

The crowded effects can be also noticed in the water blowdown simulation, (fig.127 to 130). where for an averaged ϕ value of 1.2E-3 ,the first pressure minimum is underpredicted.Generally the model underpredicts the long term pressure history,after the pressure recovery and this could be due to the vast bubble production and fast increase of the void fraction (see fig. 107),which results in an early stop of the nucleation process.Nevertheless it improves the metastable region prediction by improving the pressure minimum and the pressure recovery to a maximum pressure simulation.

Figures 131 and 132 illustrate the comparison between the theoretical and experimental prediction of the void fraction for the R12 tests.The measured void fraction in the present experiments is believed to be greater than the real one and this is due to the way it was measured (see discussion chapter 5). Taking into account the above comment,the discrepancy between the predicted void fraction, from the constant bubble size phase non-equilibrium model, is not quite as big as it is shown in figure 131.On the other hand,the nucleation model prediction of the void fraction is not quite as close as in figure

132.Generally the void fraction prediction looks quite well,with quite good similarity of the history profile.An interesting observation is that the rapid increase of the void fraction,which can be seen in the water experiments, is not present in the R12 ones and probably this is because of the perspex vessel (fewer nucleation sites).

6.4 COMPARISON OF THE PARTIALLY FULL VESSEL MODEL

The main empirical parameter involved in the present model is the slip ratio between the two phases at the interface between the mixture and the escaped gas. Figures 133 and 134 illustrate the effect of different slip ratios (VE) on the initial and long term depressurisation.A VE=0.99 denotes an almost zero slip at the interface.This means that most of the produced vapor is trapped in the mixture increasing its pressure quickly (see fig 133 and 134).If the vapor velocity is double the liquid one (VE=0.5), the pressure maximum, built in the mixture phase, slightly decreases, allowing more vapor to escape to the vapor phase.For greater differences, in the pressure maximum ,to be noticed, VE has to go down to 0.1,which means that the vapor velocity is ten times greater than the liquid's.Hence for realistic values of the VE,the effect of this parameter on the pressure history is quite small.From figure 134,one may notice that VE affects only the first 10 msec of the total event time.This is because the interfacial model is in use for as long as the interface is in the vessel.The value of VE chosen is 0.5.C_d is assumed to be one,since the large inertia of the vapor,initially in the vessel,helps to a clearer break of the diaphragm.Even so the flow losses at the exit are not zero and the pressure underprediction at the long depressurisation history can be partially blamed on the assumption of $C_d = 1$.The heterogeneous factor was found to be 1.2E-3 if the experimental data were to be quite well predicted.

Figures 135 to 140 illustrate the pressure predictions at the three pressure stations during blowdown process of an initially half full vessel. Generally both the initial and long term

expansion histories of the mixture phase are predicted quite well,taking into account the simplicity of the interfacial model,to cover for any vapor escape from the interface due to i) evaporation and ii) bubble slip.One of the discrepancies of the model is the small overprediction of the maximum pressure in all pressure stations.But the rate of the initial depressurisation and the minimum pressure are predicted quite closely,even at the top pressure transducer,which initially is in the vapor phase.As it was expected, the discrepancy is greater at the middle pressure station, which is in the vicinity of the mixture-vapor interface.For the long term expansion,the theoretical pressure is initially somewhat greater than the experimental one,but as the influence of the nucleation dies out,it becomes smaller.For all the pressure traces, the pressure plateaus are quite well predicted. The present model did not seem capable of predicting the pressure oscillations due to the complex movement of the interface,especially at the middle pressure station.It is believed that the nucleation produced at the vicinity of the minimum pressure dumps out any pressure waves produced by the interfacial movement and also increases the pressure to a maximum somewhat greater than the experimental one.

A blowdown from a partially full vessel with an extension pipe (0.2 m in length) was also simulated.Figures 141 to 148 present the above simulation.It is believed that generally the theoretical pressure predictions are quite agreeable with the experimental ones,with respect to the minimum pressure,the rate of pressure recovery,the maximum pressure,the pressure plateau and the total event time.The rate of the liquid's rapid depressurisation is also quite well predicted,except the bottom pressure trace.This last discrepancy it is believed to have nothing to do with the present modelling.An early start of the nucleation in the vicinity of the bottom pressure transducer probably resulted to a slow down of the depressurisation rate,for the individual experiment.

Figures 147 and 148 illustrate the pressure trace (initial and long term expansion history respectively) for the pressure station 6 cm from the exit inside the vent pipe.In figure 147 one can see the good agreement in the first pressure increase,due to the shock wave passing by

and the quite good prediction of the pressure reduction to a minimum and then increase to a maximum as the mixture-vapor interface reaches the pressure station.Also figure 148 illustrates the good simulation of the experimental pressure history.One has to keep in mind the rather simplified assumption of the ideal vapor phase.It is well-known that this is not true,since there are also dispersed droplets,which carry on evaporating or condensing depending on the local conditions.

Generally it is believed that the present model gives a good idea of what the flow variation will be in the case of a blowdown from a partially full vessel,with or without a vent pipe at the exit.

Concluding,any discrepancies,especially the underprediction of the pressure history towards the end of the expansion of the two phase mixture for all three models,can be attributed to the two main assumptions of the models i.e. i) the bubbly flow and ii) the zero slip.When the void fraction becomes large, both above assumptions become unrealistic.For example a vapor-droplet mixture would result in i) slower increase of the void fraction and ii) interfacial forces due to slip,which could prolong the pressure plateau.Furthermore, the individuality of the opening of the diaphragm produces further discrepancies, noticed in almost all pressure history comparisons for the exit pressure station.

CHAPTER 7

CONCLUSIONS - FUTURE RECOMMENDATIONS

1. To model the initial phase of a transient release of a saturated or subcooled liquid requires the non-equilibrium effect to be included as well as a physically based heterogeneous nucleation model.

2. For longer term conditions it is essential to correctly model the flow exit boundary condition.Any discrepancies between theory and experiments are due to the omission of droplet-vapor mixture within the vessel.

3. For a partially full vessel the vapor escape at the free surface needs to be allowed for.

4. It has also been postulated that the presence of large growing bubbles and small critical bubbles influence the rate of nucleation. A theory to explain this has been presented.

5. In conjunction with experimental data the heterogeneous factor in freon 12 and water has been determined and shown to be a function of the initial liquid temperature in the vessel and the degree of superheat of the liquid.

6. The model freon 12 experiments have shown that an increase in the initial liquid temperature results in higher maximum pressures and shorter event times.Different vessel material and roughness of the internal surface affect the event time and also the long term depressurisation,resulting in flatter pressure plateau,observed after the pressure has reached its maximum. The effect of partially full vessel with liquid, prior the blowdown, has been shown to affect the pressure maximum (lower),the pressure plateau (shorter) and the time for

the phenomenon completion. Another factor,which increases the mass hold up in the vessel,is the presence of a vent pipe at the exit, which was attributed to phase transition phenomena in the pipe and friction effects.

RECOMMENDATIONS FOR FURTHER WORK

Further improvements in the modelling might be achieved by

1. allowing for slip between the phases

2. allowing for a transition between a vapor - liquid mixture and a vapor - droplet - liquid mixture when the void fraction is in excess of 0.7.

3. Future experiments should attempt to monitor the diaphragm opening time ,or to devise a more repeatable opening mechanism.This would greatly improve the analysis of data.

REFERENCES

ARDON, K., H., DUFFEY, R., B., (1978), Acoustic wave propagation in a flowing liquid-vapor mixture.Int. J. multiphase flows,4 303-322

VAN DEN AKKER, H.,E.,A., (1986), Discharge of saturated liquified gases from pressure vessels-nonequilibrium phenomena to flashing. Provisional lecture notes for the VKI-course on two phase flows in major technological hazards,Rhode-st-Genese (Belgium), 1-77

ALAMGIR, MD., LIENHARD, J., H., (1981), Correlation of pressure undershoot during hot-water depressurisation.J heat transfer,103 52-55

ALAMGIR, MD., KAN, C.,Y., LIENHARD, J., H., (1980), An experimental study of the rapid depressurisation of hot water.J. heat transfer, 102 433-438

ALAMGIR, MD., LIENHARD, J., H., (1978), The temperature dependence of surface tension of pure fluids.J. heat transfer,100 324-329

ARUBERG, B., T.,et.al., (1974), Discharge coefficient correlations for circular-arc venturi flowmeter.J. fluid eng.,96 111

BENSON, R., S., (1966), Advanced Thermodynamics. Pergamon press

BIRD, R., B., STEWART,W.,E.,LIGHTFOOT,E.,N.,(1960) ,Transport phenomena,Wiley

BANKOFF,S.,G.,(1960),A variable density single-fluid model for two phase flow with particular reference to steam-water flow. J. heat transfer,265-272

BANERJEE,S.,(1978),A surface renewal model for interfacial heat and mass transfer in transient two phase flow.Int. J. Multiphase flow,4 571-573

BANERJEE,S.,HANCOX,W.,T.,(1978),On the development of methods for analysing transient flow boiling.Int. J. multiphase flows,4 437-460

BANERJEE,S.,HANCOX,W.,T.,SULATISKY,M.,T.,(1978),Transient two phase flow and heat transfer during blowdown from subcooled conditions with heat addition.The American institute of chemical engineers,141-148

BANERJEE,S.,(1978),The dynamics of two phase flow in a duct. Proc.6th international heat transfer conference,Toronto (August) 345-350

BENEDICT,R.,P.et.al.,(1974),Generelized discharge coefficient for different pressure type fluid meter.J. eng. for power,96 440

BOURE',J.,A.,(1979),On the form of the pressure terms in the momentum and energy equations of two phase flow models.Int. J. multiphase flows,5 159-164

BOURE',J.,A.,(1975),On a unified presentation of the non-equilibrium two phase flow models.Non-equilibrium Two phase Flows ,ASME,New York,1-9

BANERJEE,S.,CHAN,A.,M.,(1980),Separated flow models-I.Analysis of the averaged and local instantaneous formulations.Int. J. multiphase flows,1-24

BIESHEUVEL,VAN WIJNGAARDEN,(1984), Two phase flow equations for a dilute dispersion of gas bubbles in liquid.J. Fluid Mech., 148 301-318

BLANDER,M.,KATZ,J.,L.,(1975),Bubble nucleation in liquids. AIChE J.,21 833-848

BROWN,E.,A.,(1959),Experiments on the explosive decompression of water.Armour research foundation report ARF 4132-9

COLLIER,J.,G.,(1972),Convective boiling and condensation, McGraw Hill

DREW,A.,D.,LAHEY,R.,T.,(1979),Application of general constitutive principles to the derivation of multidemensional two phase flow equations.Int. J. multiphase flow,5 243-264

DREW,D.,A.,(1983),Mathematical modelling of two phase flow. Ann. Rev. fluid mech.,15 261-291

DELHAYE,J.,M.,(1974),Jump conditions and entropy sources in two phase systems.Local instant formulation.Int. J. multiphase flows,1 395-409

DREW,D.,CHENG,L.,LAHEY,R.,T.,(1979),The analysis of virtual mass effects in two phase flow.Int. J. multiphase flows,5 233-242

DORING,W.,(1937),Z. PHYS. CHEM.,36 371-386
EDWARDS,A.R.,O'BRIEN,T.P.,(1970),Studies of phenomena connected with the depressurisation of water reactors.J.Br. nuclear energy,9 125-135
EDWARDS,A.,R.,(1968),Conduction controlled flashing of a fluid ,and the prediction of critical flow rates in one-dimensional system. UKAEA,AHSB(S),report R 147,1-37
EDWARDS,A.,R.,JONES,C.,(1972),An analysis of phase IIA blowdown tests - the discharge of high enthalpy water from a simple volume into a containment volume.UKAEA,SRD,report R27,1-31
FORD,W.D.,FAUSKE,H.K.,BANKOFF,S.G.,(1971),The slug expulsion of freon 113 by rapid depressurisation of a vertical tube.Int. J. heat mass transfer,14 133-140
FLETCHER,B.,(1984),Flashing flow through orifices and pipes. Chemical engineering progress,(March) 76-81
FERCH,R.,L.,(1979),Method of characteristic solutions for non-equilibrium transient flow boiling.Int. J. multiphase flows,5 265-279
FISHER,J.,C.,(1948),The fracture of liquids.J. applied physics, 19 1062-1067
FRIEDEL,L., (1986), Thermohydraulics during venting of two phase systems.Provisional lecture notes on Two phase flows in major technological hazards, Rhode-st-Genese (Belgium), 1-52
GIDASPOW,D.,(1978),A set of hyperbolic incompressible two phase flow equations for two components.The American institute of chemical engineers,186-190
HANCOX,W.,T.,MATHERS,W.G.,KAWA,D.,(1978),Analysis of transient flow boiling:application of the method of characteristics.The American institute of chemical engineers,175-183
HUNT,D.,L.,(1970),The effect of delayed bubble growth on the depressurisation of vessels containing high temperature water. UKAEA,AHSB(S),REPORT R.189,1-17
HUTCHERSON,M.,N.,HENRY,R.,E.,WOLLERSHEIM,D.,E.,(1983), Two phase vessel blowdown of an initially saturated liquid-part 1: experimental.J. heat transfer,105, 687-699
HUTCHERSON,M.,N.,HENRY,R.,E.,WOLLERSHEIM,D.,E.,(1983), Two phase vessel blowdown of an initially saturated liquid-part2: analytical
HANCOX,W.,T.,FERCH,R.,L.,LIU,W.,S.,NIEMAN,R.,E.,(1980),One dimensional models for transient gas-liquid flows in ducts. Int. J. multiphase flows,6 25-40
HAYWOOD,R.,W.,(1969),A simplified presentation of equations for the thermodynamic properties of dichlorodifluoromethane, (freon 12).J. mechanical eng. science,11 376-383
HENRY,R.,E.,(1968),A study of one and two component ,two phase critical flows at low qualities.ANL-7430,Argonne National Laboratory
HODGSON,A.,W.,(1984),Homogeneous nucleation.Adv. colloid & interface sci.,21 303-327
ISHII,M.,RIZNIC,J.,R., (1989), Bubble number density and vapor generation in flashing flow.Int. J. Heat Mass Transfer, 32 1821-1833
ISHII,M.,MISHIMA,K.,KATAOKA,I.,KOCAMUSTAFAOGULLARI,G.,(1982), Two fluid model and importance of the interfacial area in two phase flow analysis.Proc. 9th U.S. national congress of applied mechanics IEHACA New York,73-80
ISHII,M.,(1975),Thermo-fluid dynamic theory of two-phase flow.Eyrolles,Paris
KAGAN,YU.,(1960),The kinetics of boiling of a pure liquid. Russian J. phys. chem.,34 42-46
KENNING,D.B.R.,THIRUNAVUKKARASU,K.,(1970),Bubble nucleation following a sudden pressure reduction in water.34th Intl. heat transfer conf.,(B.29) 1-10
KENDOUSH,A.,A.,(1989),The delay time during depressurisation of saturated water.Int. J. heat mass transfer,32 2149-2154
KELLY,J.,E.,KAZIMI,M.,S.,(1982),Interfacial exchange relations for two fluid vapor-liquid flow : a simplified regime-map approach. Nuclear science and engineering,81 305-318
KOCAMUSTAFAOGULLARI,G.,ISHII,M.,(1983),Interfacial area and nucleation site density in boiling systems.Int.J. heat mass transfer ,26 1377-1387
KANTROWITZ,A.,(1951),Nucleation in very rapid vapor expansions. J.chem. phys.,19 1097-1100
LEVY,S.,ABDOLLAHIAN,D.,(1982),Homogeneous non-equilibrium critical flow model.Int. J. heat mass transfer,25 759-770
LYCZKOWSKI,R.,W.,GRIMESEY,R.,A.,SOLBRIG,C.,W.,(1978), Pipe blowdown analysis using explicit numerical schemes, The American institute of chemical engineers,129-139
LYCZKOWSKI,R.,W.,(1976), Numerical techniques for the computation of transient unequal phase velocity, unequal phase temperature two phase flow and heat transfer.Two phase transport and reactor safety, vol II, Proc. Two phase flow and heat transfer Symp.-Workshop,839
LYCZKOWSKI,R.,W.,GIDASPOW,D.,SOLBRIG,C.,W.,HUGHES,E.,D.,(1977), Characteristics and stability analysis of transient one dimensional two phase flow equations and their difference approximations.Nuclear science and engineering,66 378-396

LYCZKOWSKI,R.,W.,MECHAM,D.,C.,SOLBRIG,C.,W.,(1979), Network computations using a transient two phase velocity difference model.Nuclear science and engineering,69 279-289
LIENHARD,J.,H.,ALAMGIR,MD.,TRELA,M.,(1978),Early response of water to sudden release from high pressure.J. heat transfer,100 473-479
LEE,Y.,SHEN,W.,Q.,(1987),Effect of surface roughness on the rewetting process.Int. J. multiphase flows,13 857-861
LOOMIS,J.,REED,W.,SCHOR,A.,STEWART,M.,WOLF,L., (1981),THERMIT: A computer program for 3-D thermal-hydraulic analysis of light water reactor cores.EPRI NP-2032
MALNES,D.,(1975),Critical two phase flow based on non-equilibrium effects.In Non-equilibrium Two phase Flows (edited by R.T. Lahey and G.B.Wallis).ASME,New York
MOKEYEV,YU.,G.,(1977),Effect of particle concentration on their
MOORE,K.,V.,RETTING,W.,H.,(1973),"RELAP4" - A computer program for transient thermal-hydraulic analysis.ANCR-1127,Aerojet Nuclear company drag and induced mass.Fluid mech. sov. res.,6 161
MARKATOS,N.,C.,RAWNSLEY,S.,M.,TATCHELL,D.,G.,(1983),Analysis of a small break loss-of-coolant accident in a pressurised water reactor.C103/83 IMechE,121-134
MOODY,F.,J.,(1965),Maximum flow rate of a single component two phase mixture.J. heat transfer,87 134
NIGMATULIN,R.,I.,(1979),Spatial averaging in the mechanics of heterogeneous and dispersed systems.Int. J. multiphase flows, 5 353-385
PATTON,D.,L.,(1978),Semiscale MOD-3 test program and system descriptions.TREE-NUREG-1212
RIZINC,J.,R.,ISHII,M.,(1989),Bubble number density and vapor generation in flashing flow.Int.J. heat transfer,32 1821-1833
ROUSSEAU,J.,C.,FERCH,R.,L.,(1979),A note on two phase separated flow models.Int. J. multiphase flows,5 489-493
REEDER,D.,L.,(1978),Loft system and test description NUREG/CR-0247. TREE-1208
REED,W.,H.,KIRCHNER,W.,L.,(1977),Fluid dynamics and heat transfer methods for the TRAC code.C205/77 IMechE,97-101
ROGERS,G.,F.,C.,MAYHEW,Y.,R.,(1980),Thermodynamic and transport properties of fluids.Basil Blackwell
SKRIPOV,V.,P.,(1974),Metastable liquids,Wiley
SOLBRIG,C.W.,McFADDEN,J.H.,LYCZKOWSKI,R.W.,HUGHES,E.D.,(1978), Heat transfer and friction correlations required to describe steam-water behaviour in nuclear safety studies.The American institute of chemical engineers,100-127
SOLBRIG,C.,W.,MORTENSEN,G.,A.,LYCZKOSKI,R.,W.,(1976), An unequal phase velocity ,unequal phase temperature theory applied to two phase blowdown from a horizontal pipe, Proceedings of 25th Heat transfer and fluid mechanics, California, 60-76
SHA,W.,T.,SOO,S.,L.,(1979),On the effect of $p\nabla\alpha$ term in multiphase mechanics.Int.J. multiphase flows,153-158
TRAVIS,J.,R.,HARLOW,F.,H.,AMSDEN,A.,A.,(1976),Numerical calculation of two phase flows.Nuclear science and engineering,61 1-10
TRAPP,J.,A.,(1986),The mean flow character of two-phase flow equations.Int. J. multiphase flows,12 263-276
TONG,L.,S.,(1965),Boiling heat transfer and two phase flow, McGrow Hill
VOLMER,M.,WEBER,A.,(1926),Nucleus formation in supersaturated systems. Z. phys. chem.,119 277-301
WHITE,F.,M.,(1974),Viscous fluid flow,Mc Grow Hill
WINTERS,W.S.,MERTE,H.,(1979),Experiments and nonequilibrium analysis of pipe blowdown.J.Nuclear science and engineering,69 411-429
WINTERS,W.,S.,(1978),Non equilibrium blowdown in long pipes. PhD thesis,The university of Michigan,Ann Arbor
WOLFERT,K.,(1976),The simulation of blowdown processes with consideration of thermodynamic nonequilibrium within the control volumes.DECD/NEA meeting on transient two phase flow,Toronto,156-198
VAN WIJNGAARDEN,L.,(1976),Hydrodynamic interaction between gas bubbles in liquid.J.fluid mech.,77 27-44
ZUBER,N.,FINDLAY,J.,A.,(1965),Average volumetric concentration in two phase flow systems.J. heat transfer,453-468

ZUBER,N.,STAUB,F.,W.,BIJWAARD,G.,(1966),Vapor void fraction in subcooled boiling and in saturated boiling systems.Proc. 3rd Int. heat transfer conf.,V 24-38
ZUBER,N.,(1964),On the dispersed two phase flow in the laminar flow regime.Chem. eng.sci.,19 897-903
ZUCROW,M.,J.,HOFFMAN,J.,D.,(1976),Gas dynamics (vol I). McGrow Hill

TABLES

TEST No	DISTANCE FROM BOTTOM mm	DELAY msec	INITIAL CONDITION		U m/sec	SPACE RANGE mm	TIME RANGE msec
100	19	14.8	P^{in} = 5.4bar	GROUP	2.5	19-43	14.8-24.4
103	43	24.4	T^{in} = 18.15°C	1			
110	40	10.45	P^{in} = 5.2bar	GROUP	1.62	40-43	10.45-12.3
111	43	12.3	T^{in} = 16.9°C	2			
113	0.5	0.73	P^{in} = 5.2bar	GROUP	1.05	0.5-4	0.73-4.05
114	4	4.05	T^{in}_{in} = 17.2°C	3	1.44	4-10	4.05-8.2
115	10	8.2			1.87	10-16	8.2-11.4
116	16	11.4			0.8	16-19.5	11.4-15.8
117	19.5	15.8					

TABLE 1a. SINGLE LASER BEAM MEASUREMENTS. Bottom laser tests.

TEST No	DISTANCE FROM MIDDLE mm	DELAY msec	INITIAL CONDITION		U m/sec	SPACE RANGE mm	TIME RANGE msec
104	40	8.6	P^{in} = 5.4bar		7.86	40-51	8.6-10
105	51	10	T^{in}_{in} = 18.2°C		2.03	51-59	10-13.95
107	59	13.95					

TABLE 1b. SINGLE BEAM MEASUREMENTS. Middle laser tests.

TEST No	DISTANCE FROM BOTTOM mm	LASER SPLITTER RANGE mm	DELAY msec	INITIAL CONDITION	U m/sec	TIME RANGE msec
168	3	6	4.05	P^{in} = 5.4bar T^{in} = 18.2°C	1.48	3.3-7.35
169	18	10	11.7	P^{in} = 5.48bar T^{in} = 18.6°C	0.86	11.3-23
170	18	10	10.7	P^{in} = 5.46bar T^{in} = 18.5°C	0.93	12.36-21.36

TABLE 2a. DOUBLE LASER BEAM MEASUREMENTS. Bottom laser tests.

TEST No	DISTANCE FROM MIDDLE mm	LASER SPLITTER RANGE mm	DELAY msec	INITIAL CONDITION	U m/sec	TIME RANGE msec
176	36	4.5	1.1	P^{in} = 5.26bar T^{in} = 17.5°C	4.1	8.45-9.55
177	50.5	5.5	1.1	P^{in} = 5.48bar T^{in} = 18.4°C	4.82	12.5-13.6
178	63.5	4.5	1	P^{in} = 5.4bar T^{in} = 18.4°C	4.5	14.57-15.57

TABLE 2b. DOUBLE LASER BEAM MEASUREMENTS. Middle laser tests.

TEST No	DISTANCE FROM EXIT mm	DELAY TIME ms	VELOCITY m/sec	INIT.PRESS. bar	INIT.TEMPR. °C
120	60	2.475	24.24	5.37	17.85
121	60	2.075	28.9	5.37	17.9
122	60	2.095	28.64	5.34	17.65
130	60	2.495	24	5.77	17.25
171	60	3.175	18.89	5.47	18.4
172	60	2.375	25.26	5.47	18.6
186	67	4.174	16	5.58	19.4
188	60	2.374	25.27	5.52	18.9
190	60	2.424	24.75	5.46	18.55
193	67	1.795	36.7	6.9	27
209	60	2.015	29.77	5.27	17.3
213	66	1.935	34.2	6.91	27
214	56	1.983	28.24	6.9	27
218	66	3.695	17.86	5.29	17.45
219	60	2.414	24.85	5.27	17.35
222	60	2.894	20.73	6.91	27
233	66	2.672	24.7	6.91	26.8
224	56	1.923	29	6.89	26.7

TABLE 3. CALCULATED EXPANSION VELOCITY.

TEST No	NUCLEATION DELAY TIME μsec
1	210
2	-
3	-
4	540
5	-
6	200
7	420
8	650
9	-
10	-
11	-
12	510
13	440
14	560
15	520
16	360
17	600
18	600

TABLE 4. NUCLEATION DELAY TIME.

TEST No	FRAME No 1	2	3	4	5	6	7	8	9	10	11	12	13	14
1	3.0	3.0	3.25	3.25	3.5	3.5	3.5	3.5	-	-	-	-	-	-
4	0.0	0.0	0.0	0.0	0.0	0.0	0.0	0.5	-	-	-	-	-	-
12	0.37	0.37	0.37	0.37	0.5	0.5	0.5	0.5	0.5	1.0	-	-	-	-
14	1.5	1.5	1.5	1.5	1.75	1.75	1.75	2.0	2.0	2.0	2.0	2.0	2.0	2.0
15	2.5	2.75	2.75	2.75	2.75	2.5	2.9	2.75	2.75	2.5	2.5	2.5	-	-
16	2.5	2.5	2.75	2.85	2.85	3.0	3.0	3.0	3.0	3.0	3.0	3.0	-	-
17	2.25	2.25	2.5	2.5	2.5	2.5	2.5	2.5	2.75	2.25	2.5	2.5	-	-
18	2.25	2.25	2.5	2.5	2.5	2.5	2.25	2.0	2.0	2.5	2.5	2.5	2.25	2.5

TABLE 5. BUBBLE SIZE MEASUREMENTS (in mm).

TEST No	FRAME No 1	2	3	4	5	6	7	8	9	10	11	12	13	14	15	16
1	1	1	1	1	1	1.25	1.25	1.5	1.5	1.5	1.5	1.5	1.5	1.5	-	-
4	0	0	0	0	0	0	0	0	0	0	0	0	0	0	-	-
12	0	0	0	0	0	0	0	0	0	0	0	0	0	0	-	-
14	0	0	0	0	0	0	0	0	0	0	0	0	0	0	-	-
15	0.7	0.7	0.7	0.7	0.7	0.7	1	1	1	1	1	1	1	1.25	-	-
16	1.25	1.25	1.25	1.5	1.5	1.5	1.5	1.75	1.75	1.75	2	2	2	2	-	-
17	2.3	2.3	2.3	2.5	2.5	2.5	2.5	2.5	2.5	2.5	2.75	2.75	2.75	2.75	-	-
18	3.25	3.25	3.25	3.5	3.5	3.5	3.5	3.5	3.75	3.75	3.75	3.75	3.75	3.75	3.75	4

TABLE 6. DISPLACEMENT FROM THE "HOT JUNCTION" MEASUREMENT (in mm).

TEST No	BUBBLE RISE VELOCITY m/sec	TIME RANGE μsec
1	1.25	340-540
1	3.125	540-640
4	-	540
12	-	1055-1415
14	-	1690-2210
15	1.25	2320-2560
15	0.893	2560-2840
16	2.083	2900-3020
16	1.563	3020-3180
16	2.083	3180-3300
17	1.67	3600-3720
17	0.893	3720-4000
18	2.083	4500-4620
18	1.25	4620-4820
18	0.893	4820-5100

TABLE 7. BUBBLE RISE VELOCITY.

TEST No	U_{test} m/sec	U_{theor}.m/sec	TIME μsec
15	1.06	1	2600
16	1.91	1.18	3100
17	1.28	1.5	3800
18	1.41	2	5175

TABLE 8. THEORETICAL-EXPERIMENTAL BUBBLE RISE VELOCITY COMPARISON

CATEGORY	REGRESSION COEFF. "r"	PROBABILITY LEVEL ON "r"	CONSTANT	SLOPE W.R.T T_{in}
PERSPEX	0.795	> 0.999	1.56	0.092
MILD STEEL1	0.944	> 0.999	1.45	0.109
MILD STEEL2	0.964	> 0.999	1.64	0.102
MILD STEEL3	0.93	> 0.999	1.95	0.092
WINTERS	0.69	> 0.96	1.42	0.094

TABLE 9. STATISTICAL DATA.

CATEGORIES	REGRESSION COEFF. "r"	PROBABILITY LEVEL ON "r"	CONSTANT	SLOPE W.R.T P_s
OLD PERSPEX	0.874	> 0.9999	1.655	8.98E-5
NEW PERSPEX	0.319	< 0.95	-	-
MILD STEEL	0.985	> 0.9999	2.19	2.99E-5
WINTERS	0.977	> 0.9999	1.18	0.372

TABLE 10. STATISTICAL DATA.

"EXTNPIPE" (m)	REGRESSION COEFF. "r"	PROBABILITY LEVEL ON "r"	CONSTANT	SLOPE W.R.T. "FILLING"
0	0.968	> 0.9999	0.686	-0.089
0.2	0.977	> 0.9999	0.671	-0.127
0.5	0.996	> 0.9999	0.682	-0.133
1.0	0.98	> 0.9999	0.767	-0.214

TABLE 11. STATISTICAL DATA.

"EXTNPIPE" (m)	TYPE OF RELATIONSHIP
0	$SURFsts = f(filling^3)$
0.2	$SURFsts = f(filling^3)$
0.5	$SURFsts = f(filling^3)$
1.0	$SURFsts = f(filling)$

TABLE 11a (continue).

"FILLING"	REGRESSION COEFF. "r"	PROBABILITY LEVEL ON "r"	CONSTANT	SLOP W.R.T "1/EXTNPIPE"
100% FULL	0.932	> 0.9999	0.546	5.05E-7
75% FULL	0.918	> 0.9995	0.616	3.96E-7
50% FULL	0.562	< 0.95	-	-
25% FULL	0.322	< 0.95	-	-

TABLE 12. STATISTICAL DATA.

BLANK IN ORIGINAL

FIGURES

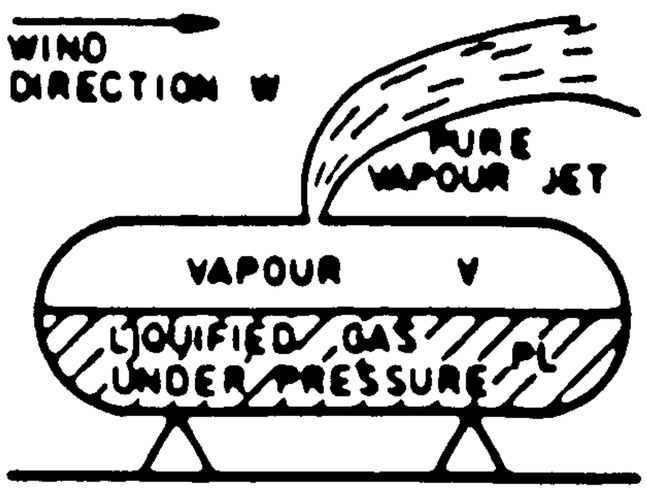

FIG 1A SMALL HOLE IN VAPOUR SPACE-PRESSURIZED TANK

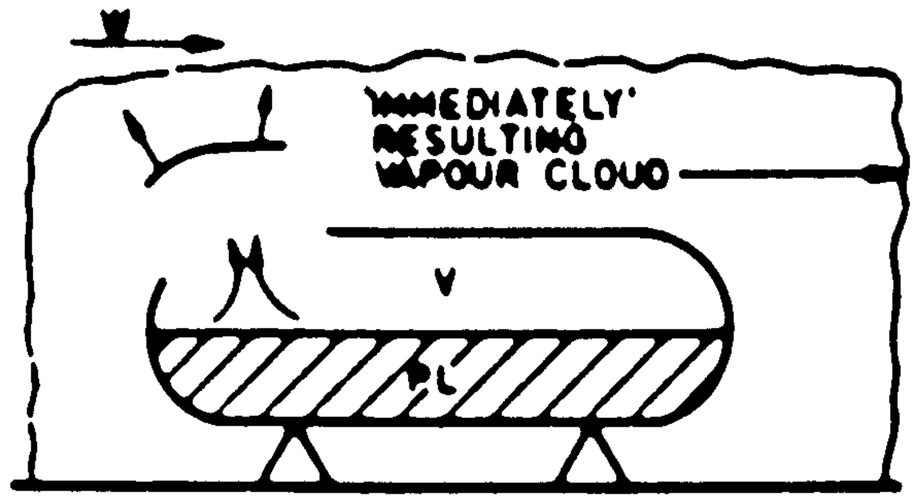

FIG 1B CATASTROPHIC FAILURE OF PRESSURIZED TANK

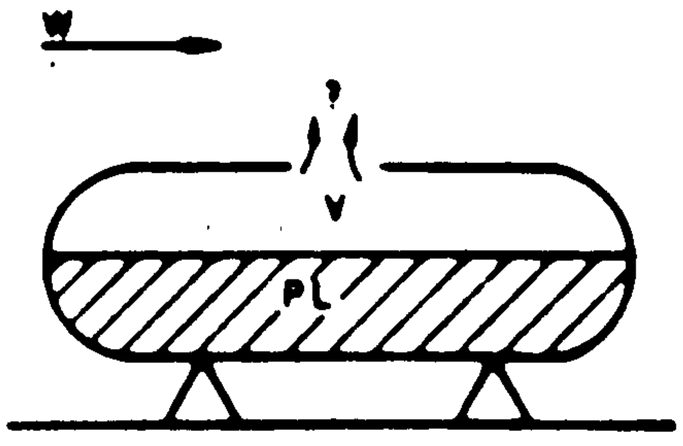

FIG 1C INTERMEDIATE HOLE IN VAPOUR SPACE-PRESSURIZED TANK

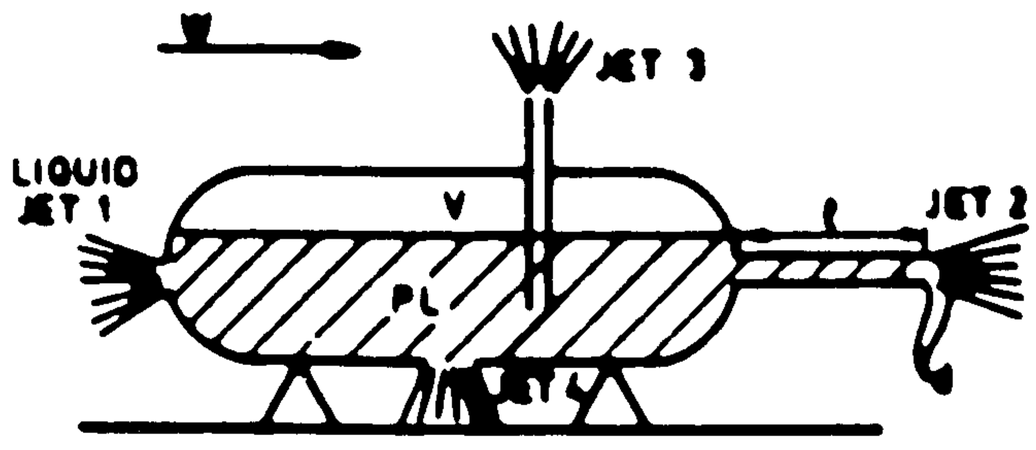

FIG 1D ESCAPE OF LIQUIFIED GAS FROM A PRESSURIZED TANK

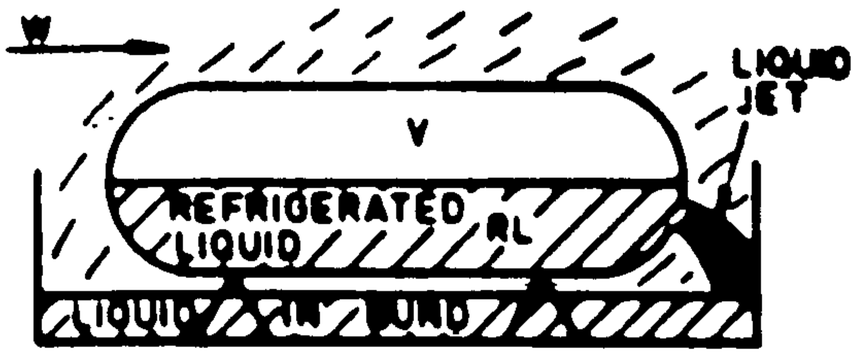

FIG 1E SPILLAGE OF REFRIGERATED LIQUID INTO BUND

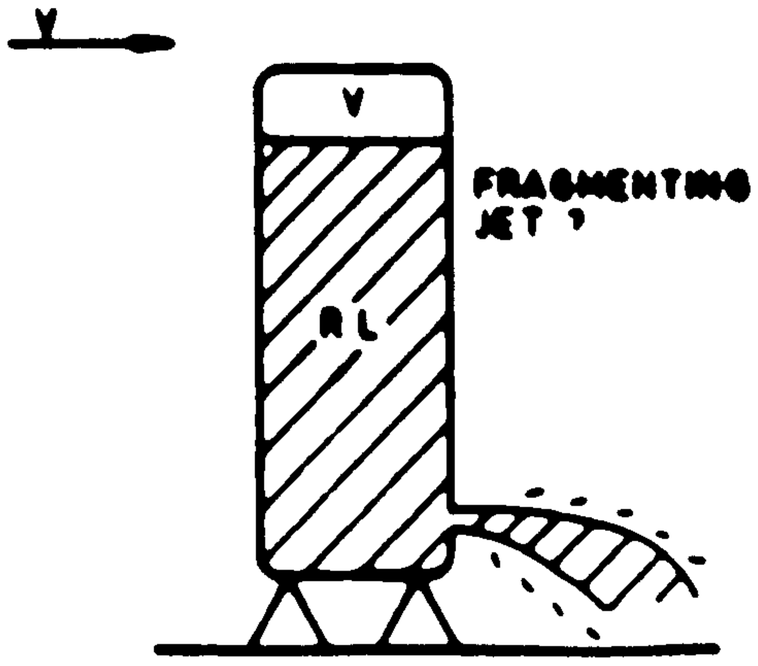

FIG 1F HIGH VELOCITY FRAGMENTING JET FROM REFRIGERATED CONTAINMENT

Figure 1. Illustration of some conceivable release mechanism.

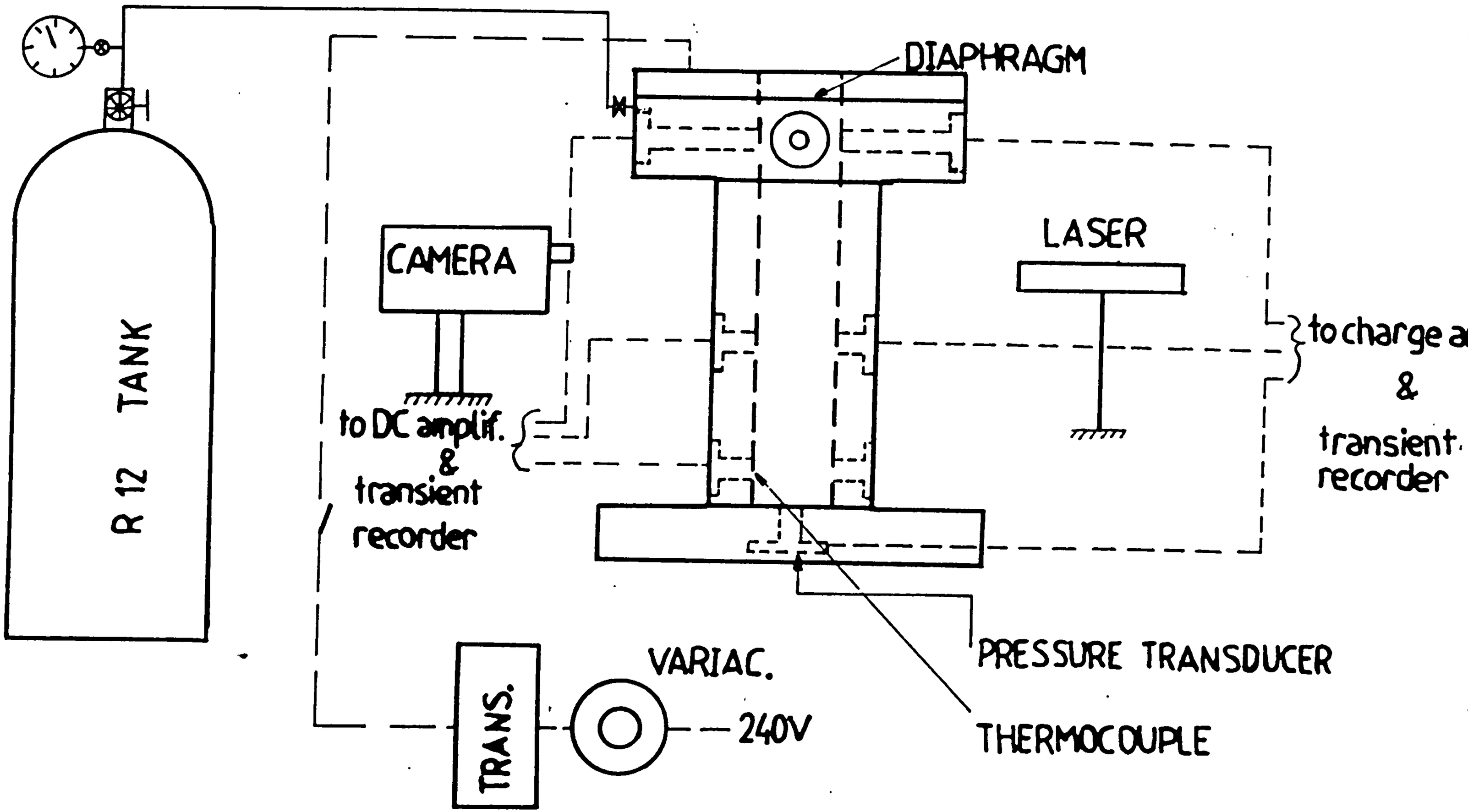

Figure 2. Schematic diagram of the experimental apparatus.

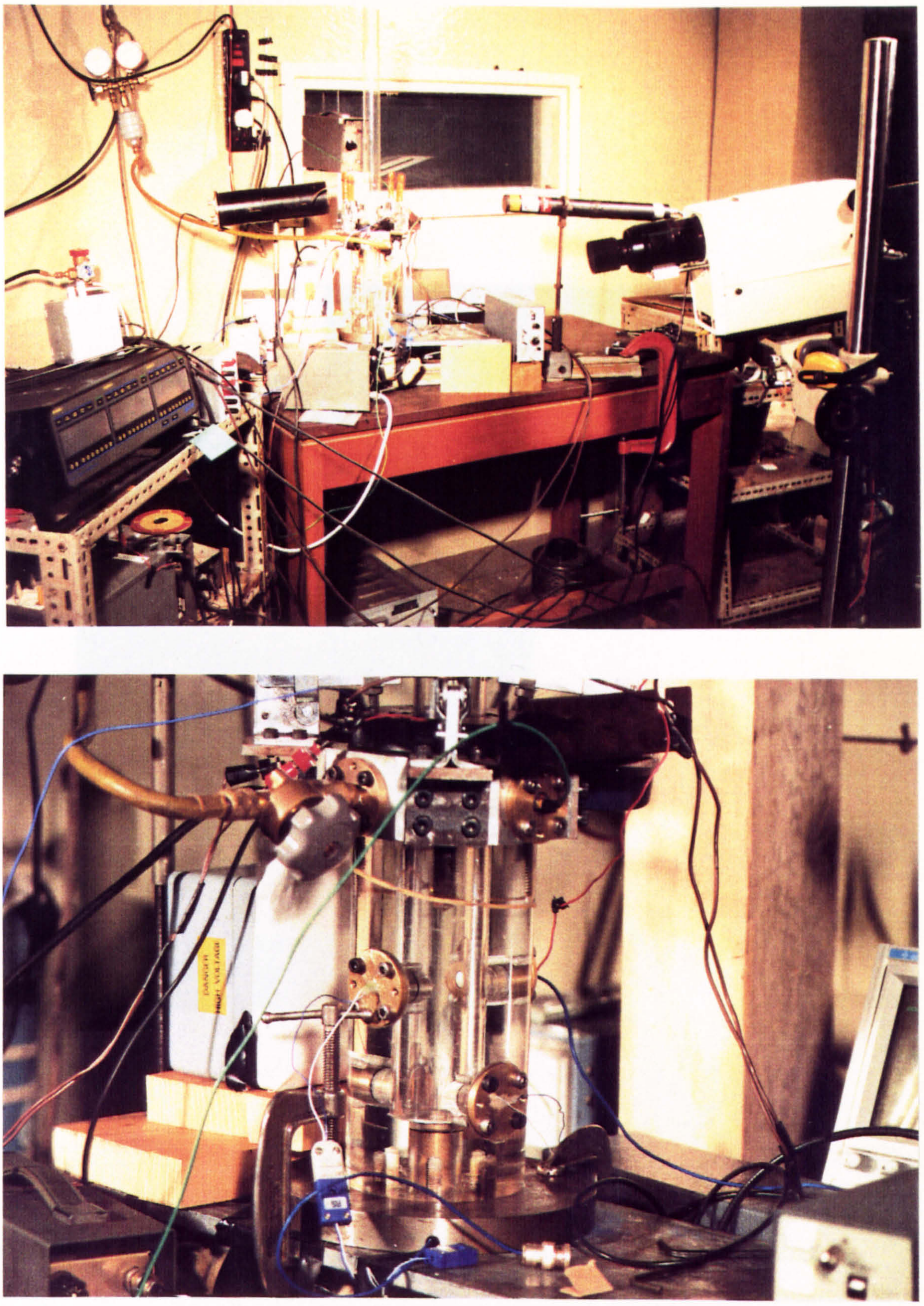

Figure 3. Photograph of the experimental rig.

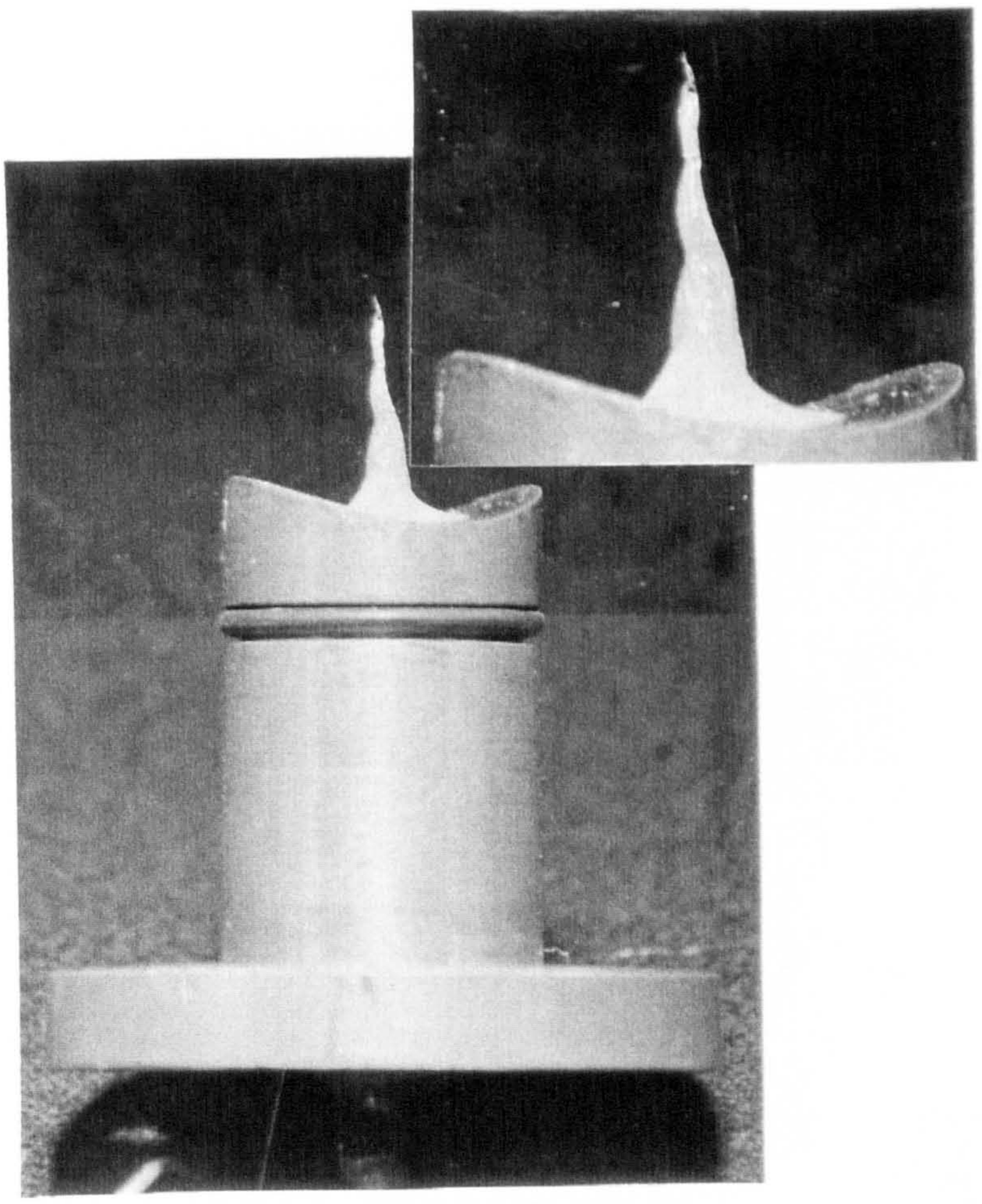

Figure 4. Photograph of the thermocouple.

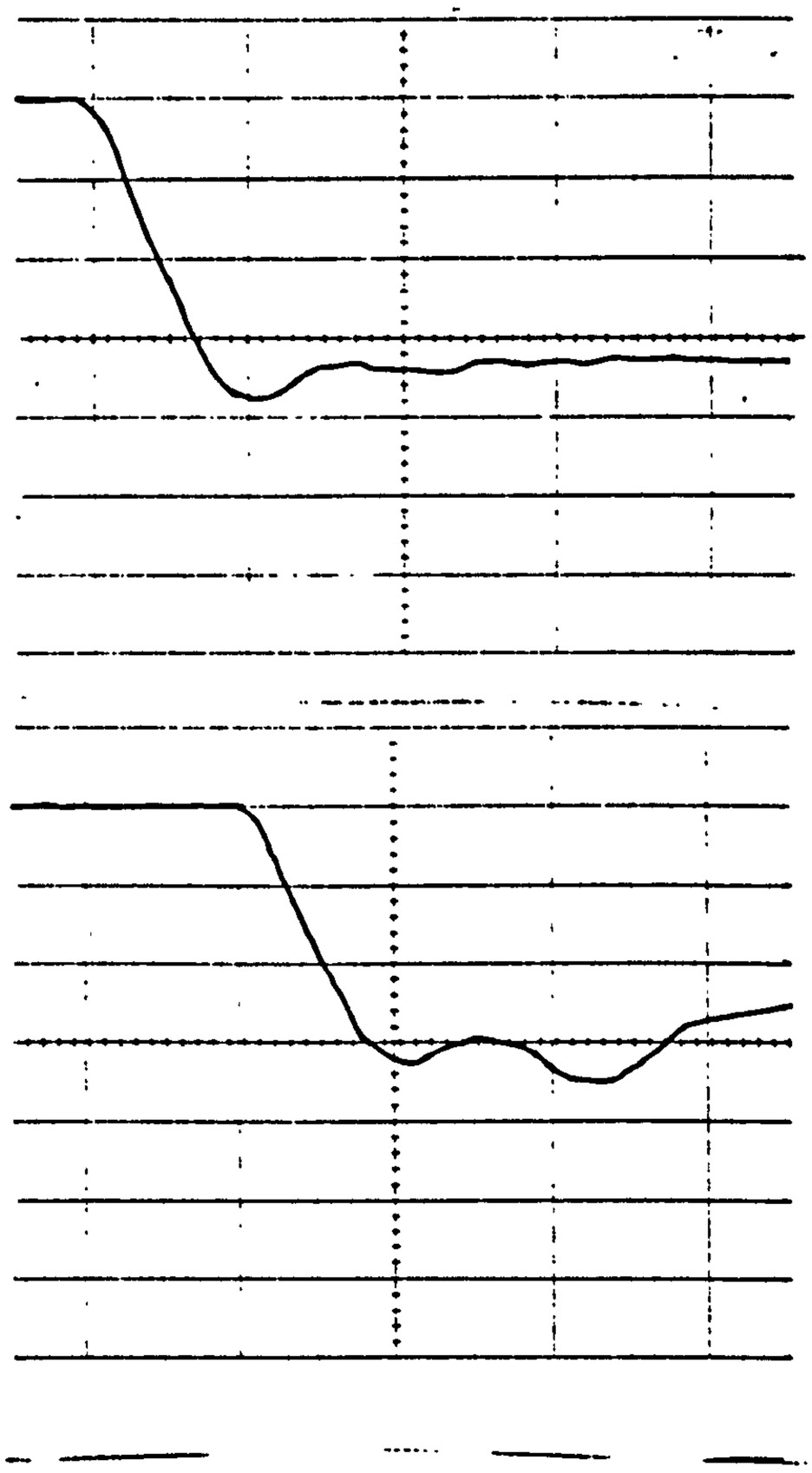

Figure 5. Typical initial decompression histories (100μsec/div) at the three (top(1bar/div),middle(1bar/div),bottom(0.845bar/div)) pressure stations (w.r.t the plots position). (test no 123,P_{in} = 5.25 bars,T_{in} = 17.2°C)

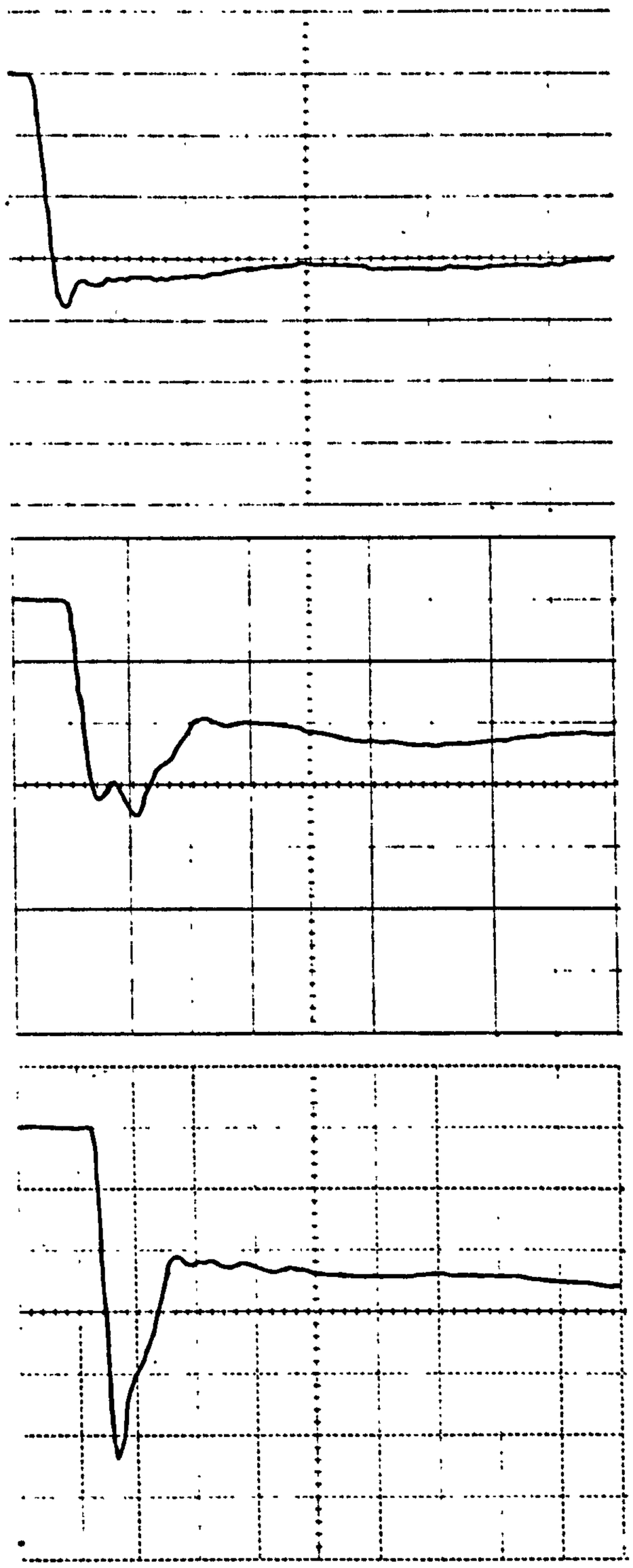

Figure 6. Typical initial decompression histories (400μsec/div) at the three (top(1bar/div),middle(1bar/div),bottom(0.845bar/div)) pressure stations (w.r.t the plots position). (test no 123,P_{in} = 5.25 bar,T_{in} = 17.2°C).

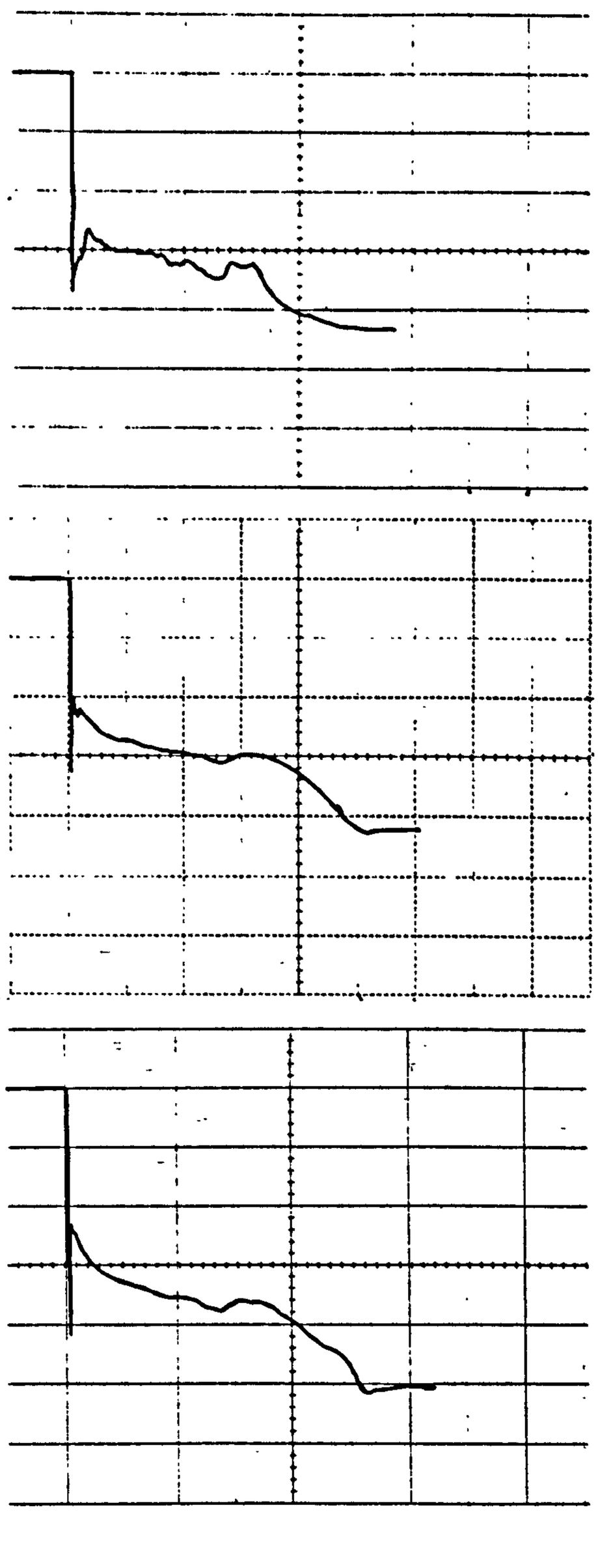

Figure 7. Typical long term depressurisation (20msec/div) at the three (top(1bar/div),middle(1bar/div),bottom(0.845/div)) pressure stations (w.r.t the plots position). (test no 123,P_{in} = 5.25 bar,T_{in} = 17.2°C).

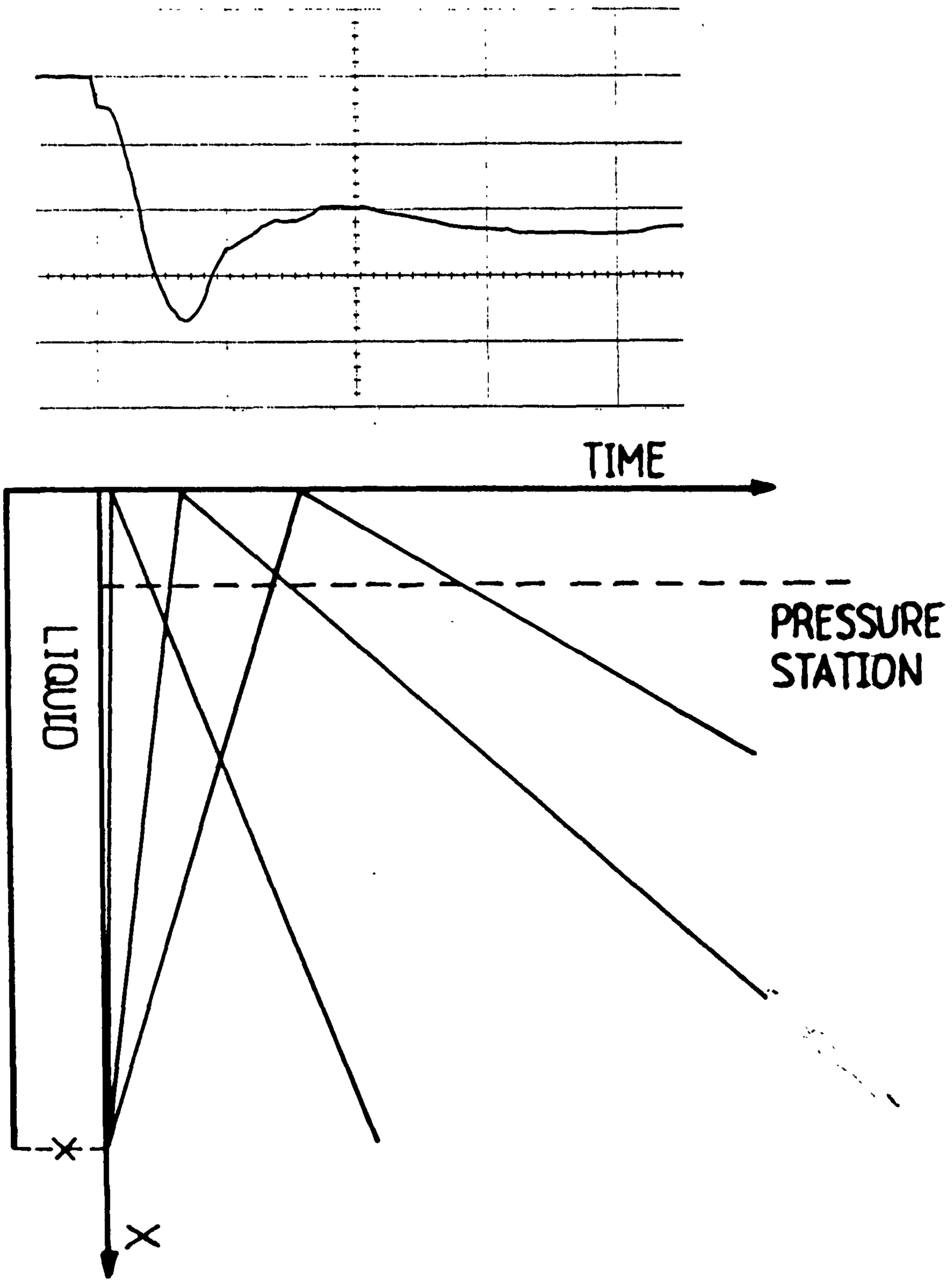

Fiqure 8. The effect of an ill-opened diaphragm,on the middle pressure trace.

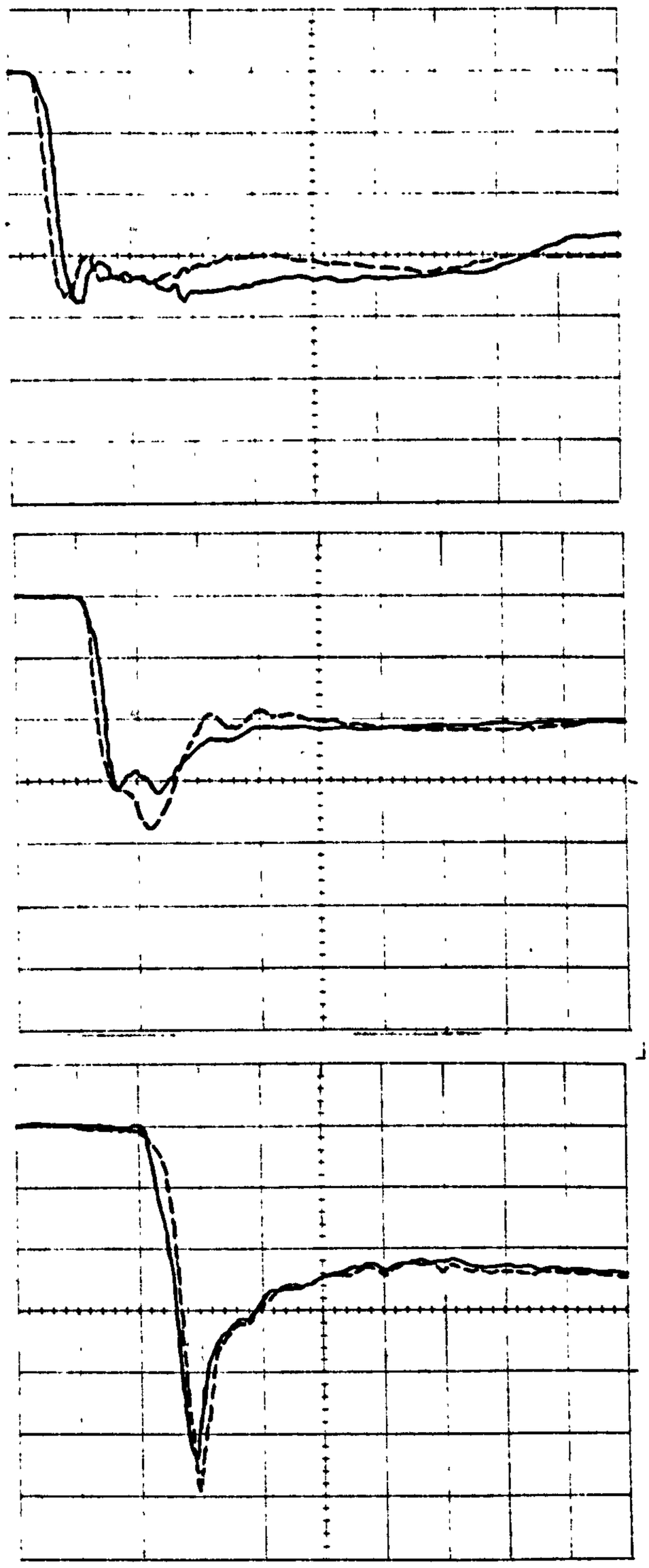

Figure 9. Reproducibility of the initial decompression (400μsec/div) at the three (top(1bar/div),middle(1bar/div),bottom(0.845bar/div)) pressure stations (w.r.t. the plots position).(test no 124,P_{in} = 5.26 bar,T_{in} = 17.23°C). (top:__test no 126,- -test no 124,middle:__test no 202,- -test no 203 ,bottom:__test no 44,- -test no 42).

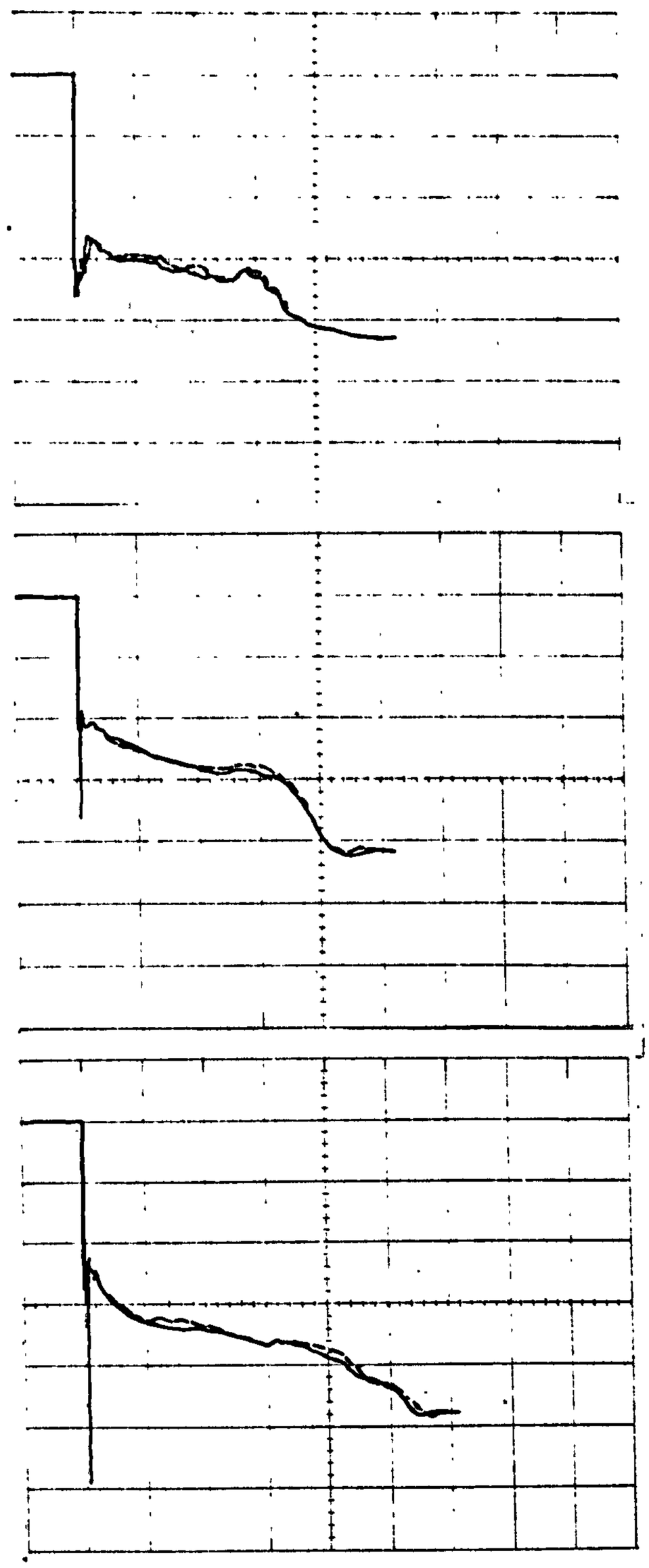

Figure 10. Reproducibility of the long term (20 msec/div) decompression at the three (top(1bar/div),middle(1bar/div),bottom (0.845bar/div)) pressure stations (w.r.t the plots position).(P_{in} = 5.26 bar,T_{in} = 17.2°C). (top:__test no 126,- -test no 124,middle:__test no 203,- -test no 202 ,bottom:__test no 42,- -test no 44).

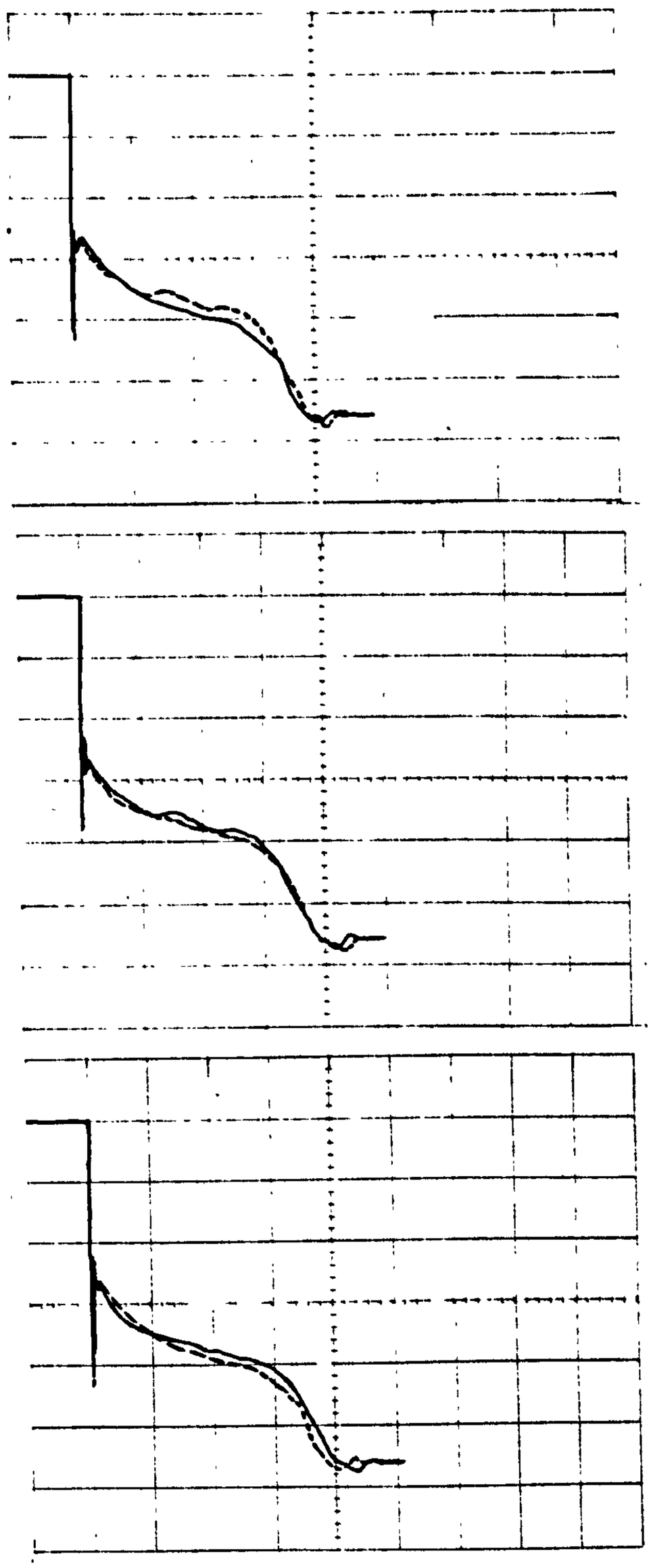

Figure 11. The roughness effect on the long term decompression(20ms/div, 1bar/div,mild steel vessel).(P_{in} = 6.91bar,T_{in} = 27.1°C). (top:__test no 199,- -test no 215,middle:__test no 215,- -test no 221 ,bottom:__test no 221,- -test no 199).

Perspex

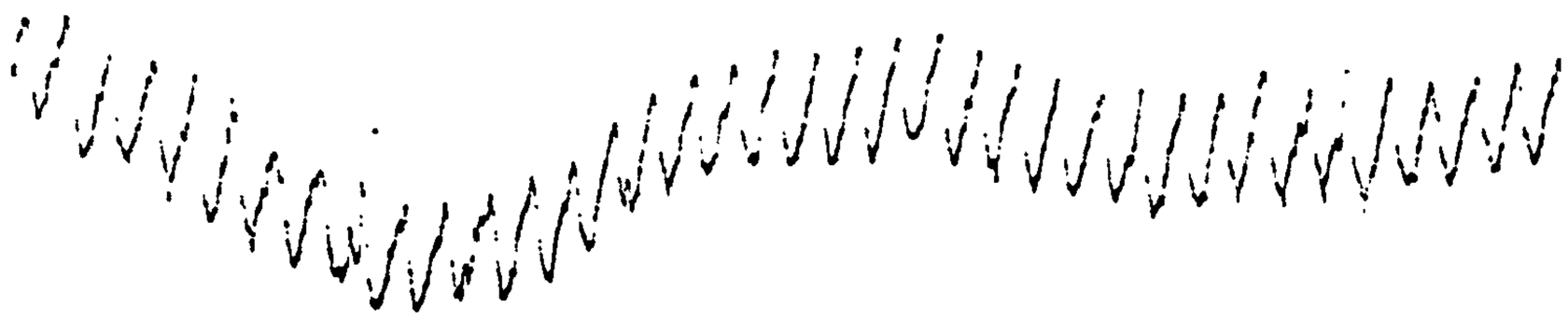

Mild steel - fine turning

Mild steel - hand polish

Figure 12. Profilometry for both perspex and mild steel vessels.

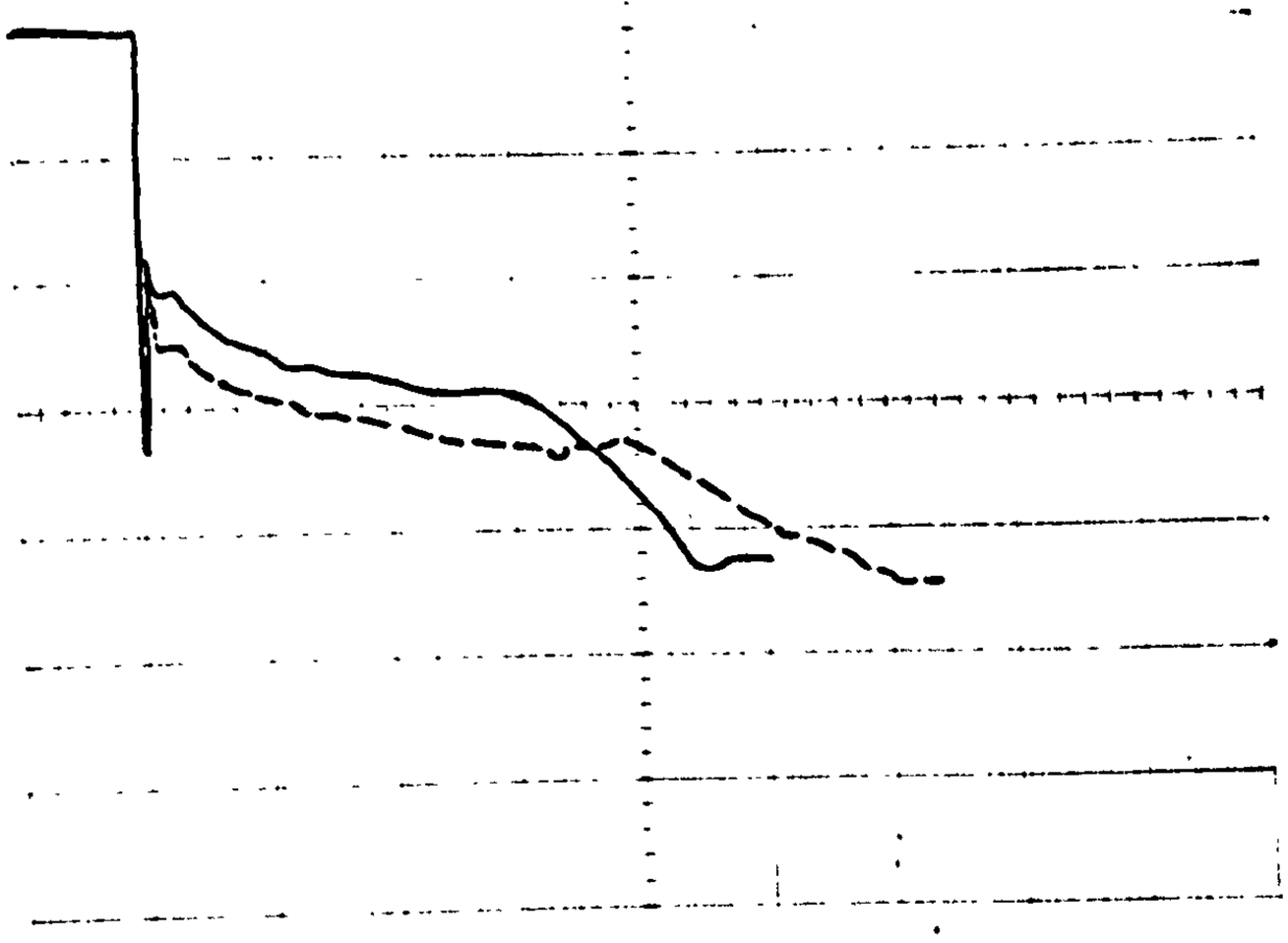

Fiqure 13. The effect of different material on the long term depressurisation (20msec/div,1bar/div).(P_{in} = 5.32bar, T_{in} = 17.5°C).(__test no 216 (mild steel),- -test no 8 (perspex)).

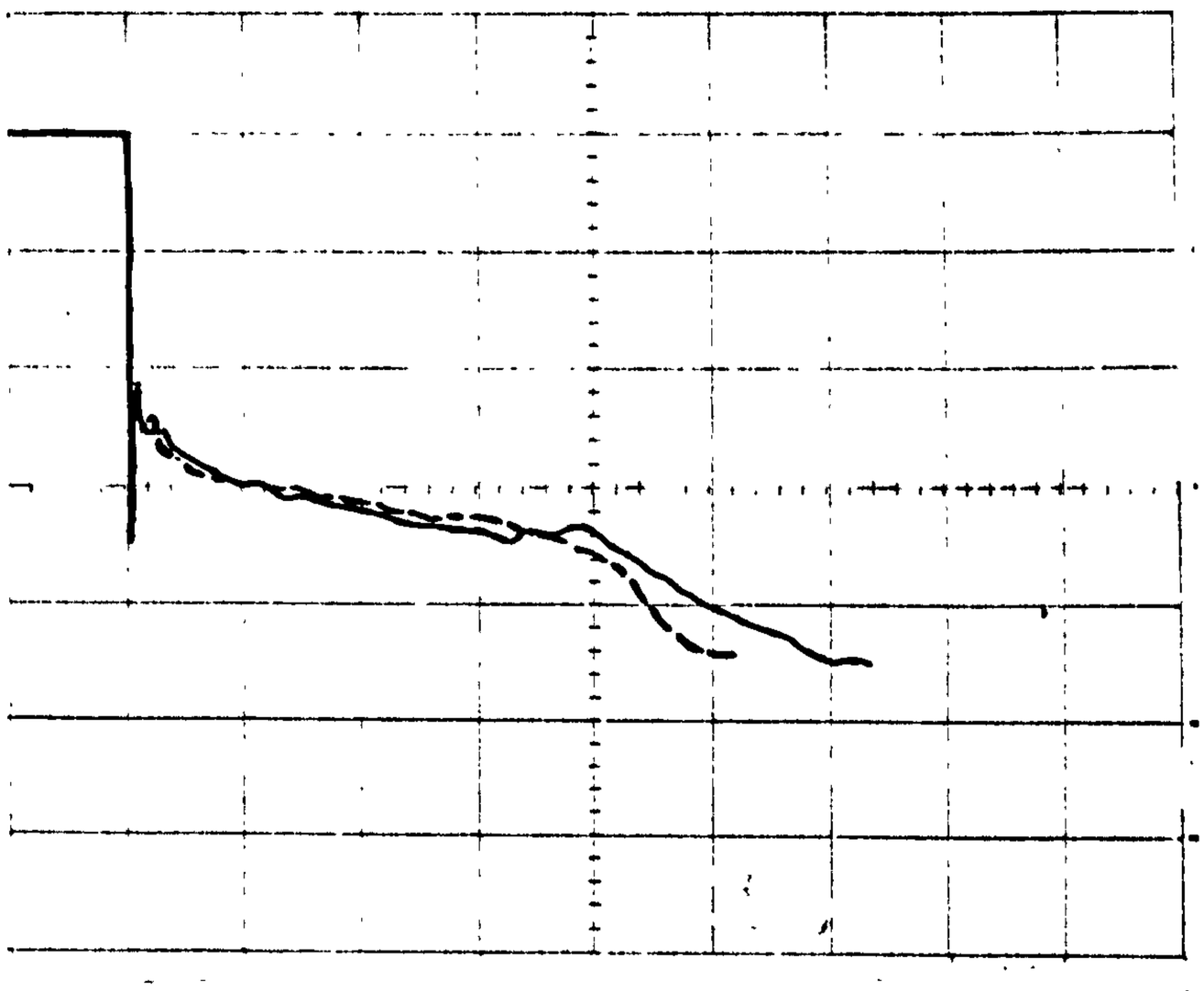

Figure 14. The roughness effect on the long term depressurisation history (20msec/div,1bar/div,perspex vessel).(P_{in} = 5.32bar, T_{in} = 17.5°C,__test no 8,- -test no 124).

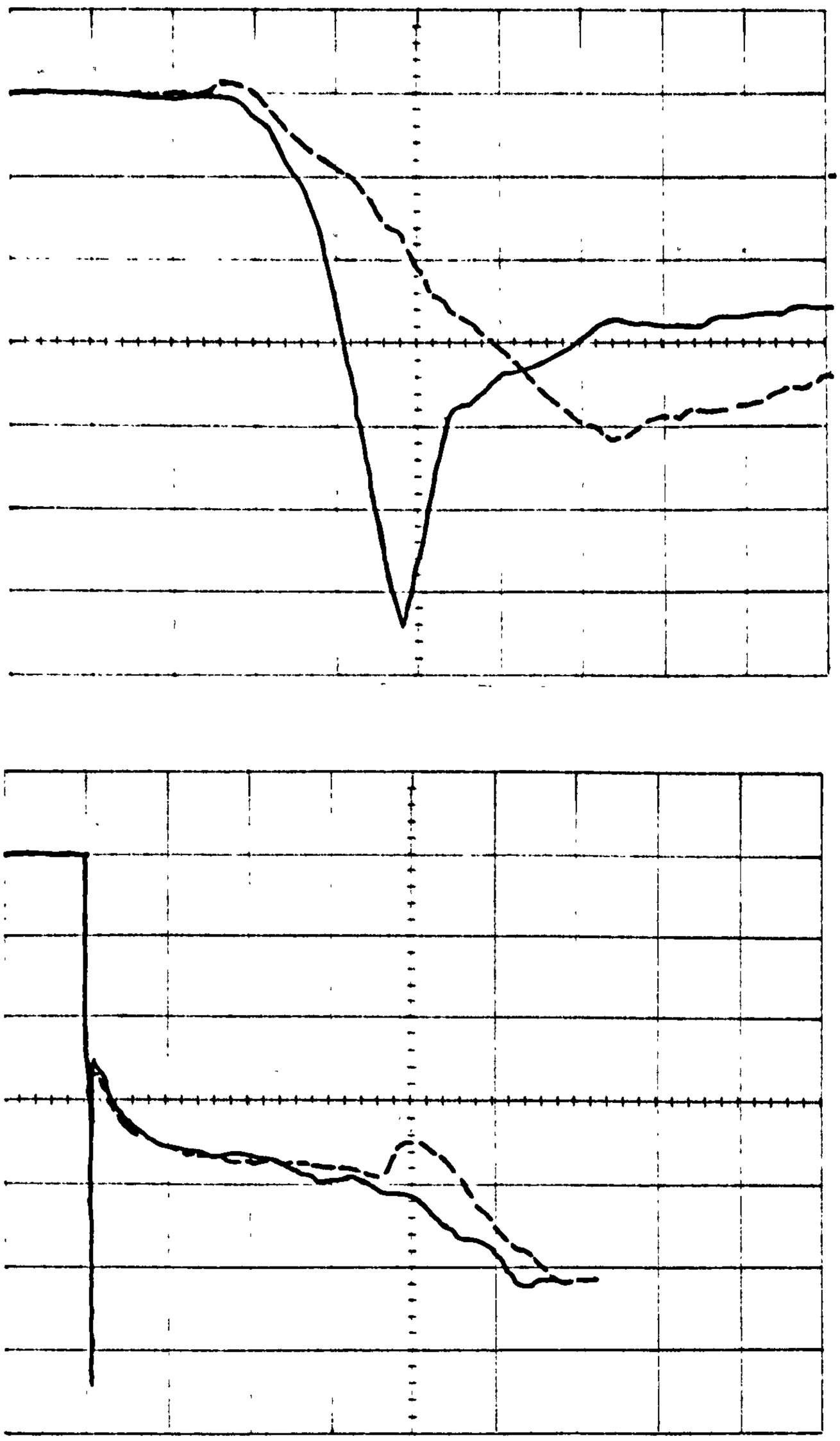

Figure 15. The orientation (vertical-horizontal) effect on the initial (100μsec/div) and long (20msec/div) term decompression at the bottom pressure station (0.85bar/div),(w.r.t. the plots position). (P_{in} = 5.2 bar, T_{in} = 17°C, __ test no 51 (vertical) ,- -test no 14 (horizontal)).

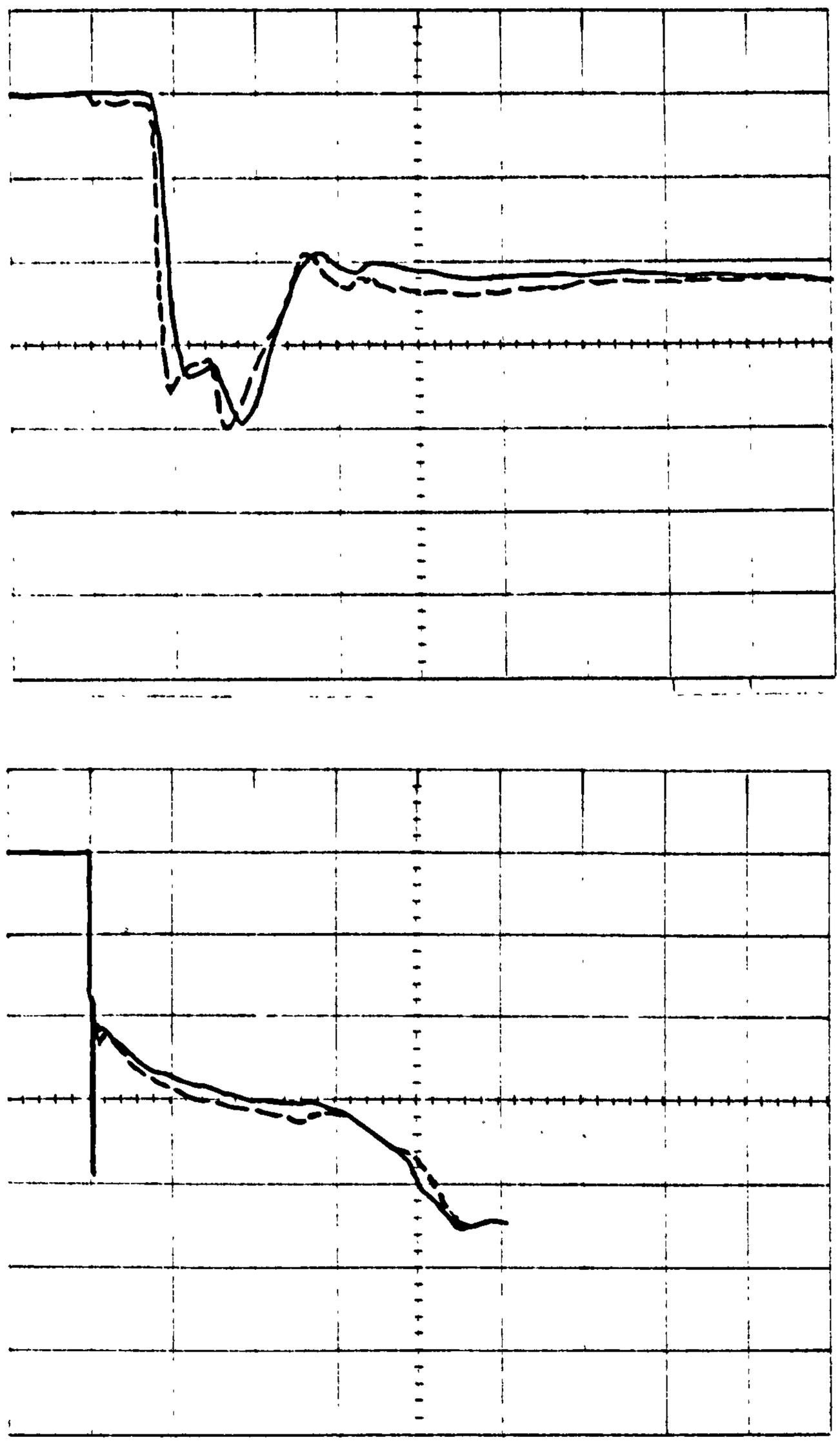

Figure 16. The orientation (vertical-horizontal) effect on the initial (400μsec/div) and long (20msec/div) term decompression,at the middle pressure station (1bar/div), (w.r.t the plots position).(P_{in} = 5.5 bar,T_{in} = 18.8°C ,__test no 228 (vertical),- -test no 233 (horizontal)).

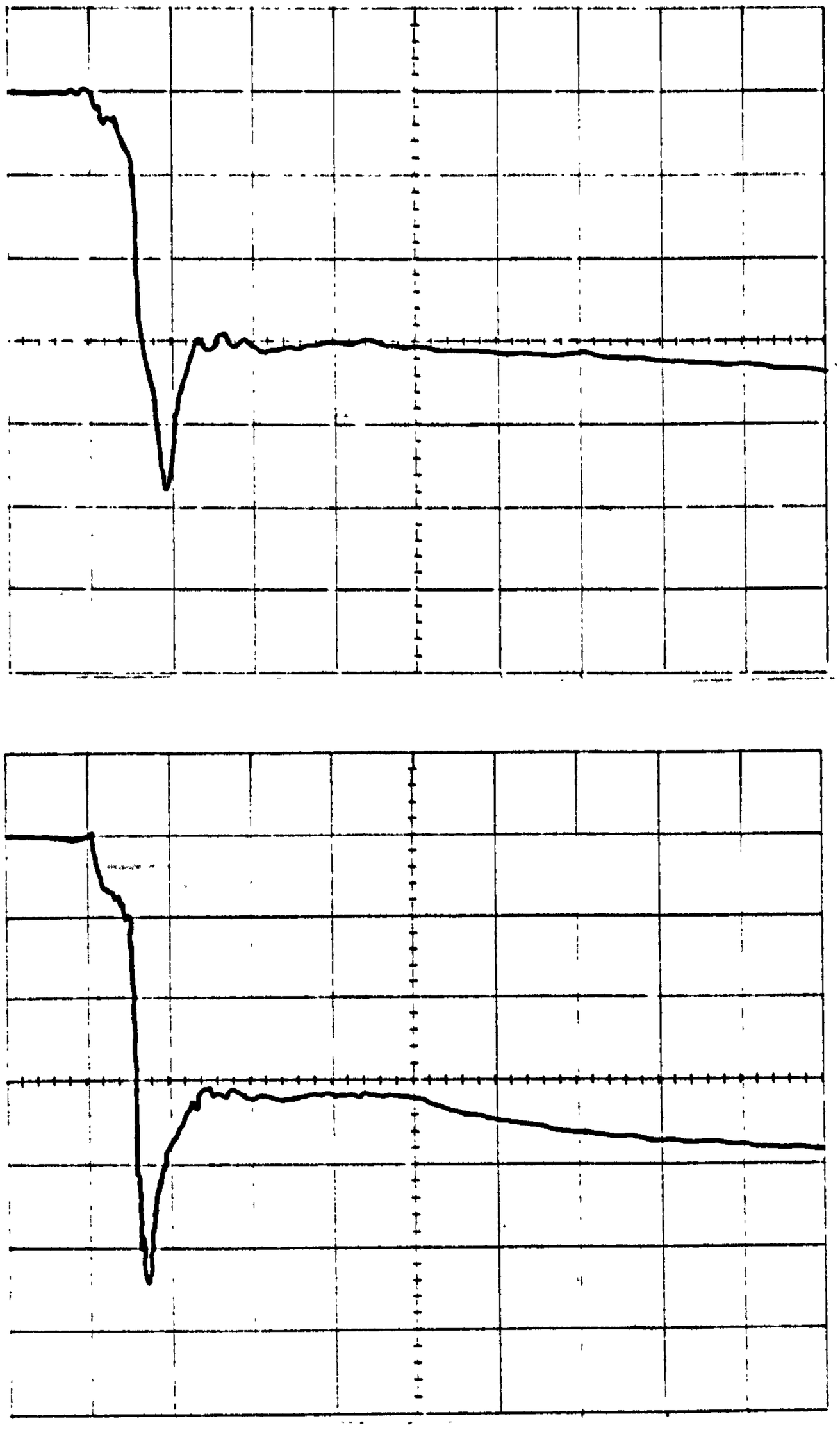

Figure 17. Typical initial decompression history (1msec/div) at the two (middle(1bar/div),bottom(0.845bar/div)) pressure stations (w.r.t. the plots position), during blowdown from a vessel with horizontal orientation. (P_{in} = 6 bar, T_{in} = 17.45°C).

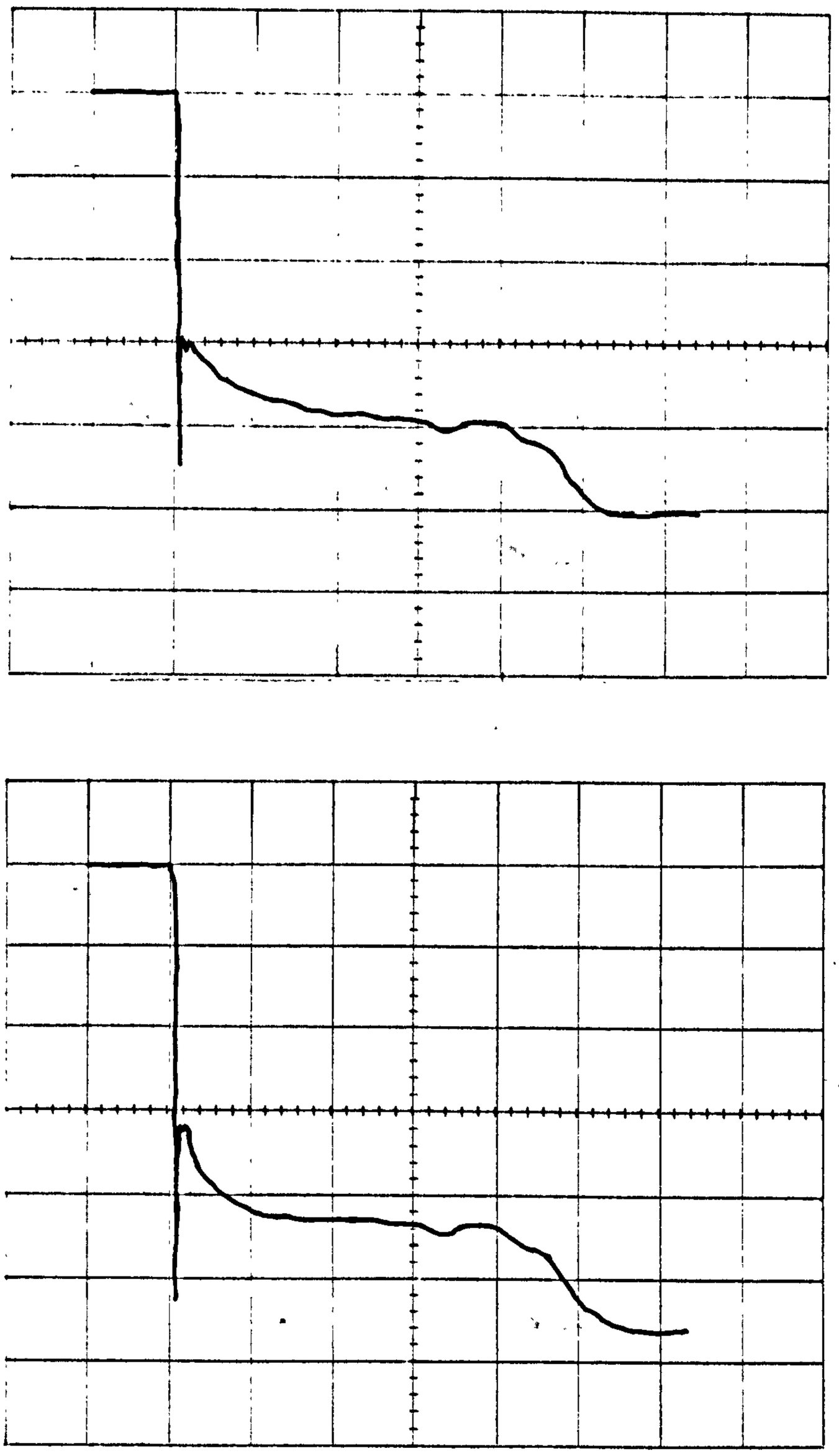

Figure 18. Typical long term depressurisation (20msec/div) at the two (middle(1bar/div),bottom(0.845bar/div)) pressure stations (w.r.t the plots position),during blowdown from a vessel with horizontal orientation. (P_{in} = 6bar,T_{in} = 17.45°C).

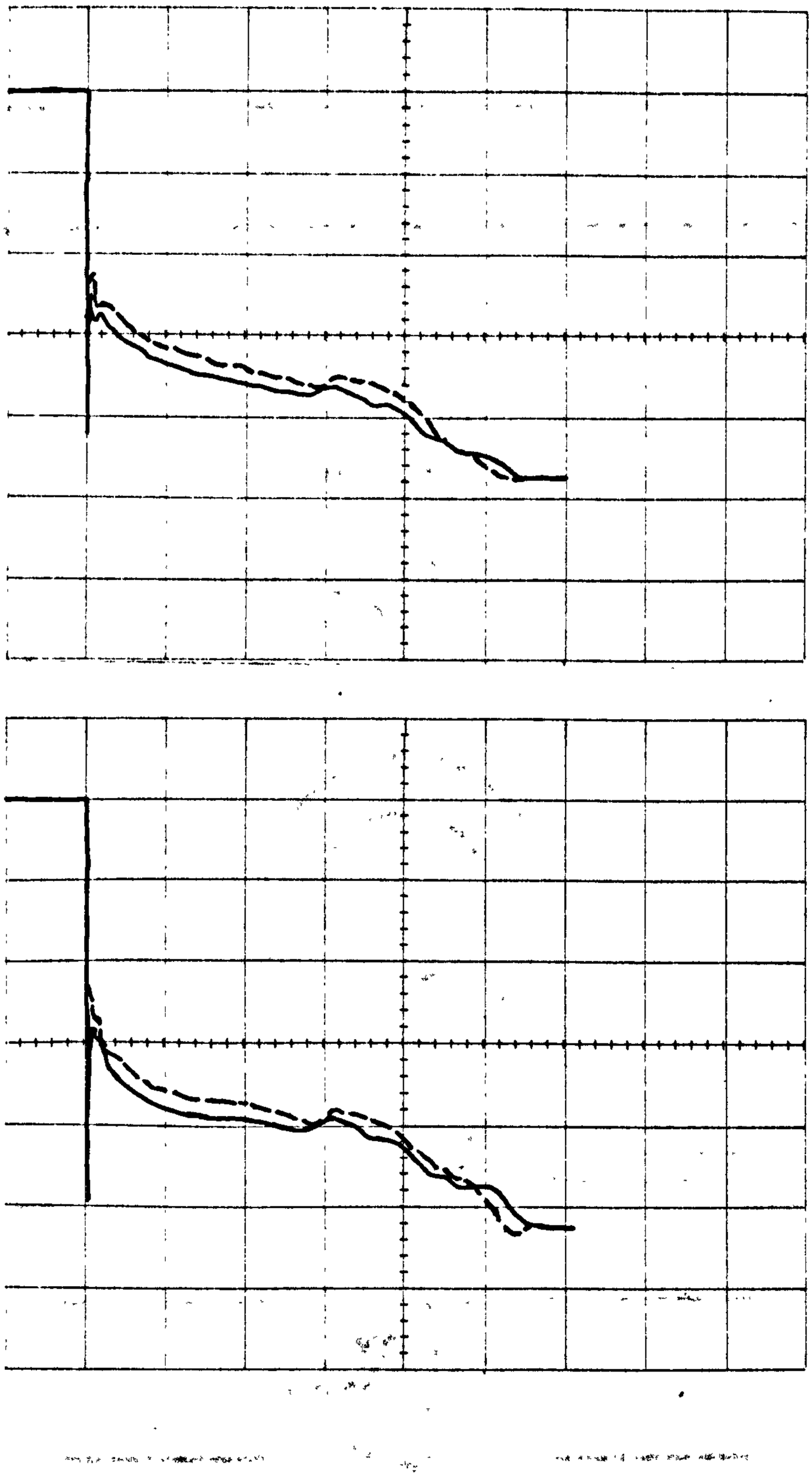

Fiqure 19. The effect of varing the initial temperature on the long term pressure history (20msec/div), at the two (middle(1bar/div),bottom(0.845bar/div)) pressure stations (w.r.t the plots position). (P_{in} = 5.7bar,__test no 19 (T_{in} = 17.8°C),- -test no 58 (T_{in} = 20.15°C)).

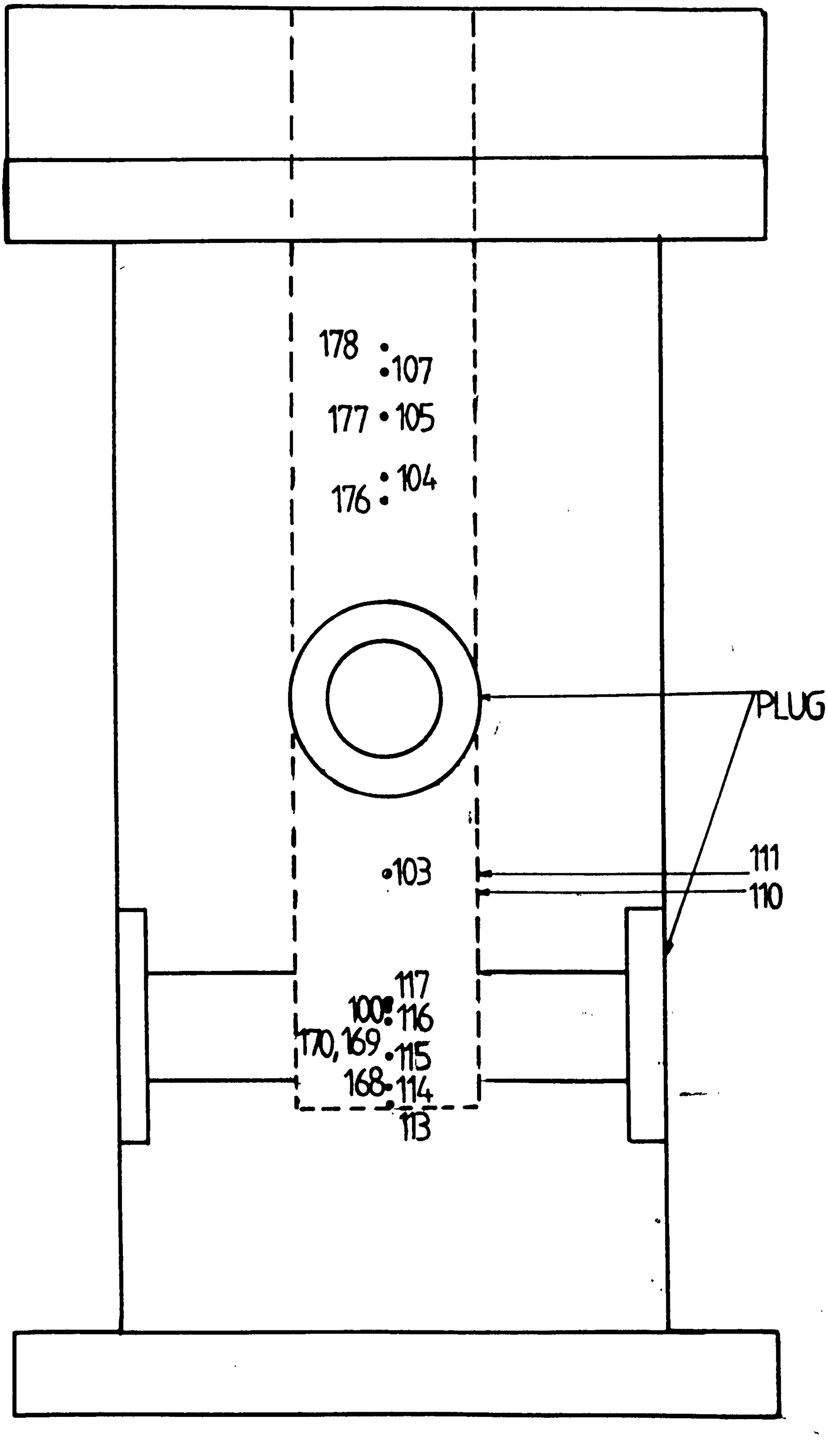

Figure 20. Illustrating diagram of the laser measurments set up.

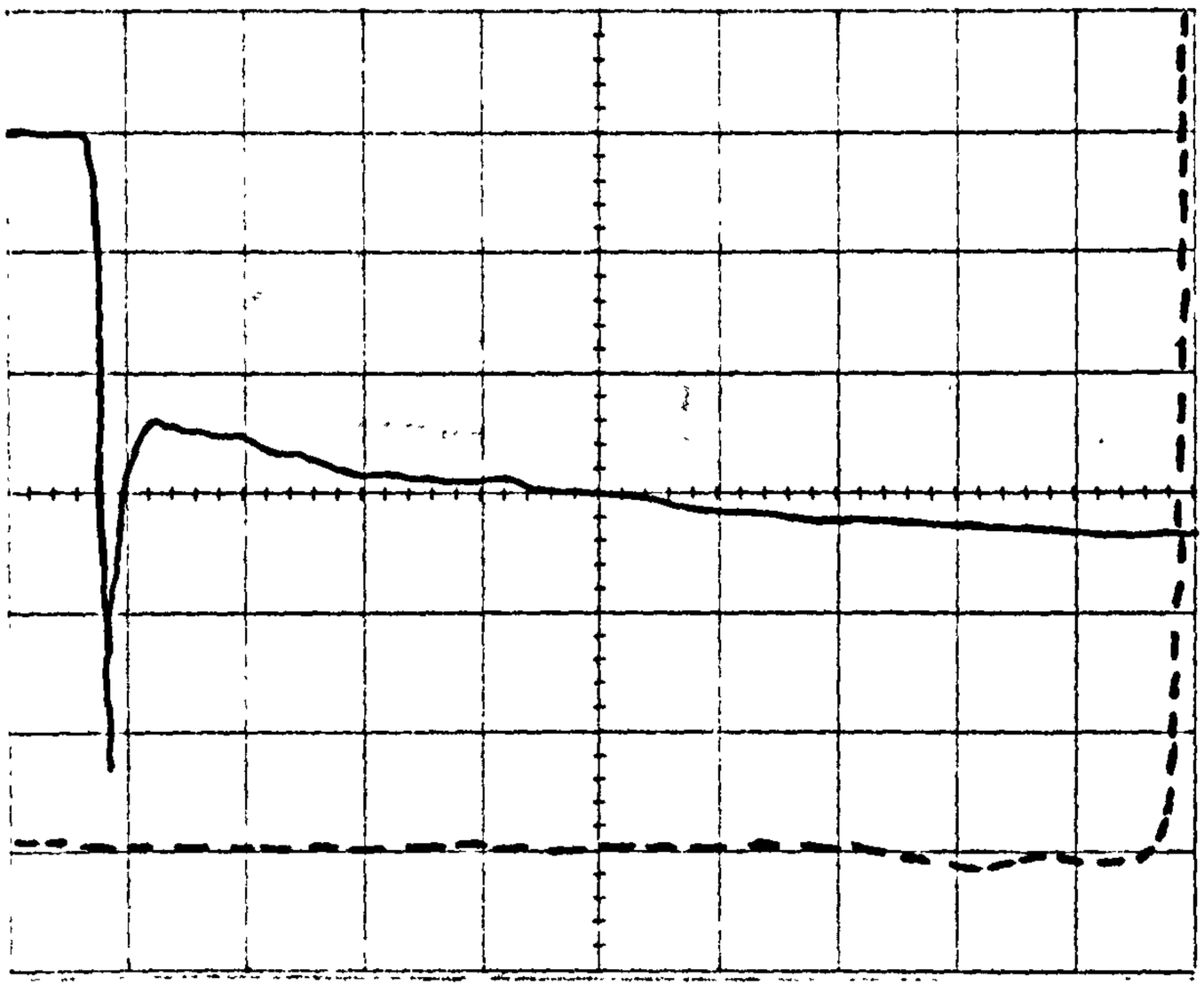

Figure 21. A typical laser output. (__pressure trace,- -laser output).

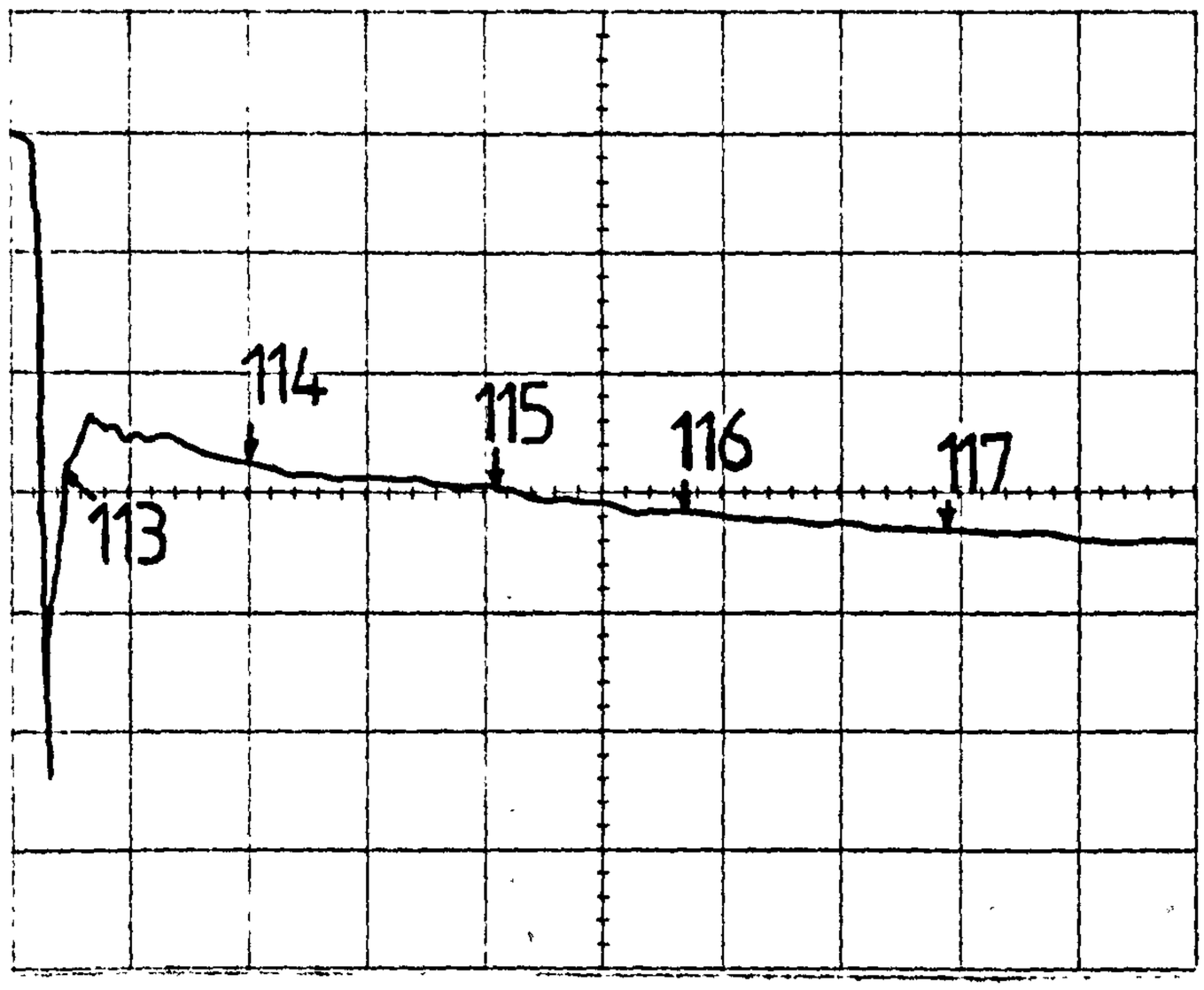

Figure 22. The laser beam block off delay time,illustrated on a typical initial decompression history. (0.845bar/div,2msec/div).

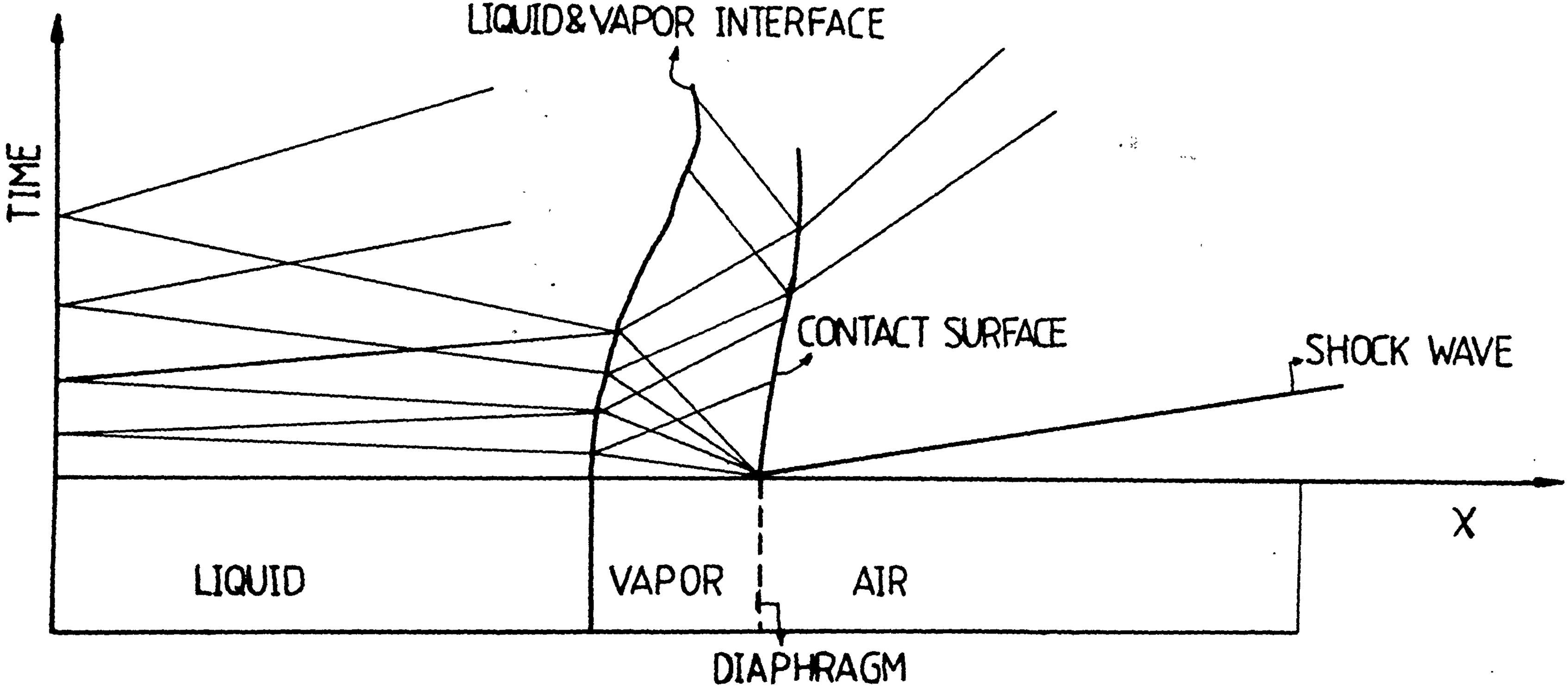

Figure 23. Typical wave action on a x-t plane,encountered in a typical shock tube problem.

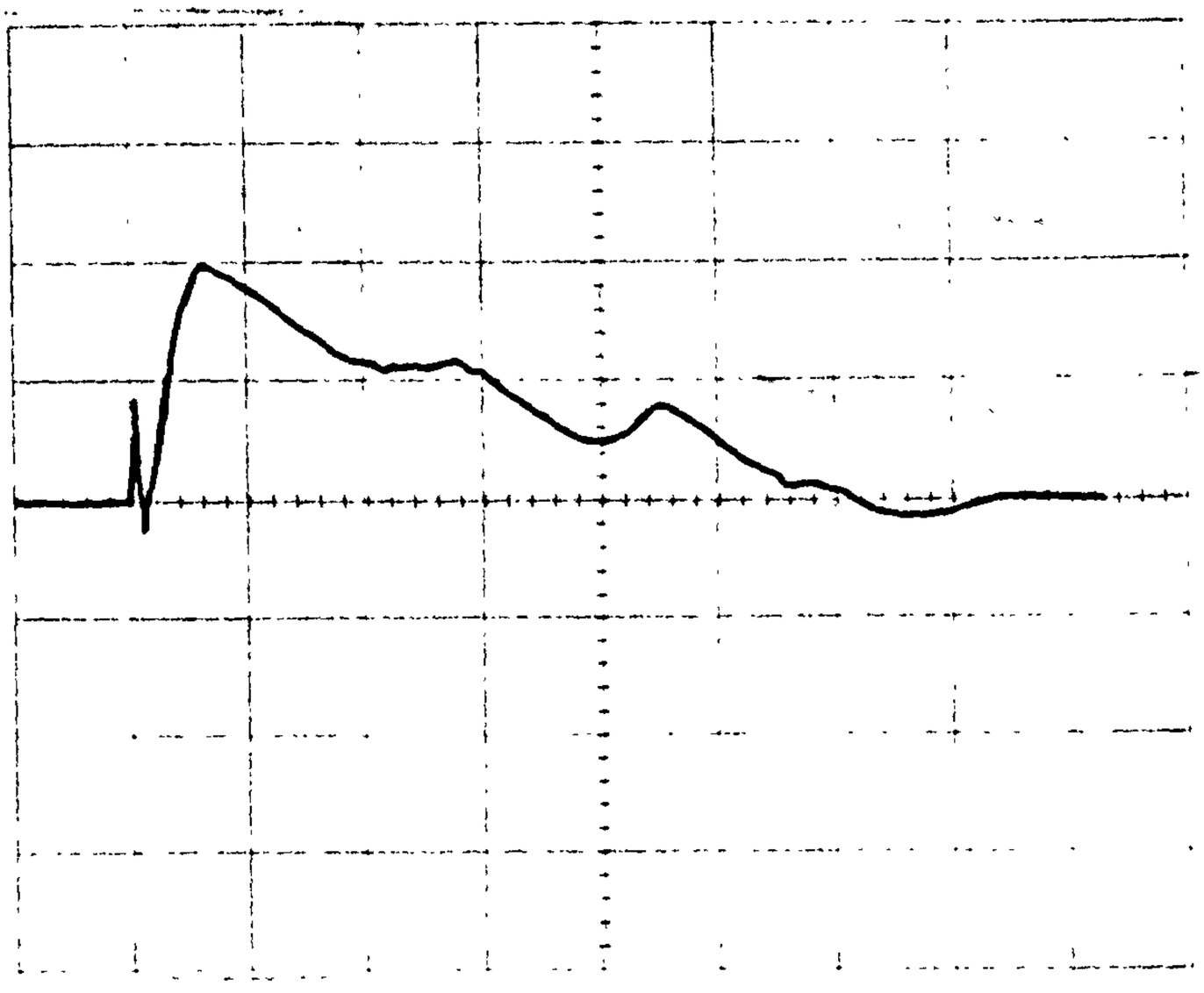

Figure 24. Typical long term decompression recorded by the vent pipe pressure station.(0.833bar/div,20msec/div).

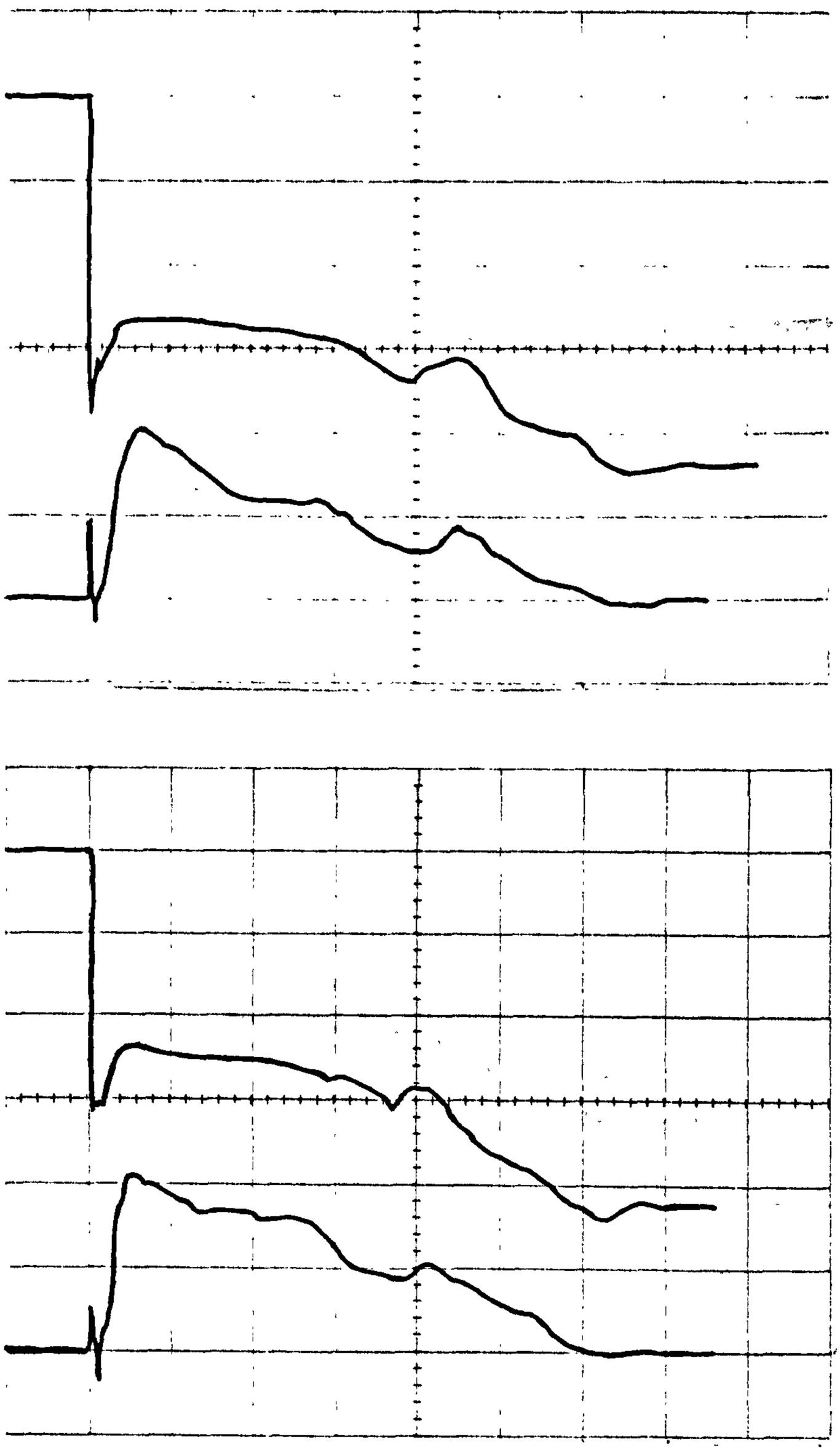

Figure 25. Coplot of long term decompressions (20msec/div),recorded by both the top (1bar/div) and the vent pipe (top:0.833bar/div,bottom: 1.52bar/div) pressure stations. (P_{in} = 5.25bar,T_{in} = 17.1°C)

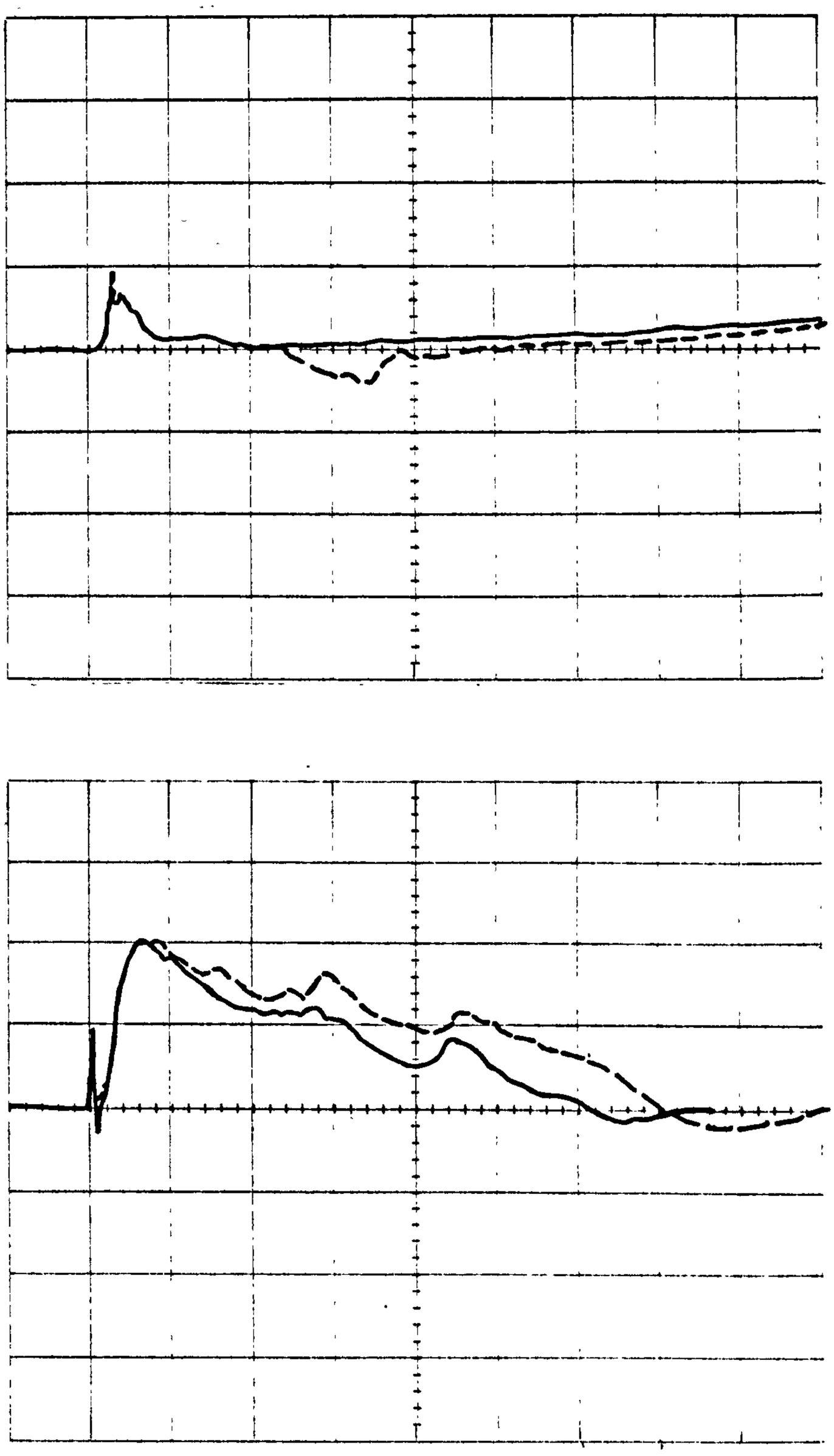

Figure 26. The effect of varing the vent pipe length on the pressure trace,recorded in the vent pipe region (initial (400μsec/div) and long (20msec/div) term decompression (0.833bar/div) respectivelly).(P_{in} = 5.25bar ,T_{in} = 17.1°C,__test no 139 (vent pipe length:1m),- -test no 141 (vent pipe length:0.5m)).

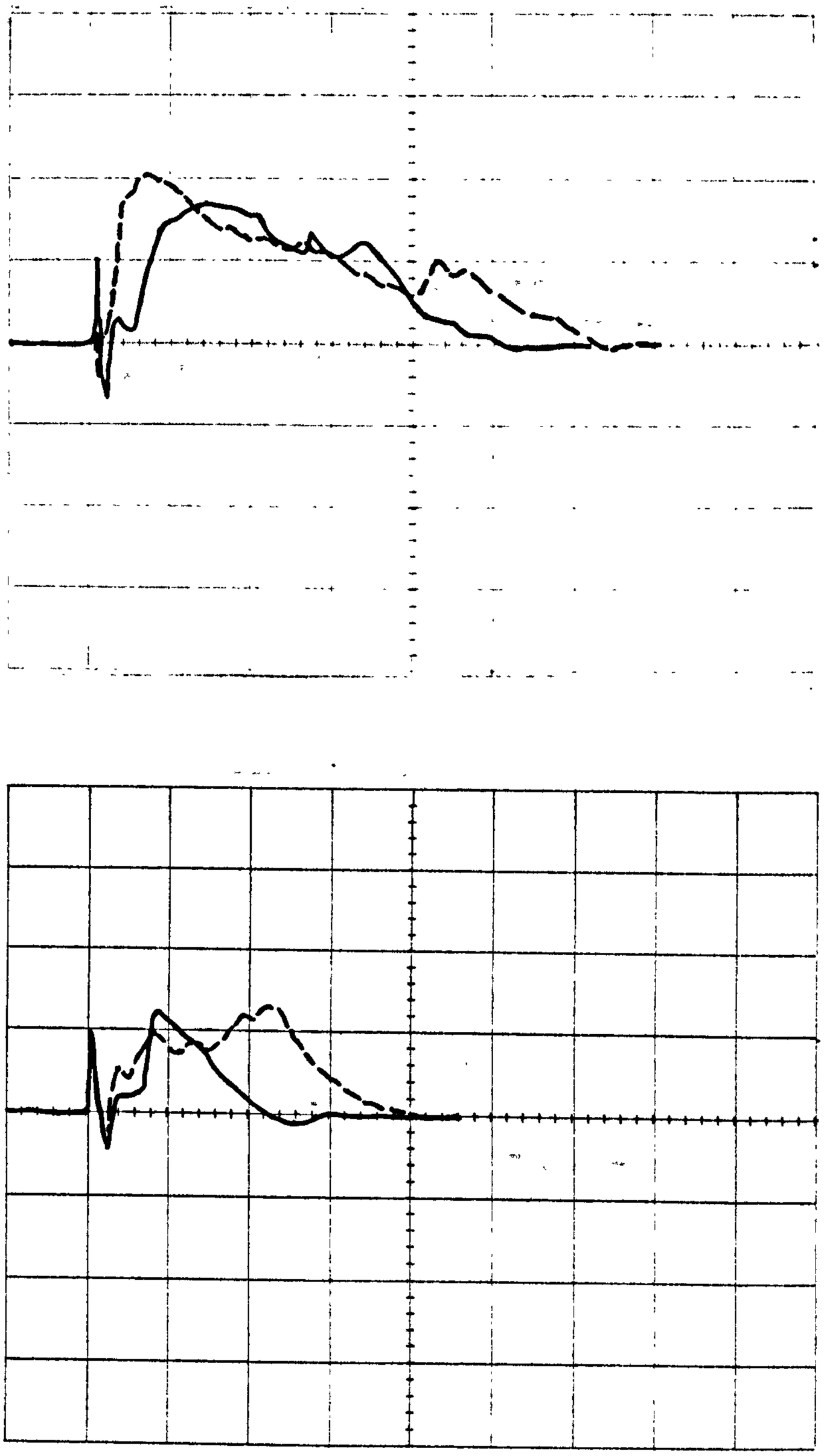

Figure 27. The effect of a "partially full" vessel blowdown on the vent pipe pressure history (long term (20msec/div)). Vent pipe length:0.2m.(0.833bar/div,top:__100%full,--75%full, bottom:__25%full,- -50%full).

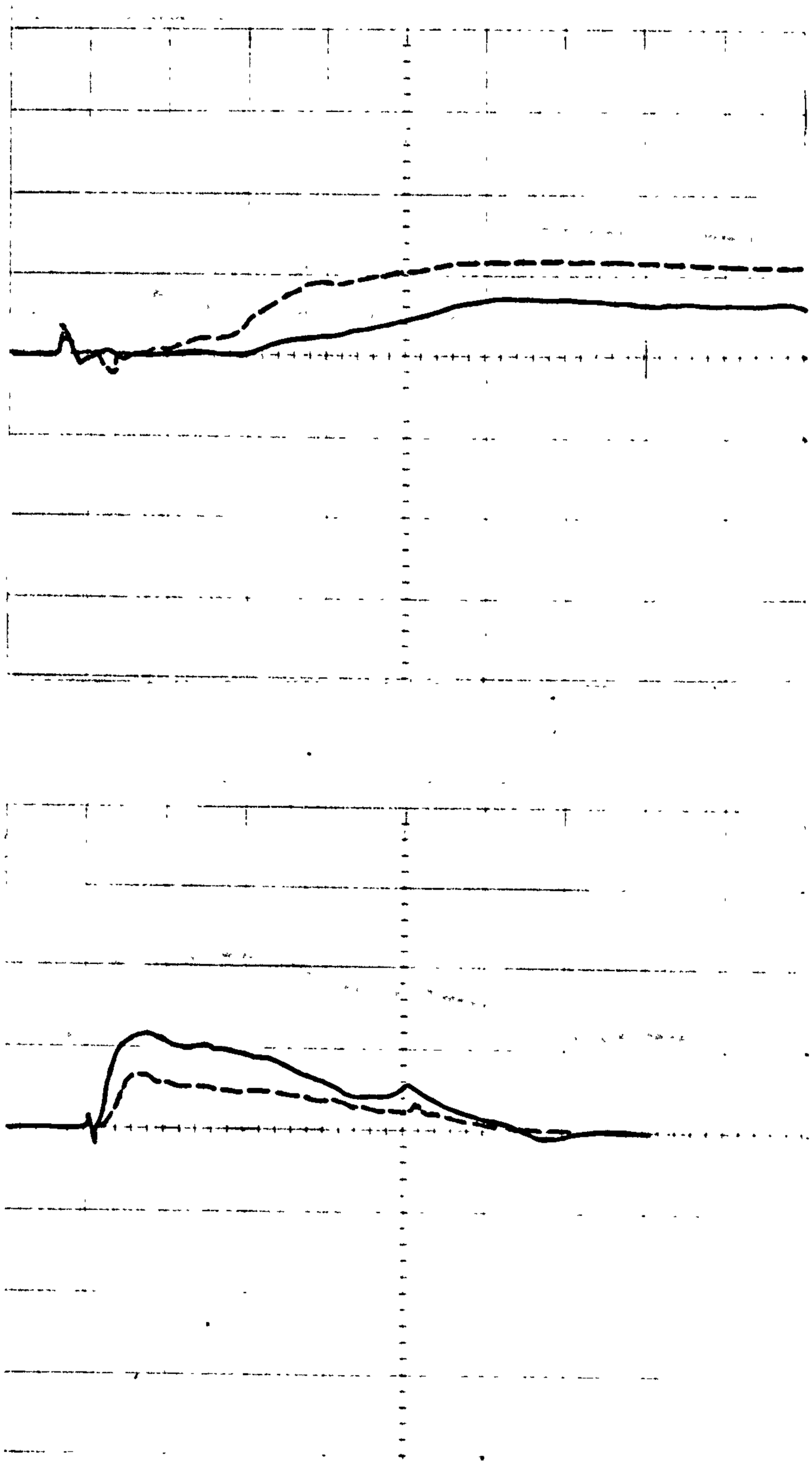

Figure 28. Comparison of two pressure traces,recorded at different locations along the vent pipe axis,(initial (2msec/div) and long (20msec/ div) term pressure (1.6bar/div) histories respectivelly).Vent pipe length:0.2 m.(__pressure station 60mm from diaphragm,--pressure station 163mm from diaphragm).

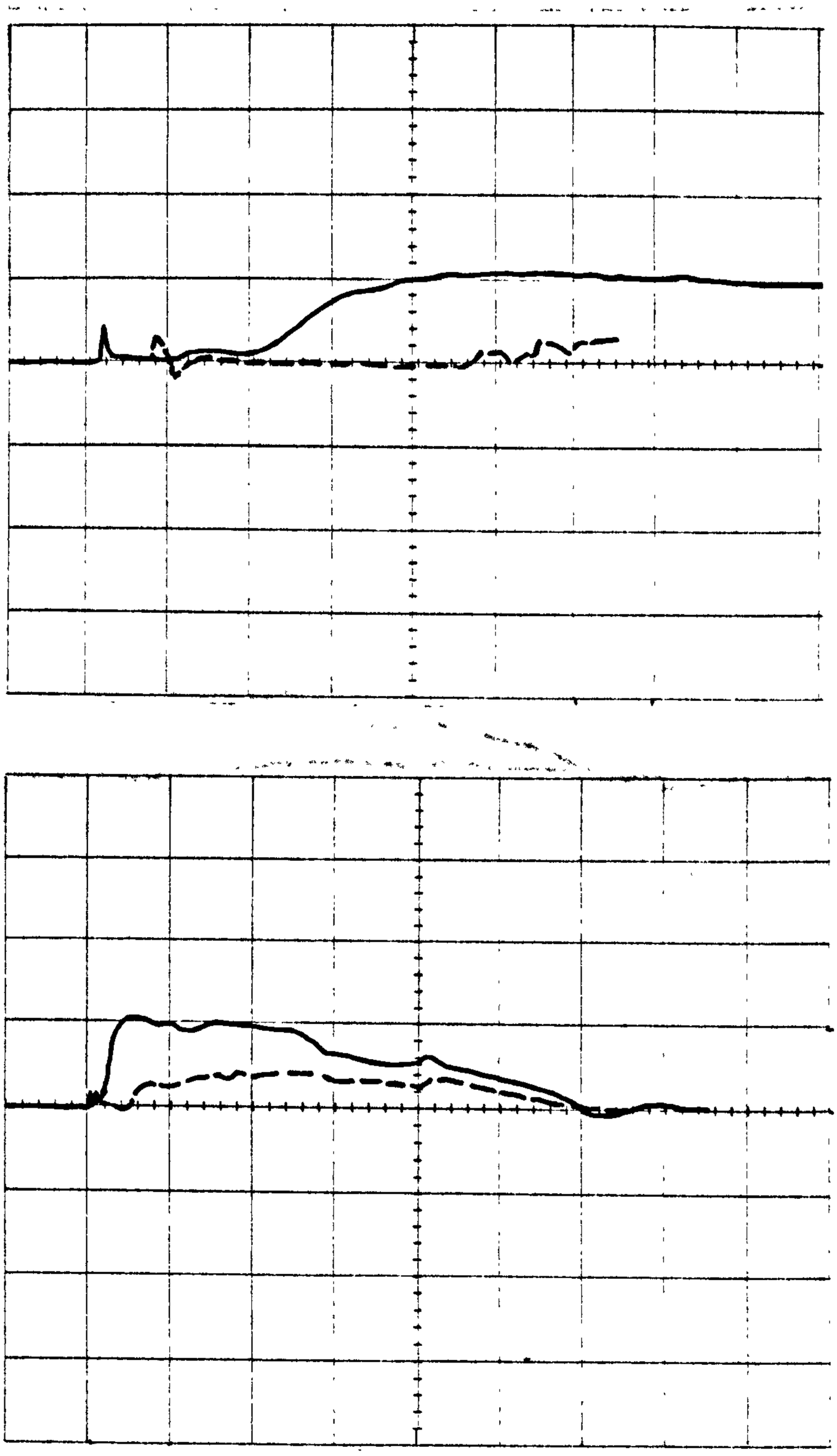

Figure 29. Comparison of two pressure traces,recorded at different locations along the vent pipe axis (initial (2msec/div) and long (20msec/ div) term pressure (1.6bar/div) histories respectivelly).Vent pipe length:0.5m.(__pressure station 66mm from diaphragm,--pressure station 457mm from diaphragm).

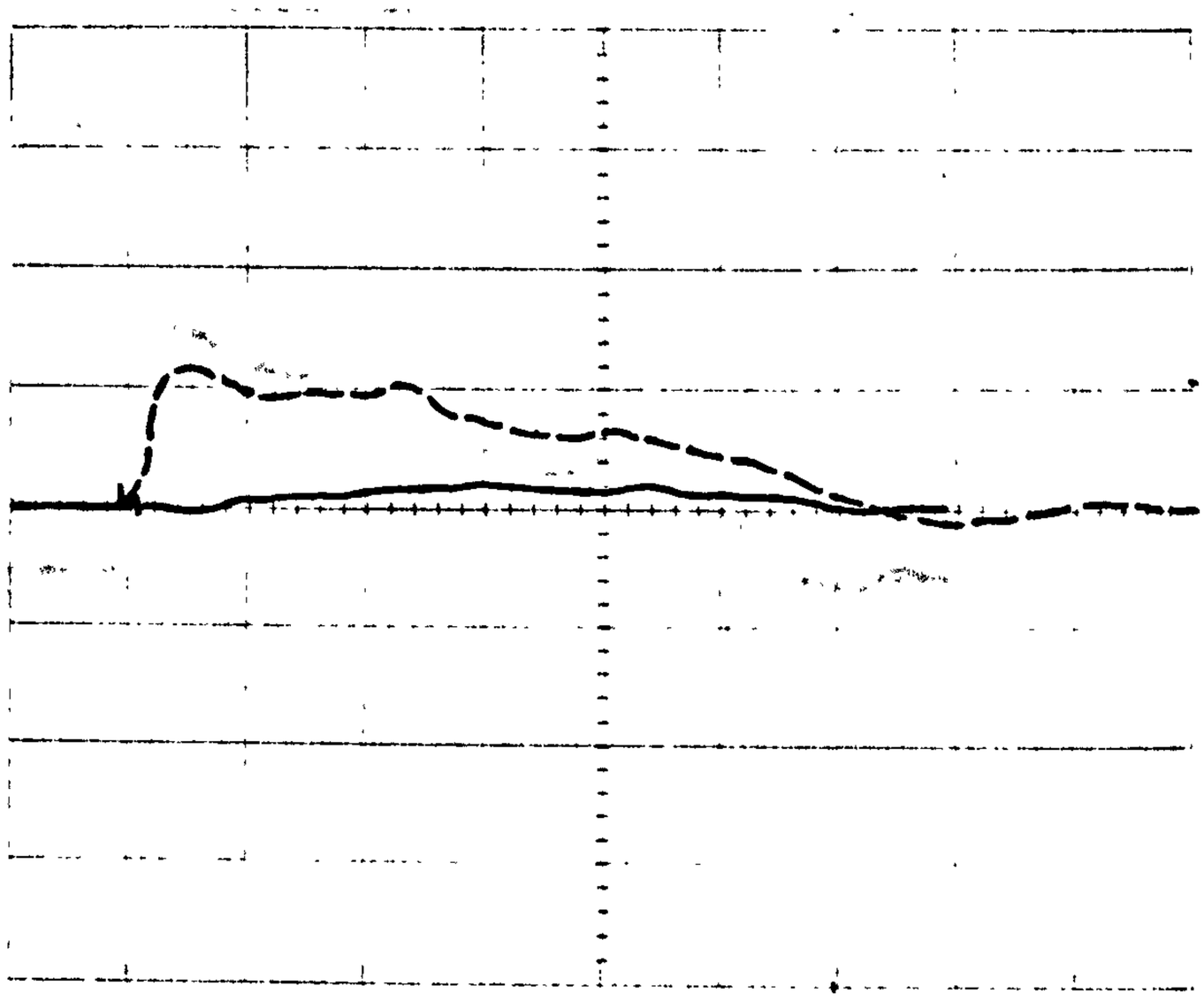

Figure 30. Comparison of two pressure traces recorded at different locations along the vent pipe axis, (long (20msec/div) term depressurisation (1.6bar/div)) Vent pipe length: 1.0m.(__pressure station 955mm from diaphragm,- - pressure station 60mm from diaphragm).

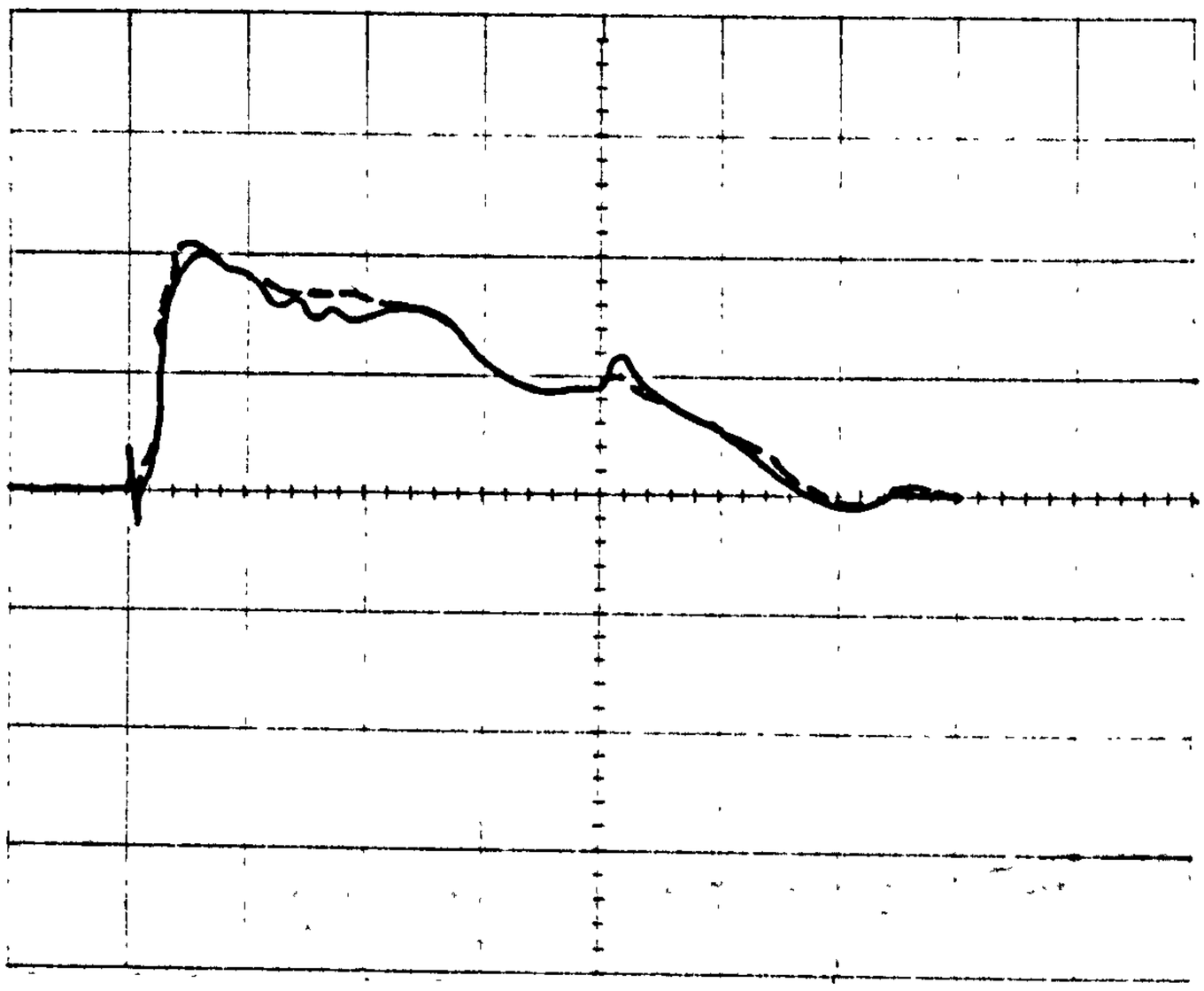

Fiqure 31. The effect of roughness on the long (20msec/div) term decompression (1.52bar/div) ,recorded by the vent pipe pressure station.Vent pipe length:0.2m.

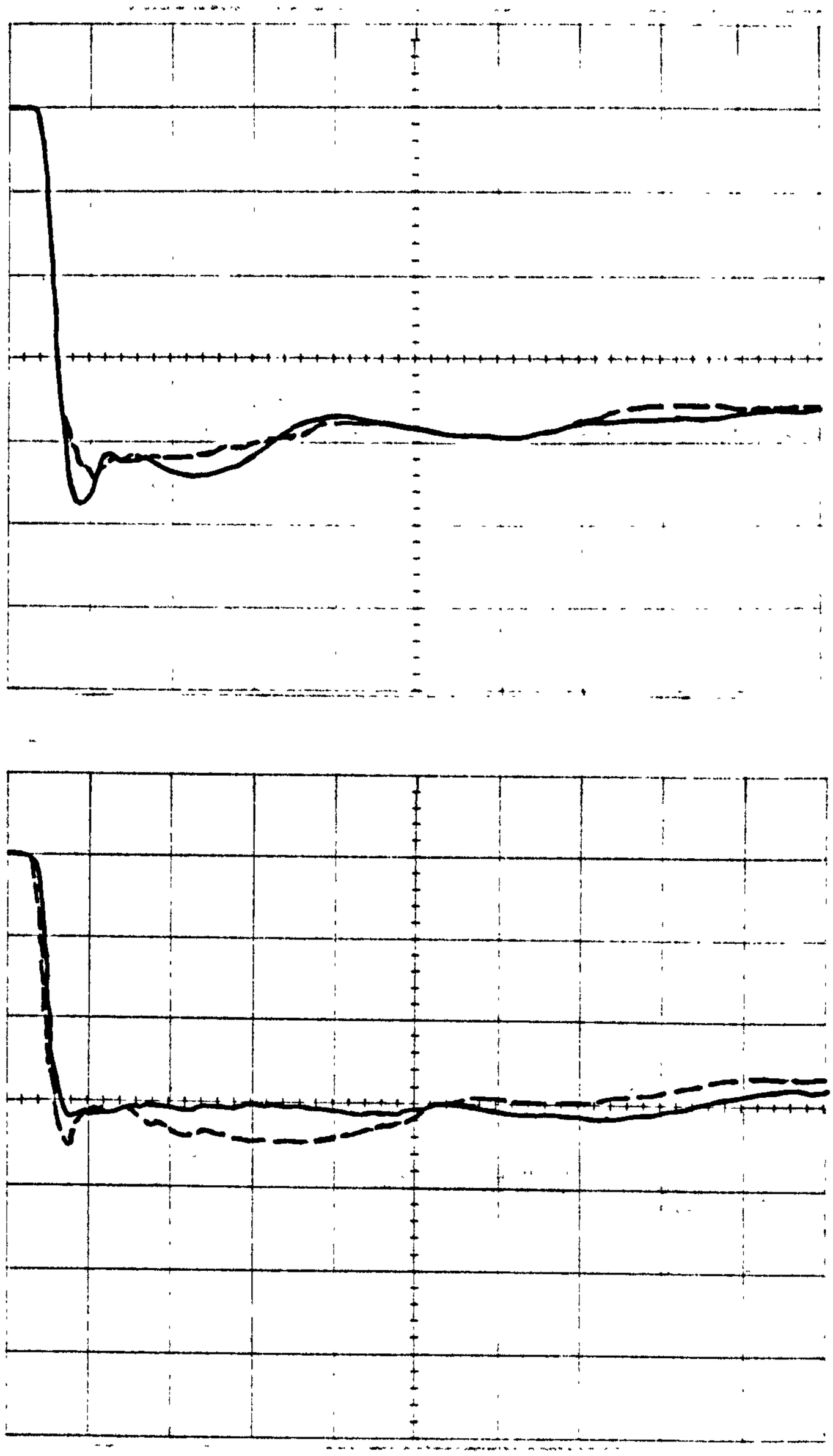

Figure 32. Initial (400μsec/div) depressurisation (1bar/div) history recorded by the top pressure station.(top:__test no 219,- -test no 209 ,bottom:__test no 193,- -test no 222).

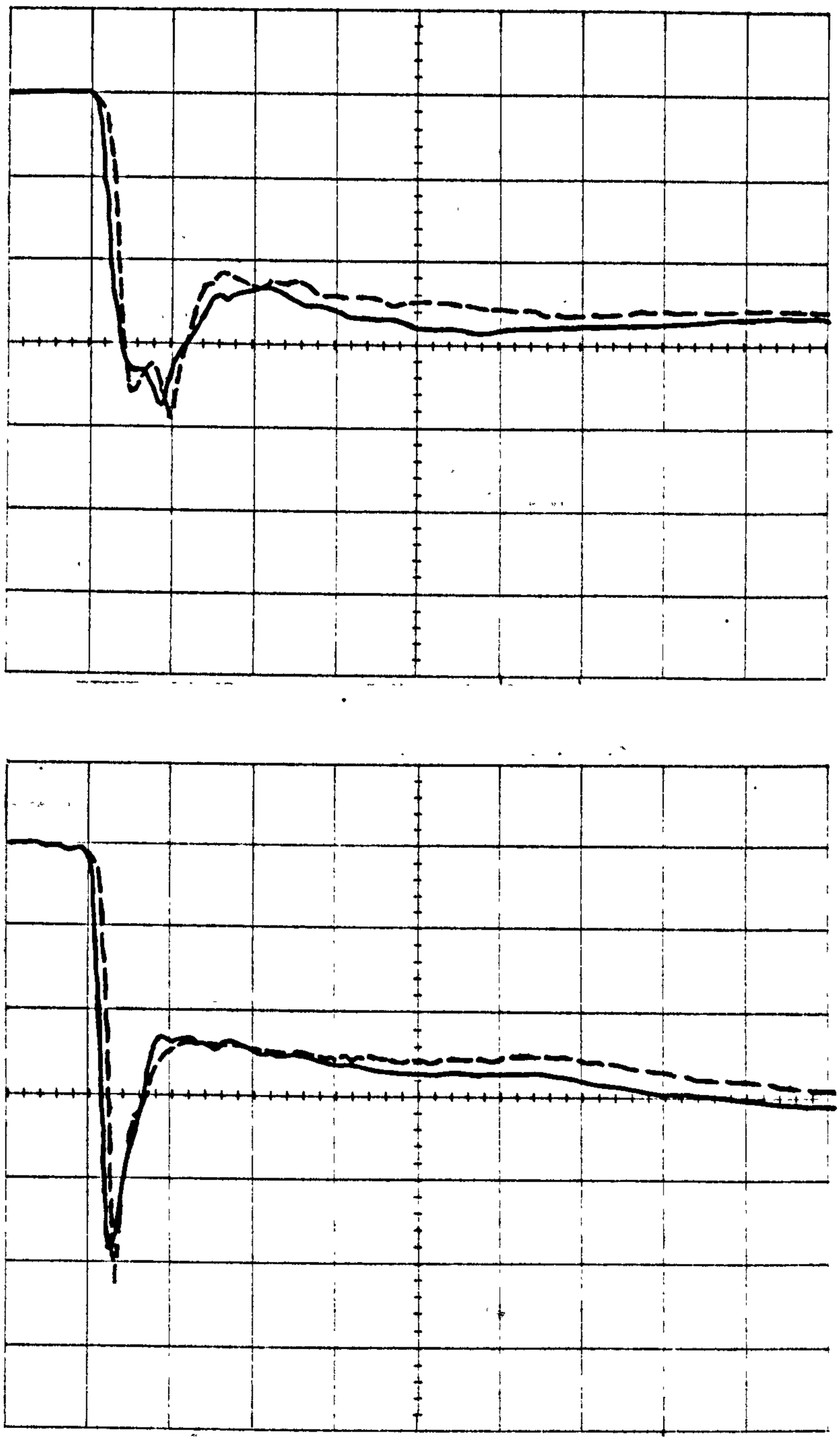

Figure 33. The effect of the "vacuum" pressure at the exit of the vessel,on the initial (500μsec/div) decompression, at the two (middle(1bar/div),bottom(0.89bar/div)) pressure stations (w.r.t. the plots position).(__test no 24(144mmHg pressure at the exit),- -test no 30(atmospheric conditions at the exit)).

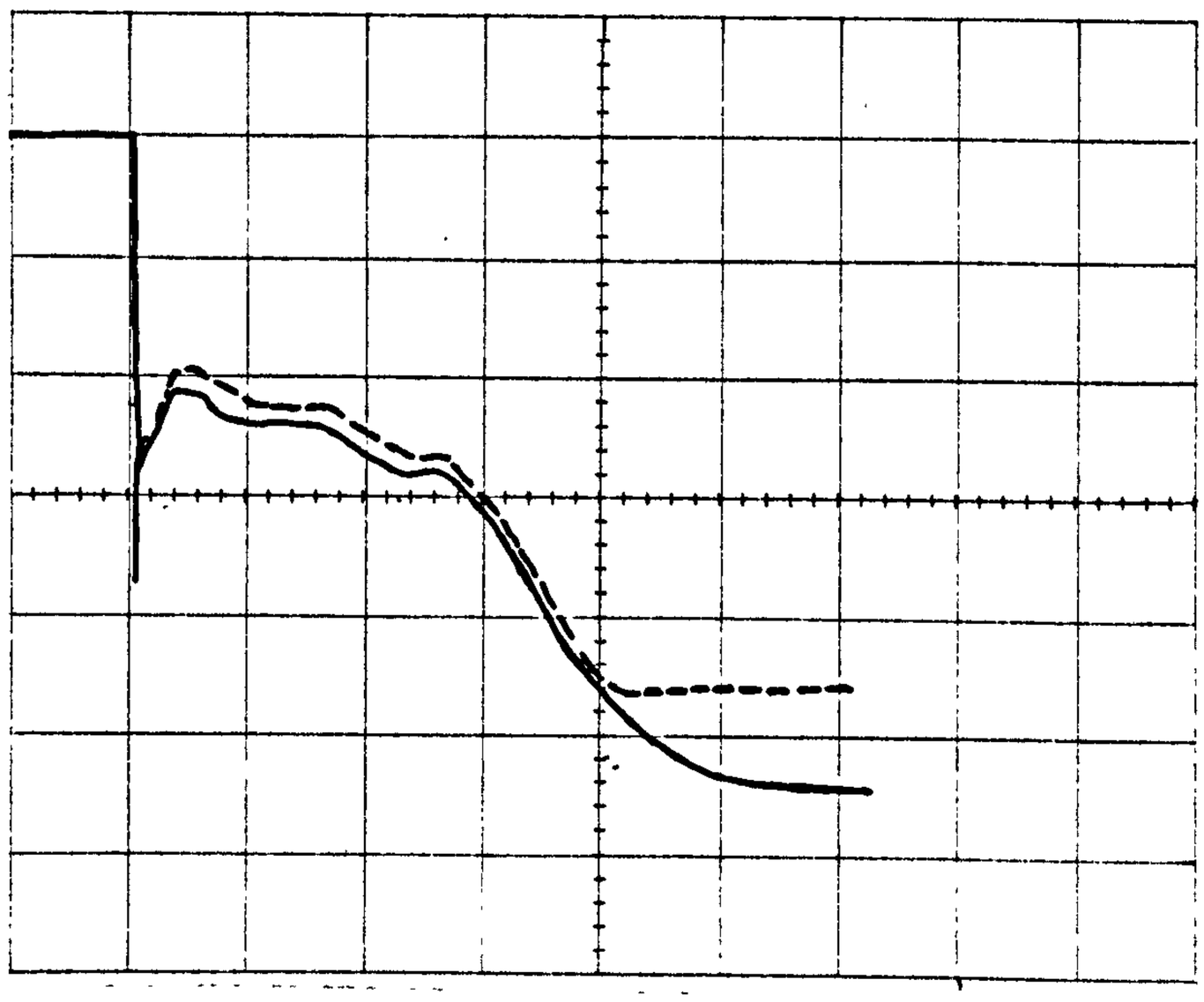

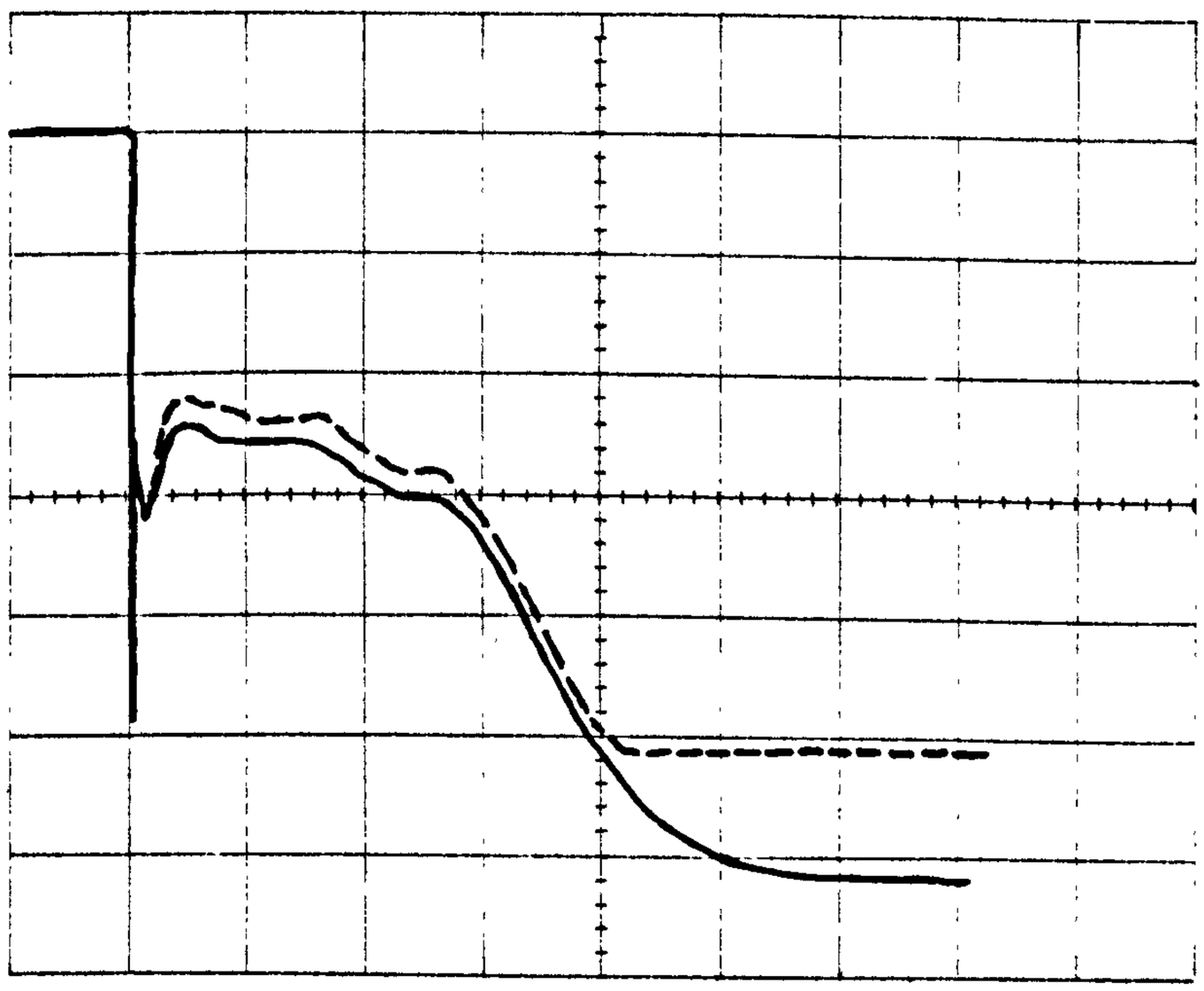

Figure 34. The effect of the "vacuum" pressure at the exit of the vessel,on the long (50msec/div) term decompression ,at the two (middle(1bar/div),bottom(0.89bar/div) pressure stations (w.r.t. the plots position).(top:__test no 24(144mm Hg pressure at the exit),--test no 30(atmosheric conditions at the exit)).

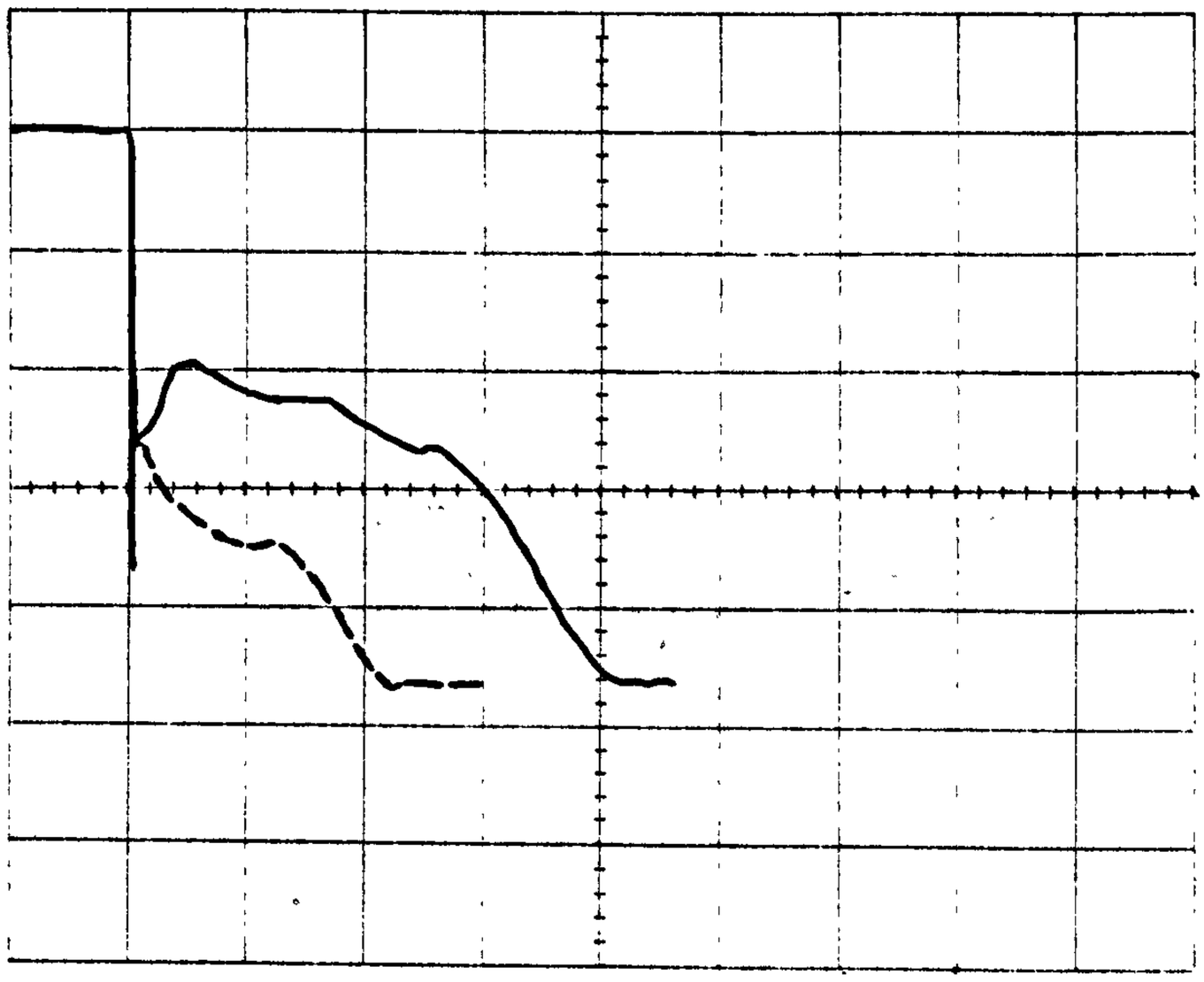

Figure 35. The effect of a bent vent pipe on the long (50msec/div) term decompression (1bar/div), recorded by the middle pressure station.(__test no 30(with bent vent pipe),- -test no 58(without bent vent pipe)).

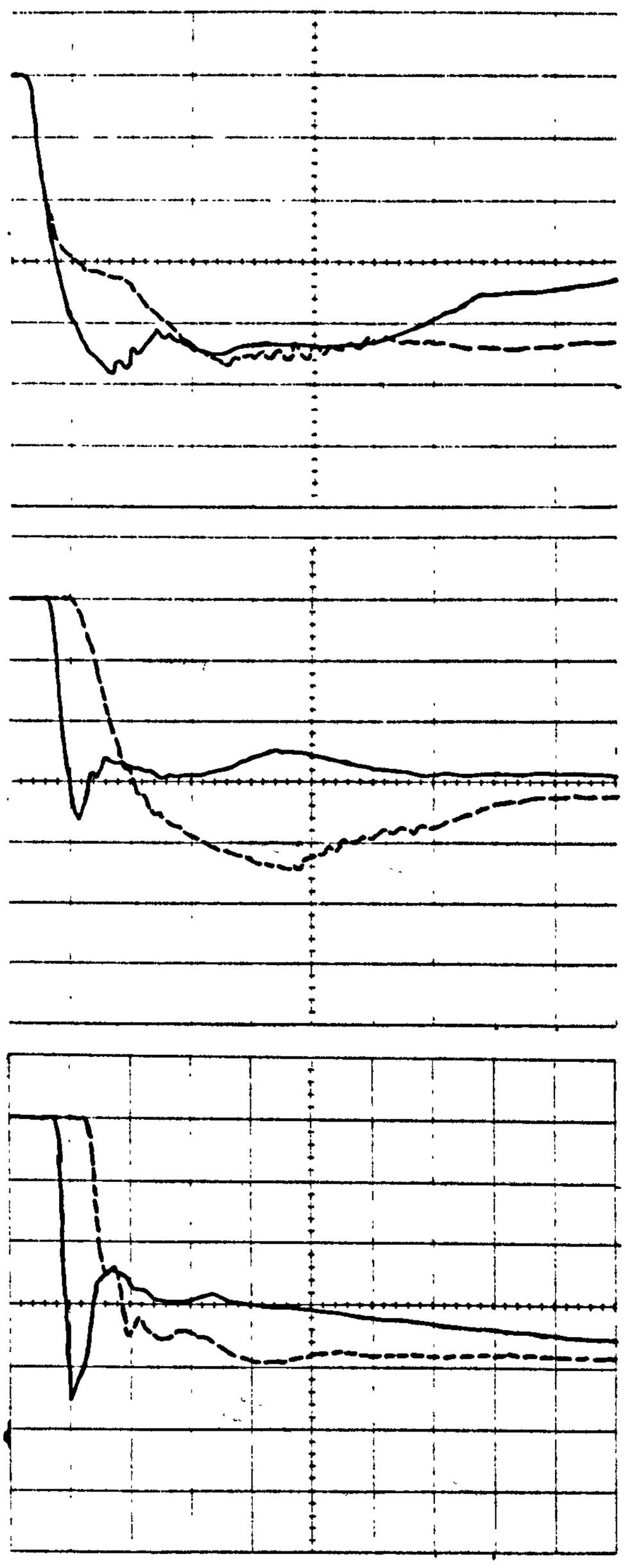

Figure 36. The a effect of a partially full vessel blowdown on the initial (1msec/div) decompression history ,at the three (top(1bar/div),middle(1bar/div),bottom(0.866bar/div)) pressure stations (w.r.t. the plots position).(__test no 143(75%full) , - -test no 145(25%full)).

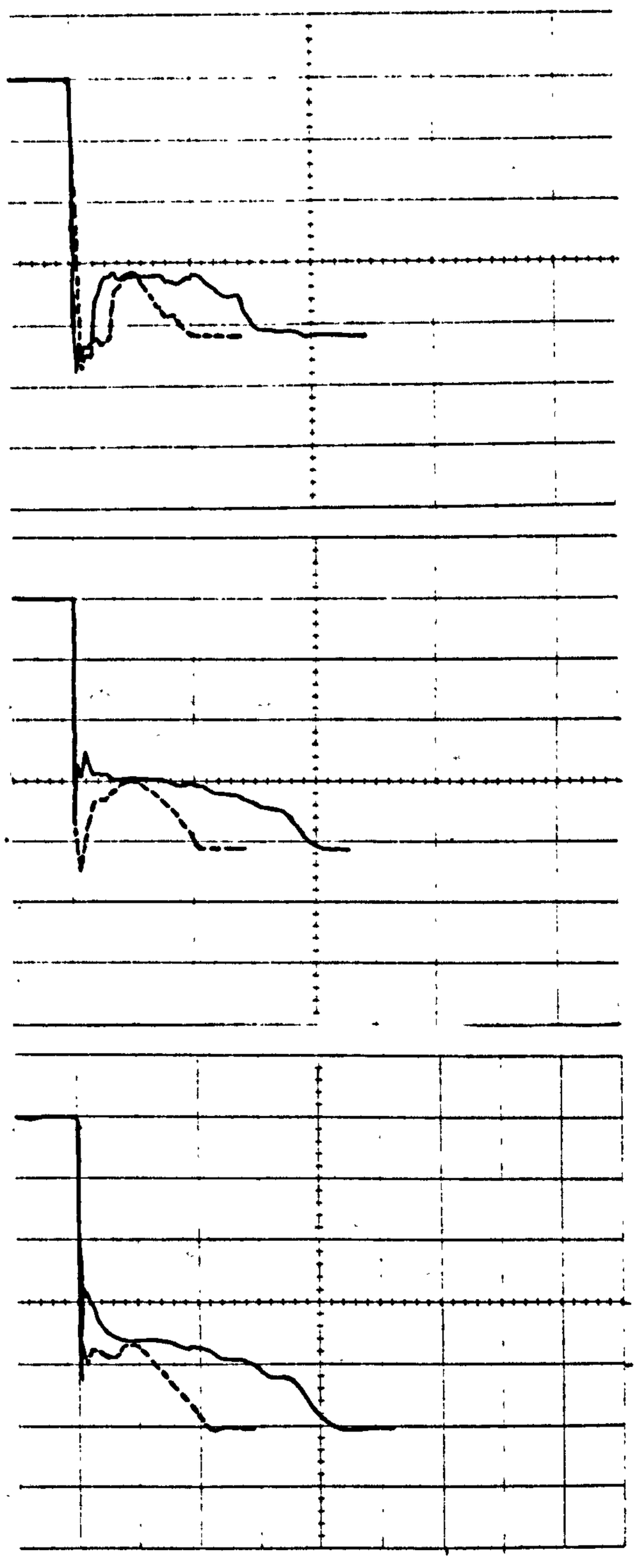

Figure 37. The effect of a partially full vessel blowdown,on the long (20msec/div) term decompression ,at the three (top(1bar/div),middle(1bar/div),bottom(0.866bar/div)) pressure stations (w.r.t. the plots position).(__test no 143(75%full),- -test no 145(25%full)).

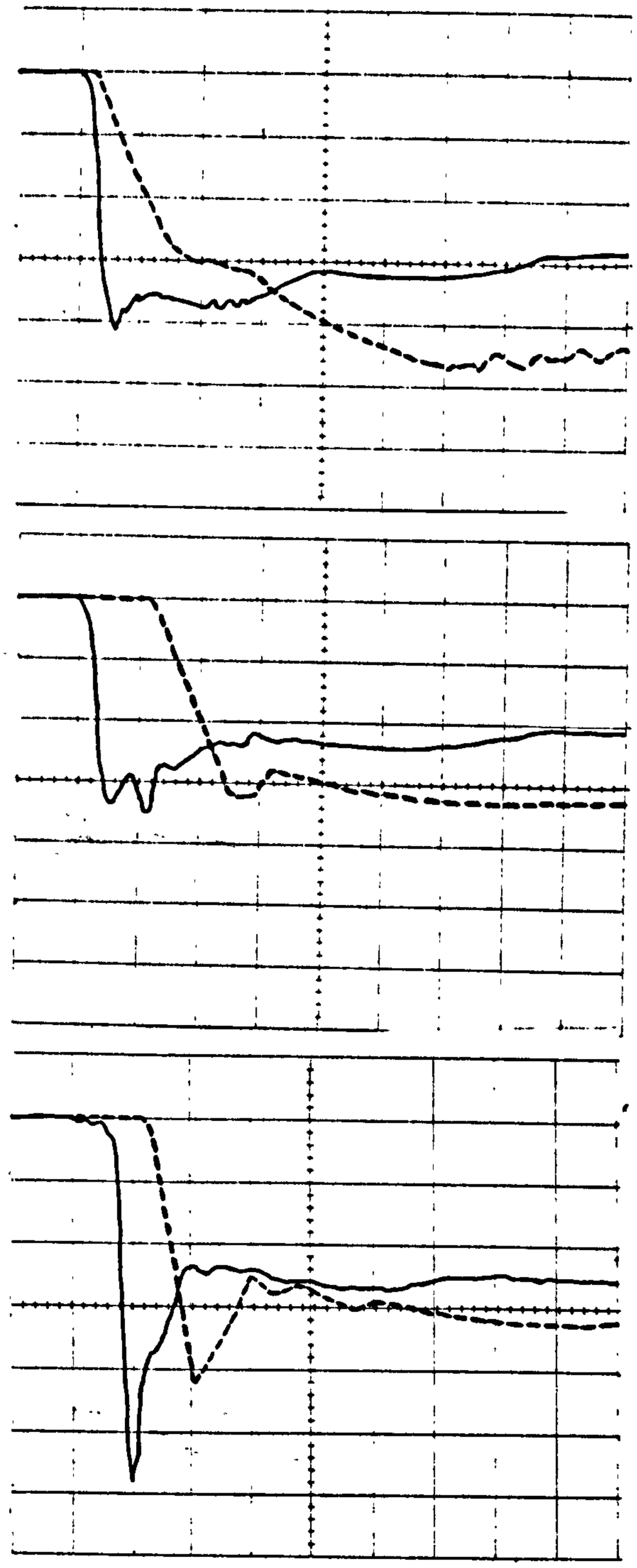

Figure 38. The effect of partially full vessel blowdown on the initial (400μsec/div) decompression ,at the three (top(1bar/div),middle(1bar/div),bottom(0.866bar/div)) pressure stations (w.r.t. the plots position).(__test no 142(100%full),- -test no 137(50 %full)).

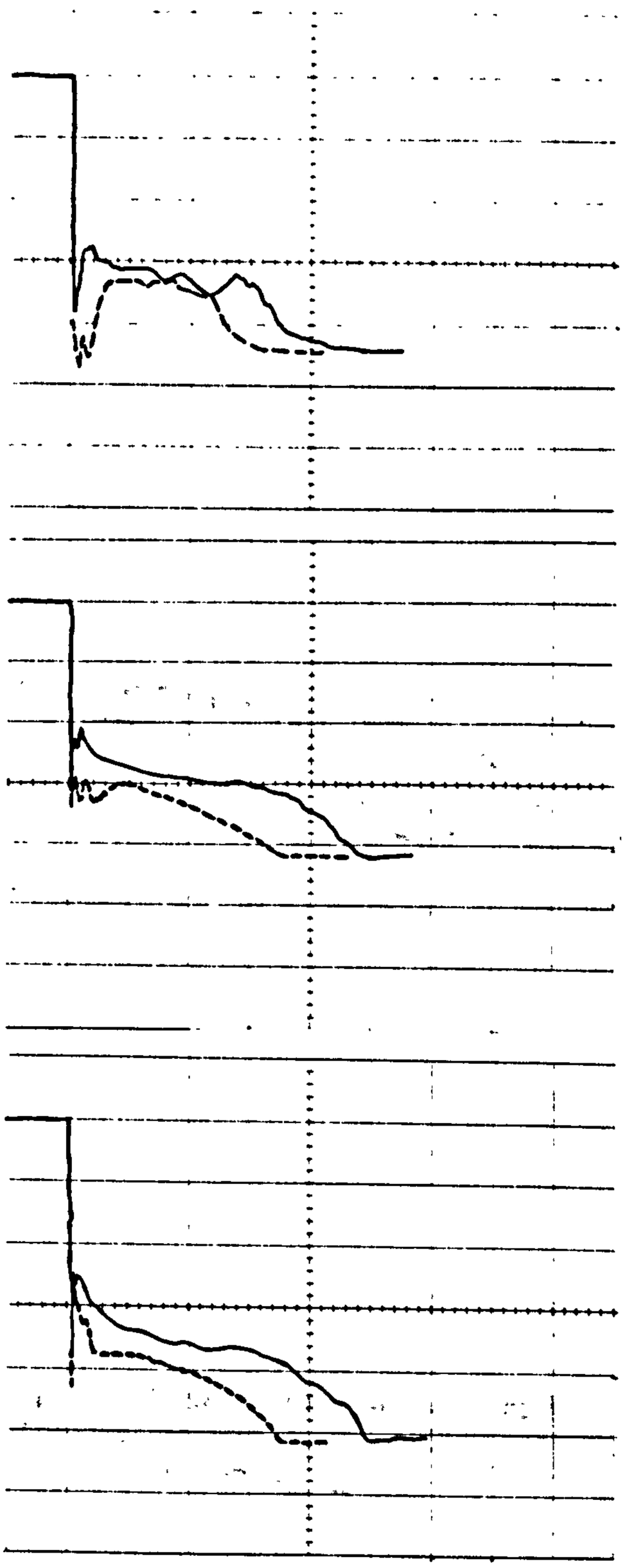

Figure 39. The effect of a partially full vessel blowdown on the long (20msec/div) term decompression,at the three (top(1bar/div), bottom(0.866bar/div)) presure stations (w.r.t. the plots position).(__test no 142(100%full),- -test no 137(50%full)).

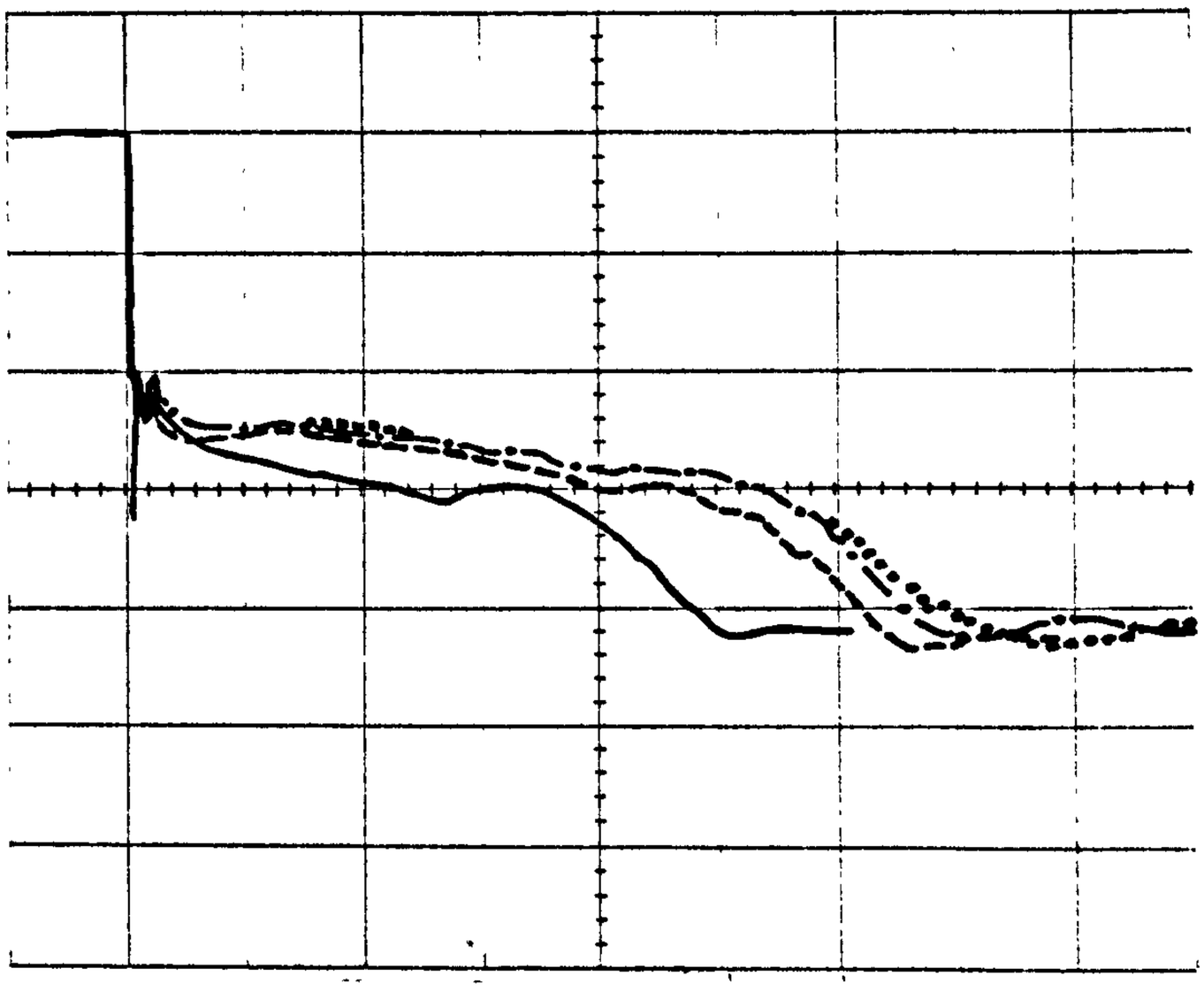

Figure 40. The effect of varing the vent pipe length on the long (20msec/div) term decompression (middle pressure station (1bar/div)-perspex).(__test no 123(no vent pipe),--test no 139(0.2m long vent pipe),_ . _test no 140(0.5m long vent pipe),. .test no 141(1m long vent pipe)).

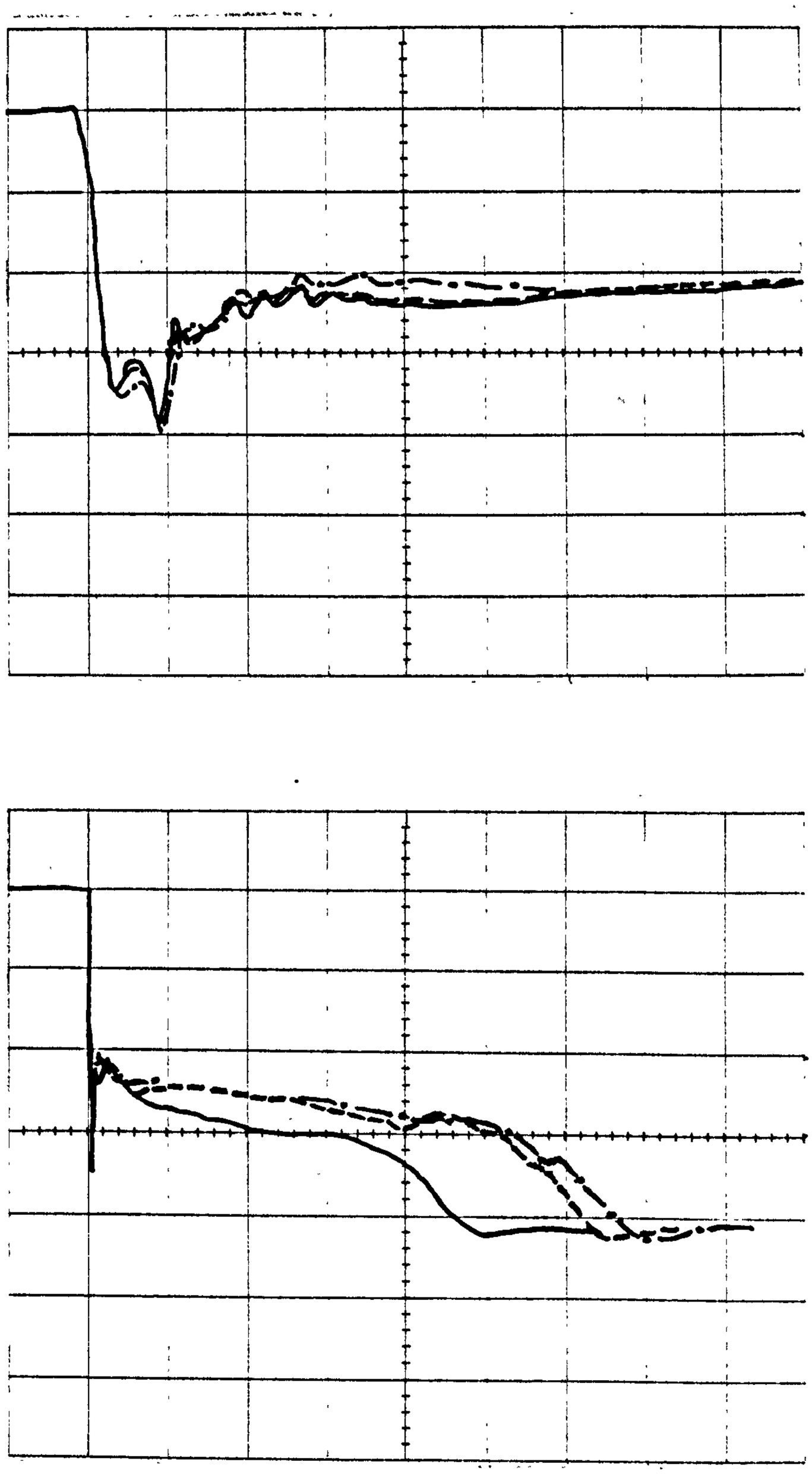

Figure 41. The effect of varing the vent pipe length on both the initial (400μsec/div) and long (20 msec/div) term depressurisation (middle pressure station (1bar/div)-perspex).(__test no 150(no vent pipe),- -test no 147(0.2m long vent pipe),_ . _test no 148(0.5m long vent pipe)).

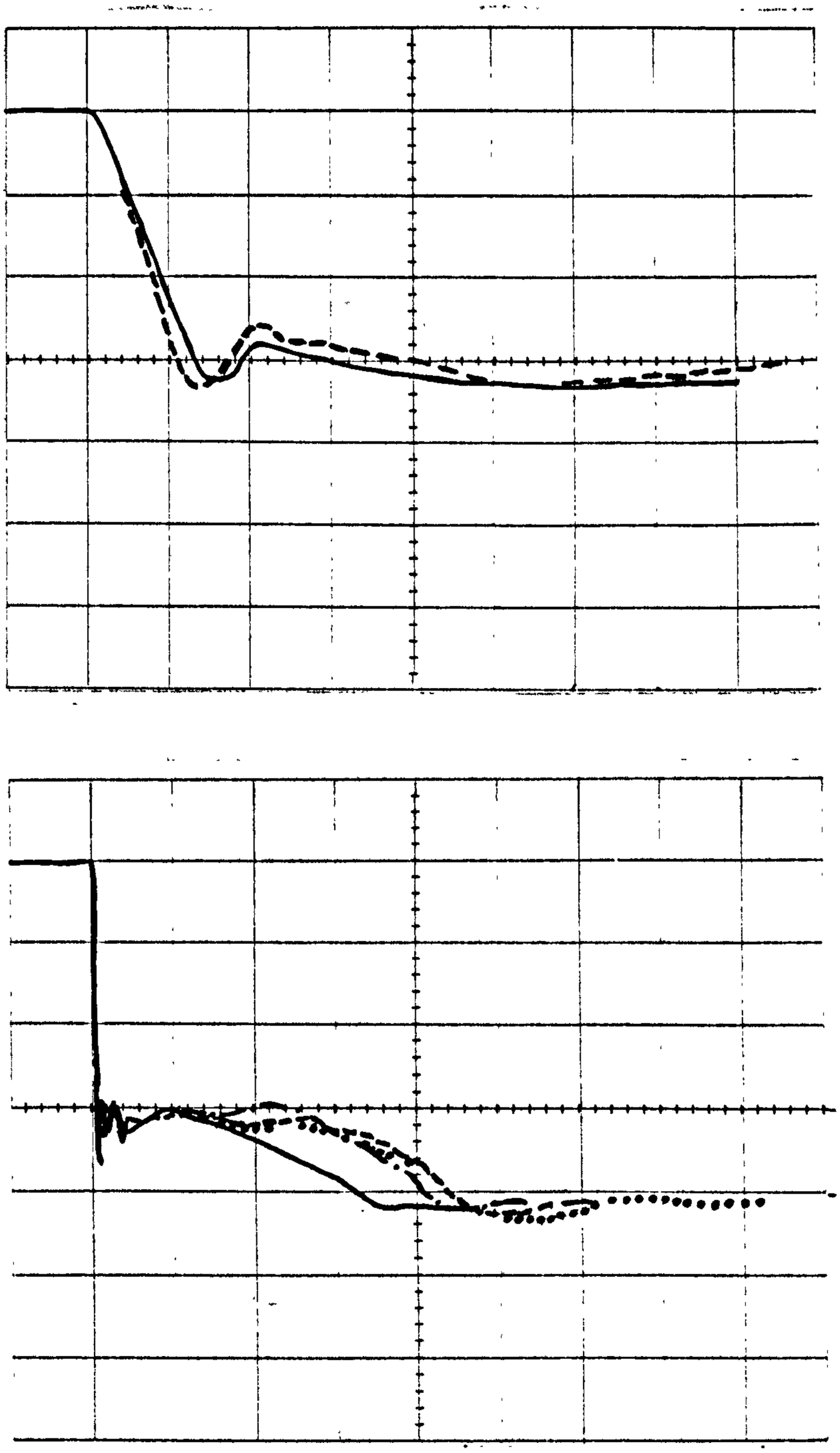

Figure 42. The effect of varing the vent pipe length for the case of a 50% full vessel.Initial (400μsec/div) and long (20msec/div) term decompression (middle pressure station (1bar/div)-perspex). (__test no 137(no vent pipe),- -test no 135(0.5m long vent pipe), _ . _test no 156(0.2m long vent pipe),. .test no 159(1m long vent pipe)).

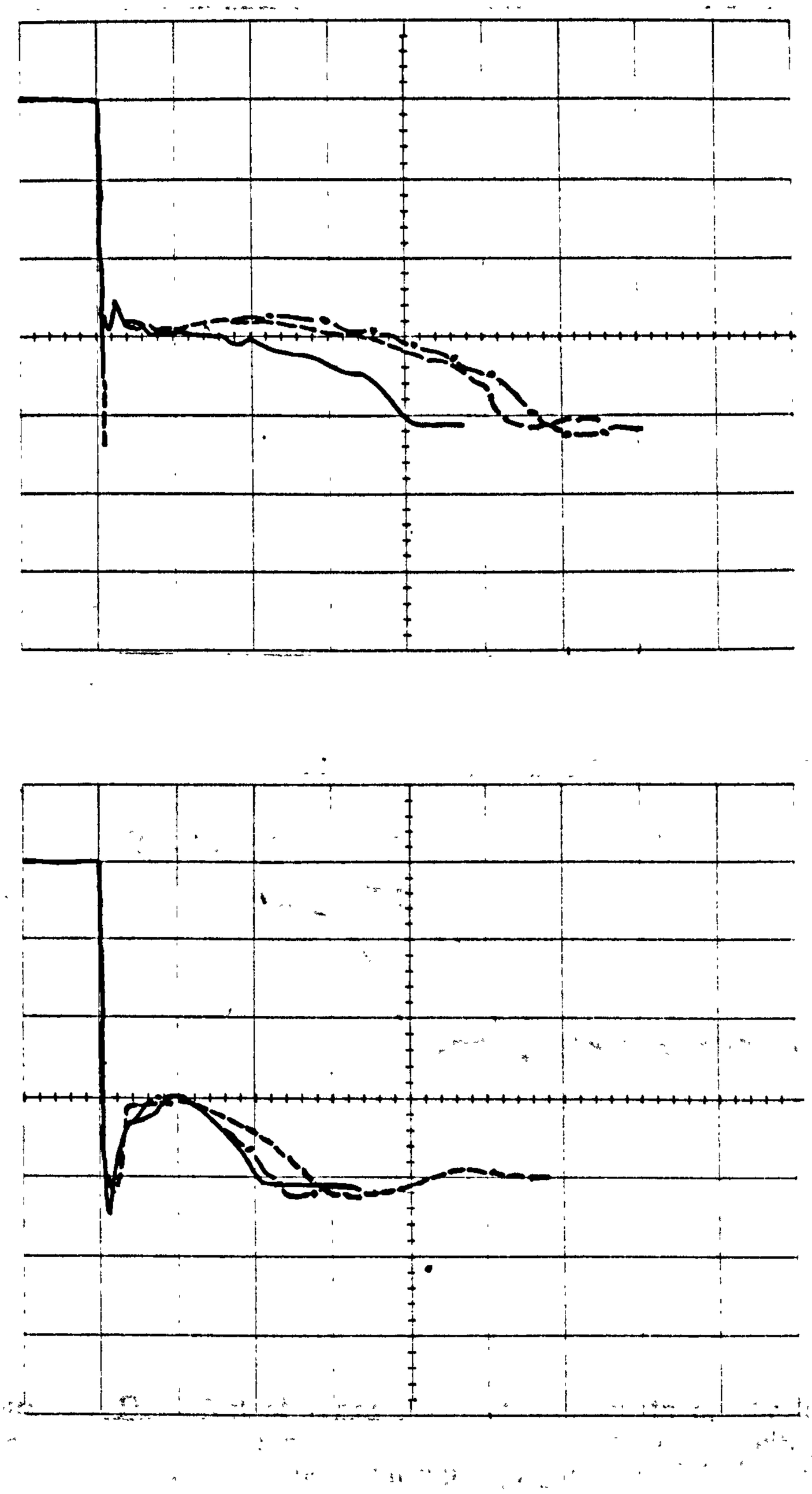

Fiqure 43. The effect of varing the vent pipe length for the cases of 75% (top plot) and 25% (bottom plot) full vessel.Long (20msec/div) term decompression (1bar/div).(top:__test no 143(no vent pipe),- -test no 155(0.2m long vent pipe),_ . _test no 134(1m long vent pipe),bottom: __test no 145(no vent pipe),- -test no 160(1m long vent pipe),_ . _test no 157(0.2m long vent pipe)).

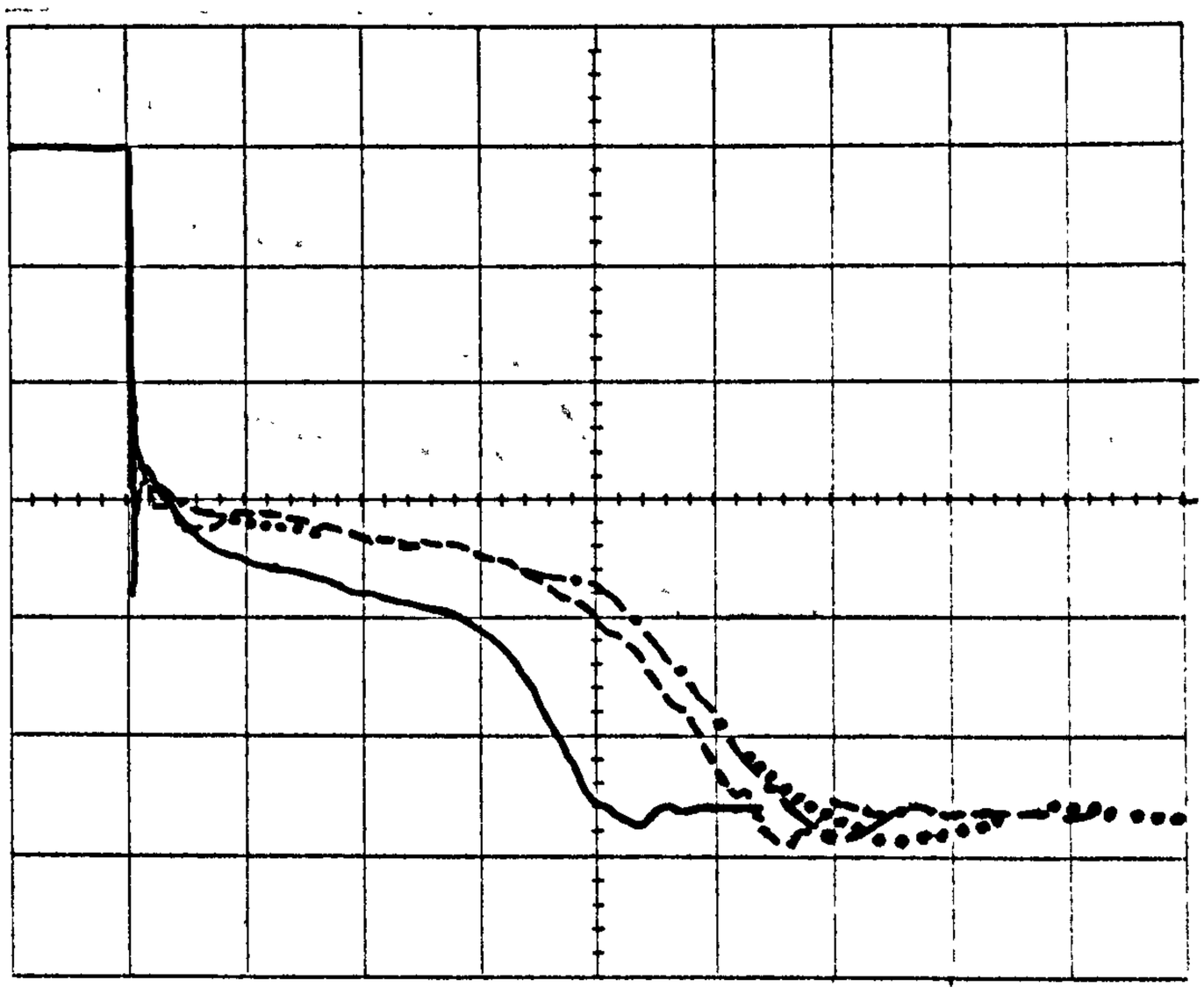

Figure 44. The effect of varing the vent pipe length on the long (20msec/div) term depressurisation (middle pressure station (1bar/div)-mild steel).(__test no 221(no vent pipe),- -test no 222(0.2m long vent pipe),_ . _test no 223(0.5m long vent pipe),. .test no 224(1m long vent pipe)).

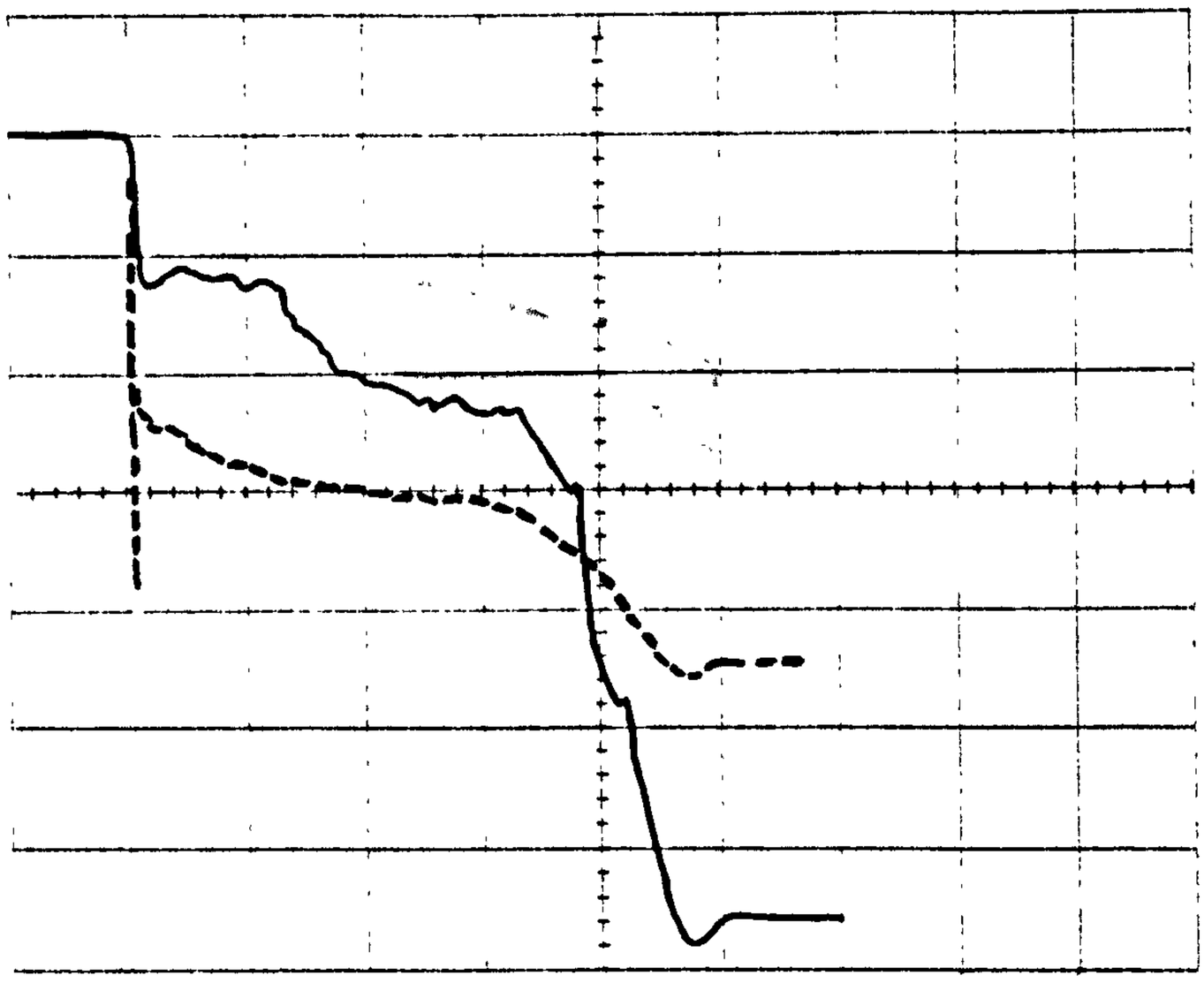

Figure 45. Similarity of the response time for both pressure and temperature measurements.(20msec/div,pressure trace:1bar/div,temperature trace:2.54°C/div).

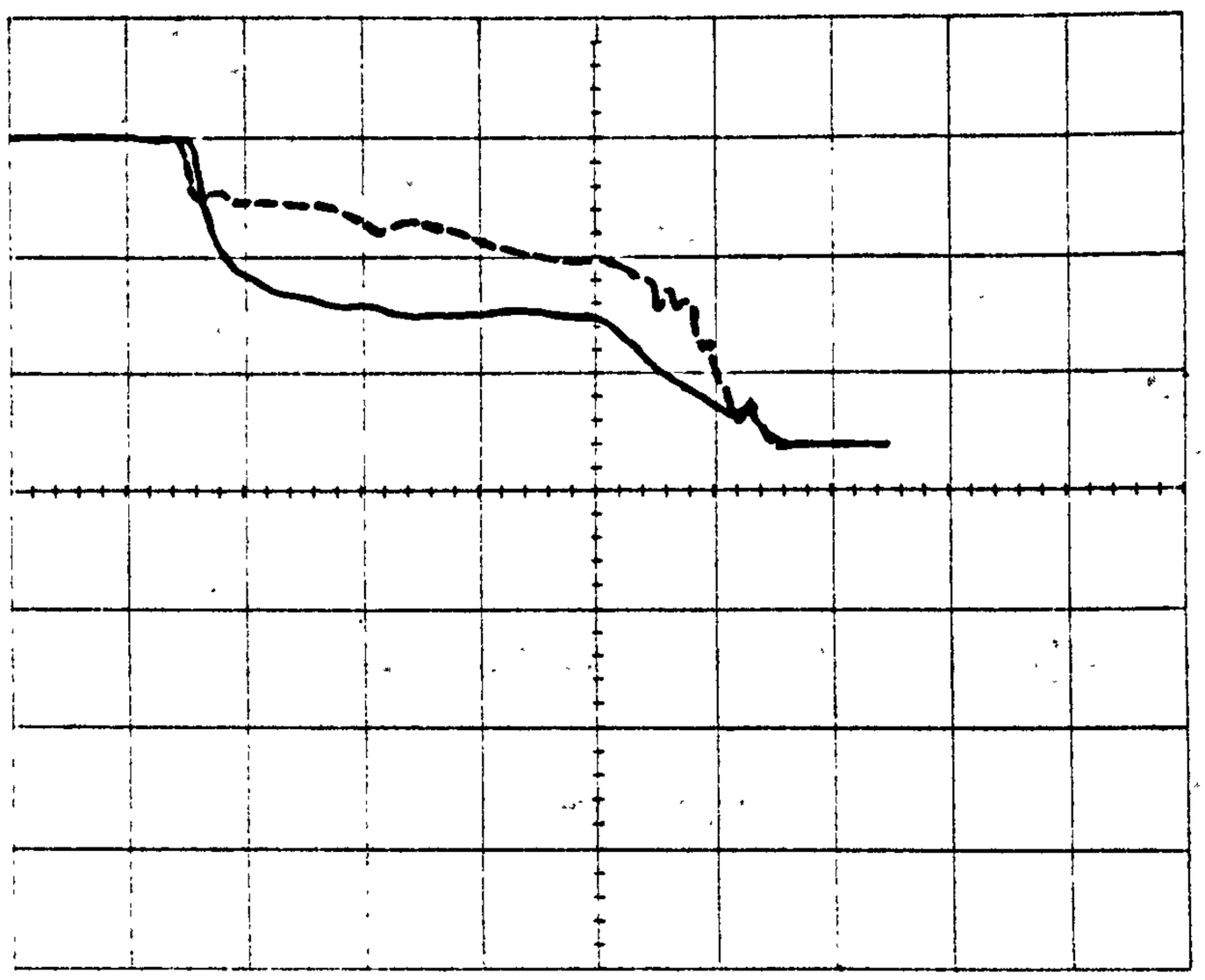

Figure 46. Typical temperature measurements ("short" thermocouple). (20msec/div, 12.88°C/div, __middle temperature station, - -bottom temperature station).

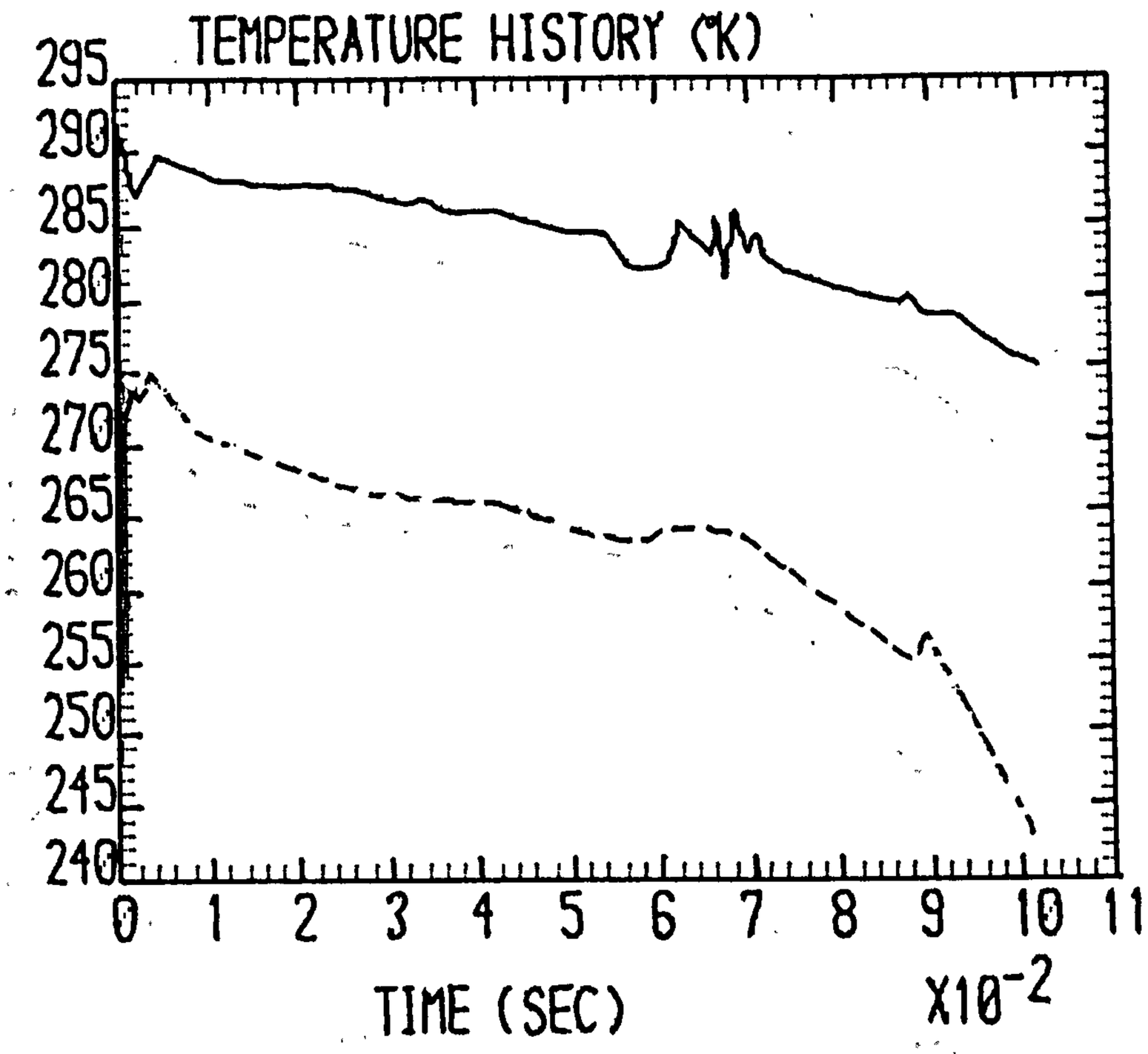

Figure 47. Comparison of the temperature measurements (____) with the saturation temperature (- - -) , corresponding to the local pressure measurements.

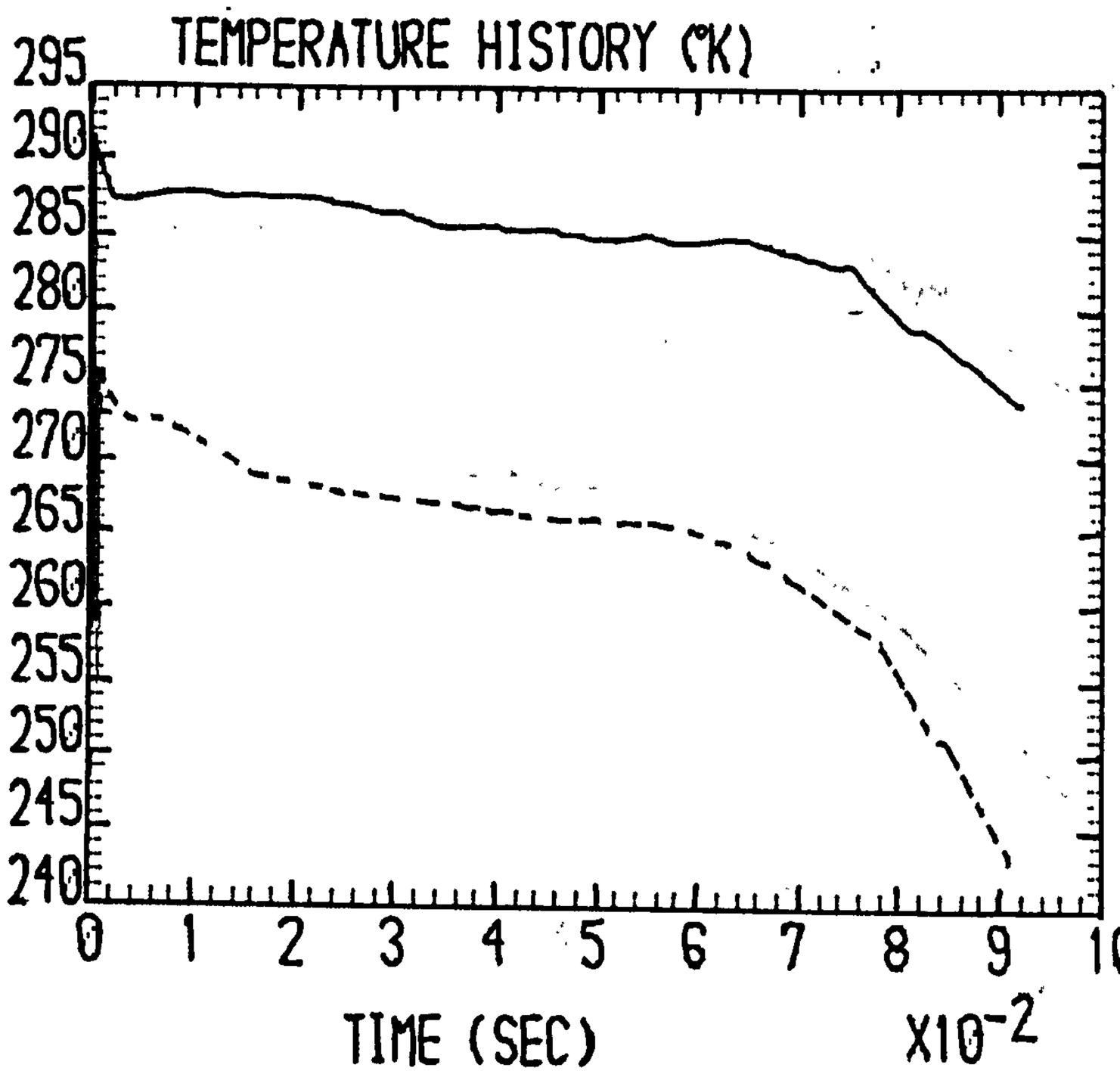

Figure 48. Comparison of the temperature measurements (___) with the saturation temperature (- - -) ,corresponding to the local pressure measurements.

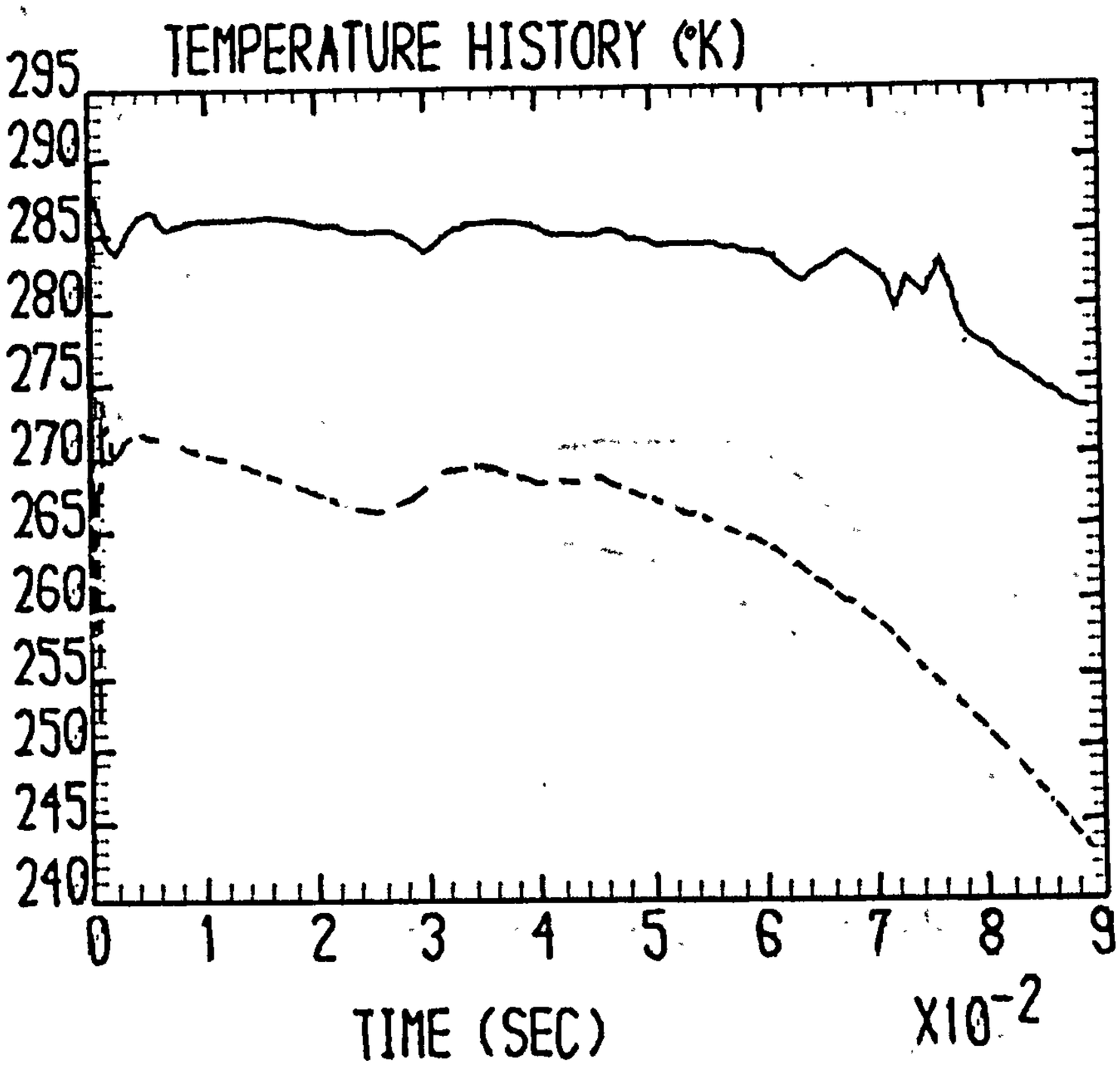

Figure 49. Comparison of the temperature measurements (___) with the saturation temperature (- - -) ,corresponding to the local pressure measurements.

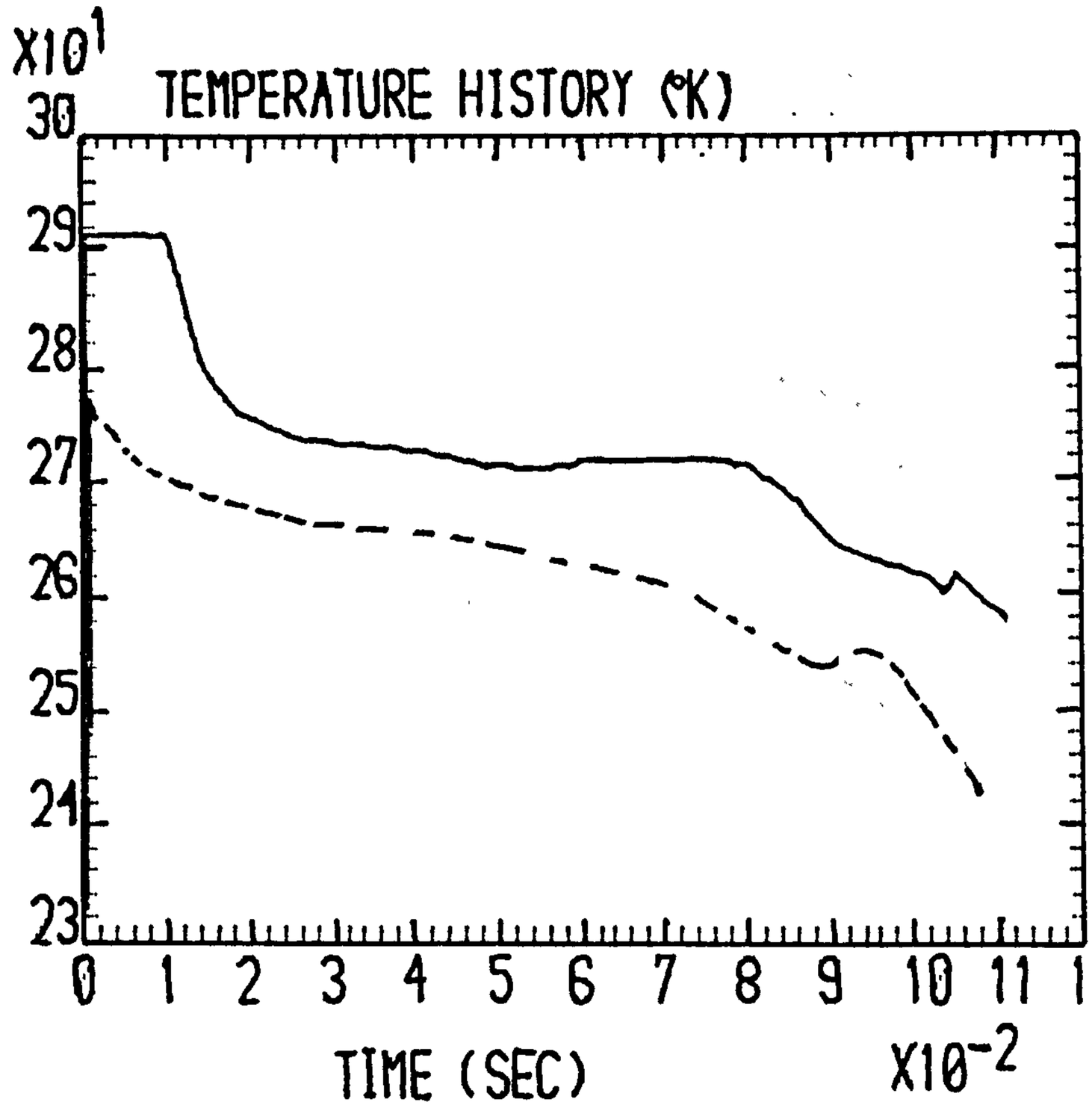

Figure 50. Comparison of the temperature measurements (___) with the saturation temperature (- - -) ,corresponding to the local pressure measurements.

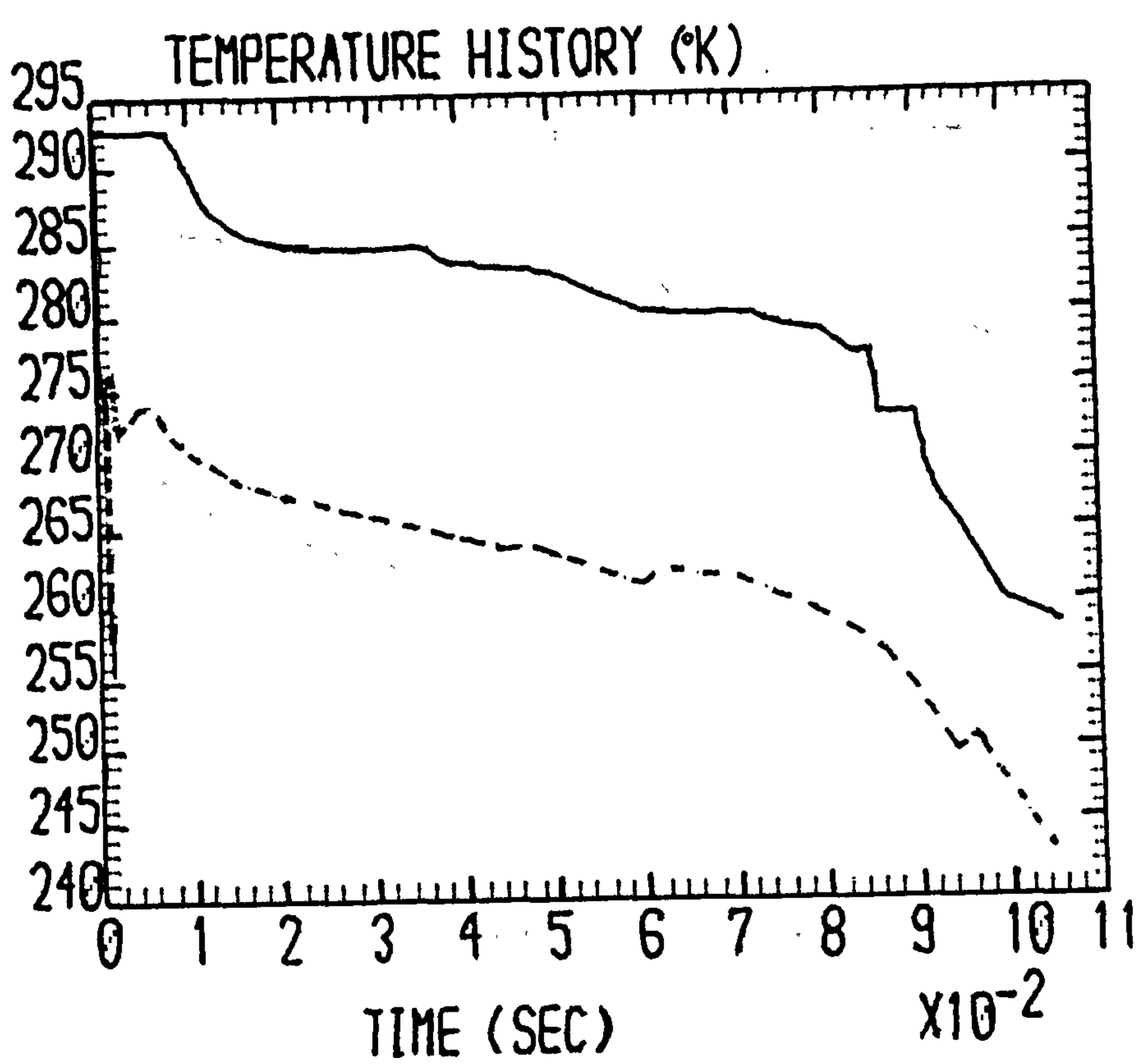

Figure 51. Comparison of the temperature measurements (___) with the saturation temperature (- - -) ,corresponding to the local pressure measurements.

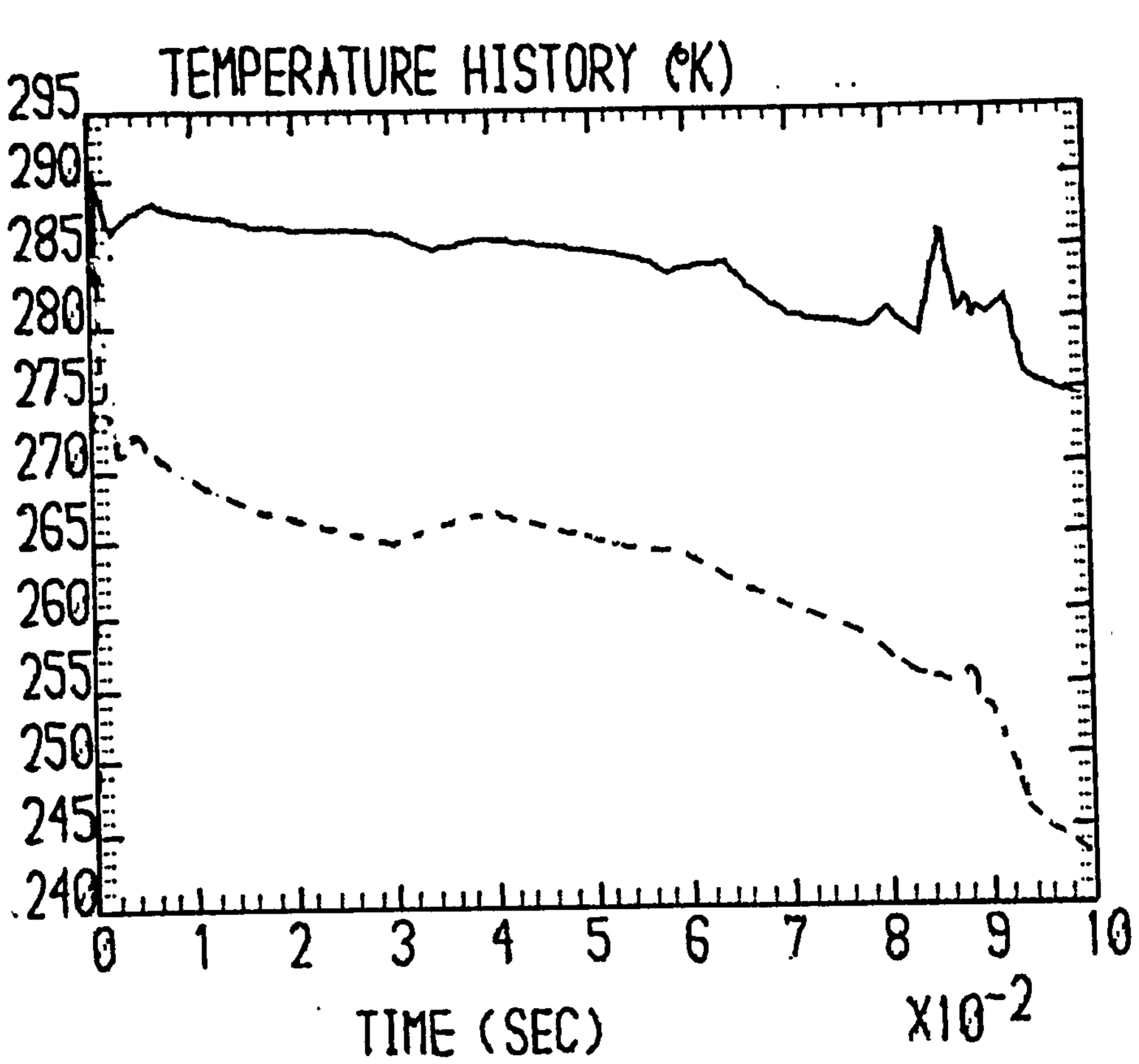

Figure 52. Comparison of the temperature measurements (___) with the saturation temperature (- - -) ,corresponding to the local pressure measurements.

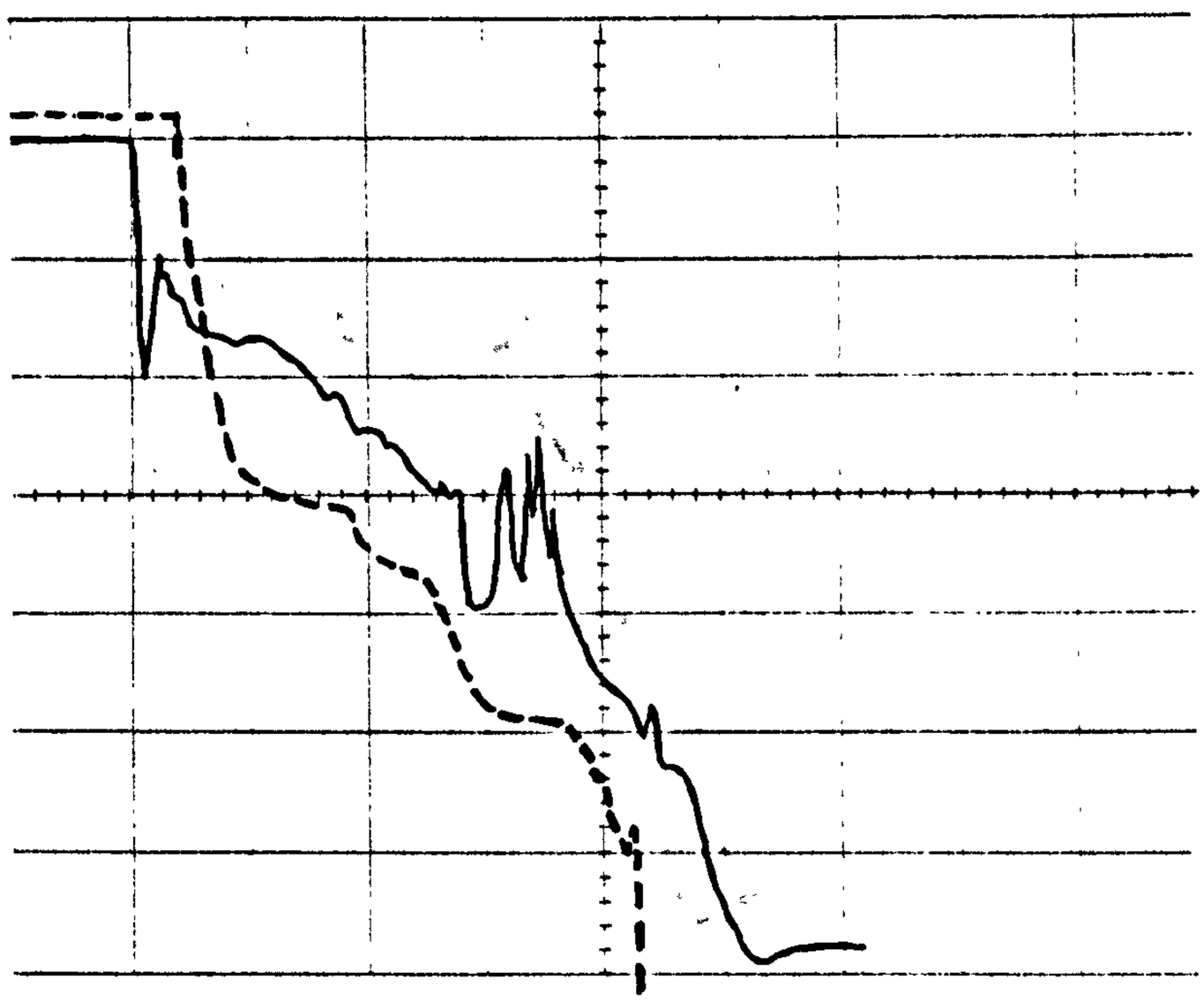

Figure 53. Comparison of temperature measurements obtained with two different thermocouple lengths (middle temperature station (2.54°C /div,20msec/div).(__"long" thermocouple,- -"short" thermocouple).

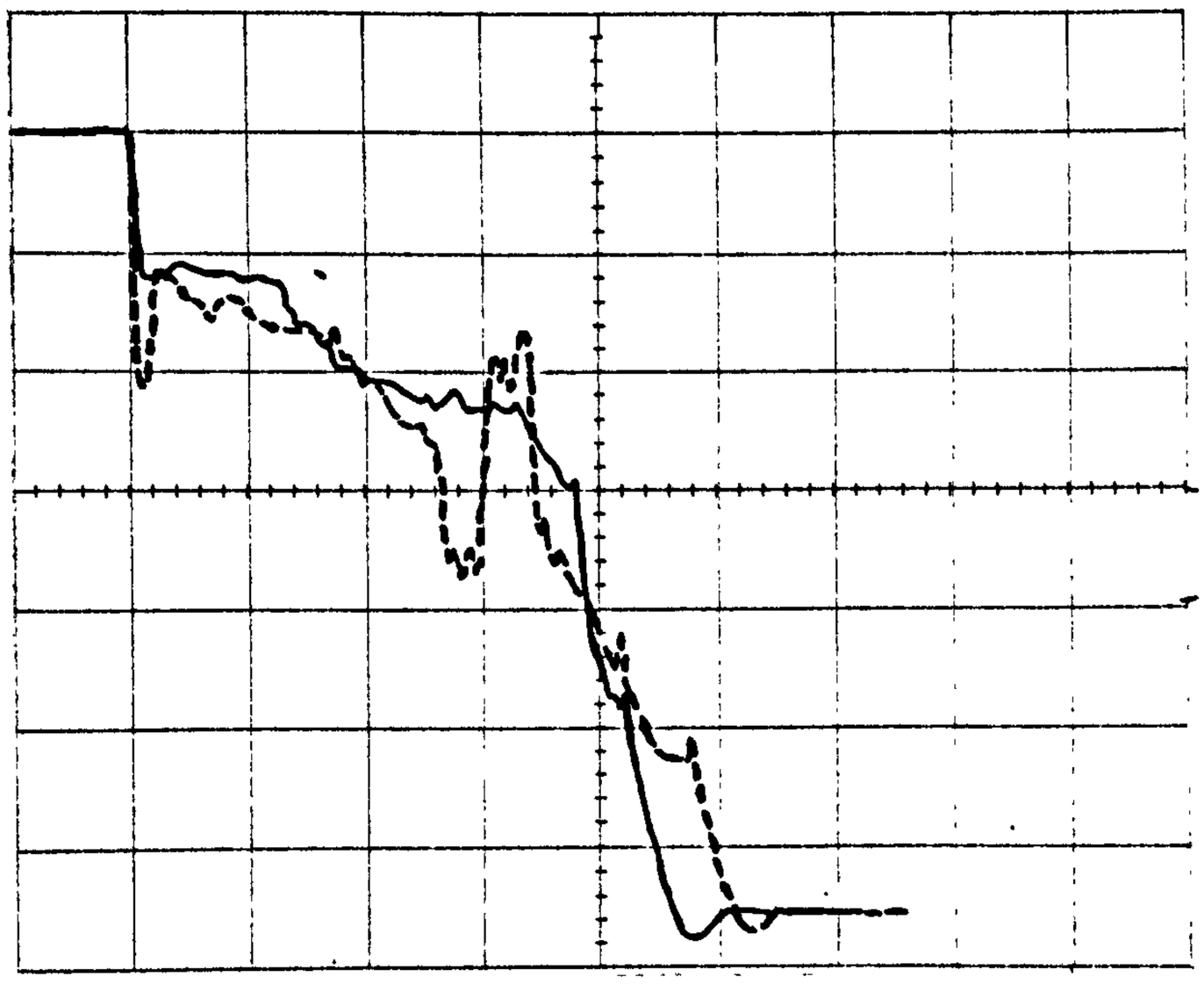

Fiqure 54. The effect of the different vessel material on the temperature history (2.54°C/div,20msec/div).(__ "mild steel",- - "perspex").

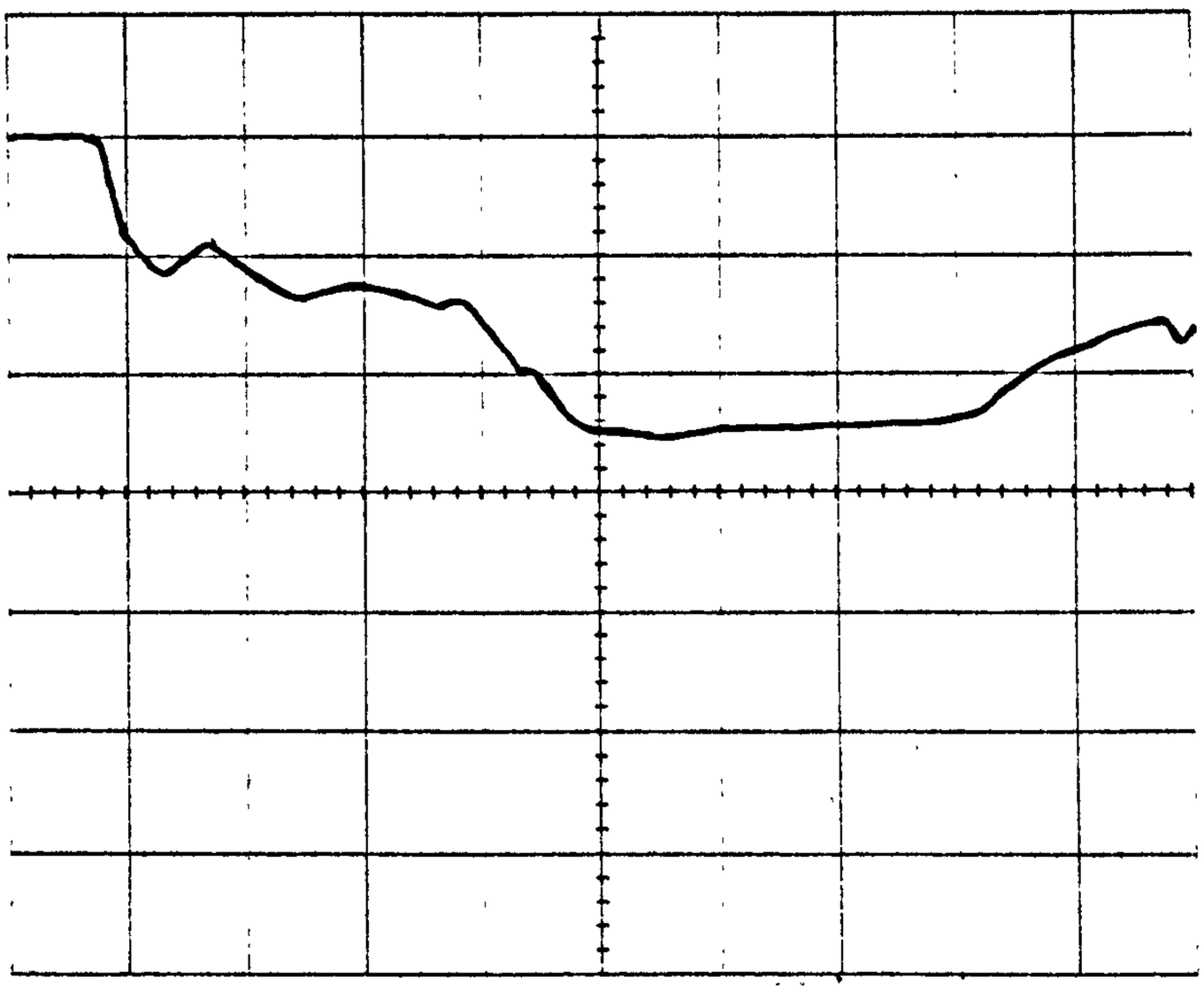

Fiqure 55. Typical temperature history,obtained with the "short" thermocouple (bottom temperature station (12.88°C/div,20msec/div).

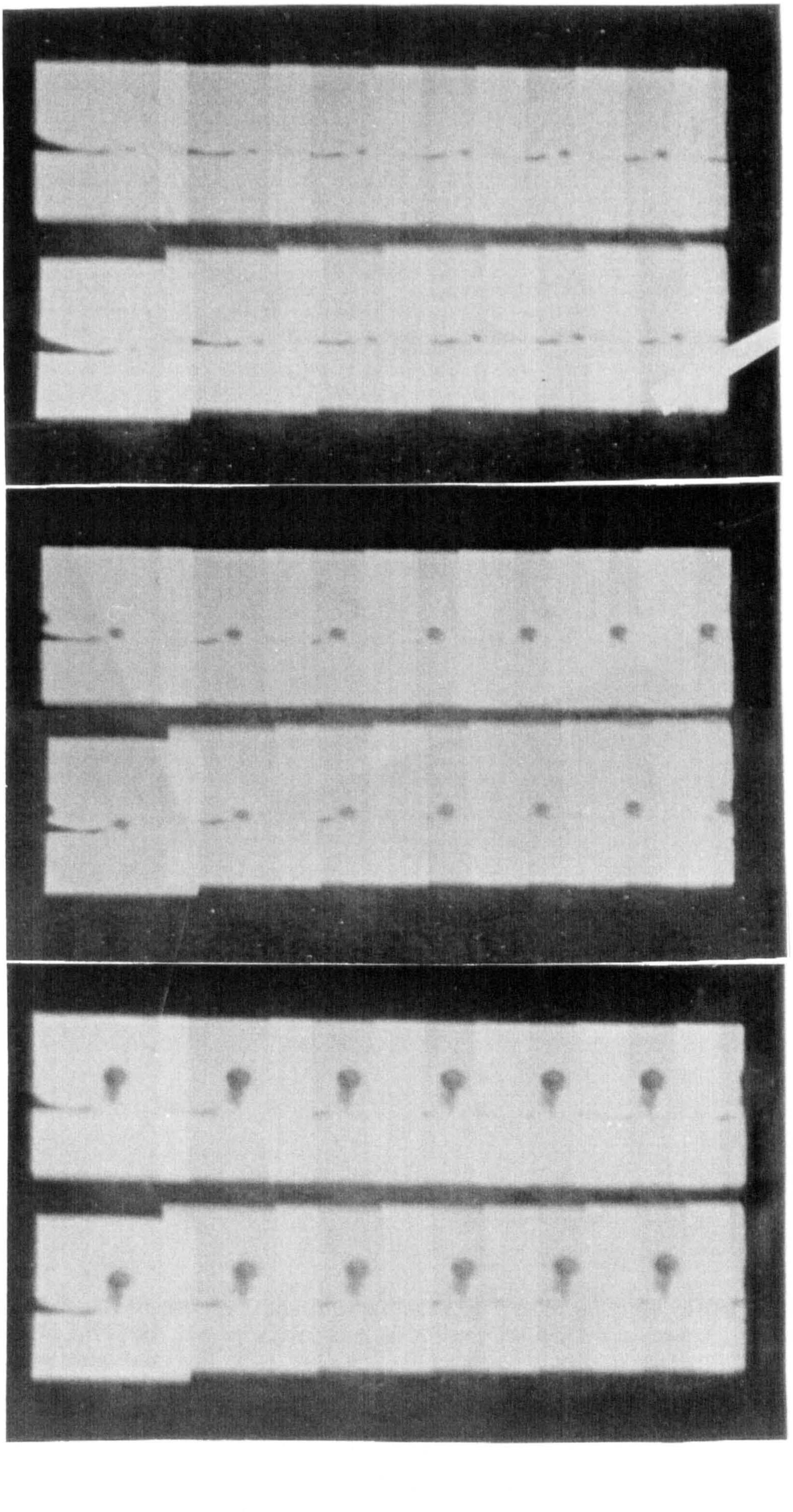

Figure 56. Photographic sequence of the bubble growth history. (top:test no 12PH,middle:test no 14PH,bottom:test no 17PH).

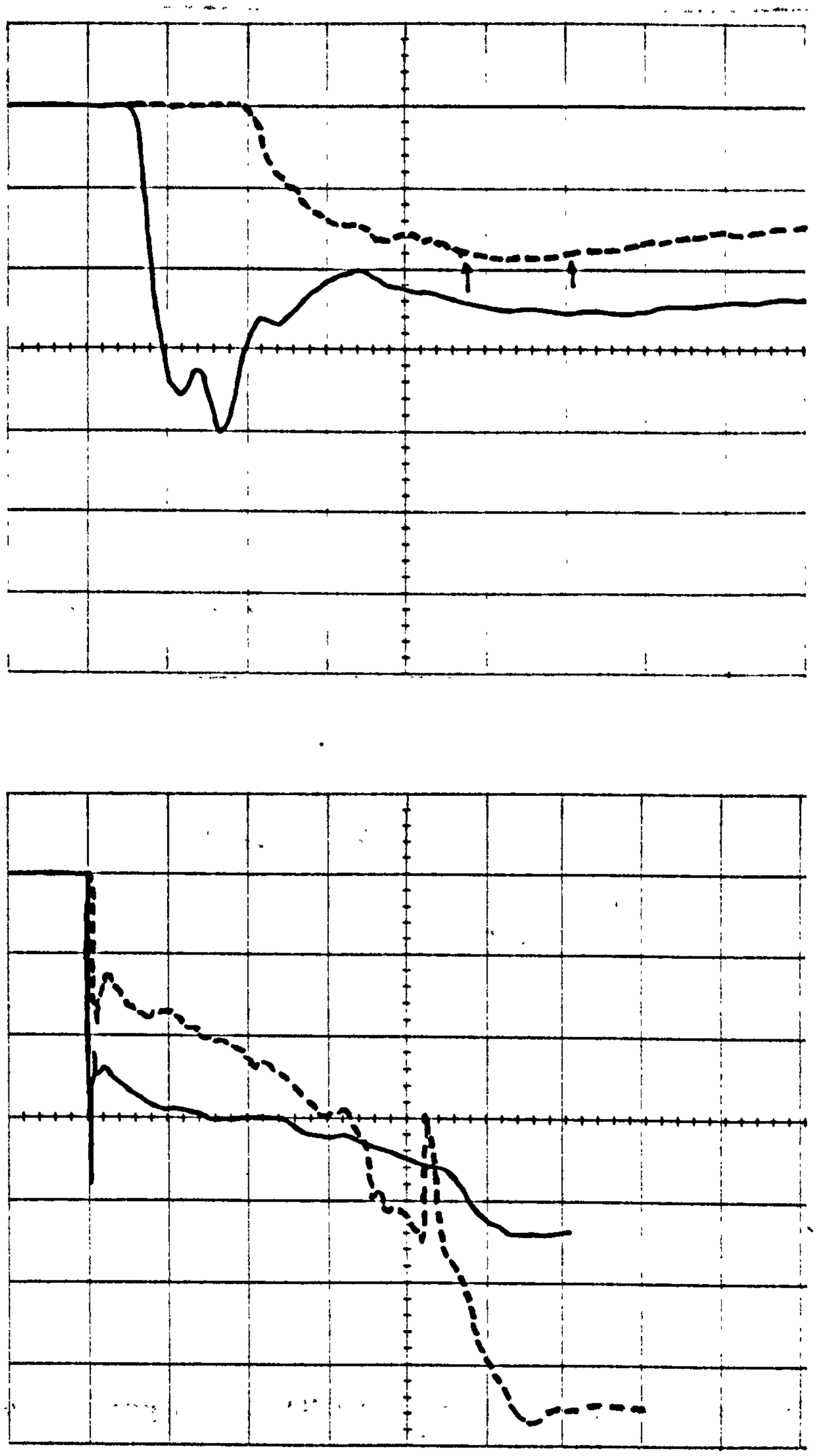

Figure 57. Initial (400μsec/div) and long (20msec/div) term pressure (1bar/div) and temperature (2.54°C/div) history during the use of the "IMACON" camera.(__pressure trace,- -temperature trace).

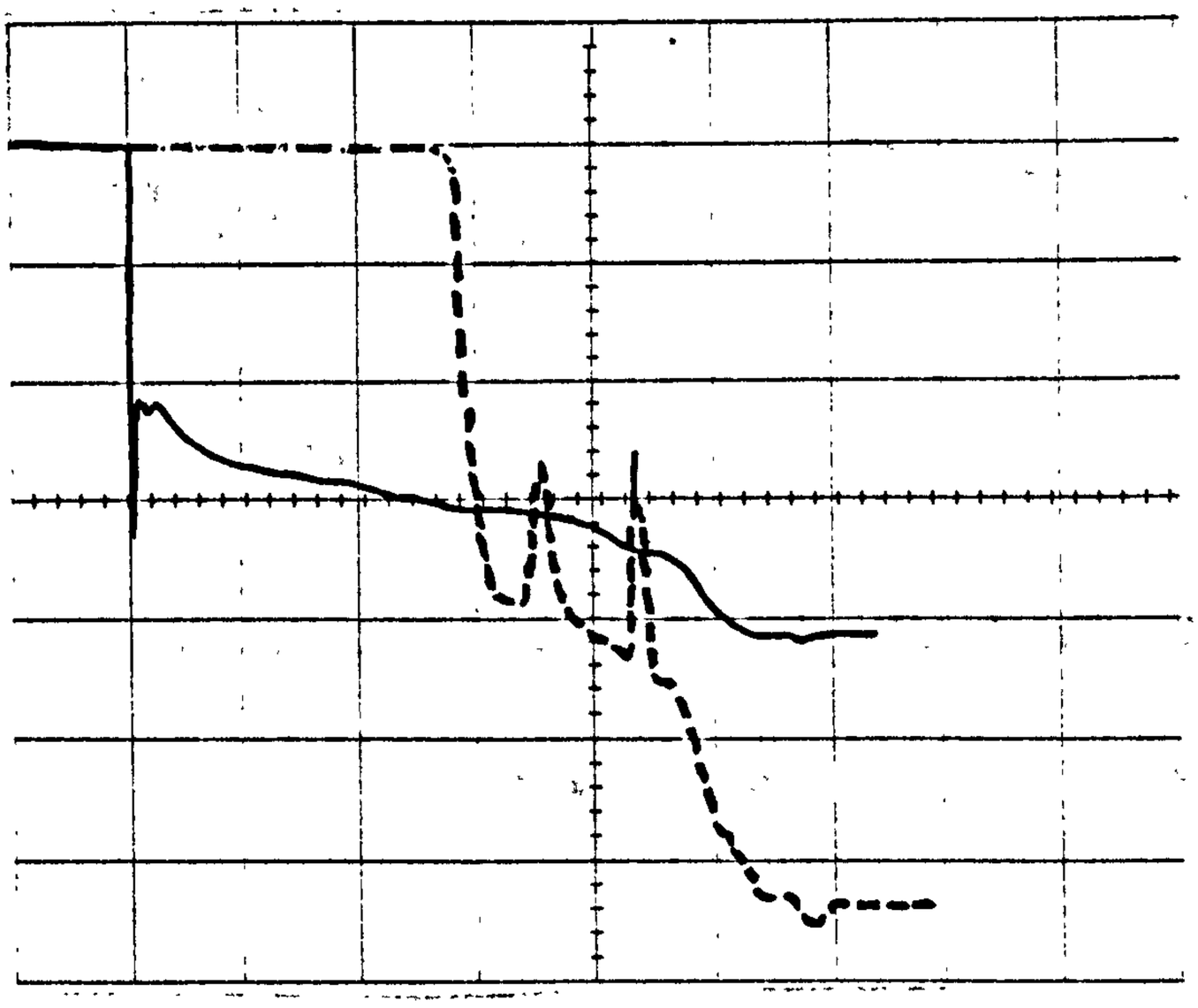

Figure 58. Long (20msec/div) term pressure (1bar/div) and temperature (2.54°C/div) history,during the use of the "IMACON" camera.(__pressure trace,- -tempreture trace).

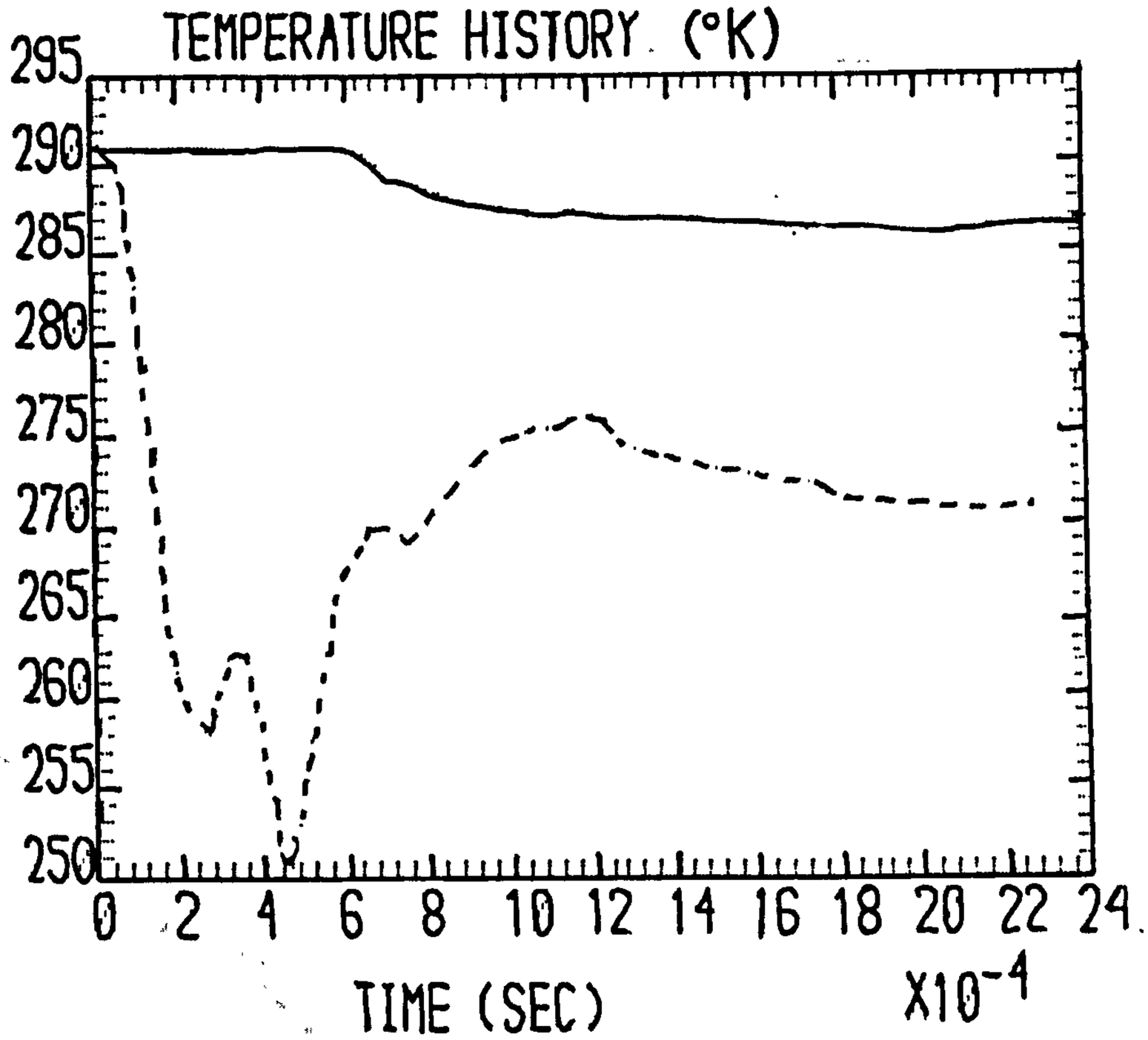

Fiqure 59. Comparison of the initial term temperature history (___) with the saturation temperature (- - -) ,corresponding to the local pressure.

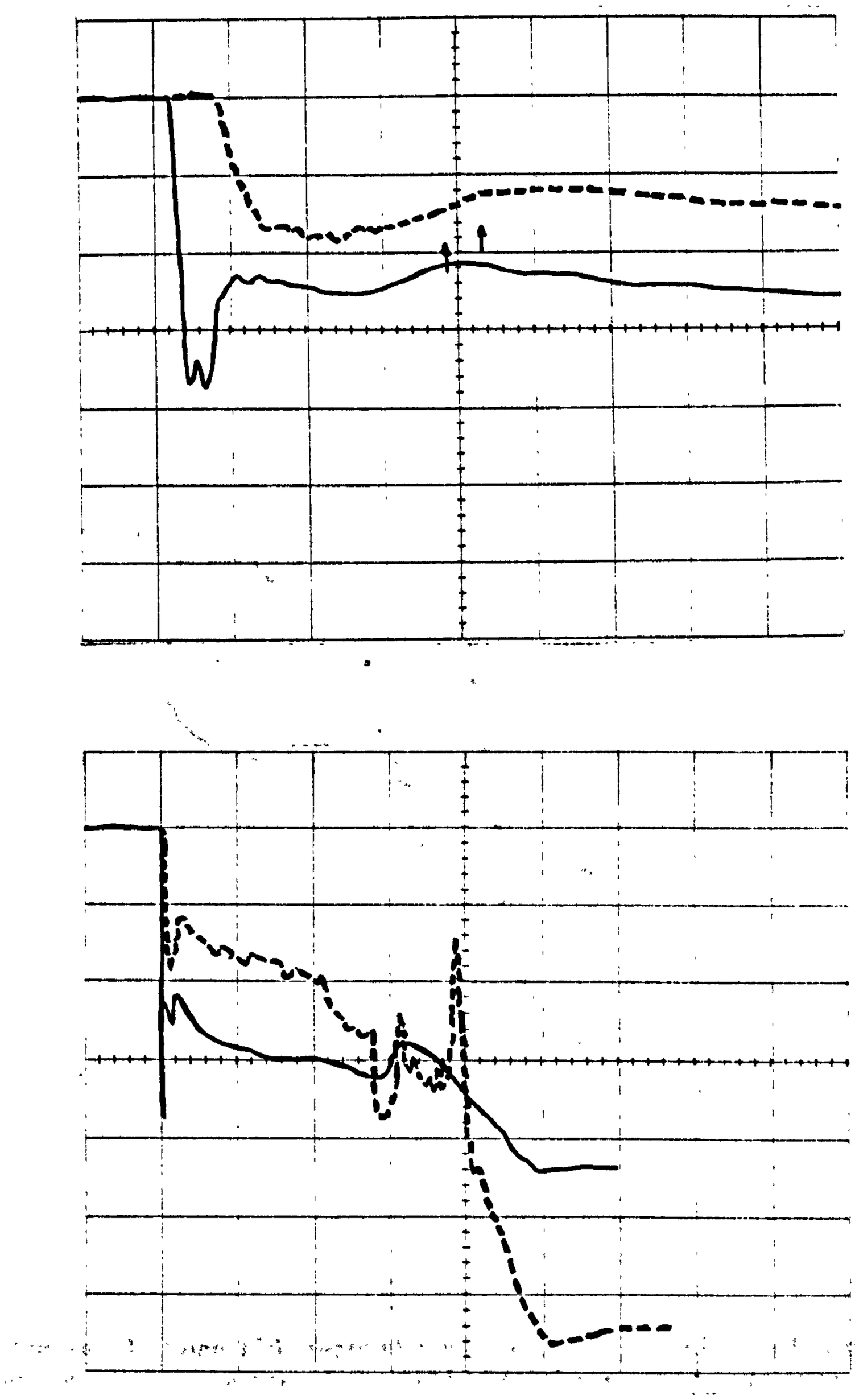

Figure 60. Initial (1msec/div) and long (20msec/div) term pressure (1bar/div) and temperature (2.54°C/div) history,during the use of the "IMACON" camera. (___pressure trace,- - -temperature trace).

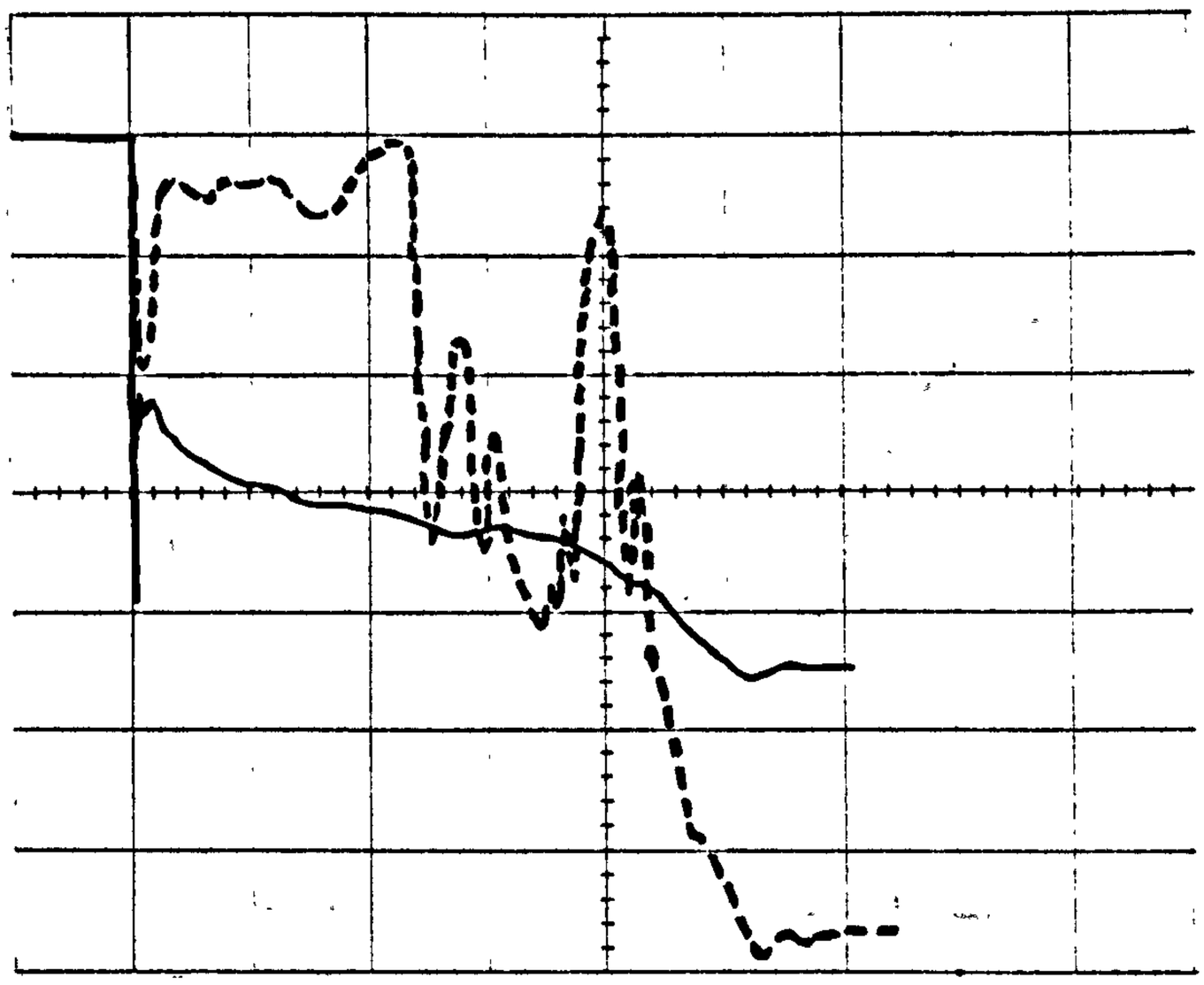

Fiqure 61. Long (20msec/div) term pressure (1bar/div) and temperature (2.54°C/div) history during the use of the "IMACON" camera.(___pressure trace,- - -temperature trace).

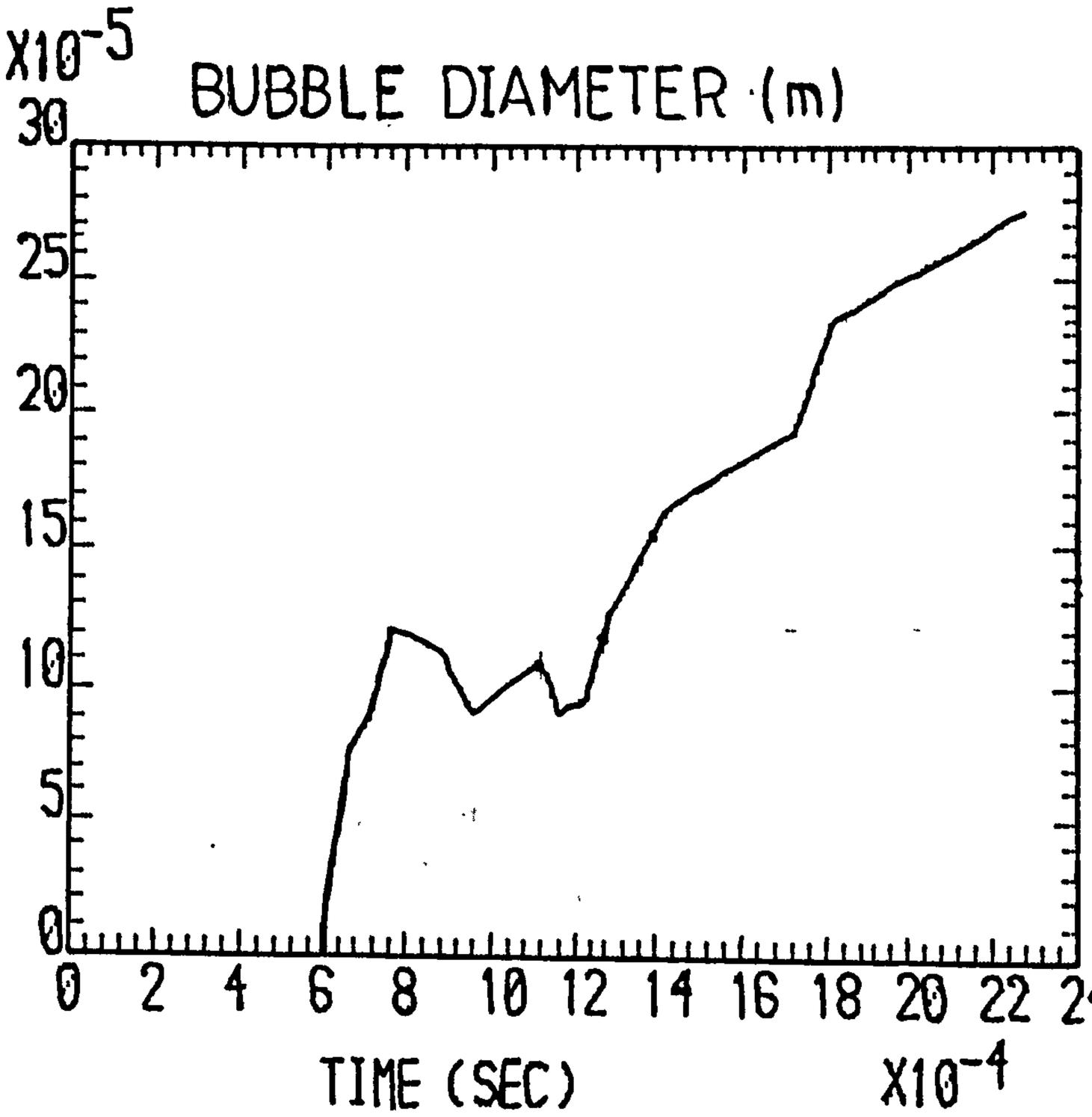

Figure 62. Bubble growth history.(test no 14PH,bubble diameter in m).

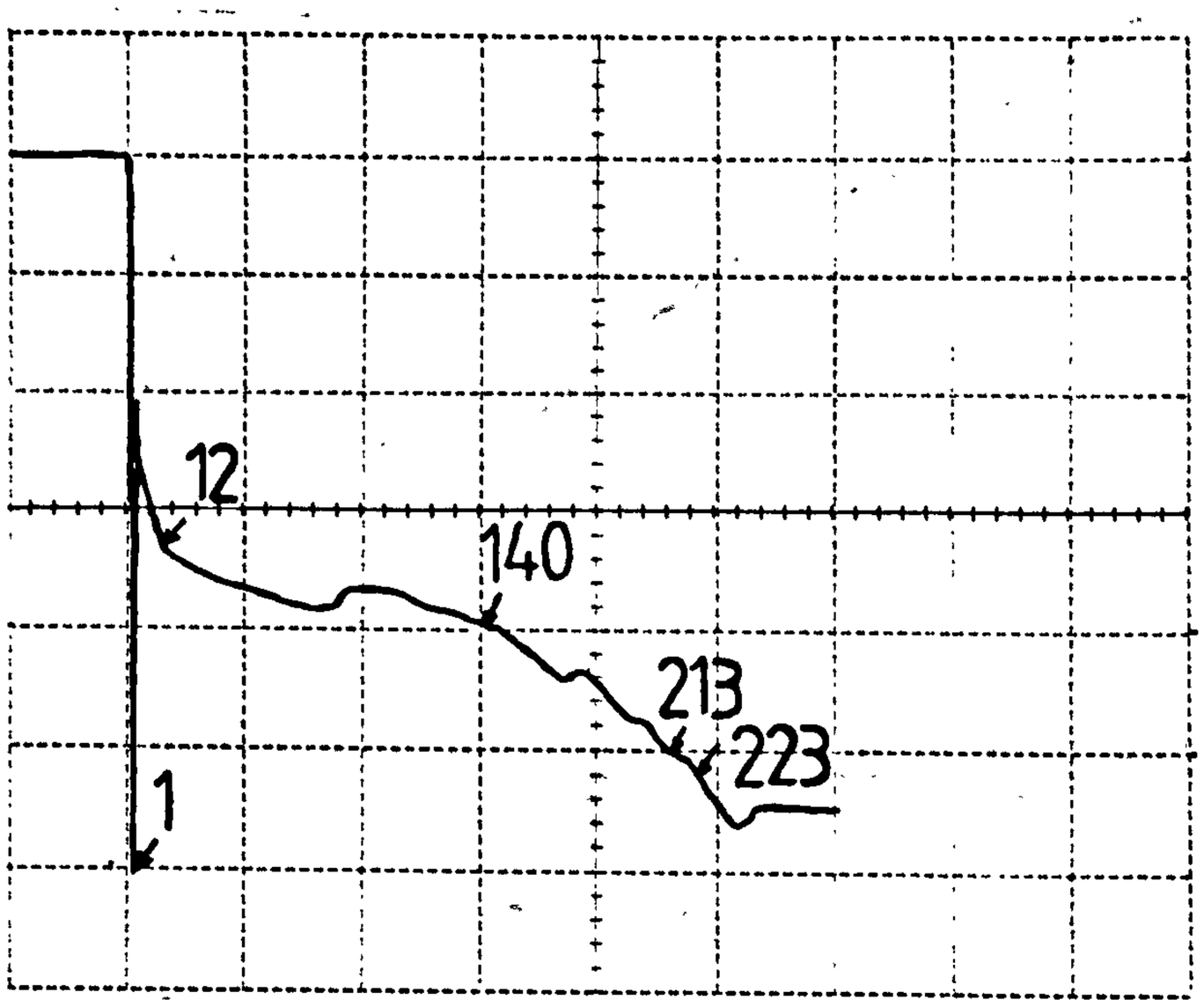

Fiqure 63. Long term decompression recorded by the bottom pressure station,during filming I.(0.845bar/div,20msec/div).

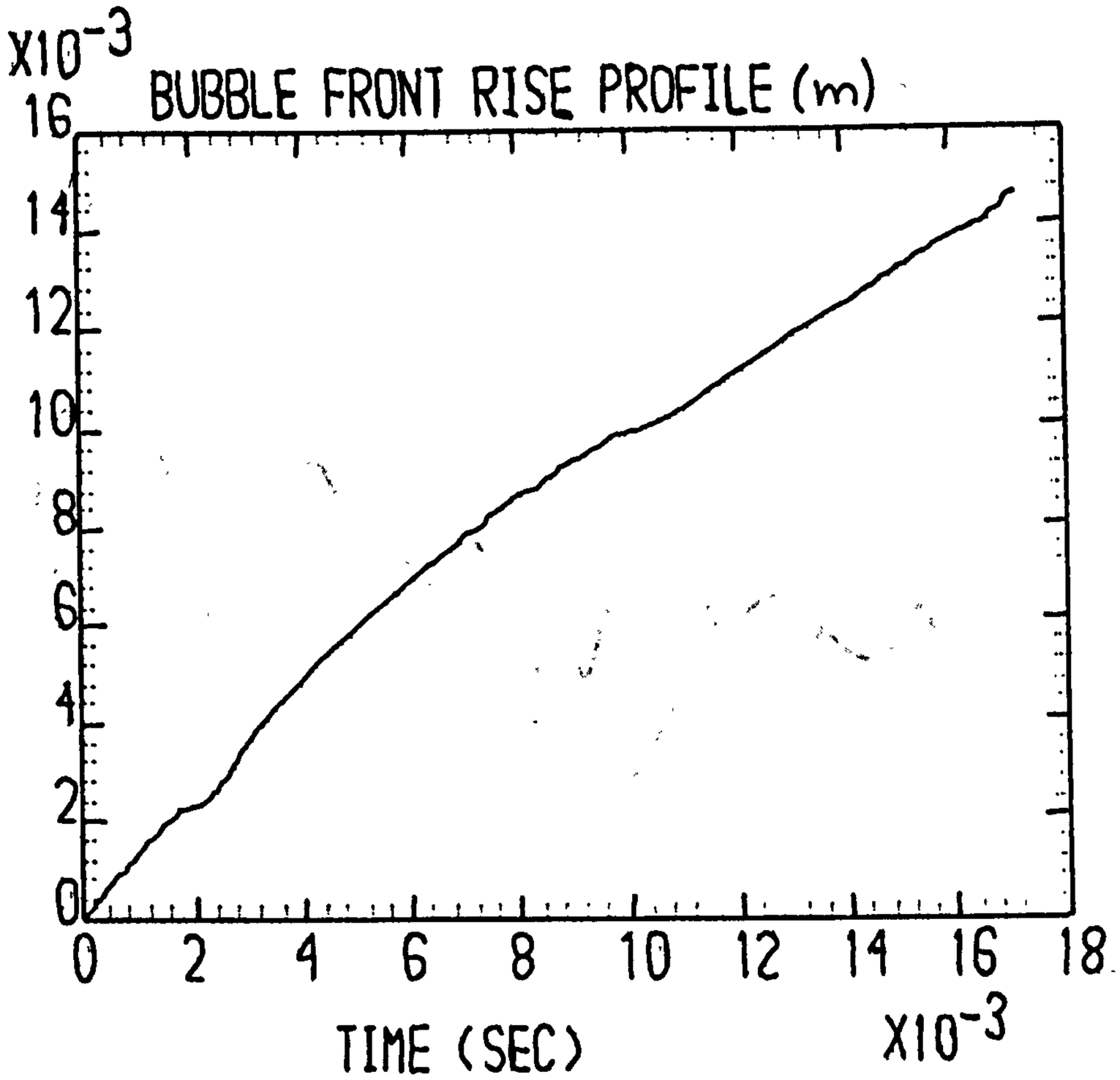

Figure 64. Evaluated bubble front rise (in m).Film I.

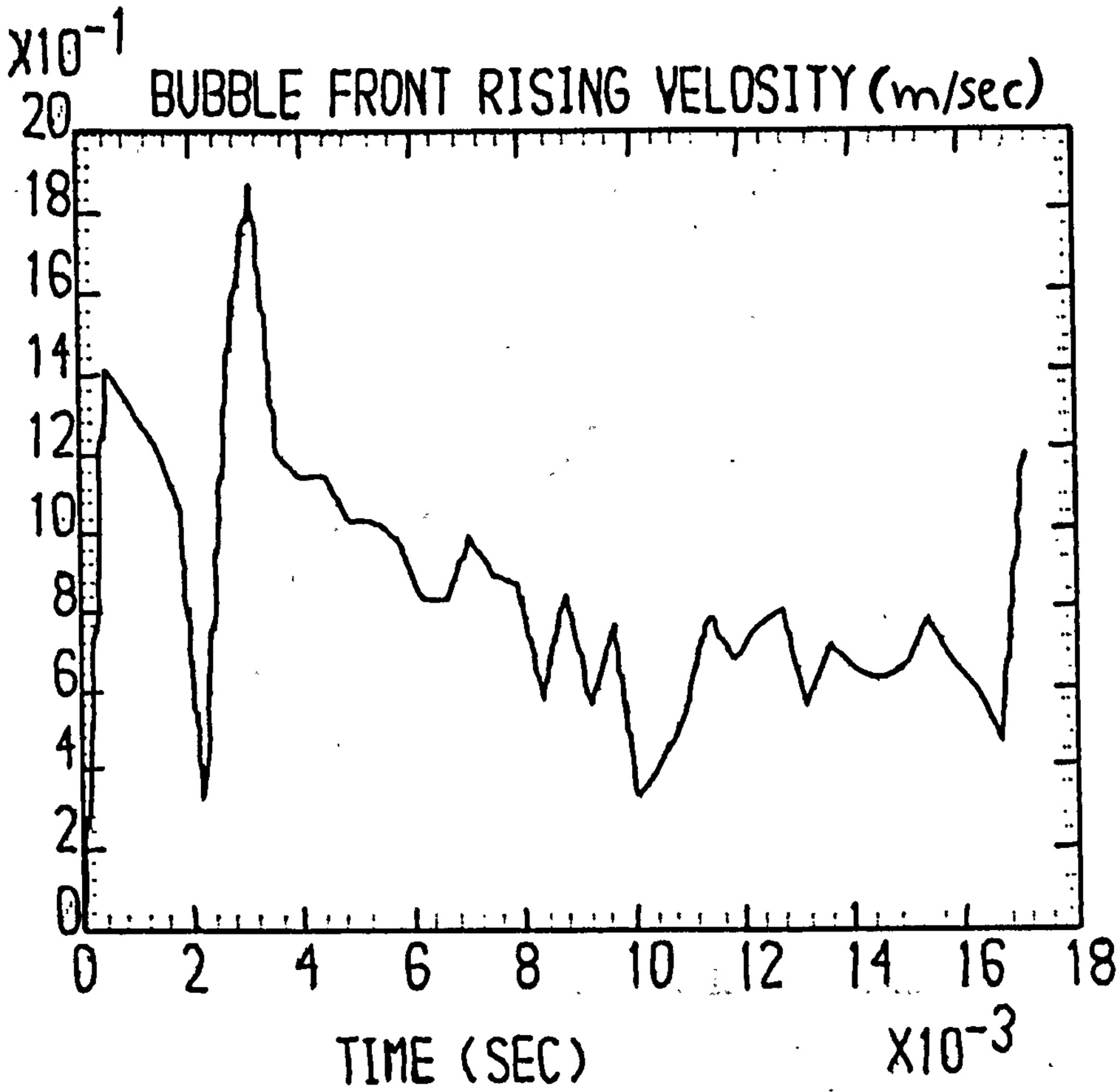

Figure 65. Evaluated bubble front rising velocity (in m/sec).Film I.

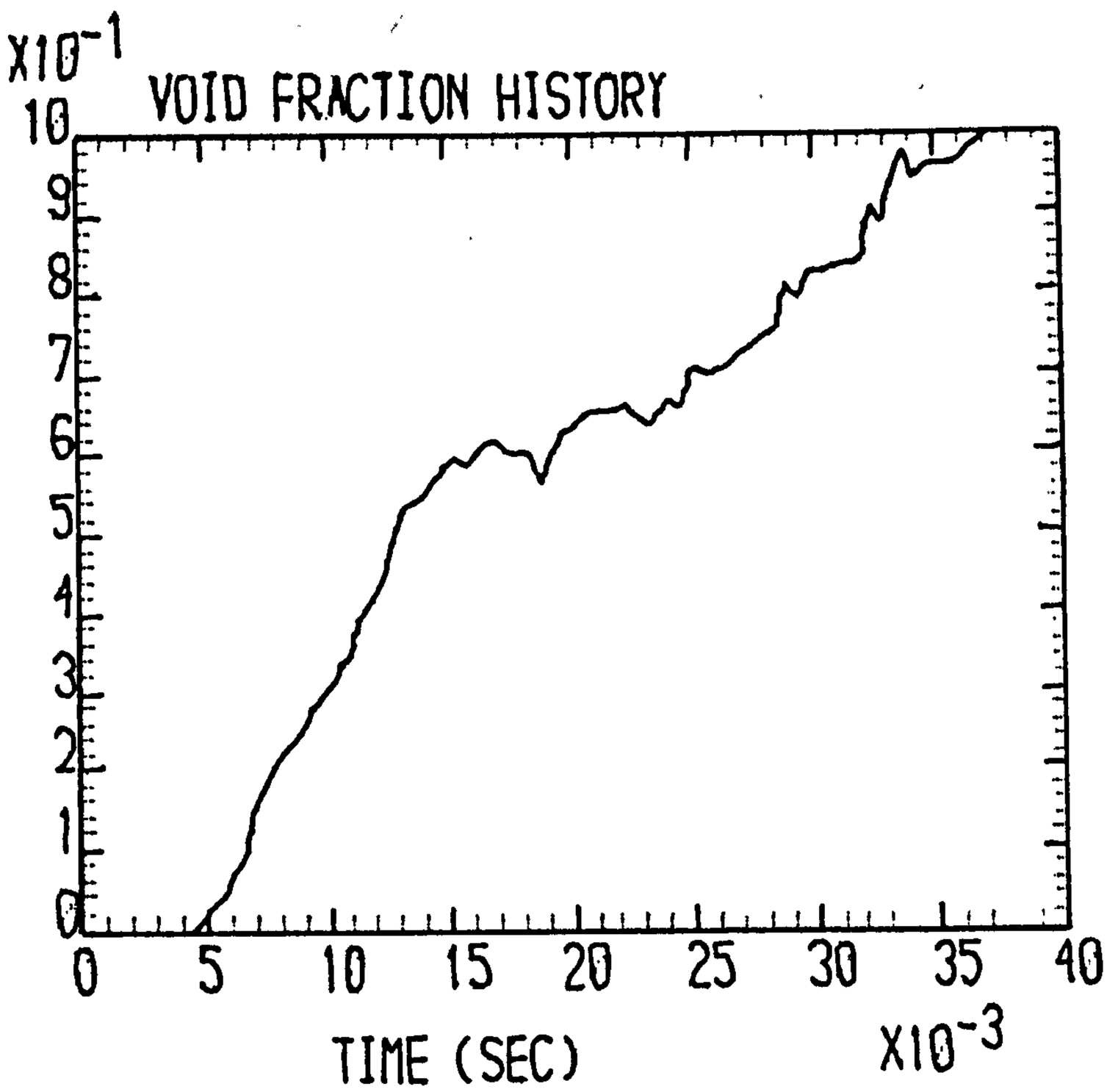

Figure 66. Evaluated void fraction history.Film I.

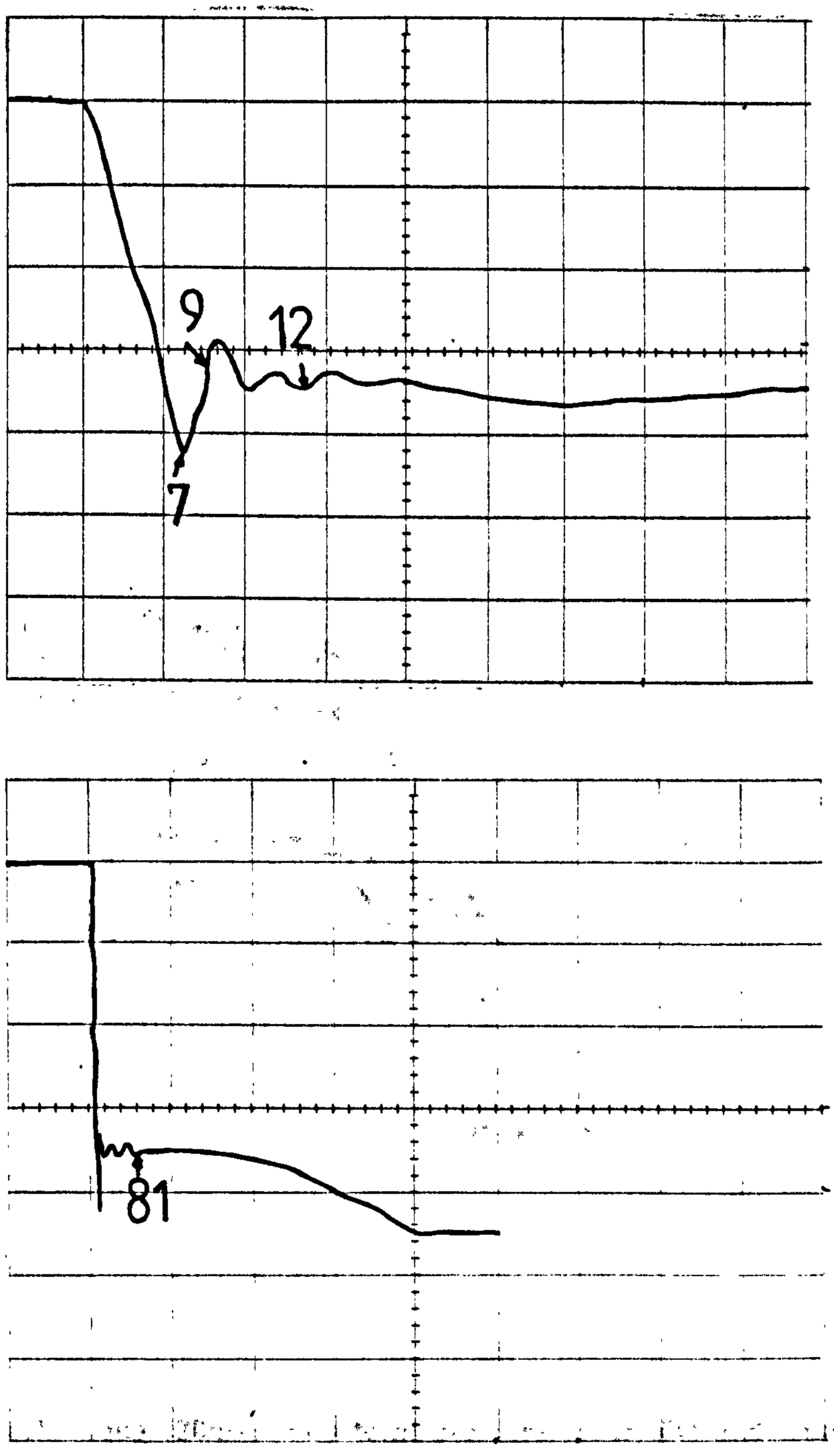

Figure 67. Initial (400μsec/div) and long (20msec/div) term decompression (1bar/div),during filming II.

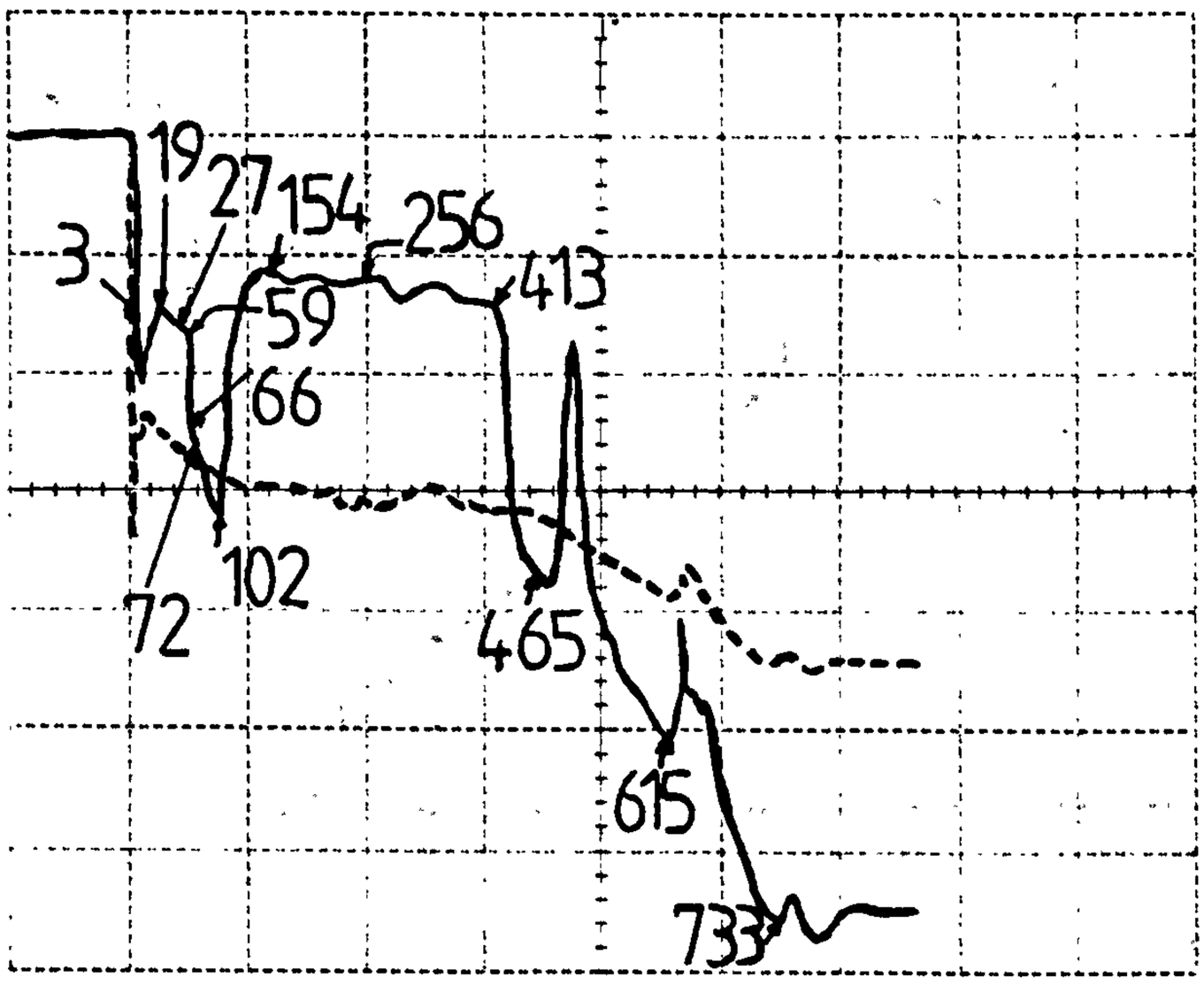

Figure 68. Long (20msec/div) term pressure (1bar/div) and temperature (2.54°C/div) measurements during filming IV.(___temperature trace,- - -pressure trace).

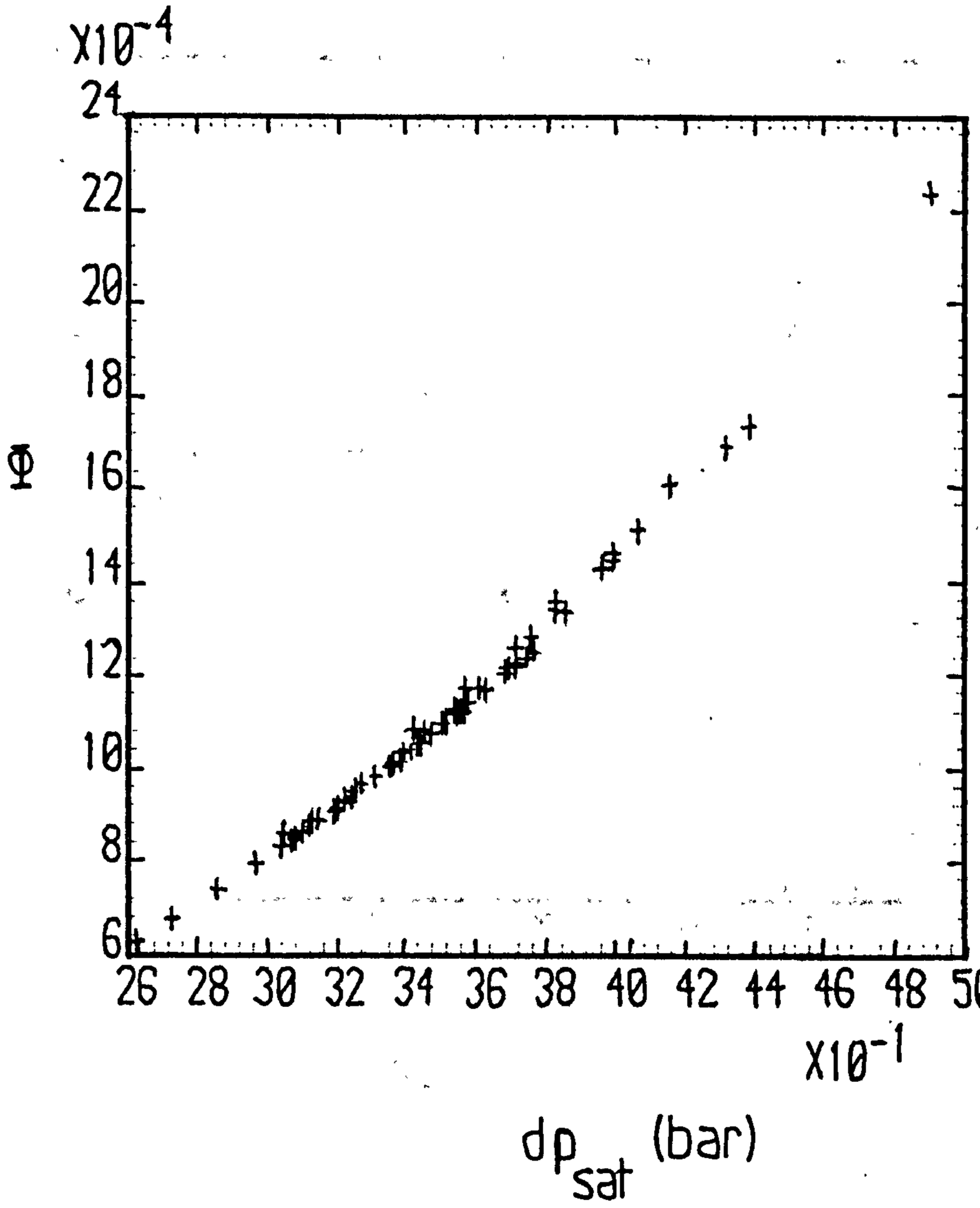

Figure 69. Heterogeneous factor,"Φ",correlation with respect to dp_{sat} (freon 12).

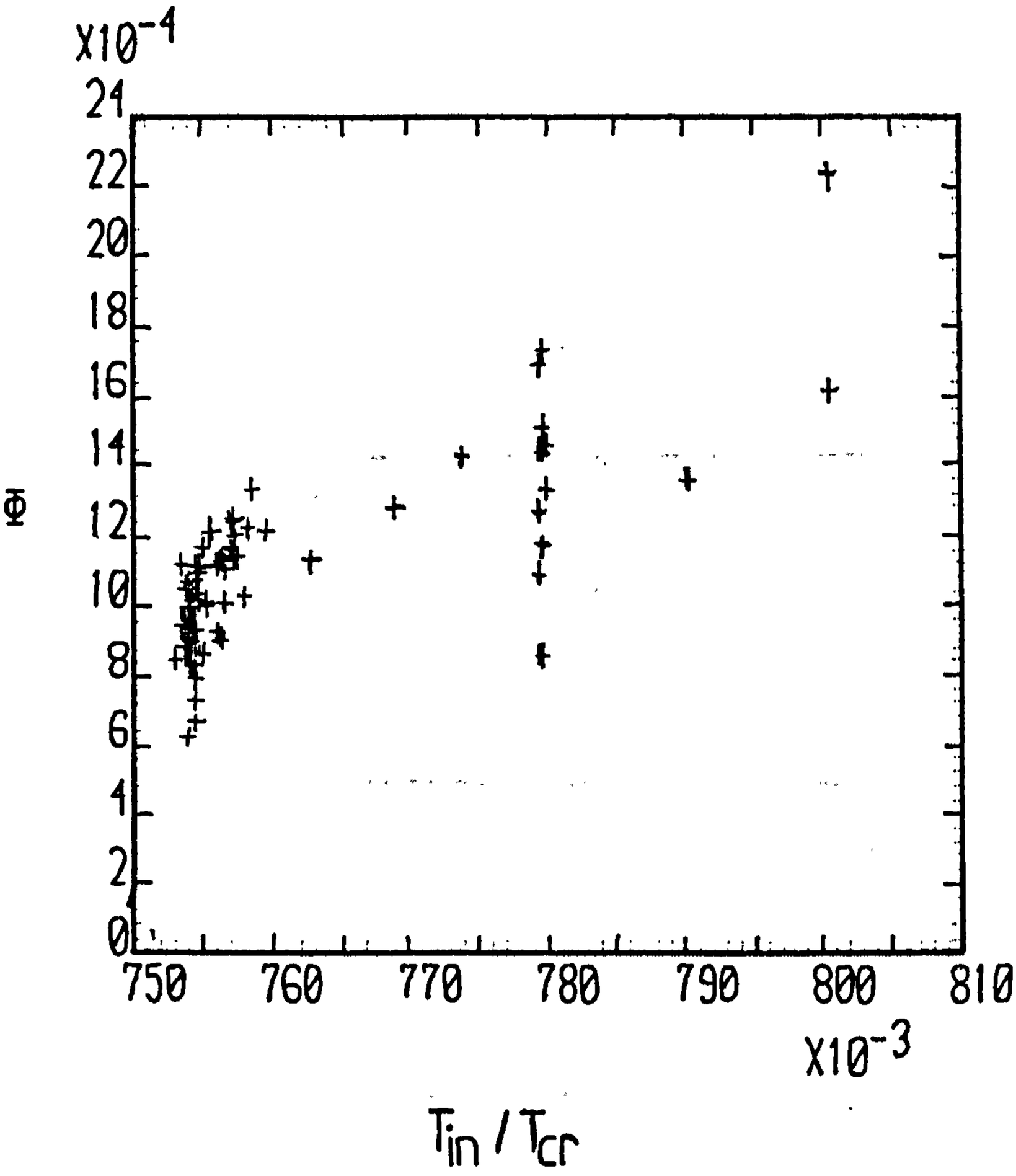

Figure 70. Heterogeneous factor,"Φ",correlation with respect to T_{in}/T_{cr} (freon 12).

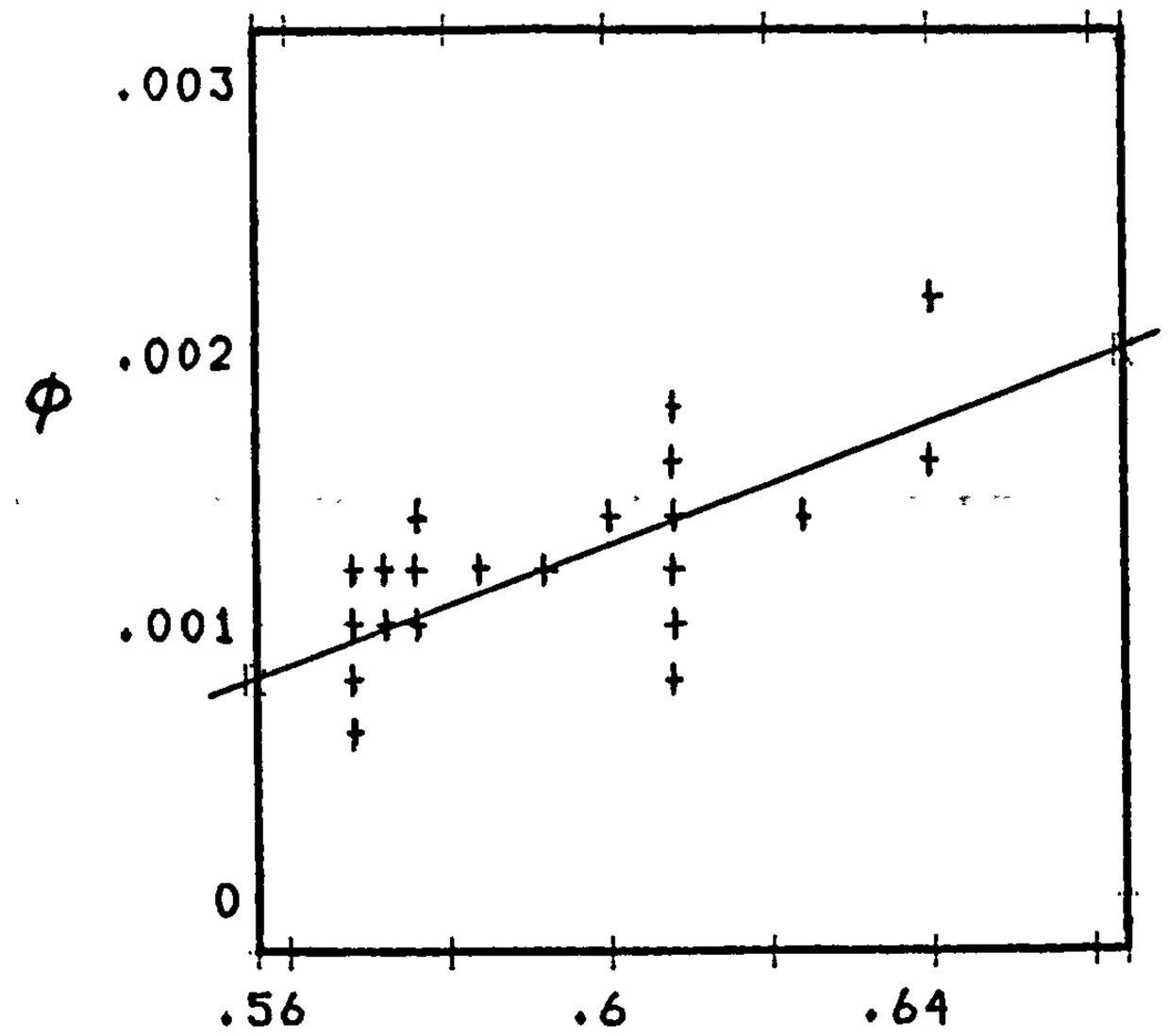

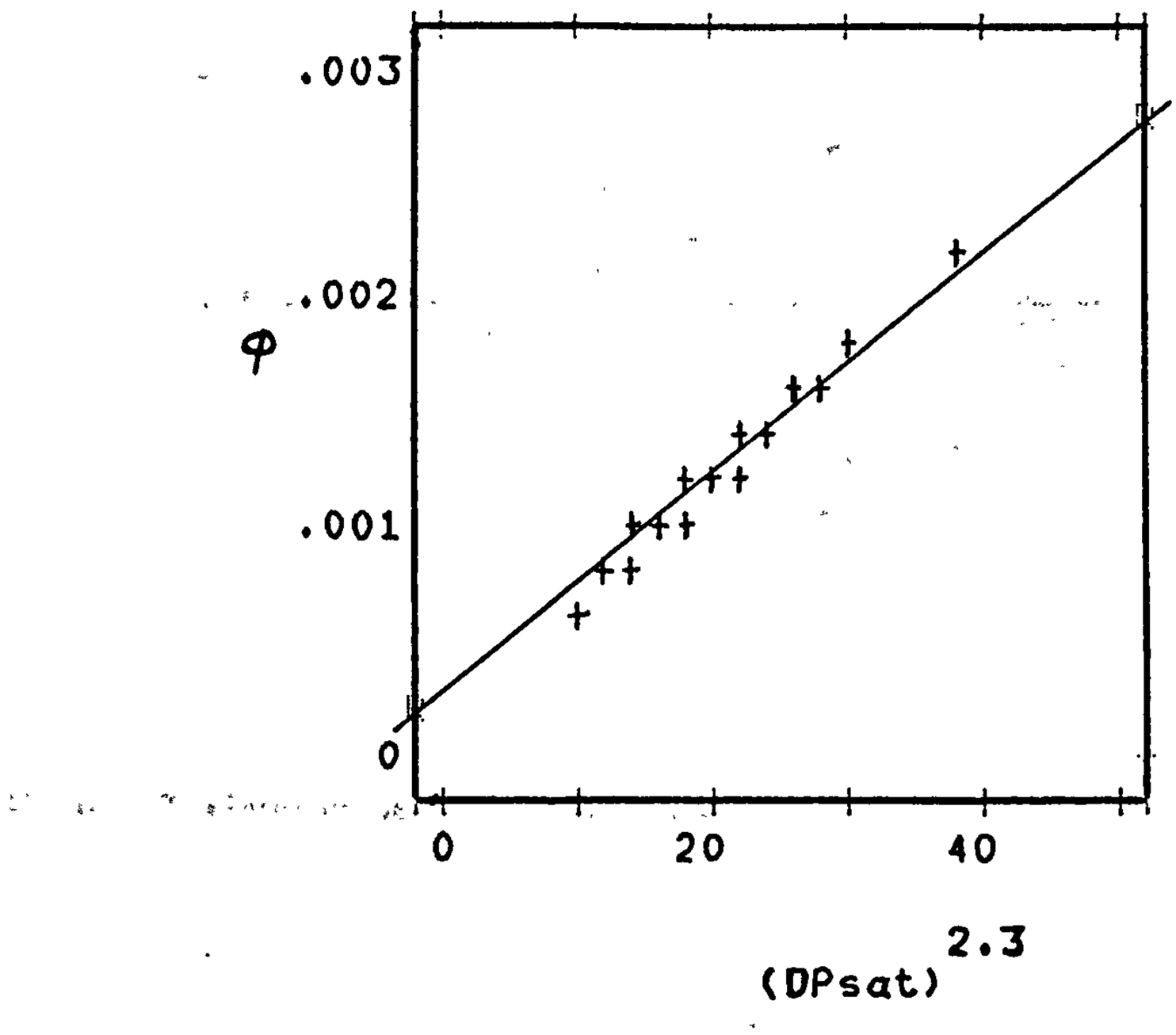

Figure 71. Linearise correlation of Φ with respect to $(T_{in}/T_{cr})^2$ (top) and $(dp_{sat})^{2.3}$ (bottom).

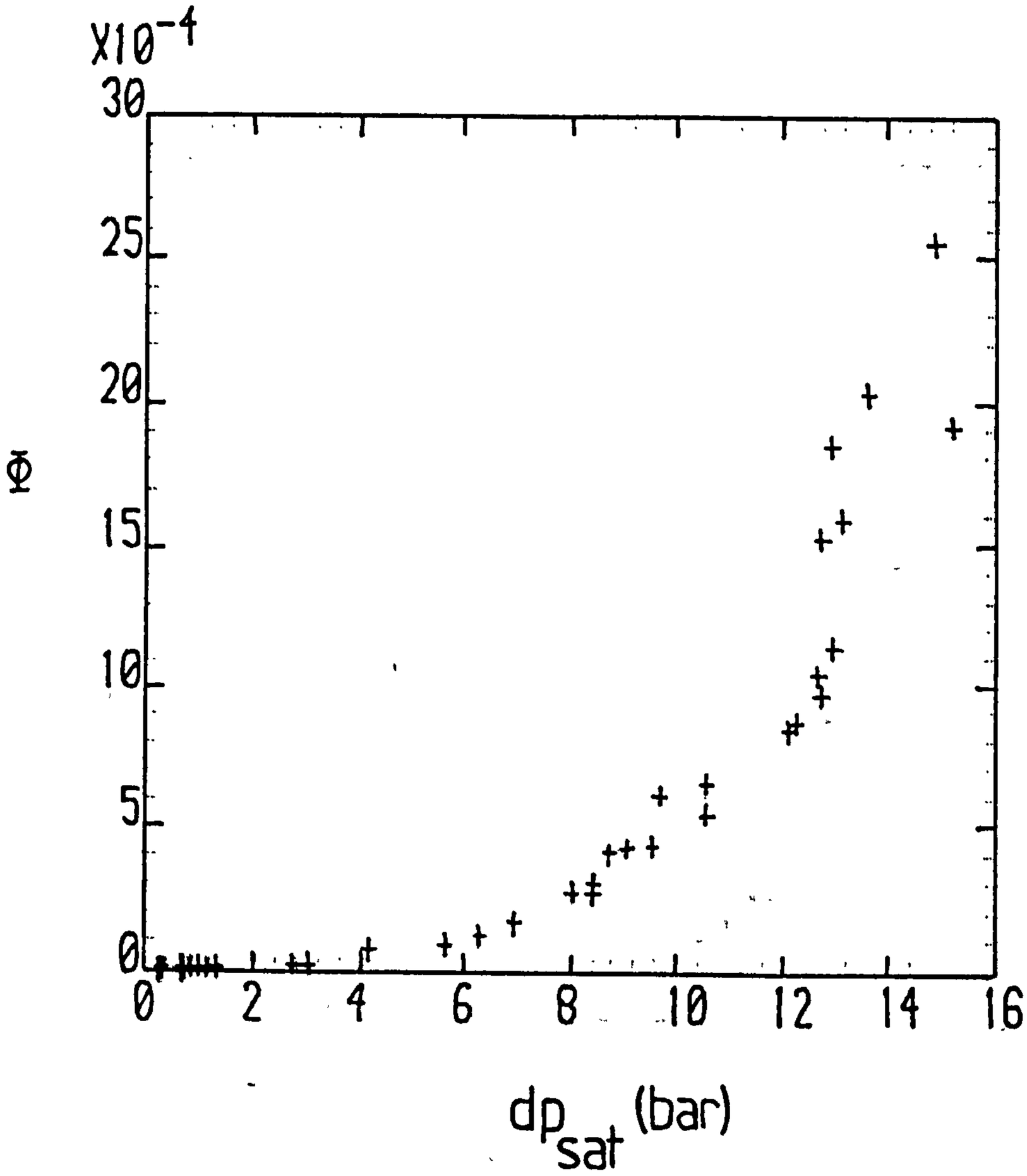

Figure 72. Heterogeneous factor,"Φ",correlation with respect to dp_{sat} (water).

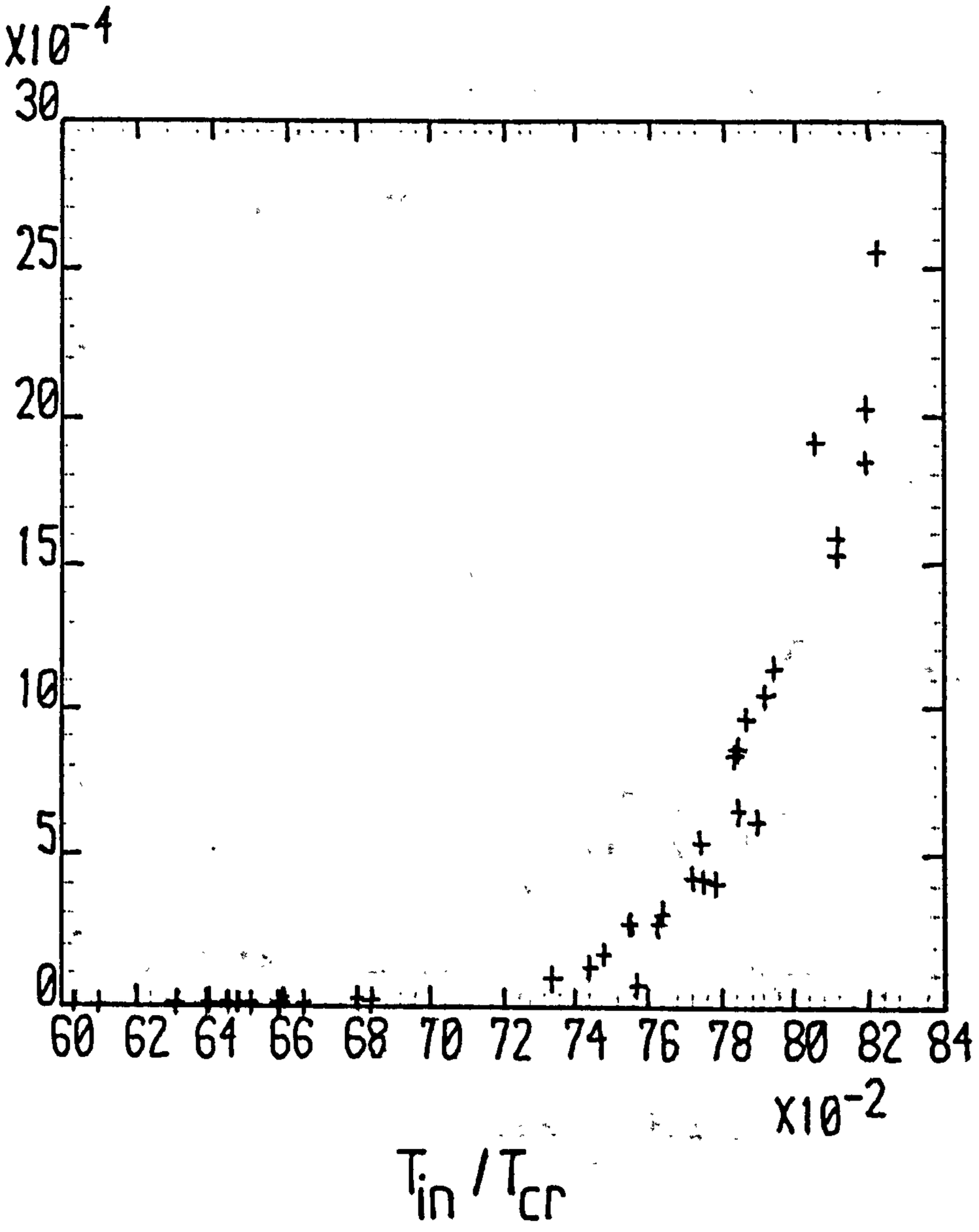

Figure 73. Heterogeneous factor,"Φ",correlation with respect to T_{in}/T_{cr} (water).

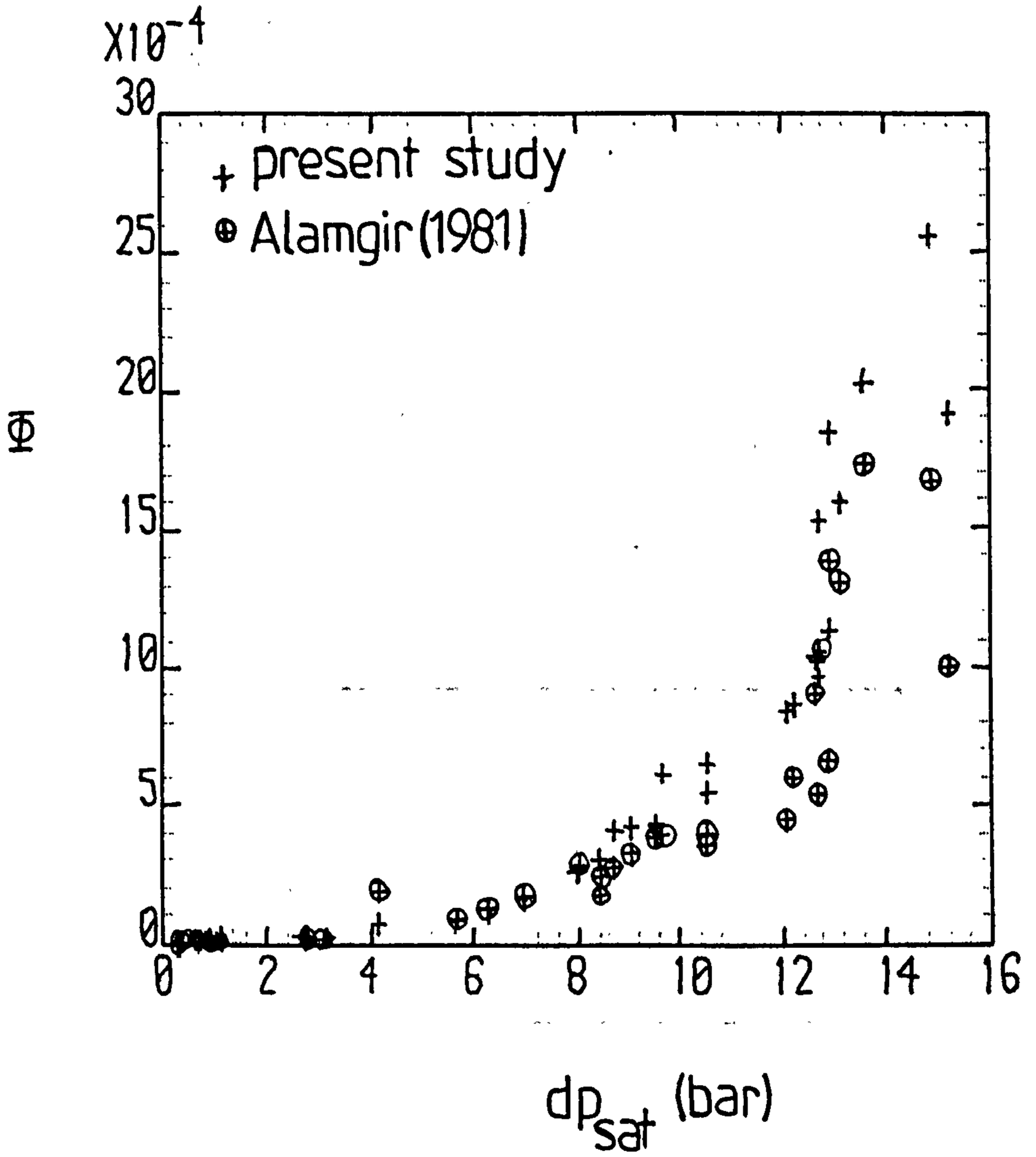

Figure 74. Comparison of the "Φ- dp_{sat}" correlation ,provided by the present and Alamgir's method.

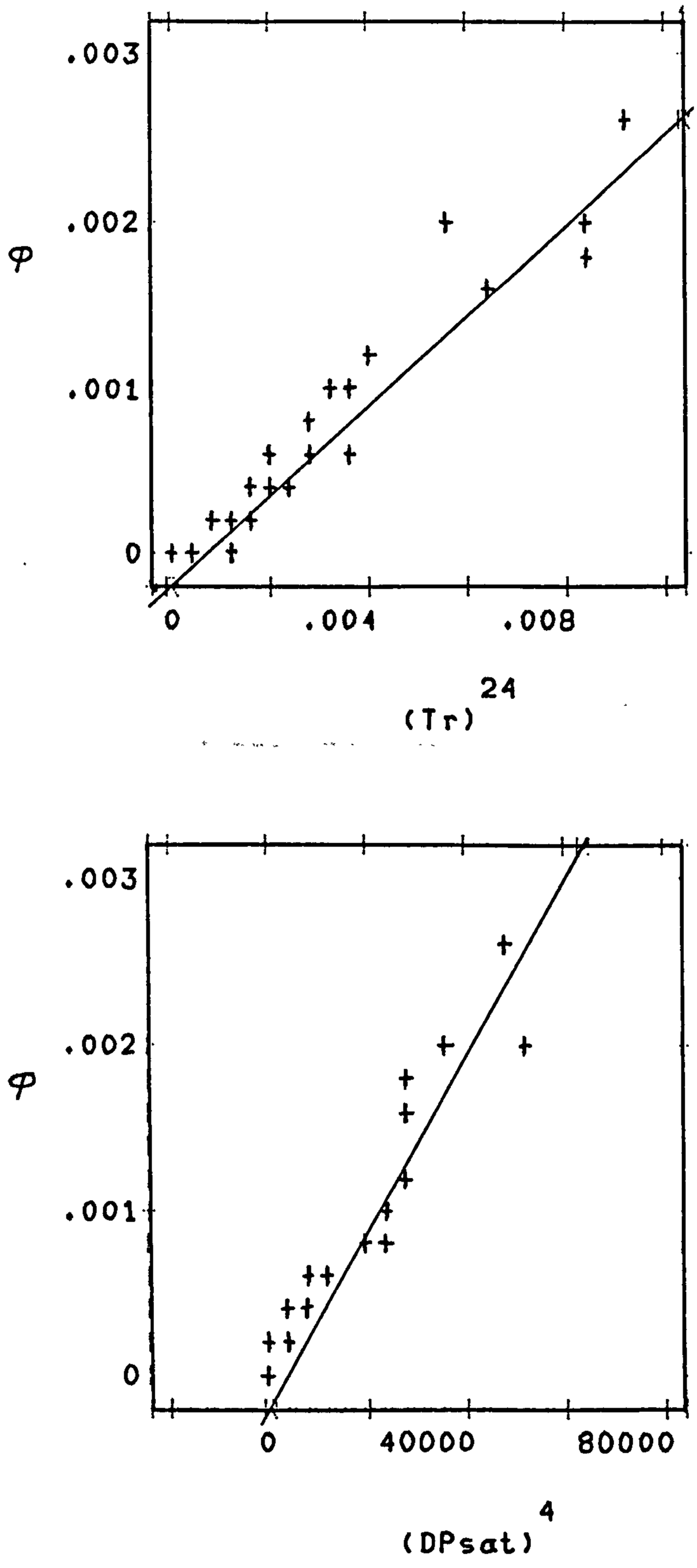

Figure 75. Linearise correlation of "Φ" with respect to $(T_{in}/T_{cr})^{24}$ (top) and $(dp_{sat})^4$ (bottom) (water).

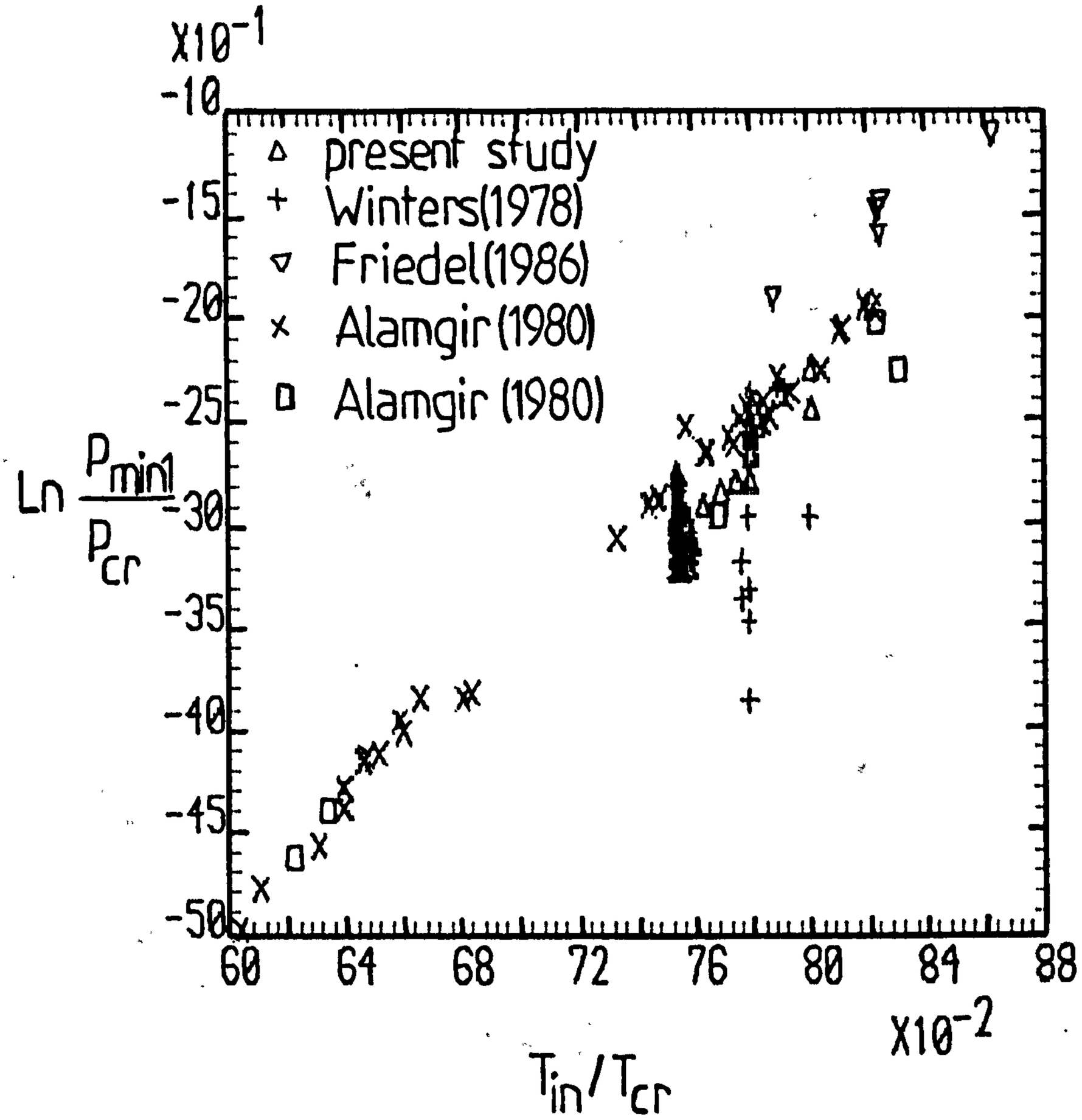

Figure 76a. Illustration of the p_{min1} dependence on the initial temperature (water and freon 12).

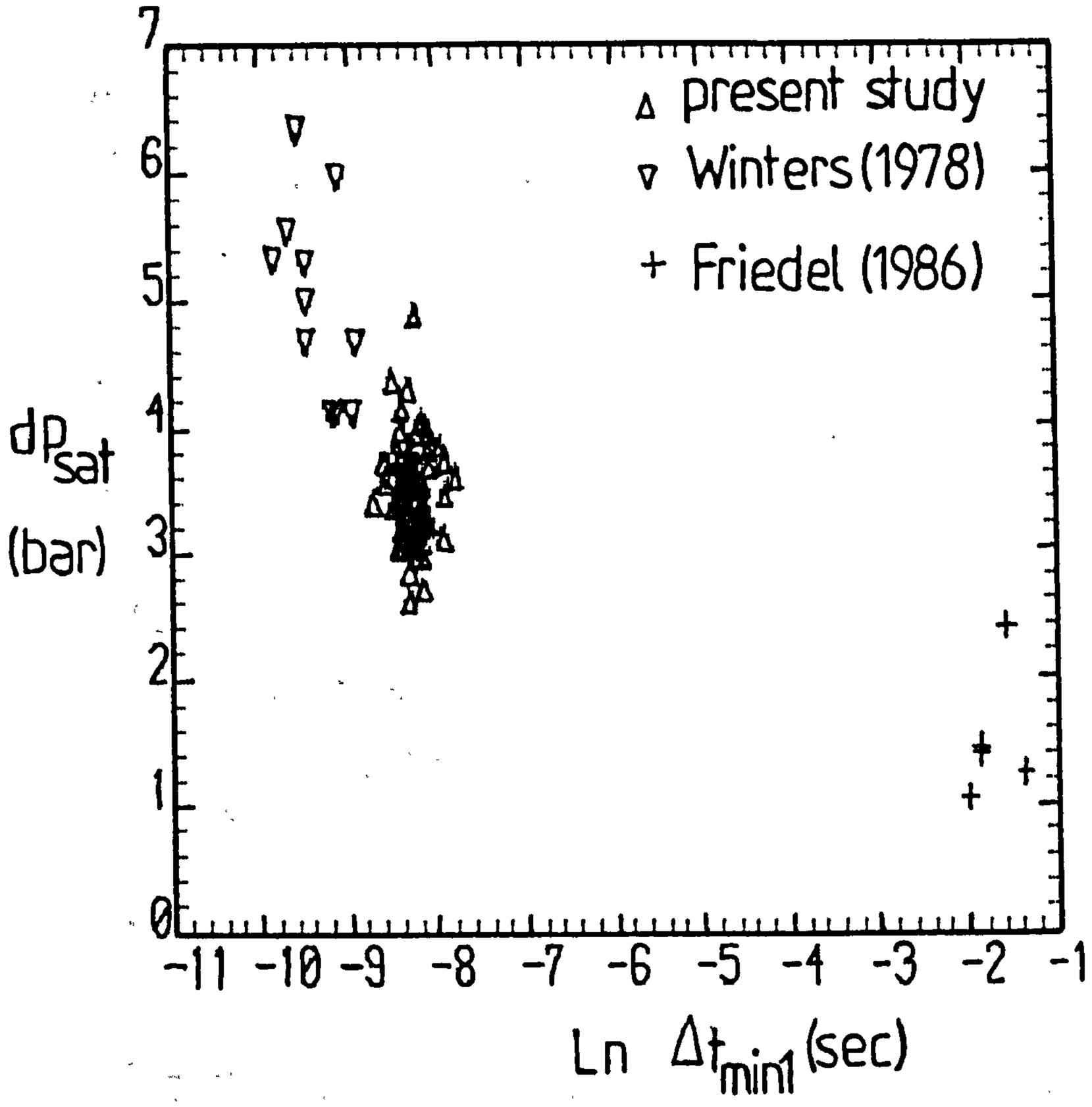

Figure 76b. Illustration of the dp_{sat} dependence on the Δt_{min1} (freon 12).

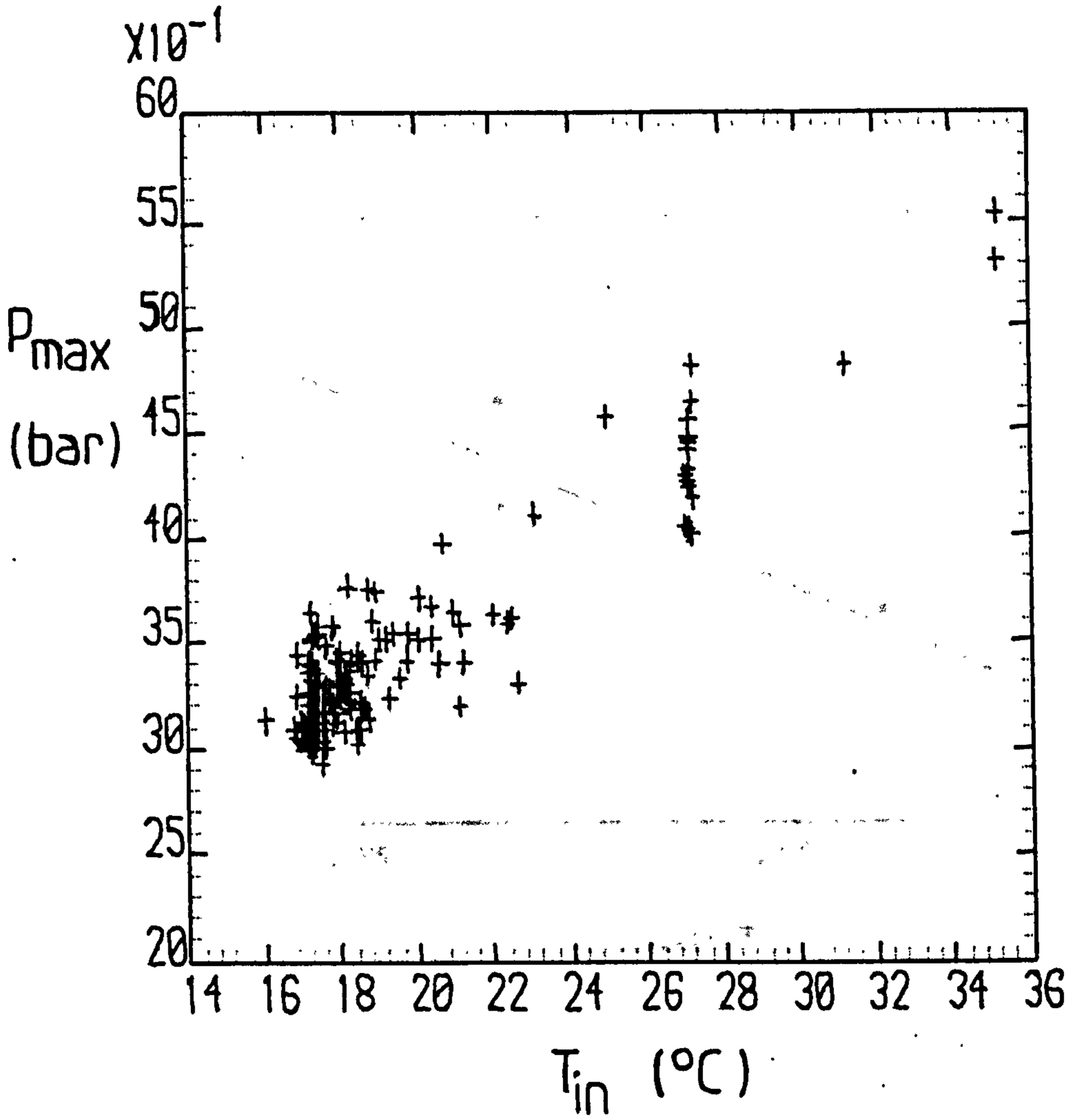

Figure 77. Illustration of the p_{max} dependence on the initial temperature (freon 12).

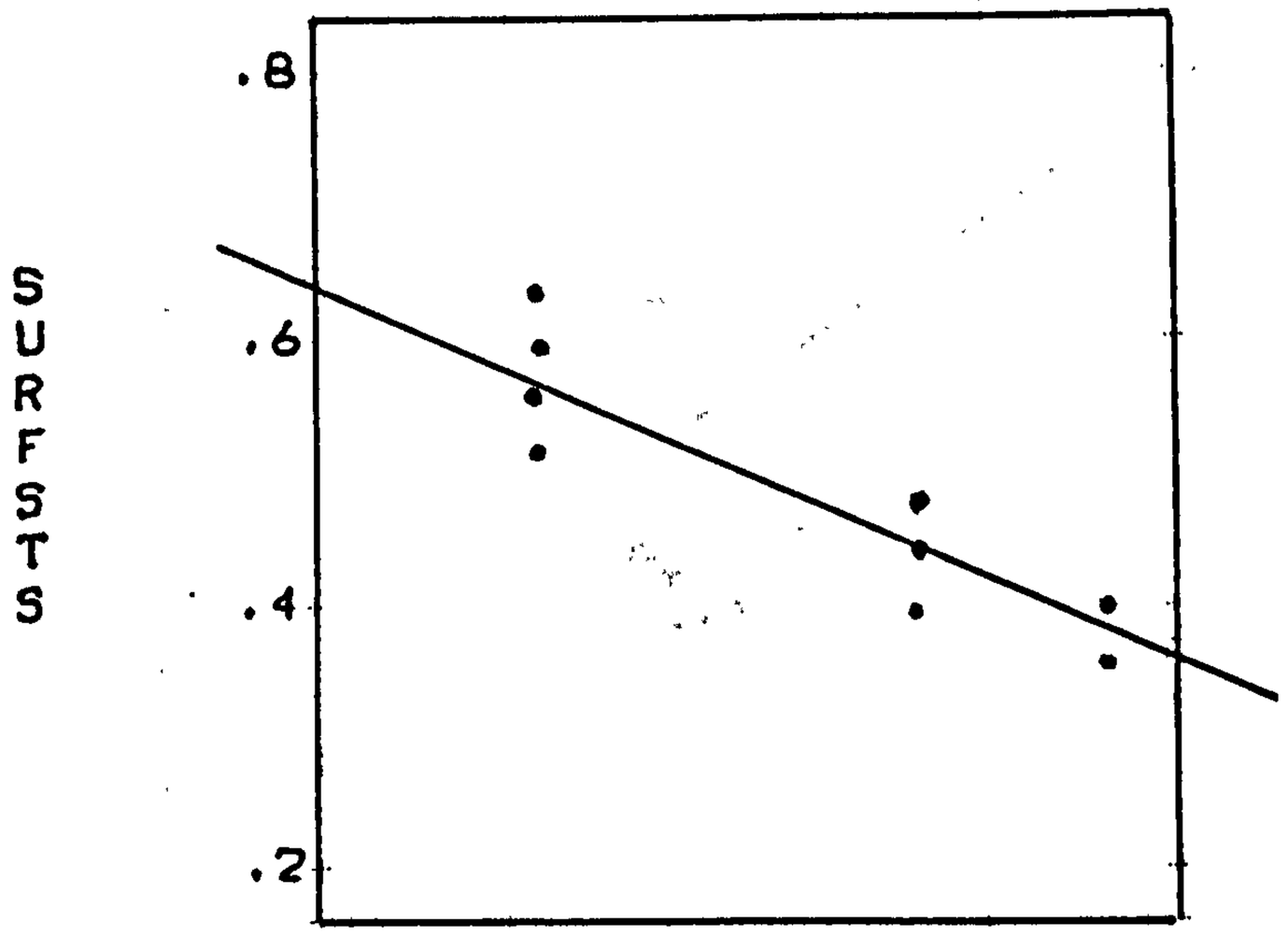

Figure 78: Linearise correlation of the standarized average pressure in the vessel,"surfsts",with respect to ("size")$^{0.3}$

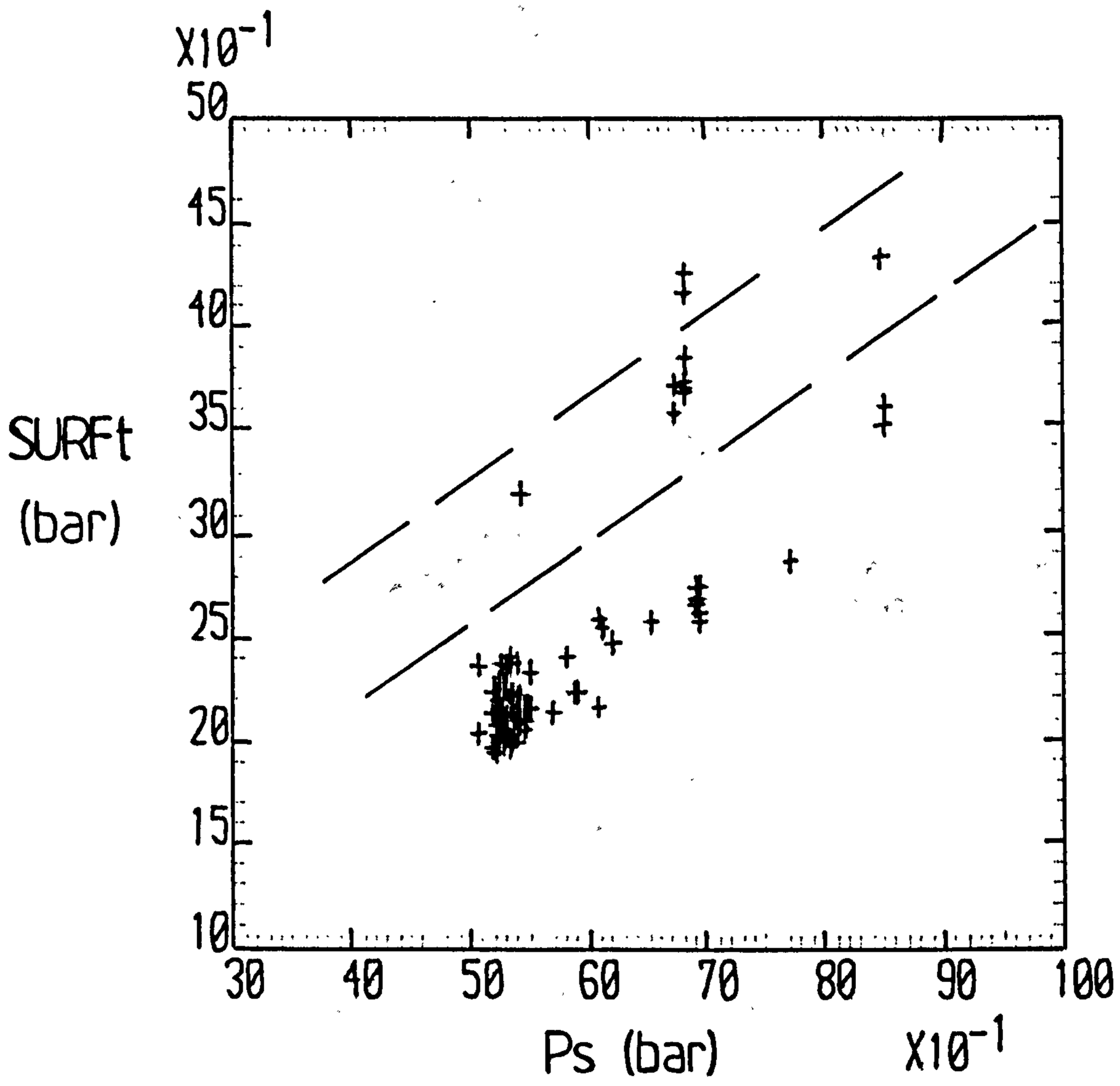

Figure 79. Illustration of the average pressure in the vessel,"surft" dependence on the saturation pressure,corresponding to the initial temperature (all materials-all sizes).

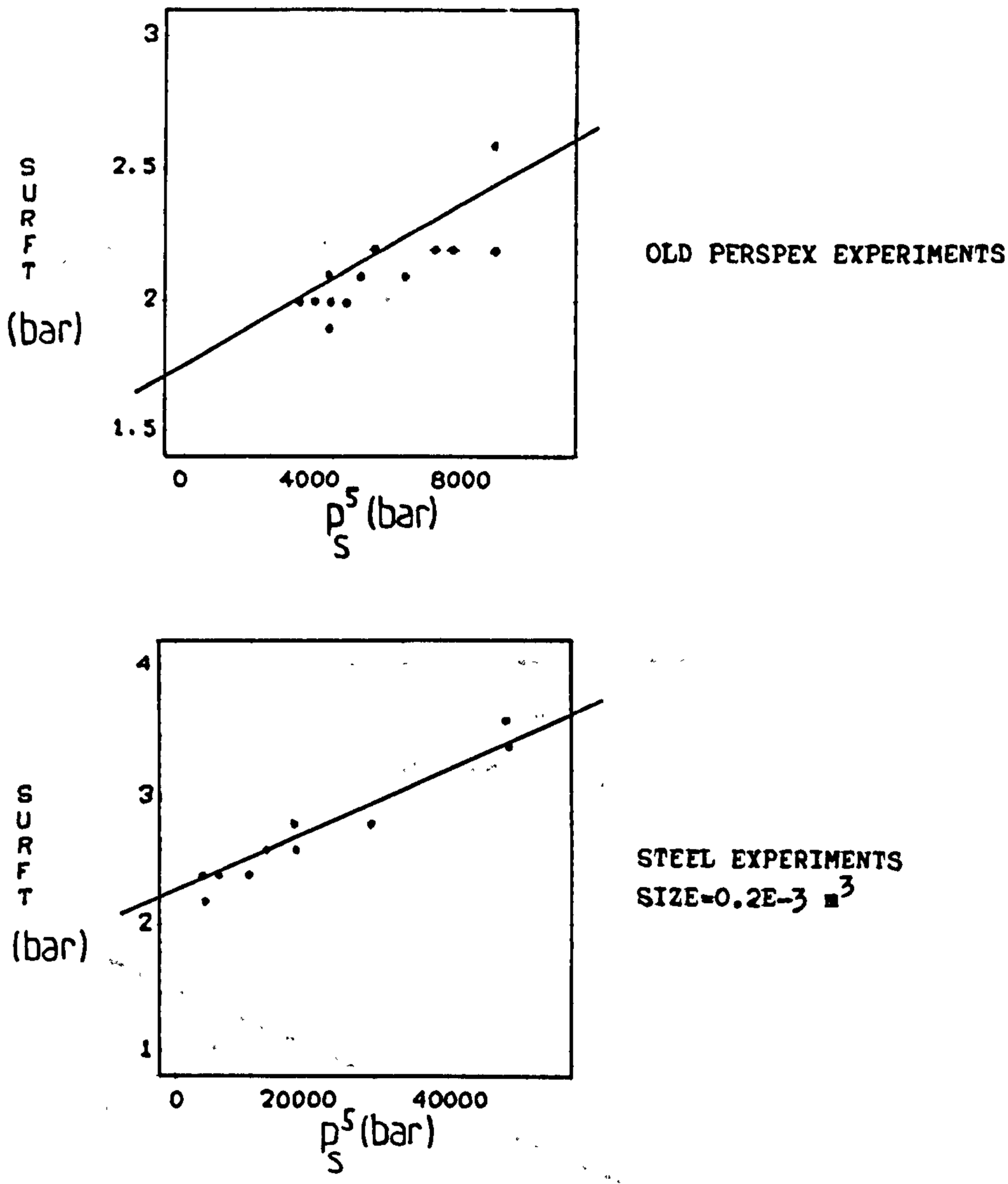

Figure 80. Illustration of the average pressure in the vessel dependence on the saturation pressure,corresponding to the initial temperature.

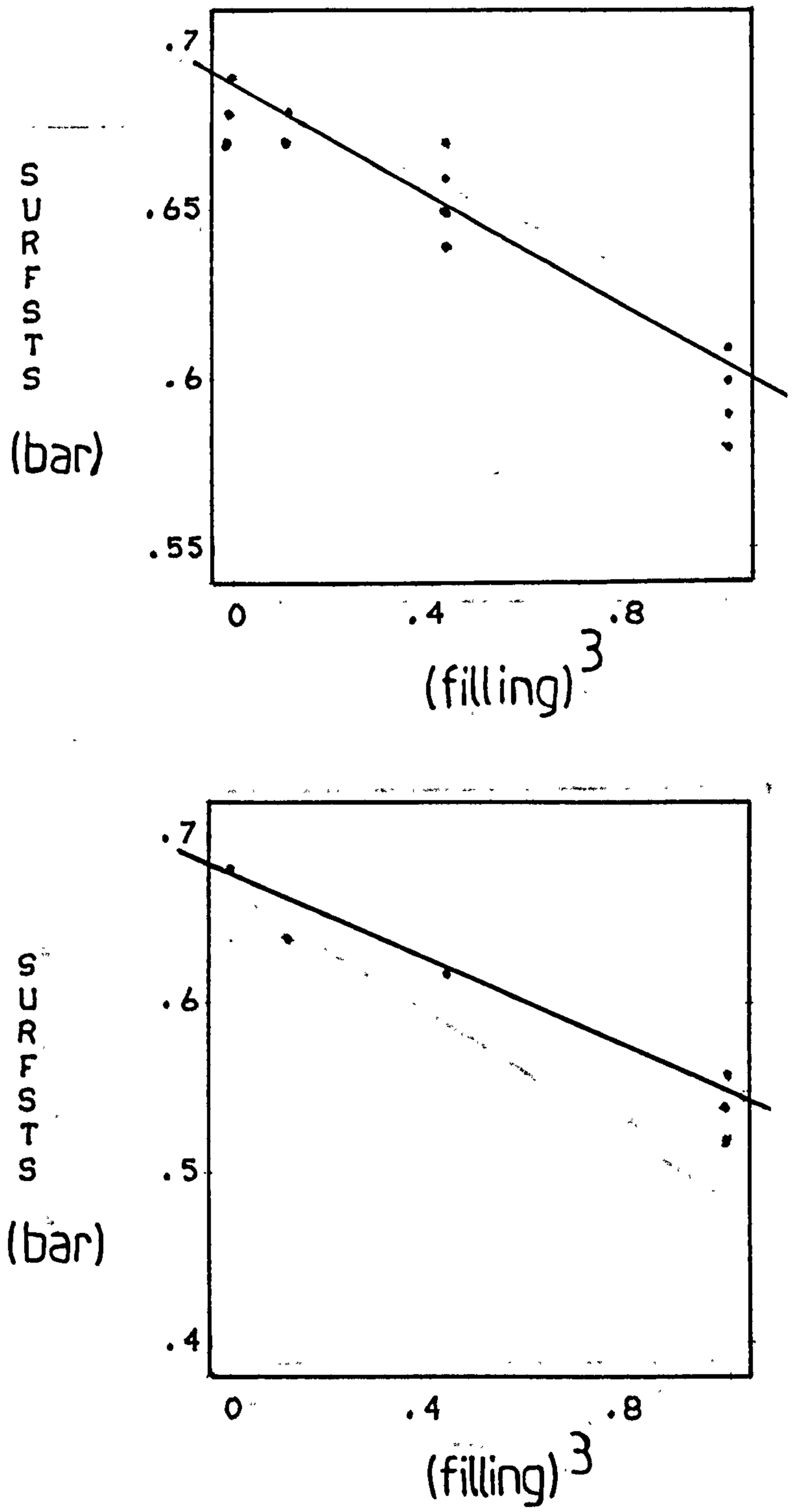

Figure 81. Illustration of the effect of a "partially full" vessel blowdown,on the standarized average pressure,"surfsts".Vent pipe length equals to 0m (top) and 0.2m (bottom).

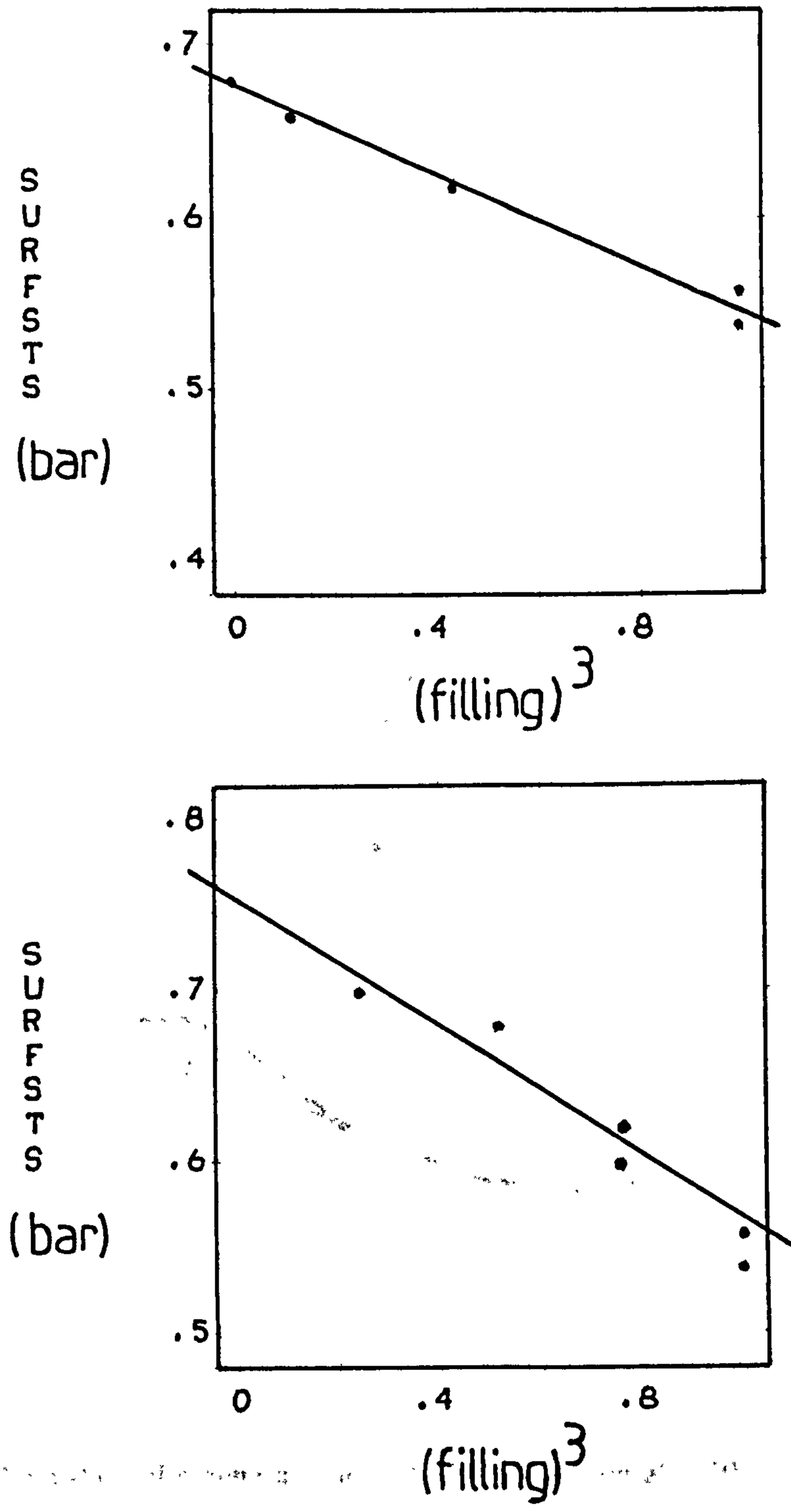

Figure 82. Illustration of the effect of a "partially full" vessel blowdown,on the standarized average pressure,"surfsts".Vent pipe length equals to 0.5m (top) and 1m (bottom).

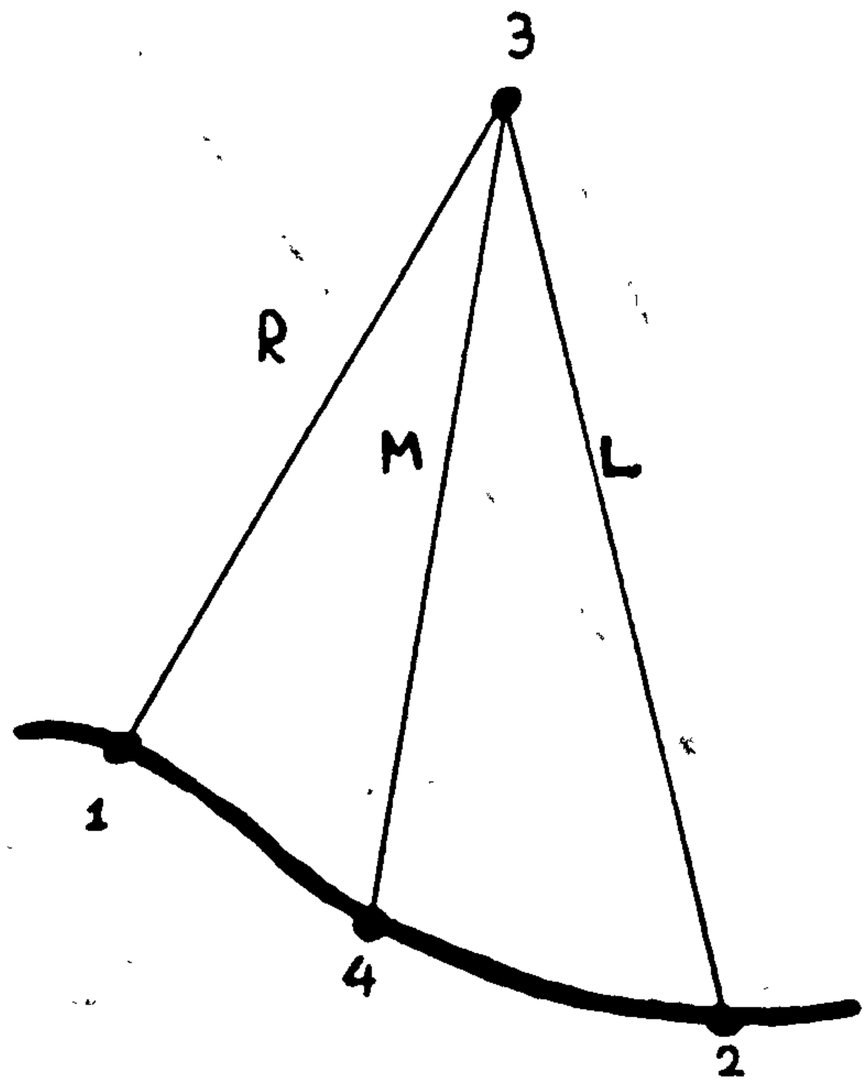

Figure 83. Illustration of a general "characteristic" solution algorithm.

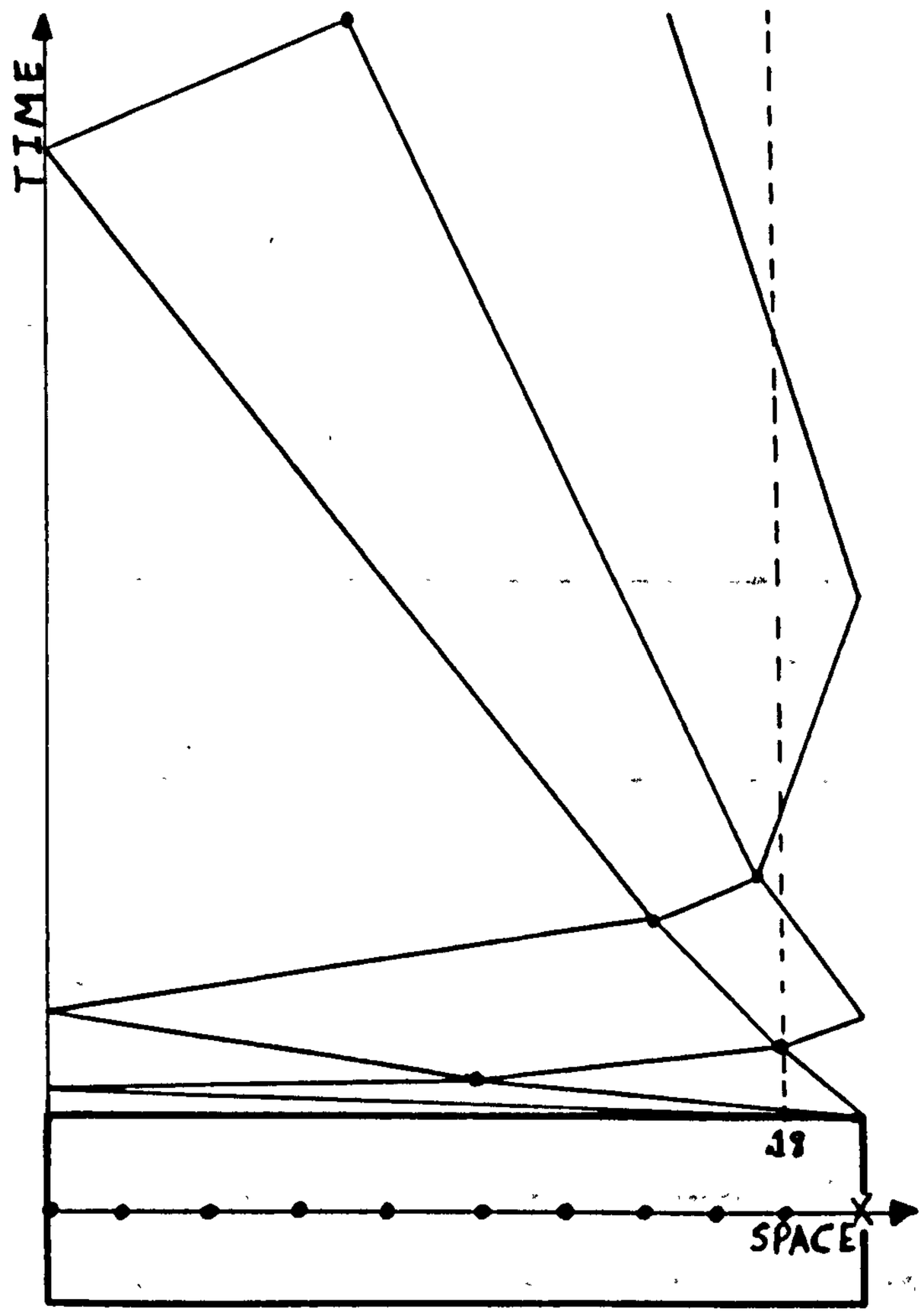

Figure 84. Wave tracing type of solution.Method of "characteristics".

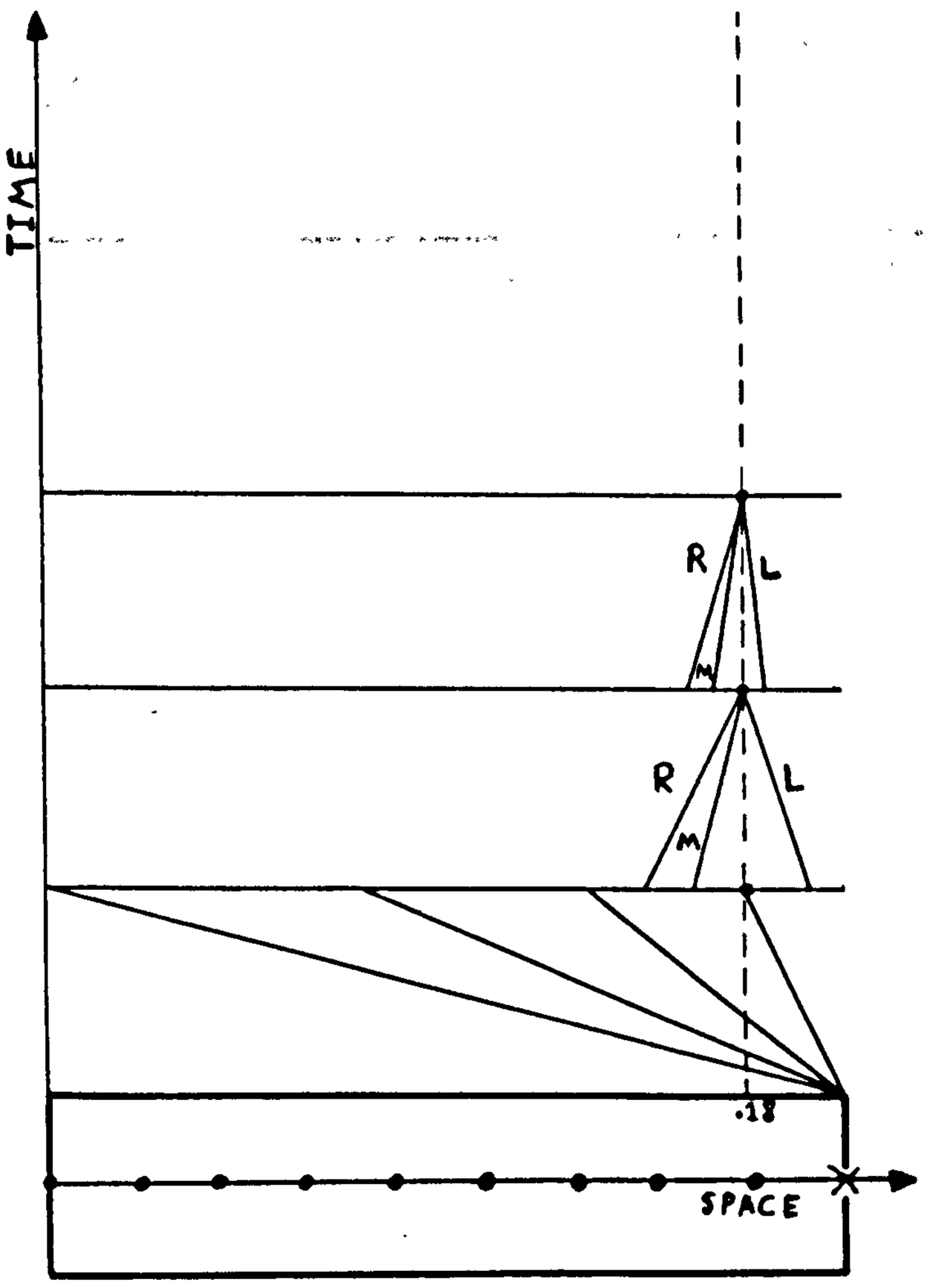

Figure 85. Constant mesh point type of solution.Method of "characteristics".

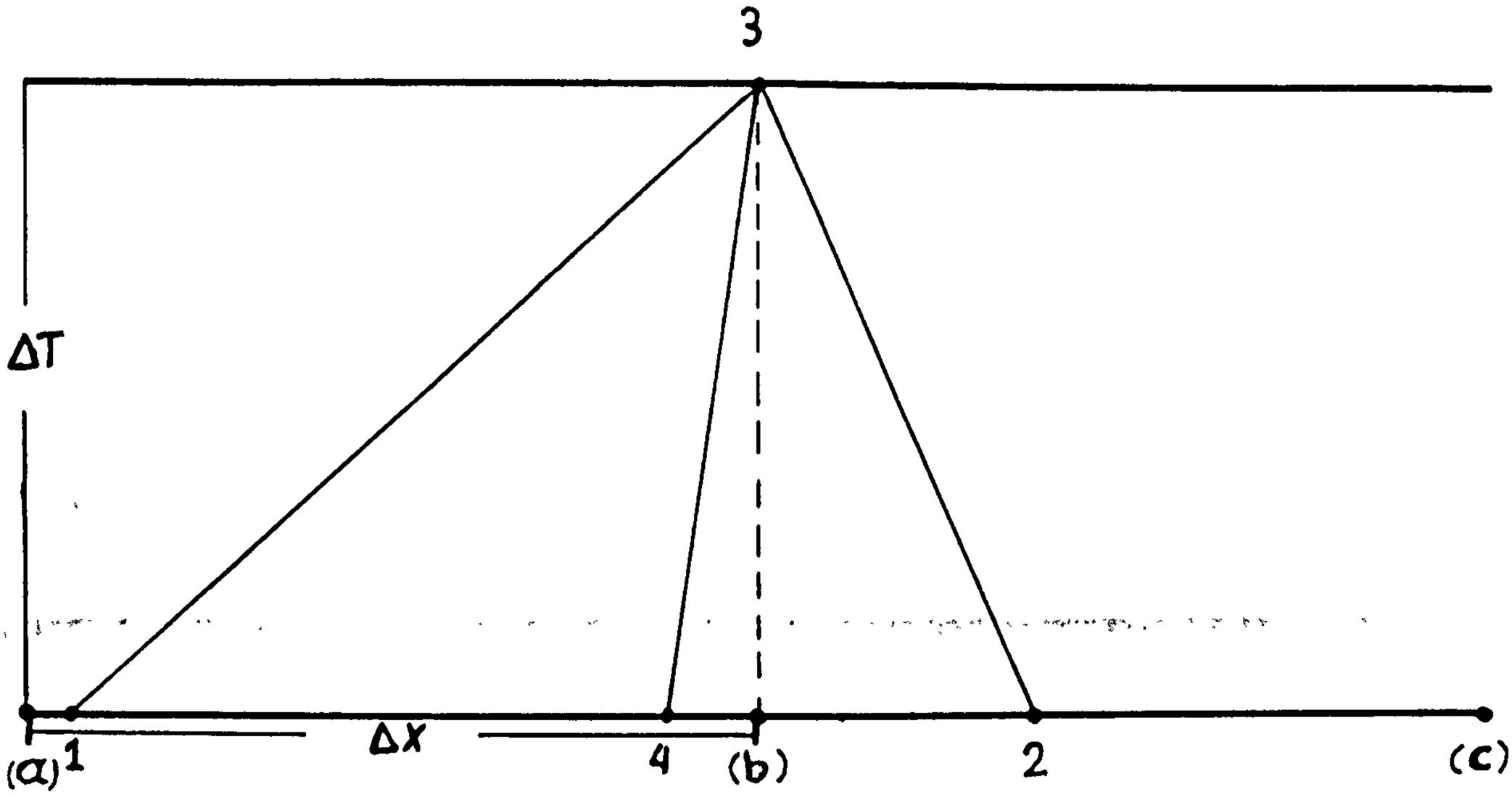

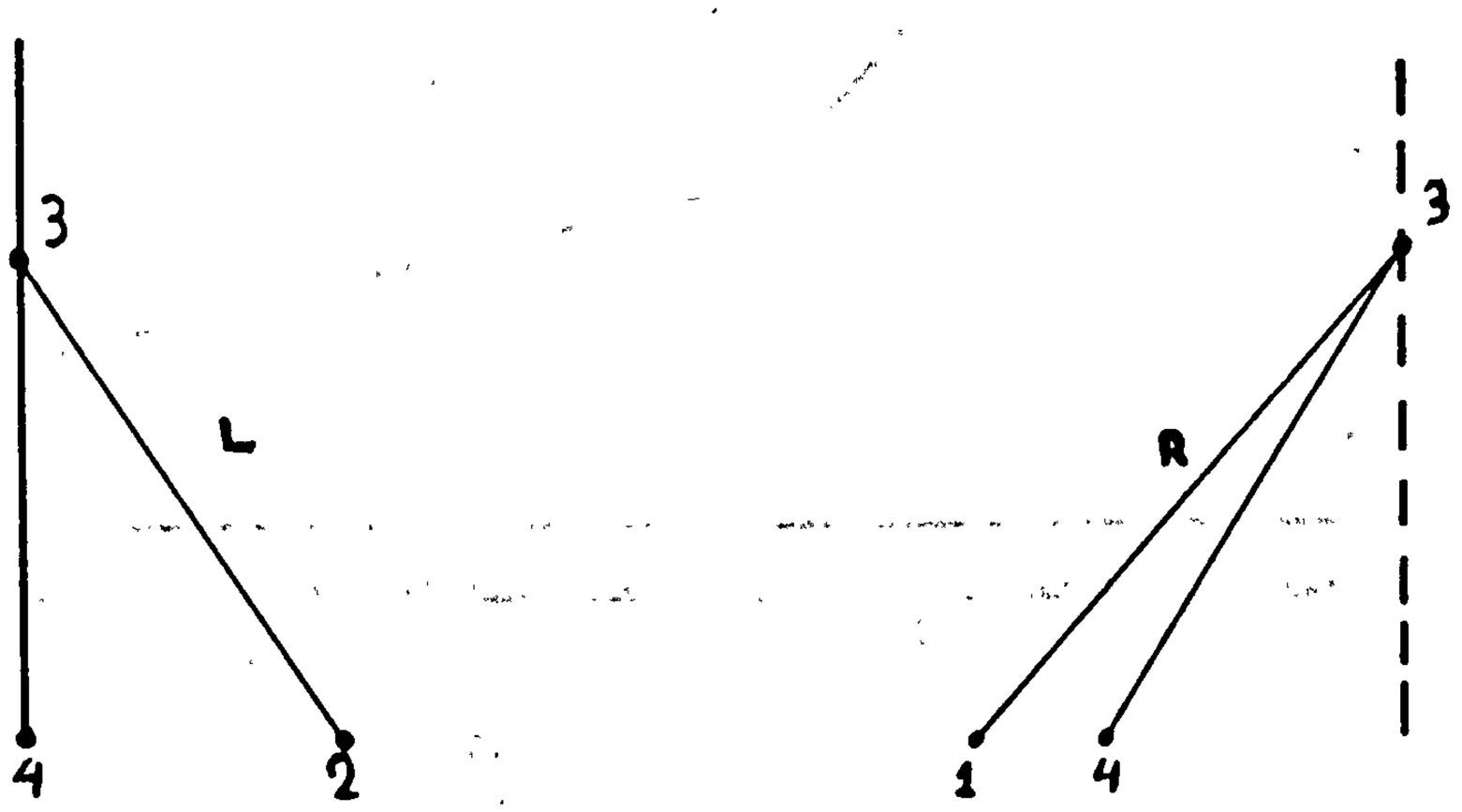

Figure 86. Solution technique for the middle and boundary mesh points. Method of "Characteristics".

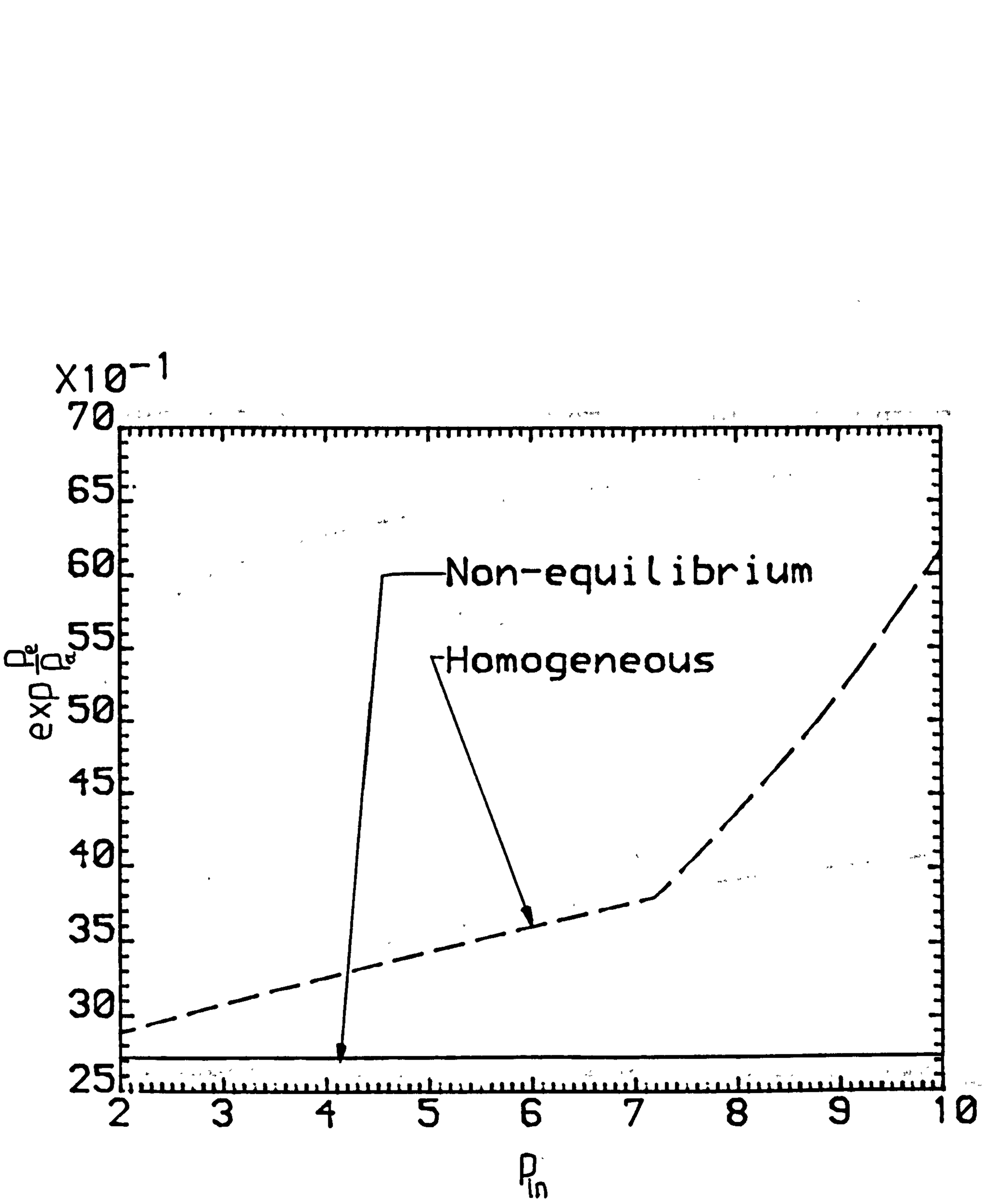

Figure 87. The effect of the initial pressure (bar),in the driving section of a shock tube,on the ratio of the expansion pressure to the atmospheric pressure (___thermal non-equilibrium model,- - -homogeneous model).

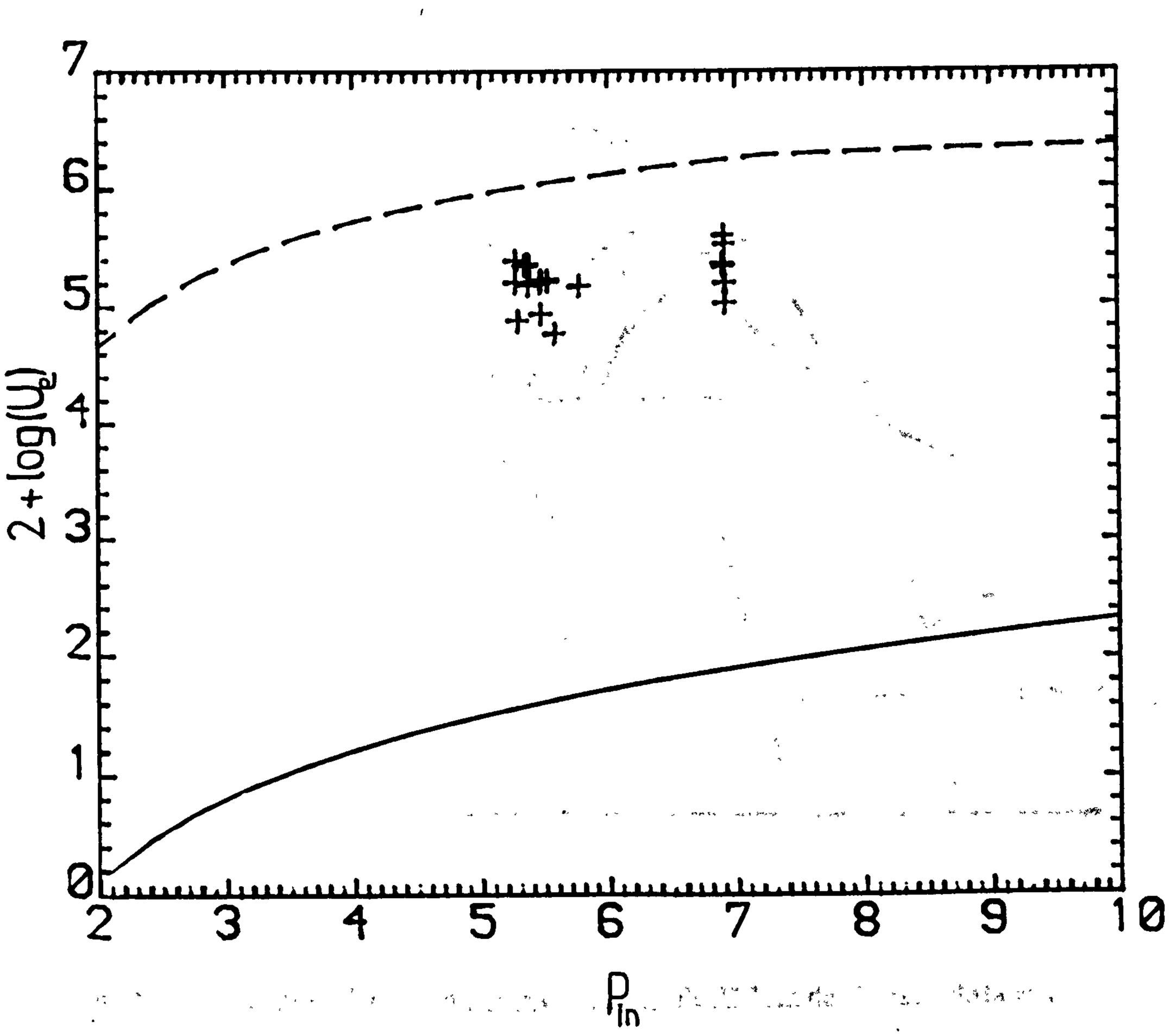

Figure 88. The effect of the initial pressure (bar),in the driving section of a shock tube,on the expansion material velocity (___thermal non-equilibrium model, - - -homogeneous model).Comparison with experimental data (+).

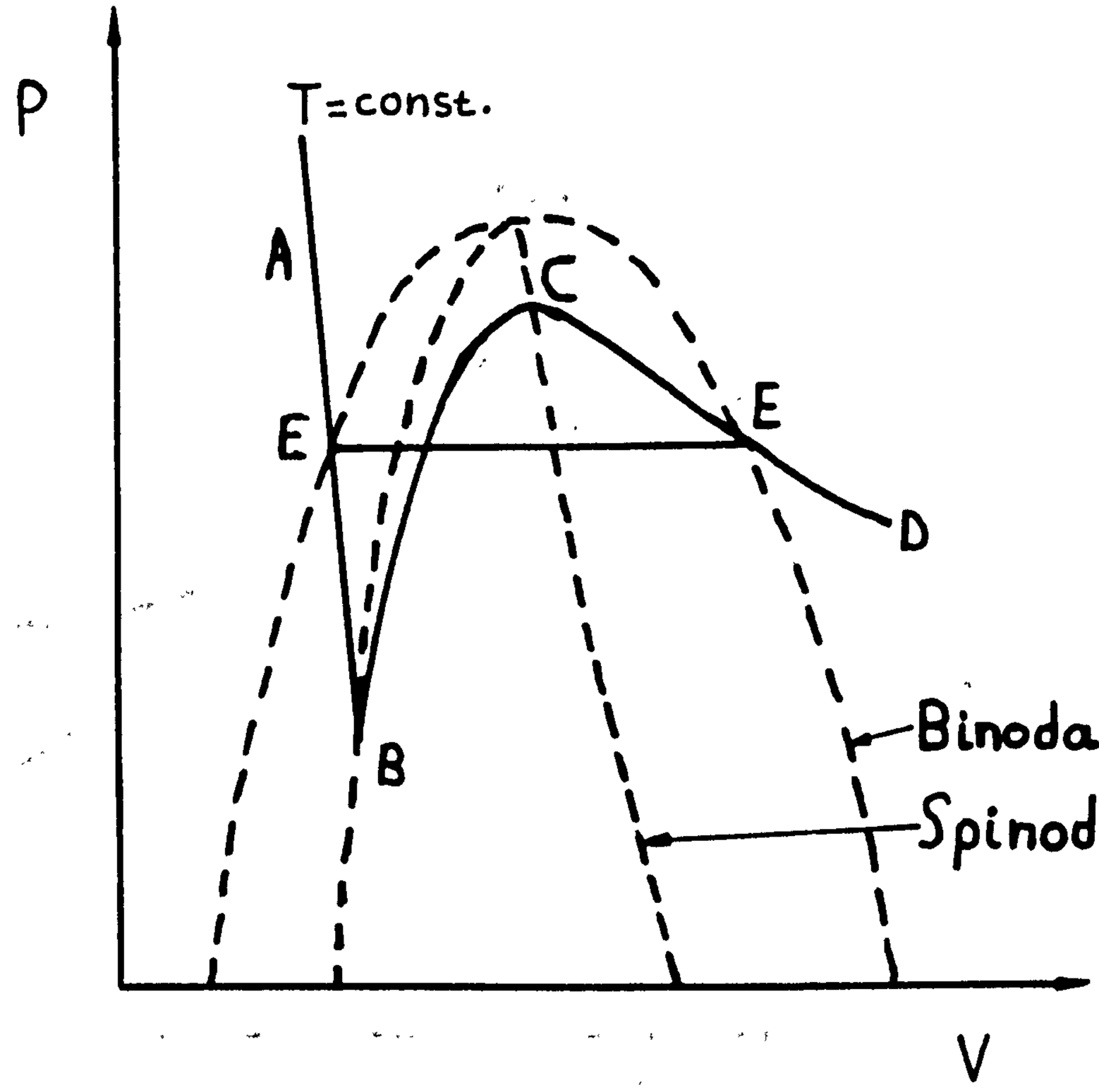

Figure 89. P-V diagram.Isothermal process of an "ideal" Van der Waal substance.

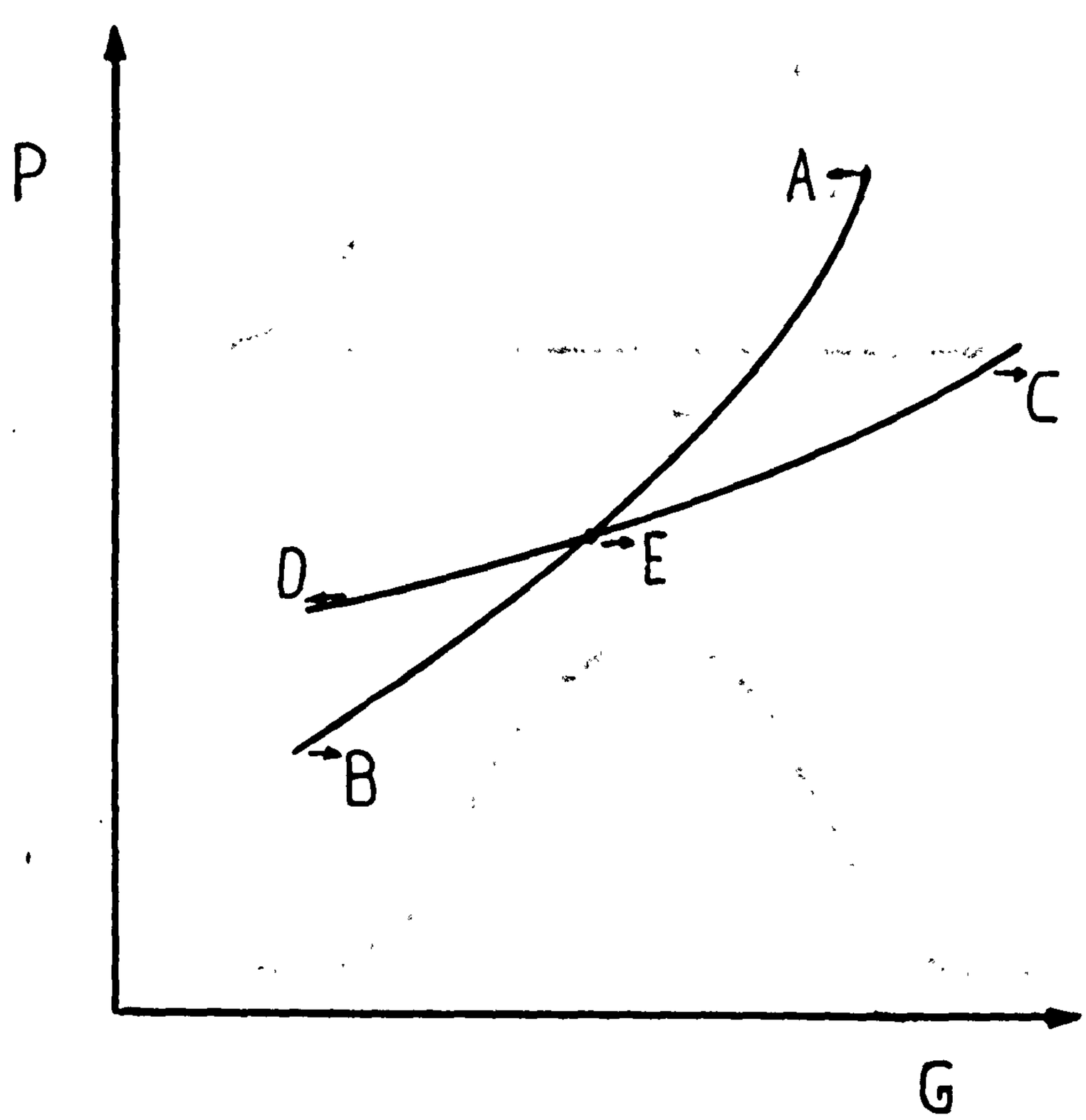

Figure 90. Illustration of the effect of pressure on the Gibb's free energy.

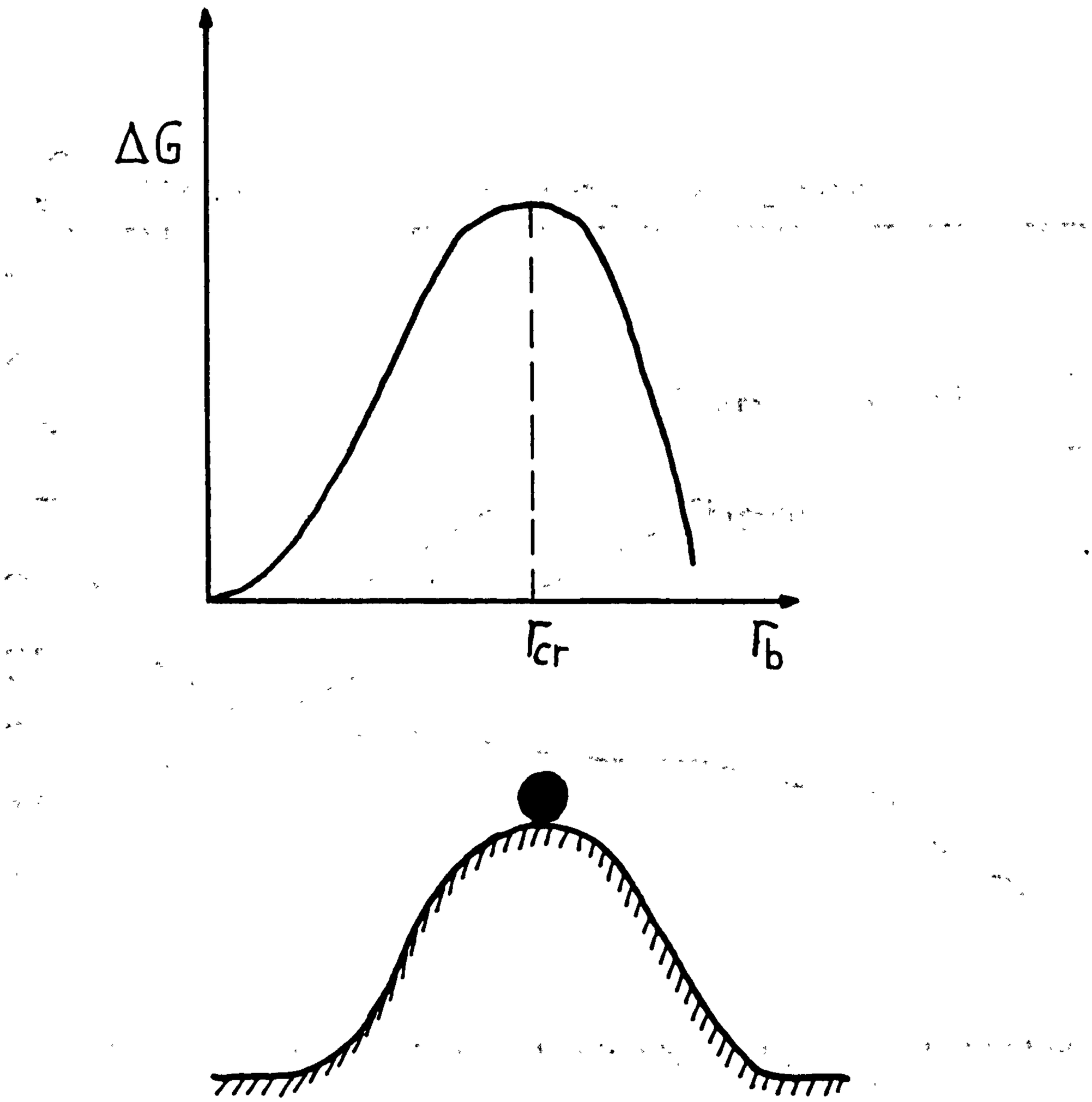

Figure 91. Illustration of the stability state of the nucleation process.

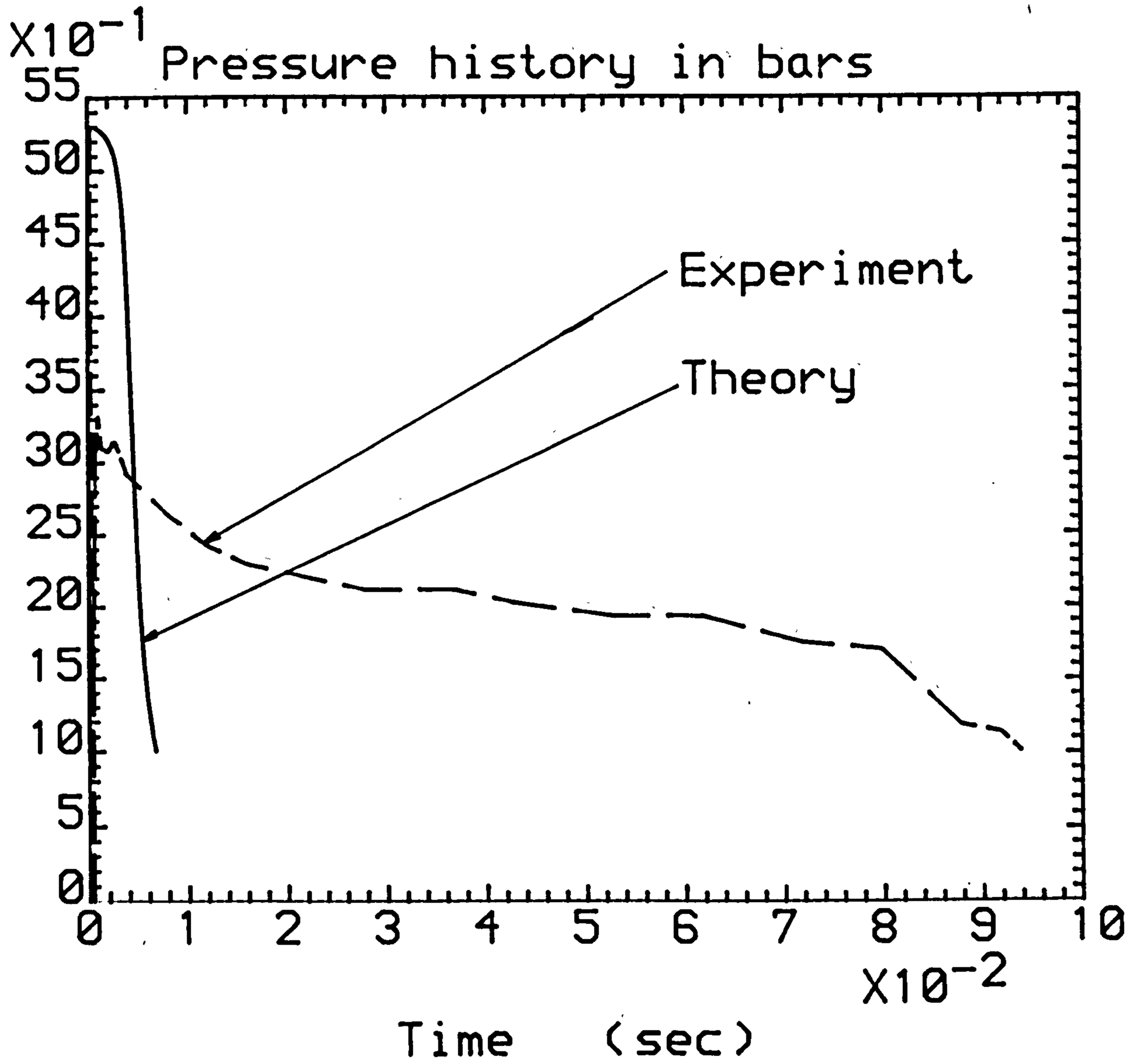

Figure 92. Comparison of the homogeneous model analysis with R 12 vessel blowdown data.Long term decompression (perspex vessel,bottom pressure station).(Initially saturated liquid of 5.3 bar).

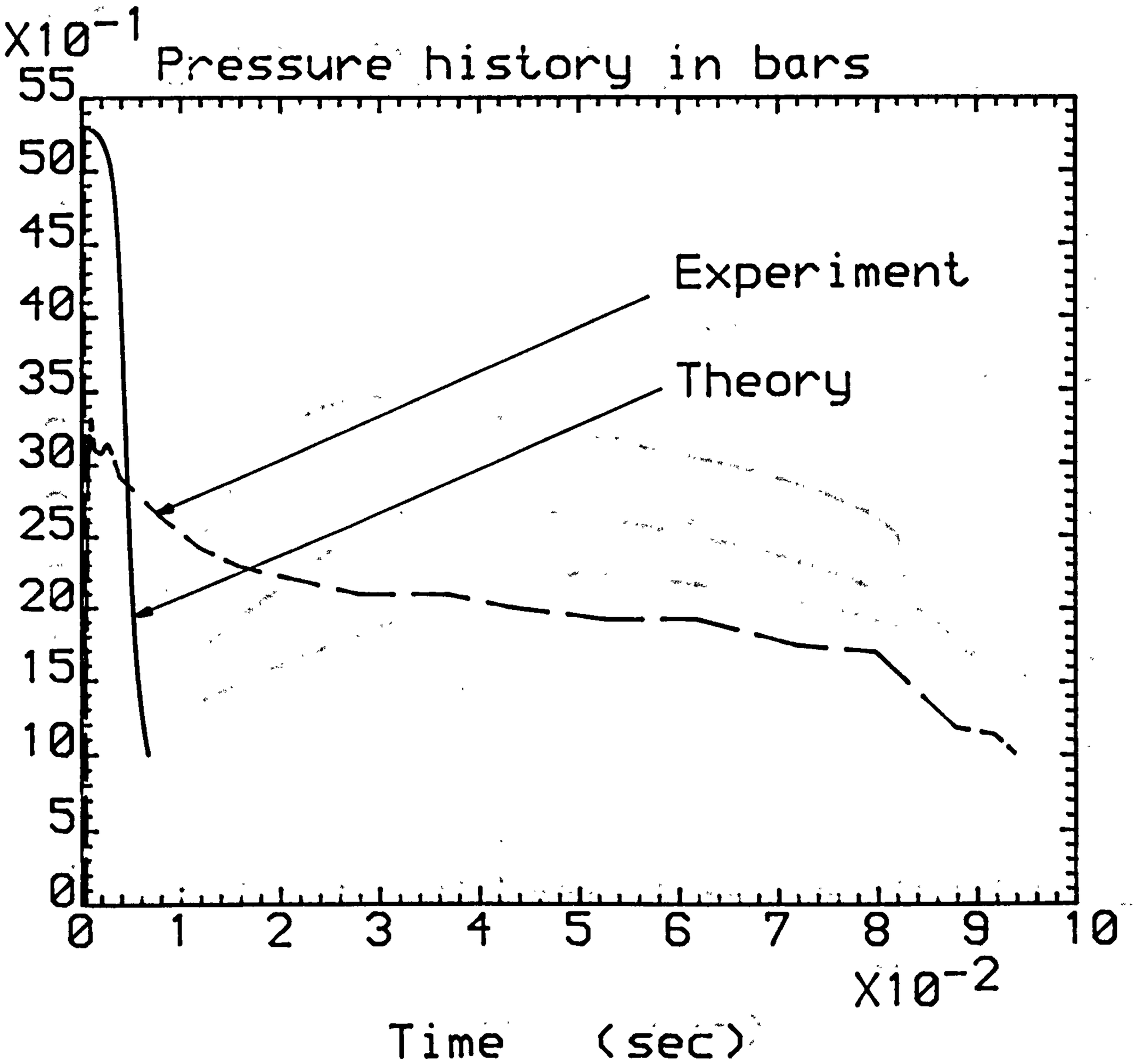

Figure 93. Comparison of the homogeneous model analysis with R 12 vessel blowdown data.Long term decompression (perspex vessel,middle pressure station).(Initially saturated liquid of 5.3 bar).

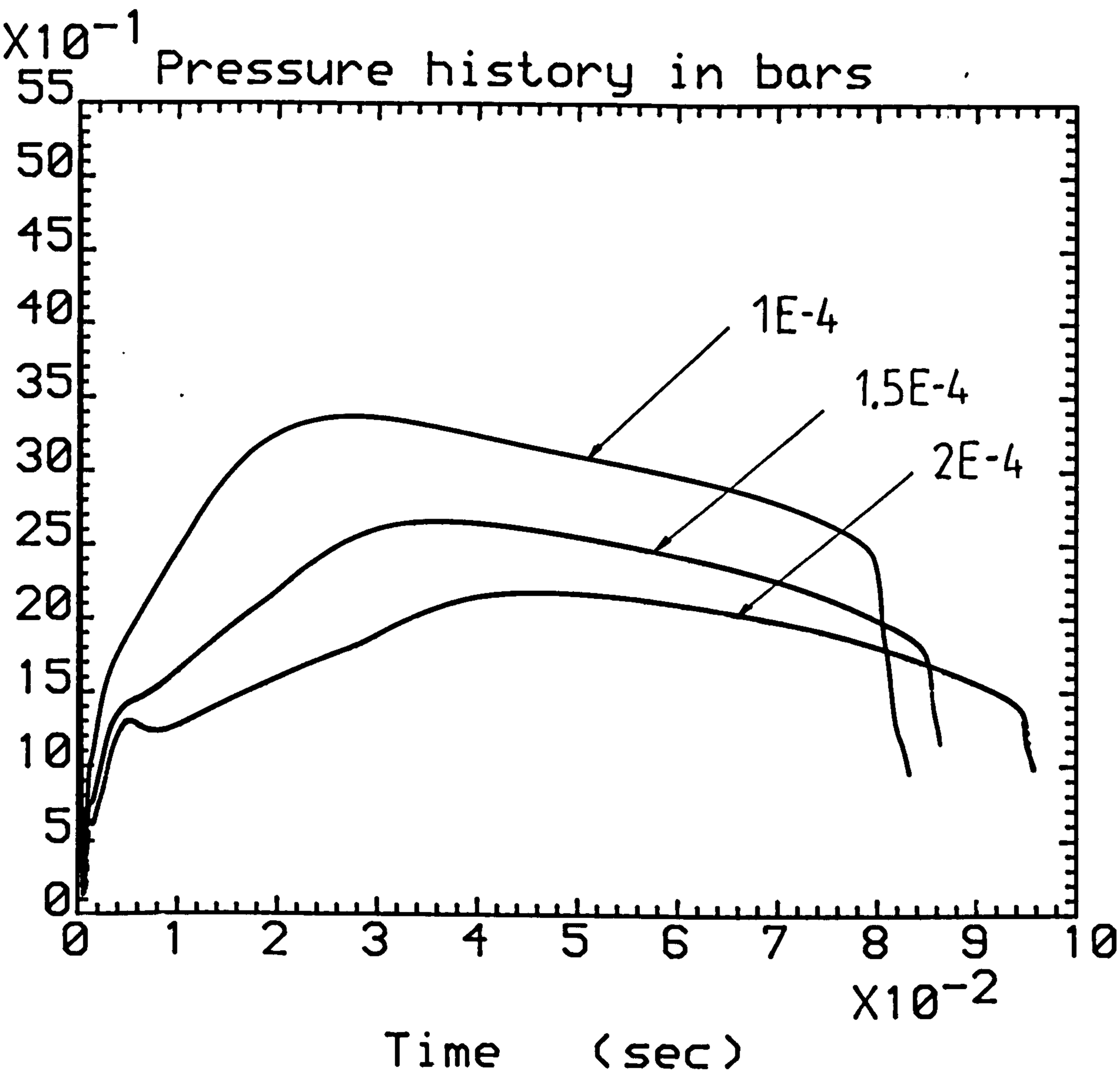

Figure 94. Influence of the bubble size,R_b,on the thermal non-equilibrium blowdown model pressure predictions ($C_d = 0.4$).

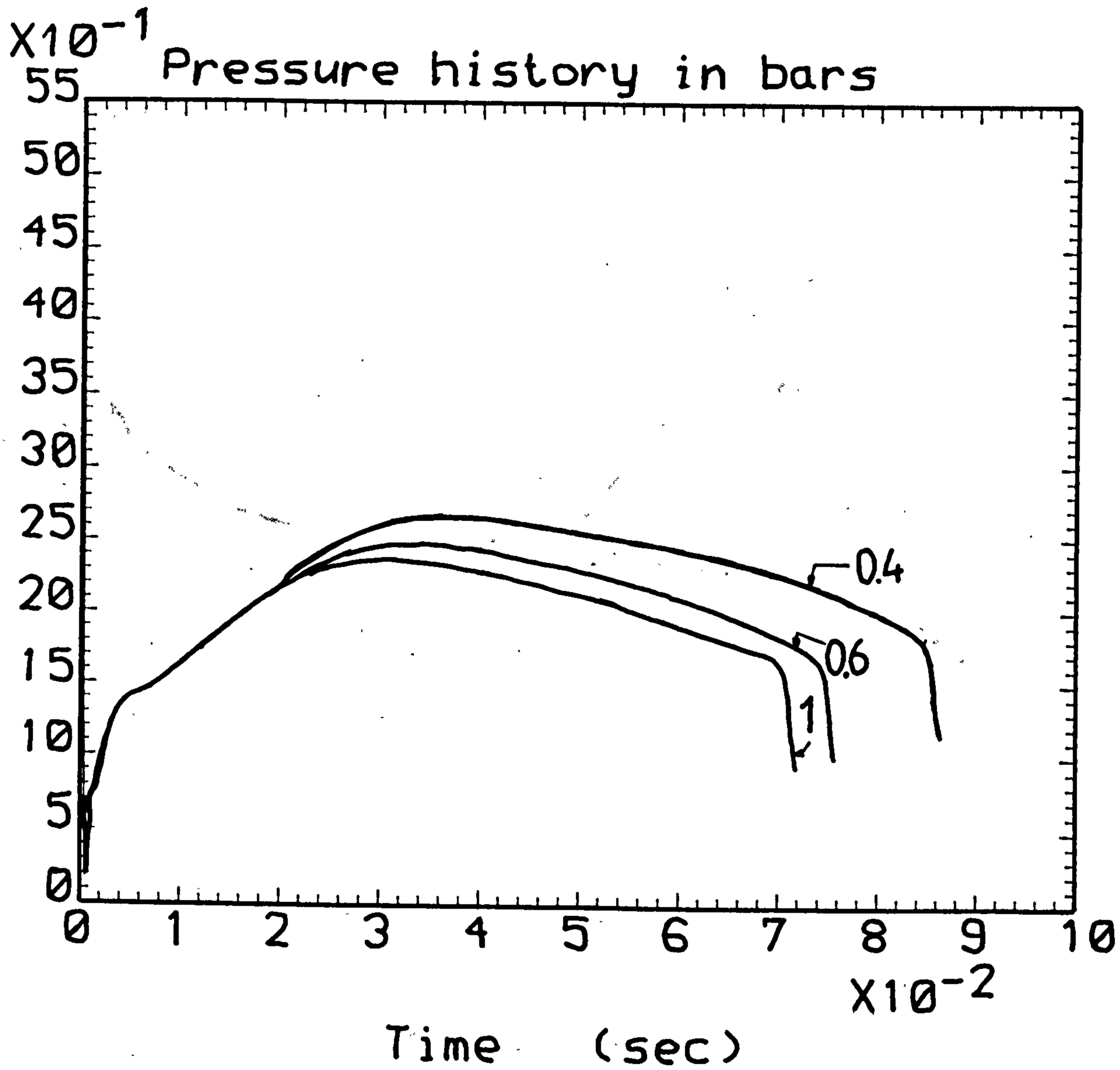

Figure 95. Influence of the discharge coefficient, C_d, on the thermal non-equilibrium blowdown model pressure predictions (R_b = 1.5E-4m).

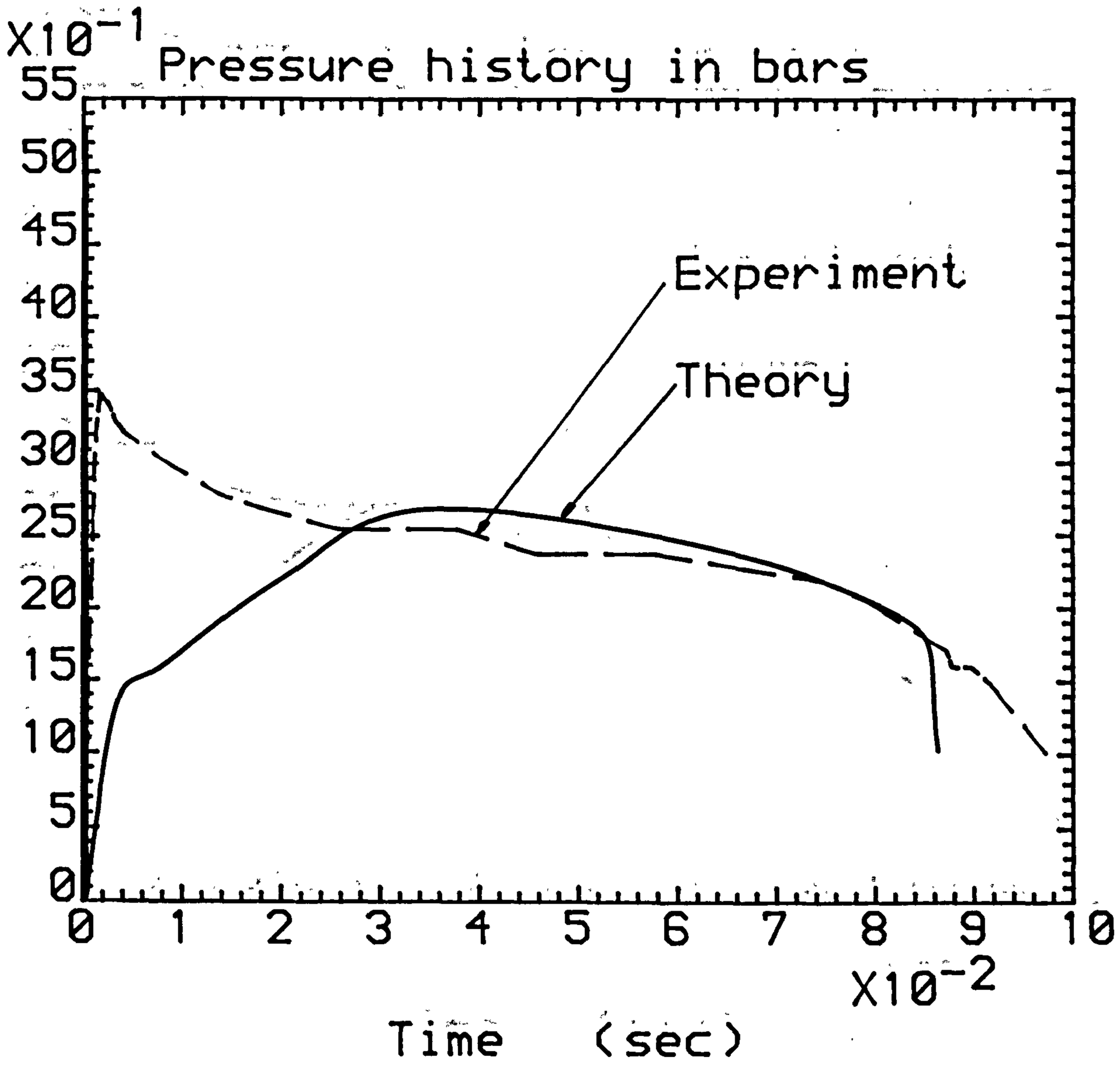

Figure 96. Comparison of the thermal non-equilibrium model analysis with R 12 vessel blowdown data.Long term decompression (mild steel,bottom pressure station). (Initially saturated liquid of 5.3 bar,C_d = 0.4,R_b = 1.5E-4m).

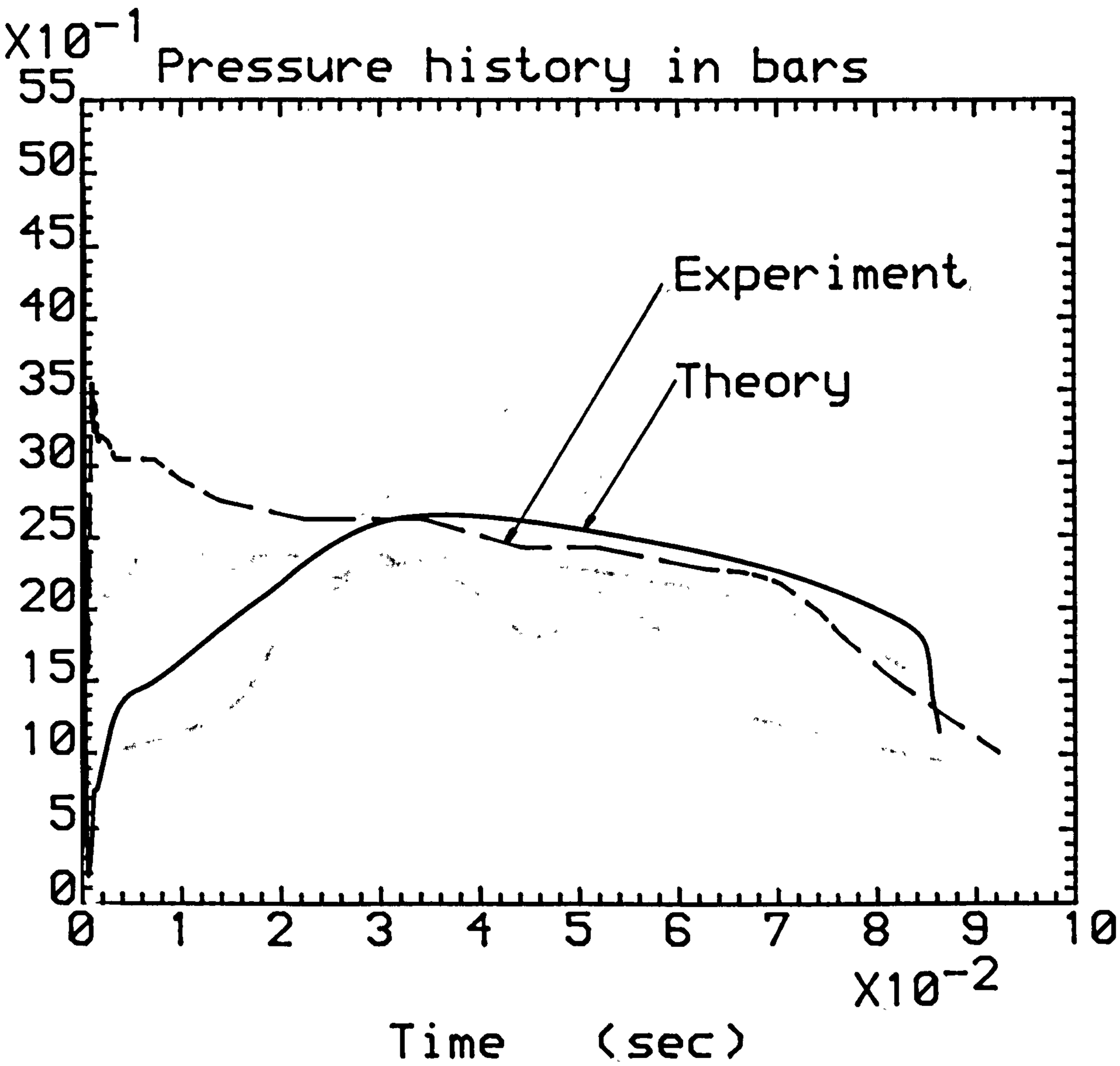

Figure 97. Comparison of the thermal non-equilibrium model analysis with R 12 vessel blowdown data.Long term decompression (mild steel vessel,middle pressure station).(Initially saturated liquid of 5.3 bar,$C_d = 0.4$,$R_b = 1.5E\text{-}4m$).

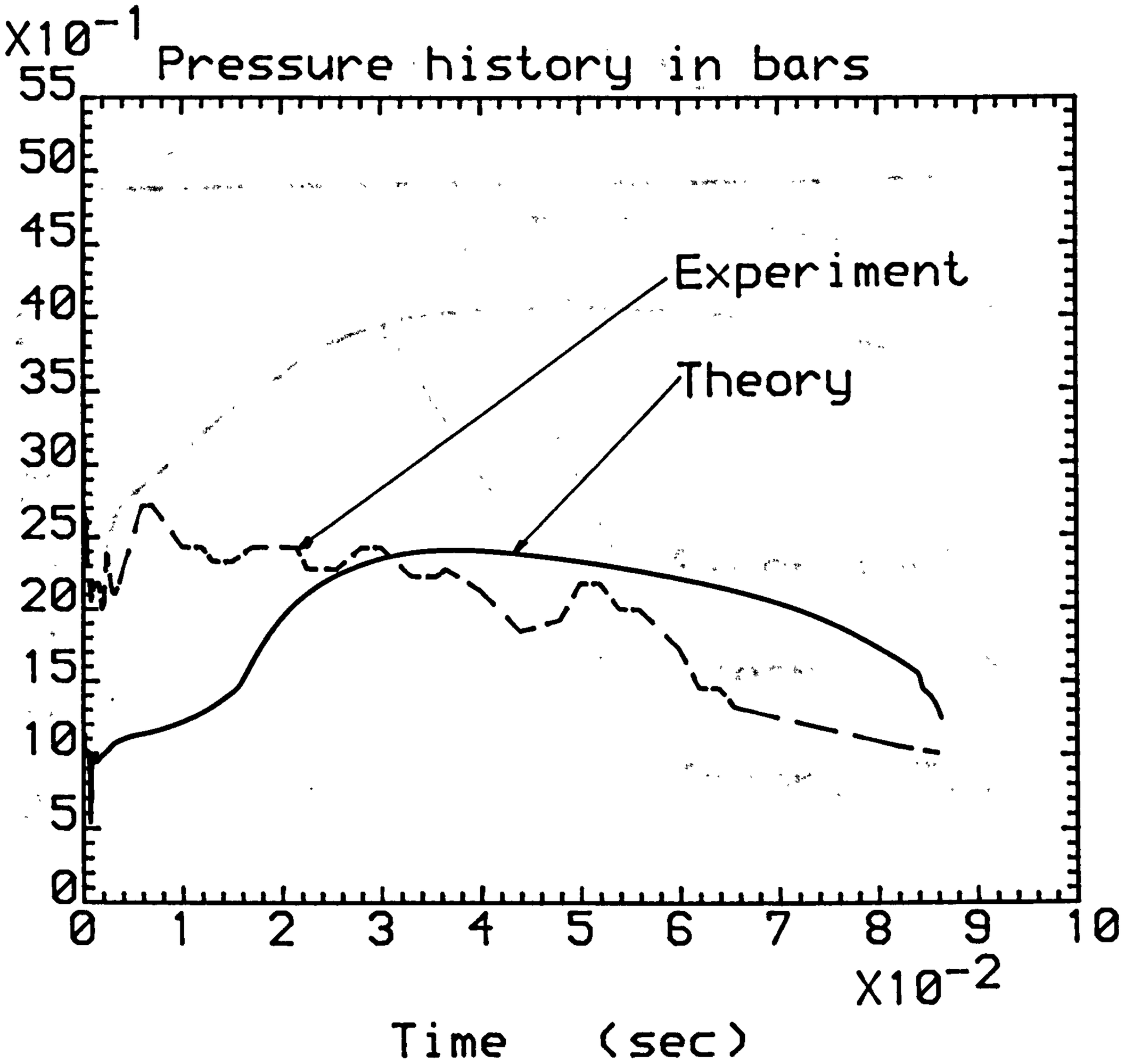

Figure 98. Comparison of the thermal non-equilibrium model analysis with R 12 vessel blowdown data.Long term decompression (mild steel vessel,top pressure station). (Initially saturated liquid of 5.3 bar,$C_d = 0.4$,$R_b = 1.5E\text{-}4m$).

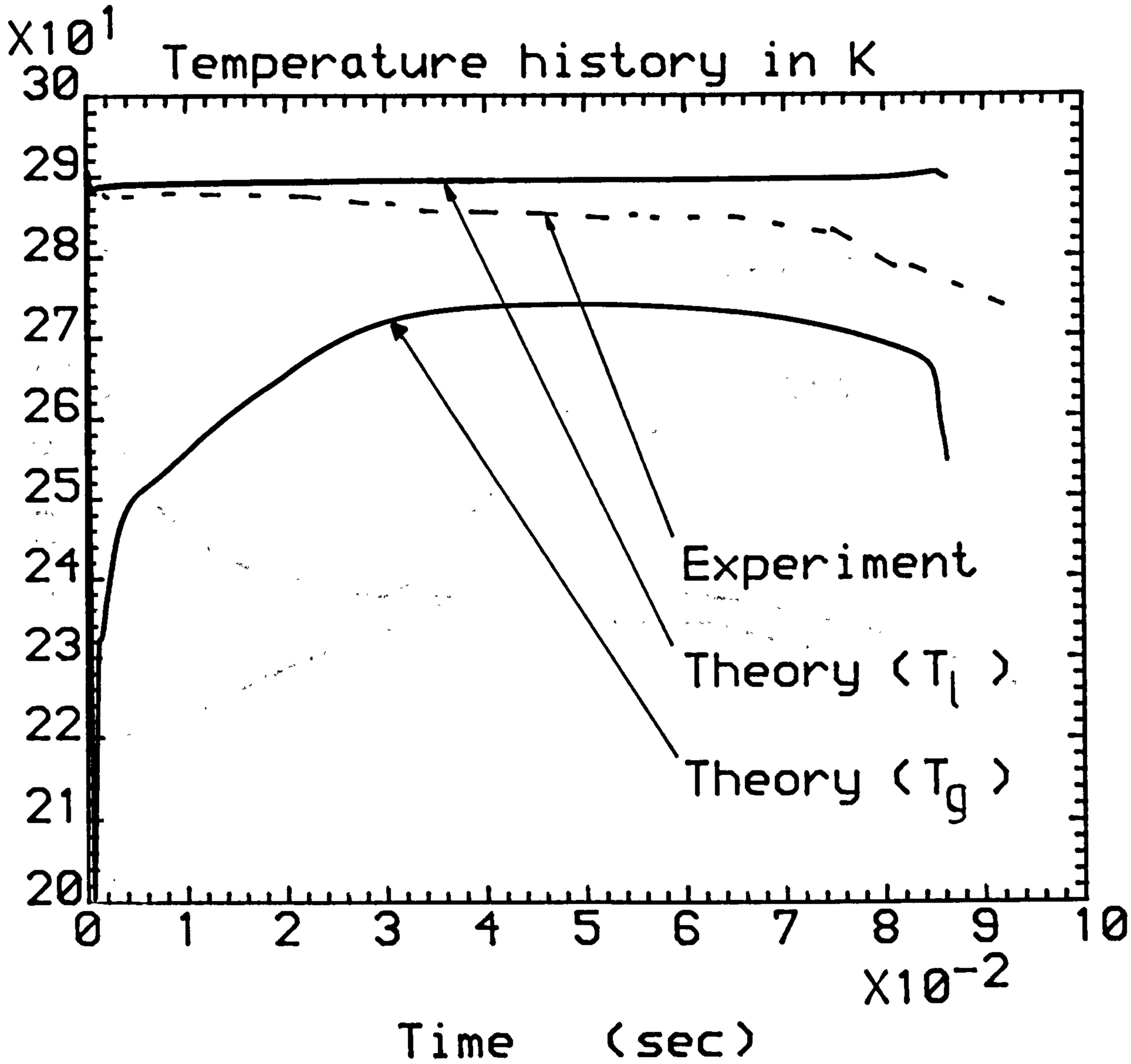

Figure 99. Comparison of the thermal non-equilibrium model analysis with R 12 vessel blowdown data.Long term temperature history (mild steel vessel,middle temperature station).(Initially saturated liquid of 5.3 bar,C_d = 0.4,R_b = 1.5E-4m).

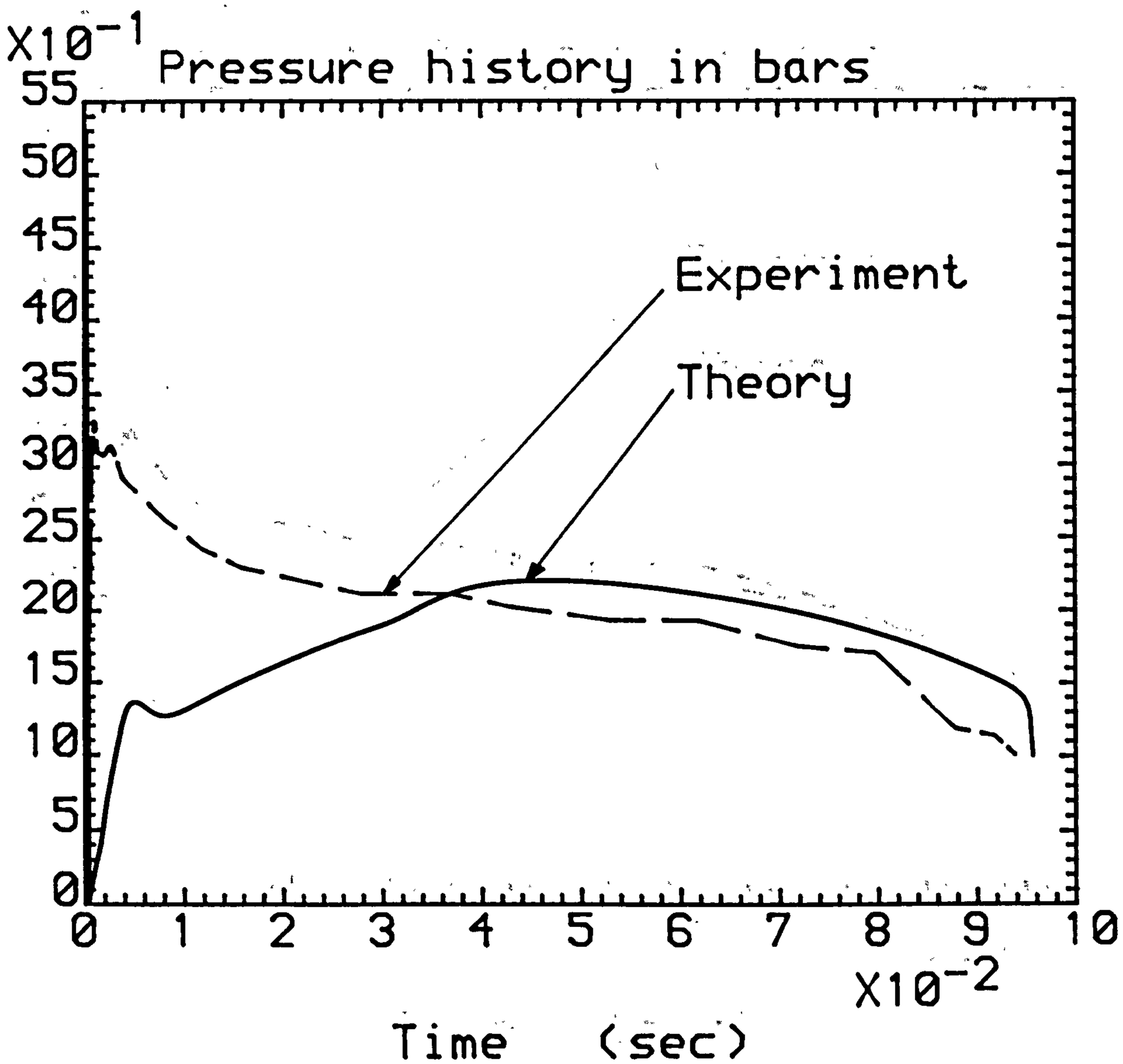

Figure 100. Comparison of the thermal non-equilibrium model analysis with R 12 vessel blowdown data.Long term decompression (perspex vessel,bottom pressure station). (Initially saturated liquid of 5.3 bar,$C_d = 0.4$,$R_b = 2E\text{-}4m$).

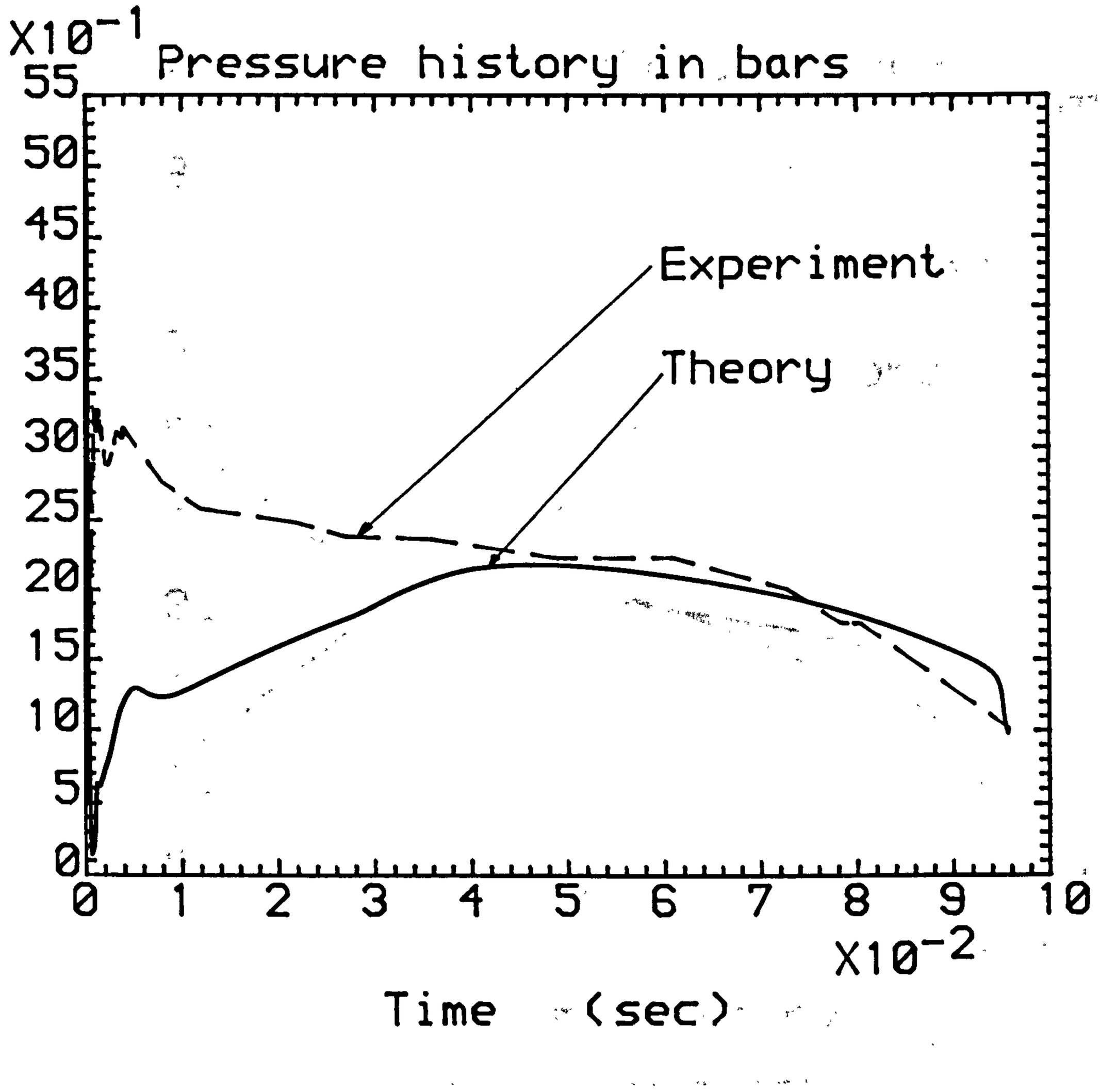

Figure 101. Comparison of the thermal non-equilibrium model analysis with R 12 vessel blowdown data.Long term decompression (perspex vessel,middle pressure station). (Initially saturated liquid of 5.3 bar,$C_d = 0.4$,$R_b = 2E\text{-}4$).

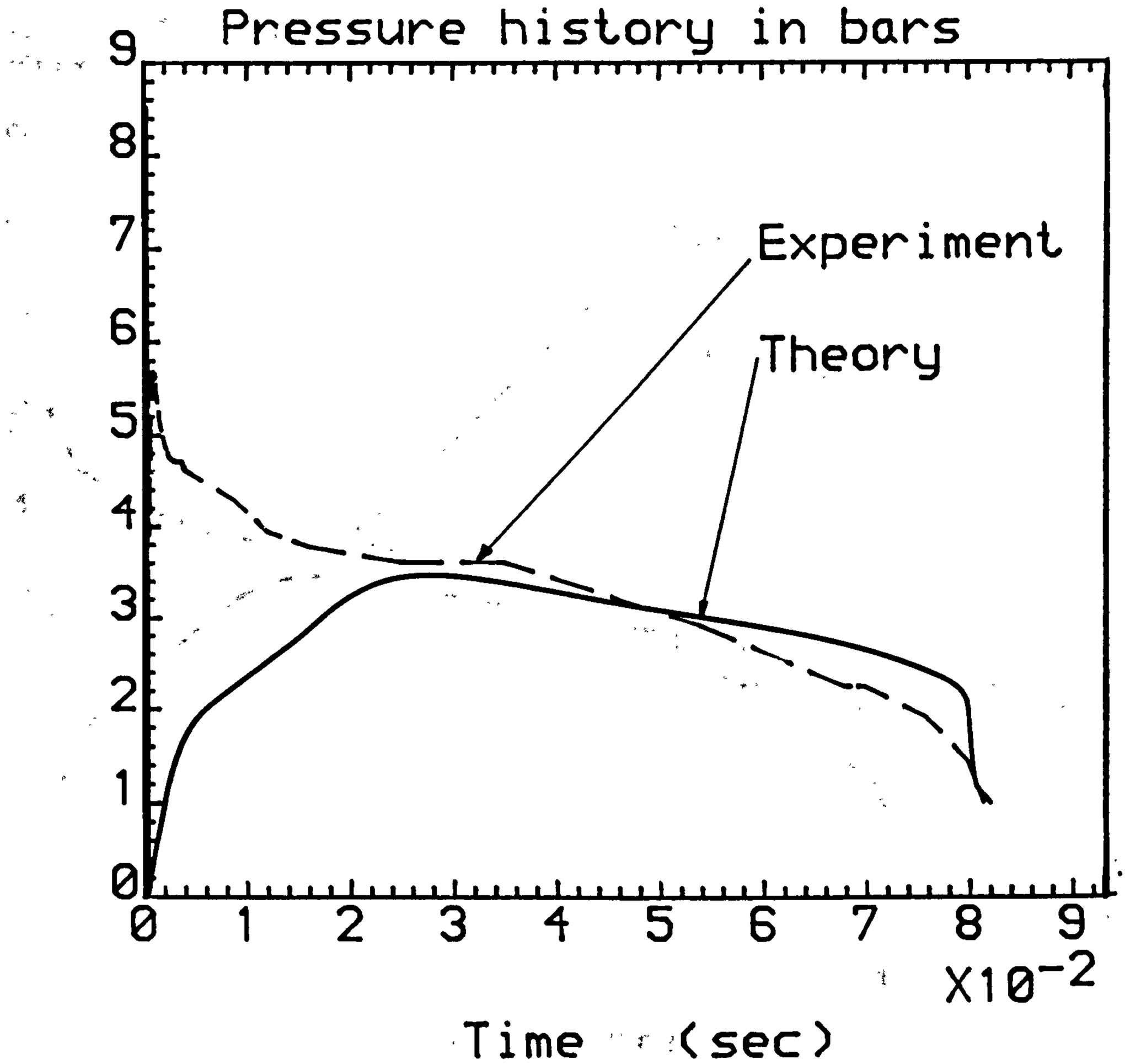

Figure 102. Comparison of the thermal non-equilibrium model analysis with R 12 vessel blowdown data.Long term decompression (mild steel vessel,bottom pressure station).(Initially saturated liquid of 8.5 bar,$C_d = 0.4$,$R_b = 1.5E\text{-}4m$).

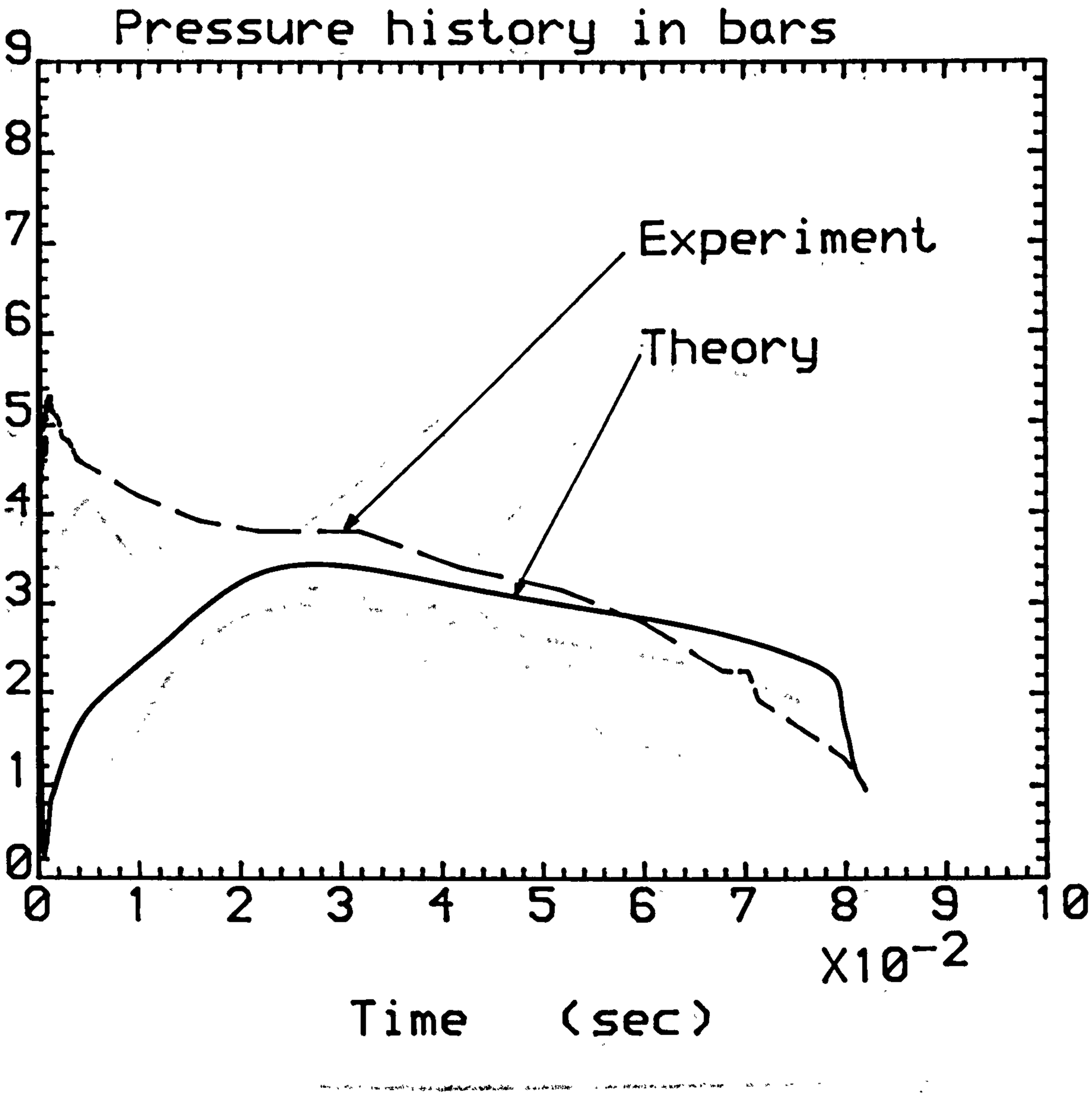

Figure 103. Comparison of the thermal non-equilibrium model analysis with R 12 vessel blowdown data.Long term decopression (mild steel vessel,middle pressure station).(Initially saturated liquid of 8.5 bar,$C_d = 0.4$,$R_b = 1.5E\text{-}4m$).

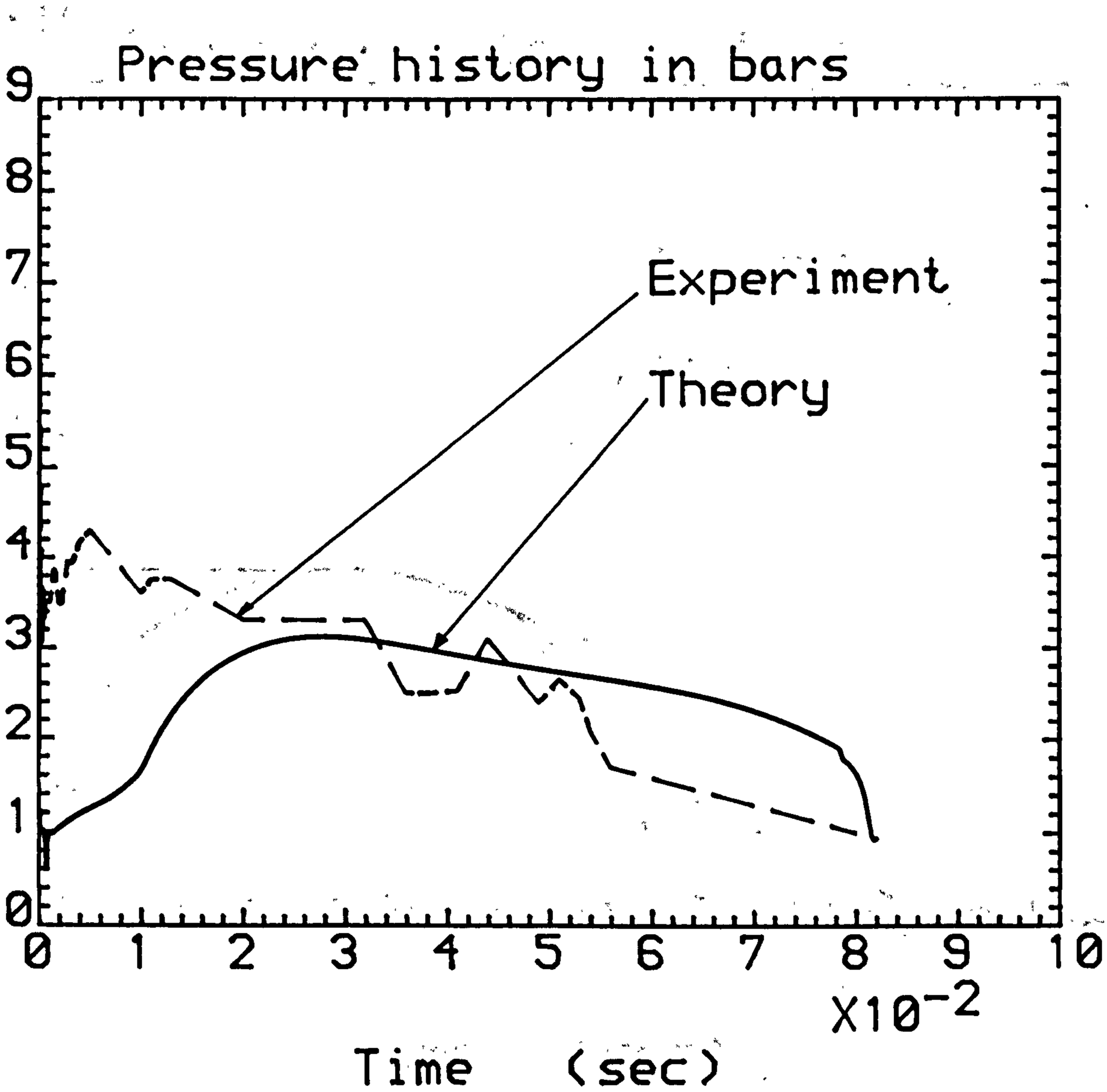

Figure 104. Comparison of the thermal non-equilibrium model analysis with R 12 vessel blowdown data.Long term decompression (mild steel vessel,top pressure station). (Initially saturated liquid of 8.5 bar,$C_d = 0.4$,$R_b = 1.5E\text{-}4m$).

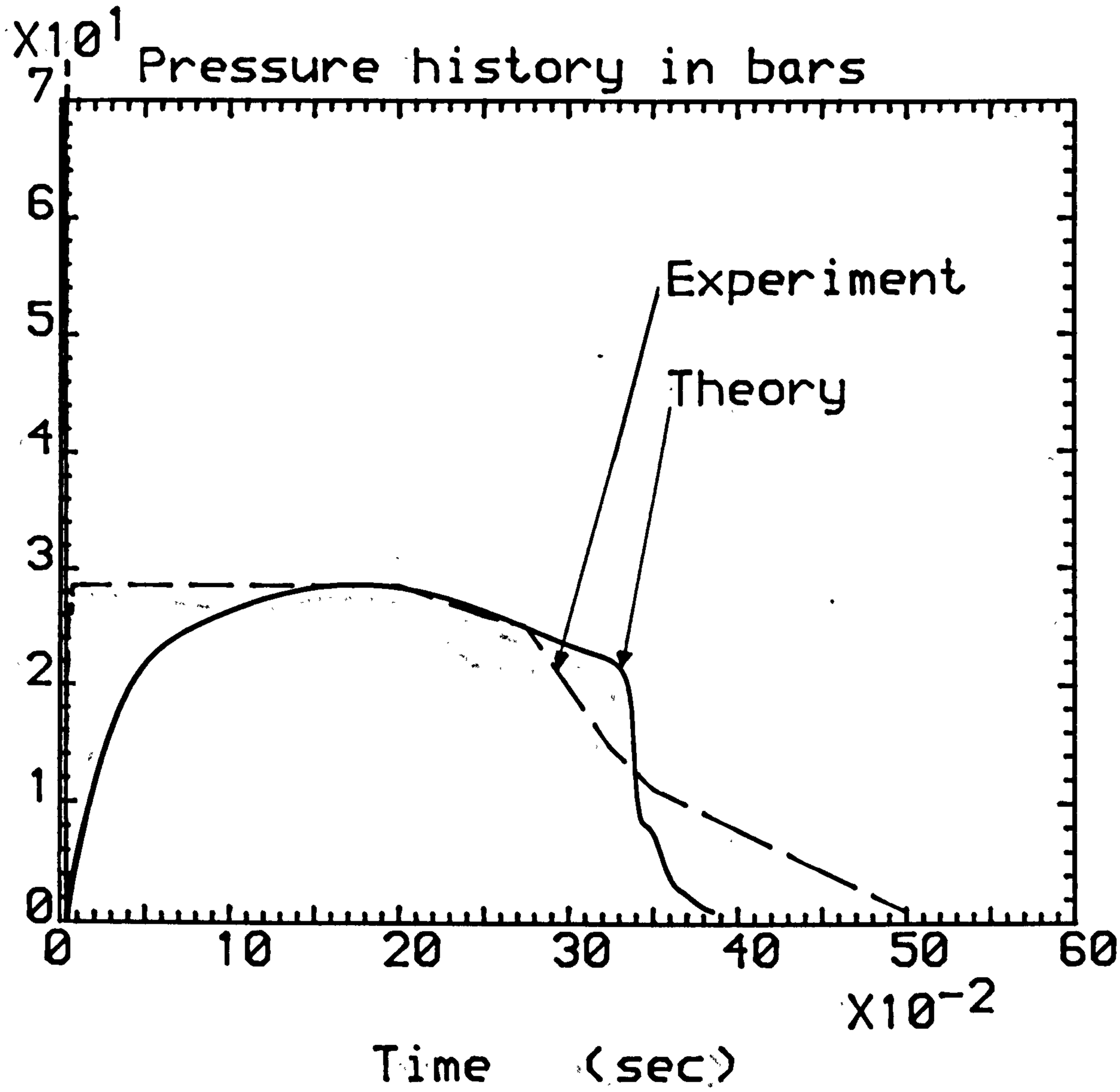

Figure 105. Comparison of the thermal non-equilibrium model analysis with water vessel blowdown data.Long term decompression (pressure station 100mm from closed end).(p_{in} = 69 bar,T_{in} = 242°C,C_d = 0.5,R_b = 4.5E-4).

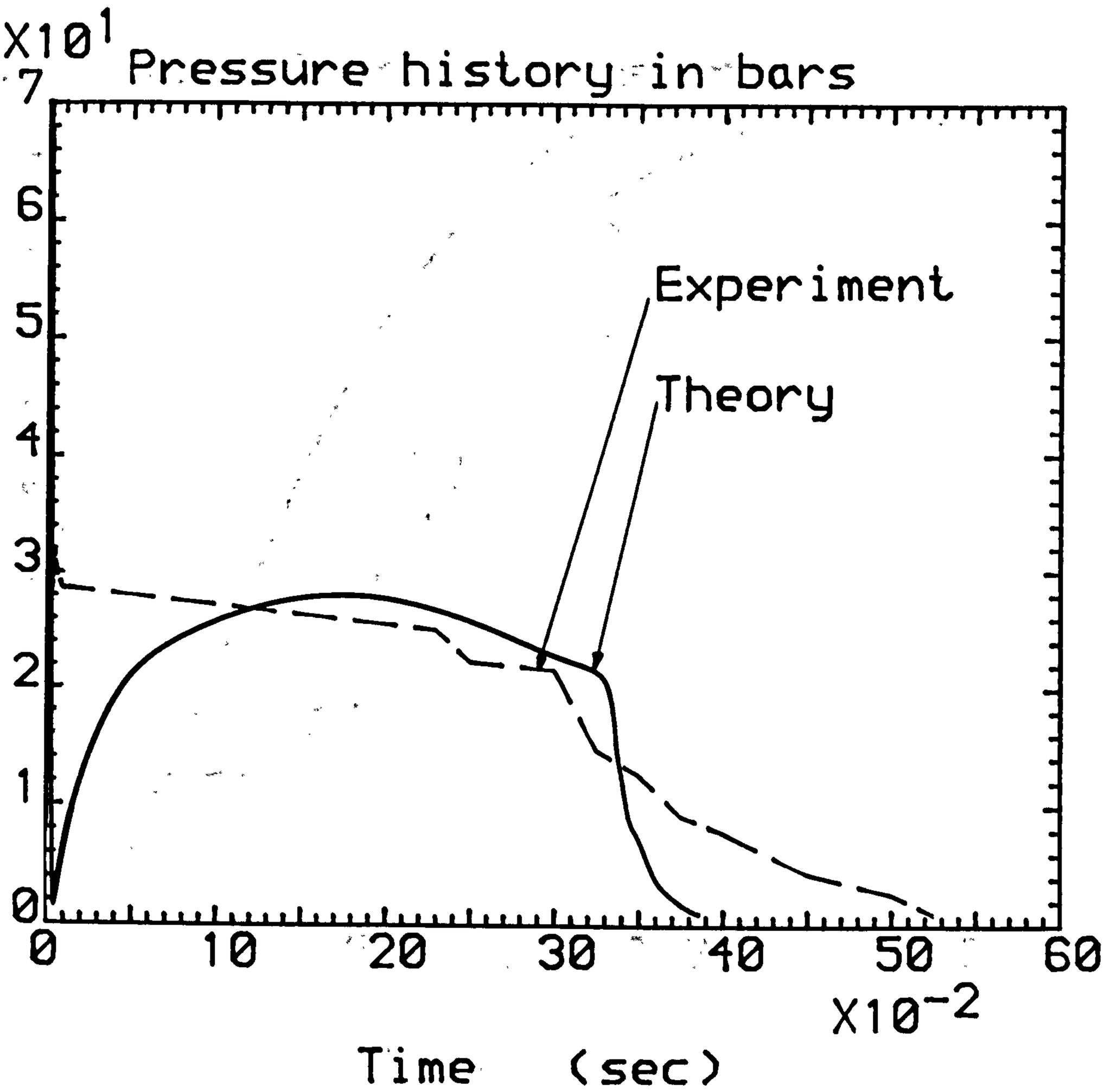

Figure 106. Comparison of the thermal non-equilibrium model analysis with water vessel blowdown data.Long term decompression (pressure station 1.5m from closed end).(p_{in} = 69 bar,T_{in} = 242°C,C_d = 0.5,R_b = 4.5E-4).

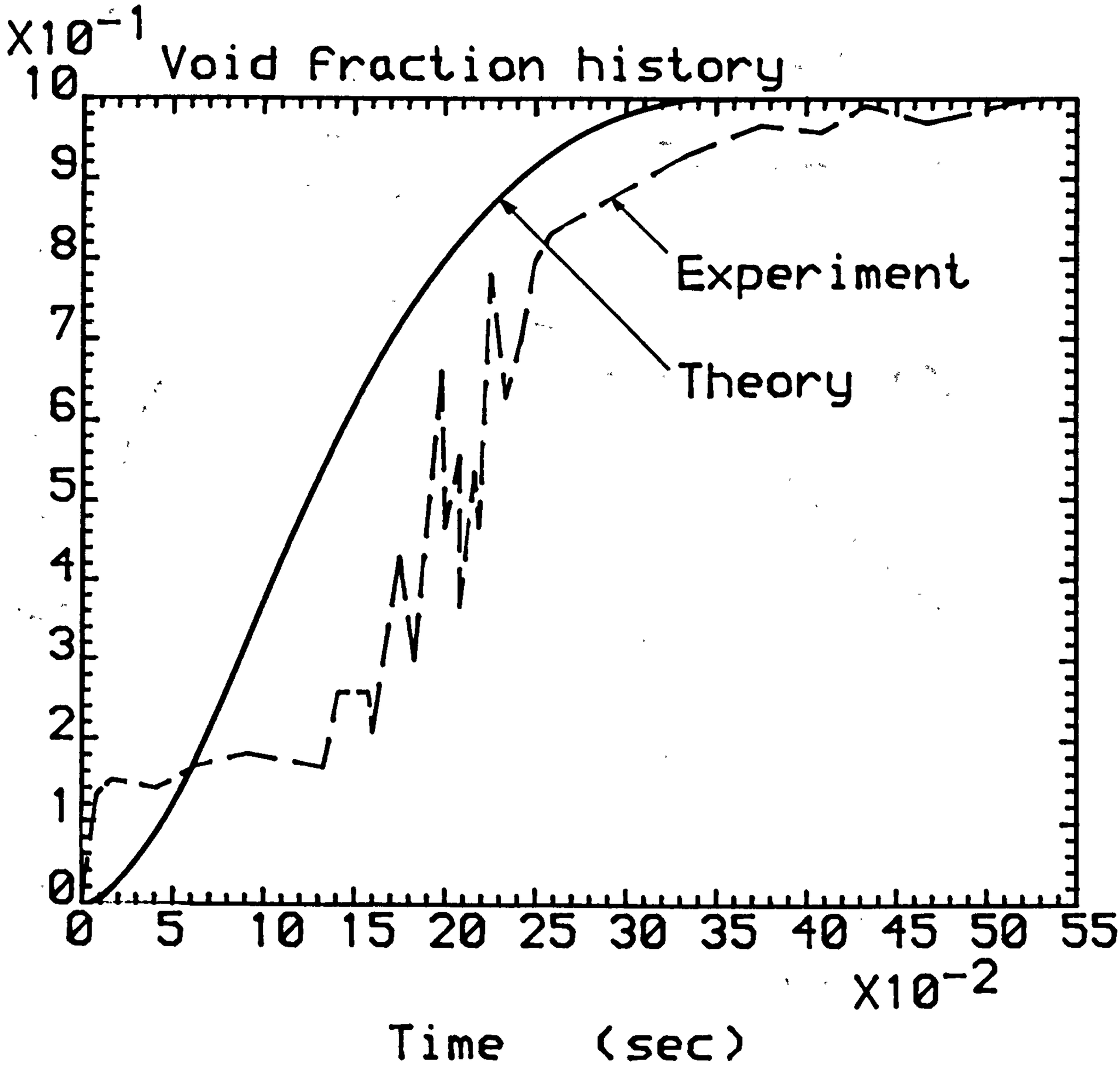

Figure 107. Comparison of the thermal non-equilibrium model analysis with water vessel blowdown data.Long term void fraction history (void fraction station 1.5m from closed end).(p_{in} = 69 bar,T_{in} = 242°C,C_d = 0.5 ,R_b = 4.5E-4m).

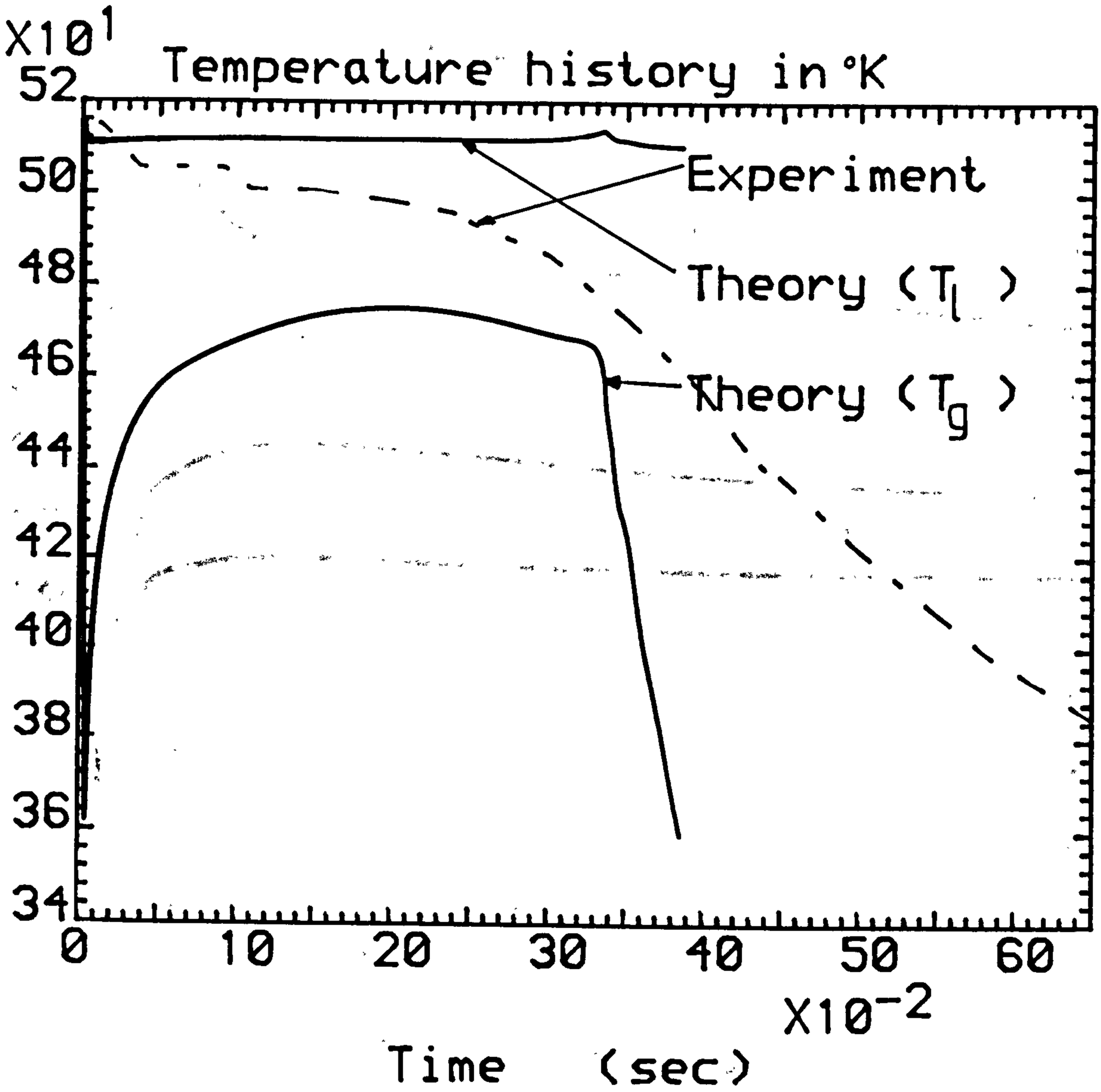

Figure 108. Comparison of the thermal non-equilibrium model analysis with water vessel blowdown data.Long term temperature history (temperature station 1.5m from closed end).(p_{in} = 69 bar,T_{in} = 242°C,C_d = 0.5,R_b = 4.5E-4m).

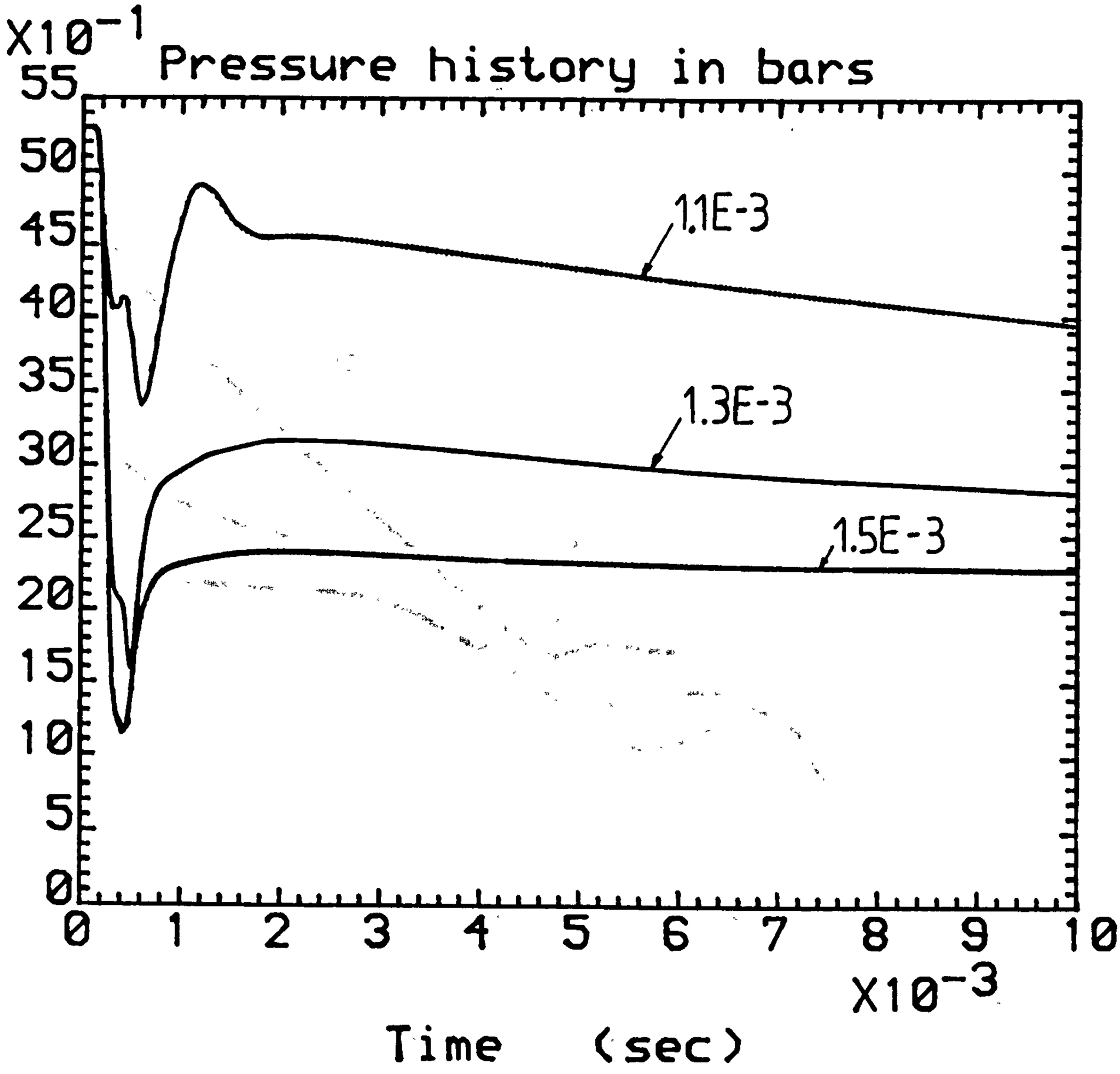

Figure 109. Influence of the heterogeneous factor,Φ,on the thermal non-equilibrium blowdown model pressure predictions.Initial decompression history ($C_d = 0.4$).

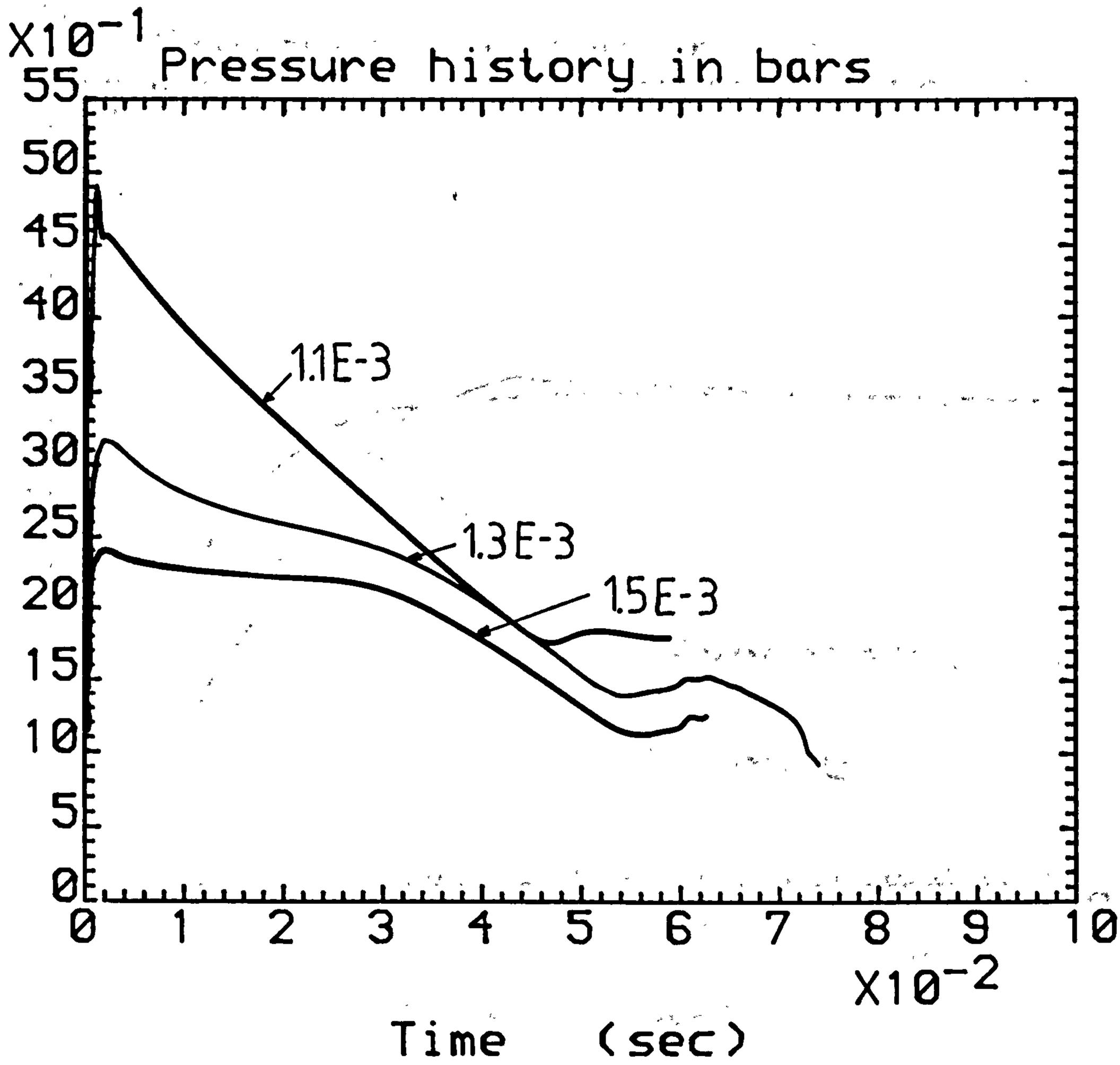

Figure 110. Influence of the heterogeneous factor,Φ,on the thermal non-equilibrium blowdown model pressure predictions.Long term decompression ($C_d = 0.4$).

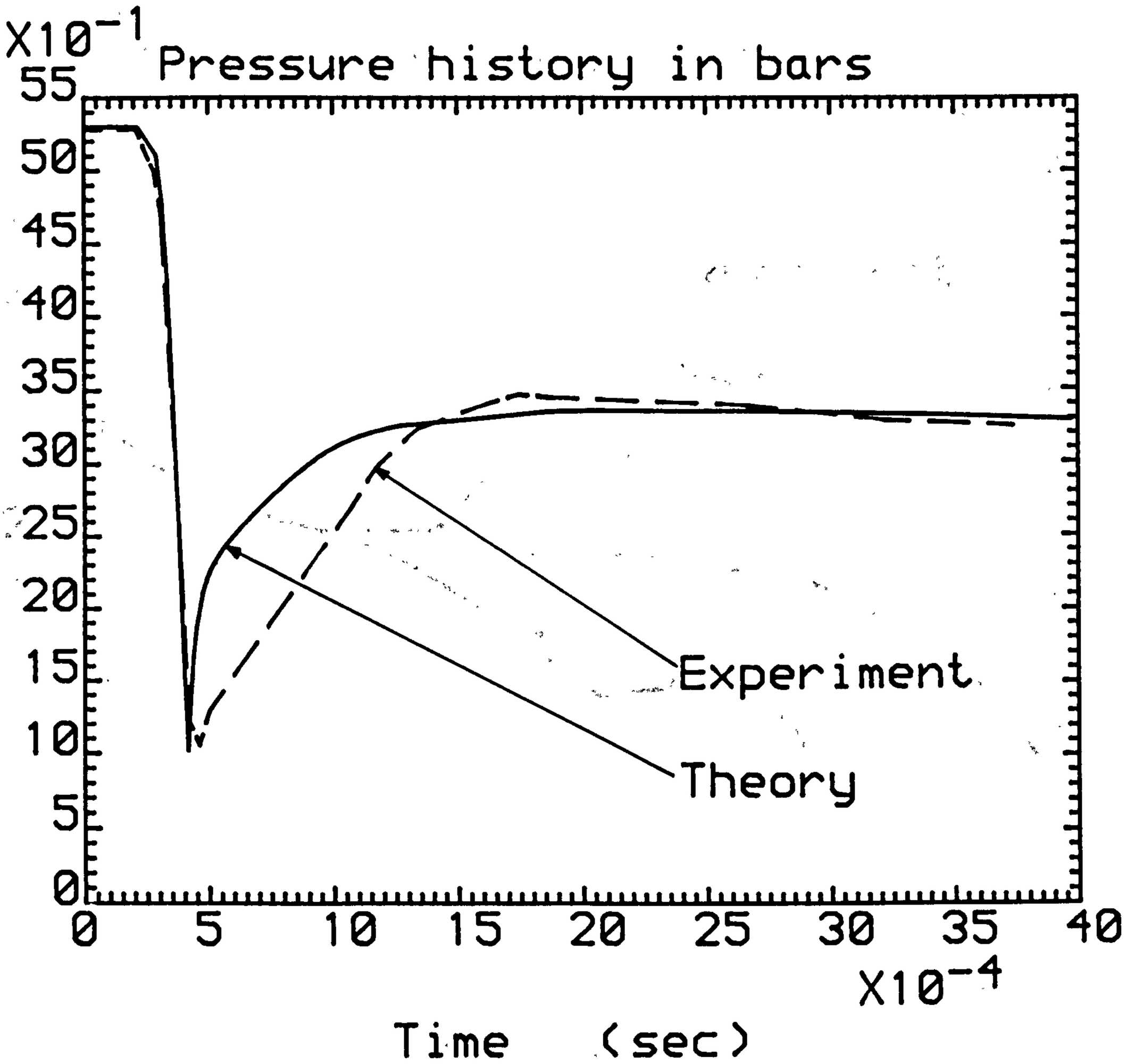

Figure 111. Comparison of the thermal non-equilibrium model analysis with R 12 vessel blowdown data.Initial depressurisation history (mild steel vessel,bottom pressure station).(Initially saturated liquid of 5.3 bar,$C_d = 0.4, \Phi = 1.3E\text{-}3$).

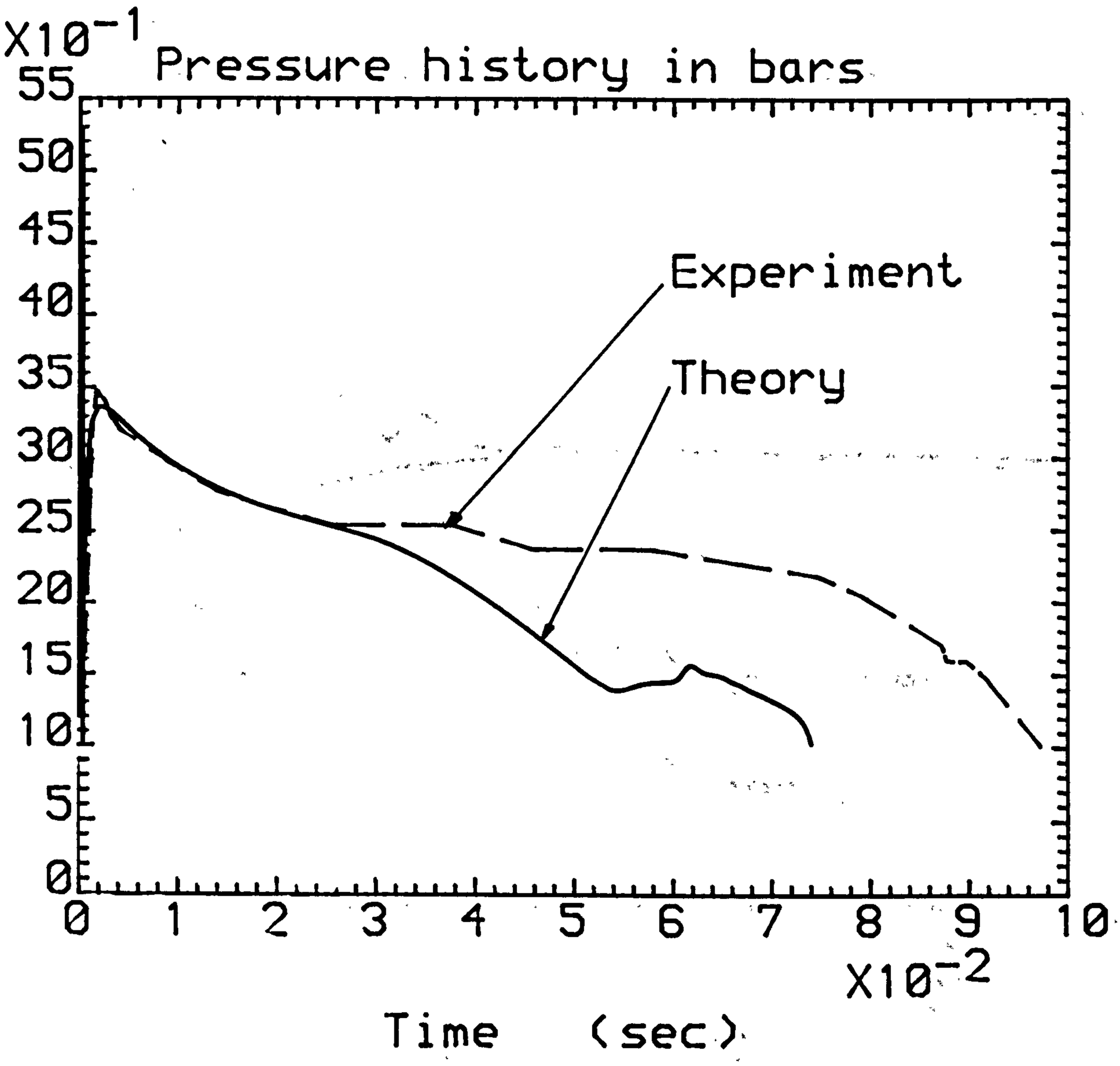

Figure 112. Comparison of the thermal non-equilibrium model analysis with R 12 vessel blowdown data. Long term decompression (mild steel vessel,bottom pressure station).(Initially saturated liquid of 5.3 bar,$C_d = 0.4, \Phi = 1.3E\text{-}3$).

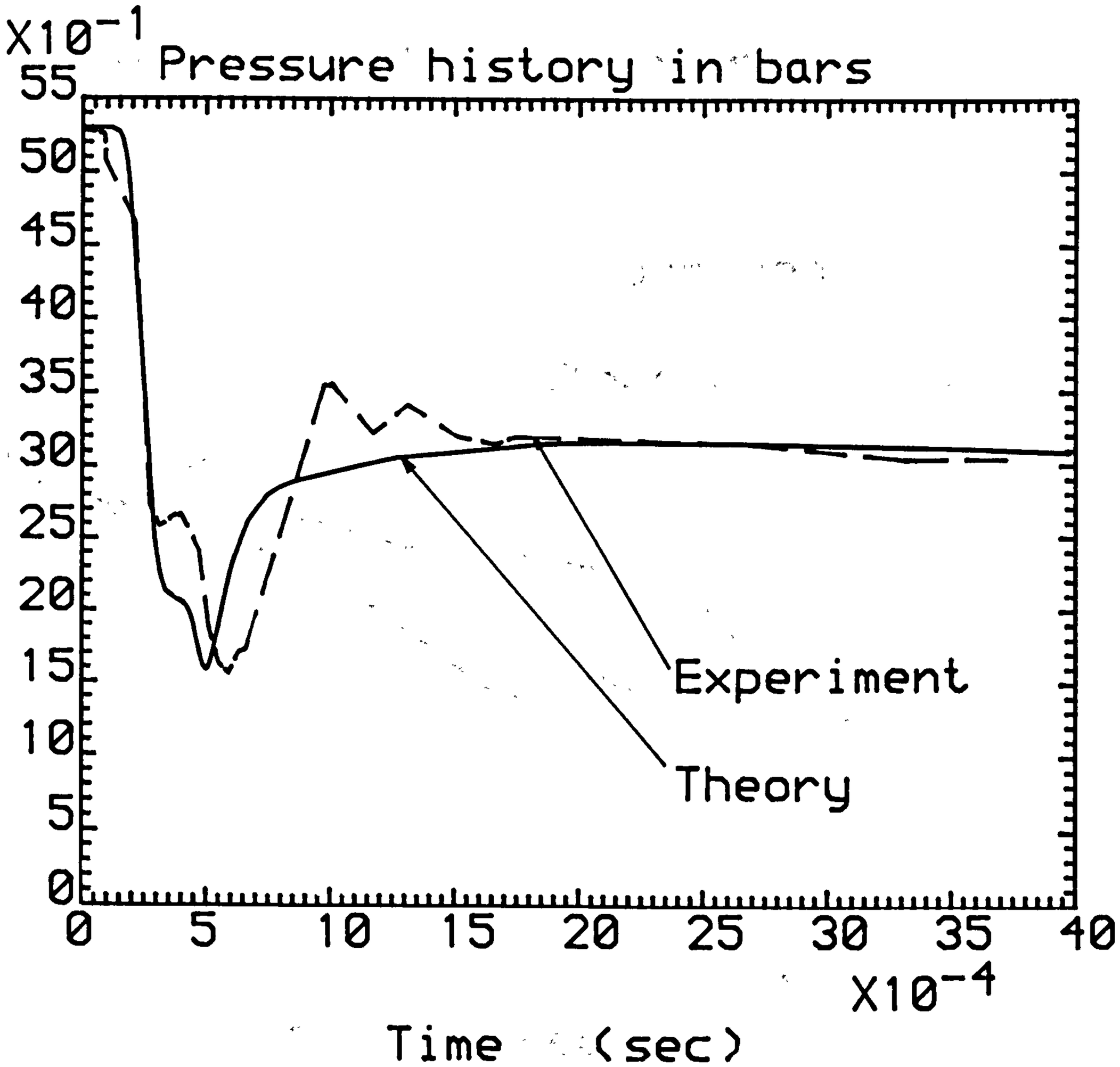

Figure 113. Comparison of the thermal non-equilibrium model analysis with R 12 vessel blowdown data.Initial depressurisation history (mild steel vessel,middle pressure station).(Initially saturated liquid of 5.3 bar,$C_d = 0.4, \Phi = 1.3E\text{-}3$).

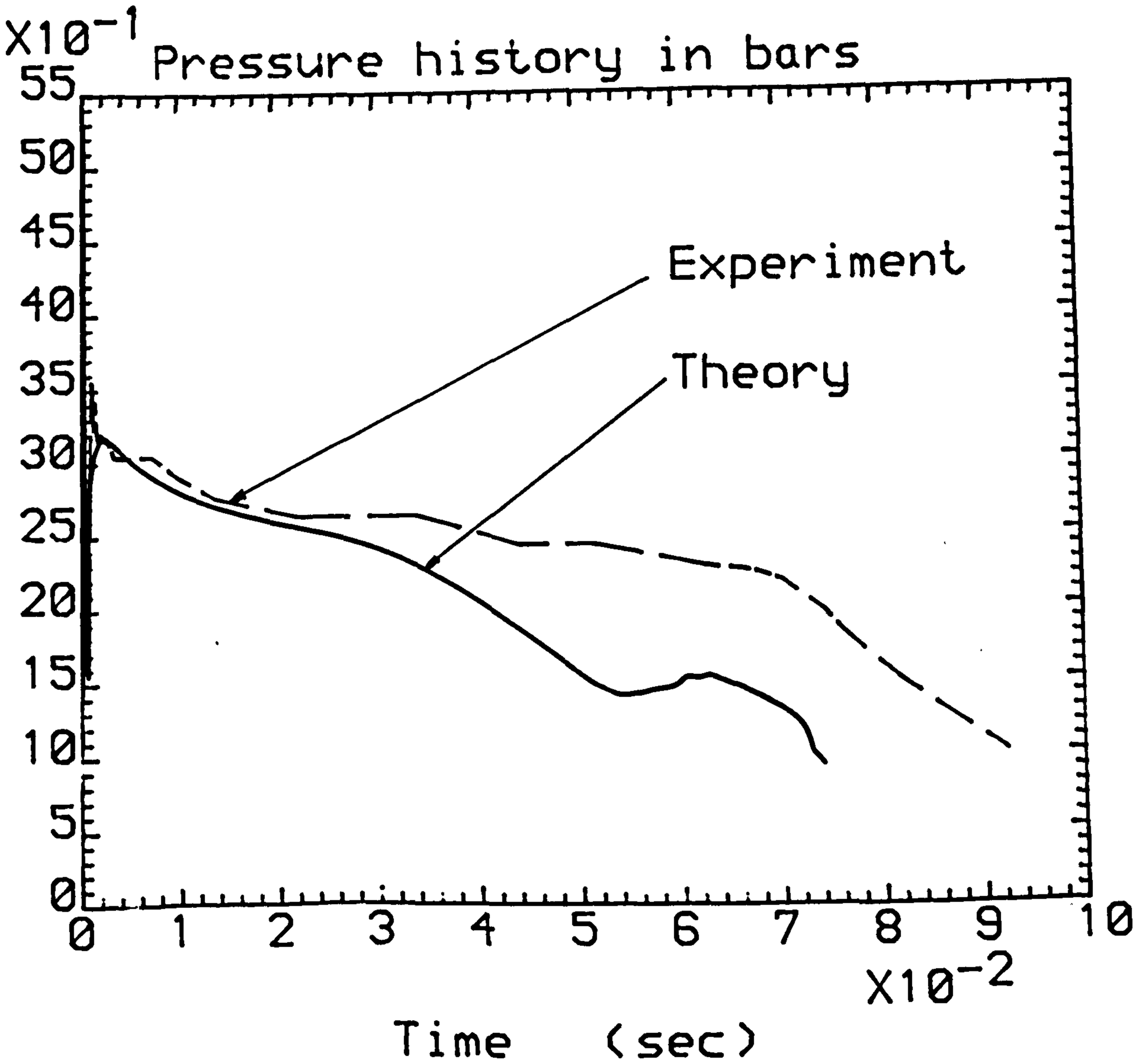

Figure 114. Comparison of the thermal non-equilibrium model analysis with R 12 vessel blowdown data.Long term decompression (mild steel vessel,middle pressure station).(Initially saturated liquid of 5.3 bar,$C_d = 0.4, \Phi = 1.3E\text{-}3$).

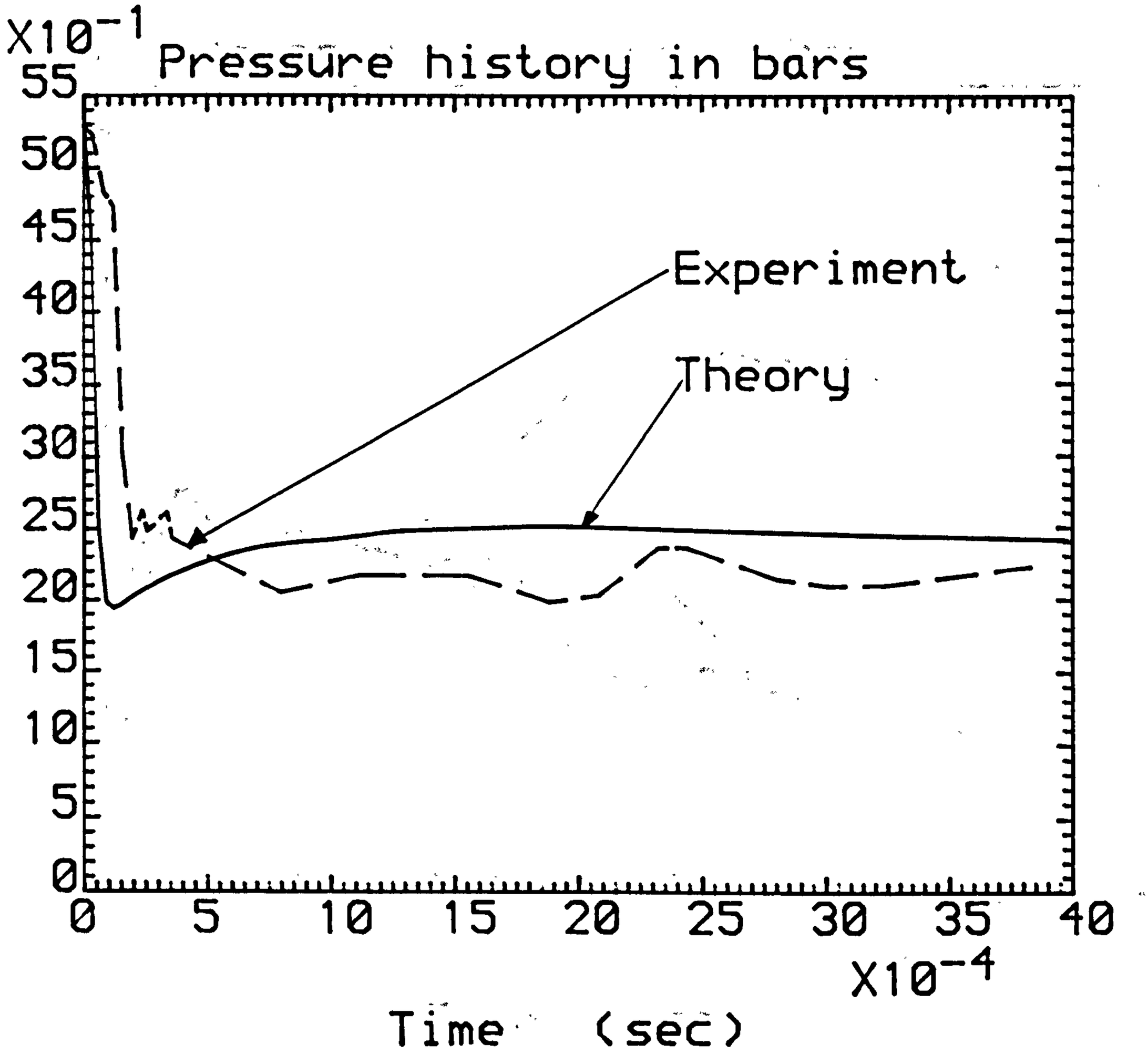

Figure 115. Comparison of the thermal non-equilibrium model analysis with R 12 vessel blowdown data.Initial depressurisation history (mild steel vessel,top pressure station).(Initially saturated liquid of 5.3 bar,$C_d = 0.4$,$\Phi = 1.3E\text{-}3$).

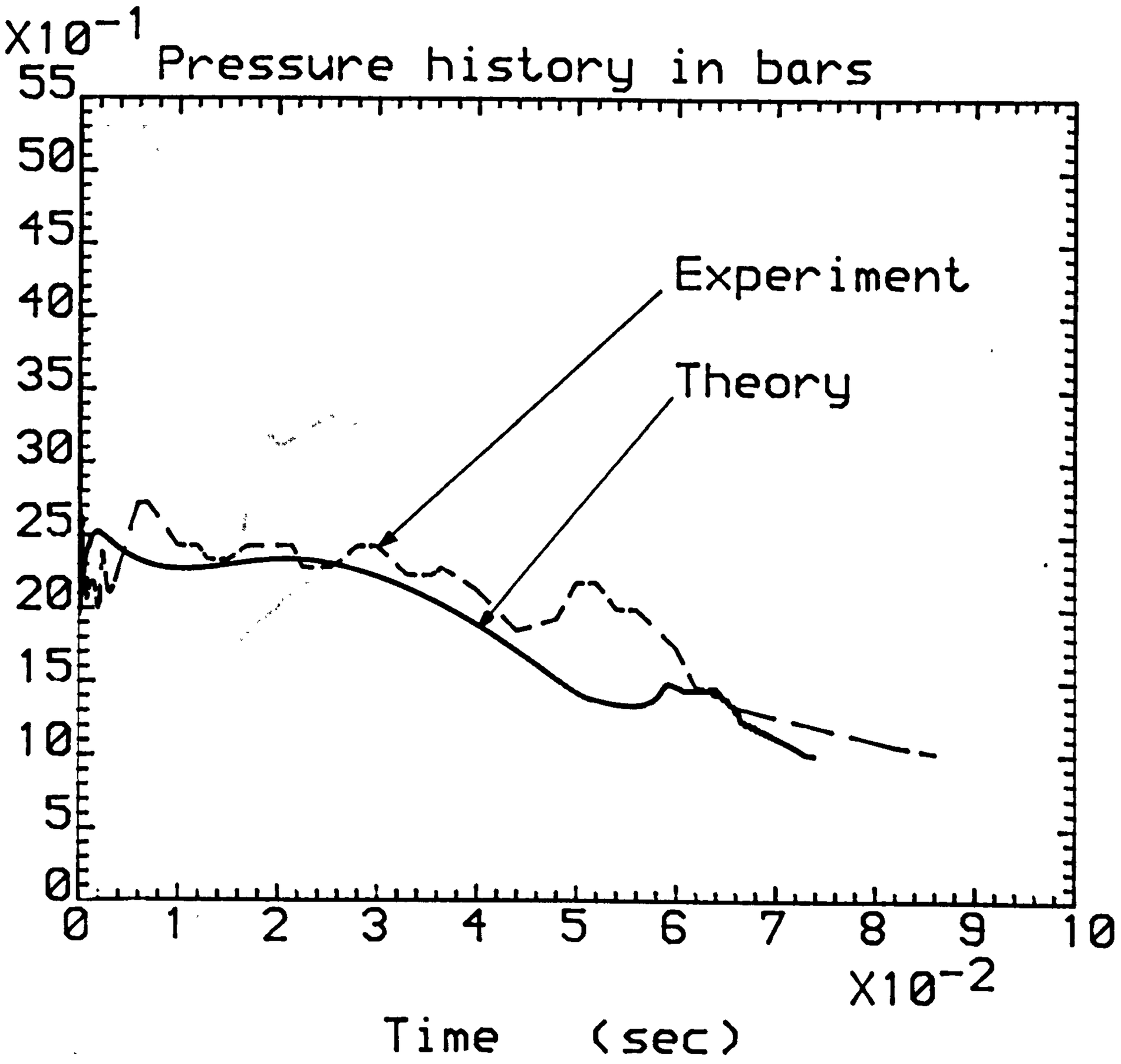

Figure 116. Comparison of the thermal non-equilibrium model analysis with R 12 vessel blowdown data.Long term decompression (mild steel vessel,top pressure station). (Initially saturated liquid of 5.3 bar,$C_d = 0.4, \Phi = 1.3E\text{-}3$).

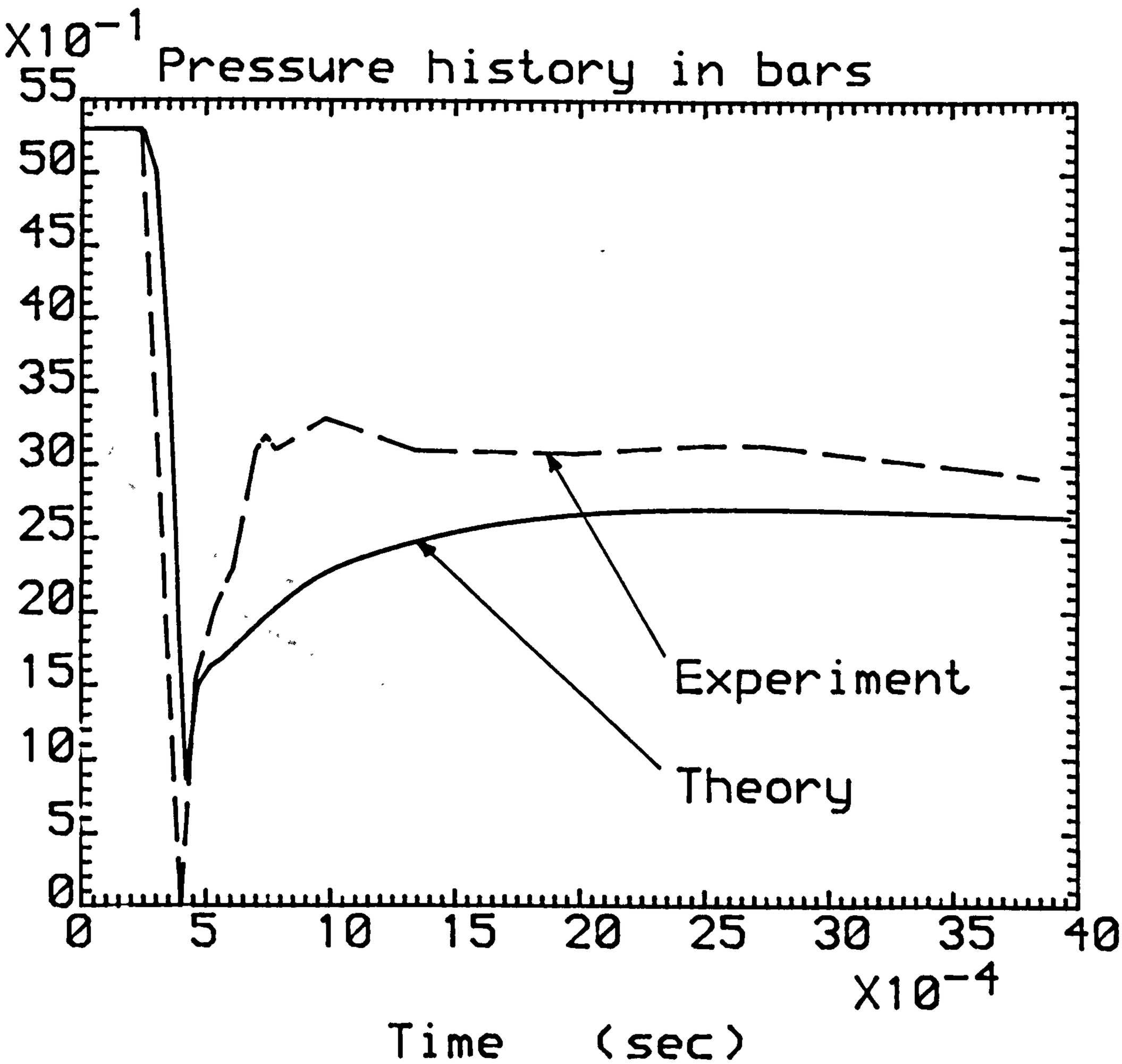

Figure 117. Comparison of the thermal non-equilibrium model analysis with R 12 vessel blowdown data.Initial depressurisation history (perspex vessel,bottom pressure station).(Initially saturated liquid of 5.3 bar,$C_d = 0.4, \Phi = 1.3E\text{-}3$).

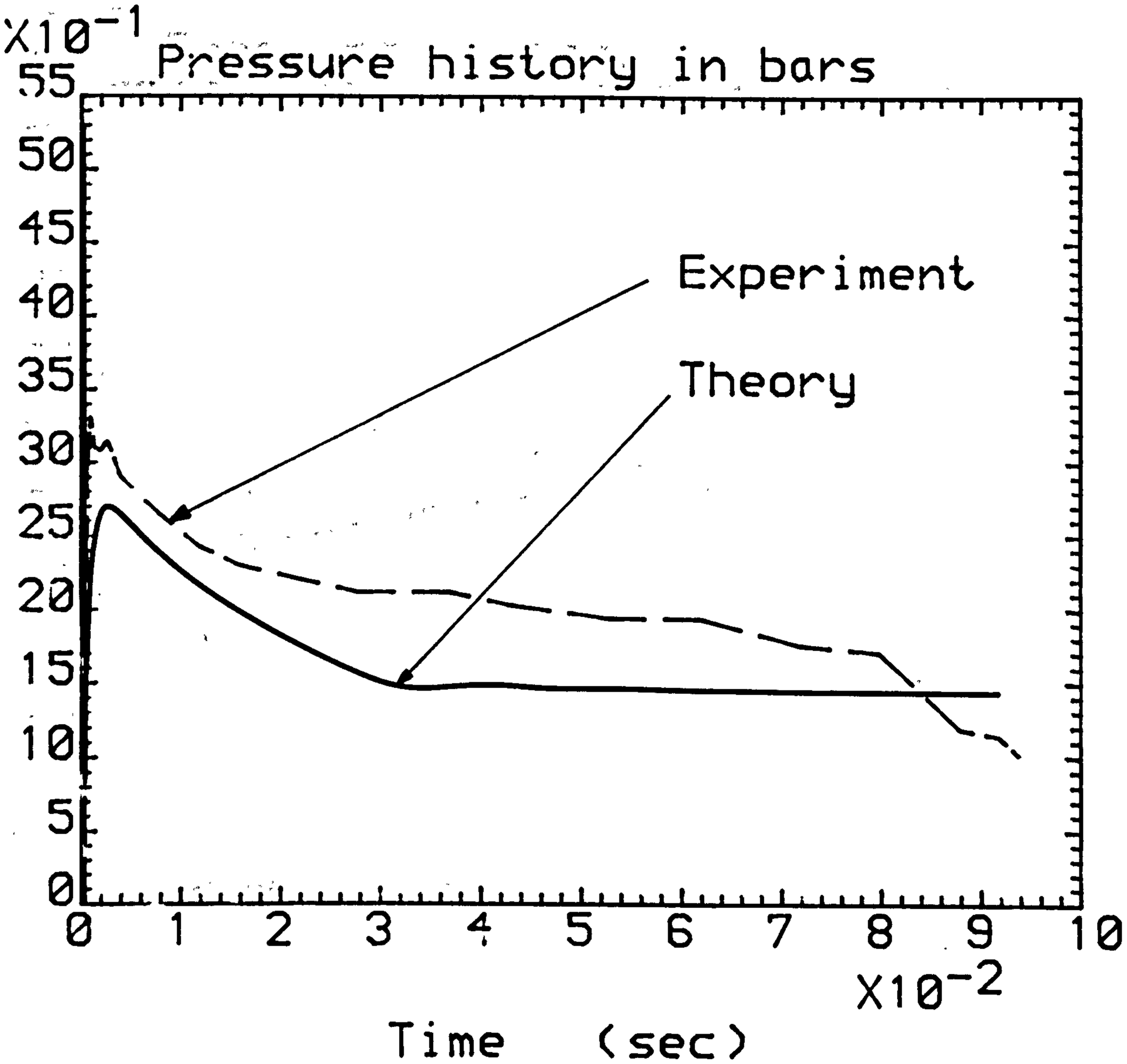

Figure 118. Comparison of the thermal non-equilibrium model analysis with R 12 vessel blowdown data.Long term decompression (perspex vessel,bottom pressure station). (Initially saturated liquid of 5.3 bar,$C_d = 0.4, \Phi = 1.3E\text{-}3$).

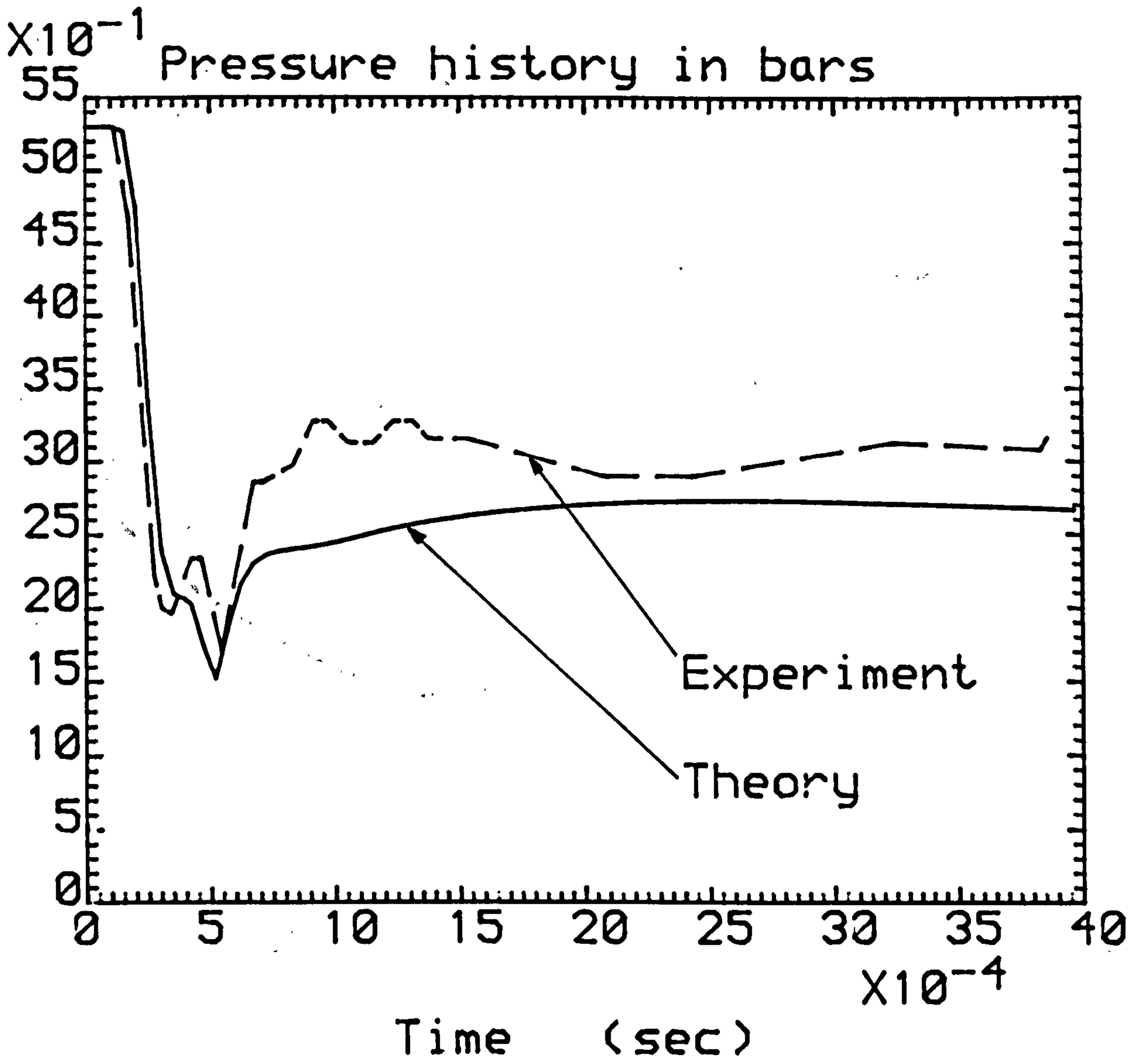

Figure 119. Comparison of the thermal non-equilibrium model analysis with R 12 vessel blowdown data.Initial depressurisation history (perspex vessel,middle pressure station). (Initially saturated liquid of 5.3 bar,$C_d = 0.4, \Phi = 1.3E\text{-}3$).

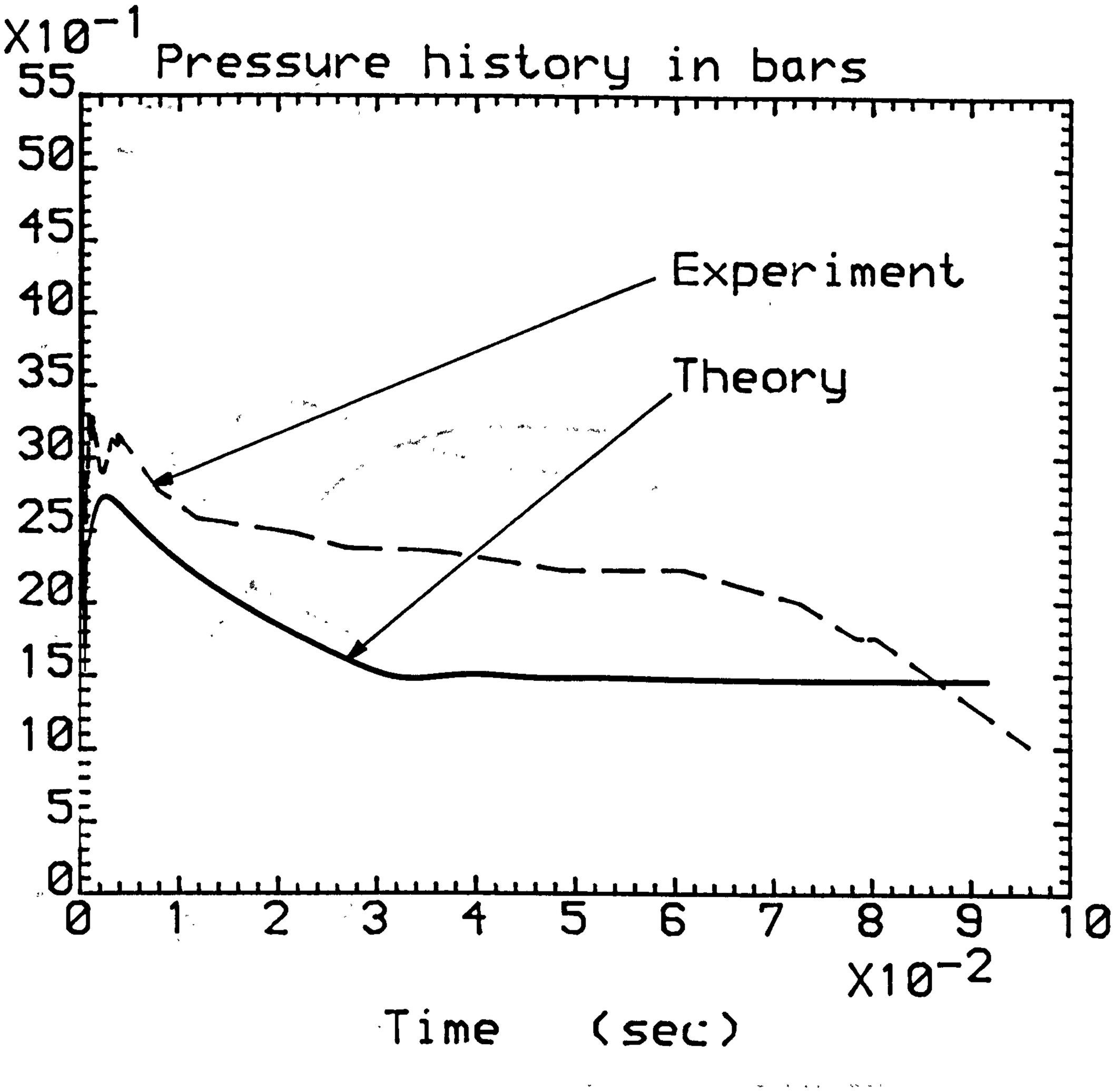

Figure 120. Comparison of the thermal non-equilibrium model analysis with R 12 vessel blowdown data.Long term decompression (perspex vessel,middle pressure station). (Initially saturated liquid of 5.3 bar,$C_d = 0.4, \Phi = 1.3E\text{-}3$).

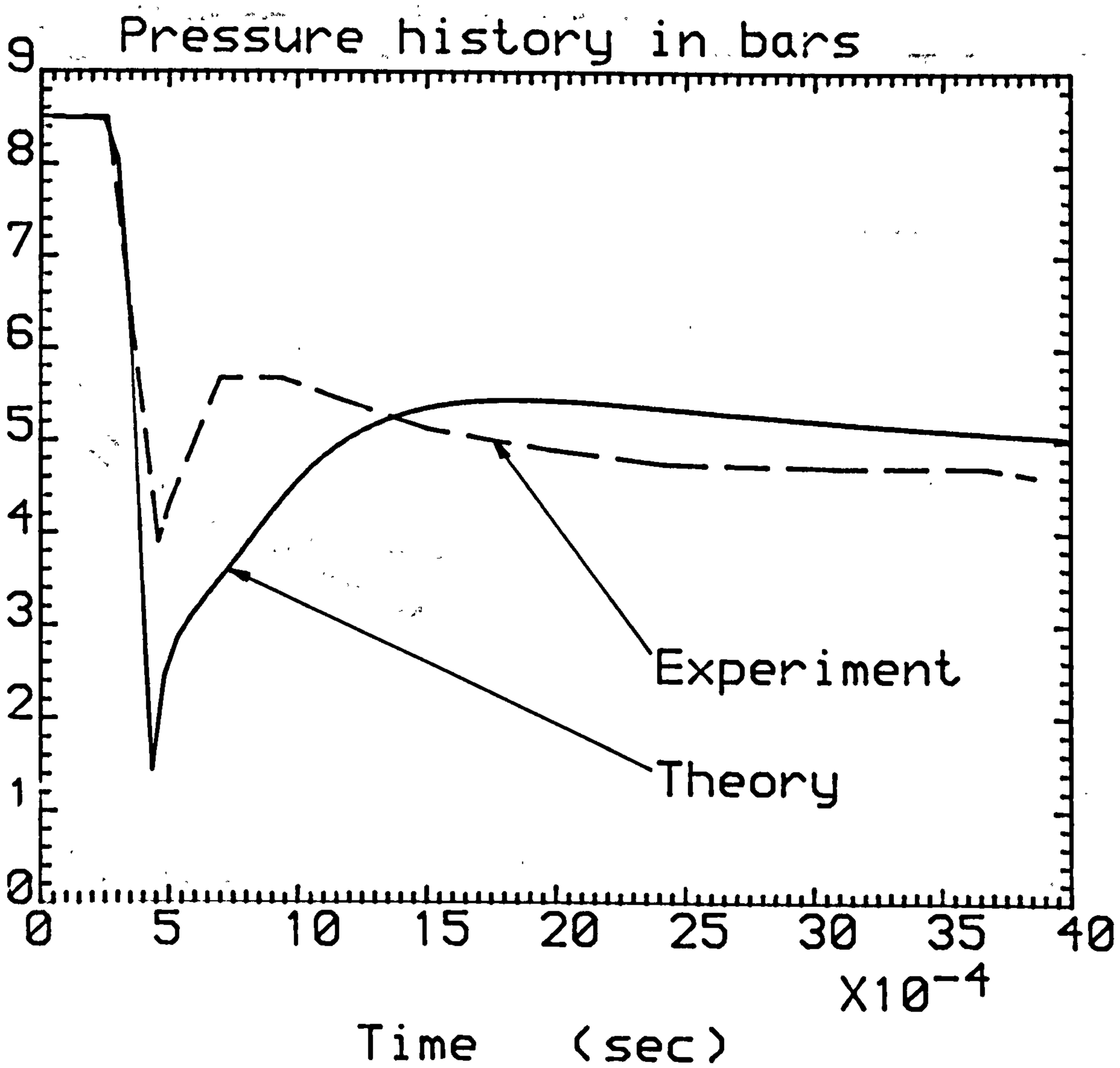

Figure 121. Comparison of the thermal non-equilibrium model analysis with R 12 vessel blowdown data.Initial depressurisation history (mild steel vessel,bottom pressure station).(Initially saturated liquid of 8.5 bar,$C_d = 0.4, \Phi = 3.7E\text{-}3$).

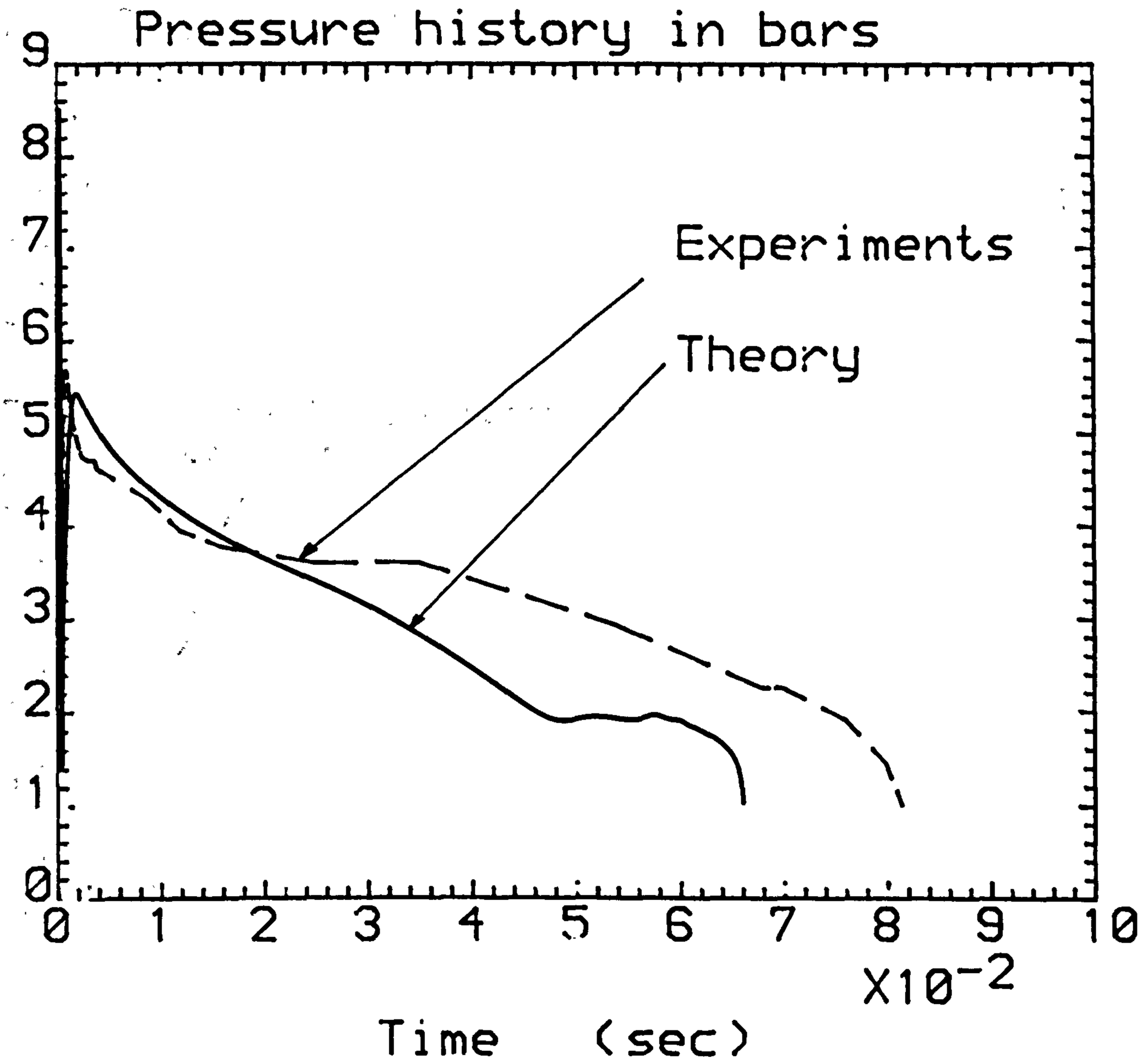

Figure 122. Comparison of the thermal non-equilibrium model analysis with R 12 vessel blowdown data. Long term decompression (mild steel vessel,bottom pressure station).(Initially saturated liquid of 8.5 bar,$C_d = 0.4, \Phi = 3.7E\text{-}3$).

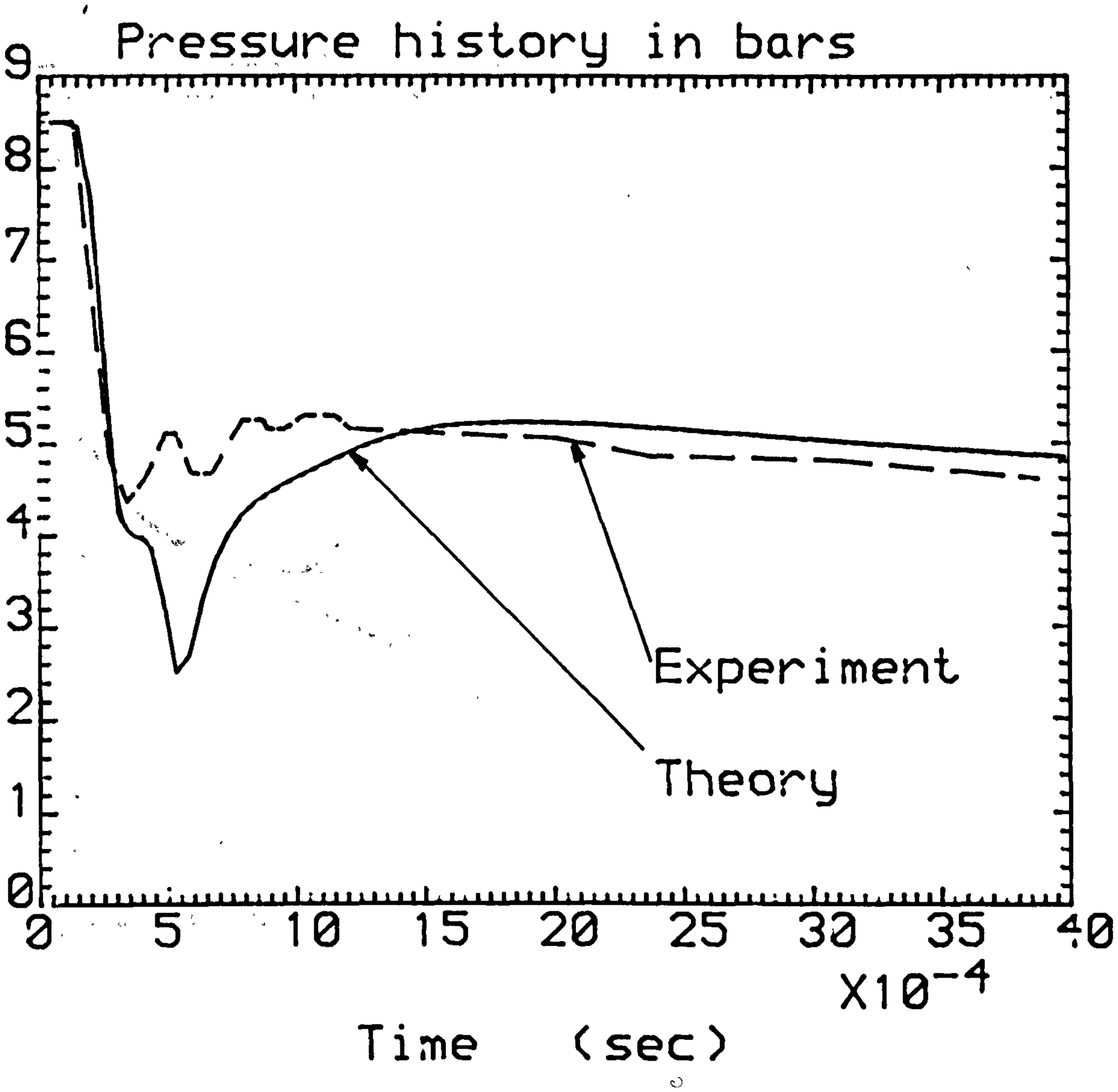

Figure 123. Comparison of the thermal non-equilibrium model analysis with R 12 vessel blowdown data.Initial depressurisation history (mild steel vessel,middle pressure station).(Initially saturated liquid of 8.5 bar,$C_d = 0.4, \Phi = 3.7E\text{-}3$).

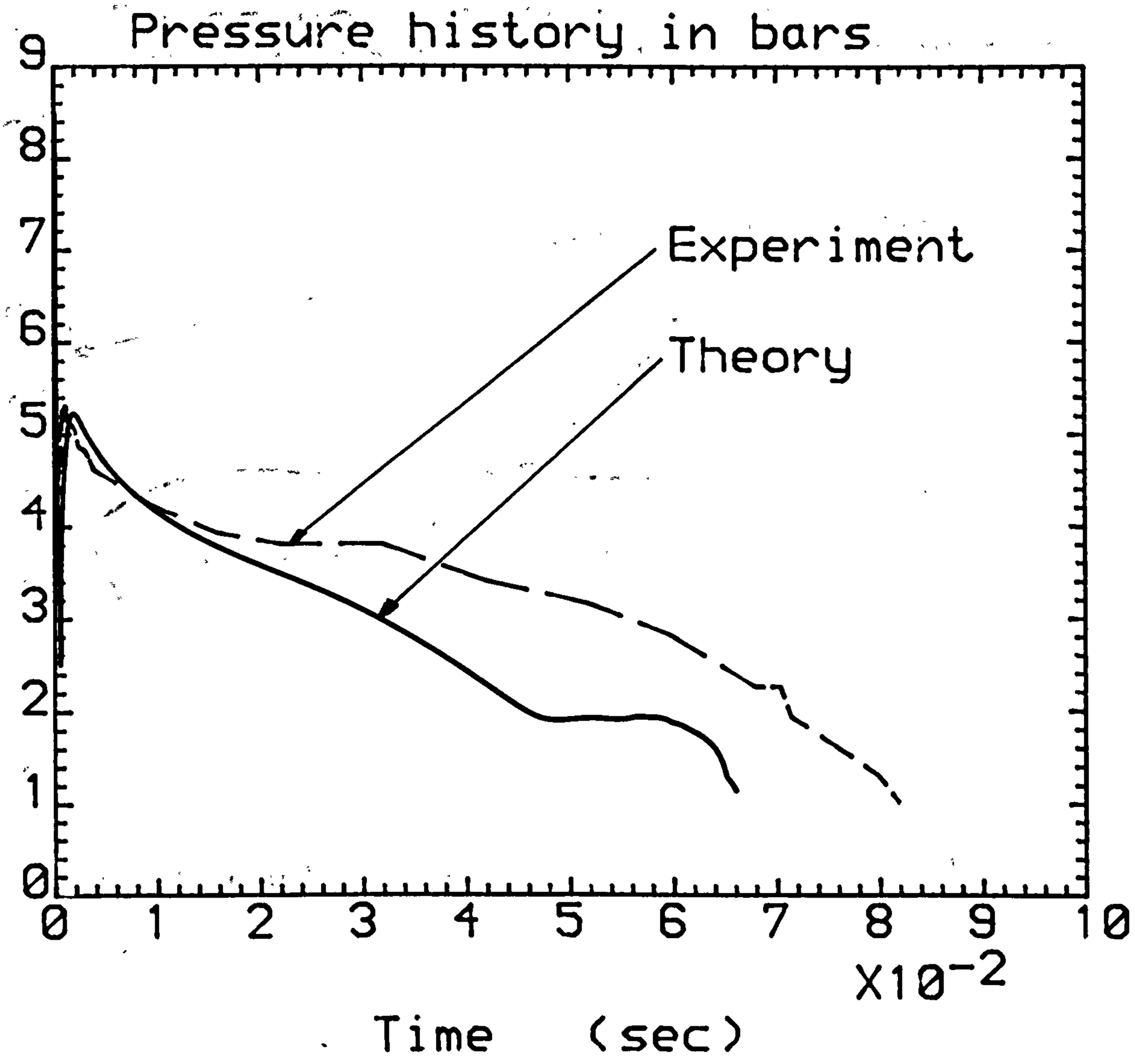

Figure 124. Comparison of the thermal non-equilibrium model analysis with R 12 vessel blowdown data.Long term decompression (mild steel vessel,middle pressure station).(Initially saturated liquid of 8.5 bar,$C_d = 0.4, \Phi = 3.7E\text{-}3$).

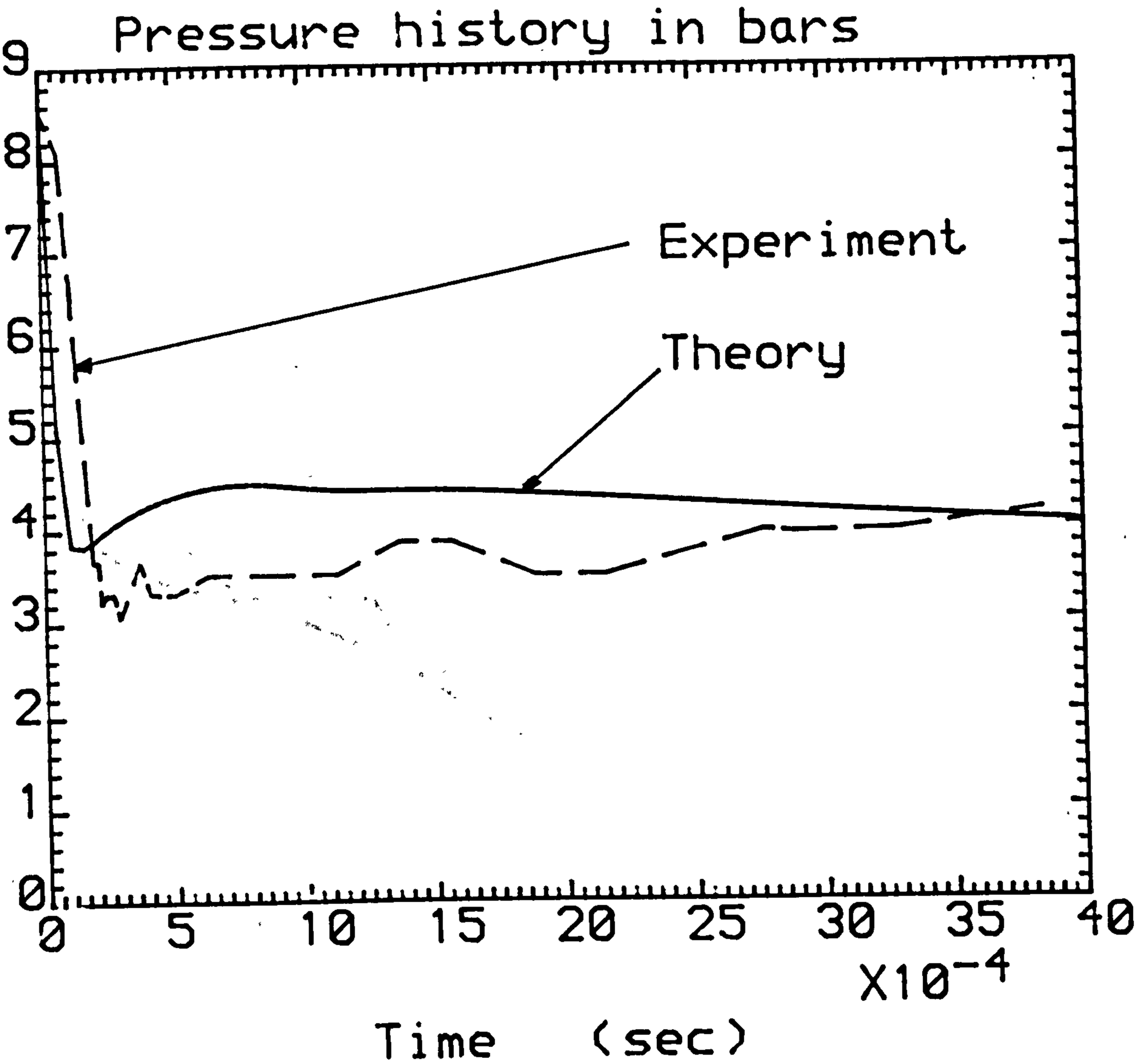

Figure 125. Comparison of the thermal non-equilibrium model analysis with R 12 vessel blowdown data.Initial .depressurisation history (mild steel vessel,top pressure station).(Initially saturated liquid of 8.5 bar,$C_d = 0.4, \Phi = 3.7E\text{-}3$).

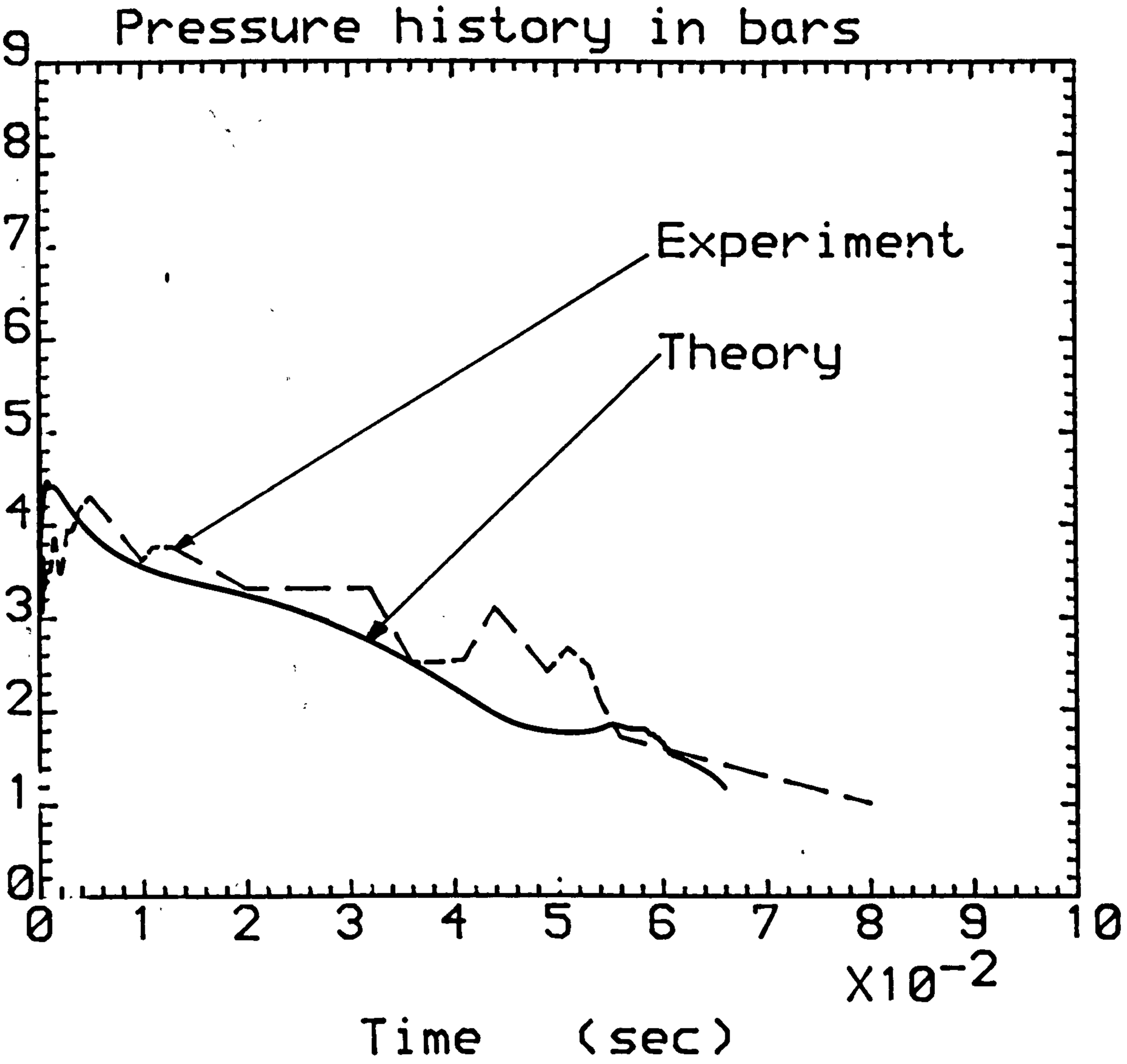

Figure 126. Comparison of the thermal non-equilibrium model analysis with R 12 vessel blodown data.Long term decompression (mild steel vessel,top pressure station). (Initially saturated liquid of 8.5 bar,$C_d = 0.4, \Phi = 3.7E\text{-}3$).

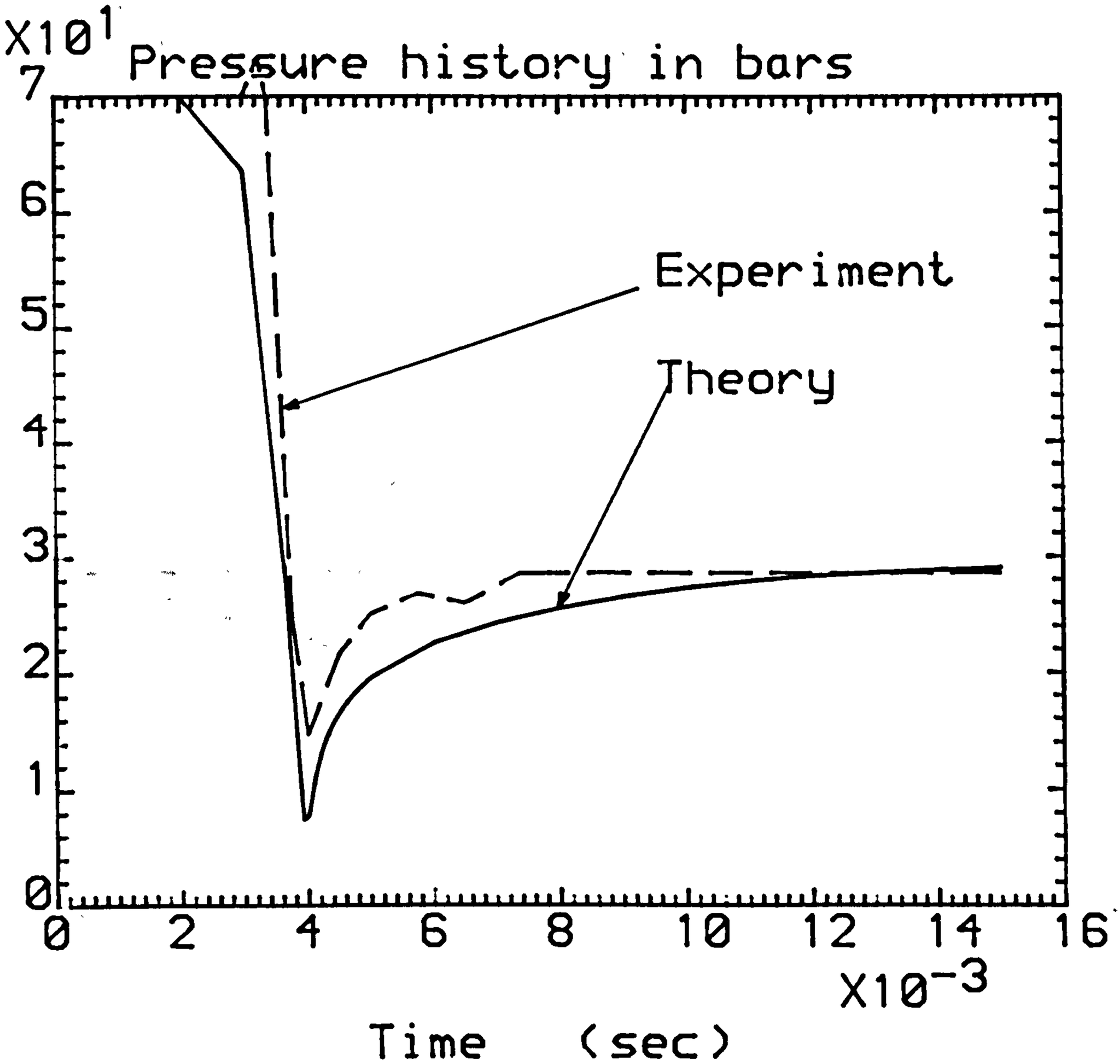

Figure 127. Comparison of the thermal non-equilibrium model analysis with water vessel blowdown data.Initial depressurisation history (pressure station 100mm from closed end).(p_{in} = 69 bar,T_{in} = 242°C,C_d = 1,Φ = 1.2E-3).

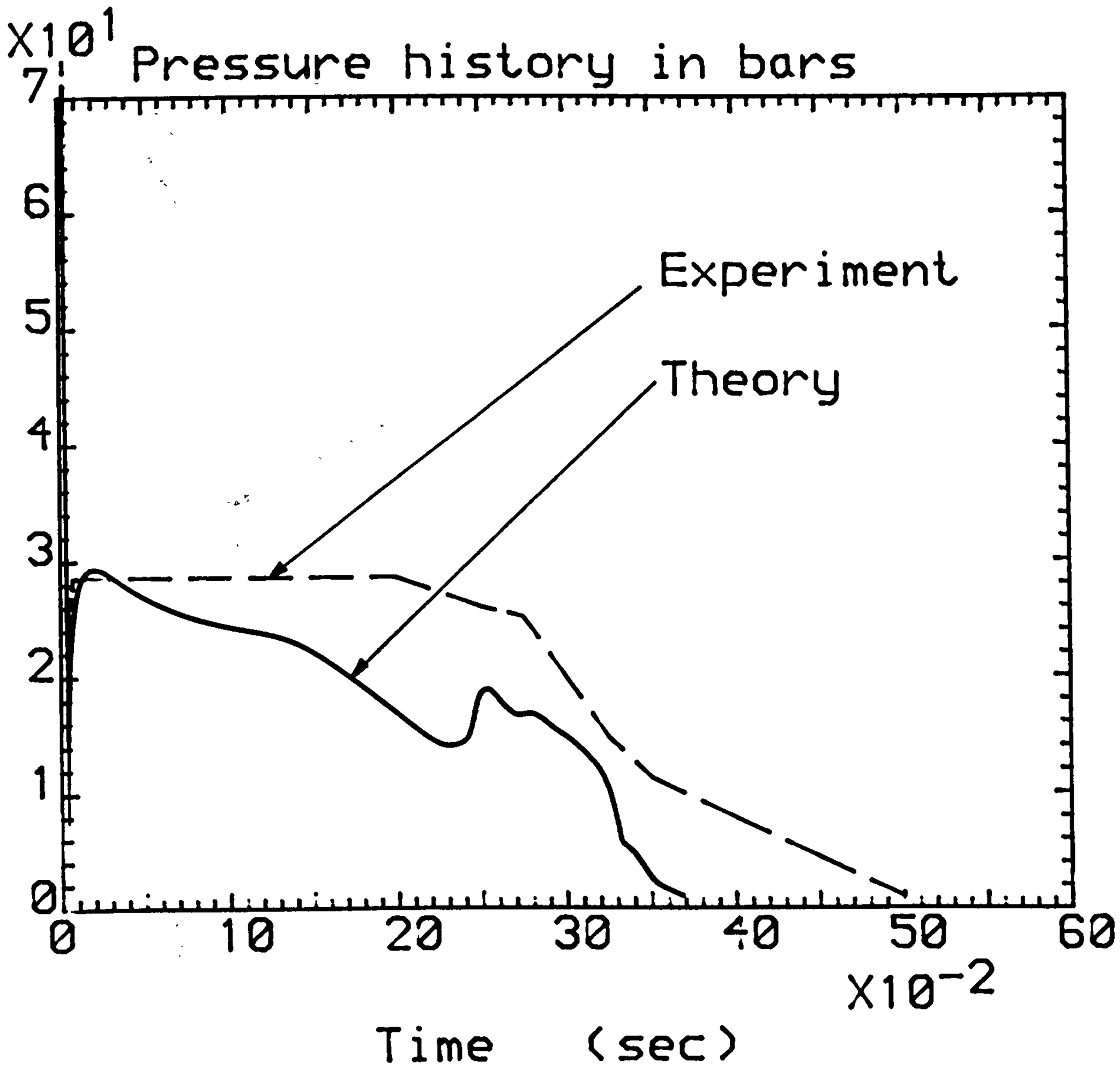

Figure 128. Comparison of the thermal non-equilibrium model analysis with water vessel blowdown data.Long term decompression (pressure station 100mm from closed end).(p_{in} = 69 bar,T_{in} = 242°C,C_d = 1,Φ = 1.2E-3).

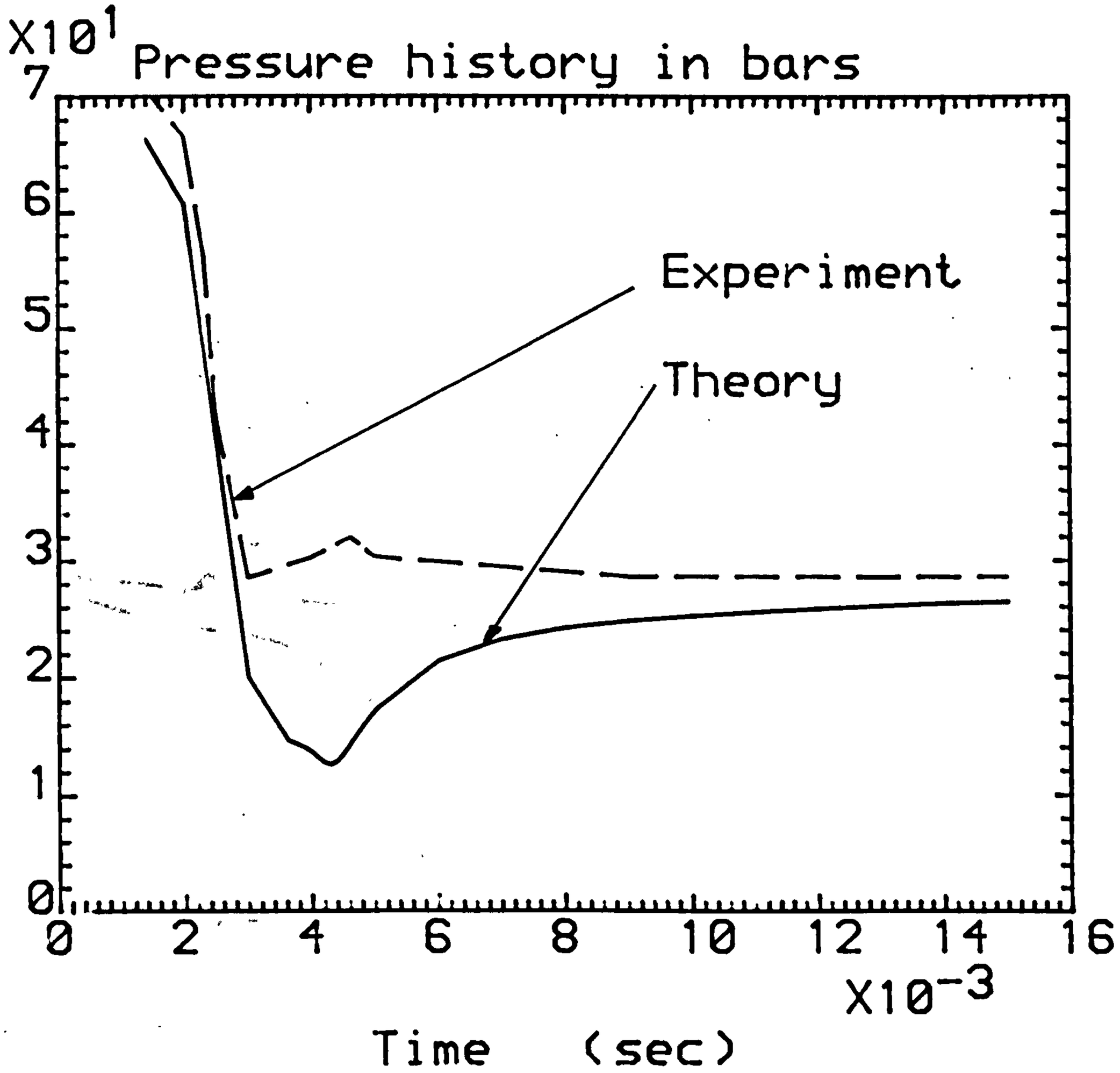

Figure 129. Comparison of the thermal non-equilibrium model analysis with water vessel blowdown data.Initial depressurisation history (pressure station 1.5m from closed end).(p_{in} = 69 bar,T_{in} = 242°C,C_d = 1,Φ = 1.2E-3).

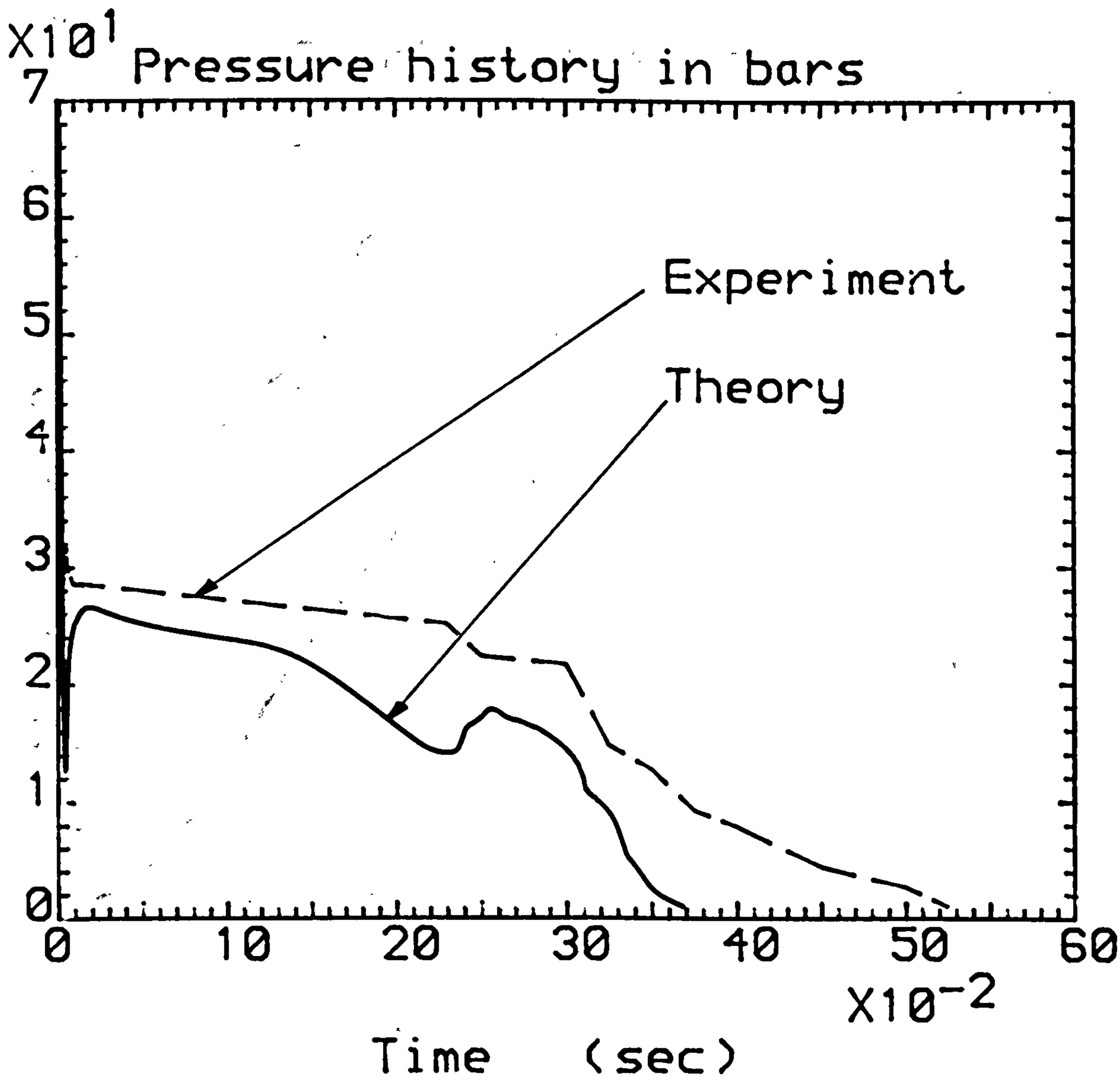

Figure 130. Comparison of the thermal non-equilibrium model analysis with water vessel blowdown data.Long term decompression (pressure station 1.5m from closed end).(p_{in} = 69 bar,T_{in} = 242°C,C_d = 1,Φ = 1.2E-3).

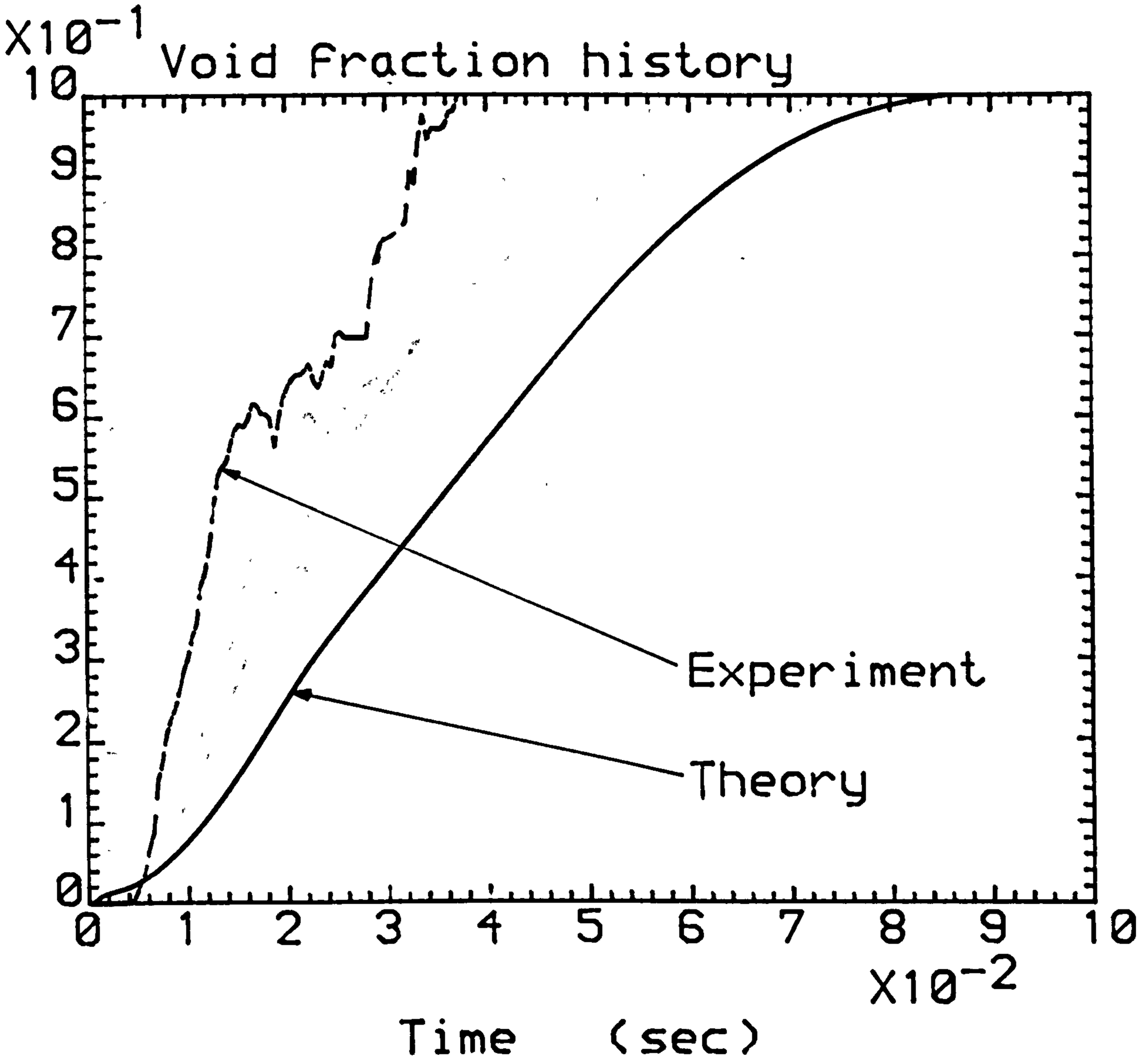

Figure 131. Comparison of the thermal non-equilibrium model analysis with R 12 vessel blowdown data.Long term void fraction history (mild steel vessel,void fraction station 20mm from closed end).(Initially saturated liquid of 5.3 bar,$C_d = 0.4$,$R_b = 1.5E\text{-}4$).

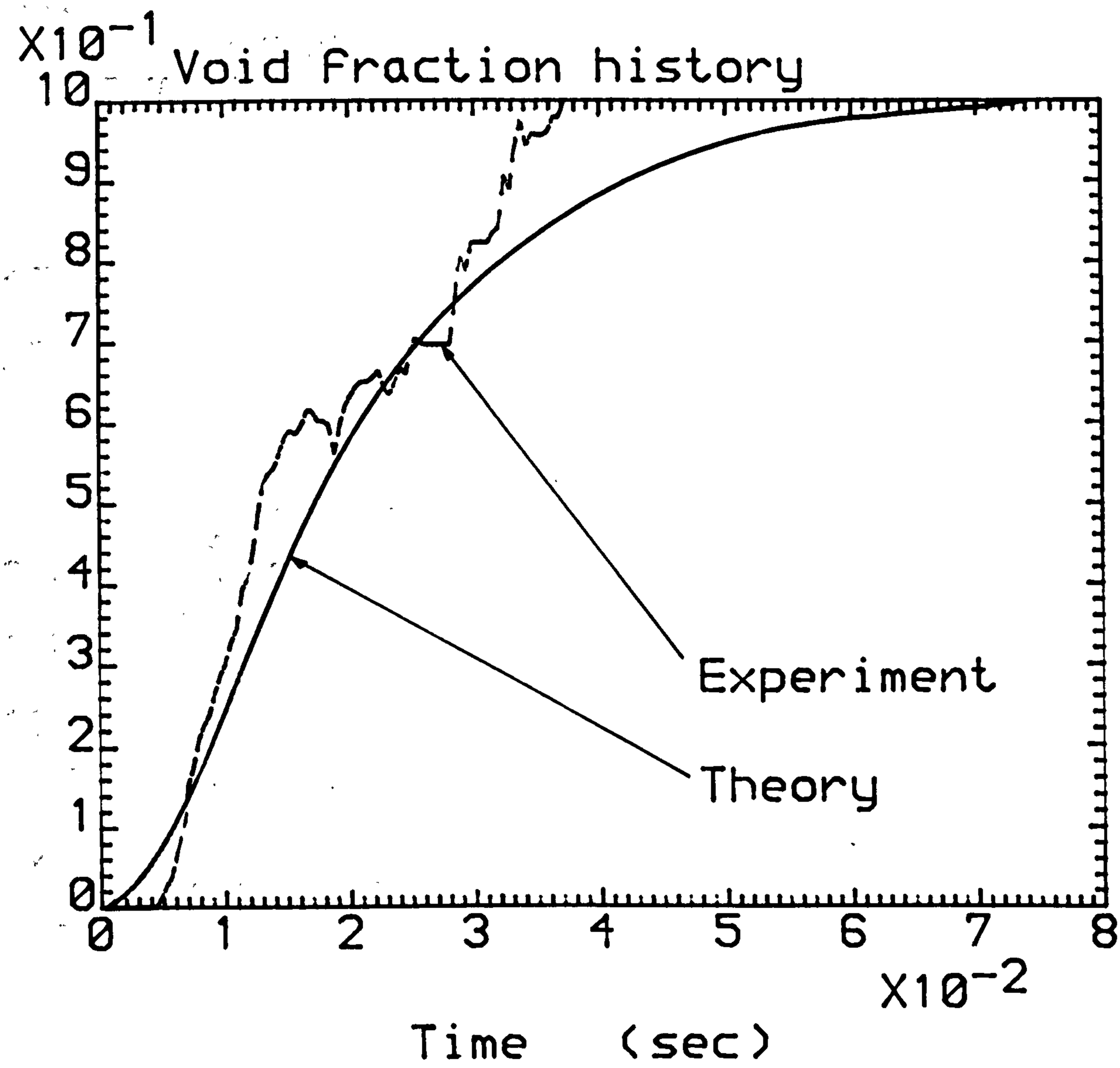

Figure 132. Comparison of the thermal non-equilibrium model analysis with R 12 vessel blowdown data.Long term void fraction history (mild steel vessel,void fraction station 20mm from closed end).(Initially saturated liquid of 5.3 bar, $C_d = 0.4, \Phi = 1.3E\text{-}3$).

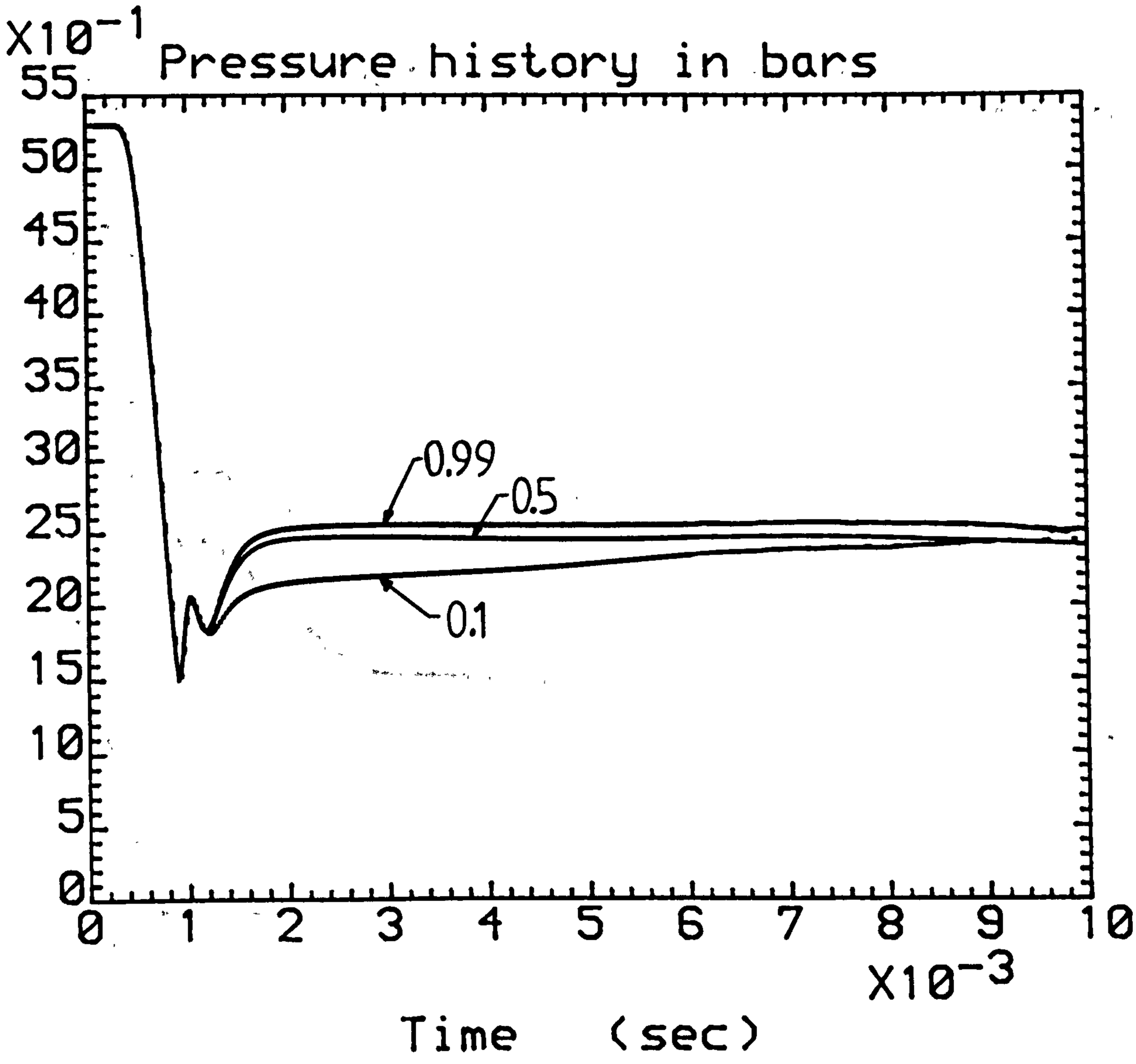

Figure 133. Influence of the slip coefficient,VE,on the thermal non-equilibrium blowdown model pressure predictions.Initial depressurisation history.

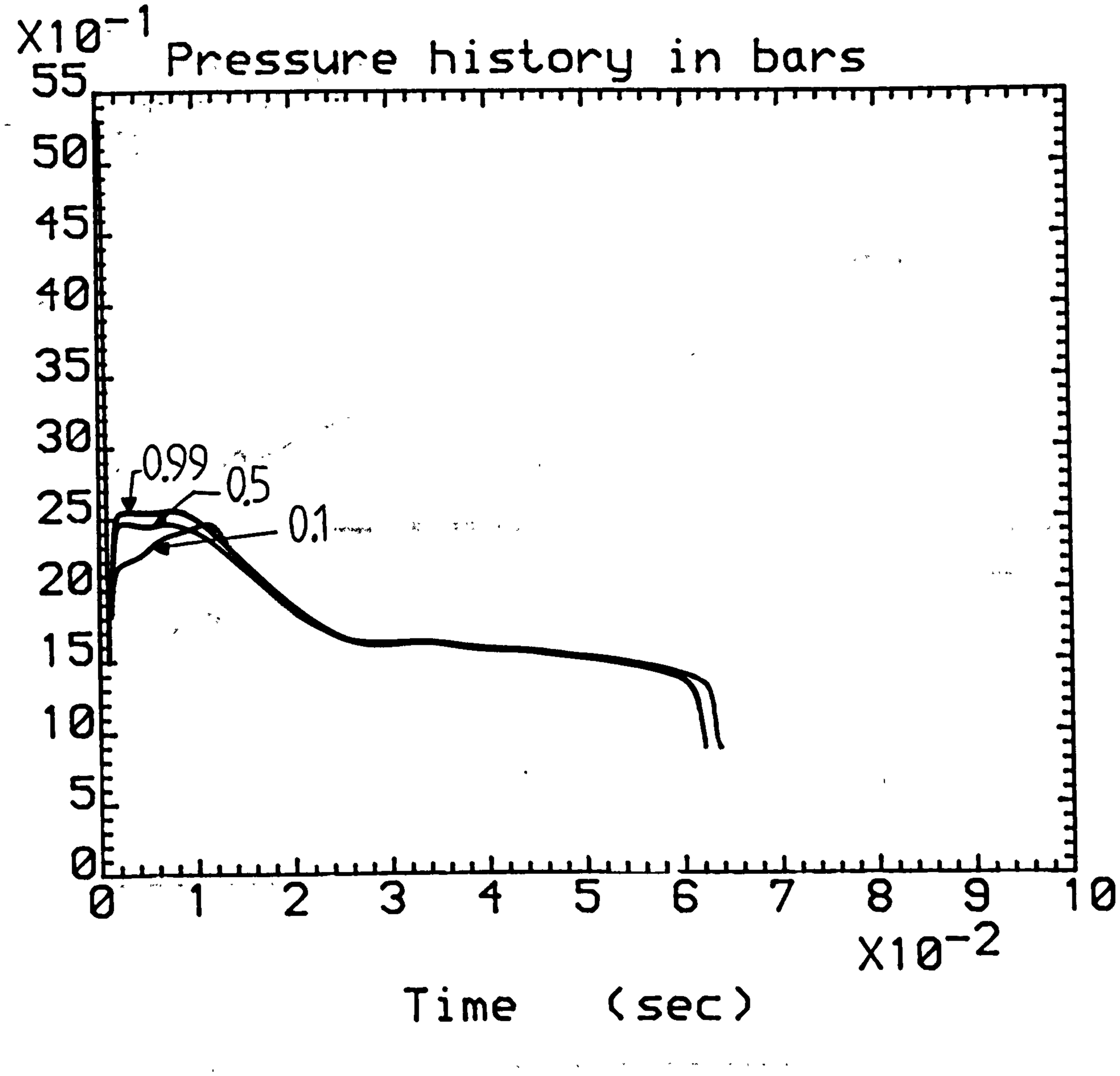

Figure 134. Influence of the slip coefficient,VE,on the thermal non-equilibrium blowdown model pressure prediction.Long term decompression.

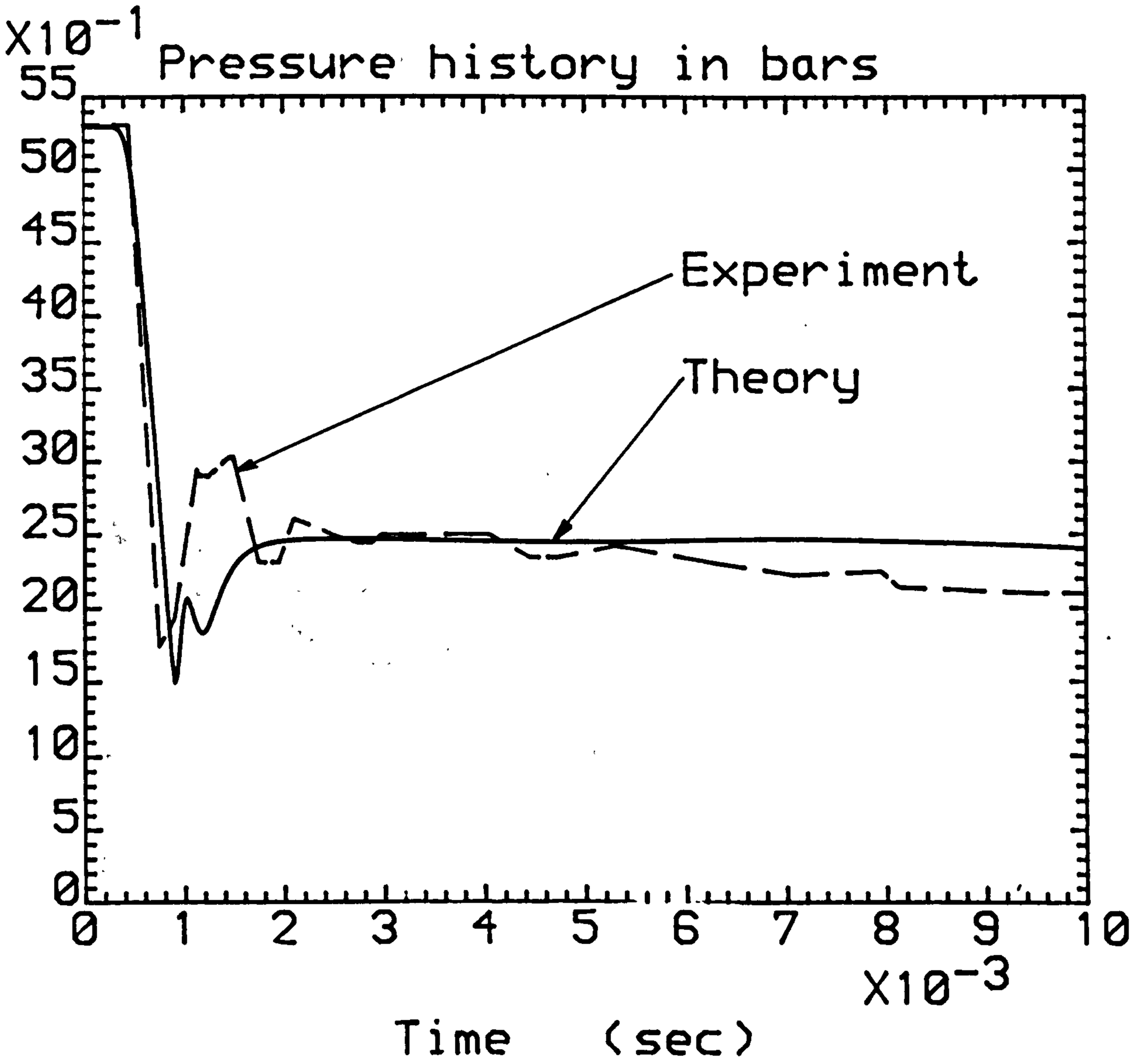

Figure 135. Comparison of the thermal non-equilibrium model analysis with R 12 vessel blowdown data.Initial depressurisation history (perspex vessel blowdown,bottom pressure station).(Initially saturated liquid of 5.3 bar,$C_d = 1, \Phi = 1.2E\text{-}3, VE = 0.5$,50%full).

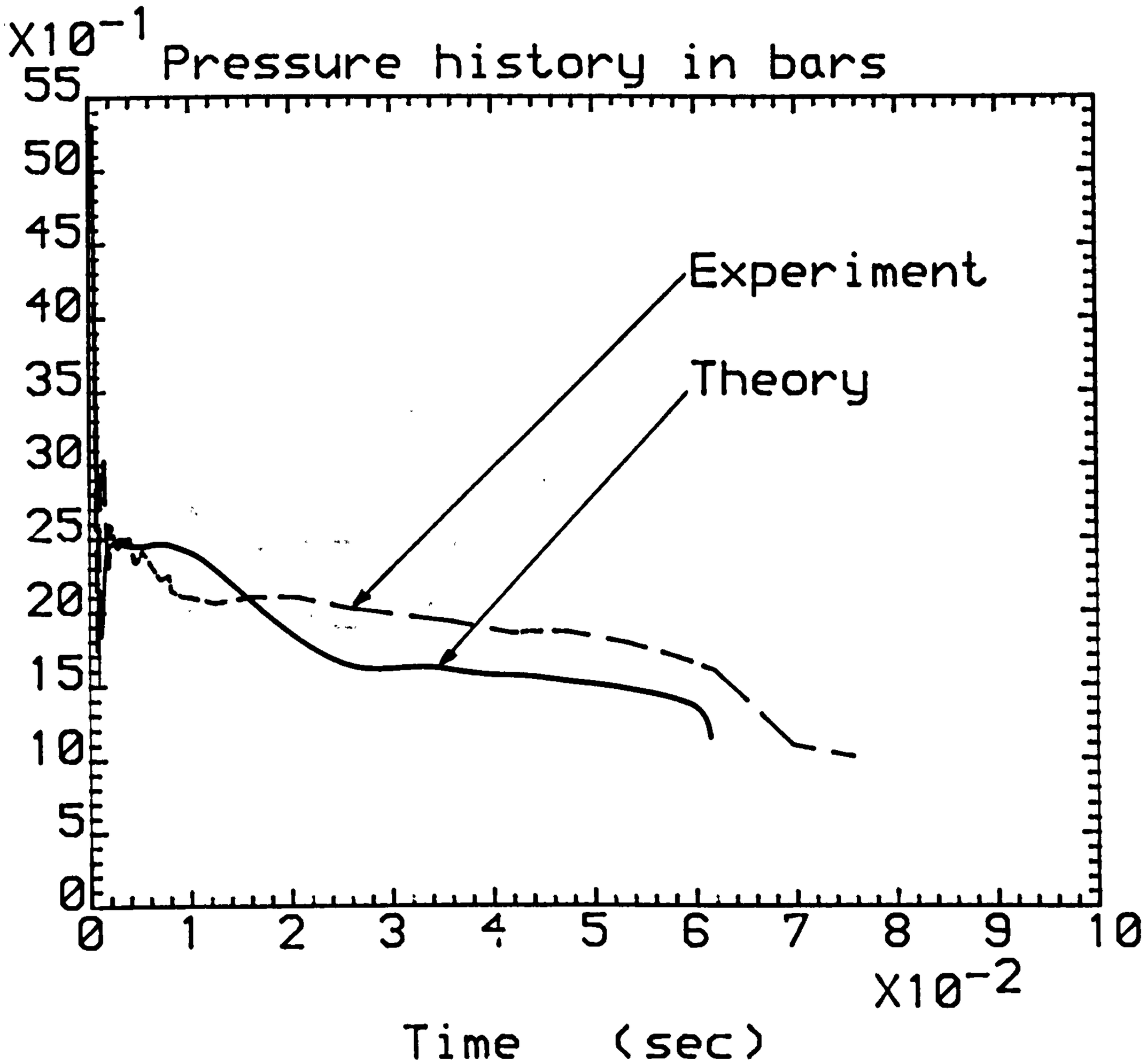

Figure 136. Comparison of the thermal non-equilibrium model analysis with R 12 vessel blowdown data.Long term decompression (perspex vessel,bottom pressure station).(Initially saturated liquid of 5.3 bar,$C_d = 1$,$\Phi = 1.2E\text{-}3$,VE = 0.5, 50%full).

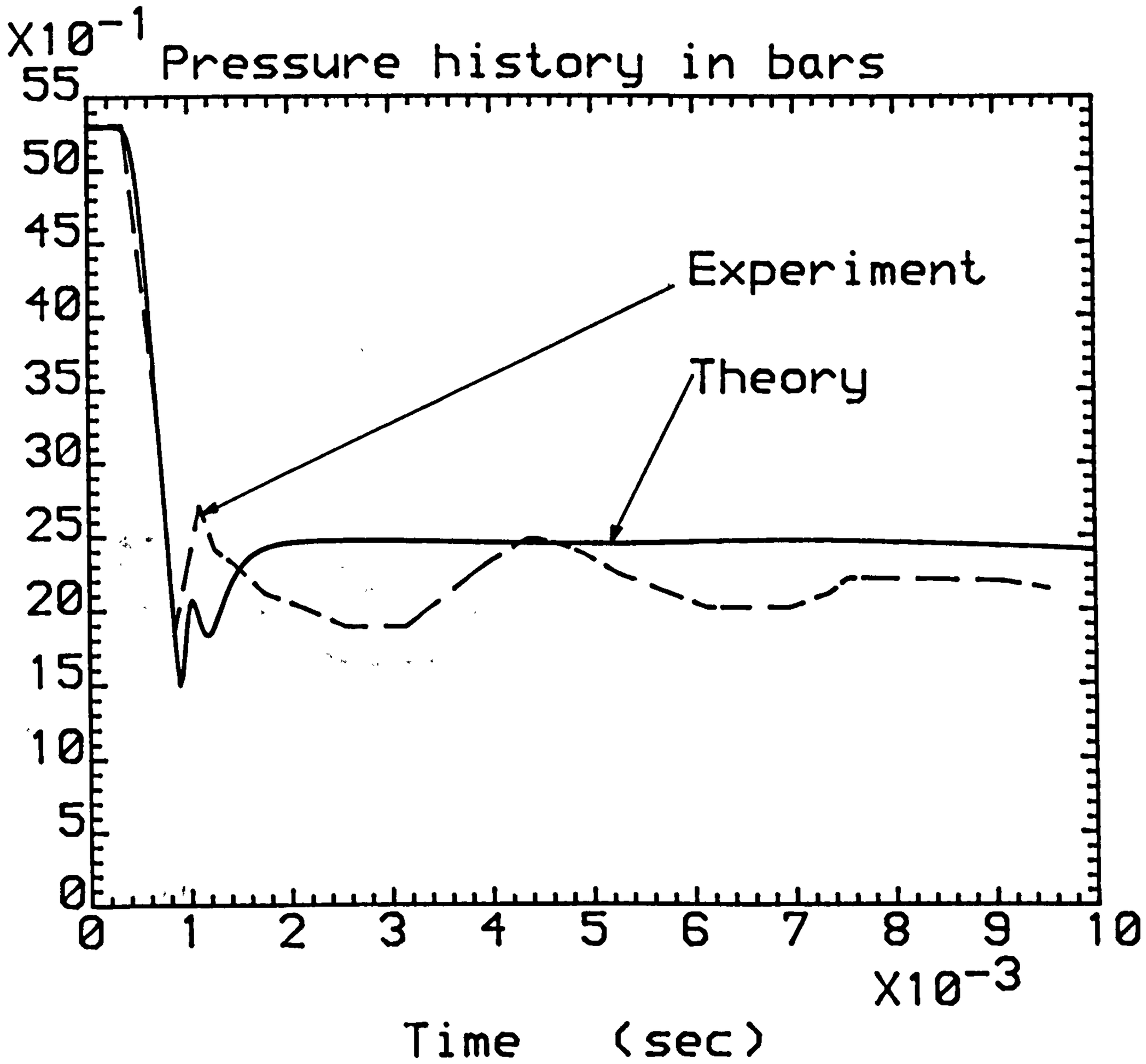

Figure 137. Comparison of the thermal non-equilibrium model analysis with R 12 vessel blowdown data.Initial depressurisation history (perspex vessel,middle pressure station).(Initially saturated liquid of 5.3 bar,$C_d = 1$,$\Phi = 1.2E\text{-}3$, VE = 0.5,50%full).

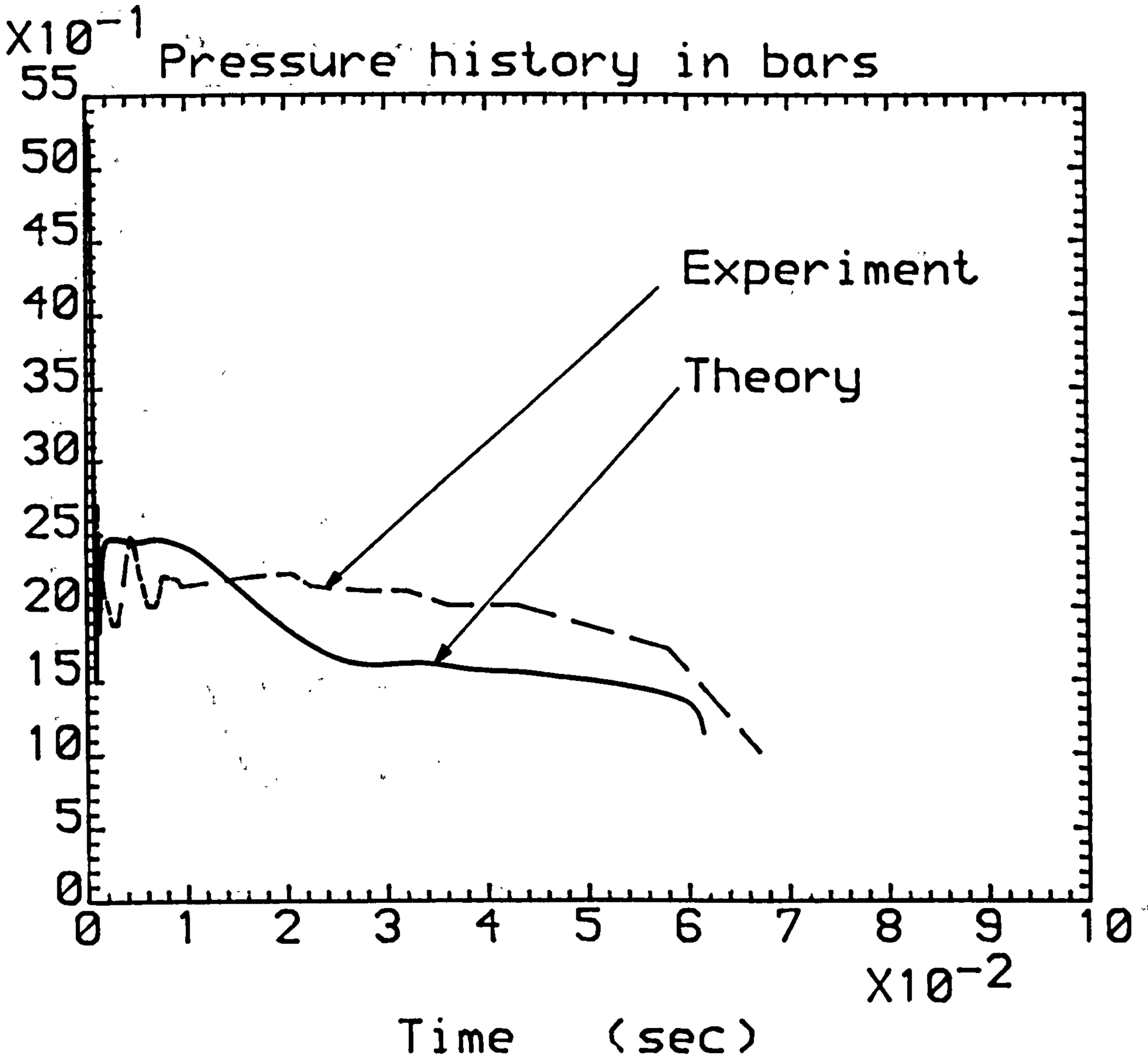

Figure 138. Comparison of the thermal non-equilibrium model analysis with R 12 vessel blowdown data.Long term decompression (perspex vessel,middle pressure station).(Initially saturated liquid of 5.3 bar,$C_d = 1, \Phi = 1.2E\text{-}3, VE = 0.5$,50%full).

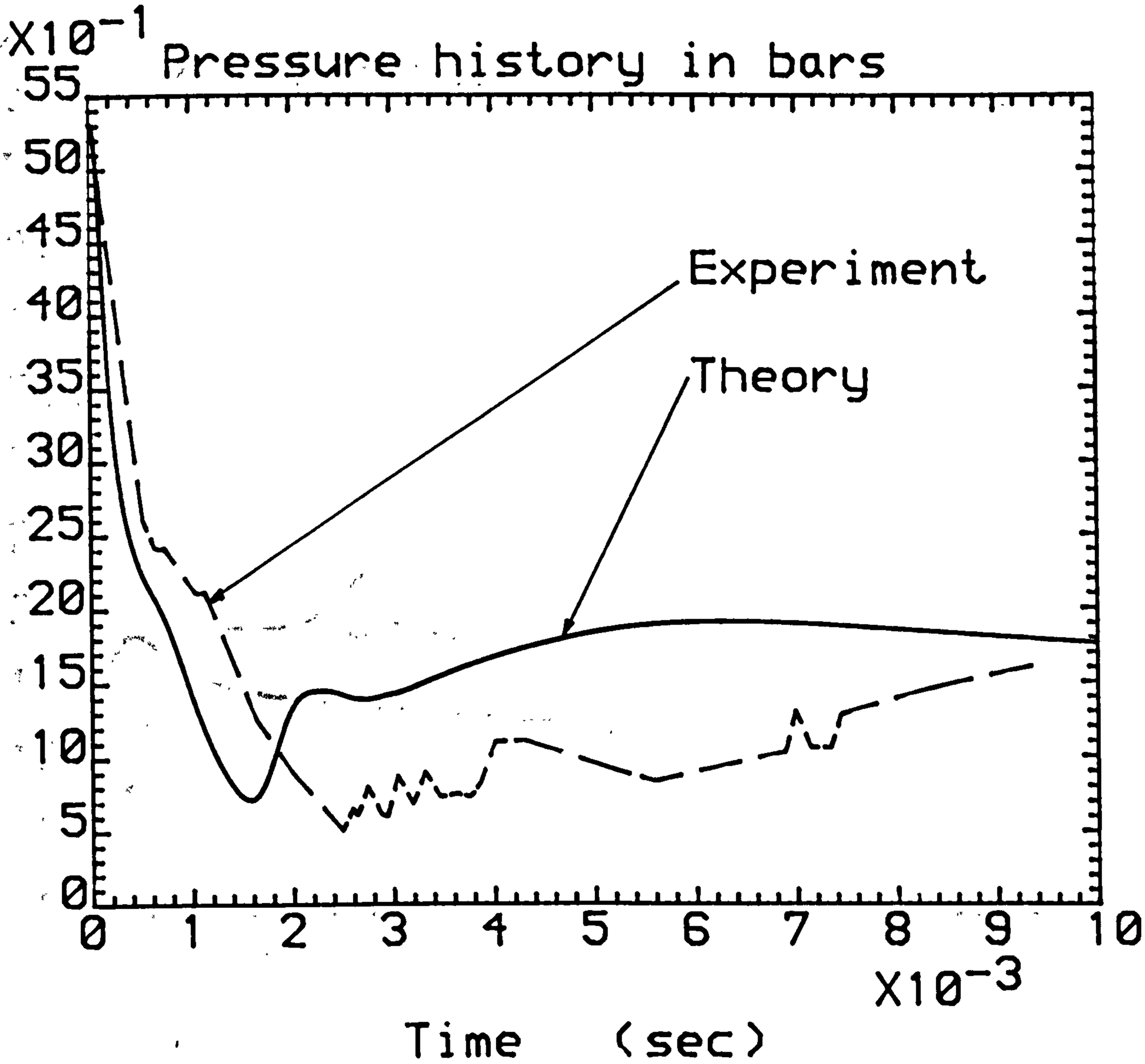

Figure 139. Comparison of the thermal non-equilibrium model analysis with R 12 vessel blowdown data.Initial depressurisation history (perspex vessel,top pressure station).(Initially saturated liquid of 5.3 bar,$C_d = 1, \Phi = 1.2E\text{-}3, VE = 0.5$,50%full).

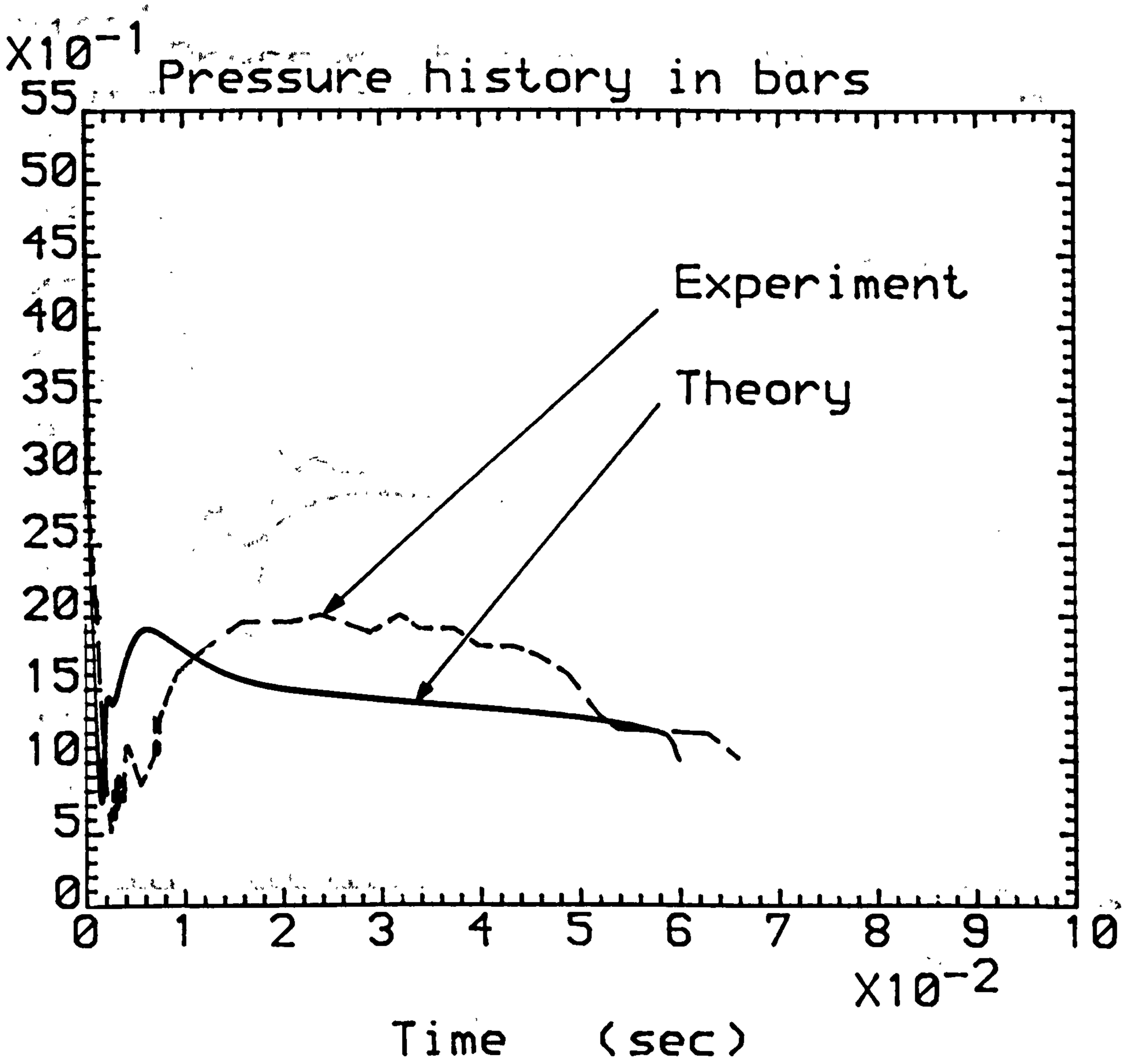

Figure 140. Comparison of the thermal non-equilibrium model analysis with R 12 vessel blowdown data.Long term decompression (perspex vessel,top pressure station). (Initially saturated liquid of 5.3 bar,$C_d = 1, \Phi = 1.2E\text{-}3, VE = 0.5$,50%full).

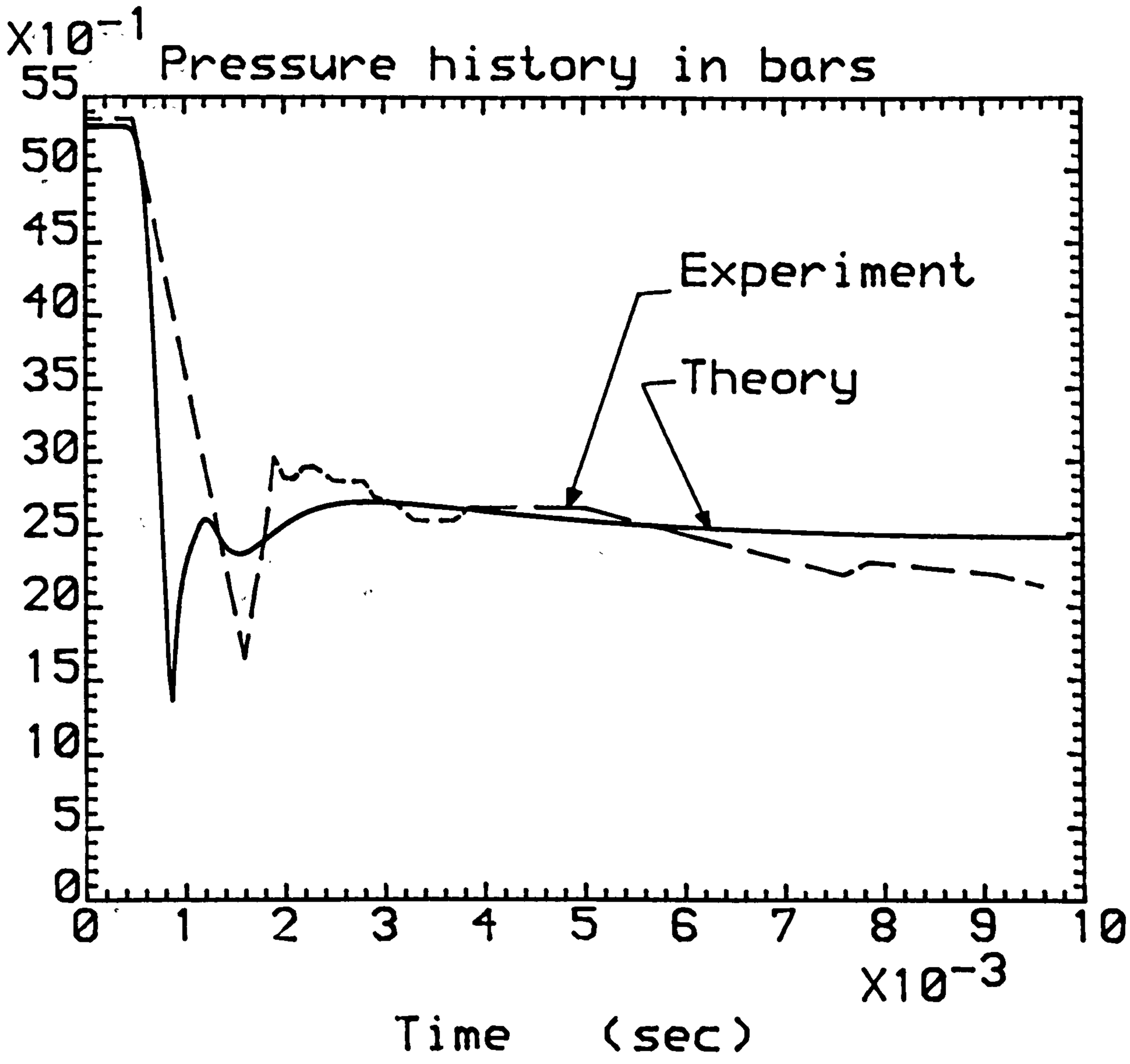

Figure 141. Comparison of the thermal non-equilibrium model analysis with R 12 vessel blowdown data.Initial depressurisation history (perspex vessel,bottom pressure station).(Initially saturated liquid of 5.3 bar,C_d = 1,Φ = 1.2E- 3,VE = 0.5,50%full,vent pipe length = 200mm).

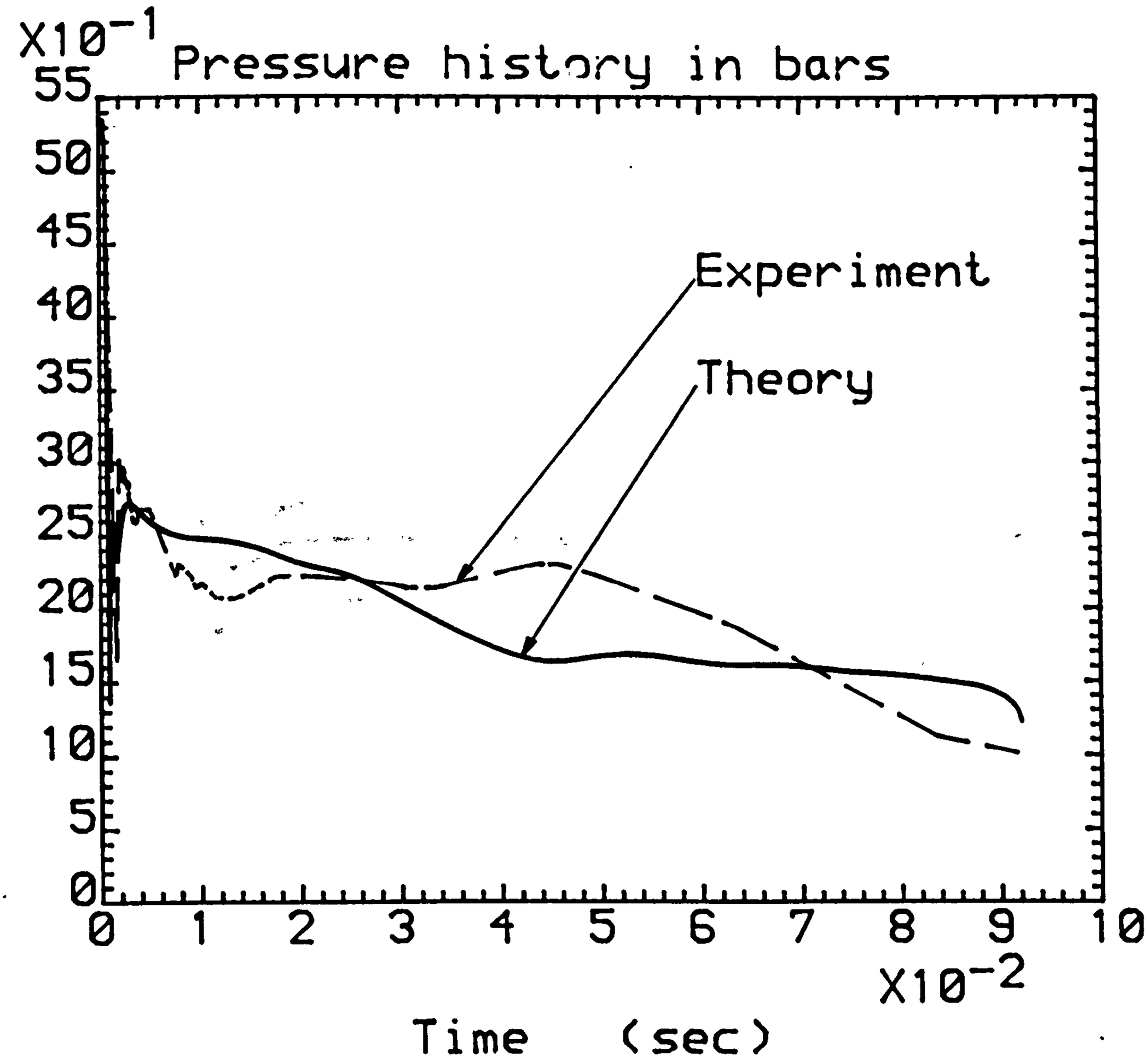

Figure 142. Comparison of the thermal non-equilibrium model analysis with R 12 vessel blowdown data.Long term decompression (perspex vessel,bottom pressure station). (Initially saturated liquid of 5.3 bar,C_d = 1,Φ = 1.2E-3,VE = 0.5,50% full,vent pipe length = 200mm).

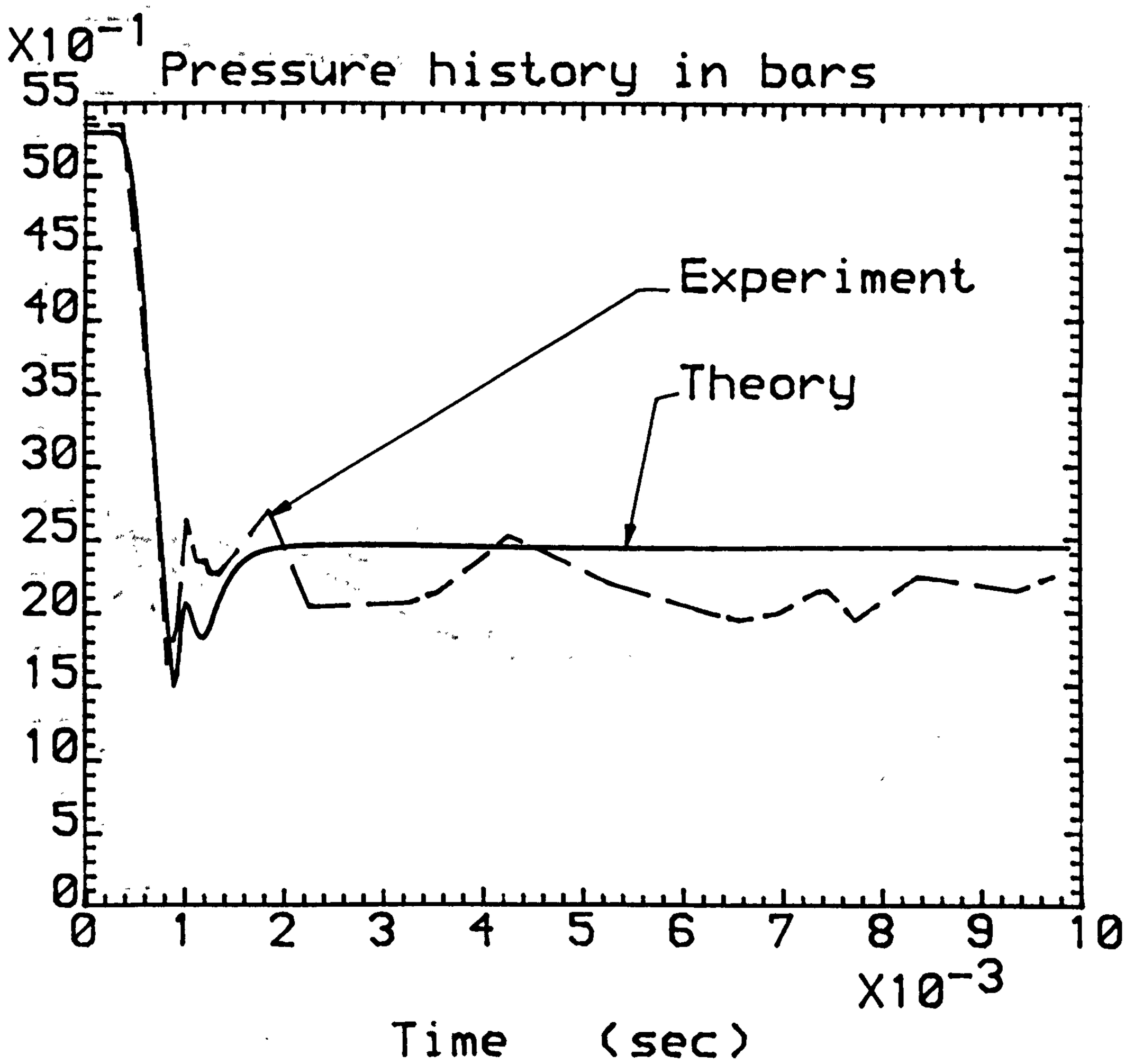

Figure 143. Comparison of the thermal non-equilibrium model analysis with R 12 vessel blowdown data.Initial depressurisation history (perspex vessel,middle pressure station).(Initially saturated liquid of 5.3 bar,C_d = 1,Φ = 1.2E-3, VE = 0.5,50%full,vent pipe length = 200mm).

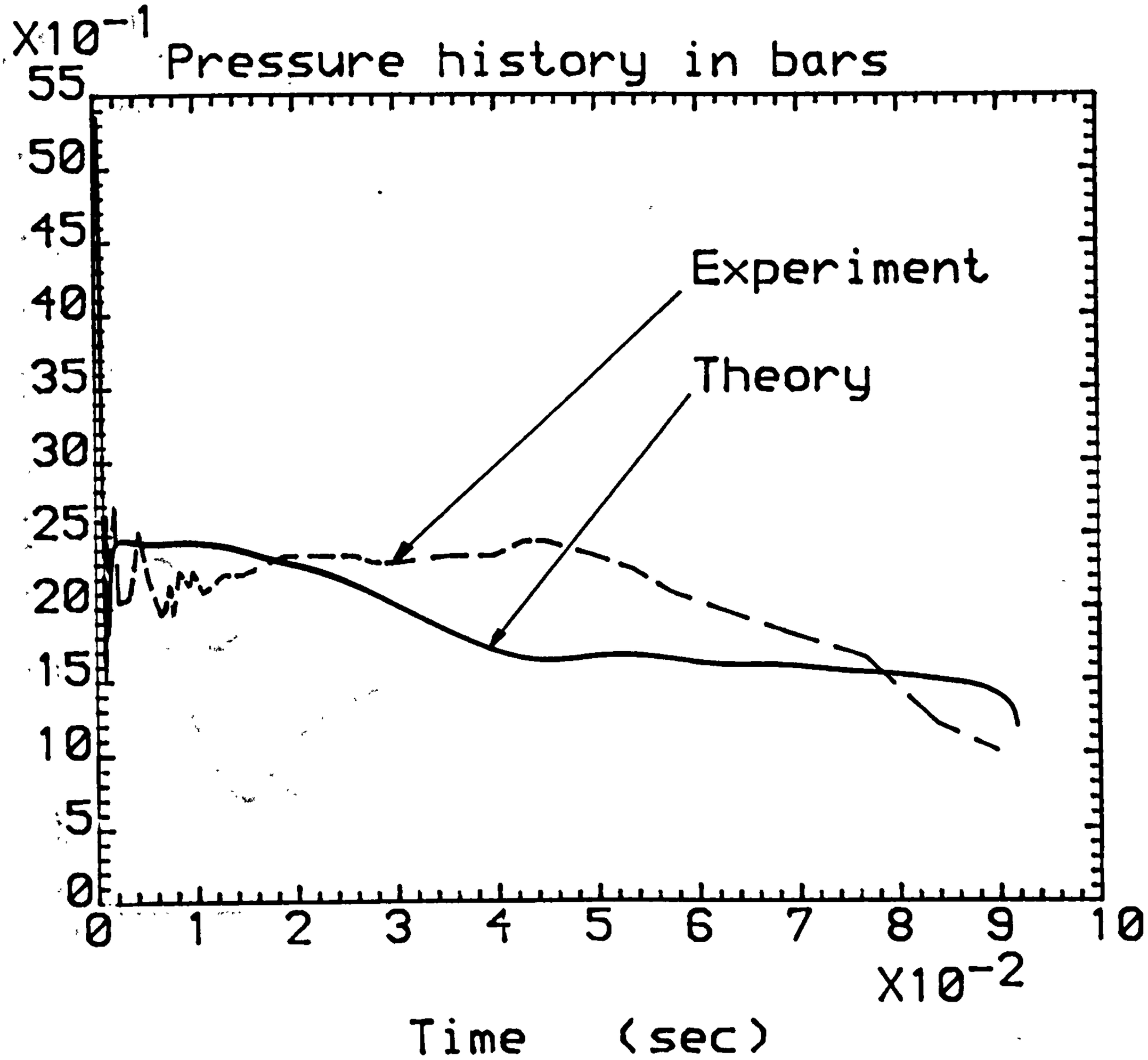

Figure 144. Comparison of the thermal non-equilibrium model analysis with R 12 vessel blowdown data.Long term decompression (perspex vessel,middle pressure station). (Initially saturated liquid of 5.3 bar,$C_d = 1$,$\Phi = 1.2E\text{-}3$,VE = 0.5, 50%full,vent pipe length = 200mm.)

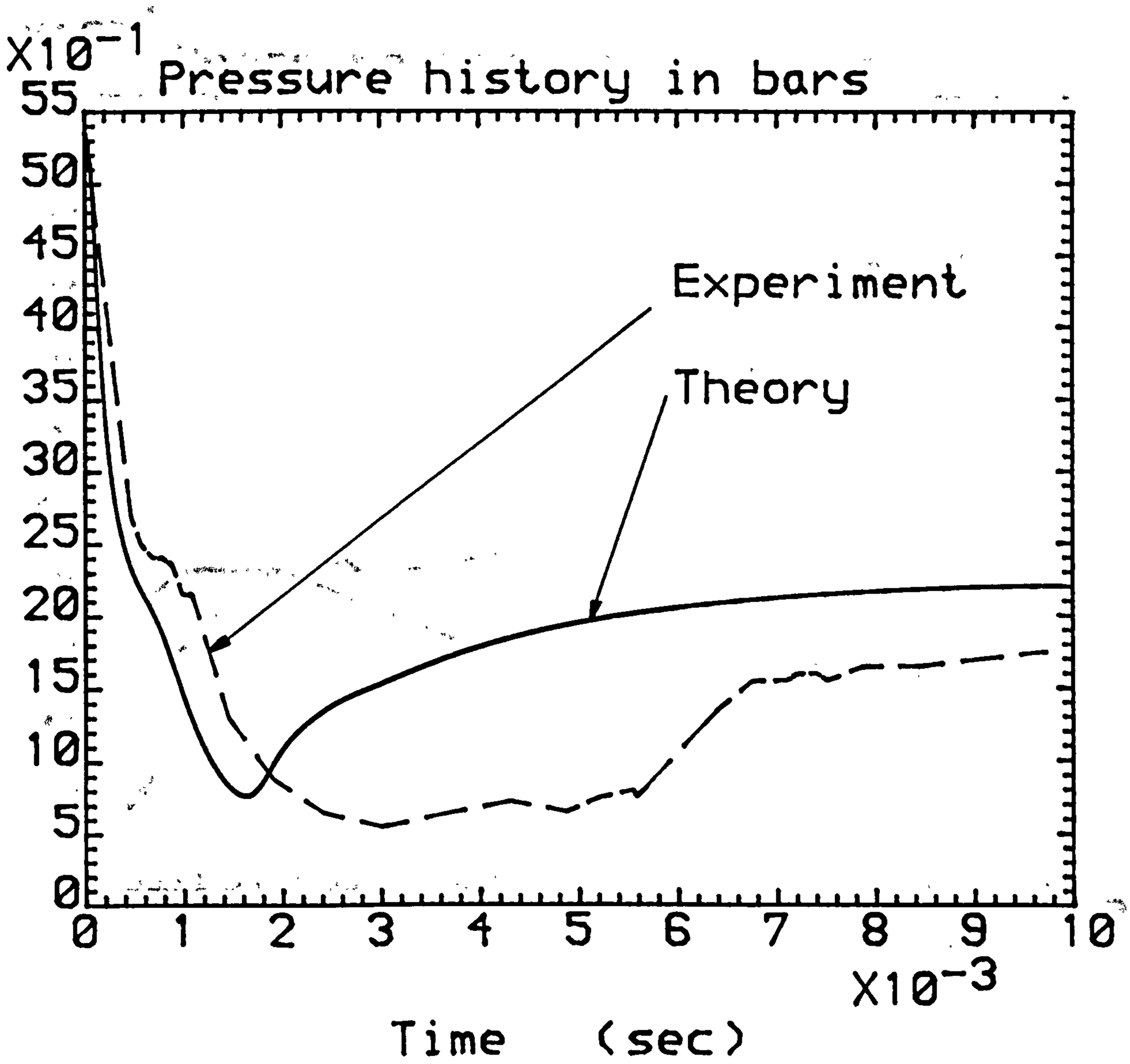

Figure 145. Comparison of the thermal non-equilibrium model analysis with R 12 vessel blowdown data.Initial depressurisation history (perspex vessel,top pressure station). (Initially saturated liquid of 5.3 bar,$C_d = 1$,$\Phi = 1.2E\text{-}3$, VE = 0.5,50%full,vent pipe length = 200mm).

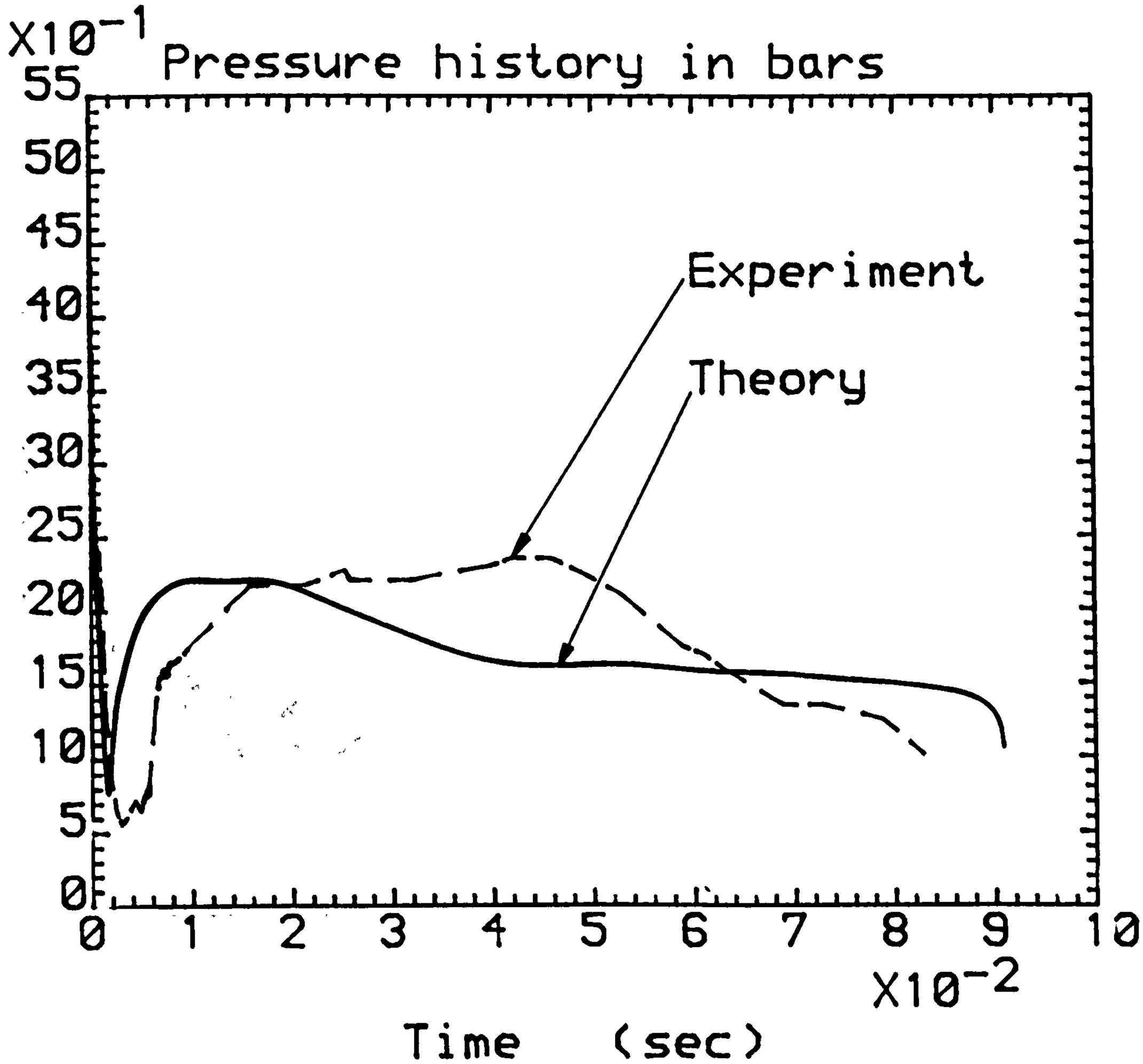

Figure 146. Comparison of the thermal non-equilibrium model analysis with R 12 vessel blowdown data.Long term decompression (perspex vessel,top pressure station). (Initially saturated liquid of 5.3 bar,$C_d = 1$,$\Phi = 1.2E\text{-}3$,VE = 0.5,50%full ,vent pipe length = 200mm).

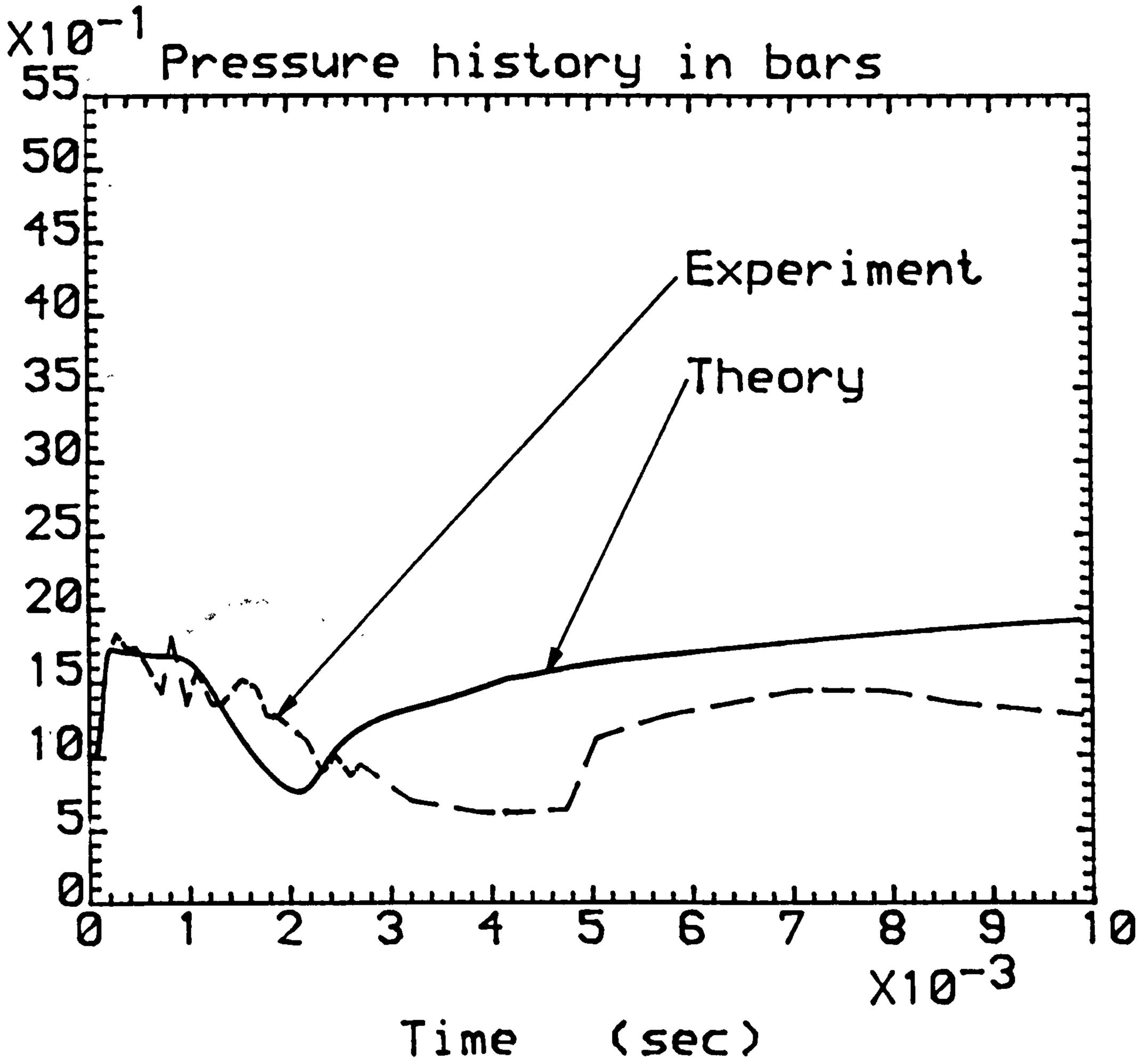

Figure 147. Comparison of the thermal non-equilibrium model analysis with R 12 vessel blowdown data.Initial pressure history (perspex vessel,pressure station 60mm from diaphragm in the vent pipe).(Initially saturated liquid of 5.3 bar,C_d = 1,Φ = 1.2E-3,VE = 0.5,50%full,vent pipe length = 200mm).

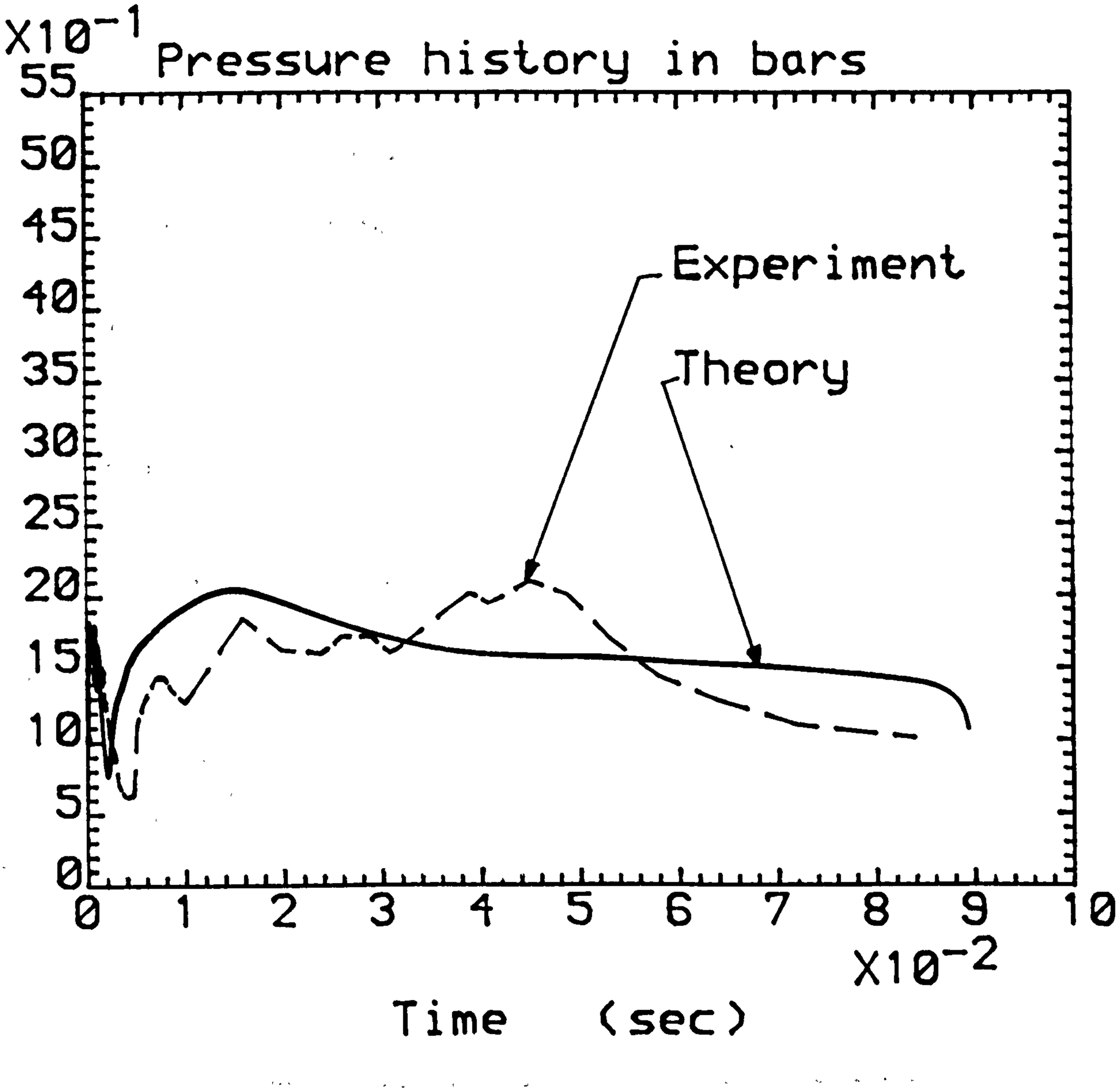

Figure 148. Comparison of the thermal non-equilibrium model analysis with R 12 vessel blowdown data.Long term pressure history (perspex vessel,pressure station 60mm from diaphragm in the vent pipe).(Initially saturated liquid of 5.3 bar, $C_d = 1, \Phi = 1.2E\text{-}3$,50%full,vent pipe length = 200mm).

APPENDIX A. COMPUTER PROGRAMS

```
C HOMOGENEOUS MODEL "DP".
      REAL XI(-1:110),PI(0:110),UI(0:110),RI(0:110),
     1AI(0:110),HI(0:110),TI(0:110),QI(0:110),RGI(0:110),CGI(0:110),
     2P(0:110),U(0:110),R(0:110),A(0:110),H(0:110),T(0:110),Q(0:110),
     3RG(0:110),CG(0:110)
        K=1
        N=0
        RL=1301.16
        CL=500.
        DX=.005
        AT=0.0
        J=40
        FI=1.1
        RGC=68.77
        CD=1.
      OPEN(UNIT=28,FILE='HIDL',STATUS='OLD')
      REWIND(28)
      DO 1111 I=0,J
      READ(28,*) PI(I),UI(I),RI(I),AI(I),HI(I),TI(I),QI(I),RGI(I),CGI(I)
1111  CONTINUE
      CLOSE(UNIT=28)
1     DT=1E-6
2     DO 30 I=0,J,1
        XI(I)=I*DX
        XI(I-1)=(I-1)*DX
        XI(I+1)=(I+1)*DX
      IF(I.EQ.0) GO TO 70
      X1=XI(I)-(UI(I)+AI(I))/((UI(I)+AI(I)-UI(I-1)-AI(I-1))/DX+1/DT)
      IF (X1.GT.XI(I).OR.X1.LT.XI(I-1)) TYPE*,'NO1',I
      XGN=(XI(I)-X1)/DX
      P1=PI(I)-(PI(I)-PI(I-1))*XGN
      H1=HI(I)-(HI(I)-HI(I-1))*XGN
      Q1=QI(I)-(QI(I)-QI(I-1))*XGN
      R1=RI(I)-(RI(I)-RI(I-1))*XGN
      RG1=RGI(I)-(RGI(I)-RGI(I-1))*XGN
      T1=TI(I)-(TI(I)-TI(I-1))*XGN
      U1=UI(I)-(UI(I)-UI(I-1))*XGN
      CG1=SQRT(T1*FI*RGC)
      A1=1/SQRT(R1**2*(Q1/(RG1*CG1)**2+(1-Q1)/(RL*CL)**2))
      IF(I.EQ.J) GO TO 204
70    X2=XI(I)-(UI(I)-AI(I))/(1/DT+(UI(I+1)-AI(I+1)-UI(I)+AI(I))/DX)
      IF (X2.LT.XI(I-1).OR.X2.GT.XI(I+1)) TYPE*,'NO2',I
      IF(X2.LT.XI(I)) THEN
      X2=XI(I)-(UI(I)-AI(I))/(1/DT+(UI(I)-AI(I)-UI(I-1)+AI(I-1))/DX)
      L=1
      ELSE IF(X2.GE.XI(I)) THEN
      L=0
      END IF
      XGN=(XI(I+1-L)-X2)/DX
      P2=PI(I+1-L)-(PI(I+1-L)-PI(I-L))*XGN
      H2=HI(I+1-L)-(HI(I+1-L)-HI(I-L))*XGN
      Q2=QI(I+1-L)-(QI(I+1-L)-QI(I-L))*XGN
      R2=RI(I+1-L)-(RI(I+1-L)-RI(I-L))*XGN
      RG2=RGI(I+1-L)-(RGI(I+1-L)-RGI(I-L))*XGN
      T2=TI(I+1-L)-(TI(I+1-L)-TI(I-L))*XGN
      CG2=SQRT(T2*RGC*FI)
      U2=UI(I+1-L)-(UI(I+1-L)-UI(I-L))*XGN
      A2=1/SQRT(R2**2*(Q2/(RG2*CG2)**2+(1-Q2)/(RL*CL)**2))
      IF(I.EQ.0) GO TO 67
      P(I)=(P2+(R2*A2)/(R1*A1)*P1+1E-5*R2*A2*(U1-U2))/(1+R2*A2/(R1*A1))
205   U(I)=(P1-P(I))*1E5/(R1*A1)+U1
      X4=XI(I)-U(I)*DT
```

```
      XGN=(X4-X1)/(X2-X1)
      H4=(H2-H1)*XGN+H1
      R4=(R2-R1)*XGN+R1
      P4=(P2-P1)*XGN+P1
202   H(I)=(P(I)-P4)*1E2/R4+H4
C     FOR SUB ROUTINE  R(I) Q(I) T(I)RG(I)
      CALL NOSUB(P(I),TT,HL,HG,RGT)
      T(I)=TT
      RG(I)=RGT
      CG(I)=SQRT(RGC*T(I)*FI)
      Q(I)=(H(I)-HL)/(HG-HL)
      IF(Q(I).GT.1.) TYPE*,'Q GT 1.',I,K
      IF(Q(I).GT.1..AND.(Q(I)-1.).GT.1E-4) THEN
      DT=DT/2.
      GO TO 2
      ELSE IF(ABS(Q(I)-1.).LE.1E-4) THEN
      Q(I)=1.
      END IF
      R(I)=1/(Q(I)/RG(I)+(1-Q(I))/RL)
      A(I)=1/SQRT(R(I)**2*(Q(I)/(RG(I)*CG(I))**2+(1-Q(I))/(RL*CL)**2))
      IF(I.EQ.J) THEN
      A(I)=A(I)*CD
      GO TO 206
      END IF
      GO TO 30
67    P(I)=P2-R2*A2*U2*1.E-5
      U(I)=0.0
      P4=PI(I)
      R4=RI(I)
      H4=HI(I)
      GO TO 202
204   P(I)=1.0133
      N=0
      IF(PI(J).GT.4.) THEN
      SP=PI(J)-1.
      ELSE IF(PI(J).LE.4.) THEN
      SP=1.
      END IF
      P2=PI(I)
      R2=RI(I)
      H2=HI(I)
      X2=XI(I)
      GO TO 205
206   IF(N.EQ.1) GO TO 132
      IF((U(I)-A(I)).LE.0.0) GO TO 30
      P(I)=P(I)+SP
      N=N+1
      GO TO 205
132   IF(ABS(U(I)-A(I)).LE.1E-2) THEN
      N=0
      GO TO 30
      ELSE  IF((U(I)-A(I)).LT.0.0) THEN
      SP=SP/1.1
      P(I)=P(I)-SP
      GO TO 205
      ELSE IF((U(I)-A(I)).GT.0.0) THEN
      SP=SP/1.1
      P(I)=P(I)+SP
      GO TO 205
      END IF
30    CONTINUE
      AT=AT+DT
      DO 1000 I=0,J,1
      PI(I)=P(I)
      UI(I)=U(I)
      HI(I)=H(I)
      RI(I)=R(I)
      QI(I)=Q(I)
      AI(I)=A(I)
      RGI(I)=RG(I)
      CGI(I)=CG(I)
      TI(I)=T(I)
1000  CONTINUE
      K=K+1
      SP=1.
```

```
      IF(AT.GE.20E-3) GO TO 10000
     GO TO 1
10000  END
```

```
C THERMAL NON-EQUILIBRIUM MODEL "EVUT1" (CONSTANT BUBBLE SIZE).
      REAL XI(-1:220),A(0:220),P(0:220),U(0:220),HG(0:220),HL(0:220)
     1,TG(0:220),TL(0:220),VF(0:220),HGL(0:220),RG(0:220),CG(0:220),
     2R(0:220),PI(0:220),AI(0:220),UI(0:220),HGI(0:220),HLI(0:220),
     3TLI(0:220),TGI(0:220),HGLI(0:220),VFI(0:220),RGI(0:220),
     4CGI(0:220),RI(0:220)
C FOR R-12
      DVL=1.93E-7
C FOR R-12
      DVG=1.62E-6
C FOR WATER      DVL=1.37E-7
C FOR WATER      DVG=5.223E-7
C FOR R-12 EXPE.
      DIA=0.034
C FOR WATER      DIA=0.073
      SP=1.
      K=1
      UN=2.
      DX=0.005
      RL=1301.16
      CL=500.
      AT=0.0
      N=0
      RGC=68.77
      CPG=0.67
      CPL=0.1807
      FI=1.1
      CK=7.264E-5
      J=40
      CD=1.
      RB=1.5E-4
      OPEN(UNIT=28,FILE='IDL1',STATUS='OLD')
      REWIND(28)
      DO 1111 I=0,J
      READ(28,*) PI(I),VFI(I),UI(I),HLI(I),HGI(I),RI(I),AI(I),TLI(I),
     1RGI(I),TGI(I),HGLI(I),CGI(I)
1111   CONTINUE
      CLOSE(UNIT=28)
1     DT=1E-6
      IF(PI(0).LE.1E-1.AND.(PM-PI(0)).GE.0.0.AND.AT.LT.10E-3) DT=1E-7
      IF(PI(0).LE.1E-2.AND.(PM-PI(0)).GE.0.0.AND.AT.LT.10E-3) DT=1E-8
      IF(PI(0).LE.1E-3.AND.(PM-PI(0)).GE.0.0) DT=1E-9
      IF(PI(0).LE.1E-1.AND.(PM-PI(0)).LT.0.0) DT=5E-7
      PM=PI(0)
2     DO 30 I=0,J,1
      XI(I)=I*DX
      XI(I-1)=(I-1)*DX
      XI(I+1)=(I+1)*DX
      IF(I.EQ.0) GO TO 70
      X1=XI(I)-(UI(I)+AI(I))/((UI(I)+AI(I)-UI(I-1)-AI(I-1))/DX+1/DT)
      IF (X1.GT.XI(I).OR.X1.LT.XI(I-1)) TYPE*,'NO1',X1,XI(I),XI(I-1)
     1,UI(I),AI(I),UI(I-1),AI(I-1)
      XGN=(XI(I)-X1)/DX
      P1=PI(I)-(PI(I)-PI(I-1))*XGN
      VF1=VFI(I)-(VFI(I)-VFI(I-1))*XGN
      HL1=HLI(I)-(HLI(I)-HLI(I-1))*XGN
      TL1=HL1/CPL
      U1=UI(I)-(UI(I)-UI(I-1))*XGN
      HG1=HGI(I)-(HGI(I)-HGI(I-1))*XGN
      HGL1=HG1-HL1
      TG1=HG1/CPG
      CG1=SQRT(FI*RGC*TG1)
      RG1=1E5*P1/(RGC*TG1)
      R1=VF1*RG1+(1-VF1)*RL
      A1=1/SQRT(R1*(VF1/(RG1*CG1**2)+(1-VF1)/(RL*CL**2)))
      IF(VF1.GE.1.) THEN
      QIG1=0.0
      ELSE IF(VF1.LT.1.) THEN
      QIG1=1.5*VF1*UN*CK*(TL1-TG1)/RB**2
      END IF
      GMI1=QIG1/HGL1
      CALL FRICTION(RL,RG1,R1,DIA,U1,DVL,DVG,VF1,TW1)
      EX1=GMI1*(1/RG1-1/RL)+(U1*TW1*1E-3*VF1)/(CPG*R1*TG1)
      IF(I.EQ.J) GO TO 204
70    X2=XI(I)-(UI(I)-AI(I))/(1/DT+(UI(I+1)-AI(I+1)-UI(I)+AI(I))/DX)
```

```
 IF (X2.LT.XI(I).OR.X2.GT.XI(I+1)) TYPE*,'NO2',X2,XI(I),XI(I+1)
1,UI(I),AI(I),UI(I+1),AI(I+1),DX,DT
 IF(X2.LT.XI(I)) THEN
 X2=XI(I)-(UI(I)-AI(I))/(1/DT+(UI(I)-AI(I)-UI(I-1)+AI(I-1))/DX)
 L=1
 ELSE IF(X2.GE.XI(I)) THEN
 L=0
 END IF
 XGN=(XI(I+1-L)-X2)/DX
 P2=PI(I+1-L)-(PI(I+1-L)-PI(I-L))*XGN
 HL2=HLI(I+1-L)-(HLI(I+1-L)-HLI(I-L))*XGN
 VF2=VFI(I+1-L)-(VFI(I+1-L)-VFI(I-L))*XGN
 TL2=HL2/CPL
 HG2=HGI(I+1-L)-(HGI(I+1-L)-HGI(I-L))*XGN
    TG2=HG2/CPG
    HGL2=HG2-HL2
    U2=UI(I+1-L)-(UI(I+1-L)-UI(I-L))*XGN
    CG2=SQRT(FI*RGC*TG2)
    RG2=1E5*P2/(RGC*TG2)
    R2=VF2*RG2+(1-VF2)*RL
    IF(VF2.GE.1.) THEN
    QIG2=0.0
    ELSE IF(VF2.LT.1.) THEN
    QIG2=1.5*VF2*UN*CK*(TL2-TG2)/RB**2
    END IF
    A2=1/SQRT(R2*(VF2/(RG2*CG2**2)+(1-VF2)/(RL*CL**2)))
    GMI2=QIG2/HGL2
    CALL FRICTION(RL,RG2,R2,DIA,U2,DVL,DVG,VF2,TW2)
    EX2=GMI2*(1/RG2-1/RL)+(U2*TW2*1E-3*VF2)/(CPG*TG2*R2)
    IF(I.EQ.0) GO TO 67
    P(I)=(P2+(R2*A2)/(R1*A1)*P1+R2*A2*1E-5*(U1+A1*EX1*DT-U2
   1+A2*EX2*DT+(TW2/R2-TW1/R1)*DT))/(1+R2*A2/(R1*A1))
205  U(I)=(P1-P(I))*1E5/(R1*A1)+U1+A1*EX1*DT-TW1*DT/R1
    X4=XI(I)-U(I)*DT
    XGN=(X4-X1)/(X2-X1)
    HL4=(HL2-HL1)*XGN+HL1
    P4=(P2-P1)*XGN+P1
    HG4=(HG2-HG1)*XGN+HG1
    HGL4=HG4-HL4
    TG4=HG4/CPG
    TL4=HL4/CPL
    VF4=(VF2-VF1)*XGN+VF1
    U4=(U2-U1)*XGN+U1
    CG4=SQRT(FI*RGC*TG4)
    RG4=1E5*P4/(RGC*TG4)
    R4=VF4*RG4+(1-VF4)*RL
202  B=VF4*(1-VF4)*(RG4*CG4**2-RL*CL**2)/(RG4*CG4**2*RL*CL**2)
    IF(VF4.GE.1.) THEN
    QIG4=0.0
    ELSE IF(VF4.LT.1.) THEN
    QIG4=1.5*VF4*UN*CK*(TL4-TG4)/RB**2
    END IF
    GMI4=QIG4/HGL4
    CALL FRICTION(RL,RG4,R4,DIA,U4,DVL,DVG,VF4,TW4)
    EX4=R4*GMI4/(RG4*RL)+(U4*TW4*1E-3*VF4)*(1-VF4)/(R4*TG4*CPG)
    VF(I)=VF4+B*(P(I)-P4)*1E5+EX4*DT
    IF(VF(I).GT.1..AND.(VF(I)-1.).GT.1E-4) THEN
    DT=DT/2.
    GO TO 2
    ELSE IF(ABS(VF(I)-1.).LE.1E-4) THEN
    VF(I)=1.
    END IF
    HL(I)=(P(I)-P4)*100/RL+HL4+U4*TW4*1E-3*DT/R4
    TL(I)=HL(I)/CPL
    HG(I)=HG4+(P(I)-P4)*1E2/RG4+U4*TW4*1E-3*DT/R4
    IF(HG(I).LT.0.0) TYPE*,I,P(I),P4,EX1,EX2
    HGL(I)=HG(I)-HL(I)
    TG(I)=HG(I)/CPG
    RG(I)=1E5*P(I)/(RGC*TG(I))
    CG(I)=SQRT(FI*RGC*TG(I))
    R(I)=VF(I)*RG(I)+(1-VF(I))*RL
    A(I)=1/SQRT(R(I)*(VF(I)/(RG(I)*CG(I)**2)+(1-VF(I))/(RL*CL**2)))
    IF(I.EQ.J) THEN
    A(I)=A(I)*CD
    GO TO 206
```

```
      END IF
      GO TO 30
67    P(I)=R2*A2*1E-5*(EX2*DT*A2-U2+TW2*DT/R2)+P2
      U(I)=0.0
      P4=PI(I)
      U4=UI(I)
      VF4=VFI(I)
      HL4=HLI(I)
      HG4=HGI(I)
      R4=RI(I)
      RG4=RGI(I)
      TG4=TGI(I)
      HGL4=HGLI(I)
      CG4=CGI(I)
      TL4=TLI(I)
      GO TO 202
204   P(I)=1.0133
      N=0
      IF(PI(J).GT.4.)THEN
      SP=PI(J)-1.
      ELSE IF(PI(J).LE.4.) THEN
      SP=1.
      END IF
      HL2=HLI(I)
      R2=RI(I)
      P2=PI(I)
      RG2=RGI(I)
      HG2=HGI(I)
      HGL2=HGLI(I)
      CG2=CGI(I)
      TG2=TGI(I)
      TL2=TLI(I)
      VF2=VFI(I)
      U2=UI(I)
      X2=XI(I)
      GO TO 205
206   IF(N.EQ.1) GO TO 132
      IF((U(I)-A(I)).LE.0.0) GO TO 30
      P(I)=P(I)+SP
      N=N+1
      GO TO 205
132   IF(ABS(U(I)-A(I)).LE.1E-2) THEN
      N=0
      GO TO 30
      ELSE IF((U(I)-A(I)).LT.0.0)  THEN
      SP=SP/1.1
      P(I)=P(I)-SP
      GO TO 205
      ELSE IF((U(I)-A(I)).GT.0.0) THEN
      SP=SP/1.1
      P(I)=P(I)+SP
      GO TO 205
      END IF
30    CONTINUE
      DO 1000 I=0,J,1
      PI(I)=P(I)
      UI(I)=U(I)
      HLI(I)=HL(I)
      HGI(I)=HG(I)
      HGLI(I)=HGL(I)
      RI(I)=R(I)
      VFI(I)=VF(I)
      AI(I)=A(I)
      RGI(I)=RG(I)
      TLI(I)=TL(I)
      TGI(I)=TG(I)
      CGI(I)=CG(I)
1000    CONTINUE
      AT=AT+DT
     K=K+1
     IF (AT.GE.50.E-3.AND.P(0).LT.1.) GO TO 10000
      GO TO 1
10000 END
```

```
C THERMAL NON-EQUILIBRIUM MODEL "EVUT5" (NUCLEATION).
      CHARACTER*3  HI(0:210),H
      REAL PI(0:210),VFI(0:210),UI(0:210),HLI(0:210)
     1,HGI(0:210),RI(0:210),AI(0:210),TLI(0:210),RGI(0:210),
     2TGI(0:210),HGLI(0:210),CGI(0:210),BNI(0:210),XI(-1:210),
     3P(0:210),U(0:210),HL(0:210),HG(0:210),HGL(0:210),R(0:210),
     4VF(0:210),BN(0:210),A(0:210),RG(0:210),TL(0:210),TG(0:210),
     5CG(0:210)
C FOR R12
      DVG=1.62E-6
C FOR R12
       DVL=1.93E-7
C FOR WATER          DVL=1.37E-7
C FOR WATER         DVG=5.223E-7
C FOR WATER         DIA=.073
C FOR R12
      DIA=0.034
        N=0
        CD=1.
        TYPE*,'F is expected '
        ACCEPT*,F
        FK1=F
        CALL SECA(FK1,S)
        S=(1-S)/2.
        DX=0.005
        SIG=1.E-2
C         TC=647.3
        CL=500.
        RL=1301.16
        RGC=68.77
        CPG=0.654
        CPL=0.226
        FI=1.1
        CK=7.264E-5
        UN=2.
        WM=120.91
        BC=1.380662E-23
        AC=6.022E26
        K=1
        AT=0.0
        J=40
      OPEN(UNIT=28,FILE='DIL',STATUS='OLD')
      REWIND(28)
      DO 1 I=0,J
      READ(28,*) PI(I),VFI(I),UI(I),HLI(I),HGI(I),RI(I),AI(I),TLI(I),
     1RGI(I),TGI(I),HGLI(I),CGI(I)
      BNI(I)=0.0
1     CONTINUE
      CLOSE(UNIT=28)
      TYPE*,'Is this a PARTIALLY NUCLEATION CITE run?'
      ACCEPT*,H
      IF(H.EQ.'YES') THEN
      DO 9 I=0,J,1
      HI(I)='NOO'
9     CONTINUE
      TYPE*,'How many NUCLEATION SITES are they '
      ACCEPT*,M
      DO 2 N=1,M,1
      TYPE*,'Which "I" is a NUCLEATION SITE '
      ACCEPT*,I
      HI(I)='YES'
2     CONTINUE
      ELSE IF(H.EQ.'NOO') THEN
      DO 8 I=0,J,1
      HI(I)='YES'
8     CONTINUE
      END IF
      DO 133 L=0,J,1
      TYPE*,HI(L),L
133   CONTINUE
7      DT=1E-6
      IF(PI(0).LE.5..AND.(PM-PI(0)).GE.0.0.AND.AT.LT.5E-3) DT=5E-7
      IF(PI(0).LE.5..AND.(PM-PI(0)).LT.0.0.AND.AT.LT.5E-3) DT=1E-6
      PM=PI(0)
6     DO 4 I=0,J,1
```

```
      XI(I)=I*DX
      XI(I-1)=(I-1)*DX
      XI(I+1)=(I+1)*DX
    IF(I.EQ.0) GO TO 70
    X1=XI(I)-(UI(I)+AI(I))/((UI(I)+AI(I)-UI(I-1)-AI(I-1))/DX+1/DT)
    IF (X1.GT.XI(I).OR.X1.LT.XI(I-1)) TYPE*,'NO1'
    XGN=(XI(I)-X1)/DX
    P1=PI(I)-(PI(I)-PI(I-1))*XGN
    HL1=HLI(I)-(HLI(I)-HLI(I-1))*XGN
    VF1=VFI(I)-(VFI(I)-VFI(I-1))*XGN
    TL1=HL1/CPL
    U1=UI(I)-(UI(I)-UI(I-1))*XGN
    HG1=HGI(I)-(HGI(I)-HGI(I-1))*XGN
    HGL1=HG1-HL1
    BN1=BNI(I)-(BNI(I)-BNI(I-1))*XGN
      TG1=HG1/CPG
      CG1=SQRT(FI*RGC*TG1)
      RG1=P1*1E5/(RGC*TG1)
      R1=VF1*RG1+(1-VF1)*RL
      A1=1/SQRT(R1*(VF1/(RG1*CG1**2)+(1-VF1)/(RL*CL**2)))
      IF(VF1.GE.1.) THEN
      HENU1=0.0
      QIG1=0.0
      ELSE IF(VF1.LT.1.) THEN
C NUCLEATION*****************************************************
      IF(HI(I).EQ.'YES') THEN
      TR=TL1
      CALL NOSUBT(TR,PS,RGS)
      IF((PS/P1).LE.1.) THEN
      HENU1=0.0
      ELSE IF((PS/P1).GT.1.) THEN
C       CALL NOSUBW(P1,TS)
C       SIG=.2358*(1-TS/TC)**1.256*(1-.625*(1-TS/TC))
      RC=2*SIG*1E-5/((PS-P1)*(1-RGS/RL))
      GE=4.1888*SIG*RC**2
      ANO=RL*(1-VF1)*AC/WM
      HENU1=ANO**(2./3.)*S*SQRT(.955*SIG*AC/(WM*F))*4/DIA*
     1EXP((-1)*(GE*F/(BC*TL1)))
      END IF
      ELSE IF(HI(I).EQ.'NOO') THEN
      HENU1=0.0
      END IF
      QIG1=3.9*BN1**(2./3.)*VF1**(1./3.)*UN*CK*(TL1-TG1)
      END IF
      GMN1=HENU1*4.1888*RC**3*RGS*F
      BCE1=GE*HENU1*1E-3*F
      GMI1=QIG1/HGL1
      CALL FRICTION(RL,RG1,R1,DIA,U1,DVL,DVG,VF1,TW1)
      EX1=(GMI1+GMN1)*(1/RG1-1/RL)+(BCE1+U1*TW1*RG1*1E-3*VF1/R1)
     1/(CPG*RG1*TG1)
      IF(I.EQ.J) GO TO 11
70    X2=XI(I)-(UI(I)-AI(I))/(1/DT+(UI(I+1)-AI(I+1)-UI(I)+AI(I))/DX)
      IF (X2.GT.XI(I+1).OR.X2.LT.XI(I-1)) TYPE*,'NO2'
      IF(X2.LT.XI(I)) THEN
      X2=XI(I)-(UI(I)-AI(I))/(1/DT+(UI(I)-AI(I)-UI(I-1)+AI(I-1))/DX)
      L=1
      ELSE IF(X2.GE.XI(I)) THEN
      L=0
      END IF
      XGN=(XI(I+1-L)-X2)/DX
      P2=PI(I+1-L)-(PI(I+1-L)-PI(I-L))*XGN
      HL2=HLI(I+1-L)-(HLI(I+1-L)-HLI(I-L))*XGN
      VF2=VFI(I+1-L)-(VFI(I+1-L)-VFI(I-L))*XGN
      TL2=HL2/CPL
      HG2=HGI(I+1-L)-(HGI(I+1-L)-HGI(I-L))*XGN
      TG2=HG2/CPG
      HGL2=HG2-HL2
      BN2=BNI(I+1-L)-(BNI(I+1-L)-BNI(I-L))*XGN
      U2=UI(I+1-L)-(UI(I+1-L)-UI(I-L))*XGN
      RG2=1E5*P2/(RGC*TG2)
      CG2=SQRT(FI*RGC*TG2)
      R2=VF2*RG2+(1-VF2)*RL
      A2=1/SQRT(R2*(VF2/(RG2*CG2**2)+(1-VF2)/(RL*CL**2)))
      IF(VF2.GE.1.) THEN
      HENU2=0.0
```

```
      QIG2=0.0
      ELSE IF(VF2.LT.1.) THEN
C NUCLEATION*****************************************************
      IF(HI(I).EQ.'YES') THEN
      TR=TL2
      CALL NOSUBT(TR,PS,RGS)
      IF((PS/P2).LE.1.) THEN
      HENU2=0.0
      ELSE IF((PS/P2).GT.1.) THEN
C       CALL NOSUBW(P2,TS)
C       SIG=.2358*(1-TS/TC)**1.256*(1-.625*(1-TS/TC))
      RC=2*SIG*1E-5/((PS-P2)*(1-RGS/RL))
      GE=4.1888*SIG*RC**2
      ANO=RL*(1-VF2)*AC/WM
      HENU2=ANO**(2./3.)*S*SQRT(.955*SIG*AC/(WM*F))*4/DIA*
     1EXP((-1)*(GE*F/(BC*TL2)))
      END IF
      ELSE IF(HI(I).EQ.'NOO') THEN
      HENU2=0.0
      END IF
      QIG2=3.9*BN2**(2./3.)*VF2**(1./3.)*UN*CK*(TL2-TG2)
      END IF
      GMN2=HENU2*4.1888*RC**3*RGS*F
      BCE2=GE*HENU2*1E-3*F
      GMI2=QIG2/HGL2
      CALL FRICTION(RL,RG2,R2,DIA,U2,DVL,DVG,VF2,TW2)
      EX2=(GMI2+GMN2)*(1/RG2-1/RL)+(BCE2+TW2*RG2*U2*1E-3*VF2/R2)
     1/(CPG*RG2*TG2)
      IF(I.EQ.0) GO TO 67
      P(I)=(P2+(R2*A2)/(R1*A1)*P1+R2*A2*1E-5*(U1+A1*EX1*DT-U2
     1+A2*EX2*DT+(TW2/R2-TW1/R1)*DT))/(1+R2*A2/(R1*A1))
205   U(I)=(P1-P(I))*1E5/(R1*A1)+U1+A1*EX1*DT-TW1*DT/R1
      X4=XI(I)-U(I)*DT
      XGN=(X4-X1)/(X2-X1)
      HL4=(HL2-HL1)*XGN+HL1
      P4=(P2-P1)*XGN+P1
      HG4=(HG2-HG1)*XGN+HG1
      HGL4=HG4-HL4
      TG4=HG4/CPG
      TL4=HL4/CPL
      VF4=(VF2-VF1)*XGN+VF1
      U4=(U2-U1)*XGN+U1
      BN4=(BN2-BN1)*XGN+BN1
      CG4=SQRT(F1*RGC*TG4)
      RG4=1E5*P4/(RGC*TG4)
      R4=VF4*RG4+(1-VF4)*RL
202   B=VF4*(1-VF4)*(RG4*CG4**2-RL*CL**2)/(RG4*CG4**2*RL*CL**2)
      IF(VF4.GE.1.) THEN
      HENU4=0.0
      QIG4=0.0
      ELSE IF(VF4.LT.1.) THEN
C NUCLEATION*****************************************************
      IF(HI(I).EQ.'YES') THEN
      TR=TL4
      CALL NOSUBT(TR,PS,RGS)
      IF((PS/P4).LE.1.) THEN
      HENU4=0.0
      ELSE IF((PS/P4).GT.1.) THEN
C       CALL NOSUBW(P4,TS)
C       SIG=.2358*(1-TS/TC)**1.256*(1-.625*(1-TS/TC))
      RC=2*SIG*1E-5/((PS-P4)*(1-RGS/RL))
      GE=4.1888*SIG*RC**2
      ANO=RL*(1-VF4)*AC/WM
      HENU4=ANO**(2./3.)*S*SQRT(.955*SIG*AC/(WM*F))*4/DIA*
     1EXP((-1)*(GE*F/(BC*TL4)))
      END IF
      ELSE IF(HI(I).EQ.'NOO') THEN
      HENU4=0.0
      END IF
      QIG4=3.9*BN4**(2./3.)*VF4**(1./3.)*UN*CK*(TL4-TG4)
      END IF
      GMN4=HENU4*4.1888*RC**3*RGS*F
      BCE4=GE*HENU4*1E-3*F
      GMI4=QIG4/HGL4
      CALL FRICTION(RL,RG4,R4,DIA,U4,DVL,DVG,VF4,TW4)
```

```
      EX4=R4*(GMI4+GMN4)/(RG4*RL)+(BCE4+U4*TW4*RG4*VF4*1E-3/R4)
     1*(1-VF4)/(RG4*CPG*TG4)
      VF(I)=VF4+B*(P(I)-P4)*1E5+EX4*DT
      IF(VF(I).GT.1..AND.(VF(I)-1.).GT.1E-4) THEN
      DT=DT/2
      GO TO 6
      ELSE IF(ABS(VF(I)-1.).LE.1E-4) THEN
      VF(I)=1.
      END IF
      IF(VF4.LT.1.) THEN
      BN(I)=BN4+BN4/VF4*(VF(I)-VF4)+BN4*1E5/(CG4**2*RG4)*(P(I)-P4)+
     1(HENU4-BN4/(RG4*VF4)*(GMI4+GMN4+(BCE4+U4*TW4*RG4*VF4*1E-3/R4)/
     2(CPG*TG4)))*DT
      HL(I)=(P(I)-P4)*100/RL+HL4-(BCE4-U4*TW4*RL*(1-VF4)*1E-3/R4)*DT/
     1(RL*(1-VF4))
      ELSE IF(VF4.GE.1.) THEN
      HL(I)=HL4+(P(I)-P4)*1E2/RL+U4*TW4*1E-3*DT/R4
      BN(I)=0.0
      END IF
      TL(I)=HL(I)/CPL
      HG(I)=HG4+(P(I)-P4)*1E2/RG4+(BCE4+U4*TW4*RG4*VF4*1E-3/R4)*DT
     1/(RG4*VF4)
      HGL(I)=HG(I)-HL(I)
      TG(I)=HG(I)/CPG
      RG(I)=1E5*P(I)/(RGC*TG(I))
      IF(TG(I).LT.0.0) TYPE*,I
      CG(I)=SQRT(TG(I)*FI*RGC)
      R(I)=RG(I)*VF(I)+(1-VF(I))*RL
      IF(VF(I).LT.0.0.OR.VF(I).GT.1.) TYPE*,I,F,N,'VF',VF(I),EX4,P(I),K
      IF(RG(I).LT.0.0) TYPE*,I,TG(I),P(I),'RG',N,SP,PI(J),K
      A(I)=1/SQRT(R(I)*(VF(I)/(RG(I)*CG(I)**2)+(1-VF(I))/(RL*CL**2)))
      IF(I.EQ.J) THEN
C     IF(N.EQ.1.AND.K1.GT.300) TYPE*,'PROBLEM WITH CHOKE MODEL'
      A(I)=A(I)*CD
      GO TO 206
      END IF
      GO TO 4
67    P(I)=R2*A2*1E-5*(EX2*DT*A2-U2+TW2*DT/R2)+P2
      U(I)=0.0
      P4=PI(I)
      U4=UI(I)
      VF4=VFI(I)
      HL4=HLI(I)
      HG4=HGI(I)
      R4=RI(I)
      RG4=RGI(I)
      TG4=TGI(I)
      HGL4=HGLI(I)
      CG4=CGI(I)
      BN4=BNI(I)
      TL4=TLI(I)
      GO TO 202
11    P(I)=1.0133
      N=0
      K1=0
      IF(PI(J).GT.4.) THEN
      SP=PI(J)-1.
      ELSE IF(PI(J).LE.4.) THEN
      SP=1.
      END IF
      HL2=HLI(I)
      R2=RI(I)
      P2=PI(I)
      RG2=RGI(I)
      HG2=HGI(I)
      HGL2=HGLI(I)
      CG2=CGI(I)
      TG2=TGI(I)
      TL2=TLI(I)
      VF2=VFI(I)
      U2=UI(I)
      BN2=BNI(I)
      X2=XI(I)
      GO TO 205
206   IF(N.EQ.1) GO TO 132
```

```
      IF((U(I)-A(I)).LE.0.0) GO TO 4
      P(I)=P(I)+SP
      N=N+1
      GO TO 205
132   IF(ABS(U(I)-A(I)).LE.1E-2) THEN
      N=0
      GO TO 4
      ELSE IF((U(I)-A(I)).LT.0.0)  THEN
      K1=K1+1
      SP=SP/1.1
      P(I)=P(I)-SP
      GO TO 205
      ELSE IF((U(I)-A(I)).GT.0.0) THEN
      K1=K1+1
      SP=SP/1.1
      P(I)=P(I)+SP
      GO TO 205
      END IF
4     CONTINUE
      DO 5 I=0,J,1
        PI(I)=P(I)
        UI(I)=U(I)
        HLI(I)=HL(I)
        HGI(I)=HG(I)
        HGLI(I)=HGL(I)
        RI(I)=R(I)
        VFI(I)=VF(I)
        AI(I)=A(I)
        RGI(I)=RG(I)
        TLI(I)=TL(I)
        TGI(I)=TG(I)
        CGI(I)=CG(I)
        BNI(I)=BN(I)
5     CONTINUE
      AT=AT+DT
      K=K+1
C       IF(AT.GT.90E-3) GO TO 10000
      IF (AT.GE.20.E-3.AND.P(0).LT.1.) GO TO 10000
      GO TO 7
10000 END
```

```
C THERMAL NON-EQUILIBRIUM MODEL 'EVUT6' (MOVING INTERFACE).
      CHARACTER*3 SWITCHM,SWITCHG,SWITCHM1,SWITCHG1,SWITCH2,SWTRL
     1,APR*3
      REAL XI(-1:100),CG(0:100),U(0:100),R(0:100),TGI(0:100),
     1UI(0:100),RI(0:100),TLI(0:100),TG(0:100),VFI(0:100),HLI(0:100),
     2HGI(0:100),HL(0:100),HG(0:100),VF(0:100),AI(0:100),A(0:100),
     3TL(0:100),HGLI(0:100),HGL(0:100),CGI(0:100),RGI(0:100),RG(0:100)
     4,PI(0:100),P(0:100),BN(0:100),BNI(0:100)
C***************INITIAL DATA*************************************
      SIG=1E-2
      F=1.2E-3
      FTR=F
      CALL SECA(FTR,S)
      S=(1-S)/2.
      CD=1.
      PL=0.4
      EL=0.2
      PV=0.1
      PMX=0.1
      TYPE*,' F IS ',F,' CD IS',CD
      SP=1.
      K=1
      DX=.005
      RL=1301.16
      CL=500.
      AT=0.0
      N=0
      NI=0
      RGC=68.77
      CPG=.67
      CPL=.1807
      FI=1.1
      FIG=1.4
      RGCG=287.
      CK=7.264E-5
      UN=2.
      WM=120.91
      AC=6.022E26
      BC=1.380662E-23
      DIA=0.034
      IF(EL.NE.0.0) THEN
      TYPE*,'The ambience temperature  (in Kelvin) ?'
      ACCEPT*,TAMB
      END IF
      IF(PMX.LT.PL) THEN
      TYPE*,'VE(velocity slip ratio at the liq. interface) ?'
      ACCEPT*,VE
      END IF
      K1=PMX/DX
      K2=(PMX+PV)/DX
      J=PL/DX
      OPEN(UNIT=28,FILE='IDL',STATUS='OLD')
      REWIND(28)
      DO 2 I=0,K1,1
      READ(28,*) PI(I),VFI(I),UI(I),HLI(I),HGI(I),RI(I),AI(I),TLI(I),
     1RGI(I),TGI(I),HGLI(I),CGI(I)
      BNI(I)=0.0
2     CONTINUE
      CLOSE(UNIT=28)
      IF(PV.NE.0.0) THEN
      OPEN(UNIT=29,FILE='IDVI',STATUS='OLD')
      REWIND(29)
      DO 3 I=(K1+1),K2,1
      READ(29,*) PI(I),UI(I),RGI(I),TGI(I),CGI(I)
3     CONTINUE
      CLOSE(UNIT=29)
      END IF
      IF(EL.NE.0.0) THEN
      DO 4 I=(K2+1),J,1
      PI(I)=1.0133
      UI(I)=0.0
      RGI(I)=1.23
      TGI(I)=TAMB
      CGI(I)=SQRT(FIG*RGCG*TAMB)
4     CONTINUE
```

```
      END IF
      XGB=(PMX+PV)
      XMB=PMX
      PMB=PI(K1)
      PGB=PI(K2)
      UMBM=UI(K1)
      UMBG=UMBM
      UGB=UI(K2)
      BNMBM=0.0
      VFMBM=VFI(K1)
      HLMBM=HLI(K1)
      HGMBM=HGI(K1)
      RMBM=RL
      AMBM=AI(K1)
      TLMBM=TLI(K1)
      TGMBM=TGI(K1)
      TGMBG=TGI(K1)
      RGMBM=RGI(K1)
      RGMBG=RGI(K1)
      HGLMBM=HGLI(K1)
      CGMBM=CGI(K1)
      CGMBG=SQRT(FIG*RGC*TGMBG)
      TGGBG=TGI(K2)
      RGGBG=RGI(K2)
      CGGBG=SQRT(FIG*RGC*TGGBG)
      IF(EL.NE.0.0) THEN
      TGGBA=TAMB*(PGB/1.0133)**.286
      RGGBA=1E5*PGB/(RGCG*TGGBA)
      CGGBA=SQRT(FIG*RGCG*TGGBA)
      END IF
C*SWITCHM='INS' WHEN THE LIQUID INTERFACE IS STILL INSIDE THE VESSEL
C*WHEN THE INTERFACE IS UP TO THE EXIT OF THE VESSEL THE 'M' SWITCH
C*IS EQUAL TO OUT THE SAME DEFINITION HOLDS FOR THE 'G' SWITCH
C*WHEN ANY OF THE INTERFACES(LIQUID OR VAPOR) WHICH ARE INITIALLY
C*INSIDE,REACH THE EXIT SWITCHI(M OR G) WILL SWITCH THE CONTROL OF
C*THE PROGRAM TO A SPECIAL PART WHICH CONTROLS THE NEXT TIME STEP
C*SWITCHS 2 AND TRL ARE USED AS SPECIAL ITERATION INTICATORS
      IF(EL.EQ.0.0) THEN
      IF(PV.EQ.0.0) THEN
      TYPE*,'This is a full vessel BLOWDOWN simulation'
      SWITCHM='OUT'
      SWITCHG='OUT'
      XMA=XMB
      XGA=XGB
      ELSE IF(PV.NE.0.0) THEN
      TYPE*,'This is a partially full vessel (',PMX,'liquid level)
     1 BLOWDOWN simulation'
      SWITCHM='INS'
      SWITCHG='OUT'
      XGA=XGB
      END IF
      ELSE IF(EL.NE.0.0) THEN
      IF(PV.NE.0.0) TYPE*,'This is apartially full vessel (',PMX,
     1'liquid level) with extension pipework (',EL,'m) BLOWDOWN
     2 simulation'
      IF(PV.EQ.0.0) TYPE*,'This is a full vessel with extension
     1 pipework (',EL,' m) BLOWDOWN simulation'
      SWITCHM='INS'
      SWITCHG='INS'
      END IF
      SWITCHM1='NFS'
      SWITCHG1='NFS'
      SWITCH2='ON2'
      SWTRL='OFF'
      TYPE*,'The liquid interface is ',SWITCHM,
     1'the vapor interface is ',SWITCHG,'the liquid No of
     2 nodes is ',K1,' and the vapor and total ones are ',(PV/DX),' and
     3',J
      TYPE*,'The portions of liquid and vapor into the vessel and the
     1 total length are ',PMX,PV,PL,' and the space interval is '
     2,DX
C***************TIME STEP*****************************************
6     IF(AT.LE.6E-3) DT=5E-7
      IF(AT.GT.6E-3) DT=5E-6
      IF(PI(0).LE.1E-1.AND.(PM-PI(0)).GE.0.0) DT=5E-7
```

```
      IF(PI(0).LE.1E-2.AND.(PM-PI(0)).GE.0.0) DT=1E-8
      IF(PI(0).LE.1E-1.AND.(PM-PI(0)).LT.0.0) DT=5E-7
      PM=PI(0)
7     DO 9 I=0,J,1
C*************** INTERFACE*****************************************
8     IF(I.EQ.0.AND.SWITCHM.EQ.'INS') THEN
      XMA=UMBM*DT+XMB
      IF(XMA.GT.PL) THEN
      DT=(PL-XMB)/UMBM
      XMA=PL
      TYPE*,'M INTERFACE IS OUT',K,(AT+DT)
      SWITCHM='OUT'
      SWITCHM1='FST'
      END IF
      M1=XMB/DX
      IF(INT(XMB/DX).EQ.(XMB/DX)) M1=XMB/DX-1
      XI(I-1)=M1*DX
      X1=(XMA/DT-UMBM-AMBM+XMB*((UI(M1)+AI(M1)-UMBM-AMBM)/(XI(I-1)-
     1XMB)))/(1/DT+(UI(M1)+AI(M1)-UMBM-AMBM)/(XI(I-1)-XMB))
      IF(X1.LT.XI(I-1)) THEN
      X1=(XMA/DT+XI(I-1)*((UI(M1)+AI(M1)-UI(M1-1)-AI(M1-1))/DX)-UI(M1)
     1-AI(M1))/(1/DT+(UI(M1)+AI(M1)-UI(M1-1)-AI(M1-1))/DX)
      IF(X1.GT.XMB) TYPE*,'KAIKES',I
      IF(X1.LT.(XI(I-1)-DX)) TYPE*,'NO1',K,I
      XNG=(XI(I-1)-X1)/DX
      P1=PI(M1)-(PI(M1)-PI(M1-1))*XNG
      U1=UI(M1)-(UI(M1)-UI(M1-1))*XNG
      HG1=HGI(M1)-(HGI(M1)-HGI(M1-1))*XNG
      HL1=HLI(M1)-(HLI(M1)-HLI(M1-1))*XNG
      BN1=BNI(M1)-(BNI(M1)-BNI(M1-1))*XNG
      TG1=HG1/CPG
      VF1=VFI(M1)-(VFI(M1)-VFI(M1-1))*XNG
      RG1=1E5*P1/(RGC*TG1)
      CG1=SQRT(FI*RGC*TG1)
      R1=VF1*RG1+(1-VF1)*RL
      HGL1=HG1-HL1
      GO TO 10
      END IF
      XNG=(XMB-X1)/(XMB-XI(I-1))
      P1=PMB-(PMB-PI(M1))*XNG
      U1=UMBM-(UMBM-UI(M1))*XNG
      HG1=HGMBM-(HGMBM-HGI(M1))*XNG
      HL1=HLMBM-(HLMBM-HLI(M1))*XNG
      BN1=BNMBM-(BNMBM-BNI(M1))*XNG
      TG1=HG1/CPG
      TL1=HL1/CPL
      RG1=1E5*P1/(RGC*TG1)
      CG1=SQRT(FI*RGC*TG1)
      VF1=VFMBM-(VFMBM-VFI(M1))*XNG
      R1=VF1*RG1+(1-VF1)*RL
      HGL1=HG1-HL1
10     A1=1/SQRT(R1*(VF1/(RG1*CG1**2)+(1-VF1)/(RL*CL**2)))
      IF(VF1.GE.1.) THEN
      HENU1=0.0
      QIG1=0.0
      ELSE IF(VF1.LT.1.) THEN
C********************* NUCLEATION *********************************
      TTRIAL=TL1
      CALL NOSUBT(TTRIAL,PS,RGS)
      IF((PS/P1).LE.1.) THEN
      HENU1=0.0
      ELSE IF((PS/P1).GT.1.) THEN
      RC=2*SIG*1E-5/((PS-P1)*(1-RGS/RL))
      GE=4.1888*SIG*RC**2
      ANO=RL*(1-VF1)*AC/WM
      HENU1=ANO**(2./3.)*S*SQRT(.955*SIG*AC/(WM*F))*4/DIA*
     1exp((-1)*(GE*F/(BC*TL1)))
      END IF
      QIG1=3.9*BN1**(2./3.)*VF1**(1./3.)*UN*CK*(TL1-TG1)
      END IF
      GMN1=HENU1*4.1888*RC**3*RGS*F
      BCE1=GE*HENU1*F*1E-3
      GMI1=QIG1/HGL1
      EX1=(GMI1+GMN1)*(1/RG1-1/RL)+BCE1/(CPG*RG1*TG1)
      IF(SWITCHM1.EQ.'FST') THEN
```

PAGE
NUMBERS
CUT OFF
IN
ORIGINAL

```
      PMA=1.0133
      N=0
      SP=1.
11     UMAM=(PI-PMA)*1E5/(R1*A1)+U1+A1*EX1*DT
      IF(VFMBM.GE.1.) THEN
      HENU4=0.0
      QIG4=0.0
      ELSE IF(VFMBM.LT.1.) THEN
C********************* NUCLEATION ****************************
      TTRIAL=TLMBM
      CALL NOSUBT(TTRIAL,PS,RGS)
      IF((PS/PMB).LE.1.) THEN
       HENU4=0.0
      ELSE IF((PS/PMB).GT.1.) THEN
       RC=2*SIG*1E-5/((PS-PMB)*(1-RGS/RL))
       GE=4.1888*SIG*RC**2
       ANO=RL*(1-VFMBM)*AC/WM
       HENU4=ANO**(2./3.)*S*SQRT(.955*SIG*AC/(WM*F))*4/DIA*
     1exp((-1)*(GE*F/(BC*TLMBM)))
       END IF
       QIG4=3.9*BNMBM**(2./3.)*VFMBM**(1./3.)*UN*CK*(TLMBM-TGMBM)
      END IF
      GMN4=HENU4*4.1888*RC**3*RGS*F
      BCE4=GE*HENU4*F*1E-3
      GMI4=QIG4/HGLMBM
      EX4=RMBM*(GMI4+GMN4)/(RGMBM*RL)+BCE4*(1-VFMBM)/(CPG*RGMBM*TGMBM)
      B=VFMBM*(1-VFMBM)*(RGMBM*CGMBM**2-RL*CL**2)/(RGMBM*CGMBM**2*RL*
     1 CL**2)
      VFMAM=VFMBM+B*(PMA-PMB)*1E5+EX4*DT
      IF(VFMAM.GT.1..AND.(VFMAM-1.).GT.1E-4) THEN
      DT=DT/2.
      GO TO 7
     ELSE IF(ABS(VFMAM-1.).LE.1E-4) THEN
      VFMAM=1.
      END IF
      IF(VFMBM.LT.1.) THEN
       BNMAM=BNMBM+BNMBM/VFMBM*(VFMAM-VFMBM)+BNMBM*1E5/
     1(CGMBM**2*RGMBM)*(PMA-PMB)+(HENU4-BNMBM/
     2(RGMBM*VFMBM)*(GMI4+GMN4+BCE4/(CPG*TGMBM)))*DT
       HLMAM=HLMBM+(PMA-PMB)*1E2/RL-BCE4*DT/(RL*(1-VFMBM))
       ELSE IF(VFMBM.GE.1.) THEN
       HLMAM=HLMBM+(PMA-PMB)*1E2/RL
       BNMAM=0.0
       END IF
       TLMAM=HLMAM/CPL
       HGMAM=HGMBM+(PMA-PMB)*1E2/RGMBM+BCE4*DT/(RGMBM*VFMBM)
       HGLMAM=HGMAM-HLMAM
       TGMAM=HGMAM/CPG
       RGMAM=1E5*PMA/(RGC*TGMAM)
       CGMAM=SQRT(RGC*FI*TGMAM)
       RMAM=VFMAM*RGMAM+(1-VFMAM)*RL
       AMAM=1/SQRT(RMAM*(VFMAM/(RGMAM*CGMAM**2)+(1-VFMAM)/(RL*CL**2)))
       IF((UMAM-AMAM).LE.0.0.AND.N.EQ.0) GO TO 23
       IF(N.EQ.1) GO TO 12
       PMA=PMA+SP
       N=N+1
       GO TO 11
12     IF(ABS(UMAM-AMAM).LE.1.E-3) THEN
       N=0
       GO TO 23
       ELSE IF((UMAM-AMAM).LT.0.0) THEN
        SP=SP/1.1
        PMA=PMA-SP
        GO TO 11
       ELSE IF((UMAM-AMAM).GT.0.0) THEN
        SP=SP/1.1
        PMA=PMA+SP
        GO TO 11
       END IF
       END IF
       IF(SWITCHG.EQ.'INS'.OR.SWITCHG1.EQ.'FST') THEN
        XGA=UGB*DT+XGB
       IF(XGA.GT.PL) THEN
        DT=(PL-XGB)/UGB
        XGA=PL
```

```
 TYPE*,'G INTERFACE IS OUT',K,(AT+DT)
 SWITCHG='OUT'
 SWITCHG1='FST'
 GO TO 8
 END IF
 IF(SWITCHG1.EQ.'NFS') THEN
 M2=XGB/DX
 XI(I+1)=(M2+1)*DX
 X2=(XGA/DT-UGB+CGGBA+XGB*((UI(M2+1)-CGI(M2+1)-UGB+CGGBA)/
1(XI(I+1)-XGB)))/(1/DT+(UI(M2+1)-CGI(M2+1)-UGB+CGGBA)/
2(XI(I+1)-XGB))
 IF(X2.LT.XGB) TYPE*,'KAIKES',K,I
 IF(X2.GT.PL) THEN
 SWITCH2='NO2'
 FK1=(U(J)-CG(J)-UI(J)+CGI(J))/DT
 FK2=AT+DT
 FK3=U(J)-CG(J)-2*FK1*FK2
 FK4=XGA-PL-FK2*(U(J)-CG(J))+FK1*FK2**2
IF(FK1.EQ.0.0) THEN
 P2=P(J)
 U2=U(J)
 TG2=TG(J)
 RG2=RG(J)
 CG2=CG(J)
ELSE IF(FK1.NE.0.0) THEN
 T2T1=(-FK3+SQRT(FK3**2-4*FK1*FK4))/(2*FK1)
 T2T2=(-FK3-SQRT(FK3**2-4*FK1*FK4))/(2*FK1)
 T2=0.0
IF(T2T1.GE.AT.AND.T2T1.LE.FK2) T2=T2T1
IF(T2T2.GE.AT.AND.T2T2.LE.FK2) T2=T2T2
IF(T2.EQ.0.0) TYPE*,'INTERFACE T2 FAULSE-AIR',K,I
 TA=(T2-FK2)/DT
 P2=(P(J)-PI(J))*TA+P(J)
 U2=(U(J)-UI(J))*TA+U(J)
 TG2=(TG(J)-TGI(J))*TA+TG(J)
 RG2=1E5*P2/(RGCG*TG2)
 CG2=SQRT(RGCG*FIG*TG2)
END IF
 UCTR=U(J)-CG(J)
 GO TO 13
 ELSE IF(X2.LE.PL) THEN
 IF(X2.GT.XI(I+1)) THEN
 X2=(XGA/DT-UI(M2+1)+CGI(M2+1)+XI(I+1)*((UI(M2+2)-CGI(M2+2)-
1UI(M2+1)+CGI(M2+1))/DX))/(1/DT+(UI(M2+2)-CGI(M2+2)-UI(M2+1)+
2CGI(M2+1))/DX)
 IF(X2.GT.(XI(I+1)+DX)) TYPE*,'NO2',K,I
 XNG=(X2-XI(I+1))/DX
 P2=PI(M2+1)+(PI(M2+2)-PI(M2+1))*XNG
 U2=UI(M2+1)+(UI(M2+2)-UI(M2+1))*XNG
 TG2=TGI(M2+1)+(TGI(M2+2)-TGI(M2+1))*XNG
 RG2=1E5*P2/(RGCG*TG2)
 CG2=SQRT(RGCG*FIG*TG2)
 GO TO 13
 ELSE IF(X2.LE.XI(I+1)) THEN
 XNG=(XI(I+1)-X2)/(XI(I+1)-XGB)
 P2=PI(M2+1)-(PI(M2+1)-PGB)*XNG
 U2=UI(M2+1)-(UI(M2+1)-UGB)*XNG
 TG2=TGI(M2+1)-(TGI(M2+1)-TGGBA)*XNG
 CG2=SQRT(TG2*RGCG*FIG)
 RG2=1E5*P2/(RGCG*TG2)
END IF
 END IF
 END IF
13  IF(XGB.EQ.XMB) GO TO 14
 IF(((XGB-XMB)/DX).LE.1.) THEN
 XI2=(XMA/DT-UMBG+CGMBG+XMB*(UMBG-CGMBG-UGB+CGGBG)/(XMB-XGB))/
1((UMBG-CGMBG-UGB+CGGBG)/(XMB-XGB)+1/DT)
 ELSE IF(((XGB-XMB)/DX).GT.1.) THEN
 M2=XMB/DX
 XI(I+1)=(M2+1)*DX
 XI2=(XMA/DT-UMBG+CGMBG+XMB*(UI(M2+1)-CGI(M2+1)-UMBG+CGMBG)/
1(XI(I+1)-XMB))/((UI(M2+1)-CGI(M2+1)-UMBG+CGMBG)/(XI(I+1)-XMB)
2+1/DT)
 IF(XI2.GT.XGB) TYPE*,'INT.M-XI2-WRONG'
 IF(XI2.GT.XI(I+1)) THEN
```

```
 IF(XGB.GT.(XI(I+1)+DX)) THEN
 XI2=(XMA/DT-UI(M2+1)+CGI(M2+1)+XI(I+1)*((UI(M2+2)-CGI(M2+2)-
1UI(M2+1)+CGI(M2+1))/DX))/(1/DT+(UI(M2+2)-CGI(M2+2)-UI(M2+1)+
2CGI(M2+1))/DX)
 IF(XI2.GT.XGB.OR.XI2.GT.(XI(I+1)+DX)) TYPE*,'INT.M-XI2-WRONG1'
 ELSE IF(XGB.LE.(XI(I+1)+DX)) THEN
 XI2=(XMA/DT-UI(M2+1)+CGI(M2+1)+XI(I+1)*(UGB-CGGBG-UI(M2+1)+
1CGI(M2+1))/(XGB-XI(I+1)))/(1/DT+(UGB-CGGBG-UI(M2+1)+CGI(M2+1))/
2(XGB-XI(I+1)))
 END IF
 END IF
 IF(XI2.GT.XGB) TYPE*,'INT.M-XI2-WRONG2'
 END IF
 IF(XI2.LT.XMB) TYPE*,'OUT OF RANGE M2',CGGBG,CGI(M2+1),CGMBG,
1CGI(M2+2)
 IF(XI2.GT.XGB) THEN
  XI1=(XGA/DT-UMBG-CGMBG+XMB*(UMBG+CGMBG-UGB-CGGBG)/(XMB-XGB))
1 /((UMBG+CGMBG-UGB-CGGBG)/(XMB-XGB)+1/DT)
 IF(XI1.GT.XGB) TYPE*,'OUT OF RANGE G1'
 IF(XI1.GE.XMB) THEN
  XNG=(XMB-XI1)/(XMB-XGB)
  PI1=PMB-(PMB-PGB)*XNG
  UI1=UMBG-(UMBG-UGB)*XNG
  TGI1=TGMBG-(TGMBG-TGGBG)*XNG
  RGI1=1E5*PI1/(RGC*TGI1)
  CGI1=SQRT(RGC*FIG*TGI1)
  ELSE IF(XI1.LT.XMB) THEN
14  IF(NI.EQ.0) THEN
  PI1=PMB
  UI1=UMBG
  RGI1=RGMBG
  TGI1=TGMBG
  CGI1=CGMBG
  XI1=XMB
  NI=2
  UCTL=UMBG+CGMBG
  SWTRL='ONN'
  GO TO 15
 ELSE IF(NI.EQ.2) THEN
  UCA=UMAG+CGMAG
  UCB=UMBG+CGMBG
  NUMBER=1
 CALL INTRPL(NUMBER,UCA,UCB,XGA,XMA,XMB,DT,AT,XI1,TI1,XNG)
  PI1=PMA-(PMA-PMB)*XNG
  UI1=UMAG-(UMAG-UMBG)*XNG
  TGI1=TGMAG-(TGMAG-TGMBG)*XNG
  CGI1=SQRT(RGC*FIG*TGI1)
  RGI1=1E5*PI1/(RGC*TGI1)
  UCTL=UCA
  SWTRL='ONN'
 END IF
 END IF
15  IF(SWITCHG1.EQ.'FST') THEN
  PGA=1.0133
  SP=1.
  N=0
16   UGA=(PI1-PGA)*1E5/(RGI1*CGI1)+UI1
  TGGAG=TGGBG*(PGA/PGB)**.286
  CGGAG=SQRT(FIG*RGC*TGGAG)
  IF((UGA-CGGAG).LE.0.0.AND.N.EQ.0) GO TO 18
 IF(N.EQ.1) GO TO 17
  PGA=PGA+SP
  N=N+1
  GO TO 16
17  IF(ABS(UGA-CGGAG).LE.1E-3) THEN
  N=0
  GO TO 18
 ELSE IF((UGA-CGGAG).LT.0.0) THEN
  SP=SP/1.1
  PGA=PGA-SP
  GO TO 16
 ELSE IF((UGA-CGGAG).GT.0.0) THEN
  SP=SP/1.1
  PGA=PGA+SP
  GO TO 16
```

```
      END IF
18      RGGAG=1E5*PGA/(RGC*TGGAG)
      ELSE IF(SWITCHG1.EQ.'NFS') THEN
       PGA=(P2+RG2*CG2*PI1/(RGI1*CGI1)+RG2*CG2*1E-5*(UI1-U2))/
     1 (1+RG2*CG2/(RGI1*CGI1))
       UGA=(PI1-PGA)*1E5/(RGI1*CGI1)+UI1
       TGGAG=TGGBG*(PGA/PGB)**.286
       RGGAG=1E5*PGA/(RGC*TGGAG)
       CGGAG=SQRT(FIG*RGC*TGGAG)
       TGGAA=TGGBA*(PGA/PGB)**.286
       RGGAA=1E5*PGA/(RGCG*TGGAA)
       CGGAA=SQRT(TGGAA*FIG*RGCG)
      END IF
       UCA=UGA-CGGAG
       UCB=UGB-CGGBG
       NUMBER=2
      CALL INTRPL(NUMBER,UCA,UCB,XMA,XGA,XGB,DT,AT,XI2,TI2,XNG)
       PI2=PGA-(PGA-PGB)*XNG
       UI2=UGA-(UGA-UGB)*XNG
       TGI2=TGGAG-(TGGAG-TGGBG)*XNG
       RGI2=1E5*PI2/(RGC*TGI2)
       CGI2=SQRT(RGC*FIG*TGI2)
       PMA=(PI2+RGI2*CGI2*PI/(RI*AI*VE)+RGI2*CGI2*1E-5/
     1 VE*(UI+AI*EXI*DT-UI2*VE))/(1+RGI2*CGI2/(RI*AI*VE))
       UMAM=(PI-PMA)*1E5/(RI*AI)+UI+AI*EXI*DT
       UMAG=UMAM/VE
       IF(VFMBM.GE.1.) THEN
       HENU4=0.0
       QIG4=0.0
       ELSE IF(VFMBM.LT.1.) THEN
C********************** NUCLEATION ***************************:
       TTRIAL=TLMBM
       CALL NOSUBT(TTRIAL,PS,RGS)
       IF((PS/PMB).LE.1.)THEN
       HENU4=0.0
       ELSE IF((PS/PMB).GT.1.) THEN
       RC=2*SIG*1E-5/((PS-PMB)*(1-RGS/RL))
       GE=4.1888*SIG*RC**2
       ANO=RL*(1-VFMBM)*AC/WM
       HENU4=ANO**(2./3.)*S*SQRT(.955*SIG*AC/(WM*F))*4/DIA*
     1exp((-1)*(GE*F/(BC*TLMBM)))
       END IF
       QIG4=3.9*BNMBM**(2./3.)*VFMBM**(1./3.)*UN*CK*(TLMBM-TGMBM)
       END IF
       GMN4=HENU4*4.1888*RGS*RC**3*F
       BCE4=GE*HENU4*1E-3*F
       GMI4=QIG4/HGLMBM
       EX4=RMBM*(GMI4+GMN4)/(RGMBM*RL)+BCE4*(1-VFMBM)
     1/(RGMBM*CPG*TGMBM)
       B=VFMBM*(1-VFMBM)*(RGMBM*CGMBM**2-RL*CL**2)
     1 /(RGMBM*CGMBM**2*RL*CL**2)
       VFMAM=VFMBM+B*(PMA-PMB)*1E5+EX4*DT
       IF(VFMAM.GT.1..AND.(VFMAM-1.).GT.1E-4) THEN
       DT=DT/2.
       GO TO 7
       ELSE IF(ABS(VFMAM-1.).LE.1E-4) THEN
       VFMAM=1.
       END IF
       IF(VFMBM.LT.1.) THEN
       BNMAM=BNMBM+BNMBM/VFMBM*(VFMAM-VFMBM)+BNMBM*1E5/
     1(CGMBM**2*RGMBM)*(PMA-PMB)+(HENU4-BNMBM/
     2(RGMBM*VFMBM)*(GMI4+GMN4+BCE4/(CPG*TGMBM)))*DT
       HLMAM=HLMBM+(PMA-PMB)*1E2/RL-BCE4*DT/(RL*(1-VFMBM))
       ELSE IF(VFMBM.GE.1.) THEN
       HLMAM=HLMBM+(PMA-PMB)*1E2/RL
       BNMAM=0.0
       END IF
       TLMAM=HLMAM/CPL
       HGMAM=HGMBM+(PMA-PMB)*1E2/RGMBM+BCE4*DT/(RGMBM*VFMBM)
       HGLMAM=HGMAM-HLMAM
       TGMAM=HGMAM/CPG
       RGMAM=1E5*PMA/(RGC*TGMAM)
       CGMAM=SQRT(FI*RGC*TGMAM)
       RMAM=VFMAM*RGMAM+(1-VFMAM)*RL
       AMAM=1/SQRT(RMAM*(VFMAM/(RGMAM*CGMAM**2)+(1-VFMAM)
```

```
     1/(RL*CL**2)))
      TGMAG=TGMAM
      RGMAG=RGMAM
      CGMAG=SQRT(FIG*RGC*TGMAG)
     IF(SWTRL.EQ.'ONN') THEN
      UCTLC=UMAG+CGMAG
     IF(ABS(UCTL-UCTLC).GT.1E-3) THEN
      GO TO 14
     ELSE IF(ABS(UCTL-UCTLC).LE.1E-3) THEN
      SWTRL='OFF'
      NI=0
     END IF
     END IF
     GO TO 23
     ELSE IF(XI2.LE.XGB) THEN
     IF(((XGB-XMB)/DX).LE.1.) THEN
      XNG=(XMB-XI2)/(XMB-XGB)
      PI2=PMB-(PMB-PGB)*XNG
      UI2=UMBG-(UMBG-UGB)*XNG
      TGI2=TGMBG-(TGMBG-TGGBG)*XNG
      RGI2=1E5*PI2/(RGC*TGI2)
      CGI2=SQRT(TGI2*FIG*RGC)
     ELSE IF(((XGB-XMB)/DX).GT.1.) THEN
     IF(XI2.LE.XI(I+1)) THEN
      XNG=(XI(I+1)-XI2)/(XI(I+1)-XMB)
      PI2=PI(M2+1)-(PI(M2+1)-PMB)*XNG
      UI2=UI(M2+1)-(UI(M2+1)-UMBG)*XNG
      TGI2=TGI(M2+1)-(TGI(M2+1)-TGMBG)*XNG
      RGI2=1E5*PI2/(RGC*TGI2)
      CGI2=SQRT(RGC*FIG*TGI2)
     ELSE IF(XI2.GT.XI(I+1).AND.XGB.GT.(XI(I+1)+DX)) THEN
      XNG=(XI2-XI(I+1))/DX
      PI2=PI(M2+1)+(PI(M2+2)-PI(M2+1))*XNG
      UI2=UI(M2+1)+(UI(M2+2)-UI(M2+1))*XNG
      TGI2=TGI(M2+1)+(TGI(M2+2)-TGI(M2+1))*XNG
      RGI2=1E5*PI2/(RGC*TGI2)
      CGI2=SQRT(RGC*TGI2*FIG)
     ELSE IF(XI2.GT.XI(I+1).AND.XGB.LE.(XI(I+1)+DX)) THEN
      XNG=(XI2-XI(I+1))/(XGB-XI(I+1))
      PI2=PI(M2+1)+(PGB-PI(M2+1))*XNG
      UI2=UI(M2+1)+(UGB-UI(M2+1))*XNG
      TGI2=TGI(M2+1)+(TGGBG-TGI(M2+1))*XNG
      RGI2=1E5*PI2/(RGC*TGI2)
      CGI2=SQRT(RGC*FIG*TGI2)
     END IF
     END IF
     PMA=(PI2+RGI2*CGI2*P1/(R1*A1*VE)+RGI2*CGI2*1E-5/VE
    1*(U1+A1*EX1*DT-UI2*VE))/(1+RGI2*CGI2/(R1*A1*VE))
     UMAM=(P1-PMA)*1E5/(R1*A1)+U1+A1*EX1*DT
     UMAG=UMAM/VE
     IF(VFMBM.GE.1.) THEN
     HENU4=0.0
     QIG4=0.0
     ELSE IF(VFMBM.LT.1.) THEN
C*************** NUCLEATION ************************************
     TTRIAL=TLMBM
     CALL NOSUBT(TTRIAL,PS,RGS)
     IF((PS/PMB).LE.1.) THEN
     HENU4=0.0
     ELSE IF((PS/PMB).GT.1.) THEN
     RC=2*SIG*1E-5/((PS-PMB)*(1-RGS/RL))
     GE=4.1888*SIG*RC**2
     ANO=RL*(1-VFMBM)*AC/WM
     HENU4=ANO**(2./3.)*S*SQRT(.955*SIG*AC/(WM*F))*4/DIA*
    1exp((-1)*(GE*F/(BC*TLMBM)))
     END IF
     QIG4=3.9*BNMBM**(2./3.)*VFMBM**(1./3.)*UN*CK*(TLMBM-TGMBM)
     END IF
     GMN4=HENU4*4.1888*RGS*RC**3*F
     BCE4=HENU4*GE*F*1E-3
     GMI4=QIG4/HGLMBM
     EX4=RMBM*(GMN4+GMI4)/(RGMBM*RL)+BCE4*(1-VFMBM)/
    1 (RGMBM*CPG*TGMBM)
     B=VFMBM*(1-VFMBM)*(RGMBM*CGMBM**2-RL*CL**2)/
    1 (RGMBM*CGMBM**2*RL*CL**2)
```

```
  VFMAM=VFMBM+B*(PMA-PMB)*1E5+EX4*DT
  IF(VFMAM.GT.1..AND.(VFMAM-1.).GT.1E-4) THEN
  DT=DT/2
  GO TO 7
  ELSE IF(ABS(VFMAM-1.).LE.1E-4) THEN
  VFMAM=1.
  END IF
  IF(VFMBM.LT.1.) THEN
  BNMAM=BNMBM+BNMBM/VFMBM*(VFMAM-VFMBM)+BNMBM*1E5/
2/(CGMBM**2*RGMBM)
1*(PMA-PMB)+(HENU4-BNMBM/(RGMBM*VFMBM)*(GMI4+GMN4+BCE4
2/(CPG*TGMBM)))*DT
  HLMAM=HLMBM+(PMA-PMB)*1E2/RL-BCE4*DT/(RL*(1-VFMBM))
  ELSE IF(VFMBM.GE.1.) THEN
  HLMAM=HLMBM+(PMA-PMB)*1E2/RL
  BNMAM=0.0
  END IF
  TLMAM=HLMAM/CPL
  HGMAM=HGMBM+(PMA-PMB)*1E2/RGMBM+BCE4*DT/(RGMBM*VFMBM)
  HGLMAM=HGMAM-HLMAM
  TGMAM=HGMAM/CPG
  RGMAM=1E5*PMA/(RGC*TGMAM)
  CGMAM=SQRT(FI*RGC*TGMAM)
  RMAM=RGMAM*VFMAM+(1-VFMAM)*RL
  AMAM=1/SQRT(RMAM*(VFMAM/(RGMAM*CGMAM**2)+(1-VFMAM)/(RL*CL**2)))
  TGMAG=TGMAM
  RGMAG=RGMAM
  CGMAG=SQRT(FIG*RGC*TGMAG)
  IF(((XGB-XMB) DX).LE.1.) THEN
  XII=(XGA/DT-UMBG-CGMBG+XMB*(UMBG+CGMBG-UGB-CGGBG)/(XMB-XGB))
1 /((UMBG+CGMBG-UGB-CGGBG)/(XMB-XGB)+1/DT)
 IF(XII.GT.XGB) TYPE*,'KAIKES'
 IF(XII.GE.XMB) THEN
  XNG=(XMB-XII) (XMB-XGB)
  PII=PMB-(PMB-PGB)*XNG
  UII=UMBG-(UMBG-UGB)*XNG
  TGII=TGMBG-(TGMBG-TGGBG)*XNG
  RGII=1E5*PII/(RGC*TGII)
  CGII=SQRT(RGC*FIG*TGII)
 ELSE IF(XII.LT.XMB) THEN
  UCA=UMAG+CGMAG
  UCB=UMBG+CGMBG
  NUMBER=3
 CALL INTRPL(NUMBER,UCA,UCB,XGA,XMA,XMB,DT,AT,XII,TII,XNG)
  PII=PMA-(PMA-PMB)*XNG
  UII=UMAG-(UMAG-UMBG)*XNG
  TGII=TGMAG-(TGMAG-TGMBG)*XNG
  RGII=1E5*PII/(RGC*TGII)
  CGII=SQRT(RGC*FIG*TGII)
 END IF
 ELSE IF(((XGB-XMB)/DX).GT.1.) THEN
  MI=XGB/DX
  IF(INT(XGB/DX).EQ.(XGB/DX)) MI=XGB/DX-1
  XI(I-1)=MI*DX
  XII=(XGA/DT-UGB-CGGBG+XGB*((UI(MI)+CGI(MI)-UGB-CGGBG)/(XI(I-1)
1-XGB)))/(1/DT+(UI(MI)+CGI(MI)-UGB-CGGBG)/(XI(I-1)-XGB))
 IF(XII.LT.XI(I-1)) THEN
 IF(XMB.LT.(XI(I-1)-DX)) THEN
  XII=(XGA/DT+XI(I-1)*((UI(MI)+CGI(MI)-UI(MI-1)-CGI(MI-1))/DX)
1-UI(MI)-CGI(MI))/(1/DT+(UI(MI)+CGI(MI)-UI(MI-1)-CGI(MI-1))/DX)
  IF(XII.GT.XGB.OR.XII.LT.(XI(I-1)-DX).OR.XII.LT.XMB)
1 TYPE*,'INT.G-XI-WRONGI'
  XNG=(XI(I-1)-XII)/DX
  PII=PI(MI)-(PI(MI)-PI(MI-1))*XNG
  UII=UI(MI)-(UI(MI)-UI(MI-1))*XNG
  TGII=TGI(MI)-(TGI(MI)-TGI(MI-1))*XNG
  RGII=1E5*PII/(RGC*TGII)
  CGII=SQRT(RGC*FIG*TGII)
 ELSE IF(XMB.GE.(XI(I-1)-DX)) THEN
 XII=(XGA/DT-UI(MI)-CGI(MI)+XI(I-1)*((UI(MI)+CGI(MI)-UMBG-CGMBG)/
1(XI(I-1)-XMB)))/(1/DT+(UI(MI)+CGI(MI)-UMBG-CGMBG)/(XI(I-1)-XMB))
  IF(XII.GT.XGB.OR.XII.LT.XMB) TYPE*,'INT.G-XII-WRONG2'
  XNG=(XI(I-1)-XII)/(XI(I-1)-XMB)
  PII=PI(MI)-(PI(MI)-PMB)*XNG
  UII=UI(MI)-(UI(MI)-UMBG)*XNG
```

```
      TGI1=TGI(M1)-(TGI(M1)-TGMBG)*XNG
      RGI1=1E5*PI1/(RGC*TGI1)
      CGI1=SQRT(RGC*FIG*TGI1)
      END IF
      GO TO 71
     ELSE IF(XI1.GE.XI(I-1)) THEN
      XNG=(XGB-XI1)/(XGB-XI(I-1))
      PI1=PGB-(PGB-PI(M1))*XNG
      UI1=UGB-(UGB-UI(M1))*XNG
      TGI1=TGGBG-(TGGBG-TGI(M1))*XNG
      RGI1=1E5*PI1/(RGC*TGI1)
      CGI1=SQRT(RGC*FIG*TGI1)
     END IF
     END IF
71    IF(SWITCHG1.EQ.'FST') THEN
      PGA=1.0133
      SP=1.
      N=0
19     UGA=(PI1-PGA)*1E5/(RGI1*CGI1)+UI1
      TGGAG=TGGBG*(PGA/PGB)**.286
      CGGAG=SQRT(RGC*FIG*TGGAG)
     IF((UGA-CGGAG).LE.0.0.AND.N.EQ.0) GO TO 21
     IF(N.EQ.1) GO TO 20
      PGA=PGA+SP
      N=N+1
      GO TO 19
20    IF(ABS(UGA-CGGAG).LE.1E-3) THEN
      N=0
      GO TO 21
     ELSE IF((UGA-CGGAG).LT.0.0) THEN
      SP=SP/1.1
      PGA=PGA-SP
      GO TO 19
     ELSE IF((UGA-CGGAG).GT.0.0) THEN
      SP=SP/1.1
      PGA=PGA+SP
      GO TO 19
     END IF
21     RGGAG=1E5*PGA/(RGC*TGGAG)
     ELSE IF(SWITCHG1.EQ.'NFS') THEN
      PGA=(P2+RG2*CG2*PI1/(RGI1*CGI1)+RG2*CG2*1E-5*(UI1-U2))/
    1 (1+RG2*CG2/(RGI1*CGI1))
      UGA=(PI1-PGA)*1E5/(RGI1*CGI1)+UI1
      TGGAG=TGGBG*(PGA/PGB)**.286
      RGGAG=1E5*PGA/(RGC*TGGAG)
      CGGAG=SQRT(FIG*RGC*TGGAG)
      TGGAA=TGGBA*(PGA/PGB)**.286
      RGGAA=1E5*PGA/(RGCG*TGGAA)
      CGGAA=SQRT(RGCG*FIG*TGGAA)
     END IF
     END IF
     GO TO 23
     ELSE IF(SWITCHG.EQ.'OUT') THEN
      M2=XMB/DX
      XI(I+1)=(M2+1)*DX
      X2=(XMA/DT-UMBG+CGMBG+XMB*((UI(M2+1)-CGI(M2+1)-UMBG+CGMBG)/
    1 (XI(I+1)-XMB)))/(1/DT+(UI(M2+1)-CGI(M2+1)-UMBG+CGMBG)/
    2 (XI(I+1)-XMB))
     IF(X2.LT.XMB) TYPE*,'KAIKES'
     IF(X2.GT.PL) THEN
     SWITCH2='NO2'
     FK1=(U(J)-CG(J)-UI(J)+CGI(J))/DT
     FK2=AT+DT
     FK3=U(J)-CG(J)-2*FK1*FK2
     FK4=XMA-PL-FK2*(U(J)-CG(J))+FK1*FK2**2
    IF(FK1.EQ.0.0) THEN
     P2=P(J)
     U2=U(J)
     TG2=TG(J)
     RG2=RG(J)
     CG2=CG(J)
    ELSE IF(FK1.NE.0.0) THEN
     T2T1=(-FK3+SQRT(FK3**2-4*FK1*FK4))/(2*FK1)
     T2T2=(-FK3-SQRT(FK3**2-4*FK1*FK4))/(2*FK1)
     T2=0.0
```

```
      IF(T2T1.GE.AT.AND.T2T1.LE.FK2) T2=T2T1
      IF(T2T2.GE.AT.AND.T2T2.LE.FK2) T2=T2T2
      IF(T2.EQ.0.0) TYPE*,'INTERFACE T2 FAULSE-GAS'
       TA=(T2-FK2)/DT
       P2=(P(J)-PI(J))*TA+P(J)
       U2=(U(J)-UI(J))*TA+U(J)
       TG2=(TG(J)-TGI(J))*TA+TG(J)
       RG2=1E5*P2/(RGC*TG2)
       CG2=SQRT(RGC*FIG*TG2)
      END IF
       UCTR=U(J)-CG(J)
       GO TO 22
      ELSE IF(X2.LE.PL) THEN
      IF(X2.GT.XI(I+1)) THEN
       X2=(XMA/DT-UI(M2+1)+CGI(M2+1)+XI(I+1)*((UI(M2+2)-CGI(M2+2)-
     1UI(M2+1)+CGI(M2+1))/DX))/(1/DT+(UI(M2+2)-CGI(M2+2)-UI(M2+1)+
     2CGI(M2+1))/DX)
       IF(X2.GT.(XI(I+1)+DX)) TYPE*,'NO2',K,I
       XNG=(X2-XI(I+1))/DX
       P2=PI(M2+1)+(PI(M2+2)-PI(M2+1))*XNG
       U2=UI(M2+1)+(UI(M2+2)-UI(M2+1))*XNG
       TG2=TGI(M2+1)+(TGI(M2+2)-TGI(M2+1))*XNG
       RG2=1E5*P2/(RGC*TG2)
       CG2=SQRT(TG2*RGC*FIG)
       GO TO 22
      ELSE IF(X2.LE.XI(I+1)) THEN
       XNG=(XI(I+1)-X2)/(XI(I+1)-XMB)
       P2=PI(M2+1)-(PI(M2+1)-PMB)*XNG
       U2=UI(M2+1)-(UI(M2+1)-UMBG)*XNG
       TG2=TGI(M2+1)-(TGI(M2+1)-TGMBG)*XNG
       CG2=SQRT(RGC*FIG*TG2)
       RG2=1E5*P2/(RGC*TG2)
      END IF
      END IF
22     PMA=(P2+RG2*CG2*P1/(R1*A1*VE)+RG2*CG2*1E-5/VE
     1*(U1+A1*EX1*DT-U2*VE))/(1+RG2*CG2/(R1*A1*VE))
       UMAM=(P1-PMA)*1E5/(R1*A1)+U1+A1*EX1*DT
       UMAG=UMAM/VE
       IF(VFMBM.GE.1.) THEN
       HENU4=0.0
       QIG4=0.0
       ELSE IF(VFMBM.LT.1.) THEN
C**************: NUCLEATION **********************
       TTRIAL=TLMBM
       CALL NOSUBT(TTRIAL,PS,RGS)
       IF((PS/PMB).LE.1.) THEN
       HENU4=0.0
       ELSE IF((PS/PMB).GT.1.) THEN
       RC=2*SIG*1E-5/((PS-PMB)*(1-RGS/RL))
       GE=4.1888*SIG*RC**2
       ANO=RL*(1-VFMBM)*AC/WM
       HENU4=ANO**(2./3.)*S*SQRT(.955*SIG*AC/(WM*F))*4/DIA*
     1exp((-1)*(GE*F/(BC*TLMBM)))
       END IF
       QIG4=3.9*BNMBM**(2./3.)*VFMBM**(1./3.)*UN*CK*(TLMBM-TGMBM)
       END IF
       GMN4=HENU4*4.1888*RGS*F*RC**3
       BCE4=HENU4*GE*F*1E-3
       GMI4=QIG4/HGLMBM
       EX4=RMBM*(GMI4+GMN4)/(RGMBM*RL)+BCE4*(1-VFMBM)/
     1 (RGMBM*CPG*TGMBM)
       B=VFMBM*(1-VFMBM)*(RGMBM*CGMBM**2-RL*CL**2)/
     1 (RGMBM*CGMBM**2*RL*CL**2)
       VFMAM=VFMBM+B*(PMA-PMB)*1E5+EX4*DT
       IF(VFMAM.GT.1..AND.(VFMAM-1.).GT.1E-4) THEN
       TYPE*,'VFMAM>1',K,XGA
       DT=DT/2.
       GO TO 7
       ELSE IF(ABS(VFMAM-1.).LE.1E-4) THEN
       VFMAM=1.
       END IF
       IF(VFMBM.LT.1.) THEN
       BNMAM=BNMBM+BNMBM/VFMBM*(VFMAM-VFMBM)+BNMBM*1E5/
     3(CGMBM**2*RGMBM
     1)*(PMA-PMB)+(HENU4-BNMBM/(RGMBM*VFMBM)*(GMI4+GMN4+BCE4/
```

```
2(CPG*TGMBM)))*DT
  HLMAM=HLMBM+(PMA-PMB)*1E2/RL-BCE4*DT/(RL*(1-VFMBM))
  ELSE IF(VFMBM.GE.1.) THEN
  BNMAM=0.0
  HLMAM=HLMBM+(PMA-PMB)*1E2/RL
  END IF
  TLMAM=HLMAM/CPL
  HGMAM=HGMBM+(PMA-PMB)*1E2/RGMBM+BCE4*DT/(RGMBM*VFMBM)
  TGMAM=HGMAM/CPG
  HGLMAM=HGMAM-HLMAM
  RGMAM=1E5*PMA/(RGC*TGMAM)
  CGMAM=SQRT(RGC*TGMAM*FI)
  RMAM=VFMAM*RGMAM+(1-VFMAM)*RL
  AMAM=1/SQRT(RMAM*(VFMAM/(RGMAM*CGMAM**2)+(1-VFMAM)/(RL*CL**2)))
      TGMAG=TGMAM
      RGMAG=RGMAM
      CGMAG=SQRT(FIG*RGC*TGMAG)
     END IF
     END IF
23    XI(I)=I*DX
     XI(I-1)=(I-1)*DX
     XI(I+1)=(I+1)*DX
     IF(XI(I).GT.XMA.AND.XI(I).LE.XGA) GO TO 45
     IF(XI(I).GT.XGA) GO TO 37
C*****************MIXTURE*****************************************
     IF(ABS(XI(I)-XMA).LT.5E-6.AND.(SWITCHM.EQ.'INS'
    1.OR.SWITCHM1.EQ.'FST')) THEN
      U(I)=UMAM
      P(I)=PMA
      R(I)=RMAM
      A(I)=AMAM
      HG(I)=HGMAM
      HL(I)=HLMAM
      TG(I)=TGMAM
      TL(I)=TLMAM
      RG(I)=RGMAM
      CG(I)=CGMAM
      VF(I)=VFMAM
      BN(I)=BNMAM
      HGL(I)=HGLMAM
      GO TO 9
      END IF
      IF(I.EQ.0) GO TO 70
      IF(XMB.GE.XI(I)) GO TO 24
      X1=(XI(I)/DT-UMBM-AMBM+XMB*((UI(I-1)+AI(I-1)-UMBM-AMBM)/
    1(XI(I-1)-XMB)))/((UI(I-1)+AI(I-1)-UMBM-AMBM)/(XI(I-1)-XMB)+1/DT)
      IF(X1.LT.XI(I-1).OR.X1.GT.XI(I)) TYPE*,'NOL1-B-M-IM',I,K
      IF(X1.LE.XMB) THEN
      XNG=(XMB-X1)/(XMB-XI(I-1))
      P1=PMB-(PMB-PI(I-1))*XNG
      HL1=HLMBM-(HLMBM-HLI(I-1))*XNG
      HG1=HGMBM-(HGMBM-HGI(I-1))*XNG
      TG1=HG1/CPG
      TL1=HL1/CPL
      RG1=1E5*P1/(RGC*TG1)
      CG1=SQRT(RGC*FI*TG1)
      VF1=VFMBM-(VFMBM-VFI(I-1))*XNG
      BN1=BNMBM-(BNMBM-BNI(I-1))*XNG
      R1=VF1*RG1+(1-VF1)*RL
      U1=UMBM-(UMBM-UI(I-1))*XNG
      HGL1=HG1-HL1
      T1=AT
      ELSE IF(X1.GT.XMB) THEN
      UCA=UMAM+AMAM
      UCB=UMBM+AMBM
      NUMBER=4
      CALL INTRPL(NUMBER,UCA,UCB,XI(I),XMA,XMB,DT,AT,X1,T1,XNG)
      P1=PMA-(PMA-PMB)*XNG
      U1=UMAM-(UMAM-UMBM)*XNG
      HG1=HGMAM-(HGMAM-HGMBM)*XNG
      TG1=HG1/CPG
      RG1=1E5*P1/(RGC*TG1)
      CG1=SQRT(FI*RGC*TG1)
      HL1=HLMAM-(HLMAM-HLMBM)*XNG
      VF1=VFMAM-(VFMAM-VFMBM)*XNG
```

```
      BN1 = BNMAM-(BNMAM-BNMBM)*XNG
      R1 = RG1*VF1 + (1-VF1)*RL
      TL1 = HL1/CPL
      HGL1 = HG1-HL1
      END IF
      A1 = 1/SQRT(R1*(VF1/(RG1*CG1**2) + (1-VF1)/(RL*CL**2)))
      IF(VF1.GE.1.) THEN
      VF1 = 1
      QIG1 = 0.0
      HENU1 = 0.0
      ELSE IF(VF1.LT.1.) THEN
C***************** NUCLEATION ************************
      TTRIAL = TL1
      CALL NOSUBT(TTRIAL,PS,RGS)
      IF((PS/P1).LE.1.) THEN
      HENU1 = 0.0
      ELSE IF((PS/P1).GT.1.) THEN
      RC = 2*SIG*1E-5/((PS-P1)*(1-RGS/RL))
      GE = 4.1888*SIG*RC**2
      ANO = RL*(1-VF1)*AC/WM
      HENU1 = ANO**(2./3.)*S*SQRT(.955*SIG*AC/(WM*F))*4/DIA
     1*exp((-1)*(GE*F/(BC*TL1)))
      END IF
      QIG1 = 3.9*BN1**(2./3.)*VF1**(1./3.)*UN*CK*(TL1-TG1)
      END IF
      GO TO 25
24    X1 = XI(I)-(UI(I) + AI(I))/((UI(I) + AI(I)-UI(I-1)-AI(I-1))/DX + 1/DT)
      IF (X1.GT.XI(I).OR.X1.LT.XI(I-1)) TYPE*,'NOL1-B-M-M',K,I,XMA,XMB
     1,X1,XI(I-1),XI(I),UI(I),AI(I),UI(I-1),AI(I-1),DX,DT
      XNG = (XI(I)-X1)/DX
      P1 = PI(I)-(PI(I)-PI(I-1))*XNG
      HL1 = HLI(I)-(HLI(I)-HLI(I-1))*XNG
      VF1 = VFI(I)-(VFI(I)-VFI(I-1))*XNG
      BN1 = BNI(I)-(BNI(I)-BNI(I-1))*XNG
      TL1 = HL1/CPL
      HG1 = HGI(I)-(HGI(I)-HGI(I-1))*XNG
      TG1 = HG1/CPG
      RG1 = 1E5*P1/(RGC*TG1)
      CG1 = SQRT(RGC*FI*TG1)
      R1 = RG1*VF1 + (1-VF1)*RL
      U1 = UI(I)-(UI(I)-UI(I-1))*XNG
      HGL1 = HG1-HL1
      A1 = 1/SQRT(R1*(VF1/(RG1*CG1**2) + (1-VF1)/(RL*CL**2)))
      T1 = AT
      IF(VF1.GE.1.) THEN
      VF1 = 1
      QIG1 = 0.0
      HENU1 = 0.0
      ELSE IF(VF1.LT.1.) THEN
C***************** NUCLEATION ******************
      TTRIAL = TL1
      CALL NOSUBT(TTRIAL,PS,RGS)
      IF((PS/P1).LE.1.) THEN
      HENU1 = 0.0
      ELSE IF((PS/P1).GT.1.) THEN
      RC = 2*SIG*1E-5/((PS-P1)*(1-RGS/RL))
      GE = 4.1888*SIG*RC**2
      ANO = RL*(1-VF1)*AC/WM
      HENU1 = ANO**(2./3.)*S*SQRT(.955*SIG*AC/(WM*F))*4/DIA
     1*exp((-1)*(GE*F/(BC*TL1)))
      END IF
      QIG1 = 3.9*BN1**(2./3.)*VF1**(1./3.)*UN*CK*(TL1-TG1)
      END IF
25    GMN1 = HENU1*4.1888*RGS*RC**3*F
      GMI1 = QIG1/HGL1
      BCE1 = HENU1*GE*F*1E-3
      EX1 = (GMI1 + GMN1)*(1/RG1-1/RL) + BCE1/(CPG*TG1*RG1)
      IF(I.EQ.J) GO TO 34
70    IF(XMB.GE.XI(I + 1)) GO TO 28
      IF(XMB.LE.XI(I)) GO TO 26
      X2 = (XI(I)/DT-UMBM + AMBM + XMB*((UI(I)-AI(I)-UMBM + AMBM)/
     1(XI(I)-XMB)))/((UI(I)-AI(I)-UMBM + AMBM)/(XI(I)-XMB) + 1/DT)
      IF(X2.GT.XMB) THEN
26    UCA = UMAM-AMAM
      UCB = UMBM-AMBM
```

```
      NUMBER=5
      CALL INTRPL(NUMBER,UCA,UCB,XI(I),XMA,XMB,DT,AT,X2,T2,XNG)
      IF(X2.LT.XMB.AND.XMB.LE.XI(I)) THEN
      X2=(XI(I)/DT-UI(I-1)+AI(I-1)+XI(I-1)*(UI(I-1)-AI(I-1)-UMBM+AMBM
     1)/(XI(I-1)-XMB))/(1/DT+(UI(I-1)-AI(I-1)-UMBM+AMBM)/(XI(I-1)-XMB))
      XNG=(X2-XI(I-1))/(XMB-XI(I-1))
      P2=PI(I-1)+(PMB-PI(I-1))*XNG
      U2=UI(I-1)+(UMBM-UI(I-1))*XNG
      HL2=HLI(I-1)+(HLMBM-HLI(I-1))*XNG
      HG2=HGI(I-1)+(HGMBM-HGI(I-1))*XNG
      VF2=VFI(I-1)+(VFMBM-VFI(I-1))*XNG
      BN2=BNI(I-1)+(BNMBM-BNI(I-1))*XNG
      T2=AT
      ELSE IF(X2.GE.XMB) THEN
      P2=PMA-(PMA-PMB)*XNG
      U2=UMAM-(UMAM-UMBM)*XNG
      HL2=HLMAM-(HLMAM-HLMBM)*XNG
      HG2=HGMAM-(HGMAM-HGMBM)*XNG
      VF2=VFMAM-(VFMAM-VFMBM)*XNG
      BN2=BNMAM-(BNMAM-BNMBM)*XNG
      END IF
      HGL2=HG2-HL2
      TG2=HG2/CPG
      TL2=HL2/CPL
      RG2=1E5*P2/(RGC*TG2)
      CG2=SQRT(RGC*FI*TG2)
      R2=VF2*RG2+(1-VF2)*RL
      GO TO 27
      ELSE IF(X2.LE.XMB) THEN
      IF(X2.LT.XI(I)) GO TO 29
      XNG=(XMB-X2)/(XMB-XI(I))
      P2=PMB-(PMB-PI(I))*XNG
      HL2=HLMBM-(HLMBM-HLI(I))*XNG
      VF2=VFMBM-(VFMBM-VFI(I))*XNG
      BN2=BNMBM-(BNMBM-BNI(I))*XNG
      TL2=HL2/CPL
      HG2=HGMBM-(HGMBM-HGI(I))*XNG
      TG2=HG2/CPG
      HGL2=HG2-HL2
      CG2=SQRT(RGC*FI*TG2)
      RG2=1E5*P2/(RGC*TG2)
      R2=VF2*RG2+(1-VF2)*RL
      U2=UMBM-(UMBM-UI(I))*XNG
      T2=AT
      END IF
   27  A2=1/SQRT(R2*(VF2/(RG2*CG2**2)+(1-VF2)/(RL*CL**2)))
      IF(VF2.GE.1.) THEN
      VF2=1
      QIG2=0.0
      HENU2=0.0
      ELSE IF(VF2.LT.1.) THEN
C***************** NUCLEATION ****************************
      TTRIAL=TL2
      CALL NOSUBT(TTRIAL,PS,RGS)
      IF((PS/P2).LE.1.) THEN
      HENU2=0.0
      ELSE IF((PS/P2).GT.1.) THEN
      RC=2*SIG*1E-5/((PS-P2)*(1-RGS/RL))
      GE=4.1888*SIG*RC**2
      ANO=RL*(1-VF2)*AC/WM
      HENU2=ANO**(2./3.)*S*SQRT(.955*SIG*AC/(F*WM))*4/DIA
     1*exp((-1)*(GE*F/(BC*TL2)))
      END IF
      QIG2=3.9*BN2**(2./3.)*VF2**(1./3.)*UN*CK*(TL2-TG2)
      END IF
      GO TO 30
   28  X2=XI(I)-(UI(I)-AI(I))/(1/DT+(UI(I+1)-AI(I+1)-UI(I)+AI(I))/DX)
      IF(X2.LT.XI(I)) THEN
   29   X2=XI(I)-(UI(I)-AI(I))/(1/DT+(UI(I)-AI(I)-UI(I-1)+AI(I-1))/DX)
       L1=1
      ELSE IF(X2.GE.XI(I)) THEN
       L1=0
      END IF
      XNG=(XI(I+1-L1)-X2)/DX
      P2=PI(I+1-L1)-(PI(I+1-L1)-PI(I-L1))*XNG
```

```
      HL2=HLI(I+1-L1)-(HLI(I+1-L1)-HLI(I-L1))*XNG
      VF2=VFI(I+1-L1)-(VFI(I+1-L1)-VFI(I-L1))*XNG
      BN2=BNI(I+1-L1)-(BNI(I+1-L1)-BNI(I-L1))*XNG
      TL2=HL2/CPL
      HG2=HGI(I+1-L1)-(HGI(I+1-L1)-HGI(I-L1))*XNG
      TG2=HG2/CPG
      RG2=1E5*P2/(RGC*TG2)
      R2=VF2*RG2+(1-VF2)*RL
      HGL2=HG2-HL2
      CG2=SQRT(FI*RGC*TG2)
      U2=UI(I+1-L1)-(UI(I+1-L1)-UI(I-L1))*XNG
      A2=1/SQRT(R2*(VF2/(RG2*CG2**2)+(1-VF2)/(CL**2*RL)))
      T2=AT
      IF(VF2.GE.1.) THEN
      VF2=1.
      QIG2=0.0
      HENU2=0.0
      ELSE IF(VF2.LT.1.) THEN
C***************** NUCLEATION ************************:
      TTRIAL=TL2
      CALL NOSUBT(TTRIAL,PS,RGS)
      IF((PS/P2).LE.1.) THEN
      HENU2=0.0
      ELSE IF((PS/P2).GT.1.) THEN
      RC=2*SIG*1E-5/((PS-P2)*(1-RGS/RL))
      GE=4.1888*SIG*RC**2
      ANO=RL*(1-VF2)*AC/WM
      HENU2=ANO**(2./3.)*S*SQRT(.955*SIG*AC/(WM*F))*4/DIA
     1*exp((-1)*(GE*F/(BC*TL2)))
      END IF
      QIG2=3.9*BN2**(2./3.)*VF2**(1./3.)*UN*CK*(TL2-TG2)
      END IF
30    GMN2=HENU2*4.1888*RC**3*RGS*F
      BCE2=HENU2*GE*1E-3*F
      GMI2=QIG2/HGL2
      EX2=(GMI2+GMN2)*(1/RG2-1/RL)+BCE2/(CPG*TG2*RG2)
C       EX2=GMI2*(1/RG2-1/RL)
      IF(I.EQ.0) GO TO 33
      P(I)=(P2+(R2*A2)/(R1*A1)*P1+R2*A2*1E-5*(U1+A1*EX1*(AT+DT
     1-T1)-U2+A2*EX2*(AT+DT-T2)))/(1+R2*A2/(R1*A1))
31    U(I)=(P1-P(I))*1E5/(R1*A1)+U1+A1*EX1*(AT+DT-T1)
      IF(T1.GT.AT.OR.T2.GT.AT) THEN
      T4=(XI(I)-X1+T1*(X1-X2)/(T1-T2)-U(I)*(AT+DT))/((X1-X2)/
     1(T1-T2)-U(I))
      X4=X1+(T4-T1)*(X1-X2)/(T1-T2)
      ELSE IF(ABS(T1-AT).LE.1E-6.AND.ABS(T2-AT).LE.1E-6) THEN
      T4=AT
      X4=XI(I)-U(I)*DT
      END IF
      XNG=SQRT((T4-T1)**2+(X4-X1)**2)/SQRT((T2-T1)**2+(X2-X1)**2)
      HL4=(HL2-HL1)*XNG+HL1
      P4=(P2-P1)*XNG+P1
      HG4=(HG2-HG1)*XNG+HG1
      HGL4=HG4-HL4
      TG4=HG4/CPG
      TL4=HL4/CPL
      CG4=SQRT(RGC*FI*TG4)
      RG4=1E5*P4/(RGC*TG4)
      VF4=(VF2-VF1)*XNG+VF1
      BN4=(BN2-BN1)*XNG+BN1
      R4=VF4*RG4+(1-VF4)*RL
      U4=(U2-U1)*XNG+U1
32    B=VF4*(1-VF4)*(RG4*CG4**2-(RL*CL**2))/(RG4*CG4**2*
     1RL*CL**2)
      IF(VF4.GE.1.) THEN
      VF4=1
      QIG4=0.0
      HENU4=0.0
      ELSE IF(VF4.LT.1.) THEN
C************: NUCLEATION ************:
      TTRIAL=TL4
      CALL NOSUBT(TTRIAL,PS,RGS)
      IF((PS/P4).LE.1.) THEN
      HENU4=0.0
      ELSE IF((PS/P4).GT.1.) THEN
```

```
RC=2*SIG*1E-5/((PS-P4)*(1-RGS/RL))
GE=4.1888*SIG*RC**2
ANO=RL*(1-VF4)*AC/WM
HENU4=ANO**(2./3.)*S*SQRT(.955*SIG*AC/(WM*F))*4/DIA
1*exp((-1)*(GE*F/(BC*TL4)))
END IF
QIG4=3.9*BN4**(2./3.)*VF4**(1./3.)*UN*CK*(TL4-TG4)
END IF
GMN4=HENU4*4.1888*RC**3*RGS*F
BCE4=HENU4*GE*1E-3*F
GMI4=QIG4/HGL4
EX4=R4*(GMI4+GMN4)/(RG4*RL)+BCE4*(1-VF4)/(RG4*CPG*TG4)
VF(I)=VF4+B*(P(I)-P4)*1E5+EX4*(AT+DT-T4)
IF(VF(I).GT.1..AND.(VF(I)-1.).GT.1E-4) THEN
DT=DT/2.
GO TO 7
ELSE IF(ABS(VF(I)-1.).LE.1E-4) THEN
VF(I)=1.
END IF
IF(VF4.LT.1.) THEN
BN(I)=BN4+BN4/VF4*(VF(I)-VF4)+BN4*1E5/(CG4**2*RG4)*(P(I)-P4)+
1(HENU4-BN4/(RG4*VF4)*(GMI4+GMN4+BCE4/(CPG*TG4)))*DT
HL(I)=(P(I)-P4)*100/RL+HL4-BCE4*DT/(RL*(1-VF4))
ELSE IF(VF4.GE.1.) THEN
HL(I)=HL4+(P(I)-P4)*1E2/RL
BN(I)=0.0
END IF
TL(I)=HL(I)/CPL
HG(I)=HG4+(P(I)-P4)*100/RG4+BCE4*DT/(RG4*VF4)
HGL(I)=HG(I)-HL(I)
TG(I)=HG(I) CPG
RG(I)=1E5*P(I)/(RGC*TG(I))
CG(I)=SQRT(FI*RGC*TG(I))
R(I)=VF(I)*RG(I)+(1-VF(I))*RL
IF(VF(I).LT.0.0.OR.VF(I).GT.1.) TYPE*,'VF',P(I),I,XMA
IF(P(I).LT.0.0) TYPE*,'P',I,K
A(I)=1/SQRT(R(I)*(VF(I)/(RG(I)*CG(I)**2)+(1-VF(I))
1/(RL*CL**2)))
IF(I.EQ.J) THEN
A(I)=A(I)*CD
GO TO 35
END IF
GO TO 9
33   P(I)=R2*A2*1E-5*(EX2*DT*A2-U2)+P2
U(I)=0.0
P4=PI(I)
U4=UI(I)
VF4=VFI(I)
BN4=BNI(I)
HL4=HLI(I)
R4=RI(I)
RG4=RGI(I)
TG4=TGI(I)
HGL4=HGLI(I)
HG4=HGI(I)
CG4=CGI(I)
TL4=TLI(I)
T4=AT
GO TO 32
34   P(I)=1.0133
N=0
IF(PI(J).GT.3.) THEN
SP=PI(J)-1.
ELSE IF(PI(J).LE.3.) THEN
SP=1.
END IF
HL2=HLI(I)
R2=RI(I)
P2=PI(I)
RG2=RGI(I)
HG2=HGI(I)
HGL2=HGLI(I)
CG2=CGI(I)
TG2=TGI(I)
TL2=TLI(I)
```

```
      VF2=VFI(I)
      BN2=BNI(I)
      U2=UI(I)
      X2=XI(I)
      T2=AT
      GO TO 31
35    IF(N.EQ.1) GO TO 36
      IF((U(I)-A(I)).LE.0.0) GO TO 9
      P(I)=P(I)+SP
      N=N+1
      GO TO 31
36    IF(ABS(U(I)-A(I)).LE.1E-2) THEN
      N=0
      GO TO 9
      ELSE IF((U(I)-A(I)).LT.0.0) THEN
      SP=SP/1.1
      P(I)=P(I)-SP
      GO TO 31
      ELSE IF((U(I)-A(I)).GT.0.0) THEN
      SP=SP/1.1
      P(I)=P(I)+SP
      GO TO 31
      END IF
C*****************AIR GAS*********************************
37    IF(ABS(XGA-XI(I)).LE.5E-6) THEN
      P(I)=PGA
      U(I)=UGA
      TG(I)=TGGAA
      RG(I)=RGGAA
      CG(I)=CGGAA
      VF(I)=0.0
      HL(I)=0.0
      HG(I)=0.0
      R(I)=0.0
      A(I)=0.0
      TL(I)=0.0
      HGL(I)=0.0
      GO TO 9
      END IF
      IF(XGB.LT.XI(I-1)) GO TO 39
      IF(XGB.GE.XI(I)) GO TO 38
      X1=(XI(I)/DT-UGB-CGGBA+XGB*((UGB+CGGBA-UI(I)-CGI(I))/(XGB-XI(I)
     1)))/(1/DT+(UGB+CGGBA-UI(I)-CGI(I))/(XGB-XI(I)))
      IF(X1.GT.XI(I)) TYPE*,'NOA1-B-IA-A',K,I
      IF(X1.LT.XGB) THEN
38    UCA=UGA+CGGAA
      UCB=UGB+CGGBA
      NUMBER=6
      CALL INTRPL(NUMBER,UCA,UCB,XI(I),XGA,XGB,DT,AT,X1,T1,XNG)
      P1=PGA-(PGA-PGB)*XNG
      U1=UGA-(UGA-UGB)*XNG
      TG1=TGGAA-(TGGAA-TGGBA)*XNG
      RG1=1E5*P1/(RGCG*TG1)
      CG1=SQRT(FIG*RGCG*TG1)
      GO TO 40
      ELSE IF(X1.GE.XGB) THEN
      XNG=(XI(I)-X1)/(XI(I)-XGB)
      P1=PI(I)-(PI(I)-PGB)*XNG
      U1=UI(I)-(UI(I)-UGB)*XNG
      TG1=TGI(I)-(TGI(I)-TGGBA)*XNG
      RG1=1E5*P1/(RGCG*TG1)
      CG1=SQRT(FIG*RGCG*TG1)
      T1=AT
      END IF
      GO TO 40
39    X1=XI(I)-(UI(I)+CGI(I))/(1/DT+(UI(I)+CGI(I)-UI(I-1)-CGI(I-1))
     1/DX)
      IF(X1.GT.XI(I).OR.X1.LT.XI(I-1)) TYPE*,'NOA1-B-A-A',K,I
      XNG=(XI(I)-X1)/DX
      P1=PI(I)-(PI(I)-PI(I-1))*XNG
      U1=UI(I)-(UI(I)-UI(I-1))*XNG
      TG1=TGI(I)-(TGI(I)-TGI(I-1))*XNG
      RG1=1E5*P1/(RGCG*TG1)
      CG1=SQRT(FIG*RGCG*TG1)
```

```
      T1=AT
40    IF(I.EQ.J) GO TO 42
      IF(XGB.LT.XI(I)) THEN
      X2=XI(I)-(UI(I)-CGI(I))/(1/DT+(UI(I+1)-CGI(I+1)-UI(I)+
     1CGI(I))/DX)
      IF(X2.GT.XI(I+1)) TYPE*,'NOA2-B-A-A',K,I
      IF(X2.LT.XI(I).AND.XGB.GE.XI(I-1)) THEN
       X2=(XI(I)/DT-UGB+CGGBA+XGB*(UGB-CGGBA-UI(I)+CGI(I))/(XGB-XI(I))
     1)/(1/DT+(UGB-CGGBA-UI(I)+CGI(I))/(XGB-XI(I)))
      IF(X2.LT.XGB) GO TO 72
       XNG=(X2-XGB)/(XI(I)-XGB)
       P2=PGB+(PI(I)-PGB)*XNG
       U2=UGB+(UI(I)-UGB)*XNG
       TG2=TGGBA+(TGI(I)-TGGBA)*XNG
       RG2=1E5*P2/(RGCG*TG2)
       CG2=SQRT(FIG*TG2*RGCG)
       T2=AT
       GO TO 73
      END IF
      IF(X2.LT.XI(I).AND.XGB.LT.XI(I-1)) THEN
      X2=XI(I)-(UI(I)-CGI(I))/(1/DT+(UI(I)-CGI(I)-UI(I-1)+CGI(I-1))/DX)
       L1=1
      ELSE IF(X2.GE.XI(I)) THEN
       L1=0
      END IF
      XNG=(XI(I+1-L1)-X2)/DX
      P2=PI(I+1-L1)-(PI(I+1-L1)-PI(I-L1))*XNG
      U2=UI(I+1-L1)-(UI(I+1-L1)-UI(I-L1))*XNG
      TG2=TGI(I+1-L1)-(TGI(I+1-L1)-TGI(I-L1))*XNG
      RG2=1E5*P2/(RGCG*TG2)
      CG2=SQRT(FIG*RGCG*TG2)
      T2=AT
      GO TO 73
      ELSE IF(XGB.GE.XI(I)) THEN
      X2=(XI(I)/DT-UGB+CGGBA+XGB*((UI(I+1)-CGI(I+1)-UGB+CGGBA)/(
     1XI(I+1)-XGB)))/((UI(I+1)-CGI(I+1)-UGB+CGGBA)/(XI(I+1)-XGB)+1/DT)
      IF(X2.GT.XI(I+1)) TYPE*,'NOA2-B-IA-A',I,K
      IF(X2.GE.XGB) THEN
      XNG=(XI(I+1)-X2)/(XI(I+1)-XGB)
      P2=PI(I+1)-(PI(I+1)-PGB)*XNG
      U2=UI(I+1)-(UI(I+1)-UGB)*XNG
      TG2=TGI(I+1)-(TGI(I+1)-TGGBA)*XNG
      RG2=1E5*P2/(RGCG*TG2)
      CG2=SQRT(FIG*RGCG*TG2)
      T2=AT
      GO TO 73
      ELSE IF(X2.LT.XGB) THEN
72     UCA=UGA-CGGAA
      UCB=UGB-CGGBA
      NUMBER=7
      CALL INTRPL(NUMBER,UCA,UCB,XI(I),XGA,XGB,DT,AT,X2,T2,XNG)
      P2=PGA-(PGA-PGB)*XNG
      U2=UGA-(UGA-UGB)*XNG
      TG2=TGGAA-(TGGAA-TGGBA)*XNG
      RG2=1E5*P2/(RGCG*TG2)
      CG2=SQRT(FIG*RGCG*TG2)
      END IF
      END IF
73     P(I)=(P2+(RG2*CG2)/(RG1*CG1)*P1+RG2*CG2*1E-5*(U1-U2))/(1+RG2*
     1CG2/(RG1*CG1))
41     U(I)=(P1-P(I))*1E5/(RG1*CG1)+U1
      IF(T1.GT.AT.OR.T2.GT.AT) THEN
      T4=(XI(I)-X1+T1*(X1-X2)/(T1-T2)-U(I)*(AT+DT))/((X1-X2)/
     1(T1-T2)-U(I))
      X4=X1+(T4-T1)*(X1-X2)/(T1-T2)
      ELSE IF(ABS(T1-AT).LE.1E-6.AND.ABS(T2-AT).LE.1E-6) THEN
      T4=AT
      X4=XI(I)-U(I)*DT
      END IF
      XNG=SQRT((T4-T1)**2+(X4-X1)**2)/SQRT((T2-T1)**2+(X2-X1)**2)
      P4=(P2-P1)*XNG+P1
      TG4=(TG2-TG1)*XNG+TG1
      TG(I)=TG4*(P(I)/P4)**.286
      RG(I)=1E5*P(I)/(RGCG*TG(I))
      CG(I)=SQRT(TG(I)*FIG*RGCG)
```

```
      VF(I)=0.0
      HL(I)=0.0
      HG(I)=0.0
      R(I)=0.0
      A(I)=0.0
      TL(I)=0.0
      HGL(I)=0.0
      IF(I.EQ.J) GO TO 43
      GO TO 9
42    P(I)=1.0133
      N=0
      SP=1.
      P2=PI(I)
      U2=UI(I)
      CG2=CGI(I)
      RG2=RGI(I)
      TG2=TGI(I)
      X2=XI(I)
      T2=AT
      GO TO 41
43    IF(N.EQ.1) GO TO 44
      IF((U(I)-CG(I)).LE.0.0) GO TO 9
      P(I)=P(I)+SP
      N=N+1
      GO TO 41
44    IF(ABS(U(I)-CG(I)).LE.1E-2) THEN
      N=0
      GO TO 9
      ELSE IF((U(I)-CG(I)).LT.0.0) THEN
      SP=SP/1.1
      P(I)=P(I)-SP
      GO TO 41
      ELSE IF((U(I)-CG(I)).GT.0.0) THEN
      SP=SP/1.1
      P(I)=P(I)+SP
      GO TO 41
      END IF
C*********************FREON GAS*********************************
45    IF((SWITCHG.EQ.'INS'.OR.SWITCHG1.EQ.'FST').AND.(XGA-XI(I))
     1.LE.5E-6) THEN
        U(I)=UGA
        P(I)=PGA
        TG(I)=TGGAG
        RG(I)=RGGAG
        CG(I)=CGGAG
        R(I)=0.0
        A(I)=0.0
        HG(I)=0.0
        HL(I)=0.0
        TL(I)=0.0
        VF(I)=0.0
        HGL(I)=0.0
        GO TO 9
       END IF
       IF(ABS(XMA-XI(I)).LE.5E-6) THEN
        P(I)=PMA
        U(I)=UMAG
        TG(I)=TGMAG
        RG(I)=RGMAG
        CG(I)=CGMAG
        R(I)=0.0
        A(I)=0.0
        HG(I)=0.0
        HL(I)=0.0
        TL(I)=0.0
        VF(I)=0.0
        HGL(I)=0.0
        GO TO 9
      END IF
      IF(XGB.LT.XI(I+1).AND.XMB.GE.XI(I-1).AND.I.NE.J) THEN
      XNG=(XMA-XI(I))/(XMA-XGA)
      P(I)=PMA-(PMA-PGA)*XNG
      U(I)=UMAG-(UMAG-UGA)*XNG
      TG(I)=TGMAG-(TGMAG-TGGAG)*XNG
      CG(I)=SQRT(FIG*RGC*TG(I))
```

```
      RG(I)=1E5*P(I)/(RGC*TG(I))
      A(I)=0.0
      VF(I)=0.0
      HL(I)=0.0
      HG(I)=0.0
      R(I)=0.0
      TL(I)=0.0
      HGL(I)=0.0
      GO TO 9
      ELSE IF(XGB.GE.XI(I+1).OR.I.EQ.J) THEN
      IF(XMB.LT.XI(I-1)) GO TO 47
      IF(XMB.GE.XI(I)) GO TO 46
      X1=(XI(I)/DT-UMBG-CGMBG+XMB*(UMBG+CGMBG-UI(I)-CGI(I))/
     1(XMB-XI(I)))/(1/DT+(UMBG+CGMBG-UI(I)-CGI(I))/(XMB-XI(I)))
      IF(X1.GT.XI(I)) TYPE*,'NOG1-B-IM-G',K,I
      IF(X1.LT.XMB) THEN
   46  UCA=UMAG+CGMAG
      UCB=UMBG+CGMBG
      NUMBER=8
      CALL INTRPL(NUMBER,UCA,UCB,XI(I),XMA,XMB,DT,AT,X1,T1,XNG)
      P1=PMA-(PMA-PMB)*XNG
      U1=UMAG-(UMAG-UMBG)*XNG
      TG1=TGMAG-(TGMAG-TGMBG)*XNG
      RG1=1E5*P1/(RGC*TG1)
      CG1=SQRT(TG1*FIG*RGC)
      GO TO 48
      ELSE IF(X1.GE.XMB) THEN
      XNG=(XI(I)-X1)/(XI(I)-XMB)
      P1=PI(I)-(PI(I)-PMB)*XNG
      U1=UI(I)-(UI(I)-UMBG)*XNG
      TG1=TGI(I)-(TGI(I)-TGMBG)*XNG
      RG1=1E5*P1/(RGC*TG1)
      CG1=SQRT(FIG*RGC*TG1)
      T1=AT
      END IF
      GO TO 48
   47 X1=XI(I)-(UI(I)+CGI(I))/(1/DT+(UI(I)+CGI(I)-UI(I-1)-CGI(I-1))
     1/DX)
      IF(X1.GT.XI(I).OR.X1.LT.XI(I-1)) TYPE*,'NOG1-B-G-G',K,I
      XNG=(XI(I)-X1)/DX
      P1=PI(I)-(PI(I)-PI(I-1))*XNG
      U1=UI(I)-(UI(I)-UI(I-1))*XNG
      TG1=TGI(I)-(TGI(I)-TGI(I-1))*XNG
      RG1=1E5*P1/(TG1*RGC)
      CG1=SQRT(FIG*RGC*TG1)
      T1=AT
   48  IF(I.EQ.J) GO TO 50
      IF(XMB.LT.XI(I)) THEN
      X2=XI(I)-(UI(I)-CGI(I))/(1/DT+(UI(I+1)-CGI(I+1)-UI(I)+
     1CGI(I))/DX)
      IF(X2.GT.XI(I+1)) TYPE*,'NOG2-B-G-G',K,I
      IF(X2.LT.XI(I).AND.XMB.GE.XI(I-1)) THEN
      X2=(XI(I)/DT-UMBG+CGMBG+XMB*(UMBG-CGMBG-UI(I)+CGI(I))/
     1(XMB-XI(I)))/(1/DT+(UMBG-CGMBG-UI(I)+CGI(I))/(XMB-XI(I)))
      IF(X2.LT.XMB) GO TO 60
      XNG=(X2-XI(I))/(XMB-XI(I))
      P2=PI(I)+(PMB-PI(I))*XNG
      U2=UI(I)+(UMBG-UI(I))*XNG
      TG2=TGI(I)+(TGMBG-TGI(I))*XNG
      RG2=1E5*P2/(RGC*TG2)
      CG2=SQRT(RGC*FIG*TG2)
      T2=AT
      GO TO 58
      END IF
      IF(X2.LT.XI(I).AND.XMB.LT.XI(I-1)) THEN
       X2=XI(I)-(UI(I)-CGI(I))/(1/DT+(UI(I)-CGI(I)-UI(I-1)+CGI(I-1))
     1/DX)
       L1=1
      ELSE IF(X2.GE.XI(I)) THEN
       L1=0
      END IF
      XNG=(XI(I+1-L1)-X2)/DX
      P2=PI(I+1-L1)-(PI(I+1-L1)-PI(I-L1))*XNG
      U2=UI(I+1-L1)-(UI(I+1-L1)-UI(I-L1))*XNG
      TG2=TGI(I+1-L1)-(TGI(I+1-L1)-TGI(I-L1))*XNG
```

```
      RG2=1E5*P2/(RGC*TG2)
      CG2=SQRT(TG2*RGC*FIG)
      T2=AT
      GO TO 58
      ELSE IF(XMB.GE.XI(I)) THEN
      X2=(XI(I)/DT-UMBG+CGMBG+XMB*(UI(I+1)-CGI(I+1)-UMBG+CGMBG)/(XI
     1(I+1)-XMB))/(1/DT+(UI(I+1)-CGI(I+1)-UMBG+CGMBG)/(XI(I+1)-XMB))
      IF(X2.GT.XI(I+1)) TYPE*,'NOG2-B-IM-G',I,K
      IF(X2.GE.XMB) THEN
      XNG=(XI(I+1)-X2)/(XI(I+1)-XMB)
      P2=PI(I+1)-(PI(I+1)-PMB)*XNG
      U2=UI(I+1)-(UI(I+1)-UMBG)*XNG
      TG2=TGI(I+1)-(TGI(I+1)-TGMBG)*XNG
      RG2=1E5*P2/(TG2*RGC)
      CG2=SQRT(TG2*RGC*FIG)
      T2=AT
      GO TO 58
      ELSE IF(X2.LT.XMB) THEN
   60  UCA=UMAG-CGMAG
      UCB=UMBG-CGMBG
      NUMBER=9
      CALL INTRPL(NUMBER,UCA,UCB,XI(I),XMA,XMB,DT,AT,X2,T2,XNG)
      P2=PMA-(PMA-PMB)*XNG
      U2=UMAG-(UMAG-UMBG)*XNG
      TG2=TGMAG-(TGMAG-TGMBG)*XNG
      RG2=1E5*P2/(RGC*TG2)
      CG2=SQRT(TG2*RGC*FIG)
      GO TO 58
      END IF
      END IF
      ELSE IF(XMB.LT.XI(I-1)) THEN
      IF(XGB.GT.XI(I+1)) GO TO 56
      IF(XGB.LE.XI(I)) GO TO 55
      X2=(XI(I) DT-UGB+CGGBG+XGB*(UI(I)-CGI(I)-UGB+CGGBG)/(XI(I)-XGB))
     1/(1/DT+(UI(I)-CGI(I)-UGB+CGGBG)/(XI(I)-XGB))
      IF(X2.LT.XI(I)) GO TO 59
      IF(X2.GT.XGB) THEN
   55  UCA=UGA-CGGAG
      UCB=UGB-CGGBG
      NUMBER=10
      CALL INTRPL(NUMBER,UCA,UCB,XI(I),XGA,XGB,DT,AT,X2,T2,XNG)
      IF(X2.LT.XGB.AND.XGB.LE.XI(I)) THEN
      X2=(XI(I)/DT-UI(I-1)+CGI(I-1)+XI(I-1)*(UI(I-1)-CGI(I-1)-UGB+
     1CGGBG)/(XI(I-1)-XGB))/(1/DT+(UI(I-1)-CGI(I-1)-UGB+CGGBG)/
     2(XI(I-1)-XGB))
       XNG=(X2-XGB)/(XI(I-1)-XGB)
       P2=PGB+(PI(I-1)-PGB)*XNG
       U2=UGB+(UI(I-1)-UGB)*XNG
       TG2=TGGBG+(TGI(I-1)-TGGBG)*XNG
       T2=AT
      ELSE IF(X2.GE.XGB) THEN
       P2=PGA-(PGA-PGB)*XNG
       U2=UGA-(UGA-UGB)*XNG
       TG2=TGGAG-(TGGAG-TGGBG)*XNG
      END IF
       RG2=1E5*P2/(RGC*TG2)
       CG2=SQRT(TG2*RGC*FIG)
      GO TO 57
      ELSE IF(X2.LE.XGB) THEN
      XNG=(X2-XI(I))/(XGB-XI(I))
      P2=PI(I)+(PGB-PI(I))*XNG
      U2=UI(I)+(UGB-UI(I))*XNG
      TG2=TGI(I)+(TGGBG-TGI(I))*XNG
      RG2=1E5*P2/(RGC*TG2)
      CG2=SQRT(FIG*RGC*TG2)
      T2=AT
      GO TO 57
      END IF
   56  X2=XI(I)-(UI(I)-CGI(I))/(1/DT+(UI(I+1)-CGI(I+1)-UI(I)+CGI(I))
     1/DX)
      IF(X2.GT.XI(I+1)) TYPE*,'FREON-GAS X2 WRONG'
   59  IF(X2.LT.XI(I)) THEN
      X2=XI(I)-(UI(I)-CGI(I))/(1/DT+(UI(I)-CGI(I)-UI(I-1)+CGI(I-1))
     1/DX)
      L1=1
```

```
      ELSE IF(X2.GE.XI(I)) THEN
      L1=0
      END IF
      XNG=(XI(I+1-L1)-X2)/DX
      P2=PI(I+1-L1)-(PI(I+1-L1)-PI(I-L1))*XNG
      U2=UI(I+1-L1)-(UI(I+1-L1)-UI(I-L1))*XNG
      TG2=TGI(I+1-L1)-(TGI(I+1-L1)-TGI(I-L1))*XNG
      RG2=1E5*P2/(RGC*TG2)
      CG2=SQRT(FIG*RGC*TG2)
      T2=AT
   57  IF(XGB.GT.XI(I)) THEN
      X1=XI(I)-(UI(I)+CGI(I))/(1/DT+(UI(I)+CGI(I)-UI(I-1)-CGI(I-1))
     1/DX)
      IF(X1.GT.XI(I).OR.X1.LT.XI(I-1)) TYPE*,'FREON-GAS X1 WRONG'
      XNG=(XI(I)-X1)/DX
      P1=PI(I)-(PI(I)-PI(I-1))*XNG
      U1=UI(I)-(UI(I)-UI(I-1))*XNG
      TG1=TGI(I)-(TGI(I)-TGI(I-1))*XNG
      RG1=1E5*P1/(TG1*RGC)
      CG1=SQRT(FIG*TG1*RGC)
      T1=AT
      GO TO 58
      ELSE IF(XGB.LE.XI(I)) THEN
      X1=(XI(I),DT-UGB-CGGBG+XGB*(UGB+CGGBG-UI(I-1)-CGI(I-1))/
     1(XGB-XI(I-1)))/(1/DT+(UGB+CGGBG-UI(I-1)-CGI(I-1))/(XGB-XI(I-1)))
      IF(X1.LT.XI(I-1)) TYPE*,'FREON-GAS X1 WRONG1'
      IF(X1.GT.XGB) THEN
      UCA=UGA+CGGAG
      UCB=UGB+CGGBG
      NUMBER=11
      CALL INTRPL(NUMBER,UCA,UCB,XI(I),XGA,XGB,DT,AT,X1,T1,XNG)
      P1=PGA-(PGA-PGB)*XNG
      U1=UGA-(UGA-UGB)*XNG
      TG1=TGGAG-(TGGAG-TGGBG)*XNG
      RG1=1E5*P1/(RGC*TG1)
      CG1=SQRT(FIG*RGC*TG1)
      GO TO 58
      ELSE IF(X1.LE.XGB) THEN
      XNG=(X1-XI(I-1))/(XI(I-1)-XGB)
      P1=PI(I-1)+(PI(I-1)-PGB)*XNG
      U1=UI(I-1)+(UI(I-1)-UGB)*XNG
      TG1=TGI(I-1)+(TGI(I-1)-TGGBG)*XNG
      RG1=1E5*P1/(RGC*TG1)
      CG1=SQRT(TG1*RGC*FIG)
      T1=AT
      END IF
      END IF
      END IF
   58   IF(I.EQ.J) GO TO 50
      P(I)=(P2+RG2*CG2*P1/(RG1*CG1)+RG2*CG2*1E-5*(U1-U2))/
     1(1+RG2*CG2/(RG1*CG1))
   49   U(I)=(P1-P(I))*1E5/(RG1*CG1)+U1
      IF(T1.GT.AT.OR.T2.GT.AT) THEN
      T4=(XI(I)-X1+T1*(X1-X2)/(T1-T2)-U(I)*(AT+DT))/((X1-X2)/(T1-T2)
     1-U(I))
      X4=X1+(T4-T1)*(X1-X2)/(T1-T2)
      ELSE IF(ABS(T1-AT).LT.1E-6.AND.ABS(T2-AT).LT.1E-6) THEN
      T4=AT
      X4=XI(I)-U(I)*DT
      END IF
      XNG=SQRT((T4-T1)**2+(X4-X1)**2)/SQRT((T2-T1)**2+(X2-X1)**2)
      P4=(P2-P1)*XNG+P1
      TG4=(TG2-TG1)*XNG+TG1
      TG(I)=TG4*(P(I)/P4)**.286
      RG(I)=1E5*P(I)/(RGC*TG(I))
      CG(I)=SQRT(RGC*FIG*TG(I))
      VF(I)=0.0
      HL(I)=0.0
      HG(I)=0.0
      R(I)=0.0
      A(I)=0.0
      TL(I)=0.0
      HGL(I)=0.0
      IF(I.EQ.J) GO TO 51
```

```
      GO TO 9
50    P(I)=1.0133
      N=0
      SP=1.
      P2=PI(I)
      U2=UI(I)
      TG2=TGI(I)
      RG2=RGI(I)
      CG2=CGI(I)
      X2=XI(I)
      T2=AT
      GO TO 49
51    IF(N.EQ.1) GO TO 52
      IF((U(I)-CG(I)).LE.0.0) GO TO 9
      P(I)=P(I)+SP
      N=N+1
      GO TO 49
52    IF(ABS(U(I)-CG(I)).LE.1E-2) THEN
      N=0
      GO TO 9
      ELSE IF((U(I)-CG(I)).LT.0.0) THEN
      SP=SP/1.1
      P(I)=P(I)-SP
      GO TO 49
      ELSE IF((U(I)-CG(I)).GT.0.0) THEN
      SP=SP/1.1
      P(I)=P(I)+SP
      GO TO 49
      END IF
C*******************END PROGRAM*****************************************
9     CONTINUE
      SWITCHM1='NFS'
      SWITCHG1='NFS'
      IF(SWITCH2.EQ.'NO2') THEN
       UCTRC=U(J)-CG(J)
      IF(ABS(UCTR-UCTRC).GT.1E-3) THEN
       GO TO 7
      ELSE IF(ABS(UCTR-UCTRC).LE.1E-3) THEN
       SWITCH2='ON2'
      END IF
      END IF
      DO 53 I=0,J,1
      PI(I)=P(I)
      UI(I)=U(I)
      HLI(I)=HL(I)
      HGI(I)=HG(I)
      HGLI(I)=HGL(I)
      RI(I)=R(I)
      VFI(I)=VF(I)
      AI(I)=A(I)
      RGI(I)=RG(I)
      TLI(I)=TL(I)
      TGI(I)=TG(I)
      CGI(I)=CG(I)
      BNI(I)=BN(I)
53    CONTINUE
      AT=AT+DT
      IF(XMB.LT.PL) THEN
      IF(ABS(XMA-XMB).GT.DX) TYPE*,'LARGE TIME STEP!'
      IF(ABS(XGA-XGB).GT.DX) TYPE*,'LARGE TIME STEP!'
      PMB=PMA
      UMBM=UMAM
      XMB=XMA
      BNMBM=BNMAM
      VFMBM=VFMAM
      HLMBM=HLMAM
      HGMBM=HGMAM
      HGLMBM=HGLMAM
      RMBM=RMAM
      AMBM=AMAM
      TLMBM=TLMAM
      TGMBM=TGMAM
      RGMBM=RGMAM
      CGMBM=CGMAM
      RGMBG=RGMAG
```

```
      CGMBG=CGMAG
      TGMBG=TGMAG
      UMBG=UMAG
      END IF
      IF(XGB.LT.PL) THEN
      XGB=XGA
      PGB=PGA
      UGB=UGA
      TGGBG=TGGAG
      RGGBG=RGGAG
      CGGBG=CGGAG
      TGGBA=TGGAA
      RGGBA=RGGAA
      CGGBA=CGGAA
      END IF
      IF(SWITCHM.EQ.'OUT') THEN
      XMA=XMA+DX
      XMB=XMA
      END IF
      IF(SWITCHG.EQ.'OUT') THEN
      XGA=XGA+DX
      XGB=XGA
      END IF
      K=K+1
      IF (AT.GE.30.E-3.AND.P(0).LT.1.) GO TO 54
      GO TO 6
54    TYPE*,AT
      END
```

```
C SUBROUTINE "FRICTION" FOR CALCULATING THE WALL FRICTION.
      SUBROUTINE FRICTION(RL,RG,R,DIA,U,DVL,DVG,VF,TW)
      REAL RL,RG,R,DIA,U,DVL,DVG,VF,TW,FR,TFM,REL,FQ,FB
      IF(ABS(U).LE.1E-6) THEN
      TW=0.0
      ELSE IF(ABS(U).GT.1E-6) THEN
      FQ=VF*RG/R
      FG=R*ABS(U)/(9.81*RL**2*(RL-RG)*DVL)**(1./3.)
      IF(RG.LT.0.0) TYPE*,'FRICTION-RG<0'
      FB=(DVG/DVL)**.2*(RL/RG)**.8
      A1=1+3.57*EXP((-0.00884)*FG)
      A2=1-EXP((-4.96)*(1-FQ))
      TFM=1+FQ*(FB-1)*A1*A2
      IF(VF.LT.1.) THEN
      REL=DIA*ABS(U)/DVL
      IF(REL.EQ.0.0) TYPE*,DIA,U,DVL,VF
      ELSE IF(VF.GE.1.) THEN
      REL=DIA*ABS(U)/DVG
      END IF
      IF(REL.LE.1462.27) THEN
      FR=64./REL
      ELSE
      FR=.046*REL**(-.2)
      END IF
      TW=2*R*FR*U*ABS(U)*TFM/DIA
      END IF
      RETURN
      END
```

```
C SUBROUTINE "SECA" USED BY THE NUCLEATION MODEL TO EVALUATE THE
C CONTACT ANGLE BETWEEN THE CRITICAL BUBBLE AND THE WALL,USING THE
C KNOWN VALUE OF THE HETEROGENEOUS FACTOR.
      SUBROUTINE SECA(FK1,XN)
      REAL XO1,XO2,FXO(2),XN,FK1,FK2,
     1FK3,FK4,X
      TYPE*,'SECA',XN
      XO1=0.0
      XO2=1.
2     DO 1 I=1,2
      IF(I.EQ.1) X=XO1
      IF(I.EQ.2) X=XO2
      FXO(I)=X**3-3*X+2-4*FK1
1     CONTINUE
      IF(FXO(1).EQ.FXO(2)) THEN
      XN=XO1
      GO TO 3
      END IF
      XN=(XO1*FXO(2)-XO2*FXO(1))/(FXO(2)-FXO(1))
      IF(ABS(XN-XO2).GE.1E-6) THEN
      XO2=XN
      GO TO 2
      END IF
      TYPE*,XN
3     RETURN
      END
```

```
C SUBROUTINE "INTRPL" USED BY THE "EVUT6" MAIN PROGRAM DURING A WAVE
C INTERACTION PROCESS.
      SUBROUTINE INTRPL(N,UA,UB,XI,XA,XB,TD,TA,X,T,XX)
      DOUBLE PRECISION XR,TR,UA,UB,XI,XA,XB,TD,TA,F1,F2,F3,F4,F5,F6,TT1
     1,TT2,SL,FK1,FK2,FK3,FK4,FK5,XN1,XN2
      REAL X,T,XX
      XR=0.0
      TR=0.0
      IF(XA.EQ.XB) THEN
      TYPE*,'XA=XB'
      F1=(UA-UB)/TD
      F2=TA+TD
      F3=UA-2*F1*F2
      F4=XI-XA-F2*UA+F1*F2**2
      F5=SQRT(F3**2-4*F1*F4)/(2*F1)
      F6=-F3/(2*F1)
      TT1=F6-F5
      TT2=F6+F5
      IF(TT1.GE.TA.AND.TT1.LE.F2) TR=TT1
      IF(TT2.GE.TA.AND.TT2.LE.F2) TR=TT2
      XR=XA
      IF(TR.EQ.0.0) TYPE*,'TIME INTRPL 0'
      GO TO 2
      END IF
      IF(UA.EQ.UB) THEN
      TYPE*,'UA=UB'
      SL=(XA-XB)/TD
      XR=(XA-SL*XI/UA)/(1-SL/UA)
      TR=TD+TA+(XR-XI)/UA
      GO TO 2
      END IF
      FK1=(UA-UB)/(XA-XB)
      FK2=TD/(XA-XB)
      FK3=-(FK1*FK2)
      IF(FK3.EQ.0.0)TYPE*,'FK3=0',UA,UB,XA,XB
      FK4=1+FK1*(TD+2*XB*FK2)-FK2*UB
      FK5=-FK1*(XB*TD+XB**2*FK2)-XI+TD*UB+XB*FK2*UB
      XN1=(-FK4+SQRT(FK4**2-4*FK3*FK5))/(2*FK3)
      XN2=(-FK4-SQRT(FK4**2-4*FK3*FK5))/(2*FK3)
      IF((XN1.LE.XA.AND.XN1.GE.XB).OR.(XN1.GE.XA.AND.XN1.LE.XB))
     1XR=XN1
      IF((XN2.LE.XA.AND.XN2.GE.XB).OR.(XN2.GE.XA.AND.XN2.LE.XB))
     1XR=XN2
      IF(XR.EQ.0.0) THEN
      IF(ABS(XA-XN1).LE.1E-6.OR.ABS(XA-XN2).LE.1E-6) THEN
      XR=XA
      TR=TA+TD
      GO TO 2
      END IF
      IF(ABS(XB-XN1).LE.1E-4.OR.ABS(XB-XN2).LE.1E-4) THEN
      XR=XB
      TR=TA
      GO TO 2
      ELSE IF((ABS(XB-XN1).GT.1E-4.OR.ABS(XB-XN2).GT.1E-4)
     1.AND.(N.EQ.10.OR.N.EQ.5)) THEN
      IF(ABS(XB-XN1).LT.ABS(XB-XN2)) XR=XN1
      IF(ABS(XB-XN2).LT.ABS(XB-XN1)) XR=XN2
      GO TO 1
      END IF
      END IF
      IF(XR.EQ.0.0) TYPE*,'SUBROUTINE INTRPL--X=0',XN1,XN2,XA,XB,XI,N
      TR=FK2*(XR-XB)+TA
2     IF(TR.GT.(TA+TD).OR.TR.LT.TA) TYPE*,'ALARM--TIME INTRPL',
     1UA,UB,XA,XB,XR,TR,N
      XX=SQRT((XA-XR)**2+(TA+TD-TR)**2)/SQRT((XA-XB)**2+TD**2)
      IF(XR.EQ.0.0.OR.TR.EQ.0.0) TYPE*,'XR=0.0 OR TR=0.0',XR,TR,N
1     X=XR
      T=TR
      RETURN
      END
```

APPENDIX B. BASIC PROPERTIES AND CONSTANTS

K 1.38 E-23 J/Kg °K

Na 6.022 E26 Kmole/Kg

Freon 12 (for the range of the initial temperatures)

MW 120.91

R 68.77 J/Kg °K

σ 1E-2 N/m

k_l 7.26 E-5 KW/m °K

ν_l 1.93 E-7 m²/sec

ν_g 1.62 E-6 m²/sec

c_l 500 m/sec

ρ_l 1300 Kg/m³

Cp 0.67 KJ/Kg °K

Water (for Edwards and O'Brien experimental conditions)

MW 18.015

R 461.5 J/Kg °K

σ $0.2358\left[1-\frac{T_{sat}}{T_{cr}}\right]^{1.256}\left[1-0.625\left[1-\frac{T_{sat}}{T_{cr}}\right]\right]$ (Alamgir,Lienhard (1978))

k_l 6.35 E-4 KW/m °K

ν_l 1.37 E-7 m²/sec

ν_g 5.22 E-7 m²/sec

c_l 1050 m/sec

ρ_l 810.8 Kg/m³

Cp 5.38 KJ/Kg °K

APPENDIX C. SUMMARY OF BLOWDOWN TESTS CONDUCTED

A. HOMOGENEOUS MODEL

EQUATIONS USED: (4.8) and (4.12)
MAIN ASSUMPTION: No temperature and velocity difference between the two phases.
SPECIAL NOTE: In figures 92 and 93 ,this model is independent of experimental parameters.

B. THERMAL NON-EQUILIBRIUM MODEL (CONST.BUBBLE SIZE)

EQUATIONS USED: (4.31) ,(4.32) ,(4.42) ,(4.51) and (4.63)
MAIN ASSUMPTIONS:a) zero slip between the two phases.
b) bubbly mixture
c) constant bubble size throughout the process.
SPECIAL NOTE: In figures 94 to 108 ,this model is indicated by the experimental parameters: R_b (bubble size) and C_d (exit loss coefficient).

C. THERMAL NON-EQUILIBRIUM MODEL (NUCLEATION PROCESS)

EQUATIONS USED: (4.31) ,(4.32) ,(4.51) ,(4.69) ,(4.70) ,(4.71) and (4.72)
MAIN ASSUMPTIONS:a) zero slip between the two phases
b) bubbly mixture
c) heterogeneous nucleation determined by

ϕ

SPECIAL NOTE: In figures 109 to 132 ,this model is indicated by the experimental parameters: ϕ (heterogeneous factor) and C_d.

D. THERMAL NON-EQUILIBRIUM MODEL (PARTIALLY FULL VESSEL)

EQUATIONS USED: (4.31) ,(4.32) ,(4.51) ,(4.69) ,(4.70) , (4.71) ,(4.72) and (4.73)
MAIN ASSUMPTIONS:a) same as before
b) the escape vapor velocity from the interface is given as: $u_{vapor} = u_{interface} / VE$.
SPECIAL NOTE: In figures 133 to 148 ,this model is

indicated by the experimental parameters: ϕ ,C_d and VE (slip ratio parameter).

APPENDIX C. SUMMARY OF BLOWDOWN TESTS CONDUCTED

	MS1	MS2	MS3	P1	P2
PARTIALLY FULL VESSEL	—	—	—	2,P	23,P,L,C
EXTENSION PIPEWORK	9,P,L	7,P,L	6,P,L	2,P	31,P,L,C
VERTICAL VESSEL	10,P,L	4,P,L	15,P,L,T	42,P,L	58,P,L,C,T
HORIZONTAL VESSEL	—	—	2,P,T	7,P	2,P
VACUUM EXIT CONDITION	—	—	—	4,P	—

P: PRESSURE MEASUREMENT

T: TEMPERATURE MEASUREMENT

L: LASER

C: HIGH SPEED CAMERA

MS1: MILD STEEL VESSEL (3.2μmRMS)

MS2: MILD STEEL VESSEL (0.8μmRMS)

MS3: MILD STEEL VESSEL (0.2μmRMS)

P1: PERSPEX VESSEL (SMOOTH)

P2: PERSPEX VESSEL (ROUGH)